МІНІСТЕРСТВО ОСВІТИ І НАУКИ УКРАЇНИ

КИЇВСЬКИЙ НАЦІОНАЛЬНИЙ УНІВЕРСИТЕТ
БУДІВНИЦТВА І АРХІТЕКТУРИ

# БУДІВЕЛЬНІ КОНСТРУКЦІЇ. ТЕОРІЯ І ПРАКТИКА

Збірник наукових праць

Випуск 17

Київ – КНУБА – 2025

Наукове фахове видання / Scientific edition
ISSN 2522-4182

Свідоцтво про державну реєстрацію / Certificate of state registration КВ 22149-12049Р від 23.05.2016.

Збірник наукових праць «Будівельні конструкції. Теорія і практика». Випуск 17.
Головний редактор О.Д.Журавський. К.:КНУБА, 2025. 232 с. DOI:10.32347/2522-4182.17.2025

На підставі Наказу Міністерства освіти і науки України №1188 від 24.09.2020, включено до **категорії «Б» Переліку наукових фахових видань України у галузі технічних наук зі спеціальностей 192, 194.**
Проіндексовано у базі даних Index Copernicus, Google Scholar, CrossRef.

**UKR** / Наведені результати наукових досліджень будівельних конструкцій, методи розрахунку будівельних конструкцій, використання нових прогресивних матеріалів в будівельних конструкціях, методи підсилення будівельних конструкцій, будівель та споруд.

Призначений для наукових працівників, спеціалістів проектних організацій та виробничих підприємств будівельної галузі, докторантів, аспірантів та студентів навчальних закладів будівельногонапрямку. Видання здійснює публікації за спеціальностями :

192 Будівництво та цивільна інженерія, 132 Матеріалознавство
194 Гідротехнічне будівництво, водна інженерія та водні технології

Scientific articles journal «Building Constructions. Theory and practice». Issue 17.
Chief editor O. Zhuravskyi. K. : KNUCA, 2025. 232 p. DOI:10.32347/2522-4182.17.2025

Based on the Order of Ministry of Education and Science of Ukraine № 1188 from 24.09.2020 the journal was included in the **category "B" of the List of scientific professional publications of Ukraine in the field of technical sciences in specialties 192, 194.**
Indexed in the database Index Copernicus, Google Scholar, CrossRef

**ENG** / This compilation «Building Constructions. Theory and practice» includes results of scientific researches of building constructions, methods of calculation of building constructions, usage of new advanced materials in building constructions, methods of building constructions of buildings.

Collection is intend for reseachers, specialists of design organizations and production enterprises of construction industry, high school teachers, post - graduate students etc.



Рекомендовано до видання вченою радою Київського національного університету будівництва і архітектури, протокол № 39 від 25.12.2025 року.

Recommended for publication by the Academic Council of Kyiv National University of Construction and Architecture, Protokol No. 39 of 25.12. 2025

Адреса редакції: к. 104, 114, КНУБА, проспект Повітряних Сил, 31, м. Київ, , 03037,
телефон редакції: (044) 241-55-04, (044)245-48-42
Editorial Office address: off 104, 114, KNUCA, Pvitrianykh Syl ave., 31, Kyiv, Ukraine, 03037,
editorial phone: (044) 241-55-04, (044)245-48-42

# ЗМІСТ

ISSN 2522-4182

DOI: 10.32347/2522-4182.17.2025.5-16
УДК 624.012.26

# STRENGTH OF REINFORCED CONCRETE CONSTRUCTIONS UNDER PUNCHING SHEAR

*Yulii KLYMOV*

Kyiv National University of Construction and Architecture
31, Povitryanykh Syl Ave., Kyiv, Ukraine, 03037
[1]yuliiklymov@gmail.com, http://orcid.org/0000-0002-4275-7058

**Abstract.** Punching is one of the possible types of failure of reinforced concrete structures and occurs when a concentrated force is applied to slab slabs through an area commensurate with the height of the slab. In particular, when columns rest on transfer slabs, foundation slabs, and others.

Existing methods for calculating the strength of reinforced concrete slabs under punching are based on an empirical approach, which does not always adequately assess the strength of slabs and the influence of the main factors. At the same time, the general nature of failure under punching and the action of shear force on bending elements allows calculations to be made based on a common model.

This paper presents a design model for the strength of reinforced concrete slabs under punching, based on a unified approach to calculating the strength of reinforced concrete elements under shear force and punching.

Within the framework of the developed model, the maximum shear force acting on the slab is determined as the sum of the maximum shear forces perceived by two mutually perpendicular beams of variable width. It is assumed that the beams are loaded with concentrated forces at a distance from the conditional support equal to the horizontal projection of the inclined cracks that form the buckling pyramid. The criterion for beam failure is considered to be the displacement of concrete in the compressed zone above the critical inclined crack, and the internal forces in the inclined section are taken as the forces in the concrete of the tensile zone, the compressed zone at the continuation of the inclined crack, and the forces in the transverse reinforcement.

The obtained dependencies were used to determine the internal forces at the stage of failure during punching and the ultimate force perceived by the slab.

As part of the testing of the developed method, a comparison was made with the design of the slab's punching resistance using the method that formed the basis of Eurocode 2.

The concrete strength class and the ratio of the length of the load transfer plate to the height of the slab were taken as variable factors. The concrete strength varied in the range C20/25...C50/60, the ratio of the load transfer plate to the slab height varied in the range $a_{sup}/d$ =0.7...3,0, and the reinforcement ratio varied in the range $\rho$ = 0.010 and 0.015.

The calculations showed that the developed method correctly reflects the effect on the strength of slabs when punching concrete strength and the relationship between the dimensions of the outer plate for load transfer and the height of the slab.

**Keywords:** punching shear; strength; design model; beams; slab; comparison

**Yulii KLYMOV**
Professor of the Department of Reinforced Concrete and Stone Structures,
Prof. D.Sc. (Eng.)

## PROBLEM STATEMENT AND ANALYSIS OF PREVIOUS RESEARCH

The failure resulting from punching is the most dangerous type of failure of reinforced concrete slabs, as it is fragile in nature and occurs as a result of the continuous development of inclined cracks forming a punching pyramid (Fig. 1, 2).

**Fig.1** Collapsed 4th floor slab at Pipers Car Park, Wolverhampton on 25/03/1997
Photo by Wood J. G.M [1]
**Рис.1** Руйнування перекриття 4-го поверху на парковці у Вулверхэмптоні 25/1997
Автор фото Wood J. G.M [1]

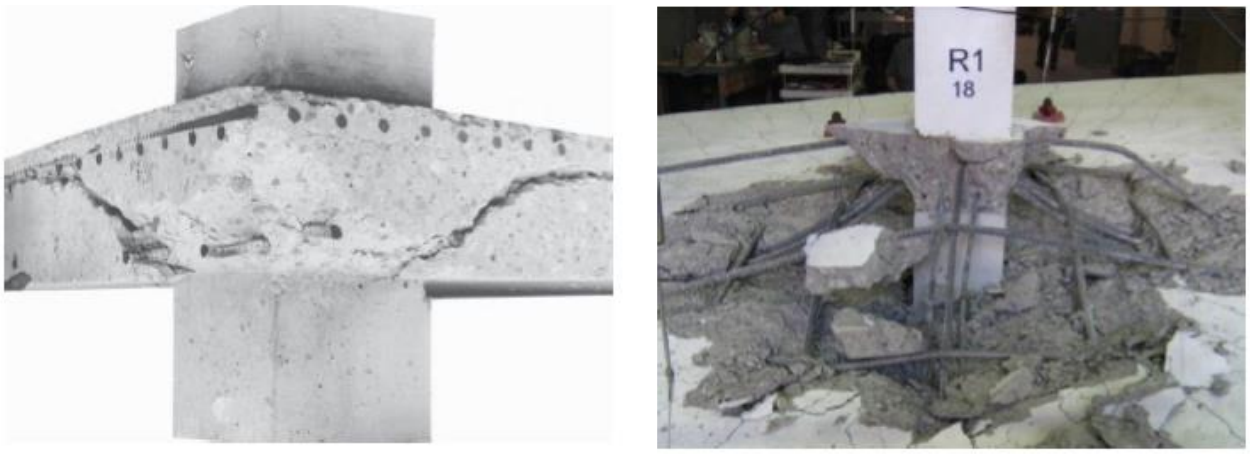


*a* *b*

**Fig. 2** Inclined cracks in a slab (a punching pyramid) after a punching shear failure.
Photo by: *a* - MacGregor, J.G [2]; *b* - Michael J. L. Egberts [3]
**Рис. 2** Похилі тріщини в плиті (піраміда продавлювання) після руйнування при продавлюванні [2,3].
Автор фото: *a* - MacGregor, J.G [2]; *b* -Michael J. L. Egberts [3]

Numerous experimental studies have been devoted to the problem of the resistance of reinforced concrete slabs to punching, including tests of column-slab connections [3-16] and foundation slabs [15,16], including under long-term [9] and dynamic loading [10].

As a result of experimental studies, the main patterns of crack formation and failure of reinforced concrete slabs during punching have been established, as well as the influence of the main factors on strength - concrete strength, ongitudinal and transverse reinforcement [3,4,6,7,8,11,16,17], concrete types and aggregate sizes [12, 13].

Based on the experimental data obtained, design models and methods for calculating the strength of reinforced concrete slabs under punching shear were developed [18,19,20], including the use of the finite element method [21]. However, these and other methods for calculating strength, including those used in regulatory codes [22-25], are far from perfect, differ from each other [16, 26,27], and consider flat vertical sections rather than inclined sections, along which failure occurs (Fig. 2).

In view of the above, further development of methods for calculating the strength of reinforced concrete slabs under punching shear,

which is the subject of this paper, appears to be a pressing task from both a scientific and practical point of view.

***The object of research*** is the strength of reinforced concrete slabs under punching shear.

***The purpose of the work*** is to develop a method for calculating the strength of reinforced concrete elements under punching based on the actual of crack formation, stress-strain state, and failure of elements, taking into account the influence of geometric dimensions, longitudinal and transverse reinforcement, and the strength characteristics of concrete and reinforcement.

## MAIN MATERIAL AND RESULTS OF RESEARCH

Existing methods for calculating the strength of reinforced concrete slabs under punching, including those used in regulatory codes [22-25], do not reflect the actual nature of crack formation and failure along inclined cracks with the formation of a punching pyramid (Fig. 1) and are based on calculations using flat vertical sections rather than failure surfaces. The latter not always allows to evaluate bearing capacity of slabs adequately especially in cases when the dimensions and support and reinforcement conditions differ from conventional. At the same time, the similarity of character of reinforced concrete slabs destruction under punching shear action and beams under shear allows to make computations more precisely on the basis of general computational model.

Particularity of reinforced concrete beams resistance to action of shear is availability of several forms of destruction which take place while distance $a$ from concentrated load point to the support is decreasing. For the relative distance of the concentrated load from the support $a/d > 1{,}5...2{,}0$ the failure happens as a result of concrete crushing in a compressed zone above a shear crack and, if $1{,}0...1{,}5 < a/d < 1{,}5...2{,}0$, as a result of the shear (diagonal tension) of concrete in a compressed zone above a shear crack and, if $1{,}0 < a/d$, as a result of concrete crushing in a inclined strut between the support and the concentrated load point. In light of above-stated, the most precision evaluation of computation of beams strength can be achieved for creation of design models applying to the concrete forms of failure.

In [28] the model is reviewed and the method of computation for case of failure as a result of crushing of concrete above a shear crack is developed. For failure of concrete as a result of crushing in a inclined strut between a support and a concentrated load point the known design model of deep beams and corbels can be used. As of case of failure of beams as a result of shear of concrete in a compressed zone above a shear crack up to now an inappropriate attention was given to creation of similar design models. At the same time, this form of beams failure is closest in character to failure of slabs under punching shear, that allows to conduct computations of beams and slabs because on the basis of a common approach.

In light of above-stated, the ultimate shear force $V_{sl}$ perceived by a slab under punching shear can be considered as the sum of ultimate shear $V_{b,1}$ and $V_{b,2}$, received by two perpendicular beams of a variable wideness (Fig. 3):

$$V_{sl} = V_{b,1} + V_{b,2} \qquad (1)$$

Here beams are considered as loaded by point concentrated force with distance to a conditional support equal to length of a sloping cut horizontal projection forming a pyramid of punching shear. Thus, the problem of shear computation of a slab is narrowed to calculation of ultimate shear received by corresponding beams for in time of failure as a result of concrete shear of a compressed zone above a shear crack.

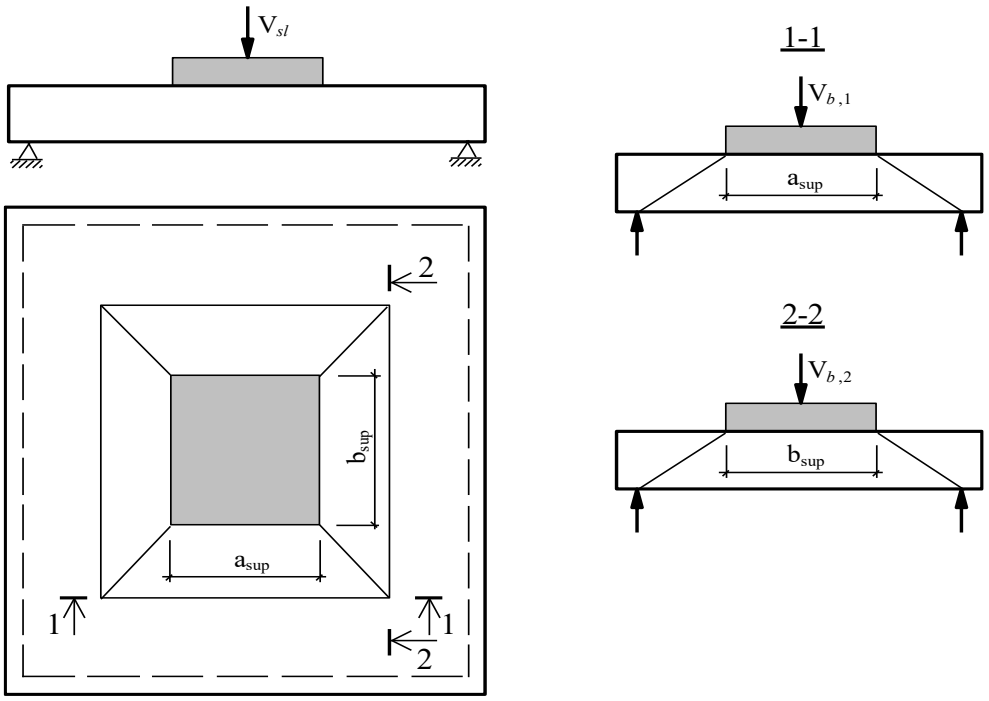


**Fig.3** Representation of a slab in form of perpendicular beams
**Рис.3** Представлення плити у вигляді перпендикулярних балок

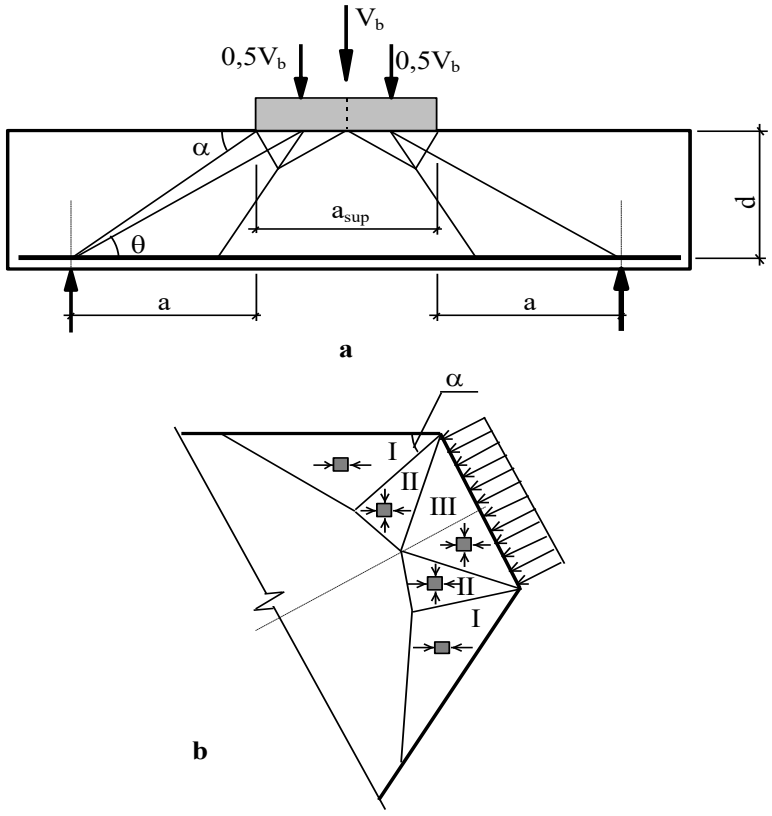


**Fig.4** A beam design model (a) and strained state of concrete in compressed zone (b)
**Рис.4** Розрахункова модель балки (а) та напружений стан бетону в зоні стиску (б)

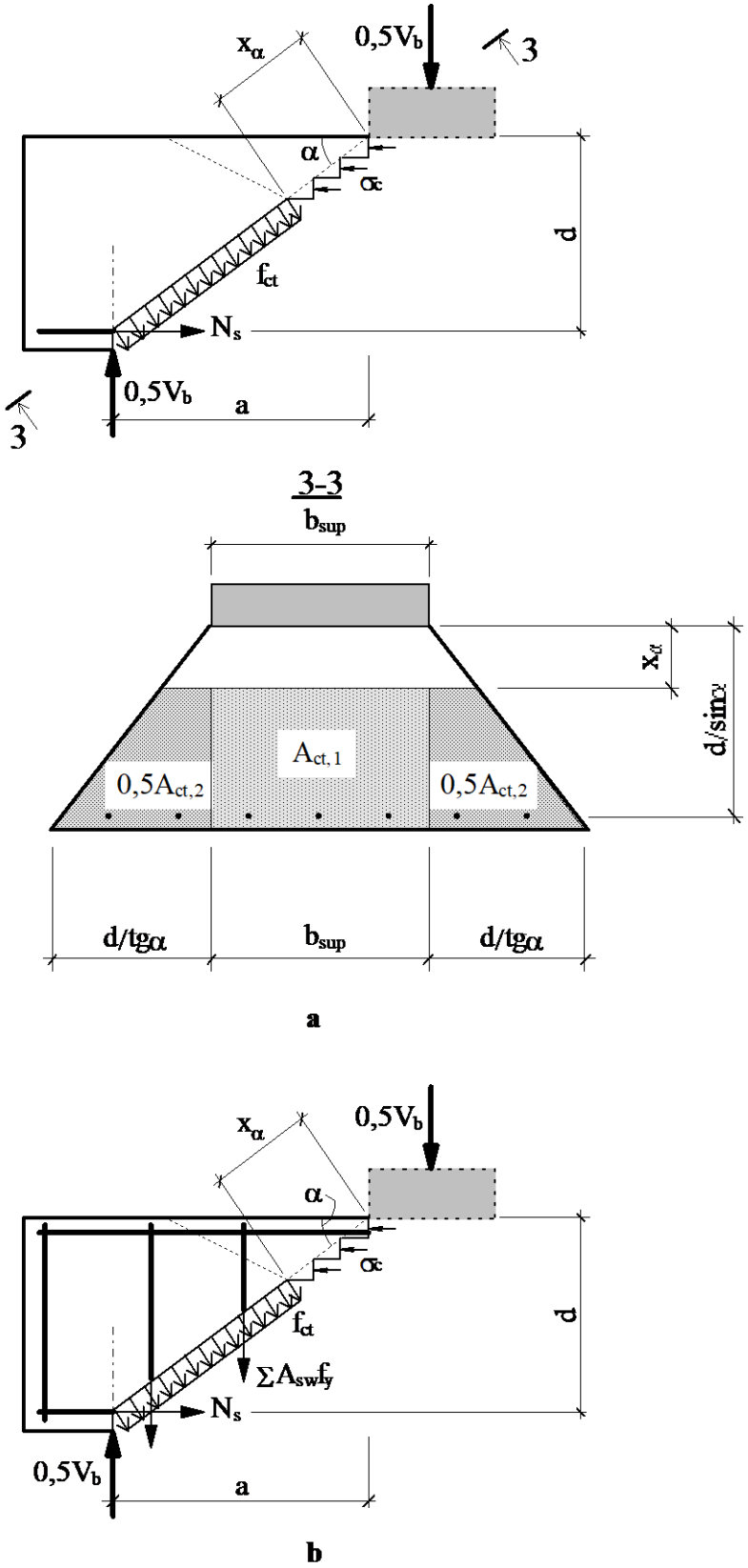


**Fig. 5** -Design model of the beam ultimate limit state in a slopping section without punching shear reinforcement *(a)* and with punching shear reinforcement *(b)*

**Рис.5** Розрахункова модель граничного стану балки в похилому перерізі без поперечного армування *(а)* і з поперечним армуванням на продавлювання *(б)*

The accepted design model of a reinforced concrete beam during failure as a result of concrete shear of a compressed zone above a shear crack shown on Fig. 4 and Fig. 5. For possibility of a correct applying of the results obtained to computation of the slab under punching shear, the case where length of the transfer platform $a_{\sup}$ of the concentrated force is commensurable with height of a beam was considered.

The character of the concrete status in a compression zone was evaluated in view of, in terms of the theory of plasticity [29,30], the problem of action of an axial proportionally distributed load on a basis of the truncated concrete wedge. As a result, it is established, that the stressed status of a concrete wedge in a plane of loading is characterized by three areas (Fig. 4b): single axial compression in direction parallel to the wedge lateral faces (area I) and bi-axial irregular compression (areas II and III). Here particularities of the compressing for movement in direction from area I to areas II and III are increase.

Such the character of failure of compressing stresses allows to come to conclusion that the top of a shear crack is located on the area I boundary and the crack itself, as it is established as a result of numerous experiments, has a strait linear trajectory. The corresponding design model of a beam is represented in Fig. 5a, where as a criterion of the ultimate limit state the reaching values of tensile strength of concrete $f_{ct}$ in a tensioned zone conterminous to the crack of a sloping section are accepted.

In light of the above-stated assumptions, the value of crack slope angle $\alpha$ and the height of concrete in a compressed zone above top of the crack (Fig. 5a) was accepted as for area I of a truncated concrete wedge (Fig. 4b).

Within the framework of an exact solution of the problem of the wedge angle $\alpha$ is determined the following formula:

$$\alpha = 0{,}5 arccos\left(\frac{0{,}5 \cdot f_{cc} - f_{ct}}{1{,}5 \cdot f_{cc}}\right) \qquad (2)$$

For concrete of classes C12/15…C50/60 the angle $\alpha$ changes in the narrow limits: $36{,}9^0$ … $37{,}9^0$ and is close to experimental values of the inclination of the faces of slabs punching shear pyramid (Fig.2).

Height of a compressed zone of concrete above a shear crack $x_\alpha$ is at the rate of a wedge in function of sizes of its basis and angle of the edges. In the case considered, for length of the platform of the concentrated force transfer $a_{\sup}$ and slopping angle $\theta$ which is equal to (Fig. 5a):

$$\theta = arctg\left(ctg\alpha + 0{,}25 \cdot \frac{a_{sup}}{d}\right) \qquad (3)$$

Value $x_\alpha$ is about 0,75 of the wedge basis length and is calculated by (Fig. 5a):

$$x_\alpha = 0{,}75 \cdot 0{,}5 \cdot a_{sup} \cdot sin\theta = \\ = 0{,}375 \cdot a_{sup} \cdot sin\theta \qquad (4)$$

Force in a tensed zone of a sloping cut is calculated as square of a corresponding signal waveform of stretching stresses by:

$$N_{ct} = N_{ct,1} + N_{ct,2} = \\ = f_{ct} \cdot A_{ct,1} + \cdot f_{ct} \cdot A_{ct,2} \qquad (5)$$

Where:

$A_{ct,1}$- square of concrete of a tensed zone in the sloping cut of the beam of a variable wideness formed by plane of the pyramid of punching shear with the slopping angle within the limits of the concentrated force transfer platform wideness (Fig. 5b):

$$A_{ct,1} = \left(\frac{d}{sin\alpha} - x_\alpha\right) \cdot b_{sup} \qquad (6)$$

$A_{ct,2}$ - the sloping cut of the beam of a variable wideness formed by plane of the pyramid of punching shear with the slopping angle out of the limits of (Fig. 5b):

$$A_{ct,2} = \left(x_\alpha \cdot cos\alpha + \frac{d}{tg\alpha}\right) \cdot \left(\frac{d}{sin\alpha} - x_\alpha\right) \qquad (7)$$

$\omega$ - coefficient of the signal waveform in a sloping cut of the beam of a variable wideness out of the limits of the external load transfer platform breadth.

For calculation of the force $N_{ct}$ by (5) the signal waveform of tensile stresses in a sloping cut of the beam was considered as an isosceles trapezoid with a rectangular site within the limits of the concentrated force transfer platform wideness and triangular sites outside of the site wideness. Such form of the signal waveform of stresses corresponds to the $\omega$ value equal 0,5.

The ultimate shear received by the beam is derived from an equilibrium equation of a sloping cut projected on a vertical axe (Fig.5a):

$$V_b = 2 \cdot N_{bt} \cdot cos\alpha \qquad (8)$$

If the punching shear reinforcement is placed, it is taken into account within the limits of length of the sloping cut tensed zone horizontal projection (Fig. 5b). Here value of an ultimate shear is calculated by:

$$V_b = 2 \cdot (N_{bt} \cdot cos\alpha + \Sigma A_{sw} \cdot f_y) \qquad (9)$$

where $\Sigma A_{sw} \cdot f_y$ - vertical force in punching shear reinforcement located within the limits of a sloping cut on length:

$$l_{sw} = (\frac{d}{sin\alpha} - x_\alpha) \cdot cos\alpha \qquad (10)$$

To verify the accuracy of the developed method and the correctness of the influence of the main factors, a comparison was made with the calculations of the punching shear strength of unreinforced slabs in accordance with the method [30], which is based on Eurocode 2 [25].

The concrete strength class and the ratio of the length of the load transfer plate to the height of the slab were taken as variable factors. The concrete strength varied in the range C20/25...C50/60, the ratio of the load transfer plate to the slab height varied in the range $a_{sup}/d$ =0.7...3,0, and the reinforcement ratio varied in the range $\rho = 0.010$ and 0.015.

The results of the comparison as the schedules of relations of relative bearing capacity of the slabs and concrete strength and relative dimensions of the concentrated force transfer platform are indicated on Fig. 6.

The analysis of the results obtained has allowed to establish the following.

The results of the developed method are close to the calculations in [31] and correctly reflect the effect on the strength of slabs when the concrete strength is punched through (Fig. 6a, 6b) and the relationship between the dimensions of the external load transfer plate and the slab height (Fig. 6c). In this case, the design is based on [31] gives higher values strength of slabs, which is increased as the concentrated force transfer plate dimensions being increased (if $\rho = 0{,}010$) from 1…3 % if $a_{\text{sup}}/d = 0{,}7$ up to 28 … 38 % if $a_{\text{sup}}/d =$ 3,0. This may be due to the fact that [31] indirectly takes into account the increase in slab strength due to the dowel force in the longitudinal reinforcement by introducing a longitudinal reinforcement coefficient into the calculation. Within the framework of the developed method, the dowel action in the longitudinal reinforcement of slabs can be taken into account based on a general approach to determining transverse forces in the longitudinal reinforcement of reinforced concrete elements under shear [32,33].

## CONCLUSIONS

The beams model of design of punching shear forces in reinforced concrete slabs on the basis the general approach to strength computation of shear appearing under punching shear is developed. Within the framework of the developed method the ultimate shear received by a slab under punching shear is determined as the sum of the ultimate shear received by two perpendicular beams of a variable wideness, see Fig.3. The ultimate shear force $V_{sl}$ perceived by a slab under punching shear can be considered as the sum of ultimate shear $V_{b1}$ and $V_{b2}$, received by two perpendicular beams of a variable wideness by (2).

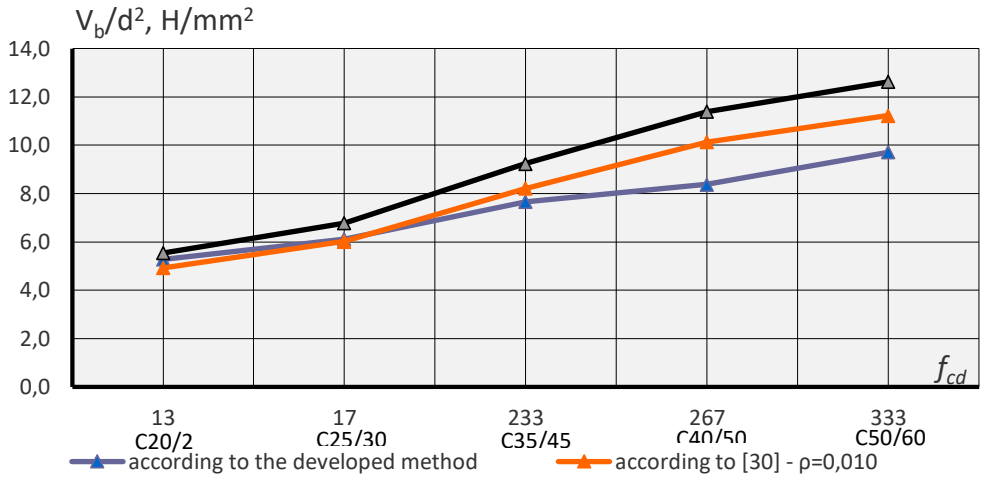


*a*

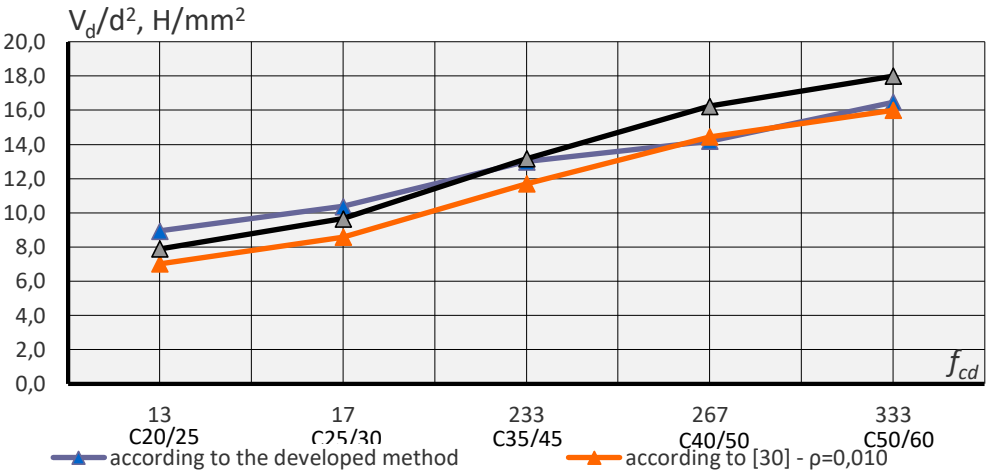


*b*

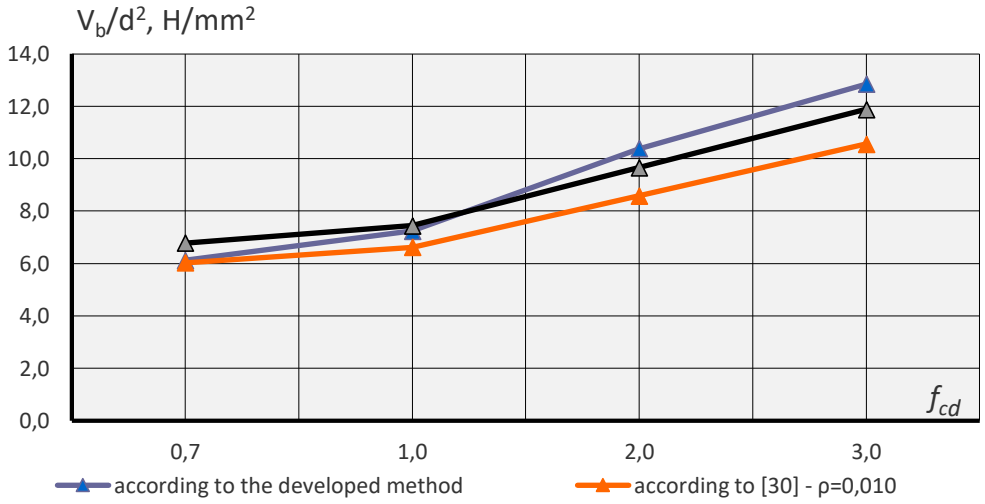


*c*

**Fig.6** Dependence strength of slab under punching shear on concrete strength at $a_{sup}/d = 0{,}7$ ***(a)*** and at $a_{sup}/d = 2{,}0$ ***(b)*** and relative dimensions of the concentrated force transfer plate *(c)*.

**Рис.6** Залежність міцності плити при продавлюванні від міцності бетону при $a_{sup}/d = 0{,}7$ ***(а)*** і при $a_{sup}/d = 2{,}0$ ***(б)*** і відносного розміру площадки передачі зосередженої сили ***(с)***.

The character of the concrete status in a compression zone was evaluated in view of, in terms of the theory of plasticity [29], the problem of action of an axial proportionally distributed load on a basis of the truncated concrete wedge, (Fig.4b). Criterion of the ultimate limit state the reaching values of tensile strength of concrete $f_{ct}$ in a tensioned zone conterminous to the crack of a sloping section are accepted (Fig. 5b). Force in a tensed zone of a sloping cut is calculated as square of a corresponding signal waveform of stretching stresses by (5). The ultimate shear received by the beam is derived from an equilibrium equation of an a sloping cut projected on a vertical axe by (8).

The design value of the strength of slabs under punching shear according to the developed method is quite close to the results of the calculation according to [31], which is based on Eurocode 2 [25], but since the developed method is based on a general model of the ultimate state of elements under shear forces [28] and the theory of plasticity of reinforced concrete [29,30], unlike empirical relationships [31], it has broader application prospects.

## REFERENCES


1. **Wood J. G.M.** Pipers Row Car Park, *Wolverhampton Quantitative Study of the Causes of the Partial Collapse on 20th March 1997, SS&D Contract Report to HSE, 2002*. [in English]
2. **Wight, J.K, MacGregor, J.G**, (2009). Reinforced Concrete *Pearson Prentice Hall, New Jersey, , 1157 p*. [in English]
3. **Michael J. L. Egberts**, (2009). Preventing Progressive Collapse of Flat Plate Structures with Irregular Layout of Structural Integrity Reinforcement, thesis, *Department of Civil Engineering and Applied Mechanics, McGill University, Montreal,,105 p*. [in English]
4. **Alaa G Sherif G.A, Walter H. Dilger**, (2000). Tests of full-scale continuous reinforced concrete flat slabs, *ACI Structural Journal, (97), No. 3, 455-467* [in English]
5. **Ramana N.V.** (2017).Review on punching shear strength of slabs, I*nt. J. International Journal of Engineering Research and Development, (13), (10),1–25*. [in English]
6. **Baskaran. K, Morly. C.T,** (2004). A new approach testing reinforced concrete flat slab, *Magazine Concrete Research, (56), No. 6, 367-374.* [in English]
7. **Muttoni A.** (2008). Punching Shear Strength of Reinforced Concrete Slabs without Transverse Reinforcement, *ACI Structural Journal/July-August, pp.440-450*. [in English]
8. **Jahangir Alam, A. K. M. Amanat Khan Mahmud, Salek M. Seraj** (2008). An Experimental Study on Punching Shear Behavior of Concrete Slabs, *Structural Engineering (12) No. 2, 257-265.* [in English]
9. **Gilbert R.I, Guo X. H.** (2005).Time –dependent deflection and deformation of reinforced concrete flat slabs – An experimental study, *ACI Structural Journal, (102), NO. 3, 363-373.* [in English]
10. **Russell, J.M., Owen, J.S., Hajirasouliha**, **I.** (2015). Experimental investigation on the dynamic response of RC flat slabs after a sudden column loss, *Engineering Structures (99), 28-41* [in English]
11. **Eva O.L. Lantsoght Cor van der Veen, Joost Walraven, Ane de Boer,** (2015). Experimental investigation on shear capacity of reinforced concrete slabs with plain bars and slabs on elastomeric bearings, *Engineering Structure, (103), 1–14.* [in English]
12. **Kwang-Soo Youm, Jung J. Kim, Jiho Moon**, (2014). Punching shear failure of slab with lightweight aggregate concrete (LWAC) and low reinforcement ratio, *Construction and Building Materials (65), 92-102.* [in English]
13. **Youm K.S., Jeon, H. K.; Park, Y.S.; Lee, S. H.; Moon, J**. Experimental study on punching shear of lightweight concrete, P*roceedings of the Thirteenth East Asia-Pacific Conference on Structural Engineering and Construction (EASEC-13), September 11-13, 2013, Sapporo, Japan, E-6-4., E-6-4* [in English]
14. **Fernandez Ruiz M., Muttoni, A. Sagaseta, J.** (2015). Shear strength of concrete members without transverse reinforcement: A mechanical approach to consistently account for size and strain effects, *Engineering Structures (99), 360-372.* [in English]
15. **Siburg, C., Hegger, J.** (2014). Experimental investigations on the punching behavior of reinforced concrete footings with structural dimensions. *Structural Concrete, 15(3), 331–339.* [in English]
16. **Siburg, C., Ricker, M., Hegger J**. (2014). Punching shear design of footings: critical review of different code provisions., *Structural Concrete., 15(4), 497–508.* [in English]

17. **Mitchell, D., Cook, W.D., Dilger, W.** (2005). Effect of size, geometry and material properties on punching shear resistance, *ACI Special Issue on Punching Shear in Reinforced Concrete Slabs, American Concrete Institute, SP-232-3,. 39–56.* [in English]
18. **Kueres, D., Siburg, C., Herbrand, M**., **Classen, M., & Hegger, J.** (2017). Uniform design method for punching shear in flat slabs and column bases. *Engineering Structures, 136(1), 149–164.* [in English]
19. **Bogdandy, B., & Hegedus, I.** (2016). Determination of the punching cross-section of reinforced concrete flat slabs. *Periodica Polytechnica Civil Engineering., 60(3), 405–411.* [in English]
20. **Muttoni, A. Fernández Ruiz M., Simões J.T. (**2017). The theoretical principles of the critical shear crack theory for punching shear failures and derivation of consistent closed-form design expressions, *Structural concrete, pp. 1-17.* [in English]
21. **Jahangir Alam1, A. K. M., Amanat Khan Mahmud**, (2013). Analysis on The Effect of flexural steel on punching shear of slabs, *International Journal of Engineering Research & Technology, (2),* (*6), 2878-2901.* [in English]
22. **SIA**, 262 Code for Concrete Structures, *Swiss Society of Engineers and Architects, Zurich, Switzerland, 2003, 94 p.* [in English]
23. **FIB**, Punching of Structural Concrete Slabs, *fib Bulletin 12, Lausanne, Switzerland, 2001, 307 p.* [in English]
24. **ACI Committee 318 2014** Building code requirements for structural concrete (ACI 318-14): an ACI standard : commentary on building code requirements for structural concrete (ACI 318R-14), an *ACI report, Michigan, United State: American Concrete Institute, 524 p.* [in English]
25. **EN 1992-1-1:2023 Eurocode 2.** -Design of concrete structures – Part-1-1 General rules and rules for building, *Bridges and civil engineering structures, 402 p.* [in English]
26. **Ricker, M., & Siburg, C.** (2016). Punching shear strength of flat slabs—critical review of *Eurocode 2 and fib Model Code 2010 design provisions. Structural Concrete, 17(3),457–468.* [in English]
27. **Alexander, S. D. B., Hawkins, N. M.,** A Design Perspective on Punching Shear, *SP-232, M. A. Polak, ed., American Concrete Institute, Farmington Hills, MI, 2005, pp. 97-108.* [in English]
28. **Klymov Yu.**, (1999) New Design Models of the Shear Strength of Reinforcement Concrete Member," Structural Concrete - *The Bridge Between People, fib Symposium, Viacon, Prague, (1), 319-324.* [in English]
29. **Klimov, Yu., Kozak**, **A. (**2025) Theoretical foundations for design of reinforced concrete under plane stress states, *Strength of Material and Theory of Structures, (114), 311-318.* [in English] https://doi.org/10.32347/2410-2547.2025.114.311-318
30. **Klymov, Yu., Smorkalov, D.** (2025). Experimental and theoretical researches of strength of compressed reinforced concrete elements with indirect reinforcement by welded meshes, *Building Constructions, Theory and practice,* (16), 22-32 [in English] https://doi.org/10.32347/2522-4182.16.2025.22-32
31. **Litzner H.-U.**Design of Concrete Structures of ENV *1992-Eurocode 2, Ernst and Sohn, 1995, 308 p.* [in English]
32. **Klimov, Yu., Smorkalov, D.V., Kozak A.A.** (2024). Behavior to shear force of a reinforced bar in the concrete *Strength of Material and Theory of Structures, (113), 320-328* [in English] https://doi.org/10.32347/2410-2547.2024.113.320-328
33 **Klymov, Yu., Smorkalov, D.** (2024) Experimental researches of the strength of reinforced concrete elements under transverse forces. *Building Constructions, Theory and practice,* (14), 4-14 [in Ukrainian] https://doi.org/10.32347/2522-4182.14.2024.4-18


## LITERATURE


1. **Wood J. G.M.** Pipers Row Car Park, *Wolverhampton Quantitative Study of the Causes of the Partial Collapse on 20th March 1997, SS&D Contract Report to HSE, 2002*.
2. **Wight, J.K, MacGregor, J.G**, (2009). Reinforced Concrete *Pearson Prentice Hall, New Jersey, , 1157 p*.
3. **Michael J. L. Egberts**, (2009). Preventing Progressive Collapse of Flat Plate Structures with Irregular Layout of Structural Integrity Reinforcement, thesis, *Department of Civil Engineering and Applied Mechanics, McGill University, Montreal,,105 p.*

4. **Alaa G Sherif G.A, Walter H. Dilger**, (2000). Tests of full-scale continuous reinforced concrete flat slabs, *ACI Structural Journal, (97), No. 3, 455-467*
5. **Ramana N.V.** (2017).Review on punching shear strength of slabs, I*nt. J. International Journal of Engineering Research and Development, (13), (10),1–25*.
6. **Baskaran. K, Morly. C.T,** (2004). A new approach testing reinforced concrete flat slab, *Magazine Concrete Research, (56), No. 6, 367-374.*
7. **Muttoni A.** (2008). Punching Shear Strength of Reinforced Concrete Slabs without Transverse Reinforcement, *ACI Structural Journal/July-August, pp.440-450.*
8. **Jahangir Alam, A. K. M. Amanat Khan Mahmud, Salek M. Seraj** (2008). An Experimental Study on Punching Shear Behavior of Concrete Slabs, *Structural Engineering (12) No. 2, 257-265.*
9. **Gilbert R.I, Guo X. H.** (2005).Time –dependent deflection and deformation of reinforced concrete flat slabs – An experimental study, *ACI Structural Journal, (102), NO. 3, 363-373.*
10. **Russell, J.M., Owen, J.S., Hajirasouliha**, **I.** (2015). Experimental investigation on the dynamic response of RC flat slabs after a sudden column loss, *Engineering Structures (99), 28-41*
11. **Eva O.L. Lantsoght Cor van der Veen, Joost Walraven, Ane de Boer,** (2015). Experimental investigation on shear capacity of reinforced concrete slabs with plain bars and slabs on elastomeric bearings, *Engineering Structure, (103), 1–14.*
12. **Kwang-Soo Youm, Jung J. Kim, Jiho Moon**, (2014). Punching shear failure of slab with lightweight aggregate concrete (LWAC) and low reinforcement ratio, *Construction and Building Materials (65), 92-102.*
13. **Youm K.S., Jeon, H. K.; Park, Y.S.; Lee, S. H.; Moon, J**. Experimental study on punching shear of lightweight concrete, P*roceedings of the Thirteenth East Asia-Pacific Conference on Structural Engineering and Construction (EASEC-13), September 11-13, 2013, Sapporo, Japan, E-6-4., E-6-4*
14. **Fernandez Ruiz M., Muttoni, A. Sagaseta, J.** (2015). Shear strength of concrete members without transverse reinforcement: A mechanical approach to consistently account for size and strain effects, *Engineering Structures (99), 360-372.*
15. **Siburg, C., Hegger, J.** (2014). Experimental investigations on the punching behavior of reinforced concrete footings with structural dimensions. *Structural Concrete, 15(3), 331–339.*
16. **Siburg, C., Ricker, M., Hegger J**. (2014). Punching shear design of footings: critical review of different code provisions., *Structural Concrete., 15(4), 497–508.*
17. **Mitchell, D., Cook, W.D., Dilger, W.** (2005). Effect of size, geometry and material properties on punching shear resistance, *ACI Special Issue on Punching Shear in Reinforced Concrete Slabs, American Concrete Institute, SP-232-3,. 39–56.*
18. **Kueres, D., Siburg, C., Herbrand, M**., **Classen, M., & Hegger, J.** (2017). Uniform design method for punching shear in flat slabs and column bases. *Engineering Structures, 136(1), 149–164.*
19. **Bogdandy, B., & Hegedus, I.** (2016). Determination of the punching cross-section of reinforced concrete flat slabs. *Periodica Polytechnica Civil Engineering., 60(3), 405–411.*
20. **Muttoni, A. Fernández Ruiz M., Simões J.T. (**2017). The theoretical principles of the critical shear crack theory for punching shear failures and derivation of consistent closed-form design expressions, *Structural concrete, pp. 1-17.*
21. **Jahangir Alam1, A. K. M., Amanat Khan Mahmud**, (2013). Analysis on The Effect of flexural steel on punching shear of slabs, *International Journal of Engineering Research & Technology, (2),* (*6), 2878-2901*.
22. **SIA**, 262 Code for Concrete Structures, *Swiss Society of Engineers and Architects, Zurich, Switzerland, 2003, 94 p.*
23. **FIB**, Punching of Structural Concrete Slabs, *fib Bulletin 12, Lausanne, Switzerland, 2001, 307 p.*
24. **ACI Committee 318 2014** Building code requirements for structural concrete (ACI 318-14): an ACI standard : commentary on building code requirements for structural concrete (ACI 318R-14), an *ACI report, Michigan, United State: American Concrete Institute, 524 p.*
25. **EN 1992-1-1:2023 Eurocode 2.** -Design of concrete structures – Part-1-1 General rules and rules for building, *Bridges and civil engineering structures, 402 p.*
26. **Ricker, M., & Siburg, C.** (2016). Punching shear strength of flat slabs—critical review of *Eurocode 2 and fib Model Code 2010 design provisions. Structural Concrete, 17(3),457–468.*
27. **Alexander, S. D. B., Hawkins, N. M.,** A Design Perspective on Punching Shear, *SP-232, M. A. Polak, ed., American Concrete Institute, Farmington Hills, MI, 2005, pp. 97-108.*

28. **Klymov Yu.**, (1999) New Design Models of the Shear Strength of Reinforcement Concrete Member," Structural Concrete - *The Bridge Between People, fib Symposium, Viacon, Prague, (1), 319-324.*
29. **Klimov, Yu., Kozak**, **A. (**2025) Theoretical foundations for design of reinforced concrete under plane stress states, *Strength of Material and Theory of Structures, (114), 311-318.* https://doi.org/10.32347/2410-2547.2025.114.311-318
30. **Klymov, Yu., Smorkalov, D.** (2025). Eksperymentalno-teoretychni doslidzhennia mitsnosti stysnutykh zalizobetonnykh elementiv z nepriamym armuvanniam zvarnymy sitkamy. *Budivelni konstruktsii. Teoriia i praktyka, (16), 22–32., (16), 22-32* https://doi.org/10.32347/2522-4182.16.2025.22-32
31. **Litzner H.-U.**Design of Concrete Structures of ENV *1992-Eurocode 2, Ernst and Sohn, 1995, 308 p.* [in English]
32. **Klimov, Yu., Smorkalov, D.V., Kozak A.A.** (2024). Behavior to shear force of a reinforced bar in the concrete *Strength of Material and Theory of Structures, (113), 320-328* [in English] https://doi.org/10.32347/2410-2547.2024.113.320-328
33. **Klymov, Yu., Smorkalov, D.** (2024) Eksperi-mentalni doslidzhennya micnosti zalizobetonnih elementiv pri diyi poperechnih sil. *Budivelni konstrukciyi. Teoriya i praktika. (14), 4-14* https://doi.org/10.32347/2522-4182.14.2024.4-18

## МІЦНІСТЬ ЗАЛІЗОБЕТОННИХ КОНСТРУКЦІЙ ПРИ ПРОДАВЛЮВАННІ

*Юлій КЛІМОВ*

**Анотація.** Продавлювання є одним із можливих видів руйнування залізобетонних конструкцій і виникає при прикладенні зосередженої сили до плит перекриття через площу, спів розмірну з висотою плити. Зокрема, коли колони спираються плити на перекриття, фундаментні плити та інші.

Існуючі методи розрахунку міцності залізобетонних плит на продавлювання базуються на емпіричному підході, який не завжди адекватно оцінює міцність плит і вплив основних факторів. Водночас загальний характер руйнування при продавлюванні та дії поперечних сил на згинальні елементи дозволяє проводити розрахунки на основі загальної моделі.

У цій статті представлено модель розрахунку міцності залізобетонних плит при продавлюванні засновану на загальному підході до розрахунку міцності залізобетонних елементів при дії поперечної сили та продавлюванні.

У рамках розробленої моделі максимальна поперечна сила, що діє на плиту, визначається як сума максимальних поперечних сил, що сприймають дві взаємно перпендикулярні балки змінної ширини. Вважається, що балки навантажені зосередженими силами на відстані від умовної опори, що дорівнює горизонтальній проекції похилих тріщин, які утворюють піраміду продавлювання. Критерієм руйнування балки вважається зсув бетону в стиснутій зоні над критичною похилою тріщиною, а у якості внутрішніх зусиль у похилому перерізі приймаються зусилля в бетоні розтягнутої зони, стиснутої зони на продовженні похилої тріщини і зусилля у поперечній арматурі.

В якості варійованих факторів були прийняті клас бетону за міцністю і відношення довжини площадки передачі зосередженої сили до висоти плити. Міцність бетону варіювалася в діапазоні С12/15…С40/50, відношення розмірів площадки до висоти плити приймалося в діапазоні $a_{sup}/d$ =0.7...3,0, а коефіцієнт армування $\rho =$ 0,010 і $\rho =$=0,015.

В результаті розрахунків встановлено, що розроблений метод правильно відображає вплив на міцність плит при продавлюванні міцності бетону та співвідношення між розмірами зовнішньої пластини для передачі навантаження та висотою плити.

**Ключові слова:** продавлювання; міцність; розрахункова модель; балка; плита; співставлення

***Received:*** *September 8, 2025.*
***Accepted:*** *November 30, 2025.*

ISSN 2522-4182

DOI: 10.32347/2522-4182.17.2025.17-29
UDC 624.012.45

# IMPACT OF BLAST WAVE ARRIVAL DELAY ON THE DYNAMIC BEHAVIOR OF PROTECTIVE STRUCTURES

*Anatoly PERELMUTER[1], Taliat AZIZOV[2], Dmytro KOCHKAREV[3], Nataliia SRIBNIAK[4]*

[1]LLC SCAD Soft
24-B Zhukova St, Kyiv, Ukraine, 02166
[2,4]Sumy National Agrarian University
160 Herasym Kondratiev Street, Sumy, Ukraine, 40021
[3]National University of Water and Environmental Engineering
11 Soborna St., Rivne, Ukraine, 33028
[1]avp@scadsoft.com, https://orcid.org/0000-0001-9537-2728
[2]azizov.taliat@snau.edu.ua, https://orcid.org/0000-0001-9621-9805
[3]d.v.kochkarev@nuwm.edu.ua, https://orcid.org/0000-0002-4525-7315
[4]nataliia.sribniak@snau.edu.ua, https://orcid.org/0000-0003-3205-433X

**Abstract.**The article examines methods for calculating protective structures under the action of a blast wave, the pressure of which reaches different points at different times. A phase-by-phase calculation approach is considered, in which the action of a series of forces with different arrival times is treated as separate phases of vibration. The initial conditions of the current phase are taken as the final conditions (displacements and velocities) of the previous phase.

The study focuses in detail on a single-degree-of-freedom (SDOF) system subjected to forces with varying arrival times. At each phase, the constants of the particular and general solutions of the SDOF differential equation are determined based on the known right-hand side of the differential equation. Once all constants are obtained, the displacements at each phase are calculated.

It is shown that the advantage of this approach lies in the fact that, regardless of the number of intervals during which forces act at different times, only one differential equation with its own initial conditions and force set is solved at each phase. Consequently, the constants for the particular and general solutions are determined for each phase in

dependently. Therefore, the number of intervals can be arbitrarily chosen by the engineer, and there is no added complexity in the numerical implementation even for systems with multiple forces.

It is demonstrated that for a single-mass system, different arrival times of the dynamic force do not increase the system response. However, this scheme is used when a multi-degree-of-freedom (MDOF) system is analyzed via modal decomposition, treating each mode as an SDOF system with consideration of the different force arrival times, and then summing the responses.

**Anatoly PERELMUTER**
Head of Research and Development, SCAD Software,
D.Sc. (Eng.)

**Taliat AZIZOV**
Professor, Department of Building Structures,
D.Sc. (Eng.)

**Dmytro KOCHKAREV**
Professor, Department of Urban Construction and Public Utilities,
D.Sc. (Eng.)

**Nataliia SRIBNIAK**
Associate Professor, Department of Building Structures,
PhD (Eng.)

It is shown why, in linear systems, summing the modal responses at specific times is correct, whereas simply summing the maximum responses is not.

The study confirms that the phase-by-phase consideration of system vibrations is correct, though more cumbersome. For multi-mass systems under impulsive loading, an analytical formula for the total response to impulses reaching different points at different times is provided. Both a triangular impulse with finite duration and an instantaneous impulse are considered.

**Keywords:** blast wave; vibration phase; single-degree-of-freedom (SDOF) system; equation of motion; impulse.

## INTRODUCTION

Protective structures play an important role in safeguarding the population during air attacks. When conventional munitions are employed, protective structures must shield occupants from the blast wave and from fragmentation. This necessitates performing specific calculations, namely:

- the analysis of the load-bearing and enclosing elements of protective structures under the action of a blast shock wave;
- the analysis of the enclosing elements of protective structures under the action of fragments.

It should be noted that there are also certain types of structures that are designed to withstand the direct impact of individual munitions. As a rule, these are specialized facilities of critical importance. Additional, specialized calculations are performed for such structures, which are not considered in this article.

The structural analysis of the enclosing elements of protective buildings and facilities under blast-wave loading may be performed using one of three methods:

- the direct integration method of the equations of motion;
- the impulse (shock-impulse) method;
- the quasi-static method.

Each of these methods is characterized by its own type of loading. Recently, attention has also been drawn to the question of whether the non-uniform (non-simultaneous) arrival of blast-wave pressure affects the dynamic displacements and internal forces in protective-structure components.

## ANALYSIS OF PREVIOUS RESEARCH

A considerable number of studies have been devoted to the investigation of blast wave effects. One of the key issues is the analysis of the shape and function of blast wave pressure [2, 12, 25]. In calculations, including those specified in regulatory documents, both curvilinear and simplified linear functions are used [5, 23, 24]. Additionally, computational tools for determining blast wave parameters are also available [13].

Research has shown that accounting for the negative phase of pressure leads to changes in dynamic forces in elements of protective structures [1, 14]. However, in many regulatory documents, calculations are performed considering only the positive phase of blast wave pressure.

There is extensive discussion and debate regarding the choice of calculation method: the direct integration of motion equations, the impulse method, and the quasi-static method. In Ukrainian standards [5], the quasi-static method is adopted. This approach is the simplest, though the least precise, but it allows relatively rapid determination of results. In the US standards [23, 24], the choice among direct integration, impulse, or quasi-static methods depends on the ratio of the positive phase duration of the blast to the natural period of structural vibration. Experimental and numerical studies [9, 17, 26, 27] have demonstrated the influence of various factors on the resistance of reinforced concrete and steel structures to blast wave action [7, 8, 16, 19]. The effect of damping devices on the system response to blast waves has also been investigated, considering different models and various pressure waveform shapes [3, 6,11, 20].

In many calculation methods, complex multi-degree-of-freedom systems are reduced to a single-degree-of-freedom system, and the solution of a known differential equation is considered, the right-hand side of which

depends on the adopted blast wave pressure profile.

It is known that, although the duration of blast wave action is extremely short [2, 12, 13, 25], the pressure does not reach different points of the structure simultaneously. The extent to which this affects the response of the dynamic system is an important consideration for accurate structural analysis.

## PURPOSE AND METHODS

An important and theoretically underexplored issue is the investigation of the influence of differing arrival times of blast-wave pressure at various points of a structure, which may affect the displacements and internal forces in structural elements either positively or negatively. It is necessary to determine which analytical method should be used for structural assessment in such cases. In view of the above, the aim of this article is to analyze the effect of blast-pressure arrival time at different points of a structure and to develop a methodology for performing such calculations.

The study employs a comprehensive set of methods aimed at an in-depth analysis of the behavior of protective structures subjected to blast loading that reaches different points at different times. The core of the work is an analytical approach to solving the differential equations of motion describing the vibrations of an SDOF system. For each time interval in which a force with a distinct arrival time acts, a phase-by-phase calculation method is applied: the equation of motion is solved separately for each phase, with the final conditions of the preceding phase—displacement and velocity—used as the initial conditions for the subsequent one. This enables a sequential and accurate determination of all constants of the particular and general solutions and provides a complete time-dependent response of the system regardless of the number of loading intervals.

For multi-degree-of-freedom systems, modal analysis is employed, allowing the complex system to be represented as a set of independent SDOF models. For each mode, the response is determined with consideration of the differing force arrival times, after which the modal displacements are superposed in the time domain. The study provides a detailed justification for why time-domain summation of modal responses is valid for linear systems, while summation of the modal peak values leads to erroneous results.

Additionally, a comparative analysis of results obtained using different approaches is performed, allowing the assessment of how temporal mismatch in force application influences the magnitude of the structural response. For impulsive loads, analytical expressions are derived for the total response to a series of impulses arriving at different points at different times. When necessary, the analytical solutions can be validated through direct numerical integration of the equations of motion, providing a computational verification of the accuracy of the proposed methodology.

This integrated methodological framework enables a thorough investigation of the influence of non-simultaneous blast-load arrival on structural systems and establishes a universal approach for their analysis and design.

## MAIN PART

Let a vertical cantilever be given, with $n$ lumped masses attached to it. It is known that such a multi-mass system can be reduced to a system with a single equivalent mass [2, 3, 16]. Let us consider this vertical cantilever of height $L$ as a single-degree-of-freedom system with an equivalent mass $m = m_e q v$ at its free end.

A force $F_1(t) = P_1(1 - t/\tau)$ acts on it at a height a above ground level, and a force

$F_2(t) = P_2(1 - t/\tau)$ acts at a height $b$, where force $F_1$ begins to act at time $t = 0$, while force $F_2$ is applied with a delay, at time $t = \delta_t$ (Fig. 1).

Given that the distance from the explosion epicenter to different points along the height of a structure varies, it is necessary to investigate the extent to which the non-simultaneous arrival of the blast wave affects the stress–strain state of the system.

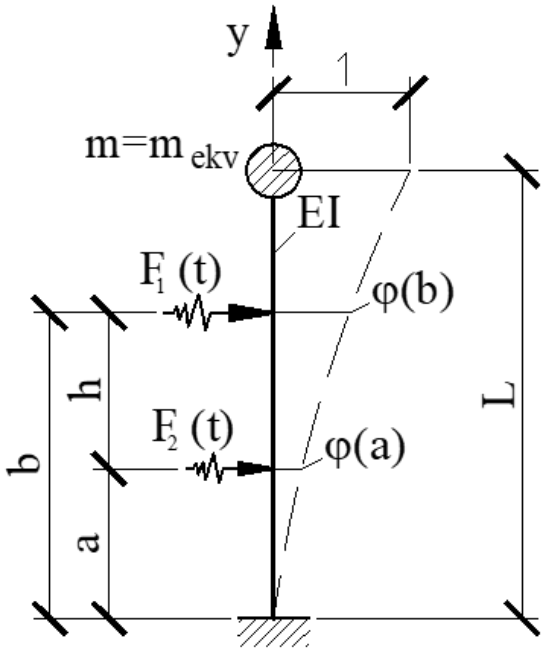


**Fig. 1** SDOF system diagram with differential arrival of dynamic forces
**Рис. 1** Схема системи з однією масою з різним приходом динамічних сил

If the cantilever is a homogeneous rod, the equivalent mass is known to be determined by the expression $m_e qv = 0.243 \cdot m_{tot}$,

where $m_{tot}$ is the total mass of the rod.

Several remarks should be made here.

1.A specified pressure is considered, and we do not address which specific type of pressure generates the forces $F_1$ and $F_2$—whether incident, reflected, etc.—because our primary objective is to determine whether the delay in force application has an influence or not.

2.We analyze a simple scheme with two forces, because such a simplified model allows us to clearly demonstrate this effect numerically. The essence of the analysis does not change when a different number of forces is considered.

Let us perform the analysis on the basis of the following theoretical approach.

The well-known differential equation without damping takes the form:

$$m \cdot \ddot{x} + k \cdot x = Q(t) \qquad (1)$$

where $x = x(t)$ is the generalized coordinate, taken here as the horizontal displacement of mass $m$; $k$ is the stiffness coefficient of the cantilever, which in our case is $k = 3 \cdot EJ / L^3$,

where $EJ$ is the bending stiffness of the rod; and $Q(t)$ is the generalized force (the coefficient corresponding to the virtual displacement of the generalized coordinate).

The delay of the second force, $\delta_t$, will be considered smaller than the duration of the positive phase of the blast wave, τ, as will be briefly discussed below. At the beginning of the calculation, the value of δt can be chosen such that $\tau = n \cdot \delta_t$. Let us illustrate this with an example where $n = 4$. In this case, several phases of vibration must be considered:

Phase 1*:*

$0 \le t \le \delta_t$ — only force $F_1$ acts; $F_2 = 0$.

Phase 2:

$\delta_t \le t \le \tau$ — both forces $F_1$ and $F_2$ act; however, the second force begins at $t = \delta_t$.

Phase 3:

$\tau \le t \le \tau + \delta_t$ — only force $F_2$ acts;

$F_1 = 0$.

Phase 4:

$t \ge \tau + \delta_t$ — free vibration phase;

$F_1 = F_2 = 0$.

Taking into account the definition of the generalized force $Q(t)$, the differential equation of motion (1) for all phases can be written as follows:

$$\ddot{x} + \omega^2 \cdot x = \frac{1}{m}\left[ P_1\left(1-\frac{t}{\tau}\right)\varphi(a) + P_2\left(1-\frac{t}{\tau}\right)\varphi(b)\right] \quad (2)$$

where, as is known, ω is the circular frequency; *φ(a)* and *φ(b)* are the normalized displacements at points *a* and *b*, corresponding to the application points of forces $F_1$ and $F_2$, respectively, which are determined from the assumed bending shape of the cantilever.

$$\varphi(\mathrm{y}) = \frac{y^2(3L-y)}{2L^3} \quad (3)$$

where *y* is the coordinate along the rod (see Fig. 1). Function (3) is chosen such that at $y = L$ we have $\varphi(y) = 1$, and it corresponds to the bending shape of a simple cantilever beam.

The general solution of the equation of motion in each phase ($i = 1 \ldots 4$) is assumed in the form:

$$x_i(t) = C_{i,1}Cos(\omega \cdot t) + C_{i,2}Sin(\omega \cdot t) + A_i + B_i t \quad (4)$$

The particular solutions are expressed as linear functions with undetermined coefficients:

$$x_i^*(t) = A_i + B_i \cdot t \quad (5)$$

The constants $A_i$ and $B_i$ are determined depending on the right-hand side of expression (2) in each phase of vibration (see above). In the fourth phase, the constants $A_4$ and $B_4$ are absent. The constants $C_{i,1}$ and $C_{i,2}$ are determined from the initial conditions of each phase:

Phase 1: initial conditions are zero:

$$x_1(0) = 0; \quad \dot{x}_1(0) = 0$$

Phase 2: initial conditions are:

$$x_2(\delta_t) = x_1(\delta_t); \quad \dot{x}_2(\delta_t) = \dot{x}_1(\delta_t)$$

Phase 3: initial conditions are:

$$x_3(\tau) = x_2(\tau); \quad \dot{x}_3(\tau) = \dot{x}_2(\tau)$$

Phase 4: initial conditions are:

$$x_4(\tau+\delta_t) = x_3(\tau+\delta_t); \qquad \dot{x}_4(\tau+\delta_t) = \dot{x}_3(\tau+\delta_t)\,.$$

That is, the initial conditions for the *i*-th phase are taken equal to the final values of displacement and velocity from the $(i-1)$-th phase, for which the solution has already been obtained.

The problem is solved according to the following algorithm:

In each phase, first, depending on the right-hand side of (2) and assuming a particular solution in the form of (5), the constants $A_i$ and $B_i$ are determined by equating coefficients of like powers of *t*. Then, using the general solution with the right-hand side (4) and applying the initial conditions (see above), the constants $C_{i,1}$ and $C_{i,2}$ are determined. Having all constants, all displacement values in each phase are calculated. The initial conditions for the next phase are the final conditions (displacement and velocity) of the previous phase. This procedure is repeated until the end of the fourth phase.

For a larger number of forces $F_1, F_2, \ldots F_n$, as well as for different durations of the positive phase $\tau_i$ of these forces, the essence of the calculation does not change. In this case, the differential equation (2) takes the form:

$$\ddot{x} + \omega^2 \cdot x = \frac{1}{m}\left[ P_1\left(1-\frac{t_1}{\tau_1}\right)\varphi(y_1) + \ldots + P_n\left(1-\frac{t_n}{\tau_n}\right)\varphi(y_n)\right] \quad (6)$$

where $y_1, \ldots, y_n$ are the distances from the base of the cantilever to the force $F_n$. In this case, the equation (6) should be considered sequentially; $t_i$ is the time at the beginning of the i-th segment of the analysis of equation (6), which is determined by the formula:

$$t_i = t - (i-1)\delta_t \quad (7)$$

That is, for each time segment, a new variable $t_i$ is introduced. In this case, the right-hand side of equation (6) will include the number $P_i$ depending on the arrival time $t_i$ of force $F_i$, the durations of forces $F_1, F_2, \ldots F_{i-1}$, as well as times $t_{i+1}, t_{i+2}, \ldots t_n$.

The number of considered phases depends on the number of segments dividing the total time, $t_{tot} = n \cdot \boldsymbol{\delta_t}$. The initial conditions for each *i*-th phase are taken as the final conditions

(displacement and velocity of the mass) at the end of the $(i-1)$-th phase.

It should be particularly noted that, regardless of the number of segments, only one differential equation (6) is solved in each phase, with its own initial conditions and its own set of forces $F_i$. Therefore, the constants $A_i$ and $B_i$ from the particular solution of the equation (see expression 5) are determined each time. As a result, the number of segments can be chosen arbitrarily by the engineer, and there is no particular difficulty in the numerical implementation of the calculation for a system with many applied forces.

The problem is significantly simplified if the loading is considered as an instantaneous impulse. Then, if n impulses $J_1, J_2, \dots J_n$ act sequentially, each applied after a time interval $\boldsymbol{\delta_t}$, the differential equation takes the form of equation (1) with a zero right-hand side. The solutions of these equations for the action of the $i$-th impulse are expressed as:

$$x_i(t) = \frac{J_i \cdot \phi_i}{m \cdot \omega} Sin(\omega \cdot t); \quad \dot{x}_i(t) = \frac{J_i \cdot \phi_i}{m} Cos(\omega \cdot t) \tag{8}$$

The difference for all the equations lies in the initial conditions. Thus, for two impulses, the initial conditions for the first impulse are $x(0) = 0;\ \dot{x}(0) = J_1\phi(a)/m$, where $\varphi(a)$ is determined from expression (3). The initial conditions for the second impulse are:

$$x(\delta_t) = \frac{J_1\phi(a)}{m \cdot \omega} Sin(\omega \cdot \delta_t); \dot{x}(\delta_t) = \frac{J_1\phi(a)}{m \cdot \omega} Cos(\omega \cdot \delta_t) + \frac{J_2\phi(b)}{m} \tag{9}$$

Under the action of $n$ impulses, the initial conditions for the n-th impulse are as follows:

$$x(n \cdot \delta_t) = \frac{J_1\phi_1}{m \cdot \omega} Sin(\omega \cdot \delta_t) + \frac{J_1\phi_2}{m \cdot \omega} Sin(\omega \cdot 2 \cdot\cdot \delta_t) + \dots + \frac{J_n\phi_n}{m \cdot \omega} Sin(\omega \cdot n \cdot \delta_t) \tag{10}$$

$$\dot{x}(n \cdot \delta_t) = \frac{J_1\phi_1}{m \cdot \omega} Cos(\omega \cdot \delta_t) + \dots + \frac{J_{n-1}\phi_{n-1}}{m \cdot \omega} Cos(\omega \cdot (n-1) \cdot \delta_t) + \frac{J_n\phi_n}{m} \tag{11}$$

where $\varphi_1, \dots, \varphi_n$ denote the functions (3) corresponding to the locations of the *1st* … *n*-th impulses.

Thus, at the moment the impulse with index $k$ is applied, the initial displacement is equal to the sum of the displacements of the free vibrations from impulses $1, \dots, k-1$ according to the first expression in (8), and the initial velocity is equal to the sum of the velocities from these impulses according to the second expression in (8), plus the initial velocity generated by the $k$-th impulse itself.

It is known that if the system is considered not as one with a single equivalent mass but as one with the actual number of masses equal to $n$, then after modal analysis one can obtain $n$ separate differential equations of type (1). Solving them yields a set of expressions $x_i(t)$ for each mode of vibration. The total response of the system (for example, the total displacement of the $i$-th mass) is simply the sum of the displacements $x_i(t)$ for all modes at the considered time $t$.

Reducing a system with $n$ masses to a system with a single equivalent mass, as discussed above, provides an approximate solution; however, it allows the effect of delayed force arrival to be taken into account.

Calculations show that, for a single-mass system, the delay in force application does not increase the system's response. However, for multi-mass systems, this effect may either increase or decrease the total response. The analysis of multi-mass systems can be performed using the methodology developed above, but with the application of modal decomposition, where each mode is treated as an SDOF system while still accounting for the delayed arrival of forces.

The methodology proposed above involves a multiphase treatment of the problem. The use of the Duhamel integral for solving the equations of motion with forces applied at different times makes it unnecessary to consider initial conditions at each phase. Let us examine an approach for analyzing a multi-mass system subjected to impulses applied with time shifts $\tau_i$, using the Duhamel integral. Since the response maxima occur at different moments in time, a simple summation of these maxima sum not the maxima, but the modal responses evaluated at the same time instant *t*. For the mode with index *r*, we obtain the following differential equation:

$$m_r\ddot{\eta}_r + k_r\eta_r = F_r(t), \qquad (12)$$

where $\eta_r = \eta_r(t)$ is the generalized coordinate in the r-th mode, determined by the well-known Duhamel integral:

$$\eta_r(t) = \frac{1}{m_r\omega_r}\int_0^t F_r(\tau)sin(\omega_r(t-\tau))d\tau. \qquad (13)$$

where $m_r$ is the modal mass;
$k_r = m_r\,\omega_r^2$ is the stiffness in the *r*-th mode.

$$F_j(\tau) = p(t-\tau_j)A_j \qquad (14)$$

where *p(t)* is the triangular impulse generated by the blast wave; $\tau_j$ is the arrival time of the wave at node *j*; $A_j$ is the area from which the load is collected for that node.

$$p(t) = \begin{cases} p_0\left(1-\frac{t}{t_+}\right), 0 \le t \le t_+ \\ 0, t > t_+. \end{cases} \qquad (15)$$

where $p_0$ is the amplitude; $t_+$ is the duration of the impulse.

Substituting into the Duhamel integral for a single node j gives us the expression:

$$\eta_{rj}(t) = \frac{p_0\,A_j\varphi_r(x_j)}{m_r\omega_r}\int_{\tau_j}^t\left(1-\frac{t-\tau_j}{t_+}\right)\times sin(\omega_r(t-\tau))d\tau \qquad (16)$$

Let us introduce a new variable:

$$u=\tau-\tau j,\ d\tau=du \qquad (17)$$

Then we will have:

$$\eta_{rj}(t) = \frac{p_0\,A_j\varphi_r(x_j)}{m_r\omega_r}\int_0^{u*}(1-\frac{u}{t_+})\,sin(\omega_r(t-\tau_j)-\omega_r u)d\tau \qquad (18)$$

where $u*=min(t-\tau_j, t+)$; is introduced;
$\varphi_r$ –is the *r*-th mode shape.

In addition, let us denote $\alpha=\omega_r(t-\tau_j)$. Then the integral can be written as follows:

$$J(\alpha,u^*) = \int_0^{u*}(1-\frac{u}{t_+})sin(\alpha-\omega_r u)du \qquad (19)$$

After expanding the integrand, applying integration by parts, imposing the limits from *0* to *u**, and performing the necessary transformations, we finally obtain:

$$J(\alpha,u^*) = \frac{1}{\omega}\,[\cos(\alpha-\omega\cdot u^*)-cos\alpha] - \frac{1}{t_+}(-\frac{u^*}{\omega}\cos(\alpha-\omega\cdot u^*) + \\ + \frac{1}{\omega^2}sin(\alpha-\omega\cdot u^*) - \frac{1}{\omega^2}sin\alpha) \qquad (20)$$

Then the final formula for the response in the *r*-th mode takes the form:

$$\eta_r(t) = \frac{1}{m_r\omega_r}\sum p_0 A_j \varphi_r(x_j) \cdot J(\omega_r(t - -\tau_j), u_j^*) \quad (21)$$

Let us now explain the reason why the responses can be summed. Solution (12) is presented in the form of (13). In this case, the modal force is determined as the sum over the segments:

$$F_r(t) = \sum_{i=1}^{N} P_{rj} S\left(t - \tau_j\right), \quad (22)$$

where $P_{rj} = p_0 A_j \phi_r(x_j)$.

From the linearity of the integral, we have:

$$\eta_r(t) = \sum_{i=1}^{N} \frac{P_{rj}}{m_r\omega_r} \int_0^t S(\tau - \tau_j) \times sin(\omega_r(t - \tau))d\tau. \quad (23)$$

Let us make the substitution $u=\tau-\tau_j$ and obtain the shifted response function:

$$\eta_r(t) = \sum_{i=1}^{N} \frac{P_{rj}}{m_r\omega_r} J_r(t - \tau_j), \quad (24)$$

where:

$$J_r(\xi) = \int_0^{min(\xi,t+)} S(u) \cdot sin(\omega_r(\xi - u))du, \quad (25)$$

$$J_r(\xi) \equiv 0 \text{ при } \xi < 0 \quad (26)$$

Here, $J_r(\xi)$ is a time-dependent function. It is zero before arrival and then varies according to a sine function.

We sum the values of these functions at the same time *t*:

$$\eta_r(t) = \sum \frac{P_{rj}}{m_r\omega_r} J_r(t - \tau_j) \quad (27)$$

This summation is correct for a linear system.

In the considered method, *J* is not a number, but a time-dependent function (a convolution kernel). To avoid interpreting *J* as a number, we fix the notation as follows:

$$\eta_r(t) = \sum_{i=1}^{N} \frac{p_0 A_j \phi_r\left(x_j\right)}{m_r\omega_r} J_r\left(t - \tau_j\right),$$

$$J_r(\xi) = H(\xi) \int_0^{min(\xi,t+)} S(u)\sin(\omega_r(\xi - u))$$

where $H(\xi)$ is the well-known unit Heaviside function. For a very short pulse $\omega_r t_+ \ll 1$, for $Jr(\xi)$ we obtain:

$$J_r(\xi) \approx \frac{t_+}{2} sin(\omega_r\xi)H(\xi) \quad (28)$$

and then we have:

$$\eta_r(t) = \sum_{j=1}^{N} \frac{P_{rj}}{m_r\omega_r} \frac{t_+}{2} sin(\omega_r(t - \tau_j)) \quad (29)$$

$$\eta_r(t) = \sum_{j=1}^{N} \frac{P_{rj}}{m_r \omega_r} \frac{t_+}{2} \sin\left(\omega_r\left(t-\tau_j\right)\right) \eta_r(t) = \frac{1}{m_r \omega_r} P_r sin(\omega_r t) \quad (30)$$

Thus, in the form (29) we obtained the total response of the system without performing a phase-by-phase computation, as was shown above. This is the advantage of such an approach. However, for calculations that take the system's nonlinearity into account, one should still use the phase-by-phase procedure, in which, as shown earlier, the initial conditions of each subsequent phase are taken as the final conditions of the preceding phase of oscillations.

**Example of Calculation.**

A vertical three-story cantilever beam is considered, with lumped masses *m=3000 kg* at each floor level. The applied forces are arranged as shown in Fig. 2. The cross-section is *b×h=0.5×1 m*, the modulus of elasticity is *E=25,000 MP*, and the TNT charge mass is *W=100 kg*. For the first force, the following parameters are adopted: $P_1$*=1184.67 kN*, $t_{01}$*=0.00715 s* (the duration of force $P_1$), $t_{A1}$*=0 s* (arrival time of $P_1$). For the second force, the parameters are: $P_2$*=725.25 kN*, $t_{02}$*=0,00737 s* (the duration of the force $P_2$), $t_{A2}$*=0.001 s* (arrival time of $P_2$). For the third force, the adopted parameters are: $P_3$*=303.66 kN*, $t_{03}$*=0,00781 s* (the duration of force $P_3$), $t_{A3}$*=0.004 s* (arrival time of $P_3$).

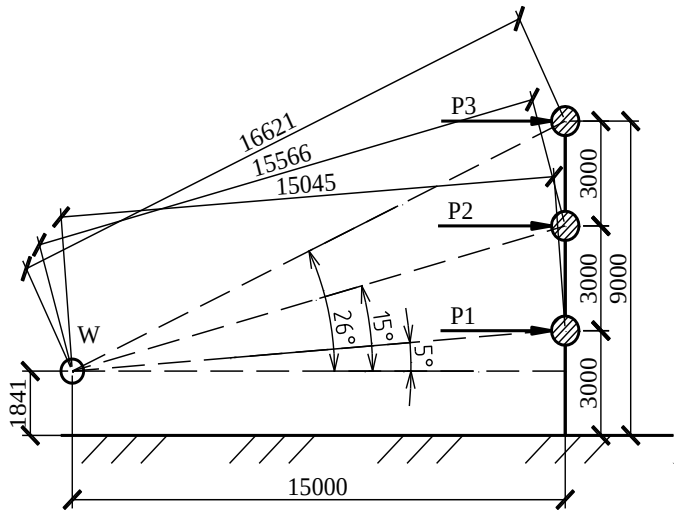


**Fig. 2** Diagram of a single-mass system subjected to dynamic forces with different arrival times
**Рис. 2** Схема системи з однією масою з різним приходом динамічних сил

**Solution.**The fundamental vibration period of the cantilever beam shown in Fig. 2 is *T=0.191 s.* The arrival times of forces $P_2$ and $P_3$ are $t_{A2}$*=0.001 s<< T= 0.191 s* and $t_{A3}$*=0.004 s<< T = 0.191 s* respectively. Therefore, the internal force values in the beam for the case of simultaneous arrival of the forces and for the case with the specified delays will be practically identical.

In the analysis of the beam under the assumption of simultaneous force arrival, the computed maximum bending moment at the fixed support is $M_{max}$*=280 kN·m*. When the delay in force application is taken into account using the proposed methodologies, the maximum bending moment is obtained as *283.26 kN·m,* corresponding to a relative error of *1.15%.*

When the force arrival times are increased to $t_{A2}$*=0.004 s* and $t_{A3}$*=0.008 s*, the calculations

yield a bending moment of *341.27 kN·m* , with a relative error of *21.88%.*

Further increasing the arrival times to $t_{A2}=0.008$ *s* and $t_{A3}=0.016$ *s* results in a bending moment of *310.56 kN·m*, corresponding to a relative error of *10.9%.*

For the arrival times $t_{A2}=T/6=0.0318$ *s* and, $t_{A3}=T/3=0.0637$ s, the calculations yield a bending moment of *270.87 kN·m,* corresponding to a relative error of *–3.37%.*

For the arrival times $t_{A2}=T/3=0.0637$ *s* and $t_{A3}=T/2=0.0955$ *s*, the bending moment is 251.45 *kN·m,* with a relative error of *–11.14%.*

Thus, we have demonstrated that accounting for delayed force arrival on subsequent floors may lead to either an increase or a decrease in the dynamic internal forces. This effect depends on factors such as the duration of the positive phase of the pressure, the delay time of the forces, and the vibration period of the system.

## CONCLUSIONS AND RECOMMENDATIONS

The proposed methodology for analyzing structural response under blast loading accounts for the non-simultaneous arrival of the blast wave at different points of the structure. The maximum response may occur during different phases of the mass motion. A phase-by-phase analysis is presented, in which the initial conditions of each subsequent phase are taken as the final conditions of the previous vibration phase. An analytical expression for the total response under multiple impulses acting on different masses of the system at different times is also derived. It is demonstrated why, in linear systems, the superposition of modal responses at a specific moment of vibration is valid. For SDOF systems, the influence of force delay has a minor effect on the system's response.

However, for multi-mass systems, the effect of delayed forces may lead either to an increase or a decrease in the overall response, depending on the ratio $t_0/T$ and the delay time.

## REFERENCES


1. **Azizov T.N., Kochkarev D.V., Galinska T.A.** (2025). Buildings and Structures Calculations for Air Shock Wave Effect from Conventional Weapons. *IOP Conference Series: Earth and Environmental Science*, 1499(1), 012012. https://doi.org/10.1088/1755-1315/1499/1/012012
2. **Baker W.E.** (1973). Explosions in Air. Univ. of Texas Press, Austin, TX, USA, 268 *pp.*
3. Blast effects on buildings. Design of buildings to optimize resistance to blast loading. (1995). *International Journal of Rock Mechanics and Mining Sciences & Geomechanics Abstracts, 32(7), 348–349.* https://doi.org/10.1016/0148-9062(95)92584-5
4. **Clough R.W., Penzien J. (2015).** Dynamics of Structures. *New Delhi: McGraw-Hill Education, 319.*.
5. **DBN V.2.2-5:2023. (2023).** Tsivilni zakhysni konstruktsii [Civil defense protective structures]. *[Chynnyi vid 1.11.2023]*, K*yiv: Ministerstvo rozvytku hromad, terytoriy ta infrastruktury Ukrayiny, 122 s. Redaktsiya stanom na 25.12.2024.*. [in Ukrainian]
6. **Dennis A.A., Rigby S.E.** (2024). The direction-encoded neural network: a machine learning approach to rapidly predict blast loading in obstructed environments. *Int. J. Protect. Struct., 15(3), 455–483.* https://doi.org/10.1177/20414196231177364
7. **Task Committee on Blast Resistant Design of the Petrochemical Committee of the Energy Division of the American Society of Civil Engineers.** (2010). *Design of blast-resistant buildings in petrochemical facilities. pp. 447*
8. **Ekström J., Rempling R., Plos M.** (2016). Spalling in concrete subjected to shock wave blast. *Engineering Structures, 122, 72–82.* https://doi.org/10.1016/j.engstruct.2016.05.002
9. **Fan Y., Chen T., Yang G., Cui X., Lu W., Wang G., Tian B.** (2024). Experimental investigation on dynamic response of concrete gravity dam under shock wave and bubble pulsation. *Engineering Structures, 318, 118796*. https://doi.org/10.1016/j.engstruct.2024.118796
10. **Isaac O.S., Alshammari O.G., Pickering E.G., Clarke S.D., Rigby S.E.** (2023). Blast wave interaction with structures—an overview. *Int. J. Protect. Struct., 14(4), 584–630*. https://doi.org/10.1177/20414196221118595
11. **Jin R., Gou Y**. (2018). Motion response analysis of large-scale structures with small-scale cylinders under wave action. O*cean Engineering, 155, 65–74.* https://doi.org/10.1016/j.oceaneng.2018.02.032
12. **Karlos V., Solomos G.** (2013). Calculation of blast loads for application to structural

components. *JRC Technical Report, EUR 26456 EN, 58 pp.* https://doi.org/10.2788/61866

13. **Kingery C.N., Bulmash G**. (1984). Technical report ARBRL-TR-02555: Air blast parameters from TNT spherical air burst and hemispherical burst. A*D-B082 713, U.S. Army Ballistic Research Laboratory, Aberdeen Proving Ground, MD, 51 p.*
14. **Kochkarev D., Azizov T., Galinska T**. (2024). Calculation of Buildings and Structures for Air Blasts Using Explosion Accelerograms. *Lecture Notes in Civil Engineering, 604 LNCE, pp. 245–256.* https://doi.org/10.1007/978-3-031-67576-8_22
15. **Kochkarev D., Azizov T., Galinska T**. (2024). Calculation of Enclosures of Defence Structures Based on the Quasi-static Method. *Lecture Notes in Civil Engineering, 469 LNCE, pp. 50–58.* https://doi.org/10.1007/978-3-031-55068-3_4
16. **Koliakova V., Dumych A., Sumak A.** (2023). Stress-Strain State of Shelter Structures under the Action of Air Shock Wave. *Sworld-Us Conference Proceedings, (1) (usc22-01), 49–56.* [in Ukrainian] https://doi.org/10.30888/2709-2267.2024-22-00-020
17. **Kumar V., Kartik K.V., Iqbal M.A.** (2020). Experimental and numerical investigation of reinforced concrete slabs under blast loading. *Engineering Structures, 206, 110125.* https://doi.org/10.1016/j.engstruct.2019.110125
18. **Wang L., Kong D. (**2023). Influence of Ground Impedance on Explosive Shock Wave Test Accuracy. *International Journal of Impact Engineering, 171, 104395* https://doi.org/10.1016/j.ijimpeng.2022.104395
19. **Li Q., Wang Y., Li L., Hao H., Wang R., Li J**. (2023). Prediction of BLEVE loads on structures using machine learning and CFD. *Process Safety and Environmental Protection, 171, 914–925.* https://doi.org/10.1016/j.psep.2023.02.008
20. **Cormie D., Smith P.D., Mays G.C**. (2019). Blast Effects on Buildings: Design of Buildings to Optimize Resistance to Blast Loading. 3rd ed., *ICE Publishing / Emerald Publishing, 344 .*
21. **Moon K.** (2011). Structural Design of Double Skin Facades as Damping Devices for Tall Buildings. *Procedia Engineering, 14, 1351–1358.* https://doi.org/10.1016/j.proeng.2011.07.170
22. **Xiao S.Y., et al**. (2021). Prediction of warhead explosion location based on explosion shock wave. *Military Automation, 40(5), 90–93.* https://doi.org/ 10.7690/bgzdh.2021.05.020
23. **U.S. Department of Defense.** (2018, change 3 — 24 May 2024). UFC 4-010-01, DoD Minimum Antiterrorism Standards for Buildings. *Washington, DC. pdf, 95*
24. **U.S. Army Corps of Engineers, Naval Facilities Engineering Command, Air Force Civil Engineer Support Agency**. (2014, Change 2 — 01 September 2014). UFC 3-340-02, Structures to Resist the Effects of Accidental *Explosions. Washington, DC. pdf, 99*
25. **Karlos V., Solomos G.** (2013). Calculation of blast loads for application to structural components. *Luxembourg: Publications Office of the European Union, 58 .* https://doi.org/ 10.2788/61866
26. **Vivek P., Sitharam T.G.** (2019). Response of Embedded Structures in Granular Material to Air-Blast Wave Loading. *In: Granular Materials Under Shock and Blast Loading, 95–109.* https://doi.org/10.1007/978-981-15-0438-9_6
27. **Wang Z., Gong X., Xiong J., Yong H.** (2014). Studying an engineering model on an air blast wave. Structures Under Shock and Impact XIII, 1, 217–227. https://doi.org/10.2495/susi140191

## LITERATURE

1. **Azizov T.N., Kochkarev D.V., Galinska T.A.** (2025). Buildings and Structures Calculations for Air Shock Wave Effect from Conventional Weapons. *IOP Conference Series: Earth and Environmental Science*, 1499(1), 012012. https://doi.org/10.1088/1755-1315/1499/1/012012
2. **Baker W.E.** (1973). Explosions in Air. Univ. of Texas Press, Austin, TX, USA
3. Blast effects on buildings. Design of buildings to optimize resistance to blast loading. (1995). International Journal of Rock Mechanics and *Mining Sciences & Geomechanics Abstracts, 32(7), 348–349.* https://doi.org/10.1016/0148-9062(95)92584-5
4. **Clough R.W., Penzien J. (2015).** Dynamics of Structures. *New Delhi: McGraw-Hill Education, 319*
5. **DBN V.2.2-5:2023. (2023).** Tsivilni zakhysni konstruktsii. *Kyiv: Ministerstvo rozvytku hromad, terytoriy ta infrastruktury Ukrayiny,* 122 s. Redaktsiya stanom na 25.12.2024.
6. **Dennis A.A., Rigby S.E.** (2024). The direction-encoded neural network: a machine learning approach to rapidly predict blast loading in obstructed environments. *Int. J. Protect. Struct., 15(3), 455–483.*

https://doi.org/10.1177/20414196231177364

7. **Task Committee on Blast Resistant Design of the Petrochemical Committee of the Energy Division of the American Society of Civil Engineers.** (2010). *Design of blast-resistant buildings in petrochemical facilities.. 447*

8. **Ekström J., Rempling R., Plos M.** (2016). Spalling in concrete subjected to shock wave blast. *Engineering Structures, 122, 72–82.* https://doi.org/10.1016/j.engstruct.2016.05.002

9. **Fan Y., Chen T., Yang G., Cui X., Lu W., Wang G., Tian B.** (2024). Experimental investigation on dynamic response of concrete gravity dam under shock wave and bubble pulsation. *Engineering Structures, 318, 118796.* https://doi.org/10.1016/j.engstruct.2024.118796

10. **Isaac O.S., Alshammari O.G., Pickering E.G., Clarke S.D., Rigby S.E.** (2023). Blast wave interaction with structures—an overview. *Int. J. Protect. Struct., 14(4), 584–630.* https://doi.org/10.1177/20414196221118595

11. **Jin R., Gou Y**. (2018). Motion response analysis of large-scale structures with small-scale cylinders under wave action. *Ocean Engineering, 155, 65–74.* https://doi.org/10.1016/j.oceaneng.2018.02.032

12. **Karlos V., Solomos G.** (2013). Calculation of blast loads for application to structural components. *JRC Technical Report, EUR 26456 EN, 58.* https://doi.org/10.2788/61866

13. **Kingery C.N., Bulmash G**. (1984). Technical report ARBRL-TR-02555: Air blast parameters from TNT spherical air burst and hemispherical burst. *AD-B082 713, U.S. Army Ballistic Research Laboratory, Aberdeen Proving Ground, MD, 51.*

14. **Kochkarev D., Azizov T., Galinska T**. (2024). Calculation of Buildings and Structures for Air Blasts Using Explosion Accelerograms. *Lecture Notes in Civil Engineering, 604 LNCE, pp. 245–256.* https://doi.org/10.1007/978-3-031-67576-8_22

15. **Kochkarev D., Azizov T., Galinska T**. (2024). Calculation of Enclosures of Defence Structures Based on the Quasi-static Method. *Lecture Notes in Civil Engineering, 469 LNCE,. 50–58.* https://doi.org/10.1007/978-3-031-55068-3_4

16. **Koliakova V., Dumych A., Sumak A.** (2023). Napruzheno-deformovanyi stan konstruktsii ukryttia pry dii povitrianoi udarnoi khvyli *Sworld-Us Conference Proceedings,(1) usc22-01, 49–56.* https://doi.org/10.30888/2709-2267.2024-22-00-020

17. **Kumar V., Kartik K.V., Iqbal M.A.** (2020). Experimental and numerical investigation of reinforced concrete slabs under blast loading. *Engineering Structures, 206, 110125.* https://doi.org/10.1016/j.engstruct.2019.110125

18. **Wang L., Kong D. (**2023). Influence of Ground Impedance on Explosive Shock Wave Test Accuracy. *International Journal of Impact Engineering, 171, 104395.* https://doi.org/10.1016/j.ijimpeng.2022.104395

19. **Li Q., Wang Y., Li L., Hao H., Wang R., Li J**. (2023). Prediction of BLEVE loads on structures using machine learning and CFD. *Process Safety and Environmental Protection, 171, 914–925*. https://doi.org/10.1016/j.psep.2023.02.008

20. **Cormie D., Smith P.D., Mays G.C**. (2019). Blast Effects on Buildings: Design of Buildings to Optimize Resistance to Blast Loading. 3rd ed., *ICE Publishing / Emerald Publishing, 344 pp.*

21. **Moon K.** (2011). Structural Design of Double Skin Facades as Damping Devices for Tall Buildings. P*rocedia Engineering, 14, 1351–1358.* https://doi.org/10.1016/j.proeng.2011.07.170

22. **Xiao S.Y., et al**. (2021). Prediction of warhead explosion location based on explosion shock wave. *Military Automation, 40(5), 90–93.* https://doi.org/10.7690/bgzdh.2021.05.020

23. **U.S. Department of Defense.** (2018, change 3 — 24 May 2024). UFC 4-010-01, DoD Minimum Antiterrorism Standards for *Buildings. Washington, DC. pdf, 95*

24. **U.S. Army Corps of Engineers, Naval Facilities Engineering Command, Air Force Civil Engineer Support Agency**. (2014, Change 2 — 01 September 2014). UFC 3-340-02, Structures to Resist the Effects of Accidental *Explosions. Washington, DC. pdf, 99*

25. **Karlos V., Solomos G.** (2013). Calculation of blast loads for application to structural components. *Luxembourg: Publications Office of the European Union, 58 .* https://doi.org/202010.2788/61866

26. **Vivek P., Sitharam T.G.** (2019). Response of Embedded Structures in Granular Material to Air-Blast Wave Loading. In: *Granular Materials Under Shock and Blast Loading, pp. 95–109.* https://doi.org/10.1007/978-981-15-0438-9_6

27. **Wang Z., Gong X., Xiong J., Yong H.** (2014). Studying an engineering model on an air blast wave. *Structures Under Shock and Impact XIII, 1, 217–227.* https://doi.org/10.2495/susi140191

ISSN 2522-4182

# ВПЛИВ ЗАПІЗНЕННЯ ПРИХОДУ ВИБУХОВОЇ ХВИЛІ НА ДИНАМІЧНУ ПОВЕДІНКУ ЗАХИСНОЇ СПОРУДИ

*Анатолій ПЕРЕЛЬМУТЕР*
*Талят АЗІЗОВ*
*Дмитро КОЧКАРЬОВ*
*Наталія СРІБНЯК*

**Анотація.** В статті розглянуто методики розрахунку захисних споруд за дії вибухової хвилі, тиск якої приходить до різних точок в різний час. Розглянуто пофазовий спосіб розрахунку, коли дію серії сил з різним часом приходу розглядають як окремі фази коливань. За початкові умови поточної фази приймаються кінцеві умови (переміщення і швидкості) попередньої фази. Докладно розглянуто систему з однією масою (SDOF-систему), на яку діють сили з різним часом приходу. На кожній фазі спочатку в залежності від правої частини відомого диференціального рівняння знаходять константи частинного і загального рішення диференціального рівняння SDOF-системи. Маючі всі константи, визначають всі значення переміщень на кожній фазі.

Показано, що перевага такого підходу полягає в тому, що незважаючи на будь яку кількість ділянок, на які діють сили в різний час, на кожній фазі вирішується лише одне диференціальне рівняння зі своїми початковими умовами і своїм набором сил. Тому кожний раз знаходяться свої константи з частинного рішення та загального рішень рівняння. Тому кількість ділянок може бути визначена будь якою на думку інженера і якоїсь складності в чисельній реалізації розрахунку система з багатьма розглядуваними силами немає.

Показано, що для одномасової системи різний час приходи динамічної сили не збільшує відгук системи, але така схема використовується, коли багатомасову систему за допомогою модального розкладення розглядають як SDOF-систему для кожної окремої моди з врахуванням різного часу приходу сили, а потім складають відгуки простим підсумовуванням. Показано, чому в лінійних системах підсумовування модальних відгуків в конкретний час коливань є правильним, але просте підсумовування максимальних відгуків не є правильним.

Показано, що пофазовий розгляд коливань системи є правильним, але більш громіздким. Для багатомасових систем за дії імпульсу наведено аналітичну формулу сумарного відгуку на імпульси, які приходять до різних точок в різний час. При цьому розглянуто трикутний імпульс з кінцевим часом дії, а також миттєвий імпульс.

**Ключові слова:** вибухова хвиля; фаза коливань; SDOF-система; рівняння коливань; імпульс.

.

***Received:*** *October 10, 2025.*
***Accepted:*** *November 30, 2025.*

ISSN 2522-4182

DOI: 10.32347/2522-4182.17.2025.30-40
UDC 624.011.620-178.2

# EXPERIMENTAL STUDIES OF PRESTRESSED SOLID TIMBER BEAMS

*Denys MYKHAILOVSKYI[1], Petro GOMON[2]*

[1,2] Kyiv National University of Construction and Architecture
31, Povitryanykh Syl Ave., Kyiv, Ukraine, 03037
[1] mykhailovskyi.dv@knuba.edu.ua, https://orcid.org/0000-0003-3151-8630
[2] p.s.homon@nuwm.edu.ua, https://orcid.org/0000-0002-5312-0351

**Abstract.** The article presents the results of comprehensive experimental and theoretical studies on the behavior of timber beams with combined reinforcement, in which both steel and composite reinforcement are simultaneously used. This approach combines the high strength and stiffness of steel with the low weight of composite materials, ensuring rational material use and improved structural efficiency.

Particular attention is given to the development and practical implementation of a method for creating prestressing in composite strip reinforcement located in the tensile zone of the beam. The proposed technique is technologically simple, does not require complex or expensive specialized equipment, and can be implemented both in laboratory conditions and in small- or medium-scale production facilities. The sequence of operations for prestressing the composite reinforcement, anchoring it within the timber base, and fabricating test specimens is described in detail.

The study provides a detailed experimental methodology, including the loading scheme, types of measuring devices, and methods for recording displacements and deformations. The deformation patterns and failure modes of prestressed timber beams with combined reinforcement are identified. Experimental relationships of the "moment–curvature" and "moment–deflection" types are constructed, allowing for quantitative evaluation of the influence of prestressing on the stiffness and strength of the elements.

The research results confirm that introducing prestressing into the composite reinforcement significantly increases the load-bearing capacity and stiffness of timber elements, reduces deflections, and ensures a more uniform stress distribution across the section.

The obtained results have important practical significance and can be applied in the design of new or reconstruction of existing timber structures, particularly in buildings and facilities with large spans, as well as in the development of new design standards, guidelines, and methodological materials for the calculation, manufacturing, and strengthening of timber structures with combined reinforcement.

**Keywords:** timber beams; combined reinforcement; composite reinforcement; prestressing.

**Denys MYKHAILOVSKYI**
Professor of the Department of Metal and Timber Structures, D.Sc. (Eng.)

**Petro GOMON**
Doctoral Student, Department of Metal and Timber Structures, PhD (Eng.)

## INTRODUCTION

Wood is a modern environmentally friendly material and one of the most in-demand renewable natural resources. Due to its numerous advantages, it has long been used as a construction material.

Today, solid (unprocessed) timber is rarely used in construction - it has been largely replaced by glued laminated timber (glulam), manufactured using advanced technologies that eliminate the main drawbacks of natural wood.

The application of glulam in large-scale engineering structures, such as halls, bridges, and stadiums, has created the need to enhance its load-bearing capacity in order to reduce cross-sectional height and limit deflections. One of the most effective ways to address this issue is by reinforcing the cross-section with materials of higher strength and stiffness.

## ANALYSIS OF PREVIOUS RESEARCH

Under wartime conditions, many authors devote their research to the strengthening of metal [1-3], reinforced concrete [4-5], and timber structures. Researchers have actively investigated the use of various materials - in particular, steel and composite reinforcement - to strengthen timber elements [6–10]. The introduction of stiffer materials into the cross-section contributes to an overall increase in beam stiffness, which, in turn, reduces deflections [11–15]. Experimental results have demonstrated the effectiveness of using composite materials based on synthetic fibers to improve the mechanical performance of timber structures. Advances in the production of fiber-reinforced polymers (FRPs) and the growing availability of synthetic fibers have made composite reinforcement a promising and efficient alternative for strengthening timber elements [16–21]. Current Ukrainian standards [22–25] for wood construction do not provide recommendations for the design and calculation of such elements, making the study of these structures relevant.

Previous studies conducted by the authors [20-21] examined the simultaneous use of steel and composite reinforcement in timber beams, which resulted in a significant increase in stiffness and load-bearing capacity. However, the idea emerged to further enhance the performance of such beams by introducing prestressing into the composite reinforcement located in the tensile zone. The proposed approach does not require complex or specialized equipment and can be implemented sequentially in several simple stages.

Therefore, the aim of this study is to determine the deformation behavior of a timber beam with combined reinforcement, in which the composite strip reinforcement in the tension zone is subjected to prestressing.

## PURPOSE AND METHODS

In the laboratory of the Department of Industrial and Civil Engineering at the National University of Water and Environmental Engineering, a prestressed bending element made of solid timber with combined reinforcement was manufactured for the first time.

A known method for prestressing bar reinforcement in the tensile zone during the production of prestressed glued laminated timber beams, which can also be applied to solid timber beams, involves the use of a special collet–clamping mechanism (CCM-1). This mechanism ensures the fixation of reinforcement ends in the beam's end faces and allows for the application of prestress to both steel and non-metallic bar reinforcement.

However, this technique requires the mandatory use of expensive specialized mechanisms and devices to create the prestressing force, as well as significant labor costs to perform the tensioning process.

The beam models developed using the new prestressing method can be made of either solid or glued laminated timber. In the proposed beams, the main objective is to reduce deflection by introducing prestressing into the composite strip reinforcement. This process is carried out in several simple stages without the use of any complex or costly specialized devices or equipment.

The designed initial deflection in $f_1$ the timber beam is created by applying an external load, as shown in Fig. 1. The height of the deflection is preliminarily calculated and specified by the designer, and its value is denoted as $f_1$. In this stressed state, a carbon fiber composite strip Sika CarboDur S-512 with a cross-section of 50 × 1.2 mm is installed in the future tensile zone of the timber element

(Fig. 1). The strip is bonded to the timber surface using Sikadur-30 adhesive. The element is maintained in this prestressed condition for 7 days until the adhesive is fully cured.

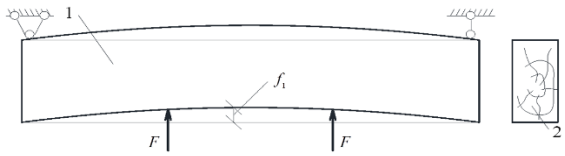


**Fig. 1** Creation of the deflection of a bending element to introduce prestressing: 1 – bending timber element; 2 – cross-section of the bending timber element; $f_1$ – initial curvature of the element; F – concentrated load

**Рис. 1** Створення вигину згинального елементу для створення попереднього напруження: 1 – згинальний дерев'яний елемент; 2 – поперечний переріз згинального дерев'яного елементу; $f_1$ – попередній вигин елемента; F– зосереджена сила

The third stage involves the removal of the concentrated external load F, which was previously applied to create the deflection in the bending timber element. As a result, the timber element reinforced with the carbon fiber strip tends to return to its initial shape. However, this movement is resisted by the bonded Sika CarboDur S-512 carbon strip, which becomes engaged in the work of the structure and counteracts the elimination of the initial deflection (Fig. 2).

Due to this effect, the solid timber bending element reinforced with the Sika CarboDur S-512 strip in the future tensile zone becomes prestressed and retains a residual deflection. In this state, the manufacturing process of the combined prestressed solid timber beam is completed by bonding steel reinforcement in the future compressive zone of the beam. The reinforcement is installed by embedding two Ø12 A500C steel bars into pre-cut grooves and fixing them with a composite mixture of epoxy adhesive and cleaned dry sand (Fig. 3).

After the adhesive mixture has fully cured, the prestressed solid timber beams with combined reinforcement are ready for testing and further structural application.

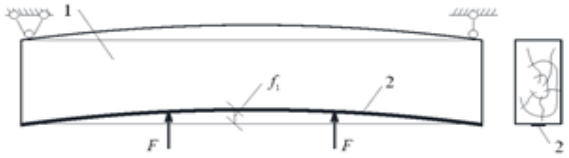


**Fig. 2** Bonding of a reinforcing element into the tension zone of a bending timber member: 1 – bending timber element; 2 – reinforcing material; $f_1$ – initial curvature of the element; F – concentrated load

**Рис. 2** Вклеювання армуючого елемента в розтягнуту зону згинального дерев'яного еле-менту: 1 – згинальний дерев'яний елемент; 2 – армуючий матеріал; $f_1$ – попередній вигин елемента; F– зосереджена сила

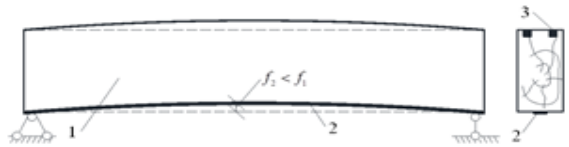


**Fig. 3** Bonding of a reinforcing element into the compression zone of a bending timber member: 1 – bending timber element; 2 – reinforcement of the tension zone; 3 – reinforcement of the compression zone; $f_1$ – deflection of the element; $f_2$ – residual deflection; F – concentrated load

**Рис. 3** Вклеювання армуючого елемента в стиснуту зону згинального дерев'яного елементу: 1 – згинальний дере-в'яний елемент; 2 – арматура розтяг-нутої зони; 3 – арматура стиснутої зони; $f_1$ – вигин елемента; $f_2$ – залиш-ковий вигин; F – зосереджена сила

According to this method, two prestressed beam specimens were manufactured, each with a total length of 3 meters and a cross-sectional size of 10 × 15 cm. The beams were reinforced with a carbon fiber strip Sika CarboDur S-512 and steel reinforcement 2Ø12 A500C. The prestressing of the SRB30 (Prst) beam was performed at a load level equal to 30% of the ultimate load, while the SRB45 (Prst) beam was prestressed at 45% of the ultimate load. The value of the ultimate load was determined during the testing of similar unreinforced

specimens.The process of bonding the carbon fiber strip under load is shown in Figure 4

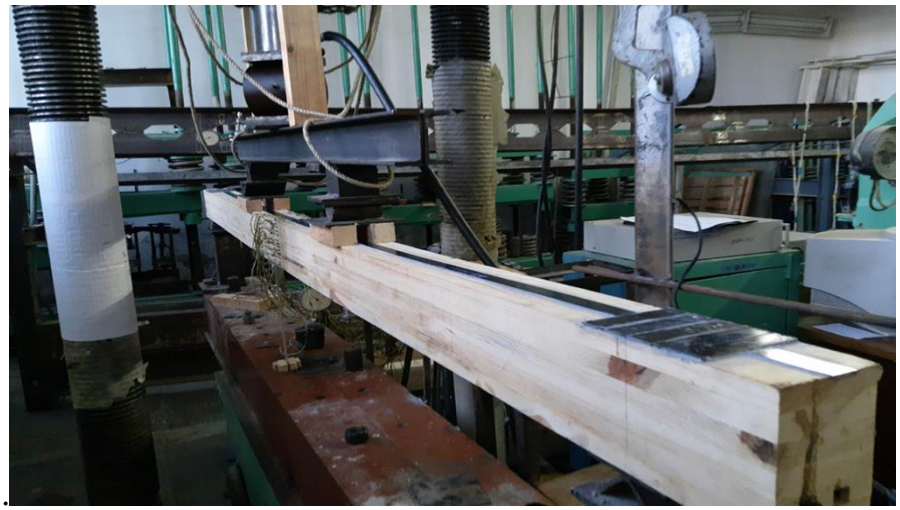

**Fig. 4** The curing process of the adhesive when bonding the composite strip reinforcement Sika CarboDur S-512 to the timber beam. Photo by Gomon, 2022
**Рис. 4** Процес твердіння клею при приклеюванні композитної стрічкової арматури Sika CarboDur S-512 до деревини балки. Фото П. Гомон, 2022

## EXPERIMENTAL STUDIES TEST SETUP

The manufactured and prepared beams made of solid and glued timber, as well as those with passive and prestressed combined reinforcement, were installed in the testing setup on hinged movable and fixed supports. In this position, all necessary measuring instruments were mounted and fixed, allowing the measurement of deflections, relative deformations of the timber in different layers along the beam height, and control of the composite action between the reinforcement and the timber.

The structural model corresponded to a simply supported beam subjected to two concentrated loads, each applied at a certain distance from the supports (four-point bending of flexural elements) (Fig. 5), in accordance with the recommendations EN 408:2007 [24].

Dial indicators ИЧ-10m were installed on the supports to measure the deformation resulting from the settlement of the beam supports under loading. A deflectometer model 6-PAO was positioned at midspan to record beam deflection.

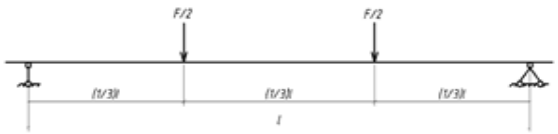


**Fig. 5** Timber beam scheme for calculations
**Рис. 5** Розрахункова схема дерев'яних балок

To measure possible slippage deformations of the steel reinforcement bars and the composite carbon fiber strip reinforcement Sika CarboDur S-512, dial-type indicators ИЧ-10n were mounted at the beam ends. All instruments were fixed on specially designed holders placed at predetermined points along the beam's cross-section (Fig. 6).

Before testing each specimen, its geometrical dimensions were verified, and the initial readings from all instruments were recorded in the experimental testing logbook. The instruments used during the experimental investigations had previously undergone official state calibration.

The prestressed solid timber beams with combined reinforcement, after verifying their geometrical dimensions, were installed in the testing setup. Subsequently, all necessary instruments were mounted and adjusted to their operational condition.

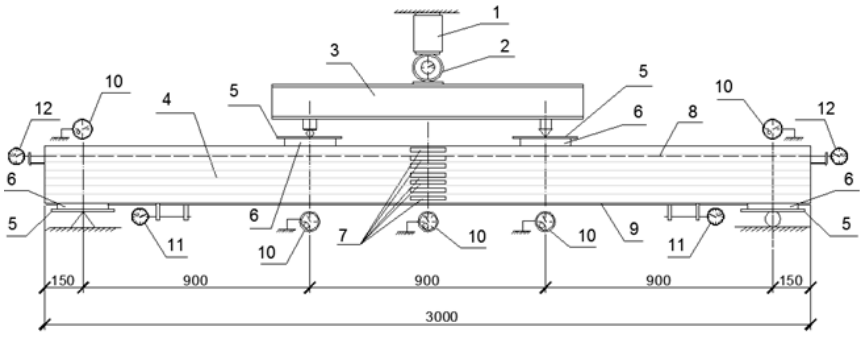


**Fig. 6** Test setup scheme for bending tests of timber beams: 1) jack; 2) dynamometer; 3) steel crosshead; 4) tested beam; 5) steel pad; 6) wooden pad; 7) strain gauges; 8) steel reinforcement 2 Ø A500C; 9) composite strip reinforcement Sika CarboDur S-512; 10) deflectometer 6-PAO; 11) indicator ICh-10n; 12) indicator ICh-10n

**Рис. 6** Схема дослідної установки для випробування дерев'яних балок на згин: 1) домкрат; 2) динамометр; 3) металева траверса; 4) досліджувана балка; 5) металева підкладка; 6) дерев'яна підкладка; 7) тензодатчики; 8) сталева арматура 2 Ø A500C; 9) композитна стрічкова арматура Sika CarboDur S-512; 10) прогиномір 6-ПАО; 11) індикатор ИЧ-10н; 12) індикатор ИЧ-10н

The loading was applied incrementally in steps of 500–1000 N, using a hydraulic jack model DOSM-5. After each successive loading step, a pause of up to 5 minutes was made to record readings from the dial indicators, deflectometer, and strain gauges. All obtained data were recorded in the test logbook.

When the applied load reached over 90% of the expected ultimate load, the measuring instruments were removed to prevent possible damage in case of sudden failure of the tested specimens.

## RESEARCH RESULTS

*Stage of Prestressing Creation.* The ultimate bending moment for the unreinforced beam was determined as $M_{\max} = 19{,}98 kN/m$. The prestressing level used to create the initial deflection was set for the combined reinforced beam SBR30 (Prst) at $M_{\max} = 6{,}0 kN/m$, and for the beam SBR45 (Prst) at $M_{\max} = 9{,}0 kN/m$, corresponding to 30% and 45% of the maximum load sustained by the unreinforced timber beam SB, respectively.

The behavior of the normal cross-sections can be illustrated using moment–curvature diagrams (Fig. 7, Fig. 8).

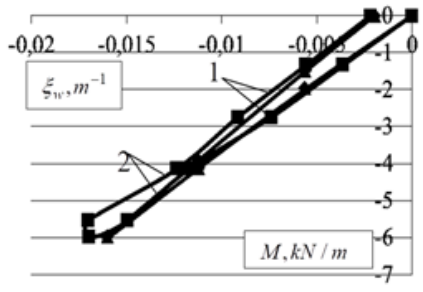


**Fig. 7** Experimental (1) and theoretical (2) "moment –curvature" graphs during loading and unloading of the SBR30(Prst) beam

**Рис. 7** Експериментальний (1) та теоретичний (2) графіки «момент-кривина» при завантаженні та розвантаженні балки SBR30(Prst)

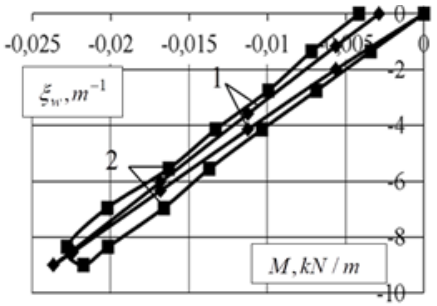


**Fig. 8** Experimental (1) and theoretical (2) "moment – curvature" graphs during loading and unloading of the SBR30(Prst) beam

**Рис. 8** Експериментальний (1) та теоретич-ний (2) графіки «момент-кривина» при завантаженні та розвантаженні балки SBR45(Prst)

The curvatures in the midspan cross-section were calculated during the loading of the SBR30 and SBR45 beams under prestressing. The curvatures of the SBR30 and SBR45 beams at the time of bonding the composite strip were $\xi_{SBR30,\mathrm{Prst}} = -0{,}017 m^{-1}$ and, $\xi_{SBR45,\mathrm{Prst}} = -0{,}017 m^{-1}$ respectively.

As shown in Fig. 7 and Fig. 8, after bonding the carbon fiber composite strip, the beam was unloaded, and the calculated model of the normal cross-section was modified to account for the addition of the carbon strip. During the first 2–3 stages of unloading, typical changes for timber are observed, indicating wood relaxation. At subsequent unloading stages, the curvature stabilizes and reaches the predicted level.

As a result of the bonded carbon fiber composite strip added to the bottom (tensile) zone, a residual deflection remains after unloading, at which the external force equals zero. The residual curvature in the SBR30 (Prst) and SBR45 (Prst) beams is

$\xi_{SBR30,0} = -0{,}0022 m^{-1}$ and,

$\xi_{SBR30,0} = -0{,}0042 m^{-1}$ respectively.

Subsequently, two Ø12 mm A500C steel reinforcement bars were bonded into the grooves of the future compressive zone of the SBR30 (Prst) and SBR45 (Prst) beams.

*Stage of Testing the Prestressed Beam.* After completing all operations for creating the prestress in the solid timber element with combined reinforcement and following the full curing of the adhesive, experimental testing of the prestressed beams SBR30 (Prst) and SBR45 (Prst) was carried out.

The results of the experimental tests were recorded in the test logbook and, after processing, are presented in Fig. 9 for the SBR30 (Prst) beam and Fig. 10 for the SBR45 (Prst) beam.

The prestressed timber beam with combined reinforcement, which was prestressed to a 0.3 load level, failed completely due to fiber rupture in the tensile zone of the timber. The failure of the second beam occurred through timber splitting along the grain. This indicates that the influence of shear stresses in prestressed combined reinforced solid timber beams is extremely significant, and therefore, a methodology for strengthening inclined cross-sections of such elements should be developed in the future.

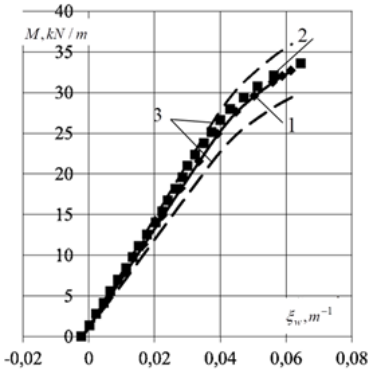


**Fig. 9** Theoretical (1) and experimental (2) curvature values depending on the applied load in the midspan section of the SBR30(Prst) beam with prestressed combined reinforcement, with deviation limits from –10% to +10% (3) of the established theoretical bending moment value
**Рис. 9** Теоретичні (1) та експериментальні значення (2) кривини в залежності від прикладеного навантаження в серед-ньому перерізі балки SBR30(Prst) з попередньо напруженим комбінова-ним армуванням з межами відхилень від -10% до +10% (3) від вста-новленого теоретичного значення згинального моменту

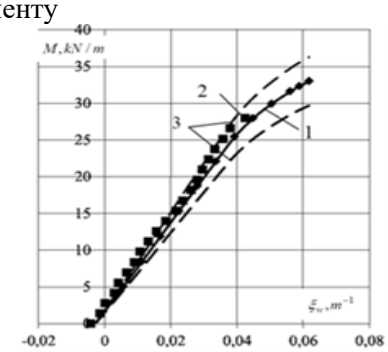


**Fig. 10** Theoretical (1) and experimental (2) curvature values depending on the applied load in the midspan section of the prestressed combined reinforced beam SBR45(Prst) (3 – range of experimental data distribution ±10%)
**Рис. 10** Теоретичні (1) та експериментальні значення (2) кривини в залежності від прикладеного навантаження в середньому перерізі попередньо напруженої комбіновано армованої балки SBR45(Prst) ( 3 – межі розподілу експериментальних значень ±10%)

The deflection–moment growth diagrams for solid timber beams are shown in Fig. 11: unreinforced beams – SB, solid timber beams with passive combined reinforcement – SBR, prestressed combined reinforced solid timber beams – SBR30 (Prst), and prestressed combined reinforced solid timber beams – SBR45 (Prst).

As a result of the study, it was established that the ultimate moment according to the second limit state, which is determined based on the ultimate deflection of the element in the tested solid timber beam, increases with the addition of reinforcement in both the compressive and tensile zones. It was also found that the creation of prestressing in the composite reinforcement of the tensile zone further increases the ultimate moment corresponding to the beam's deflection limits.

An increase in the initial curvature, which arises due to higher levels of prestressing, additionally enhances the ultimate moment according to the second limit state. The effect of increasing prestress is significant; however, it is critical not to exceed the service-level deflections of the unreinforced solid timber flexural element when applying prestress to the Sika CarboDur S-512 carbon strip.

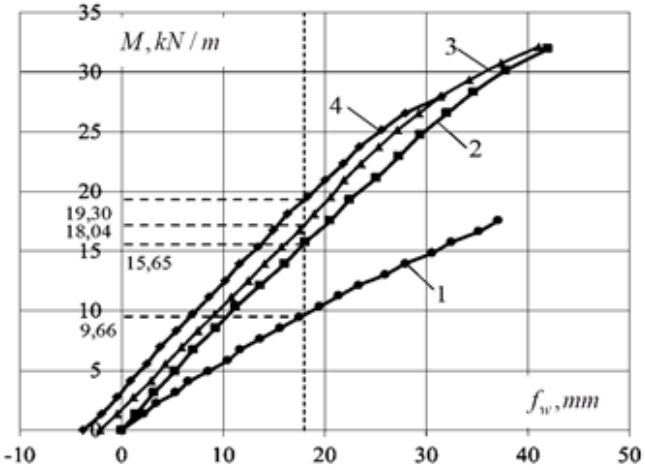


**Fig. 11** Deflection–moment diagrams for solid timber beams with graphical determination of the ultimate deflection for: 1 – SB; 2 – SBR; 3 – SBR30(Prst); 4 – SBR45(Prst)

**Рис. 11** Діаграми прогинів від зростання моментів для балок з цільної деревини з графічним встановленням граничного прогину для: 1 – SB; 2 – SBR; 3 - SBR30(Prst); 4 - SBR45(Prst)

## CONCLUSIONS AND RECOMMENDATIONS

Enhancement of the load-bearing capacity and stiffness of timber beams with combined reinforcement: The introduction of steel and composite reinforcement, as well as the application of prestressing in the composite strip, significantly increases the stiffness and load-bearing capacity of timber beams, reducing deflections and ensuring a more uniform stress distribution across the cross-section.

Effectiveness of prestressing the composite reinforcement: Creating prestress in the Sika CarboDur S-512 carbon fiber strip in the tensile zone provides residual deflection and increases the ultimate moment, allowing improved beam performance under high loads without the need for additional complex devices.

Failure characteristics: Prestressed beams with combined reinforcement exhibit different failure mechanisms: at lower levels of prestress, failure occurs through timber fiber rupture in the tensile zone, while at higher levels, splitting along the grain is observed. This indicates a significant influence of shear stresses and highlights the need for further research to strengthen inclined cross-sections.

Practical application and recommendations: The results of the study can be used for the design of new and the reconstruction of existing timber structures with large spans, as well as for the development of methodologies, regulatory documents, and guidelines regarding the reinforcement and prestressing of timber beams.

## REFERENCES


1. **Hlitin O., Bilyk S., Radetskyi S., Sonko O., Kravchenko O.** (2024). An effective method for strengthening steel beams and purlins using an elastic support in the span. *Building Constructions. Theory and Practice,. (15),174-184.* [in Ukrainian] https://doi.org/10.32347/2522-4182.15.2024.174-184
2. **Rudnieva I. V.** (2021) Technological features of strengthening steel structures by bonding high-strength fiber-reinforced systems during reconstruction. *Building Constructions. Theory and Practice,.( 8), 25-31.* [in Ukrainian] https://doi.org/10.32347/2522-4182.8.2021.32-43
3. **Hetun H., Koliakova V., Bezklyubenko I., Solomin A.** (2023) Structural solutions for blast-resistant buildings with civil protection premises. *Building Constructions. Theory and Practice,. (13), 41-50.* [in Ukrainian] https://doi.org/10.32347/2522-4182.13.2023.41-50
4. **Zhuravskyi O. D., Tymoshchuk V. A.** (2020) Calculation model of flat reinforced concrete slabs strengthened with external prestressed reinforcement. *Building Constructions. Theory and Practice,. (7), 4-11.* [in Ukrainian] https://doi.org/10.32347/2522-4182.1.2017.193-198
5. **Rudnieva I., Priadko M., Priadko H.** (2020) Features and prospects of using FRP composite technologies for strengthening building structures during reconstruction. *Building Constructions. Theory and Practice. (7), 12-22.* [in Ukrainian] https://doi.org/10.32347/2522-4182.7.2020.12-22
6. **Demchyna B. H., Surmai M. I., Kravz A. R., Bliakhar T. I.** (2010) Experience in manufacturing glued-laminated timber beams reinforced with non-metallic reinforcement. *Modern Building Materials, Structures, and Innovative Construction Technologies: Bulletin DonNABA. № 5 (85). T. II. Makiyivka: DonNABA, 193-197.* [in Ukrainian]
7. **Yermolenko D. A., Ishchenko M. S.** (2017) Strength and deformability of glued timber beams reinforced with polymer mesh. *ACADEMIC JOURNAL Series: Industrial Machine Building, Civil Engineering. — Poltava: PNTU. T. 2 (47). S. 140-147.* [in Ukrainian]
8. **Mirski R., Kuli'nski M., Dziurka D., Thomas M., Antonowicz R**. (2012) Strength properties of structural glulam elements from pine (Pinus sylvestris L.) Timber reinforced in the tensile zone with steel and basalt rods. *Materials. Vol. 14(10), Article number 2574.* https://doi.org/10.3390/ma14102574
9. **Borri A., Corradi M., Grazini A.** (2005) A method for flexural reinforcement of old wood beams with CFRP materials *Composites. Vol. 36. Pp. 143–153.* https://doi.org/10.1016/j.compositesb.2004.04.013
10. **Andor, K., Lengyel, A., Polgár, R., Fodor, T., & Karácsonyi, Z.** (2015). Experimental and statistical analysis of spruce timber beams reinforced with CFRP fabric. *Construction and Building Materials, 99, 200–207.* https://doi.org/10.1016/j.conbuildmat.2015.09.026
11. **Corradi M., Osofero A. I., Borri A. (2019)** Repair and reinforcement of historic timber structures with stainless steel — a review *Metals. Vol. 9(1). Article 106.* https://doi.org/10.3390/met9010106
12. **Soriano J., Pellis B. P., Mascia N. T.** (2016) Mechanical performance of glued-laminated timber beams symmetrically reinforced with steel bars. *Composite Structures. Vol. 150.* https://doi.org/10.1016/j.compstruct.2016.05.016
13. **Usman A., Sugiri S.** (2015) Analysis of the Strength of Timber and Glulam Timber Beams with Steel Reinforcement. *Journal of Engineering and Technological Sciences. Vol. 47. Pp. 601-611.* https://doi.org/10.5614/j.eng.technol.sci.2015.47.6.1
14. **De Luca V., Marano C.** (2012) Prestressed glulam timbers reinforced with steel bars. *Construction and Building Materials. Vol. 30. Pp. 206-217.* https://doi.org/10.1016/j.conbuildmat.2011.11.016
15. **Alam P., Ansell M.P., Smedley D.** Mecha-nical repair of timber beams fractured in flexure using bonded-in reinforcements. *Compos B Eng, 2009. Vol. 40 (2). Pp. 95-106.* https://doi.org/10.1016/j.compositesb.2008.11.010
16. **Raftery G.M. , Whelan C.** (2014) Low-grade glued laminated timber beams reinforced using improved arrangements of bonded-in GFRP rods. *Constr Build. Mater. Vol. 52. Pp. 209-220.*

https://doi.org/10.1016/j.conbuildmat.2013.11.044

17. **Gómez E.P., González M.N., Hosokawa K., Cobo A.** (2019) Experimental study of the flexural behavior of timber beams reinforced with different kinds of FRP and metallic fibers. *Compos Struct. (213), 308-316.* https://doi.org/10.1016/j.compstruct.2019.01.099
18. **Wdowiak A., Brol J.** (2019) Effectiveness of reinforcing bent non-uniform pre-stressed glulam beams with basalt fibre reinforced. *Polymers Rods. Materials. (12). Article number 3141.* https://doi.org/10.3390/ma12193141
19. **Kliger R., Haghani R., Brunner M., Harte A. M., Schober K-U.** (2016) Wood-based beams strengthened with FRP laminates: improved performance with pre-stressed systems. *Eur. J. Wood Prod. (74), 319–330.* https://doi.org/10.1007/s00107-015-0970-5
20. **Mykhailovskyi D., Komar M.** (2023) Analysis of studies on the use of composite strips for strengthening timber structures] *Budivelni konstruktsii. Teoriia i praktyka. (10),. 4-10.* [in Ukrainian] https://doi.org/10.32347/2522-4182.10.2022.4-10
21. **Mykhailovskyi D. V., Komar M. A.** (2021) Reinforcement of timber structures with composite materials: current state and prospects *Building Constructions. Theory and Practice (9), 72-80.* [in Ukrainian] https://doi.org/10.32347/2522-4182.9.2021.72-80
22. **DSTU-N B V.2.6-184:2012** "Konstruktsii z tsilnoi i kleienoi derevyny. Nastanova z proektuvannia" [Structures made of solid and glued timber. Design guidelines] [*chynnyi vid 01.04.2013*] *Kyiv, "Ukrarkhbudinform", 2013. 120 s.* [in Ukrainian]
23. **DBN V.2.6-161:2017** "Dereviani konstruktsii. Osnovni polozhennia" [Timber structures. Basic provisions] [*chynnyi vid 01.04.2017*] *Kyiv, "Ukrarkhbudinform", 2017. 111 s.* [in Ukrainian]
24. **DSTU EN 408:2012** "Konstruktsii dereviani. Konstruktsiina derevyna ta kleiena laminovana derevyna. Vyznachennia deiakykh fizychnykh ta mekhanichnykh vlasnostei" (EN 408:2003, IDT) [Timber structures. Structural timber and glued laminated timber. Determination of certain physical and mechanical properties] [*chynnyi vid 04.02.2013*] *Kyiv: Minrehion Ukrainy, 2013. 42 s.* [in Ukrainian]
25. **DSTU EN 408:2007** "Lisomaterialy konstruktsiini. Konstruktsiina ta kleiena sharuvata derevyna. Vyznachennia deiakykh fizychnykh ta mekhanichnykh vlasnostei" [Structural timber. Structural and glued laminated timber. Determination of certain physical and mechanical properties] ] [*chynnyi vid 10.10.2007*] *Kyiv: Derzhspozhystandart Ukrainy, 2012.* [in Ukrainian]

## LITERATURE

1. **Hlitin O., Bilyk S., Radetskyi S., Sonko O., Kravchenko O.** (2024). Efektyvnyi sposib pidsylennia metalevykh balok i prohoniv za dopomohoiu pruzhnoi opory v proloti. *Budivelni konstruktsii. Teoriia i praktyka. (15),174-184.* https://doi.org/10.32347/2522-4182.15.2024.174-184
2. **Rudnieva I. V.** (2021) Tekhnolohichni osoblyvosti pidsylennia metalievykh konstruktsii metodom nakleiuvannia vysokomitsnykh fibroarmovanykh system pry rekonstruktsii *Budivelni konstruktsii. Teoriia i praktyka. ( 8), 25-31.* https://doi.org/10.32347/2522-4182.8.2021.32-43
3. **Hetun H., Koliakova V., Bezklyubenko I., Solomin A.** (2023) Konstruktyvni rishennia vybukhostiikykh budivel z prymishchennaiamy tsyvilnoho zakhystu naselennia *Budivelni konstruktsii. Teoriia i praktyka. (13), 41-50.* https://doi.org/10.32347/2522-4182.13.2023.41-50
4. **Zhuravskyi O. D., Tymoshchuk V. A.** (2020) Rozrakhunkova model ploskikh zalizobetonnykh plyt, pidsilenykh zovnishnoiu napruzhenoiu armaturoiu *Budivelni konstruktsii. Teoriia i praktyka. (7), 4-11.* https://doi.org/10.32347/2522-4182.1.2017.193-198
5. **Rudnieva I., Priadko M., Priadko H.** (2020) Osoblyvosti ta perspektyvy vykorystannia tekhnolohii pidsylennia budivelnykh konstruktsii kompozytsiynymy FRP-materialamy pry rekonstruktsii sporud *Budivelni konstruktsii. Teoriia i praktyka.(7), 12-22.* https://doi.org/10.32347/2522-4182.7.2020.12-22
6. **Demchyna B. H., Surmai M. I., Kravz A. R., Bliakhar T. I.** (2010) Dosvid vyhotovlennia doshatokleienykh balk armovanykh nemetalevoiu armaturoiu. *Suchasni budivelni materialy, konstruktsii ta innovatsiyni tekhnolohii*

*zvedennia budivel i sporud: Visnyk DonNABA. № 5 (85). T. II. Makiyivka: DonNABA. S. 193-197.*

7. **Yermolenko D. A., Ishchenko M. S.** (2017) Mitsnist ta deformatyvnist kleienykh derevianykh balk, armovanykh polimernoiu sitkoiu *ACADEMIC JOURNAL Series: Industrial Machine Building, Civil Engineering. — Poltava: PNTU. T. 2 (47). S. 140-147.* http://orcid.org/0000-0001-6690-238X
8. **Mirski R., Kuli'nski M., Dziurka D., Thomas M., Antonowicz R**. (2012) Strength properties of structural glulam elements from pine (Pinus sylvestris L.) Timber reinforced in the tensile zone with steel and basalt rods. *Materials. Vol. 14(10), Article number 2574.* https://doi.org/10.3390/ma14102574
9. **Borri A., Corradi M., Grazini A.** (2005) A method for flexural reinforcement of old wood beams with CFRP materials *Composites. Vol. 36. Pp. 143–153.* https://doi.org/10.1016/j.compositesb.2004.04.013
10. **Andor, K., Lengyel, A., Polgár, R., Fodor, T., & Karácsonyi, Z.** (2015). Experimental and statistical analysis of spruce timber beams reinforced with CFRP fabric. *Construction and Building Materials, 99, 200–207.* https://doi.org/10.1016/j.conbuildmat.2015.09.026
11. **Corradi M., Osofero A. I., Borri A. (2019)** Repair and reinforcement of historic timber structures with stainless steel — a review *Metals. Vol. 9(1). Article 106.* https://doi.org/10.3390/met9010106
12. **Soriano J., Pellis B. P., Mascia N. T.** (2016) Mechanical performance of glued-laminated timber beams symmetrically reinforced with steel bars. *Composite Structures. Vol. 150.* https://doi.org/10.1016/j.compstruct.2016.05.016
13. **Usman A., Sugiri S.** (2015) Analysis of the Strength of Timber and Glulam Timber Beams with Steel Reinforcement. *Journal of Engineering and Technological Sciences. Vol. 47. Pp. 601-611.* https://doi.org/10.5614/j.eng.technol.sci.2015.47.6.1
14. **De Luca V., Marano C.** (2012) Prestressed glulam timbers reinforced with steel bars. *Construction and Building Materials. Vol. 30. Pp. 206-217.* https://doi.org/10.1016/j.conbuildmat.2011.11.016
15. **Alam P., Ansell M.P., Smedley D.**. Mechanical repair of timber beams fractured in flexure using bonded-in reinforcements. *Compos B Eng, 2009. Vol. 40 (2). Pp. 95-106.* https://doi.org/10.1016/j.compositesb.2008.11.010
16. **Raftery G.M. , Whelan C.** (2014) Low-grade glued laminated timber beams reinforced using improved arrangements of bonded-in GFRP rods. *Constr Build. Mater. Vol. 52. Pp. 209-220.* https://doi.org/10.1016/j.conbuildmat.2013.11.044
17. **Gómez E.P., González M.N., Hosokawa K., Cobo A.** (2019). Experimental study of the flexural behavior of timber beams reinforced with different kinds of FRP and metallic fibers. *Compos Struct.( 213), 308-316.* https://doi.org/10.1016/j.compstruct.2019.01.099
18. **Wdowiak A., Brol J.** (2019) Effectiveness of reinforcing bent non-uniform pre-stressed glulam beams with basalt fibre reinforced. *Polymers Rods. Materials. (12). Article number 3141.* https://doi.org/10.3390/ma12193141
19. **Kliger R., Haghani R., Brunner M., Harte A. M., Schober K-U.** (2016) Wood-based beams strengthened with FRP laminates: improved performance with pre-stressed systems. *Eur. J. Wood Prod. Vol. 74. Pp. 319–330.* https://doi.org/10.1007/s00107-015-0970-5
20. **Mykhailovskyi D., Komar M.** (2022) Analiz doslidzhen zastosuvannia kompozytnykh strichok dlia pidsylennia derevianykh konstruktsii *Budivelni konstruktsii. Teoriia i praktyka. (10),. 4-10.* https://doi.org/10.32347/2522-4182.10.2022.4-10
21. **Mykhailovskyi D. V., Komar M. A.** (2021) Armuvannia konstruktsii z derevyny kompozytnymy materialamy: stan i perspektyvy *Budivelni konstruktsii. Teoriia i praktyka.(9), 72-80.* https://doi.org/10.32347/2522-4182.9.2021.72-80
22. **DSTU-N B V.2.6-184:2012** Konstruktsii z tsilnoi i kleienoi derevyny. Nastanova z proektuvannia [*chynnyi vid 01.04.2013*] *Kyiv, "Ukrarkhbudinform", 2013. 120 s.*
23. **DBN V.2.6-161:2017** Dereviani konstruktsii. Osnovni polozhennia [*chynnyi vid 01.04.2017*] *Kyiv, "Ukrarkhbudinform", 2017. 111 s.*
24. **DSTU EN 408:2012** Konstruktsii dereviani. Konstruktsiina derevyna ta kleiena laminovana derevyna. Vyznachennia deiakykh fizychnykh ta

mekhanichnykh vlasnostei (EN 408:2003, IDT) [*chynnyi vid 04.02.2013*] *Kyiv: Minrehion Ukrainy, 2013. 42 s.*

25. **DSTU EN 408:2007** Lisomaterialy konstruktsiini. Konstruktsiina ta kleiena sharuvata derevyna. Vyznachennia deiakykh fizychnykh ta mekhanichnykh vlasnostei [*chynnyi vid 10.10.2007*] *Kyiv: Derzh-spozhystandart Ukrainy, 2012.*

## ЕКСПЕРИМЕНТАЛЬНІ ДОСЛІДЖЕННЯ ПОПЕРЕДНЬО НАПРУЖЕНИХ ДЕРЕВ'ЯНИХ БАЛОК ІЗ ЦІЛЬНОЇ ДЕРЕВИНИ

*Денис МИХАЙЛОВСЬКИЙ*
*Петро ГОМОН*

**Анотація.** У статті наведено результати комплексних експериментальних і теоретичних досліджень роботи дерев'яних балок із комбінованим армуванням, у яких одночасно використано сталеву та композитну арматуру. Такий підхід дозволяє поєднати високу міцність і жорсткість сталі з малою вагою композитних матеріалів, що забезпечує раціональне використання матеріалів і підвищення ефективності конструкції.

Основна увага приділена розробленню та практичній реалізації методу створення попереднього напруження в композитній стрічковій арматурі, розташованій у розтягнутій зоні балки. Запропонований спосіб є технологічно простим, не потребує використання складного або дорогого спеціалізованого обладнання, може бути реалізований у лабораторних умовах і на підприємствах малої та середньої потужності. Описано послідовність виконання операцій із попереднього натягування композитної арматури, фіксації її в дерев'яній основі та подальшого виготовлення зразків для випробувань.

У роботі детально представлено методику проведення експериментальних досліджень, включно з описом схеми навантаження, типів вимірювального обладнання, способів фіксації переміщень і деформацій. Визначено закономірності деформування та встановлено особливості руйнування попередньо напружених комбіновано армованих дерев'яних балок. Побудовано експериментальні залежності типу «момент–кривина» та «момент–прогин», які дозволяють кількісно оцінити вплив попе-реднього напруження на жорсткість і міцність елементів.

Результати досліджень підтвердили, що введення попереднього напруження в композитній арматурі суттєво підвищує несучу здатність та жорсткість дерев'яних елементів, зменшує прогини та забезпечує більш рівномірний розподіл напружень у перерізі.

Отримані результати мають важливе практичне значення та можуть бути використані при проєктуванні нових і реконструкції існуючих дерев'яних конструкцій, особливо в будівлях і спорудах із великими прольотами, а також при розробленні нових нормативних документів, рекомендацій і методичних матеріалів щодо розрахунку, виготовлення та підсилення дерев'яних конструкцій із комбінованим армуванням.

**Ключові слова:** дерев'яні балки; комбіноване армування; композитна арматура; попереднє напруження.

***Received:*** *November 03, 2025.*

***Accepted:*** *November 30, 2025.*

ISSN 2522-4182

DOI: 10.32347/2522-4182.17.2025.41-54
УДК 624.011

# METHODS OF EXPERIMENTAL RESEARCH OF REINFORCED CONCRETE BEAMS REINFORCED WITH POST-TENSIONED ROPES

*Dmytro SMORKALOV[1] , Volodymyr VYNOKUR[2]*

[1,2] Kyiv National University of Construction and Architecture
31, Povitryanykh Syl Ave., Kyiv, Ukraine, 03037
[1]smorkalov.dv@knuba.edu.ua, https://orcid.org/0000-0001-7890-2686
[2]vynokur_vs@knuba.edu.ua, https://orcid.org/0009-0002-3218-5620

**Abstract**. The article presents a methodology for conducting experimental studies of reinforcing reinforced concrete beams using prestressed reinforcing ropes. The developed methodology is based on the principle of reinforcing elements, which allows increasing their bearing capacity and crack resistance without the need for dismantling or significant intervention in the existing structure.

The main attention is paid to the technical aspects of implementing prestressing ropes, in particular, methods of their fastening, tension parameters, and methods of controlling the stressed state. The work presents the sequence of conducting the experiment, which includes the manufacture of a series of test specimens, their loading schemes, methods of measuring deformations and fixing the development of cracks.

At this stage of the study, the development, manufacture, and installation of a test rig designed to simulate the operation of reinforced reinforced concrete elements under various loading conditions were carried out. The created experimental base provides the possibility of further conducting a series of tests aimed at qualitative and quantitative assessment of the influence of prestressed ropes on the stressed-deformed state of beams and determining the effectiveness of the proposed reinforcement technology. The results obtained in the future will become the basis for the formation of practical recommendations and improvement of calculation methods for reinforced concrete structures.

The main goal of this work is to promote the development and implementation of this technology. The research is aimed at improving the methodology for strengthening reinforced concrete structures and creating scientific prerequisites for updating the regulatory framework, which will ensure effective design, increasing the reliability and durability of construction projects in Ukraine.

**Dmytro SMORKALOV**
Associate Professor of the Department of Reinforced Concrete and Stone Structures, Assoc. Prof., PhD (Tech. Sci.)

**Volodymyr VYNOKUR**
PhD student

**Keywords:** reinforcement; prestressing; post-tension; ropes; methodology.

## INTRODUCTION

In the conditions of modern reconstruction and technical renewal of Ukraine, the problem of restoration and strengthening of existing reinforced concrete structures that have partially or completely lost their operational characteristics is of particular relevance. Many structures erected in the second half of the 20th century today do not meet modern requirements for strength, rigidity and crack resistance.

.

The reasons for this are the natural aging of materials, corrosion of reinforcement, prolonged action of loads, as well as the influence of an aggressive environment. An additional factor that significantly complicated the situation was the destruction and damage of objects as a result of military operations, which creates an urgent need to implement quick and reliable solutions for their restoration and strengthening without complete dismantling.

Traditional strengthening methods, such as increasing the cross-section or installing steel plates, have significant disadvantages: they increase the mass of the element, complicate installation, and often require the cessation of operation of the structure. In this context, a promising direction is the use of prestressed ropes, which allow increasing the bearing capacity and crack resistance of reinforced concrete elements without significant intervention in their design. Such a method allows redistributing internal forces, reducing deformations, limiting the opening of cracks, and ensuring an increase in the service life of elements that have lost part of their bearing capacity.

At the same time, in Ukraine, relatively few studies have been carried out in the field of strengthening reinforced concrete structures using prestressing [1…13]. However, this technology is quite widespread in foreign practice [14…21]. Some works are devoted to general issues of prestressing in new construction or analysis of the operation of elements with composite reinforcement, but experimental studies of reinforcement with cables remain limited. The lack of systematized methods and scientifically based recommendations in this area necessitates the creation of our own experimental base and adaptation of world experience to Ukrainian conditions.

Thus, this work is aimed not only at improving modern design solutions, but also at scientifically substantiating and developing a methodology for experimental research of the processes of strengthening reinforced concrete elements using prestressed cables. The proposed methodology is universal and can be used both in the design of new structures and during the reconstruction or restoration of buildings with reduced load-bearing capacity or in a state of emergency.

An important direction of development of strengthening technologies in Ukraine is the systematic updating and harmonization of national regulatory documents [21…24] with modern European standards [25]. Such consistency of the regulatory framework will not only ensure compliance with international requirements, but also create the prerequisites for more effective implementation of innovative methods of strengthening existing structures, in particular with the use of pre-stressed ropes. Thanks to this, it will be possible to implement advanced technologies for restoration and reconstruction of building elements in accordance with modern safety and reliability standards.

## MAIN IDEA

The main concept of the study involves combining traditional internal reinforcement with external post-tensioning of cables, which allows to significantly increase the bearing capacity of reinforced concrete beams, reduce deflections and limit the development of cracks without significant intervention in the structural system. This approach ensures the compatible operation of materials in tension and compression zones and contributes to a more uniform redistribution of bending moments in the middle of the spans. The main scientific and practical idea is to assess the effectiveness of reinforcement for both simple single-span beams and more complex double-span structures, where the interaction of spans and the redistribution of internal forces play a significant role.

The experimental program involves testing two series of beams, each of which includes both control specimens without reinforcement and specimens with prestressed cables. Series I consists of single-span beams, which allows us to study the behavior of the elements under pure bending conditions. Series II includes double-span beams, which allows us to evaluate the effectiveness of reinforcement under conditions of redistribution of bending moments between

spans and more complex interaction of materials.

The beams are made of concrete of class C20/25, which is traditionally used in the performance of works on strengthening and repairing existing structures, and are reinforced with Ø10 A500C to ensure the compatibility of materials in the tension and compression zones. External prestressed cables Ø15.7 mm were fixed in anchor devices and tensioned to the design force determined on the basis of analytical calculations and in accordance with international design practice.

The reinforcement schemes of the beams of the first and second series are shown in Fig. 3–6. In the event of changes in loading conditions, deviations in the strength of materials, or the need to increase the accuracy of the comparative analysis of structures, the reinforcement scheme of the beams in the second series can be modified to ensure the reliability and representativeness of the experimental results.

The test scheme for single-span and double-span beams is shown in Fig. 1 and 2. The beams will be loaded using a hydraulic jack connected to a single working circuit with an oil station.

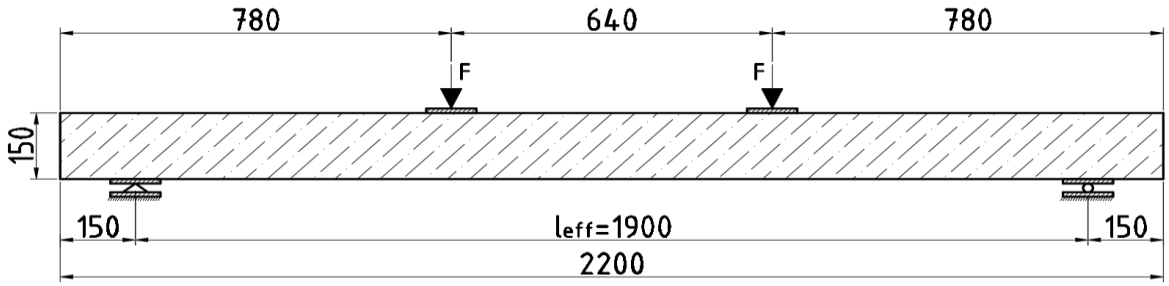


**Fig. 1** Schematic diagram of the pure bending test of single-span beams of series 1
**Рис. 1** Принципова схема випробування однопролітних балок серії 1 на чистий згин

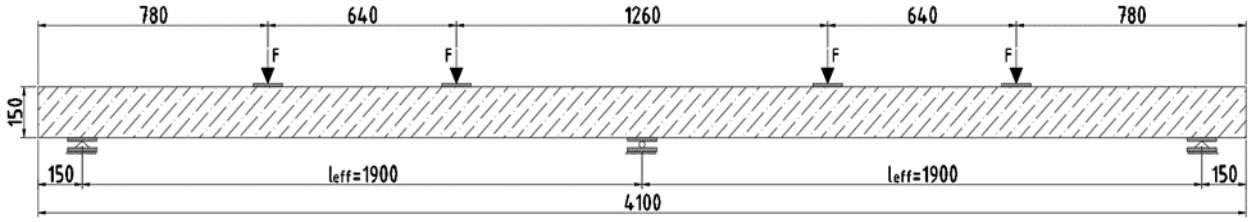


**Fig. 2** Schematic diagram of the pure bending test of two-span beams of series 2
**Рис. 2** Принципова схема випробування двоопролітних балок серії 2 на чистий згин

The loading process will be carried out in stages with a uniform increase in the load, while the indicators of all measuring devices will be constantly recorded for further analysis. This approach ensures accurate recording of the moments of formation of the first cracks, their propagation and interaction with the internal reinforcement, and also makes it possible to assess the influence of external reinforcement on the change in the stress-strain state. Additionally, the experimental scheme involves measuring deflections at key points of the span, controlling the width and development of cracks, as well as recording stresses in the ropes and internal reinforcement using sensors, which ensures high accuracy and representativeness of the obtained data.

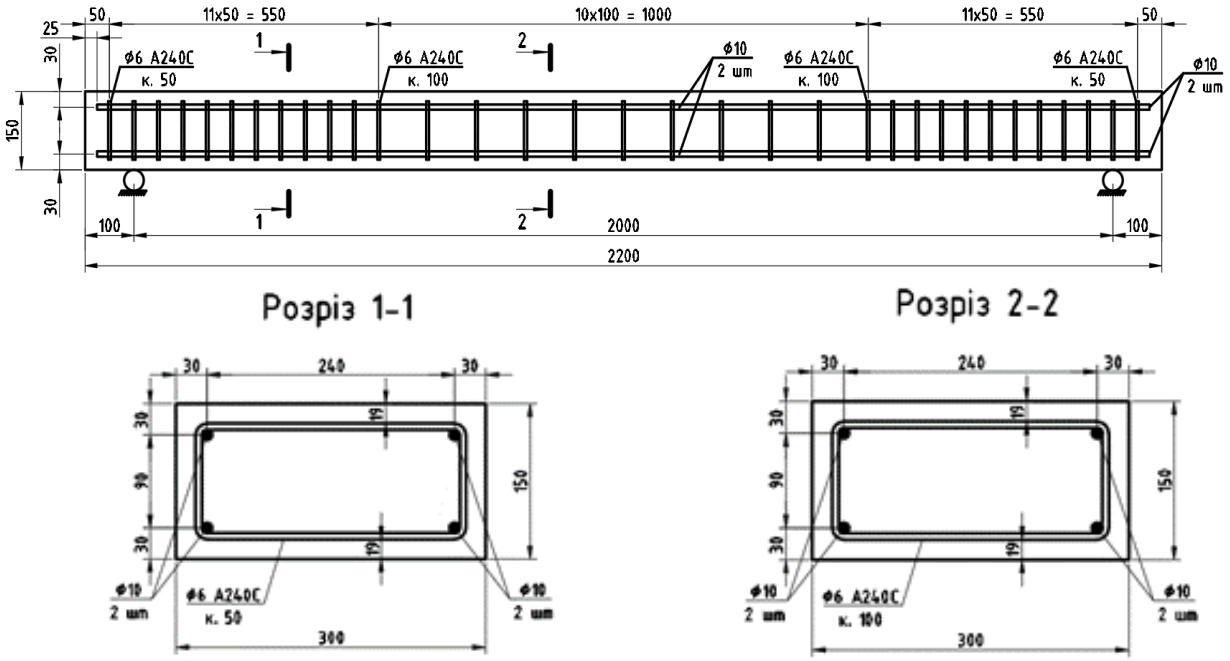


**Fig. 3** Schematic diagram of reinforcement of single-span beams B-1.1 series 1
**Рис. 3** Принципова схема армування однопролітних балок Б-1.1 серії 1

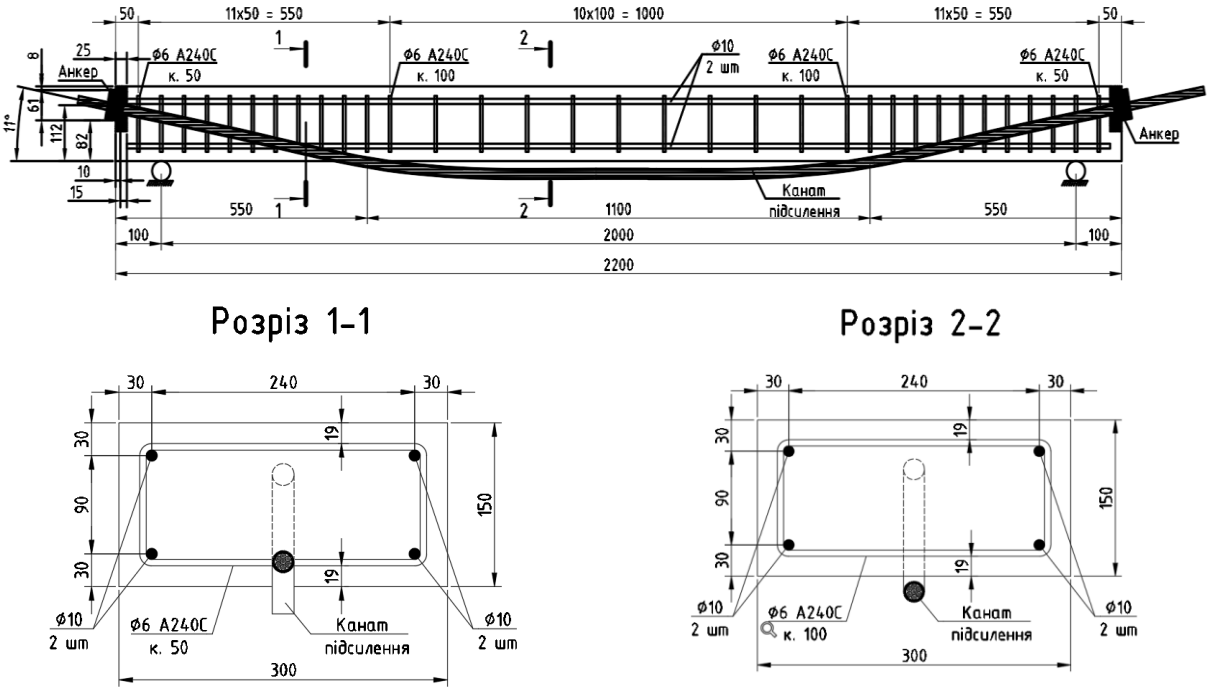


**Fig. 4** Schematic diagram of reinforcement of reinforced single-span beams B-1.2 series 1
**Рис. 4** Принципова схема армування підсилених однопролітних балок Б-1.2 серії 1

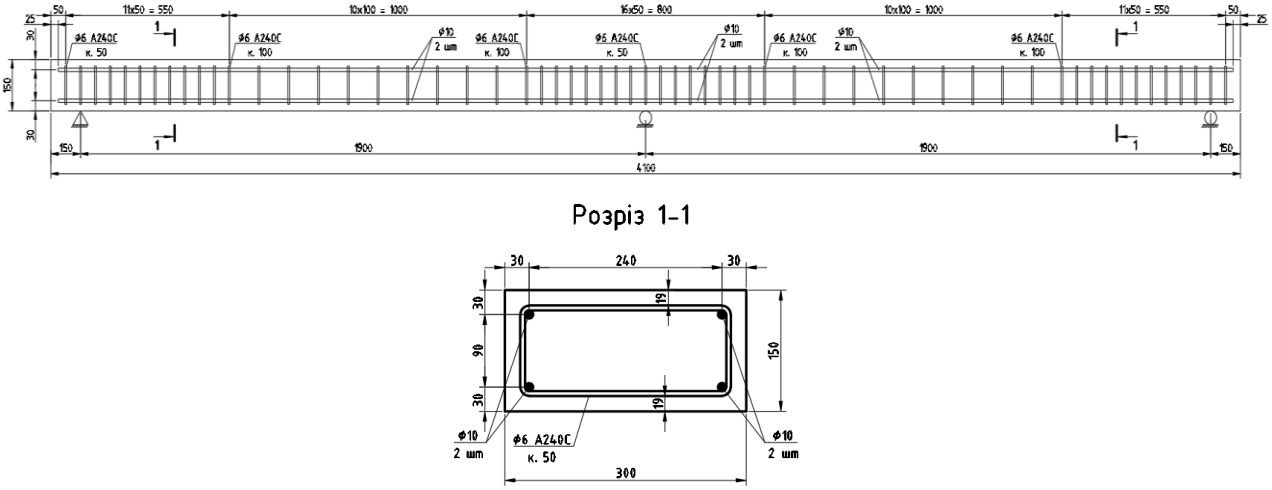


**Fig. 5** Schematic diagram of reinforcement of double-span beams B-2.1 series 2
**Рис. 5** Принципова схема армування двопролітних балок Б-2.1 серії 2

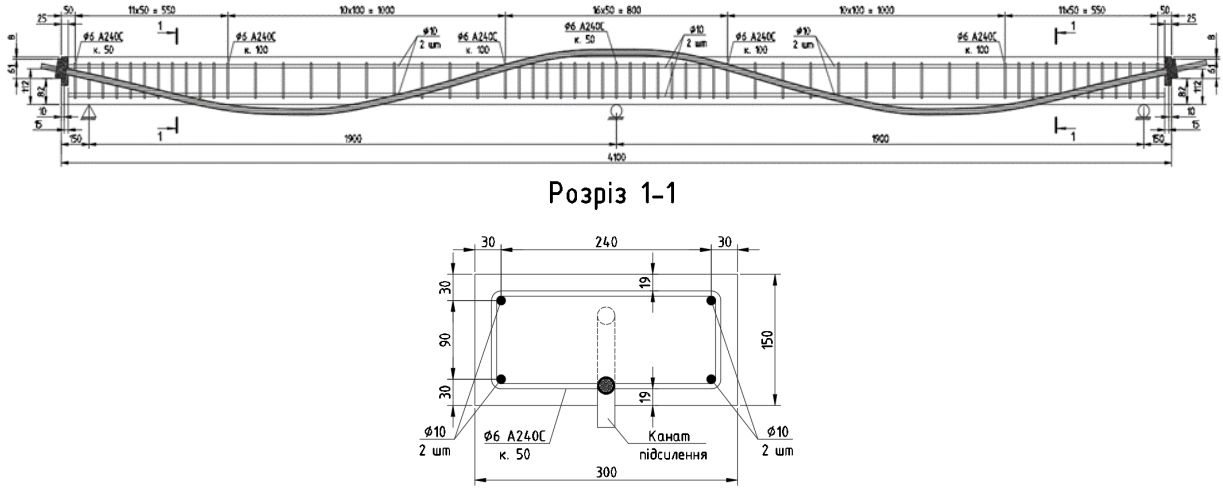


**Fig. 6** Schematic diagram of reinforcement of reinforced double-span beams B-2.2 series 2
**Рис. 6** Принципова схема армування підсилених двопролітних балок Б-2.2 серії 2

**Table 1.** Volumes and characteristics of the samples studied
**Табл. 1.** Обсяги та характеристика дослідних зразків

| Series | Marking beams | Amount | Test scheme | Notes |
|---|---|---|---|---|
| 1 | B-1.1 | 2 | 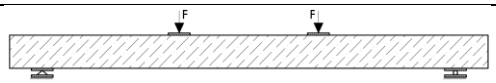 | Single-span beams without reinforcement see Fig. 7 |
| | B-1.2 | 2 | 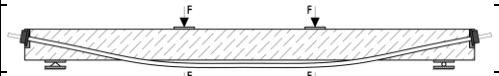 | Single-span beams with rope reinforcement see Fig. 8 |
| | B-1.3 | 2 |  | Reinforced single-span beams B-1.1 with ropes after testing |
| 2 | B-2.1 | 2 |  | Double-span beams without reinforcement see Fig. 9 |
| | B-2.2 | 2 |  | Double-span beams with rope reinforcement see Fig. 10 |
| | B-2.3 | 2 | 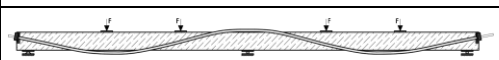 | Reinforced double-span beams B-2.1 with ropes after testing |

**Series I – single-span beams without reinforcement and with reinforcement**

Series I includes single-span beams, which are made in two versions: control specimens without reinforcement (see Fig. 7) and specimens with prestressed cables (see Fig. 8). This structure of the series allows to evaluate the effectiveness of reinforcement under simple conditions of pure bending and to form a basis for comparison with more complex structures.

Beam dimensions: 300x150(h)x2200 mm

Tasks of Series I:

- To record the relationship between the applied load, deflections and crack development.
- To determine the moment of formation of the first cracks and to trace the patterns of their propagation under the action of the load.
- To assess the stiffness and bearing capacity of beams without reinforcement and with reinforcement, which makes it possible to compare the effectiveness of the applied technology.
- To conduct a detailed analysis of the stress-strain state and the interaction of internal reinforcement and external ropes in reinforced samples.

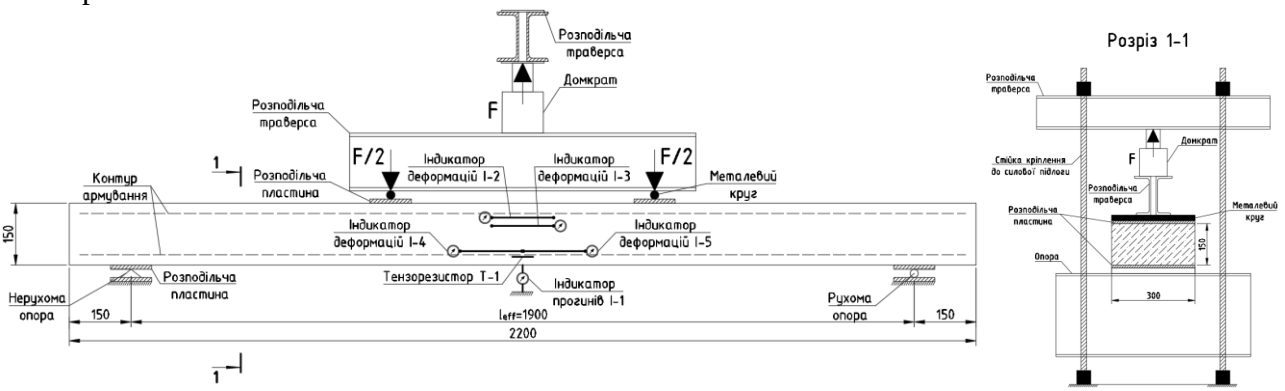


**Fig. 7** Test scheme for single-span beam B-1.1 series 1
**Рис. 7** Схема випробування однопролітної балки Б-1.1 серії 1

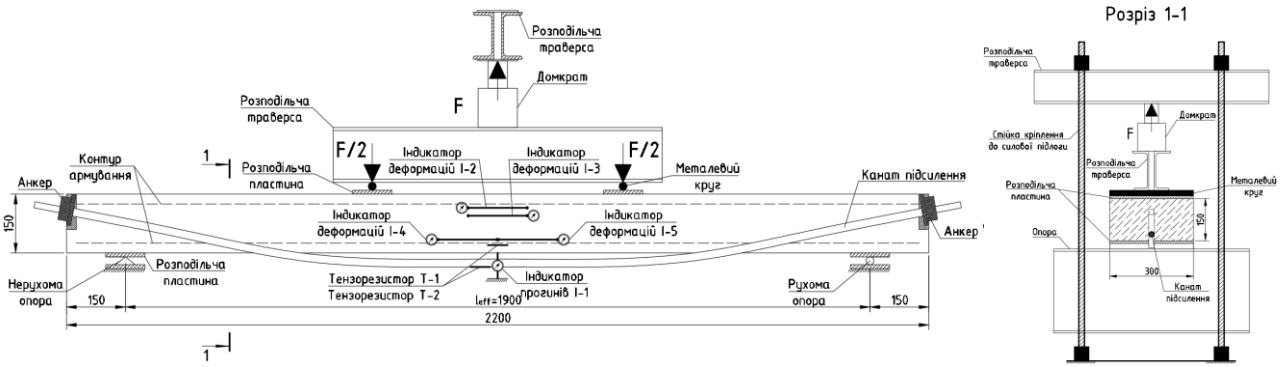


**Fig. 8** Test scheme for reinforced single-span beam B-1.2 series 1
**Рис. 8** Схема випробування підсиленої однопролітної балки Б-1.2 серії 1

**Series II – double-span beams without reinforcement and with reinforcement**

Series II involves testing two-span beams, which are also made in two versions: control specimens (see Fig. 9) and specimens with prestressed cables (see Fig. 10). The study of

two-span beams allows us to study the redistribution of bending moments between the spans and the interaction of materials in more complex structures, close to real operating conditions.

Beam dimensions: 300x150(h)x4100 mm (two spans of 1900 mm)

Tasks of Series II:

- To investigate the effect of external reinforcement on the development of cracks, deflections and redistribution of bending moments between spans.
- To determine changes in the stress-strain state and load-bearing capacity of double-span beams compared to control samples.
- To obtain data for comparing the effectiveness of reinforcement of single-span and double-span beams, which is important for the development of methodological recommendations for the reconstruction of existing buildings.

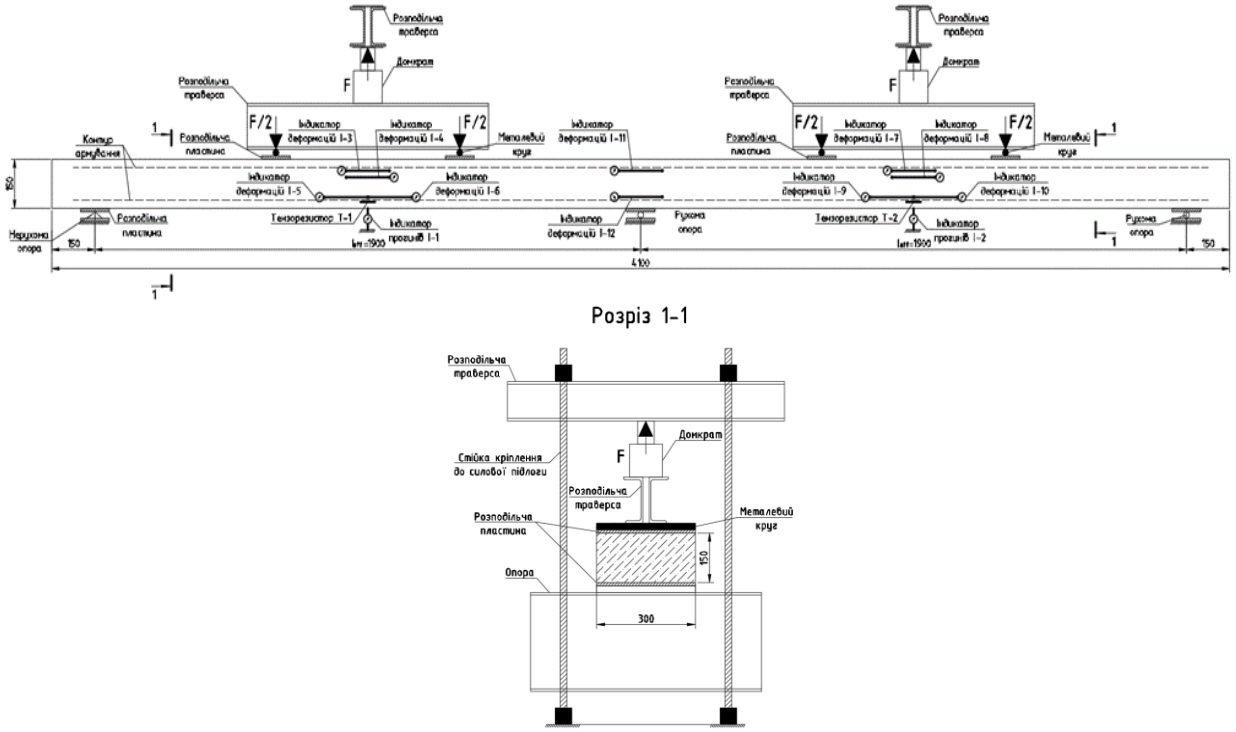


**Fig. 9** Test scheme for a double-span beam B-2.1 series 2
**Рис. 9** Схема випробування двопролітної балки Б-2.1 серії 2

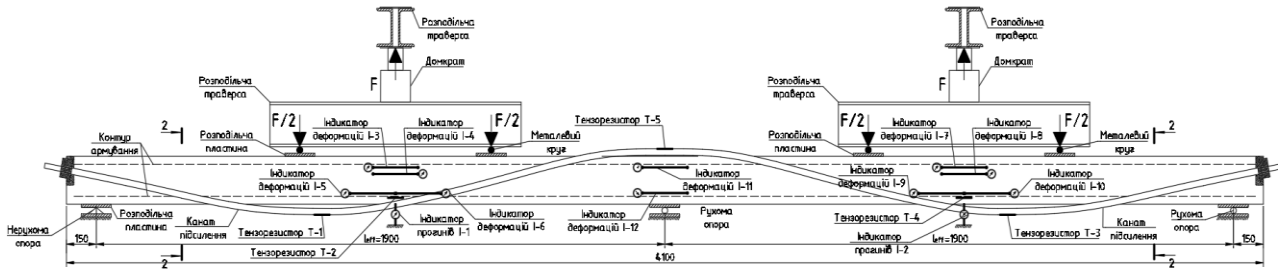


**Fig. 10.** Test scheme for reinforced double-span beam B-2.2 series 2
**Рис. 10.** Схема випробування підсиленої двопролітної балки Б-2.2 серії 2

## PREPARATORY STAGE

The preparatory stage of the experimental study involves a complex of works on the manufacture of samples, installation of the reinforcement system and arrangement of the test rig. At this stage, the pouring of reinforced concrete beams, installation of anchor devices, fastening of pre-stressed ropes and preparation of control and measuring equipment for recording deflections, cracks and stresses in materials were carried out.

For series I and series II, the beams were made of concrete of class C20/25 with internal reinforcement Ø10 A500C. During the pouring process, special attention was paid to controlling the geometric dimensions, verticality of the reinforcing frame and uniformity of concrete compaction, which ensured the accuracy of the formation of structures and minimization of internal defects. The manufacturing process Fig. 11-12.

**Fig. 11** Formwork and reinforcement arrangement before pouring experimental beams. Photo by: V.Vynokur

**Рис. 11** Влаштування опалубки та армування перед заливкою експериментаних балок. Автор фото: В. Винокур

**Fig. 12** Single-span experimental beams. Photo by: V.Vynokur

**Рис. 12** Однопролітні експериментальні балки Автор фото: В.Винокур

For the reinforced specimens, external prestressed cables Ø15.7 mm were used, fixed in anchor devices (see Fig. 13) with collets (see Fig. 14), which ensure reliable force transmission to the beam.

**Fig. 13** Rope anchor. Photo by: V.Vynokur

**Рис. 13** Анкер кріплення канату. Автор фото: В.Винокур

**Fig. 14** Collet. Photo by: V.Vynokur

**Рис. 14** Цанга. Автор фото: В.Винокур

Also at this stage, a test rig was assembled (see Fig. 15), which includes mechanisms for applying concentrated forces at points of maximum bending moment and a system for measuring deflections and cracks. The rig allows for precise loading and control over the

experimental parameters, which is critically important for the representativeness of the results.

In addition, a specialized station was used to tension the ropes, ensuring accurate application and control of the calculated prestressing force. The configuration and main components of this station are shown in Fig. 16.

**Fig. 15** Series 1 test rig. Photo by: V. Vynokur
**Рис. 15** Випробувальна установка 1 серії. Автор фото: В.Винокур

**Fig. 16** Rope tensioning station. Photo by: V.Vynokur
**Рис. 16** Станція для натягу канатів. Автор фото: В. Винокур

The main measuring devices during the experiment are clock-type deflection indicators (see Fig. 17), which ensure accurate fixation of vertical displacements of beams at key points of the span.

In addition, to determine local stresses and deformations of the material in the zone of possible crack formation, clock-type strain indicators were used (see Fig. 18), which allow monitoring changes in the stress-strain state of reinforced concrete in real time. This makes it possible to more accurately assess the behavior of the material in critical zones and establish the stages of crack development.

**Fig. 17** Deflection indicator. Photo by: V Vynokur.
**Рис. 17** Індикатор прогинів. Автор фото: В. Винокур

**Fig. 18**. Strain indicator. Photo by: V.Vynokur
**Рис. 18**. Індикатор деформацій. Автор фото: В.Винокур

Also used were strain measurement indicators of the type of extensometers (see Fig. 19), which provide high accuracy in determining the elongations or contractions of test specimens during loading. Extensometers allow direct recording of the change in the length of elements in the zone of greatest stresses, which allows for a detailed analysis of the distribution of deformations and an assessment of the effectiveness of structural reinforcement. The use of such devices is an important component of experimental studies, since they ensure the reliability of the data obtained on the stress-strain state of reinforced concrete elements.

To accurately determine the deformations in the internal reinforcement of reinforced concrete beams, the AID-4 device was used in the experiment (see Fig. 20). AID-4 is an automatic electronic strain gauge that operates on the basis of the strain gauge method, registering changes in the electrical resistance of strain gauges glued directly to the reinforcing bars.

**Fig. 19** Extensometer. Photo by: V.Vynokur
**Рис. 19** Екстензометр.
Автор фото: В. Винокур

**Fig. 19** AID-4 device (Automatic electronic strain gauge). Photo by: V.Vynokur
**Рис. 19** Прилад АИД-4 (Автоматичний електронний вимірювач деформацій).
Автор фото: В. Винокур

The AID-4 device was installed on the reinforcing bars in key areas of the span where maximum tensile deformations are expected.

## CONCLUSIONS

The article presents a methodology for experimental research into the reinforcement of reinforced concrete beams using prestressed cables. The main objective of the research is to study the effectiveness of reinforcement, which allows to increase the bearing capacity, limit the development of cracks and reduce the deflections of such structures.

At the first stage of the research, beams of the first series will be tested. This series serves as a basis for the formation of initial experimental data and verification of the reliability of the adopted methodology. The results of the first series of tests will make it possible to specify the load parameters, measurement schemes and methods of fixing deformations, which will become the basis for improving the program of further experiments.

The second series, which involves testing double-span beams, can be specified or modified based on the results of the 1st series of tests. Such a phased approach ensures scientific consistency of the research, increases the accuracy of experimental observations and allows optimizing the parameters of future tests.

The preparatory work and the created experimental setup provide accurate control of

loads and reliable fixation of the research results. The developed methodology forms a scientific basis for further testing, creating the prerequisites for developing practical recommendations for strengthening existing building structures.

Thus, the study contributes to the development of technologies for the restoration and reconstruction of reinforced concrete elements that have lost part of their load-bearing capacity, and is of great importance for increasing the reliability and safety of building infrastructure in the conditions of modern reconstruction.

## REFERENCES


1. **Smorkalov D.V.** (2022)**.** Monolithic reinforced concrete structures with prestressed cables *Building Constructions. Theory and Practice, (10), 136–142.* [in Ukrainian]. https://doi.org/10.32347/2522-4182.10.2022.136-142
2. **Smorkalov, D., & Vinokur, V.** (2024). Methods for calculating the reinforcement of reinforced concrete structures using prestressed cables using Software complexes. *Building Constructions. Theory and Practice, (15), 41–53.* [in Ukrainian]. https://doi.org/10.32347/2522-4182.15.2024.41-53
3. **Smorkalov D.V. Vinokur V.S.** (2023). Methods of calculation of monolithic reinforced concrete structures with prestressing of reinforcing ropes. *Building Constructions. Theory and Practice, (12), 73–83.* [in Ukrainian]. https://doi.org/10.32347/2522-4182.12.2023.73-83
4. **Smorkalov D.V., Zatylyuk G.A., Vinokur V.S.** (2024). Reinforcement of monolithic reinforced concrete structures using prestressed reinforcing ropes. *Modern Technologies and Methods of Calculations in Construction, (21), 224-234.* [in Ukrainian]. https://doi.org/10.36910/6775-2410-6208-2024-11(21)-24
5. **Zhuravskyi O.D., Tymoshchuk V.A.** (2017). Calculation of flat reinforced concrete slabs reinforced with external tension-ing reinforcement. *Building Constructions. Theory and Practice, (1), 193–198.* [in Ukrainian]. https://doi.org/10.32347/2522-4182.1.2017.193-198
6. **Zhuravskyi O. D., Melnyk I. V.** (2013). Work of monolithic reinforced concrete slabs with post-tensioned reinforcement. *Visnyk Natsionalnoho universytetu "Lvivska politekhnika". Teoriia i praktyka budivnytstva. (755), 135-138.* [in Ukrainian].
7. **Zhuravskyi O.D., Tymoshchuk V.A.** (2020). Research of a flat reinforced concrete slab reinforced with external tensioning reinforcement. *Building Constructions. Theory and Practice, (7), 4–11.* [in Ukrainian]. https://doi.org/10.32347/2522-4182.7.2020.4-11
8. **Yesipenko A.D., Mykhaylets O.S.** (2008). Concrete prestressing systems using wire reinforcement. *Budivelne virobnictvo. (49), 102*. [in Ukrainian].
9. **Chyrva V., Chyrva T., Panchenko O., Savchenko A., Romanenko K.** (2020). Numerical modeling of the destruction process of reinforced concrete beams of monolithic fencing and its reinforcement with carbon materials. *Building Constructions. Theory and Practice, (6), 34–41.* [in Ukrainian]. https://doi.org/10.32347/2522-4182.6.2020.34-41
10. **Petryk Yu. M.** (2017). Assessment of the state of use of monolithic reinforced concrete floors with tension of cable reinforcement on concrete (post-tensioning) in modern construction in Ukraine. *Naukovo-tekhnichnyi, vyrobnychyi ta informatsiino-analitychnyi (5), 64-67* [in Ukrainian].
11. **Petrik Yu.M.** (2016). Introduction in Ukraine of monolithic reinforced concrete structures with tension of cable reinforcement on concrete (post-tensioning) and their natural tests. *Urban Planning and Territorial Development (61), 335-342* [in Ukrainian].
12. **Petrik Yu.M., Bambura A.M.** etc.(2017). Field tests of an innovative solution for prefabricated monolithic floors with hollow prestressed slabs and hidden crossbars. *Science and Construction №2 (12), 19-25* [in Ukrainian].
13. **Murashko L.A., Kolyakova V.M., Smorkalov D.V.** (2011). Calculation of the strength of normal and inclined to the longitudinal axis sections of bending elements according to DBN V.2.6-98:2009. *Textbook, p.96.* [in Ukrainian].
14. **Zhang K., Sun Q.** Strengthening of a reinforced concrete bridge with prestressed steel wire ropes. *Civil Engineering Journal. (26), 267–285.* [in English]. https://doi.org/10.14311/cej.2017.03.0023

15. **Al-Mahmoud F., Castel A., Minh TQ., François R.** (2015). Reinforced Concrete Beams Strengthened with NSM CFRP Rods in Shear. *Adv Struct Eng (18), 74.* [in English]. https://doi.org/doi:10.1260/1369-4332.18.10.1563
16. **Elrayah Khalafala E., A Talaat I.** (2021). Strengthening of Burri box Girder Bridge by using External post Tensioning Technology (Sudan). *FES Journal of Engineering Sciences. ( 9), 49–56.* [in English]. https://doi.org/10.52981/fjes.v9i1.658
17. **Hashim H. A., Al-Zuhairi A. H.** (2021). Effect of External Post-Tensioning Strengthening Technique on Flexural Capacity of Simple Supported Composite Castellated Beam. *E3S web conferences. (318), 03006.* [in English]. https://doi.org/10.1051/e3sconf/202131803006
18. **L. Klusáček et al.** (2021). Transverse prestressing and reinforced concrete as the key to restoration of masonry arch bridges. *Engineering Structures. (245), 112898.* [in English]. https://doi.org/10.1016/j.engstruct.2021.112898
19. **Klusáček L., Svoboda A.** (2017). Strengthening of bridges by post-tensioning using monostrands in substituted cable ducts. *IOP Conference Series: Materials Science and Engineering. (236), 012057.* [in English]. https://doi.org/10.1088/1757-899x/236/1/012057
20. **Said A. I., Al-Ahmed A. H. A., Al-Fendawy D. M.** (2015). Strengthening of Reinforced Concrete T- Section Beams Using External Post-Tensioning Technique. *Journal of Engineering. (21), 139–154.* [in English]. https://doi.org/10.31026/j.eng.2015.12.09
21. **Haber Z. B., Graybeal B. A.** (2024). Strengthening of Steel Through-Girder Bridges Using UHPC and Post-Tensioning. *Journal of Bridge Engineering. (29), 62-72* [in English]. https://doi.org/10.1061/jbenf2.beeng-6272
22. **DBN V.2.6-98:2009.** Konstruktsii budynkiv i sporud. Betonni ta zalizobetonni konstruktsii. Osnovni polozhennia. [Constructions of buildings and structures. Concrete and reinforced concrete structures. Basic provisions.] *Minrehion Ukrainy. Kyiv, 2011. 71s.* [in Ukrainian].
23. **DSTU-B.V.2.6-156:2010.** Betonni ta zalizobetonni konstruktsii z vazkogo betonu. Pravyla proektuvannya. [Concrete and reinforced concrete structures made of heavy concrete. Design rules]. *Minrehion Ukrainy. Kyiv, 2011. 166s.* [in Ukrainian].
24. **DSTU-N B EN 1992-1-1:2010.** Evrokod 2 Proektuvannya zalizobetonnih konstrukcij Chastina 1-1. Zagalni pravila i pravila dlya sporud. [Eurocode 2 Design of reinforced concrete structures Part 1-1. General rules and rules for structures.]. *Minrehion Ukrainy. Kyiv, 2013. 200s.* [in Ukrainian].
25. **EN 1992-1-1:2004.** Eurocode 2: Design of concrete structures Part 1-1: General rules and rules for building. *European Committee for Standardization. Brussels, 2004. 230 s.* [in English].

## LITERATURE

1. **Smorkalov D.V.** (2022). Monolitni zalizobetonni konstruktsii z poperedno napruzhenymy kanatamy. *Budivelni konstruktsii. Teoriia i praktyka, (10), 136–142.* https://doi.org/10.32347/2522-4182.10.2022.136-142
2. **Smorkalov, D., & Vinokur, V.** (2024). Metody rozrakhunku pidsylennia zalizobetonnykh konstruktsii iz zastosuvanniam poperedno napruzhenykh kanativ z vykorystanniam prohramnykh kompleksiv. *Budivelni konstruktsii. Teoriia i praktyka, (15), 41–53.* https://doi.org/10.32347/2522-4182.15.2024.41-53
3. **Smorkalov D.V. Vinokur V.S.** (2023). Metodyky rozrakhunku monolitnykh zalizobetonnykh konstruktsii z poperednim napruzhenniam armaturnykh kanativ. *Budivelni konstruktsii. Teoriia i praktyka, (12), 73–83.* https://doi.org/10.32347/2522-4182.12.2023.73-83
4. **Smorkalov D.V., Zatylyuk G.A., Vinokur V.S.** (2024). Pidsylennia monolitnykh zalizobetonnykh konstruktsii z vykorystanniam poperedno napruzhenykh armaturnykh kanativ. *Suchasni tekhnolohii ta metody rozrakhunkiv u budivnytstvi. (21), 224-234.* https://doi.org/10.36910/6775-2410-6208-2024-11(21)-24
5. **Zhuravskyi O.D., Tymoshchuk V.A.** (2017). Rozrakhunok ploskykh zalizobetonnykh plyt, pidsylenykh zovnishnoiu napruzhenoiu armaturoiu. *Budivelni konstruktsii. Teoriia i praktyka, (1), 193–198.* https://doi.org/10.32347/2522-4182.1.2017.193-198
6. **Zhuravskyi O. D., Melnyk I. V.** (2013). Robota monolitnykh zalizobetonnykh plyt z postnapruzhenoiu armaturoiu. *Visnyk Natsionalnoho universytetu "Lvivska*

*politekhnika". Teoriia i praktyka budivnytstva. (755), 135-138.*

7. **Zhuravskyi O.D., Tymoshchuk V.A.** (2020). Doslidzhennya ploskoyi zalizobetonnoyi pliti pidsilenoyi zovnishnoyu napruzhenoyu armaturoyu. *Budivelni konstruktsii. Teoriia i praktyka, (7), 4–11.* https://doi.org/10.32347/2522-4182.7.2020.4-11
8. **Yesipenko A.D., Mykhaylets O.S.** (2008). Sistemi poperednogo napruzhennya na beton za dopomogoyu kanatnoyi armaturi. *Budivelne virobnictvo. (49), 102.*
9. **Chyrva V., Chyrva T., Panchenko O., Savchenko A., Romanenko K.** (2020). Chyselne modeliuvannia protsesu ruinuvannia zalizobetonnykh balok monolitnoho ohorodzhennia ta yoho posylennia vuhletsevymy materialamy. *Budivelni konstruktsii. Teoriia i praktyka, (6), 34–41.* https://doi.org/10.32347/2522-4182.6.2020.34-41
10. **Petryk Yu. M.** (2017). Otsinka stanu vykorystannia monolitnykh zalizobetonnykh perekryttiv z napruzhenniam kanatnoi armatury na beton (post napruzhennia) u suchasnomu budivnytstvi Ukrainy. *Naukovo-tekhnichnyi, vyrobnychyi ta informatsiino-analitychnyi (5), 64-67.*
11. **Petrik Yu.M.** (2016). Vprovadzhennya v Ukrayini monolitnih zalizobetonnih konstrukcij z napruzhennyam kanatnoyi armaturi na beton (postnapruzhennya) ta yih naturalni viprobuvannya. *Mistobuduvannya ta teritorialne planuvannya. (61), 335-342.*
12. **Petrik Yu.M., Bambura A.M.** etc. (2017). Naturni viprobuvannya innovacijnogo rishennya zbirno-monolitnogo perekrittya z pustotnimi poperedno napruzhennimi plitami ta prihovanimi rigelyami. *Nauka ta budivnictvo №2 (12), 19-25.*
13. **Murashko L.A., Kolyakova V.M., Smorkalov D.V.** (2011). Rozrahunok za micnistyu normalnih ta pohilih do pozdovzhnoyi osi pereriziv zginalnih elementiv za DBN V.2.6-98:2009. *Navchalnij posibnik, Kyiv, 96s.*
14. **Zhang K., Sun Q.** Strengthening of a reinforced concrete bridge with prestressed steel wire ropes. *Civil Engineering Journal. (26), 267–285.* https://doi.org/10.14311/cej.2017.03.0023
15. **Al-Mahmoud F., Castel A., Minh TQ., François R.** (2015). Reinforced Concrete Beams Strengthened with NSM CFRP Rods in Shear. *Adv Struct Eng (18), 74.* https://doi.org/doi:10.1260/1369-4332.18.10.1563
16. **Elrayah Khalafala E., A Talaat I.** (2021). Strengthening of Burri box Girder Bridge by using External post Tensioning Technology (Sudan). *FES Journal of Engineering Sciences. ( 9), 49–56.* https://doi.org/10.52981/fjes.v9i1.658
17. **Hashim H. A., Al-Zuhairi A. H.** (2021). Effect of External Post-Tensioning Strengthening Technique on Flexural Capacity of Simple Supported Composite Castellated Beam. *E3S web conferences. (318), 03006.* https://doi.org/10.1051/e3sconf/202131803006
18. **Klusáček L. et al.** (2021). Transverse prestressing and reinforced concrete as the key to restoration of masonry arch bridges. *Engineering Structures. (245), 112898.* https://doi.org/10.1016/j.engstruct.2021.112898
19. **Klusáček L., Svoboda A.** (2017). Strengthening of bridges by post-tensioning using monostrands in substituted cable ducts. *IOP Conference Series: Materials Science and Engineering. (236), 012057.* https://doi.org/10.1088/1757-899x/236/1/012057
20. **Said A. I., Al-Ahmed A. H. A., Al-Fendawy D. M.** (2015). Strengthening of Reinforced Concrete T- Section Beams Using External Post-Tensioning Technique. *Journal of Engineering. (21), 139–154.* https://doi.org/10.31026/j.eng.2015.12.09
21. **Haber Z. B., Graybeal B. A.** (2024). Strengthening of Steel Through-Girder Bridges Using UHPC and Post-Tensioning. *Journal of Bridge Engineering. (29), 62-72.* https://doi.org/10.1061/jbenf2.beeng-6272
22. **DBN V.2.6-98:2009.** Konstruktsii budynkiv i sporud. Betonni ta zalizobetonni konstruktsii. Osnovni polozhennia. *Minrehion Ukrainy. Kyiv, 2011. 71s.*
23. **DSTU-B.V.2.6-156:2010.** Betonni ta zalizobetonni konstruktsii z vazkogo betonu. Pravyla proektuvannya. *Minrehion Ukrainy. Kyiv, 2011. 166s.*
24. **DSTU-N B EN 1992-1-1:2010.** Evrokod 2 Proektuvannya zalizobetonnih konstrukcij Chastina 1-1. Zagalni pravila i pravila dlya sporud. *Minrehion Ukrainy. Kyiv, 2013. 200s.*
25. **EN 1992-1-1:2004.** Eurocode 2: Design of concrete structures Part 1-1: General rules and rules for building. *European Committee for Standardization. Brussels, 2004. 230 s.*

ISSN 2522-4182

# МЕТОДИКА ЕКСПЕРИМЕНТАЛЬНОГО ДОСЛІДЖЕННЯ ЗАЛІЗОБЕТОННИХ БАЛОК ПІДСИЛЕНИХ ЗА ДОПОМОГОЮ ПОСТНАПРУЖЕНИХ КАНАТІВ

*Дмитро СМОРКАЛОВ*
*Володимир ВИНОКУР*

**Анотація.** У статті представлено методику проведення експериментальних досліджень підсилення залізобетонних балок із застосуванням попередньо напружених арматурних канатів. Розроблена методика базується на принципі підсилення елементів, що дозволяє підвищити їхню несучу здатність та тріщиностійкість без необхідності демонтажу або значного втручання в існуючу конструкцію.

Основна увага приділена технічним аспектам реалізації попереднього напруження канатів, зокрема способам їх закріплення, параметрам натягу, методам контролю напруженого стану. У роботі наведено послідовність проведення експерименту, що включає виготовлення серій дослідних зразків, схеми їх навантаження, методи вимірювання деформацій і фіксації розвитку тріщин.

На даному етапі дослідження виконано розроблення, виготовлення та монтаж випробувальної установки, призначеної для моделювання роботи підсилених залізобетонних елементів у різних режимах навантаження. Створена експериментальна база забезпечує можливість подальшого проведення серії випробувань, спрямованих на якісну та кількісну оцінку впливу попередньо напружених канатів на напружено-деформований стан балок та визначення ефективності запропонованої технології підсилення. Отримані у майбутньому результати стануть основою для формування практичних рекомендацій і вдосконалення методів розрахунку підсилених залізобетонних конструкцій.

Основною метою даної роботи є сприяння розвитку та впровадженню даної технології. Дослідження спрямоване на вдосконалення методики підсилення залізобетонних конструкцій і створення наукових переду-мов для оновлення нормативної бази, що забезпечить ефективне проєктування, підвищення надійності та довговічності будівельних об’єктів в Україні.

**Ключові слова:** підсилення; попереднє напруження; постнапруження; канати; методика

***Received:*** *October 31, 2025.*
***Accepted:*** *November 30, 2025.*

ISSN 2522-4182

DOI: 10.32347/2522-4182.17.2025.55-64
UDC 624.042.8: 624.074.7: 69.059.25

# ADAPTATION OF SEISMIC RESISTANCE PRINCIPLES FOR ENSURING BLAST RESISTANCE OF HIGH-RISE BUILDINGS

*Galyna GETUN[1], Iryna BEZKLUBENKO[2]*

[1,2] Kyiv National University of Construction and Architecture
31, Povitryanykh Syl Ave., Kyiv, Ukraine, 03037
[1]galinagetun@ukr.net, http://orcid.org/0000-0002-3317-3456
[2]i.bezklubenko@gmail.com, http://orcid.org/0000-0002-9149-4178

**Abstract**. The strategic necessity and engineering mechanisms for adapting the principles of seismic-resistant design to ensure the blast resistance of multi-storey buildings in the context of the war in Ukraine are analyzed. The key goal is to prevent Progressive Collapse (PC) of structures caused by localized impulsive loads, which differ radically from cyclic seismic effects but, like them, necessitate the engagement of the plastic (post-limit) behavior of materials in building structures.

In the context of the ongoing military conflict in Ukraine, the design of high-rise buildings requires a radical restructuring, shifting the focus from traditional gravity and seismic loads (DBN V.1.1-12:2014, DBN V.2.2-41-2019) to extreme impulsive loads from explosions. The main threat is Progressive Collapse (PC), which arises after the localized failure of a key element. According to European standards (Eurocode EN 1991-1-7), the engineering objective changes: it is not to prevent damage, but to prevent its disproportionate propagation.

The introduction of the new DBN V.2.2-5:2023, which radically increased the design blast pressure to 100 kPa for protective structures, implicitly forces engineers to use Non-Linear Dynamic Analysis (NDA) methods. The article substantiates that the principles of seismic-resistant design – ductility and redundancy – are a critical basis for enhancing blast resistance, despite the differences in the frequency characteristics of the loads.

A key solution is the hybridization of national requirements with international methodologies for counteracting PC, specifically the Alternate Path (AP) method and the implementation of Tie Forces (TF), which ensure structural integrity after the removal of a vertical support by realizing the catenary action of the slabs. This requires adapting ASCE 41 acceptance criteria and utilizing innovative materials, such as Ultra-High Performance Fibre-Reinforced Concrete (UHPFRC), for effective structural strengthening. The study concludes the necessity of hybridizing Ukrainian requirements for local protective structures with international methodologies for general structural robustness to ensure comprehensive and high-level safety for high-rise buildings.

**Galyna GETUN**
Professor Department of Architectural Structures, Prof., PhD (Tech. Sci.)

**Iryna BEZKLUBENKO**
Associate Professor Department of Information Technologies and Applied Mathematics, Assoc. Prof., PhD (Tech. Sci.)

**Keywords:** high-rise buildings; blast re-sistance; progressive collapse (PC); tie force; ductili-ty.

## PROBLEM STATEMENT

The ongoing military conflict in Ukraine has radically altered the engineering require ments for high-rise building design.

While traditional design of high-rise structures historically focused on gravity, wind, and, in relevant regions, seismic loads (in accordance with DBN V.1.1-12:2014 [9, 10, 19]) and high-rise building requirements (DBN V.2.2-41-2019 [1, 13]), the focus has now shifted to extreme localized loads caused by explosions and missile strikes. These loads are impulsive in nature and fundamentally differ from inertial seismic effects.

The primary structural threat resulting from localized impulsive loading is Progressive Collapse (PC), where the localized failure of a key load-bearing element (e.g., a column or wall) due to an explosion, fire [8], or impact propagates throughout the entire building, leading to its total collapse. Thus, the engineering strategy must be changed from preventing damage to preventing the spread of damage.

The concept of structural robustness is central to the design of high-rise buildings under military threats. A building's robustness is defined as the ability of its structure to prevent the disproportionate propagation of localized failure. European standards, particularly Eurocode EN 1991-1-7 (Actions on structures: General actions) [24], clearly articulate this key principle: localized damage caused by an accidental action is acceptable, provided that it does not threaten the overall load-bearing capacity of the structure and that this capacity is maintained for a sufficient time to implement necessary emergency measures.

To achieve the required robustness (especially for buildings classified under consequence classes CC3 and CC4, which have medium and major failure consequences) [11], Eurocode recommends strategies that encompass both physical protection and structural redundancy and ductility. This requires a departure from deterministic design and a shift toward the concepts that form the basis of seismic engineering.

## ANALYSIS OF PREVIOUS RESEARCH

Seismic-resistant design possesses a number of fundamental principles that can be adapted to enhance the blast resistance of buildings. A common feature is that both types of loads are dynamic and require the structure to utilize its post-yield behavior to dissipate a significant amount of energy, in accordance with the principles of reinforced concrete design [14, 15]. However, there are significant differences. Seismic actions are cyclic and low-frequency, often causing resonance, whereas blast loading is typically impulsive—extremely fast and short-duration. A detailed comparison of these load types is provided in Table 1. In seismic events, engineers permit controlled element damage for energy dissipation; in explosions, due to their unpredictability and high intensity, the allowable damage level is often more restricted. Despite these differences, ductility and redundancy, which are core elements of seismic resistance, remain critically important for preventing blast-induced Progressive Collapse (PC).

Ukraine has taken a significant step towards enhancing civil protection by adopting the new DBN V.2.2-5:2023 "Civil Protection Protective Structures" [12], which aligns with the conclusions of previous research [3, 5, 17]. These standards substantially strengthened the requirements for mechanical strength, blast, and fire resistance, replacing the outdated 1997 norms. A key factor influencing the design methodology is the sharp increase in the design load for the load-bearing structures of protective facilities (safety capsules, bomb shelters, civil defense structures), which must withstand the external pressure of the blast wave. Previous standards (DBN V.2.2-5-97) stipulated a design peak overpressure of about 20 kPa, while the new DBN V.2.2-5:2023 [12] raised this requirement to 100 kPa. Such a radical increase in design parameters requires engineers to abandon classic simplified static calculation methods. To accurately assess structural behavior under such extreme impulsive loads and to validate an acceptable deformation level, the application of Non-Linear Dynamic Analysis

**Table 1**. Comparison of Key Characteristics of Seismic and Blast Loads
**Табл. 1** Порівняння основних характеристик сейсмічних і вибухових навантажень

| Parameter | Seismic Load | Blast Load (External/Contact) | Impact on Design |
|---|---|---|---|
| Duration | Seconds to minutes (Cyclic) | Milliseconds (Impulsive) | Requirement to consider strain rate effects Requirement for isolation systems (for seismic) or local strengthening (for blast) |
| Frequency | Low (Close to natural frequencies) | Extremely high (Shock wave) | |
| Key Stability Mechanism | Controlled energy dissipation through plastic hinges | Maintenance of structural integrity after localized failure (tie forces) | |
| Primary Risk for Multi-Storey Buildings | Large inter-storey drift | Local punching and Progressive Collapse (PC) | |

(NDA) becomes essential. These methodologies were previously the prerogative of highly seismic design or military facilities.

Thus, the requirements of the new DBN [12] implicitly compel the Ukrainian engineering community to adopt advanced analytical and structural approaches developed for seismically active areas and special facilities, as well as to integrate international methodologies for preventing Progressive Collapse (PC), such as the Alternate Path (AP) method and the Tie Force (TF) method, specified in standards like UFC 4-023-03 [26] and Eurocode EN 1991-1-7 [24].

## MAIN RESEARCH

Seismic loads are generated by inertial forces, which are a function of the building's mass and ground acceleration. They are characterized by a relatively low frequency, which often coincides with the natural frequencies of the high-rise building. This coincidence can induce resonance, leading to significant inter-storey drifts and cyclic loading of elements. The primary failure mechanism in seismic design for high-rise buildings aims at the controlled formation of plastic hinges in the beams (the "strong column – weak beam" principle), allowing the structure to dissipate energy throughout the prolonged cyclic loading [4, 16]. A detailed comparison of the key characteristics of seismic and blast loads and their impact on multi-storey building design is presented in Table 1.

In contrast to seismic activity, blast loading is impulsive. It creates a shock wave characterized by an extremely high rise time (within milliseconds), peak overpressure, and impulse. Depending on the location of the charge, distinctions are made between external blast (air shock wave) and internal blast (confinement).

The failure mechanisms under blast are localized and intense:

- *Localized impact and breach*: An explosion near an external load-bearing wall or a key column can cause instantaneous local failure.
- *Strain rate effects*: Due to the high speed of impulse application, materials (especially concrete and steel) exhibit an increase in strength, which must be accounted for in modeling.
- *Dynamic punching*: This is a critical mechanism that directly leads to Progressive Collapse (PC).

The problems arising from impulsive loading reveal a structural vulnerability often ignored in seismic design. This is particularly evident in monolithic reinforced concrete flat slabs. Studies, notably [5, 27], have shown that impulsive loading can lead to dynamic punching failure at the slab-column connection. In this scenario, failure is concentrated in a narrow zone around the column, while the rest of the slab remains practically undamaged. The critical point is that integrity rebars, traditionally used to prevent gravitational collapse, prove ineffective under impulsive loading. These reinforcement bars often fail

near the column boundary and cannot perform their function of keeping the slab from falling. This necessitates abandoning traditional node detailing methods and adopting concepts developed to counteract PC.

Despite differences in frequency characteristics, the high ductility of reinforced concrete structures (the capacity for plastic deformation without rupture) remains a key factor in the stability of framed reinforced concrete high-rise buildings [1, 14, 15].

The design of high-rise framed reinforced concrete structures must ensure a transition to plastic regime (flexure) before brittle failure (shear, block-shear). This means that connection details designed for energy dissipation under seismic cyclic loading can also work effectively under a single blast impulse, providing significant rotational capacity. However, for blast resistance, these connections must be designed to withstand significant axial tension which arises when elements transition into catenary action after support loss.

The summary in Table 1 on loads and response demonstrates why a unified approach to structural integrity must be applied to high-rise buildings subjected to dynamic loads.

Designing against Progressive Collapse is the most direct and effective adaptation of seismic principles for ensuring the blast resistance of high-rise buildings. The goal is to ensure the building's ability to remain stable despite localized failure.

The primary methodology is the Alternate Path (AP) method, detailed in international standards such as UFC 4-023-03 [26] and Eurocode EN 1991-1-7 [24]. It requires the structure to be capable of redistributing the load after the removal of a key vertical element (column or wall) without initiating global collapse. Eurocode EN 1991-1-7 [24] proposes a quantitative criterion: the damage caused by local failure should not exceed 15% of the floor area on two adjacent storeys. Ensuring this redundancy and reserve strength directly stems from seismic design principles, which demand multi-level protection systems for building structures.

For reinforced concrete structures, the key strategy for preventing PC is the implementation of an integrated system of ties (reinforcement) – the Tie Force (TF) method. This reinforcement ensures the structural integrity after the primary load-bearing elements have failed.

According to UFC 4-023-03 [26], a typical solution for reinforced concrete frames involves adding a system of ties (reinforcement) along the perimeter of the structure and across the entire area of the floor slabs. It is required that the tie forces (TF) be carried specifically in the floor slabs or roof and not concentrated in beams, girders, or perimeter bands. This allows the realization of catenary action. After the removal of a column, the slab, which previously carried the load primarily in flexure, begins to sag and act as a cable net, where the internal ties (reinforcement) work in pure axial tension, which requires a special approach to the detailing of reinforced concrete frames [16, 17]. Since standard integrity reinforcement does not withstand impulsive loading, the application of calculated TF provides the necessary robustness against dynamic punching and prevents slab failure.

Innovative materials offer significant advantages in providing dual resistance to seismic and blast loads. Ultra-High Performance Fibre-Reinforced Concrete (UHPFRC) is a cementitious composite reinforced with steel fibres that exhibits exceptional mechanical strength, ductility, low permeability, and high resistance to abrasion and fire [20]. Research has confirmed that UHPFRC and Reactive Powder Concrete (RPC) have significantly better blast resistance compared to ordinary concrete [28]. These improved characteristics are achieved through reduced free water content, the use of high-strength steel fibres, fine aggregate, and active pozzolanic materials.

UHPFRC is an especially effective material for the strengthening of existing reinforced concrete building structures. UHPFRC jacketing of columns significantly enhances their shear and axial capacity, as well as their ductility. Compared to traditional concrete jacketing, which requires a thickness of 70–100

mm, UHPFRC allows for the use of a much smaller thickness, reducing the overall mass and architectural intervention while maintaining excellent bond with the existing concrete [20].

**Table 2**. Matrix of Design Principle Transfer (from Seismic Resistance to Blast Resistance)
**Табл. 2** Матриця передачі принципів проєктування (від сейсмостійкості до вибухостійкості)

| Seismic Design Principle | Blast Resistance / PC Adaptation | Technical Rationale |
|---|---|---|
| Ductility-Based Design | Maximizing the Rotational Capacity of Connections (≈ 0.20 rad) | Ensuring plastic energy dissipation and avoiding brittle failure |
| Redundancy and Integrated Systems | Alternate Path (AP) Method and 3D Tying | Maintaining the overall load-bearing capacity after localized failure of a key element |
| Provision of Transverse Reinforcement | Implementation of Tie Forces (TF) in Slabs | Supporting the Catenary Action of slabs, preventing dynamic punching failure at slab-column nodes |
| Use of Dampers (FVD) | Hybrid Isolation and Damping Systems | Reducing drift and absorbing the high-energy impulse |
| Use of High-Strength Concrete | Application of UHPFRC for Element Strengthening | Increasing resistance to impact, improving shear strength and ductility in retrofitting |

Since designing for both seismic and blast resistance requires utilizing the post-limit (plastic) behavior of materials, linear static analysis is insufficient. For buildings classified as high-consequence category objects or those designed to withstand significant accidental loads (such as explosions), international standards require the use of either Non-Linear Dynamic Analysis (NDA) or, at minimum, Non-Linear Static Analysis (Pushover). In the context of Ukrainian design, the implementation of NDA becomes mandatory for the structures of protective facilities integrated into multi-storey buildings [12].

For realistic modeling of blast effects, Nonlinear Finite Element Method (Nonlinear FEM) must be applied, often integrated with hydrocodes (software for modeling shock wave propagation and its interaction with the structure). Hydrocodes are used to model the propagation of the blast wave and its interaction with the structure. Key aspects of advanced modeling include:

- *Constitutive Models*: The use of history- and strain-rate-dependent constitutive models for concrete and steel, considering their behavior under tension and compression, as well as the influence of the strain rate.
- *Reinforcement Modeling*: Steel reinforcement is modeled using truss or membrane elements embedded in concrete elements, assuming perfect bond.
- *Validation*: The effectiveness of such numerical simulations, which reproduce the entire process from detonation to complete failure, has been confirmed by comparison with photographs of real damage caused by terrorist attacks.

Acceptance Criteria in NDA, which were initially developed for seismic assessment (e.g., ASCE 41 [29]), are being adapted for blast resistance. They are based on strain limit states, not strength. It must be considered that the models and acceptance criteria in ASCE 41 are based on cyclic loading (for seismic), whereas blast requires modification to account for non-cyclic impulsive loading and the interaction of flexure and axial tension that occurs during PC.

## CONCLUSIONS AND PROSPECTS FOR FURTHER RESEARCH

The new Ukrainian standards, DBN B.2.2-5:2023 [12], have created a tangible opportunity to enhance the robustness of buildings, yet they necessitate a significant restructuring of design practices. The key requirement to increase the design impulsive pressure to 100 kPa directly pertains to protective structures (shelters, capsules, civil defense structures) that must now be integrated into high-rise buildings. Since this leads to the need for a substantial increase in reinforcement and displacements, static design becomes inadequate [6, 7].

DBN B.2.2-5:2023 [11] establishes stringent requirements for local protective structures, but it does not contain detailed methodologies for preventing Progressive Collapse (PC) for the entire high-rise building after an impact on an unprotected area. Given this, designers must hybridize Ukrainian requirements for local protection with international principles of structural robustness, which are the foundation of seismic design but adapted to counteract PC (AP/TF methods) (Table 2) [24, 26, 29].

Further research directions include the creation of detailed national guidelines and manuals on the application of Non-Linear Dynamic Analysis (NDA) to assess the blast resistance of high-rise buildings. These guidelines should be adapted to the specific utilization of building structures and engineering software, and must incorporate the experience gained from military actions in Ukraine [23].

## REFERENCE


1. **Getun, G. V., Kulikov, P. M., Ploskyi, V. O., et al.** (2023). Structures of Buildings and Facilities: Textbook: In 2 Books. Book 2. Non-Residential Buildings. *Kamianets-Podilskyi: Ruta Printing House.* 900. [in Ukrainian] ISBN 978-617-8221-06-5.
2. **Getun, G. V., Koliakova, V. M., Solomin, A. V., & Bezklubenko, I. S.** (2022). Features of the design of steel earthquake-resistant structures of high-rise buildings. *Building Constructions. Theory and Practice,* (11), 18-31. [in Ukrainian] https://doi.org/10.32347/2522-4182.11.2022.18-31
3. **Getun, G. V., Koliakova, V. M., Solomin, A. V., & Bezklubenko, I. S.** (2023). Structural Solutions for Blast-Resistant Buildings with Civil Protection Premises. *Building Constructions. Theory and Practice,* (13), 41-50. [in Ukrainian] https://doi.org/10.32347/2522-4182.13.2023.41-50
4. **Getun, G., Butsenko, Y., Balina, O., Bezklubenko, I., & Solomin, A.** (2019). Diffusion processes with accumulative characteristics during building exploitation. *Strength of materials and theory of structures,* (102), 243-251. [in Ukrainian] https://doi.org/10.32347/2410-2547.2019.102.243-251
5. **Getun, G., Butsenko, Y., Labzhinsky, V., Balina, O., Bezklubenko, I., & Solomin, A.** (2020). Situations forecasting and decision-making optimization based on markovs finite chains in areas with industrial pollutios. *Strength of materials and theory of structures*, (104), 164-174. [in English] https://doi.org/10.32347/2410-2547.2020.104.164-174
6. **DBN V.1.1-7-2016.** (2017). Tekhnichni normy, pravyla i standarty. Pozhezha bezpeka obiektiv budivnytstva. Zahalni vymohy [Technical Norms, Rules and Standards... Fire Safety of Construction Objects. General Requirements]. *Kyiv: Minbud Ukrainy.* [in Ukrainian]
7. **DBN V.1.1-12:2014.** (2014). Tekhnichni normy, pravyla i standarty... Budivnytstvo u seimichnykh raionakh Ukrainy [Technical Norms, Rules and Standards... Construction in Seismic Regions of Ukraine]. *Kyiv: Minrehionbud Ukrainy.* [in Ukrainian]
8. **DBN V.1.2-2:2006.** (2007). Tekhnichni normy, pravyla i standarty... Navantazhennia i vplyvy. Normy proektuvannia [Technical Norms, Rules and Standards... Loads and Impacts. Design Norms]. *Kyiv: Minbud Ukrainy.* [in Ukrainian]
9. **DBN V.1.2-14:2018.** (2018). Tekhnichni normy, pravyla i standarty. Zahalni pryntsypy zabezpechennia nadiinosti ta konstruktyvnoi bezpeky budivel... [Technical Norms, Rules and Standards... General Principles for Ensuring

Reliability and Structural Safety of Buildings]. *Kyiv: Minbud Ukrainy.* [in Ukrainian]

10. **DBN V.2.2.5:2023.** (1923). Tekhnichni normy, pravyla i standarty... Zakhysni sporudy tsyvilnoho zakhystu [Technical Norms, Rules and Standards... Civil Protection Protective Structures*]. Kyiv: Ministry for Communities, Territories and Infrastructure Development of Ukraine.* [in Ukrainian]
11. **DBN V.2.2-41-2019.** (2019). Tekhnichni normy, pravyla i standarty... Vysotni budivli. Osnovni polozhennia [Technical Norms, Rules and Standards... High-Rise Buildings. Basic Provisions]. *Kyiv: Minrehionbud Ukrainy.* [in Ukrainian]
12. **DBN V.2.6-98:2009.** (2011). Tekhnichni normy, pravyla i standarty... Betonni ta zalizobetonni konstruktsii. Osnovni polozhennia [Technical Norms, Rules and Standards... Concrete and Reinforced Concrete Structures. Basic Provisions]. *Kyiv: Minrehionbud Ukrainy.* [in Ukrainian]
13. **DSTU B V.2.6-156:2010.** (2011). Tekhnichni normy, pravyla i standarty... Betonni ta zalizobetonni konstruktsii z vazhkoho betonu. Pravyla proektuvannia [Technical Norms, Rules and Standards... Concrete and Reinforced Concrete Structures from Heavy Concrete. Design Rules]. *Kyiv: Minrehionbud Ukrainy.* [in Ukrainian]
14. **Ivanchenko, H. M., Getun, G. V., Bezklubenko, I. S., & Solomin, A. V.** (2023). Features of Designing and Calculating Complex Reinforced Concrete Frames of Buildings. *Strength of materials and theory of structures*, (110), 108-117. [in Ukrainian] https://doi.org/10.32347/2410-2547.2023.110.108-117
15. **Ivanchenko, H. M., Getun, G. V., Bezklubenko, I. S., & Solomin, A. V.** (2023). Impact of Blast Loads on Buildings and Structures for Civil Protection. *Strength of materials and theory of structures*, (111), 39-48. [in Ukrainian] https://doi.org/10.32347/2410-2547.2023.111.39-48
16. **Kulikov, P. M., Ploskyi, V. O., & Getun, G. V.** (2020). Architecture of Buildings and Facilities: Textbook: In 5 Books. Book 5: Industrial Buildings. *Kamianets-Podilskyi: Lira-K, Ruta Printing House.* 820 p. [in Ukrainian] ISBN 978-966-2771-82-4.
17. **Kulikov, P. M., Ploskyi, V. O., & Getun, G. V.** (2021). Structures of Buildings and Facilities: Textbook: In 2 Books. Book 1. *Kamianets-Podilskyi: Lira-K, Ruta Printing House.* 880 p. [in Ukrainian] ISBN 978-617-520-089-6.
18. **Lysenko, Ye. F., & Getun, G. V.** (1989). Design of Steel Fibre Reinforced Concrete Structures: Study Guide. *Kyiv, UMK VO*. 184 [in Russian].
19. **Ploskyi, V. O., & Getun, G. V.** (2017). Architecture of Buildings and Facilities: Textbook: In 5 Books. Book 2. Residential Buildings. *(3rd ed., revised and augmented)*. *Kamianets-Podilskyi: Ruta.* 736 [in Ukrainian] ISBN 978-966-2771-82-4.
20. **Ploskyi, V. O., Getun, G. V., Martynov, V. L., et al.** (2018). Architecture of Buildings and Facilities: Textbook: In 5 Books. Book 4. Technical Operation and Reconstruction of Buildings. *Kamianets-Podilskyi: Ruta Printing House*. 750 [in Ukrainian] ISBN 978-966-2771-82-4.
21. **Report** on damages to infrastructure from the destruction caused by Russia's military aggression against Ukraine as of Janua**ry 2024.** *Kyiv School of Economics (KSE).* https://kse.ua/wp-content/uploads/2024/05/Eng_01.01.24_Damages_Report.pdf.
22. **EN 1991-1-7 Eurocode 1** Accidental Actions. European Commission. Joint Research Centre. https://eurocodes.jrc.ec.europa.eu/sites/default/files/2022-06/EN1991_7_Vrouwenvelder.pdf.
23. **Shyiko, O., Kropyvnytska, T., Volianiuk, A., & Romaniuk, A.** (2024). Resistance of Structural Elements of Civil Protection Buildings and Structures to the Impact of an Explosion. *Journal of Theoretical and Applied Physics*, *6*(1), 92–99. https://doi.org/10.23939/jtbp2024.01.092 *URL:* https://science.lpnu.ua/jtbp/all-volumes-and-issues/612024/resistance-structural-elements-civil-protection-buildings-and
24. U.S. Army Corps of Engineers, Naval Facilities Engineering Command, Air Force Civil Engineer Support Agency. (2024). Unified Facilities Criteria (UFC) Design of buildings to resist progressive collapse. UFC 4-023-03 (Change 4, 10 June 2024). Retrieved from https://www.wbdg.org/FFC/DOD/UFC/ufc_4_023_03_2009_c4.pdf.
25. **Yankelevsky, D. Z., Karinski, Y. S., & Feldgun, V. R.** (2023). Damage and Failure of

a Column-Supported RC Flat Slab Subjected to Impulsive Loading. *Applied Sciences*, *13*(3): 1933. DOI: 10.3390/app13031933.

26. **Bandara, S., Wijesundara, K., & Rajeev, P.** (2023). Ultra-High-Performance Fibre-Reinforced Concrete for Rehabilitation and Strengthening of Concrete Structures: A Suitability Assessment. *Buildings*, *13*(3): 614. DOI:10.3390/buildings13030614.
27. **American Society of Civil Engineers**. (2017). ASCE/SEI 41-17: *Seismic Evaluation and Retrofit of Existing Buildings. Reston, Virginia*. ISBN 978-0-7844-1485-9.

## LITERATURE

1. **Hetun H. V.** Konstruktsii budivel i sporud: pidruchnyk: u 2 kn. Kn. 2. Nezhytlovi budivli / H. V. Hetun, P. M. Kulikov, V. O. ta in. – *Kamianets-Podilskyi: Drukarnia «Ruta», 2023 r. – 900 s.: il. ISBN 978-617-8221-06-5*
2. **Hetun H. V., Koliakova V. M., Solomin A. V., Bezklubenko I. S.** (*2022).* Osoblyvosti proiektuvannia stalevykh seismostiikykh konstruktsii vysotnykh budivel. *Budivelni konstruktsii. Teoriia i praktyka.(11), 18-31.* https://doi.org/10.32347/2522-4182.11.2022.18-31
3. **Hetun H. V., Koliakova V. M., Solomin A. V., Bezklubenko I. S.** (2023). Konstruktyvni rishennia vybukhostiikykh budivel z prymishchenniamy tsyvilnoho zakhystu naselennia. *Budivelni konstruktsii. Teoriia i praktyka.(13), 41-50.* https://doi.org/10.32347/2522-4182.13.2023.41-50
4. **Getun G., Butsenko Y., Balina O., Bezklubenko I., Solomin A.** (2019). Dyfuziini protsesy z nakopychuvalnymy kharakterystykamy pry ekspluatatsii budivel *Strength of materials and theory of structures,* (102), 243-251 https://doi.org/10.32347/2410-2547.2019.102.243-251
5. **Getun G., Butsenko Y., Labzhinsky V., Balina O., Bezklubenko I., Solomin A.** *(*2020) Situations forecasting and decision-making optimization based on markovs finite chains in areas with industrial pollutios. *Strength of materials and theory of structures(104), 164-174.* https://doi.org/10.32347/2410-2547.2020.104.164-174
6. **DBN V.1.1-7-2016:** Tekhnichni normy, pravyla i standarty. Zahalnotekhnichni vymohy do zhyttievoho seredovyshcha ta produktsii pryznachennia. Zakhyst vid nebezpechnykh heolohichnykh protsesiv, shkidlyvykh ekspluata-tsiinykh vplyviv, vid pozhezhi. Pozhezhna bezpeka obiektiv budivnytstva. Zahalni vymohy – *[Chynni vid 01.06.2017 r.]. – Kyiv: Minbud Ukrainy, 2017. – 41 s.*
7. **DBN V.1.1-12:2014:** Tekhnichni normy, pravyla i standarty. Zahalnotekhnichni vymohy do zhyttievoho seredovyshcha ta produktsii budivelnoho pryznachennia. Zakhyst vid nebezpechnykh heolohichnykh protsesiv, shkidlyvykh ekspluatatsiinykh vplyviv, vid pozhezhi. Budivnytstvo u seismichnykh raionakh Ukrai-ny – *[Chynni vid 01.10.2014 r.]. – Kyiv: Mi-nrehionbud Ukrainy, 2014. – 110 s.*
8. **DBN V.1.2-2:2006:** Tekhnichni normy, pravyla i standarty. Zahalnotekhnichni vymohy do zhyttievoho seredovyshcha ta produktsii budivelnoho pryznachennia. Systema zabez pechennia nadiinosti ta bezpeky budivelnykh obiektiv. Navantazhennia i vplyvy. Normy proektuvan-nia – *[Chynni vid 01.01.2007 r.]. – Kyiv: Minbud Ukrainy, 2007. – 60 s.*
9. **DBN V.1.2-14:2018:** Tekhnichni normy, pravyla i standarty. Zahalnotekhnichni vymohy do zhyttievoho seredovyshcha ta produktsii budivelnoho pryznachennia. Systema zabezpechen-nia nadiinosti ta bezpeky budivelnykh obiektiv. Zahalni pryntsypy zabezpechennia nadiinosti ta konstruktyvnoi bezpeky budivel, sporud, budivelnykh konstruktsii ta osnov – *[Chynni vid 01.01.2019 r.]. – Kyiv: Minbud Ukrainy, 2018.* – 30 s.
10. **DBN V.2.2.5:2023:** Tekhnichni normy, pravyla i standarty. Obiekty budivnytstva ta promyslova produktsiia budivelnoho pryznachennia. Budynky i sporudy. Zakhysni sporudy tsyvilnoho zakhystu – *[Chynni vid 01.11. 2023]. – Kyiv: «Ministerstvo rozvytku hromad, terytorii ta infra-struktury Ukrainy», 1923. – 123 s.*
11. **DBN V. 2.2-41-2019:** Tekhnichni normy, pravyla i standarty. Obiekty budivnytstva ta promyslova produktsiia budivelnoho pryznachennia. Budynky i sporudy. Vysotni budivli. Osnovni polozhennia – *[Chynni vid 01.01.2020 r.]. – Kyiv: Minrehionbud Ukrainy 2019. – 53 s.*
12. **DBN V.2.6-98:2009:** Tekhnichni normy, pravyla i standarty. Obiekty budivnytstva ta promyslova produktsiia budivelnoho

pryznachennia. Konstruktsii budynkiv i sporud. Betonni ta zalizobetonni konstruktsii. Osnovni polozhennia – *[Chynni vid 01.06.2011 r.]. – GKyiv: Minrehionbud Ukrainy, 2011. – 71 s.*

13. **DSTU B V.2.6-156:2010:** Tekhnichni normy, pravyla i standarty. Obiekty budivnytstva ta promyslova produktsiia budivelnoho pryznachennia. Konstruktsii budynkiv i sporud. Betonni ta zalizobetonni konstruktsii z vazhkoho betonu. Pravyla proektuvannia – *[Chynni vid 01.06.2011 r.]. – Kyiv: Minrehionbud Ukrainy, 2011. – 118 s.*
14. **Ivanchenko H.M. Hetun H.V., Bezklubenko I.S., Solomin A.V.** (2023). Osoblyvosti konstruiuvannia ta rozrakhunkiv skladnykh zalizobetonnykh ram budivel*. Opir materialiv i teoriia sporud. (110), 108-117.* https://doi.org/10.32347/2410-2547/2023/110/108-117
15. **Ivanchenko H.M., Hetun H.V., Bezklubenko I.S., Solomin A.V.** (2023). Vplyv vybukhovykh navantazhen na budivli ta sporudy tsyvilnoho zakhystu naselennia *Opir materialiv i teoriia sporud. (111), 39-48.* https://doi.org/10.32347/2410-2547.2023.111.39-48
16. **Kulikov P. M.** Arkhitektura budivel ta sporud: pidruchnyk: u 5 kn. – *Kn. 5: Promyslovi budivli / P. M. Kulikov, V. O. Ploskyi, H. V. Hetun. – Kamianets-Podilskyi: Drukarnia «Ruta», 2020. – 820 s.: il.* ISBN 978-966-2771-82-4**.**
17. **Kulikov, P. M., Ploskyi, V. O., & Getun, G. V.** (2021). Konstruktsii budivel i sporud: pidruchnyk: u 2 kn. Kn. 1 *Kamianets-Podilskyi: Lira-K, Ruta Printing House. 880 p.* ISBN 978-617-520-089-6.
18. **Lysenko, Ye. F., & Getun, G. V.** (1989). Proiektuvannia stalefibrobetonnykh konstruktsii: navchalnyi posibnyk Kyiv, UMK VO. 184 p.
19. **Ploskyi, V. O., & Getun, G. V.** (2017). Arkhitektura budivel ta sporud: pidruchnyk: u 5 kn. Kn. 2. Zhytlovi budynky. *(3rd ed., revised and augmented). Kamianets-Podilskyi: Ruta. 736 p.* ISBN 978-966-2771-82-4.
20. **Ploskyi, V. O., Getun, G. V., Martynov, V. L., et al.** (2018). Arkhitektura budivel ta sporud: pidruchnyk: u 5 kn. *Kn. 4. Tekhnichna ekspluatatsiia ta rekonstruktsiia budivel Kamianets-Podilskyi: Ruta Printing House. 750 p.* ISBN 978-966-2771-82-4.
21. **Report on damages to infrastructure from the destruction caused by Russia's military aggression against Ukraine as of January 2024**. *Kyiv School of Economics (KSE)*. https://kse.ua/wp-content/uploads/2024/05/Eng_01.01.24_Damages_Report.pdf.
22. **EN 1991-1-7 Eurocode 1 Accidental Actions. European Commission**. Joint Research Centre. https://eurocodes.jrc.ec.europa.eu/sites/default/files/2022-06/EN1991_7_Vrouwenvelder.pdf
23. **Shyiko O., Kropyvnytska T., Volianiuk A., Romaniuk A**. (2024) Resistance of Structural Elements of Civil Protection Buildings and Structures to the Impact of an Explosion. *Journal of Theoretical and Applied Physics.(6),(1), 92–99.* https://doi.org/10.23939/jtbp2024.01.092 URL: https://science.lpnu.ua/jtbp/all-volumes-and-issues/612024/resistance-structural-elements-civil-protection-buildings-and
24. **Yankelevsky D. Z., Karinski Y. S., Feldgun V. R**. (2023) Damage and Failure of a Column-Supported RC Flat Slab Subjected to Impulsive Loading. *Applied Sciences. (13), no. 3: 1933.* DOI: 10.3390/app13031933 https://www.mdpi.com/2076-3417/13/3/1933.
25. **Bandara S., Wijesundara K., Rajeev P**. (2023). Ultra-High-Performance Fibre-Reinforced Concrete for Rehabilitation and Strengthening of Concrete Structures: *A Suitability Assessment. Buildings. (13), no. 3: 614.* DOI: 10.3390 / buildings13030614 https://www.mdpi.com/2075-5309/13/3/614.
26. **American Society of Civil Engineers**. (2017). ASCE/SEI 41-17: *Seismic Evaluation and Retrofit of Existing Buildings. Reston, Virginia.* **ISBN** 978-0-7844-1485-9

ISSN 2522-4182

# АДАПТАЦІЯ ПРИНЦИПІВ СЕЙСМОСТІЙКОСТІ ДЛЯ ЗАБЕЗПЕЧЕННЯ ВИБУХОСТІЙКОСТІ ВИСОТНИХ БУДІВЕЛЬ

*Галина ГЕТУН*
*Ірина БЕЗКЛУБЕНКО*

**Анотація**. Проаналізовано стратегічну необхідність та інженерні механізми адаптації принципів сейсмостійкого проєктування для забезпечення вибухостійкості багатоповерхових будівель в умовах війни в Україні. Ключовою метою є запобігання прогресуючому обвалу (ПО) конструкцій, спричиненому локалізованими імпульсивними навантаженнями, які радикально відрізняються від циклічних сейсмічних впливів, але, як і вони, вимагають залучення пластичної (постграничної) поведінки матеріалів в будівельних конструкціях.

В умовах триваючого військового конфлікту в Україні проєктування висотних будівель вимагає кардинальної перебудови, зміщуючи фокус із традиційних гравітаційних та сейсмічних навантажень (ДБН В.1.1-12:2014, ДБН В.2.2-41-2019) на екстремальні імпульсивні навантаження від вибухів. Основна загроза – прогресуючий обвал (ПО), що виникає після локального руйнування ключового елемента. Згідно з європейськими стандартами (Eurocode EN 1991-1-7), інженерна мета змінюється: не запобігання пошкодженню, а запобігання його непропорційному поширенню.

Введення нових ДБН В.2.2-5:2023, які радикально підвищили розрахунковий тиск вибуху до 100 кПа для захисних споруд, неявно змушує інженерів використовувати методи нелінійного динамічного аналізу (*NDA*). У статті обґрунтовується, що принципи сейсмостійкого проєктування – дуктильність та надмірність – є критичною основою для підвищення вибухостійкості, незважаючи на відмінності у частотних характеристиках навантажень.

Ключовим рішенням є гібридизація національних вимог з міжнародними методиками протидії ПО, зокрема методами альтернативного шляху навантаження (АР) та впровадження в'яжучих зусиль (*Tie Force, TF*), які забезпечують структурну цілісність після видалення вертикальної опори, реалізуючи катанійну дію плит. Це вимагає адаптації критеріїв прийнятності ASCE 41 та використання інноваційних матеріалів, як-от Ультрависокопродуктивний сталефібробетон (UHPFRC), для ефективного посилення конструкцій.

Дослідження підсумовує необхідність гібридизації українських вимог до локальних захисних споруд з міжнародними методиками загальної структурної стійкості для забезпечення комплексної та високорівневої безпеки висотних будівель.

**Ключові слова:** висотні будівлі; вибухостійкість; прогресуючий обвал (ПО); в'яжучі зусилля (*tie force*); деформативність.

***Received:*** *October 02, 2025.*
***Accepted:*** *November 30, 2025.*

ISSN 2522-4182

DOI: 10.32347/2522-4182.17.2025.65-78
УДК 624.011

# HARDWOOD PLATE-TYPE CONNECTORS ANALYSIS FOR MULTIPANEL CLT SHEAR WALLS

*Andrii BIDAKOV[1]; Oksana PUSTOVOITOVA[2]; Viacheslav KOSMACHEVSKYI[3]; Yurii KUZUB[4]*

[1,2,3,4]O.M.Beketov National University of Urban Economy
Chornoglazivska St., Kharkiv, Ukraine, 6100217
[1]bidakov@kname.edu.ua, https://orcid.org/0000-0001-6394-2247
[2]oksana.pustovoitova@kname.edu.ua, https://orcid.org/0009-0003-4774-6686
[3]Viacheslav.Kosmachevskyi@kname.edu.ua, https://orcid.org/0009-0006-8281-3946
[4]Yurii.Kuzub@kname.edu.ua, https://orcid.org/0009-0000-7529-2069

**Abstract.** Developing multi-storey timber construction requires control and minimized deformations of both the building frame elements and their connections. This is especially important for buildings made of CLT panels, where optimizing the building frame and minimizing material consumption comes down to constructing parts of the wall panel above the window and door openings of separate elements. Also, dividing CLT panels into smaller fragments is often attempted to simplify logistics or reduce scraps when cutting a large slab in production. Such frame detailing requires monolithic connection of CLT panel elements, achieved with a large number of screws, which is extremely expensive, especially for Eastern European countries. Timber structure joints deformability is minimal in adhesive joints and joints on glued-in rods. The analysis of the rigidity and strength of CLT panels connections provided with plate elements and the test results discussed in this publication prove the efficiency and prospects of this connection type, especially manufactured with modern methods ensuring high dimensional accuracy in cutting frame parts through the application of various milling techniques.

The publication presents the results of tests conducted with oak shear-key connectors of CLT panels and compares them with the results of similar studies using aluminum shear-key and connections with a big number of screws in spline joints. Analysis of the deformation behavior of connections in multi-story building frames made of CLT panels requires special attention and the search for new solutions for connections and their components. Currently, shear-key connectors from different manufacturers offer various geometric variations that simplify their installation during building frame assembly and sometimes even allow for tightening of the connected components using wedge-shaped surfaces.

**Andrii BIDAKOV**
Assistant Professor, Department of construction design,
Dr.Sc

**Oksana PUSTOVOITOVA**
Assistant Professor,
Department of construction design,
PhD (Tech. Sci.)

**Viacheslav KOSMACHEVSKYI**
student

**Yurii KUZUB**
student

**Keywords:** cross-laminated timber (CLT); multi-panel walls; plate-type timber connector; shear-key connector.

## INTRODUCTION BACKGROUND

Intensive use of CLT panels in modern construction makes the issue of connecting frame panels to each other crucial. CLT panels are most commonly connected with screws. Minimizing the number of screws connecting CLT panels significantly reduces the cost of the building frame, which is important for promoting timber structures in Eastern European countries, including Ukraine. Timber plates made of hardwood (oak, beech or birch) were used to join logs or beams lengthwise to achieve a solid cross-section and full joint work well before the advent of timber gluing technology. As described in numerous previous references, many bridges and long-span wall designs were enabled with such connections. The old SNIP 2-25-80 standards [5], adopted in 1982, provide data for designing such connections, while the standards manual (1986) features examples of calculating such beams.

The largest number of hardwood shear-key connectors in simply supported beams is installed near the support where the maximum shear occurs.

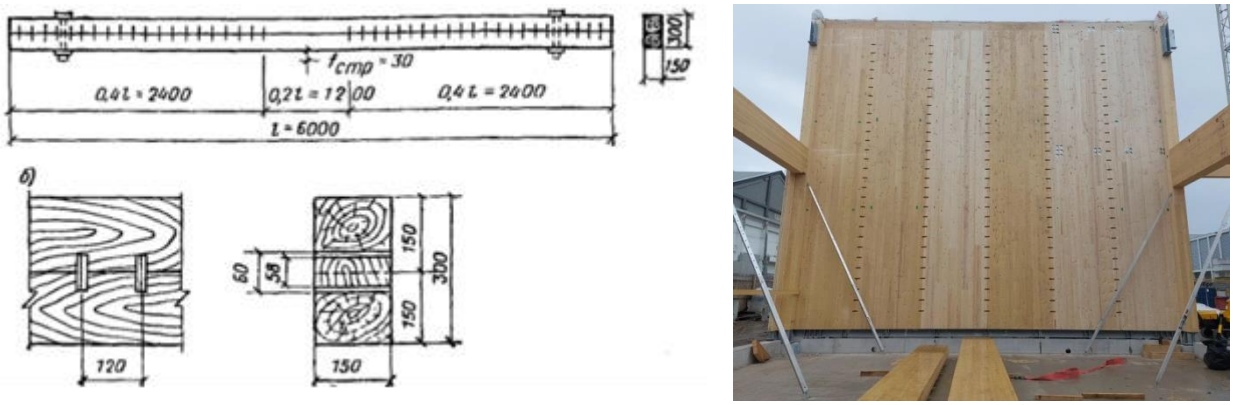


*a* *b*

**Fig. 1** Built-up beams with timber plate-type hardwood shear-key connectors (a) according to SNiP [5] and alumimium slot connector (b) manufactured by Rothoblaas [8]

**Рис. 1** Балки складеного перерізу з пластинчастими шпонками (а) згідно до СНіП [5] та алюмінієва шпонка Slot (b) виробництва компанії Rothoblaas [8]

## STATE OF THE ART

Such a timber-plate connection made of beech LVL and softwood LVL has already been widely studied by Prof. H. J. Blass and T. Schmidt (2018) for CLT panels connections, as described in their works [3, 10-13]. A similar solution, based on connecting keys, has been adapted and offered in the form of an aluminium key Slot by the Rothoblaas company [8]. This key-connection solution is widely used in engineering practice and described in the works by D. Cassagrande et al. [1, 2, 14] for multi-panel CLT shear walls, Fig. 2. The deformability is insignificant and such an easily manufacturable connection is crucial for modern construction to connect CLT wall panels [4, 15-19] and floor panels to each other along the edge, as well as to provide corner joints of CLT panels and to connect panels along the face. In this publication, the obtained testing results for oak plates deformability are compared with similar testing results for the aluminium SLOT and LVL-timber plates for a comparative analysis of deformability, as well as an analysis of changing rigidity in such joints depending on the deformations.

The plates in the wall panels' joints are placed in the upper and lower parts of the joint along the length of the vertical joint. This type of connection is both rational and effective for connecting floor slabs made of glued laminated timber independently, without fixing them to the concrete layer for timber-concrete floors.

Ductility and behaviour assessment of connections in CLT panels is very important for buildings located in seismically active regions [20-24]. Cyclic testing of CLT-panels' joints on the mechanical fasteners is conducted according to standard EN 12512:2001 [25], which lists the corresponding methods

.

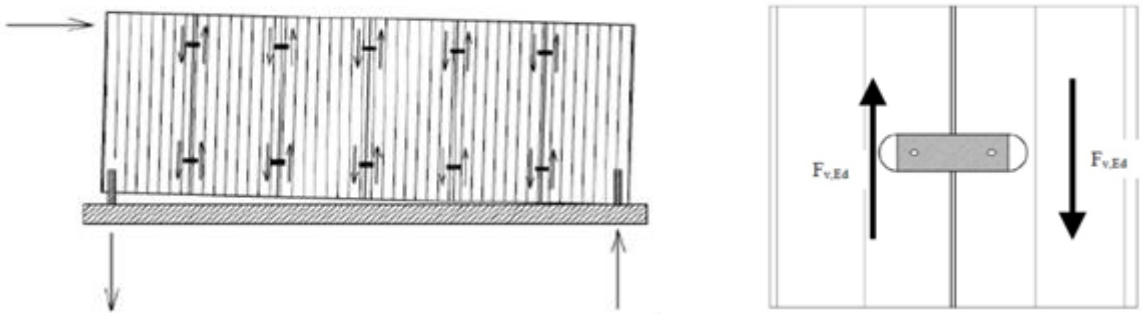


**Fig. 2** Multi-panel shear wall with shear-key or plate type stiff connector (D. Cassagrande at al. [1]).
**Рис. 2** Багатоскладна стінова панель зі шпонками у стиках або жорсткими конекторами до дії зсуву (D. Cassagrande and all [1]).

The "X-fix C" key developed by the Haaslacher company (ETA-18/0245 [6]) is formed by two plates with inclined planes. When driven into a pre-milled groove, the connected parts of the CLT panels are pulled together to minimize or eliminate the gap in the joint. This key also has widenings from the centre to the edges to retain tensile forces in such a connection. The general views of the Slot, X-fix C key and oak keys in the tested samples are shown in Fig. 3.

Joints deformations in timber structures is often a key criterion, since the horizontal displacement in wall panels cannot exceed more than h/100, where h is the height of the wall panel. The efficiency of shear-key joints in comparison with connections effected with screws installed in a row along the joint is significantly higher. Figure 4 shows a graph of the deformation of connections tested samples with an aluminium shear-key Slot and screws installed in a row (spline joint) in the same samples, obtained from the publication by D. Cassagrande [1].

The load values and deformations are reported per couple of screws. Initial slip of around .3 to .5 mm was observed as a gap between the SLOT connector and the CLT panel, but there was no initial slip in screwed joints. The number of screws was calculated to match the SLOT connector's strength and stiffness.

*a* *b* *c*

**Fig. 3** General view: Slot key (a), X-fix key (b), and oak keys in the tested samples (c)
**Рис. 3** Загальний вид алюмінієвої шпонки Slot (a), X-fix шпонка із шпонкового брусу ЛВЛ (b) та дубова шпонка яка використовувалась у дослідженні (c)

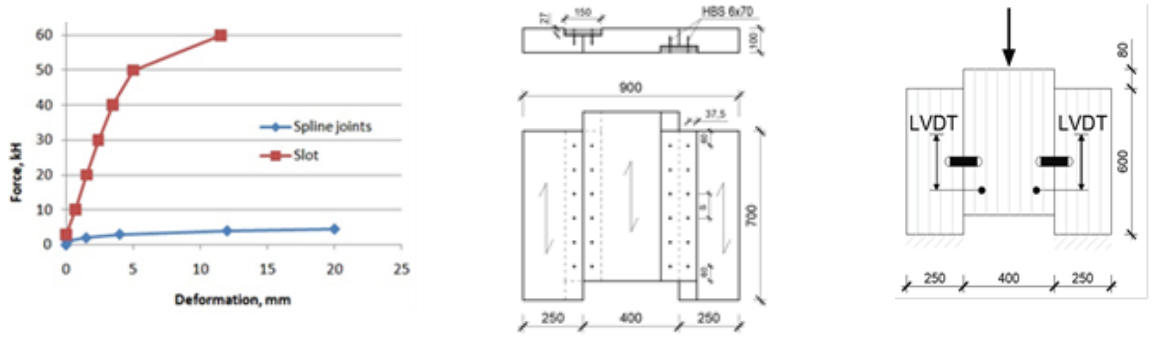


*a* *b* *c*

**Fig. 4** Force-deformation diagram (a) for aluminium Slot shear-key connection (c) and spline joint with screws (b) based on data [1].

**Рис. 4** Криві навантаження-деформація (a) для з'єднань з алюмінієвою шпонкою Slot (c) та для з'єднань з накладками та гвинтами (b) на основі експериментальних даних [1].

## DESIGN APPROACH TO CALCULATING SHEAR-KEY CONNECTORS

The characteristic values of load-bearing capacities for the SLOT connector calculated according to equation (2.1) are proposed in ETA-19/0167 [8], where $t_e$ is penetration depth which equal 60 mm -.5*$t_{gap}$ ($t_{gap}$≤5mm) and $b_{ef}$ is the effective connector depth. $b_{ef}$ = b = 89 mm for LVL and glulam, $b_{ef}$ = Σd0 + .1* (b-Σd0) for CLT, where Σd0 is accumulated layer thickness of CLT elements within width b parallel to shear force $F_{v,Ed}$.

$$F_{v,Rk} = k_{al} \cdot b_{ef} \cdot f_{c,0,k} \cdot \left( \sqrt{t_{gap}^2 + 2 \cdot (t_e - 5mm)^2} + 2 \cdot (t_e - 5mm) \right) \quad (1)$$

$$k_{al} = \begin{cases} 1 & for\ a_1 \geq 480mm\ and\ a_{3,t} \geq 480mm \\ 1 - 0{,}001 \cdot (480 - \min\{a_1; a_{3,t}\}) & for\ a_1 480 < mm\ and\ a_{3,t} < 480mm \end{cases} \quad (2)$$

Slip module per Rothoblaas Slot connector according to ETA 19/0167 [8]:

$$K_{ser} = \frac{\rho_k}{20} kN/mm \qquad \text{CLT or softwood LVL} \quad (3)$$

$$K_{ser} = \frac{\rho_k}{15} kN/mm \qquad \text{hardwood LVL or GLT} \quad (4)$$

According to the USSR norms [4, 5], reference bearing capacity in kN is calculated as follows:

$$F_{v,Rk} = 0{,}625 \cdot \delta \cdot b \quad (5)$$

where:

δ is plate thickness with the recommended value of 12 mm and b is the connector width.

The recommended hardwood shear plates width is 4.5−5*δ, which corresponds to $t_e$ value of 2.25−2.5 and which is very similar to the conclusions published by T. Schmidt and H.J. Blass [3, 10], who tested a group of specimen

series with different depth penetration te. When te exceeds 2δ, the bearing capacity does not increase.

## EXPERIMENTAL PROGRAMME. SPECIMEN GEOMETRIES AND TEST SETUPS

The shear tests were carried out to evaluate the shear resistance of CLT-to-CLT oak timber plates connections or shear-key connectors, analogous to aluminium Slot shear-key connector manufactured by Rothoblaas. The connection between two adjacent parallel panels follows the configurations in Fig. 5.

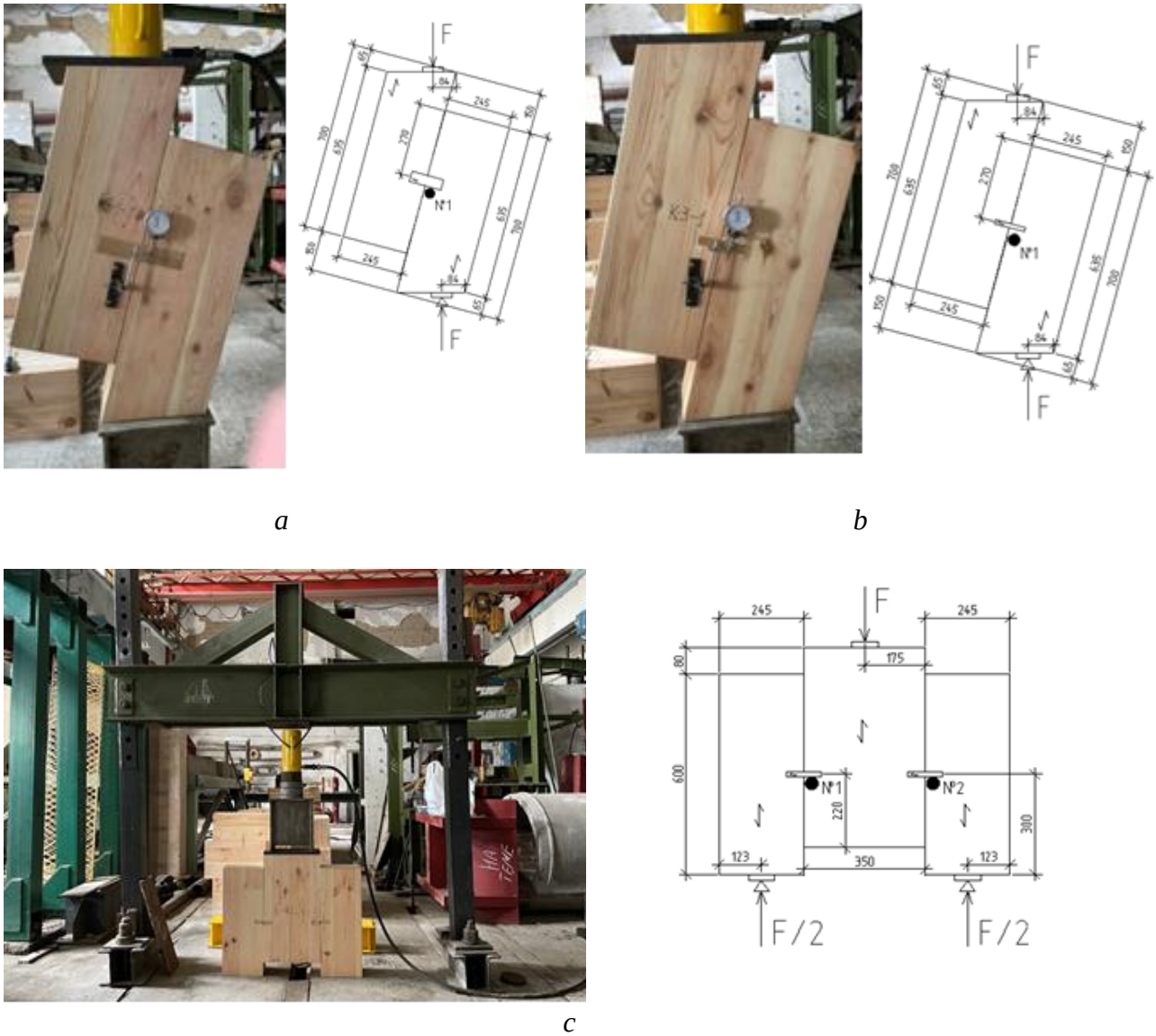


*a* *b*

*c*

**Fig. 5** Testing diagrams and geometry of the tested specimens with the shear-key oak connector:
*a* - specimen series K-1; *b* - specimen series K-3; *c* - specimen series K-4; Photo by A.Bidakov
**Рис. 5** Схема випробувань та геометричні параметри зразків з дубовими шпонками
*a* – зразки серії К-1; *b* - зразки серії К-3; *c* - зразки серії К-4; Автор фото А.Бідаков

This solution avoids the cuts needed for lap or spline joints, which are easily manufacturable on the factory production line, but challenging to obtain on-site. The experimental configuration consists of two parts, 245mm×700mm in size, joined with a shear-key connector, as shown in Fig. 5 (a, b)

as the single-shear configuration. Also, the considered three-partite double-shear K-4 configuration grants a symmetrical application of the vertical load, see Fig. 5 (c). The authors tested three different configurations, or series, each one within five iterations. Therefore, the total number of conducted tests was 3×5=15. The configurations differ by the size of shear-key oak connector and the number of shear lines in the specimen series. Tested CLT panel layouts provided the accepted thicknesses of 140 mm (40 + 20 + 20 + 20 + 40). Table 1 shows the details of the tested specimen series.

**Table 1** Tested configurations details
**Табл. 1** Параметри випробуваних зразків

| Label | CLT thickness, mm | CLT layouts, mm | Timber plate geometry, mm | Number of shear surfaces | Number of specimens |
|---|---|---|---|---|---|
| K-1 | 140 | 40-20-20-20-40 | 40*120*200 | 1 | 5 |
| K-3 | 140 | 40-20-20-20-40 | 20*120*100 | 1 | 5 |
| K-4 | 140 | 40-20-20-20-40 | 20*120*100 | 2 | 5 |

The tested 140 mm thick CLT elements were produced by the Ukrainian company Rezult, ETA-21/0914 [7]. The oak shear-key connectors had a planed, smooth surface, without any visual defects such as cracks, splits or cavities. The shear-key connectors were installed in milled grooves to a depth of 120 mm, without tolerance for the dowel thickness.

The K-1 and K-3 series of samples had undercut support elements so that the sample incline was approximately 14˚. In this case, the support centres coincided with the vertical axis passing through the shear-key centre in the samples. The oak shear-keys were located in the middle along the vertical axis of the sample, see Fig. 5 (a, b). The K-4 series of samples had the shear-keys in the middle of the vertical section of the joint. All the samples were loaded until the shear-keys began to fail

The load was applied with a constant load rate of .1 mm/s and according to EN26891 [9] the failure occurred within 300 seconds. The relative slip between the two CLT parts near the shear-key location was measured by a 250 kN load cell. A dial gauge was used to register deformations.

## RESULTS & DISCUSSION

The results obtained from testing SLOT connector joints and the screwed connections are presented in Table 2. The load-deformation diagrams for tested single-shear specimen series K-1-1…K-1-5 (thick shear-key) and tests series K-3-1…K-3-5 (thin shear-key) are shown on Fig. 6. Similar diagrams are shown on Fig. 7 for tested double-shear specimen series K-4-1…K-4-5 with two thin oak shear-key connectors.

The curves of the tested oak connectors show an initial slip around .2–.4 mm due to the imperfections and a small gap between the connector and the grooves surfaces of CLT panels' parts. Observations confirmed the oak shear-key elastic behavior and, additionally, wooden laminations failure parallel to the load direction, which was also observed for LVL connectors in tests performed by Schmidt and Blass [3, 10] and in the tests with aluminum SLOT shear-key performed by D. Casagrande [1, 2].

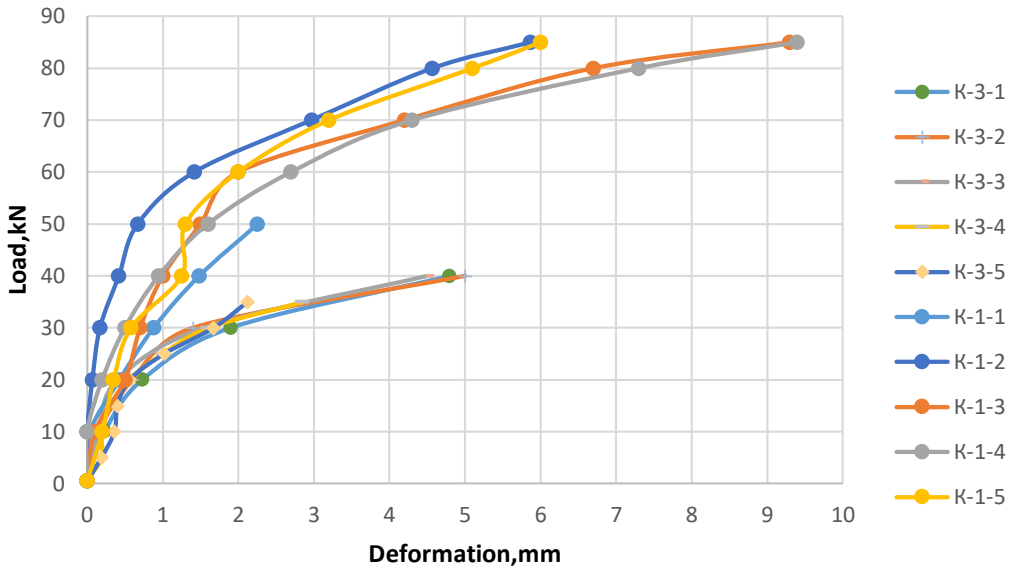


**Fig. 6** Load-deformation curves of tested series K-1 and K-3 single-shear specimens
**Рис. 6** Криві навантаження-деформація випробуваних зразків з одним стиком та однією шпонкою серій К-1 та К-3

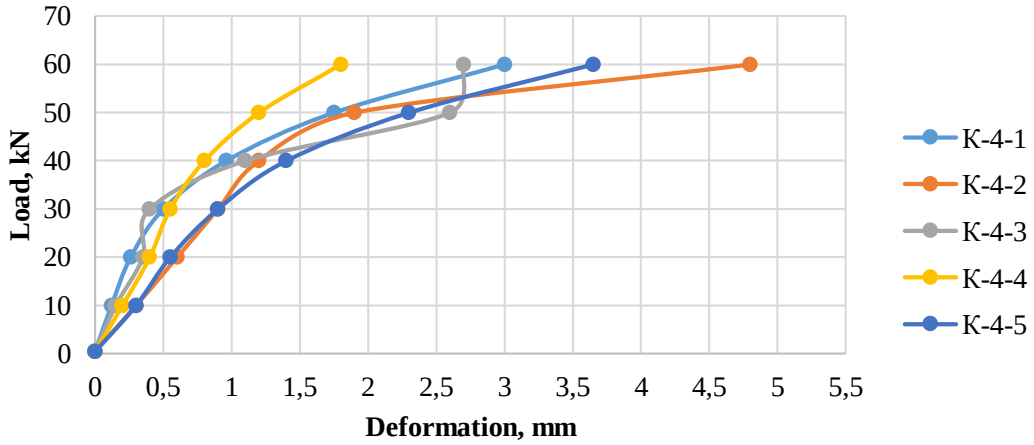


**Fig. 7** Load-deformation curves of tested series K-4 double-shear specimens
**Рис. 7** Криві навантаження-деформація випробуваних зразків з двома стиками та двома шпонками серії К-4

**Table 2** Test results of series K-1, K-3, and K-4 joints
**Табл. 2** Результати випробувань з'єднань серій зразків К-1, К-3 та К-4

| Label | Average value, $F_{max}$, kN | Average value, max. deformation, mm | SD of $F_{max}$ | COV of $F_{max}$, % |
|---|---|---|---|---|
| K-1 | 87 | 6,81 | 4,29 | 4,93 |
| K-3 | 45,22 | 3,85 | 5,41 | 11,96 |
| K-4 | 68,8 | 4,11 | 0,46 | 0,7 |


**Fig. 8** Failure mode in tested specimens:
*a*-deformation types for thick oak shear-key connector (series K-1);
*b*-deformation types for thin oak shear-key connector (series K-3);
*c*-deformations of thin oak shear-key connector (series K-4) in double-shear conditions
Photo by A.Bidakov

**Рис. 8** Види руйнувань випробуваних з'єднань зі шпонками:
*а* - типи деформацій для масивної (товстої) дубової шпонки (серія К-1);
*б* - типи деформацій для тонкої дубової шпонки (серія К-3);
*в* - деформації тонкої дубової шпонки (серія К-4) в умовах подвійного зсуву.
Автор фото А.Бідаков

The failure modes for the joints with oak shearkey connectors are shown in Fig. 8, with the observed typical failure of timber near the shear-line (Fig. 6a), i. e. compressed along the grain direction timber and bent oak shear-key. In both failure modes, a rigid body rotation with no residual plastic deformations of the connector was observed.

The test procedure and the evaluation were based on DIN EN26891 [9]. Both the ultimate load $F_{V,test}$ and the stiffness $k_s$ per connector were determined. The stiffness was determined in the 10% to 40% range of the ultimate load in the linear-elastic range.

$$k_s = K_{ser} = \frac{0{,}4 \cdot F\max - 0{,}1 \cdot F\max}{\upsilon_{04} - \upsilon_{01}} \qquad (6)$$

The low deformation of shear-key connections proves their significant advantage compared to screws, nails, pins, and bolts. Intensified deformation was observed along the line two connected CLT panels due to compression in the grain direction of the CLT panel and perpendicular to the grain of the hardwood in the shear-key itself, see Table 3 for each series of the tested specimen.

Comparative analysis diagram of CLT-panel shear-key connector slip module in shear in-plane tests with marked min/max values and mean value is presented in Fig. 9.

The load-bearing capacity of the tested K-1 series shear-keys is greater than that of the Slot aluminium key due to their greater width and length, but the character of the deformation is the same, as shown in Fig. 10.

According to equation (1), the characteristic strength $F_{v,Rk}$ equals 40.57 kN for the aluminium Slot connector in the 90 mm (24-42-24) CLT panel and 122.96kN for the 200*120*40mm oak shear-key connector in the 140 mm (40-20-20-20-40) CLT panel. Shear-key joints are versatile and they can minimize ductility and deformation of both the connections between CLT panels and between CLT and beams or columns made of glued laminated timber that need to be included in the joint work.

**Table 3** Slip module $k_{s,connector}$ for joint with dowel-type fasteners per shear plane in in-plane tests of the series K-1, K-3, and K-4 specimens

**Табл. 3** Модуль ковзання $k_{s,connector}$ для нагельних з'єднань на один стик зсуву при випробуваннях у площині панелі для зразків серій K-1, K-3 and K-4

| Number of specimen | K-1- $k_s$, kN/mm | K-3- $k_s$, kN/mm | K-4- $k_s$, kN/mm |
|---|---|---|---|
| 1 | 24.6 | 24.5 | 57.72 |
| 2 | 99.12 | 13.7 | 33.4 |
| 3 | 34.37 | 11.23 | 73.22 |
| 4 | 40.16 | 45.3 | 54.97 |
| 5 | 34.57 | 43.05 | 34.06 |

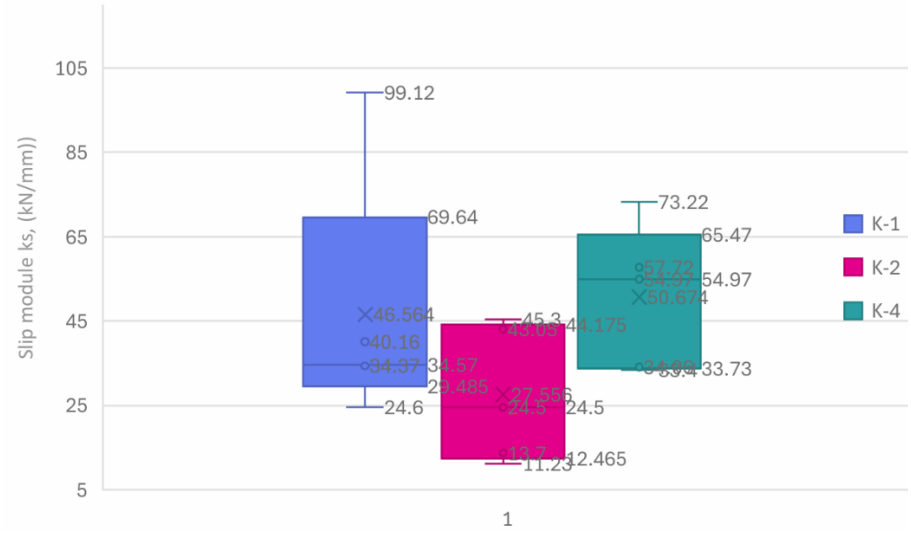


**Fig. 9** Slip module values analysis of specimens subjected to shear testing.

**Рис. 9** Аналіз величин модуля ковзання випробуваних серій зразків з дубовими шпонками при випробуваннях на зсув

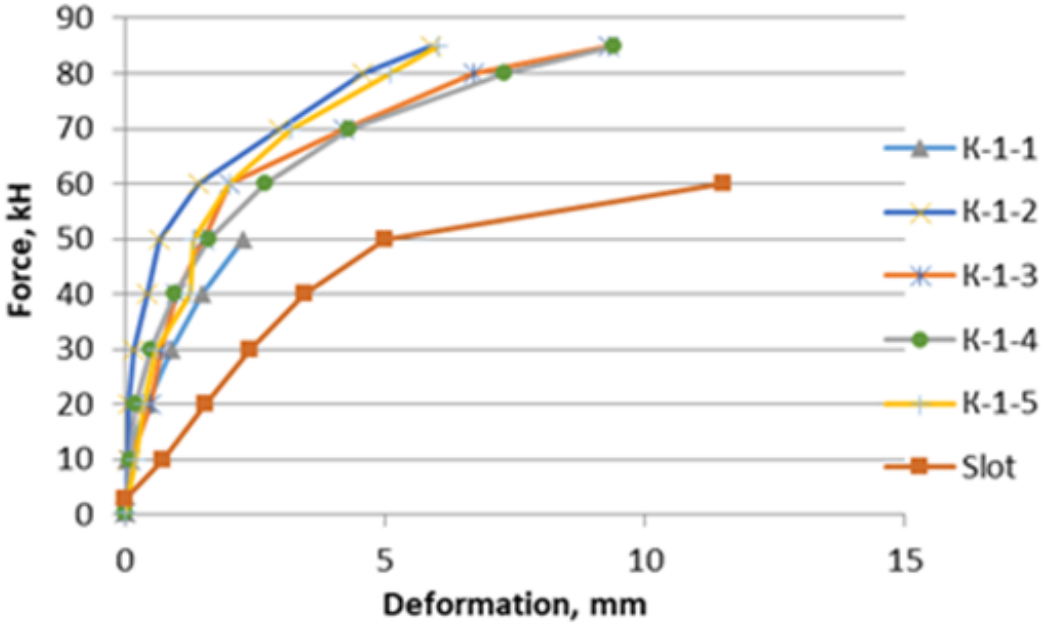


**Fig. 10** Load-deformation curves of tested single-shear specimens, series K-1 and Slot (by Casagrande et. al. [1])

**Рис. 10** Криві навантаження-деформація випробуваних зразків з одним стиком та однією шпонкою серій К-1 та Slot (by Casagrande at. all [1])

## CONCLUSIONS

This paper analyses mechanical behaviour of two types of stiff shear-key connectors made from oak and used in CLT structure joints. Static tests were carried out on 3 specimen series with one and two shear lines and yielded values of stiffness and strength, which were additionally compared with similar data for the aluminium SLOT connectors and screw spline joints, described in other publications.

The test results of oak shear-key connectors in CLT panels' shear joints showed that their strength and deformability values belong to the same range as the values for the SLOT aluminium shear-key manufactured by Rothoblaas. The the shear-key connectors at all the loading stages are characterized by a close-to-linear dependence of the force F/Fmax to deformation d/dmax ratios. The efficiency of shear-key connector joints is evident and extremely promising in comparison with screw joints, since one SLOT aluminium shear-key is equivalent to 28 screws (HBS8*100) in a half-joint joint and to 114 screws (HBS6*70) in a joint with an overlay [1]. The work of the aluminium shear-key and the thick oak shear-key is almost identical, with the oak key being twice cheaper, which is crucial for the Ukrainian market. K-1 series shear-key connectors are wider and longer, which accordingly increases their load-bearing capacity and reduces the connection flexibility in comparison with the one-size aluminium shear-key connectors.

Today, the prospects of shear-key connections application and demand for them are evident in the construction of CLT panel houses, especially in terms of the building frames' rigidity, calculated as 1/1000 of the building height for horizontal displacements. Easy installation of shear-keys in pre-milled or made in-situ grooves make this solution widely applicable. This research is continued to combine the work of glued laminated timber columns and beams with CLT diaphragm walls in the building frame.

## ACKNOWLEDGEMENTS

The work presented in the paper has been conducted in the project "Efficient connections for modular prefabricated timber buildings to

help reconstruction in Ukraine" within the programme for Academic Collaboration in the Baltic Sea Region, which is funded by The Swedish Institute (SI). We would like to thank SI for their financial support for this research project!

## REFERENCES


1. **Rigo P., Polastri A., Casagrande, D. Callegari E., Ramazzini, A. and Sestigiani L.**, (2023) "Experimental characterization of stiff aluminum connectors for multi-panel CLT shear-walls," *WCTE 2023, Oslo, pp. 2497–2503*. https://doi.org/10.52202/069179-0328
2. **Polastri A. and & Casagrande D.,** (2022) "Mechanical behaviour of multi-panel cross laminated timber shearwalls with stiff connectors," *Constr. Build. Mater.* **332**, 127275. https://doi.org/10.1016/j.conbuildmat.2022.127275
3. **Schmidt T.**, (2018) Kontaktverbindungen für aussteifende Scheiben aus Brettsperrholz, *Karlsruher Institut für Technologie (KIT), Holzbau und Baukonstruktionen, Deutschland, 249 pp.* ISBN 978-3-7315-0803-8. https://doi.org/10.5445/KSP/1000083480
4. **Bidakov, A., Jockwer, R., Just, A., Tuhkanen, E., & Kochkarev, D.** (2024). Structural behaviour of a clt connection with bondedin rods under shear loading. *Building Constructions. Theory and Practice*, (15), 156–173. https://doi.org/10.32347/2522-4182.15.2024.156-173
5. **SNiP II-25-80**. (1982) Derevyani konstructcii *TsNIISK im. Kucherenko, Stroyizdat, Moscow, 30 pp.*
6. **ETA-18/0254**, (2020) European Technical Assessment, "X-fix C. Point connector – Dovetail made of plywood for cross laminated timber," *SCHILCHER Trading & Engineering GmbH, Rangersdorf, Austria.*
7. **ETA-21/0914**, (2021) REZULT CLT. Cross laminated timber element, U*krainian Sawmill Holding Company Ltd, Kyiv, Ukraine.*
8. **ETA-19/0167**, (2019) European Technical Assessment, "Three-dimensional nailing plate (Edge connections for CLT, LVL and Glulam members)," *Rotho Blaas Slot connectors, European Organisation for Technical Approvals, Nordhavn, Denmark.*
9. **EN 26891**. Timber Structures – Joints Made with Mechanical Fasteners. *General Principles for the Determination of Strength and Deformation Characteristics*, CEN, Brussels.
10. **Schmidt T.**, (2018) Kontaktverbindungen für aussteifende Scheiben aus Brettsperrholz, *KIT Scientific Publishing, Karlsruhe*. https://doi.org/10.5445/KSP/1000083480
11. **Schmidt T. & Blass H. J.**, (2016) "Contact joints in engineered wood products," in *Proc. World Conf. on Timber Engineering (WCTE 2016)*, Vienna, Austria, Aug. 22–25. https://publikationen.bibliothek.kit.edu/1000059086
12. **Schmidt T. & Blass H. J.**, (2018) "Recent development in CLT connections. Part I: In-plane shear connection for CLT bracing elements under static loads," *Wood Fiber Sci.* **50**, 48–57. https://doi.org/10.1002/bate.201400076
13. **Schmidt T. & Blass H. J.**, (2018) "Recent development in CLT connections. Part II: In-plane shear connections for CLT bracing elements under cyclic loads," *Wood Fiber Sci.* **50**, 58–67. https://doi.org/10.22382/wfs-2018-040
14. **Casagrande D., Doudak G., Mauro L., & Polastri A.**, (2018) "Analytical approach to establishing the elastic behavior of multi-panel CLT shear walls subjected to lateral loads," *J. Struct. Eng.* 144 (2), 04017193. https://doi.org/10.1061/(ASCE)ST.1943-541X.0001948
15. **Tamagnone G. & Fragiacomo M.**, (2018) "On the rocking behavior of CLT wall assemblies," in *Proc. World Conf. on Timber Engineering (WCTE 2018)*, Seoul https://arts.units.it/handle/11368/2928709?mode=simple
16. **.Teweldebrhan B. T & Tesfamariam S.**, (2022) "Performance-based design of tall coupled cross-laminated timber wall building," *Earthq. Eng. Struct. Dyn.* 51 (7), 1677–1696. https://doi.org/10.1002/eqe.3633
17. **Chen Z. and M. Popovski**, (2020) "Mechanics-based analytical models for balloon-type cross-laminated timber (CLT) shear walls under lateral loads," *Eng. Struct.* 208, 109916. https://doi.org/10.1016/j.engstruct.2019.109916
18. **Li Z., Wang X., & He M.**, (2020) "Experimental and analytical investigations into lateral performance of cross-laminated timber (CLT) shear walls with different construction methods," *J. Earthq. Eng.*, 1–23. https://doi.org/10.1080/13632469.2020.1815609

19. **Shahnewaz M., Dickof C., & Tannert T.**, (2021) "Seismic behavior of balloon frame CLT shear walls with different ledgers," *J. Struct. Eng.* 147 (9), 04021137. https://doi.org/10.1061/(ASCE)ST.1943-541X.0003106
20. **. You T, Teweldebrhan B. T., Wang W., & S. Tesfamariam**, (2023) "Seismic loss and resilience assessment of tall-coupled cross-laminated timber wall building," *Earthq. Spectra* 39 (2), 727–747. https://doi.org/10.1177/87552930231152512
21. **Asgari H., Tannert T., Ebadi M. M., Loss C., & Popovski, M.** (2021) "Hyperelastic hold-down solution for CLT shear walls," *Constr. Build. Mater.* 289**,** 123173. https://doi.org/10.1016/j.conbuildmat.2021.123173
22. **Pozza L., Saetta, A. Savoia M., & Talledo D.**, (2018) "Angle bracket connections for CLT structures: Experimental characterisation and numerical modelling," *Constr. Build. Mater.* **191**, 95–113. https://doi.org/10.1016/j.conbuildmat.2018.09.112
23. **Rinaldi V., Casagrande D., & Fragiacomo M.**, (2022) "Verification of the behaviour factors proposed in the second generation of Eurocode 8 for cross-laminated timber buildings," *Earthq. Eng. Struct. Dyn.*. https://doi.org/10.1002
24. **.Rinaldi, V Casagrande, D. Cimini C., Follesa M., & Fragiacomo M.**, (2021) "An upgrade of existing practice-oriented FE design models for the seismic analysis of CLT buildings," *Soil Dyn. Earthq. Eng.* 149, 106802. https://doi.org/10.1016/j.soildyn.2021.106802
25. **EN 12512:2001** *(2002).* Timber Structures – Test Methods – Cyclic Testing of Joints Made with Mechanical Fasteners, *CEN, Brussels, Belgium.*
26. **Mpidi Bita H., Tannert T**. (2018) Numerical optimisation of novel connection for cross-laminated timber buildings, *Eng. Struct. 175 273– 283.* https://doi.org/10.1016/j.engstruct.2018.08.020

## LITERATURE

1. **Rigo P., Polastri A., Casagrande, D. Callegari E., Ramazzini, A. and Sestigiani L.**, (2023) "Experimental characterization of stiff aluminum connectors for multi-panel CLT shear-walls," *WCTE 2023, Oslo, pp. 2497–2503.* https://doi.org/10.52202/069179-0328
2. **Polastri A. and & Casagrande D.,** (2022) "Mechanical behaviour of multi-panel cross laminated timber shearwalls with stiff connectors," *Constr. Build. Mater.* **332**, 127275. https://doi.org/10.1016/j.conbuildmat.2022.127275
3. **Schmidt T.**, (2018) Kontaktverbindungen für aussteifende Scheiben aus Brettsperrholz, *Karlsruher Institut für Technologie (KIT), Holzbau und Baukonstruktionen, Deutschland, 249 pp.* ISBN 978-3-7315-0803-8. https://doi.org/10.5445/KSP/1000083480
4. **Bidakov, A., Jockwer, R., Just, A., Tuhkanen, E., & Kochkarev, D.** (2024). Structural behaviour of a clt connection with bondedin rods under shear loading. *Building Constructions. Theory and Practice*, (15), 156–173. https://doi.org/10.32347/2522-4182.15.2024.156-173
5. **SNiP II-25-80**. (1982) Derevyani konstructcii [Building Regulations. Wooden Structures], *TsNIISK im. Kucherenko, Stroyizdat, Moscow, 30 pp.* [In Russian]
6. **ETA-18/0254**, (2020) European Technical Assessment, "X-fix C. Point connector – Dovetail made of plywood for cross laminated timber," *SCHILCHER Trading & Engineering GmbH, Rangersdorf, Austria.*
7. **ETA-21/0914**, (2021) REZULT CLT. Cross laminated timber element, U*krainian Sawmill Holding Company Ltd, Kyiv, Ukraine.*
8. **ETA-19/0167**, (2019) European Technical Assessment, "Three-dimensional nailing plate (Edge connections for CLT, LVL and Glulam members)," *Rotho Blaas Slot connectors, European Organisation for Technical Approvals, Nordhavn, Denmark.*
9. **EN 26891**. Timber Structures – Joints Made with Mechanical Fasteners. *General Principles for the Determination of Strength and Deformation Characteristics*, CEN, Brussels.
10. **Schmidt T.**, (2018) Kontaktverbindungen für aussteifende Scheiben aus Brettsperrholz, *KIT Scientific Publishing, Karlsruhe*. https://doi.org/10.5445/KSP/1000083480
11. **Schmidt T. & Blass H. J.**, (2016) "Contact joints in engineered wood products," in *Proc. World Conf. on Timber Engineering (WCTE 2016)*, Vienna, Austria, Aug. 22–25. https://publikationen.bibliothek.kit.edu/1000059086
12. **Schmidt T. & Blass H. J.**, (2018) "Recent development in CLT connections. Part I: In-plane shear connection for CLT bracing

elements under static loads," *Wood Fiber Sci.* **50**, 48–57. https://doi.org/10.1002/bate.201400076

13. **Schmidt T. & Blass H. J.**, (2018) "Recent development in CLT connections. Part II: In-plane shear connections for CLT bracing elements under cyclic loads," *Wood Fiber Sci.* **50**, 58–67. https://doi.org/10.22382/wfs-2018-040
14. **Casagrande D., Doudak G., Mauro L., & Polastri A.**, (2018) "Analytical approach to establishing the elastic behavior of multi-panel CLT shear walls subjected to lateral loads," *J. Struct. Eng.* 144 (2), 04017193. https://doi.org/10.1061/(ASCE)ST.1943-541X.0001948
15. **Tamagnone G. & Fragiacomo M.**, (2018) "On the rocking behavior of CLT wall assemblies," in *Proc. World Conf. on Timber Engineering (WCTE 2018)*, Seoul https://arts.units.it/handle/11368/2928709?mode=simple
16. **. Teweldebrhan B. T & Tesfamariam S.**, (2022) "Performance-based design of tall coupled cross-laminated timber wall building," *Earthq. Eng. Struct. Dyn.* 51 (7), 1677–1696. https://doi.org/10.1002/eqe.3633
17. **Chen Z. and M. Popovski**, (2020) "Mechanics-based analytical models for balloon-type cross-laminated timber (CLT) shear walls under lateral loads," *Eng. Struct.* 208, 109916. https://doi.org/10.1016/j.engstruct.2019.109916
18. **Li Z., Wang X., & He M.**, (2020) "Experimental and analytical investigations into lateral performance of cross-laminated timber (CLT) shear walls with different construction methods," *J. Earthq. Eng.*, 1–23. https://doi.org/10.1080/13632469.2020.1815609
19. **M. Shahnewaz, C. Dickof, and T. Tannert**, (2021) "Seismic behavior of balloon frame CLT shear walls with different ledgers," *J. Struct. Eng.* **147** (9), 04021137. https://doi.org/10.1061/(ASCE)ST.1943-541X.0003106
20. **T. You, B. T. Teweldebrhan, W. Wang, and S. Tesfamariam**, (2023) "Seismic loss and resilience assessment of tall-coupled cross-laminated timber wall building," *Earthq. Spectra* **39** (2), 727–747. https://doi.org/10.1177/87552930231152512
21. **H. Asgari, T. Tannert, M. M. Ebadi, C. Loss, and M. Popovski**, (2021) "Hyperelastic hold-down solution for CLT shear walls," *Constr. Build. Mater.* **289**, 123173. https://doi.org/10.1016/j.conbuildmat.2021.123173
22. **L. Pozza, A. Saetta, M. Savoia, and D. Talledo**, (2018) "Angle bracket connections for CLT structures: Experimental characterisation and numerical modelling," *Constr. Build. Mater.* **191**, 95–113. https://doi.org/10.1016/j.conbuildmat.2018.09.112
23. **V. Rinaldi, D. Casagrande, and M. Fragiacomo**, (2022) "Verification of the behaviour factors proposed in the second generation of Eurocode 8 for cross-laminated timber buildings," *Earthq. Eng. Struct. Dyn.*. https://doi.org/10.1002
24. **V. Rinaldi, D. Casagrande, C. Cimini, M. Follesa, and M. Fragiacomo**, (2021) "An upgrade of existing practice-oriented FE design models for the seismic analysis of CLT buildings," *Soil Dyn. Earthq. Eng.* **149**, 106802. https://doi.org/10.1016/j.soildyn.2021.106802
25. **EN 12512:2001** *(2002).* Timber Structures – Test Methods – Cyclic Testing of Joints Made with Mechanical Fasteners, *CEN, Brussels, Belgium.*
26. **Mpidi Bita H., Tannert T**. (2018) Numerical optimisation of novel connection for cross-laminated timber buildings, *Eng. Struct. 175 273– 283.* https://doi.org/10.1016/j.engstruct.2018.08.020

## АНАЛІЗ РОБОТИ НА ЗСУВ З'ЄДНАНЬ ЗІ ШПОНКАМИ З ДЕРЕВЕНИ ТВЕРДИХ ПОРІД У СТИКАХ СТІН З ПКД ПАНЕЛЕЙ

*Андрій БІДАКОВ;*
*Оксана ПУСТОВОЙТОВА;*
*Вячеслав КОСМАЧЕВСЬКИЙ;*
*Юрій КУЗУБ*

**Анотація.** Розробка багатоповерхового дерев'яного будівництва вимагає контролю та мінімізації деформацій як елементів каркаса будівлі, так і їх з'єднань. Це особливо важливо для будівель з CLT-панелей або ПКД панелей, коли оптимізація каркаса будівлі та мінімізація витрат матеріалів зводиться до будівництва частин стінової панелі над віконними та дверними отворами у вигляді окремих деталей. Також поділ ПКД панелей на дрібні фрагменти або деталі каркасу часто проводиться для спрощення логістики чи зменшення залишків

матеріалу при розкрої великої плити у виробництві. Така деталізація каркасу вимагає досягнення монолітного з'єднання відправних марок ПКД панелей, що вимагає великої кількості гвинтів, що є надзвичайно дорогим, особливо для країн Східної Європи. Деформативність з'єднань дерев'яних конструкцій мінімальна в клейових з'єднаннях та з'єднаннях на вклеєних стрижнях. Аналіз жорсткості та міцності з'єднань між ПКД панелями на пластинчастих конекторах чи шпонках з деревини твердих листвяних порід і результати випробувань, розглянуті в цій публікації, доводять ефективність та перспективність цього типу з'єднання. Це особливо сьогодні актуально при використанні сучасних методів різання деталей каркаса з високою розмірною точністю на автоматизованих лініях різання, яке відбувається у відповідності до завантаженої моделі каркасу будівлі. Також шпонкові з'єднання можуть використовуватись у стиках колон чи балок з ПКД панелями для забезпечення сумісної роботи те економії великої кількості нагельних з'єднувальних елементів. Проведені експериментальні дослідження виконувались з урахуваннях аналогічних досліджень в інших постановках європейських дослідників і порівнювались з отримані результати (Україна).

У публікації представлені результати випробувань, проведених з дубовими шпонковими у стиках CLT-панелей, та порівнюються з результатами аналогічних досліджень з використанням алюмінієвих шпонкових з'єднань та з'єднань з великою кількістю гвинтів у з'єднаннях з накладками. Аналіз деформаційної поведінки з'єднань у каркасах багатоповерхових будівель з CLT-панелей вимагає особливої уваги та пошуку нових рішень для з'єднань та їх компонентів. Наразі шпонкові з'єднання різних виробників пропонуються з різними геометричними варіаціями, що спрощують їх монтаж під час складання каркаса будівлі, а іноді навіть дозволяють затягувати з'єднувані компоненти за допомогою клиноподібних поверхонь.

**Ключові слова**: стінові панелі; поперечно-клеєна деревина; шпонкові з'єднання; зсув з'єднань; жорсткість стиків.

***Received:*** *November 03, 2025.*
***Accepted:*** *December 05, 2025.*

ISSN 2522-4182

DOI: 10.32347/2522-4182.17.2025.79-91
UDC 624.011.1:699.812

# FIRE RESISTANCE DESIGN ANALYSIS FOR STRUCTURAL CONNECTIONS ACCORDING TO EUROCODE

*Liudmyla LAVRINENKO[1], Liudmyla AFANASIEVA[2], Vitalii TONKACHEIEV[3]*

[1,2,3] Kyiv National University of Construction and Architecture
31, Povitrianykh Syl Ave, Kyiv, Ukraina, 03037
[1] ludmila.lavrinenko@gmail.com, http://orcid.org/0000-0001-5601-0943
[2] afanasieva2709@gmail.com, http://orcid.org/0000-0001-6237-2609
[3]tonkacheiev.vg@knuba.edu.ua, https://orcid.org/0000-0002-1010-8440

**Abstract**. Correct assessment of fire resistance of building structures requires accurate mechanical modeling of material behavior, taking into account thermal creep in the stress-strain response of materials at elevated temperatures. Finite element models of fire-resistant structures using different types of coatings have been developed [6]. Using the example of timber nodal joints, the article presents a review of works and models of steel dowels. The review is based on experimental results presented in the literature and their application to models of nodal joints at elevated temperatures. The works considered in the review provide extensive factual material on the bearing capacity of a dowel joint and its stiffness. Today, these issues are actively studied by many researchers. A two-component model was analyzed in detail, on the basis of which a series of samples were compared under normal operating conditions and under fire conditions, and the corresponding stress coefficients for different degrees of fire exposure were obtained. The limit states of a dowel joint are the loss of strength due to plastic bending of the dowel in the socket when embedding wood. The analysis of numerical experiments makes it possible to verify the validity of the current design rules and standards [1, 2] and national design standards implemented in them [3-5], and also allows to identify shortcomings and limitations of the application of fire resistance design rules for this type of connection. The results emphasize the need to include the actual operation of dowels in the connections of wooden structures in modern advanced structural calculations for fire resistance and in engineering practice. The review considers an example of a symmetrical connection with two shear planes, the implementation of the finite element model and the results obtained. Today, the use of calculation methods for assessing fire resistance is associated with the introduction of the latest software computing complexes, in particular, such as LIRA-SAPR, Ansys Mechanical, Comsol Multi-physics, IdeaStatica and others [6, 8, 9]. New research allows us to improve information bases for creating tools for numerical modeling of complex structures in the direction of harmonizing international and national standards of Ukraine in the field of construction, taking into account the actual stiffness of timber structure nodes under temperature conditions [7, 39].

**Liudmyla LAVRINENKO**
Associate Professor, Department of Steel and Timber Structures,
Assoc. Prof., PhD (Tech. Sci.)

**Liudmyla AFANASIEVA**
Associate Professor, Department of Reinforced Concrete and Stone Structures,
Assoc. Prof., PhD (Tech. Sci.)

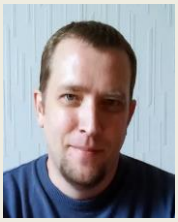

**Vitalii TONKACHEIEV**
Associate Professor, Department of Steel and Timber Structures,,
Assoc. Prof., PhD (Tech. Sci.)

**Keywords:** building structures joints; dowelled connection; fire resistance; Eurocode2; Eurocode5.

## INTRODUCTION

The progress of scientific research on the fire resistance of building structures has accelerated in recent years. This is due, not least, to the fact that fire safety is moving from regulatory [1-5] to operational solutions [6-8]. Software tools have been developed and successfully used to assess the fire resistance of steel and reinforced concrete structures. Using the "LIRA-SAPR" software (Ukraine), a method for numerically studying the fire resistance of reinforced concrete structures using non-stationary temperature fields in concrete and reinforcement, which implements the fire regime using the "Heat Conductivity" system [6], Finite element models of fire-resistant structures using various types of coatings have been developed to assess the fire resistance of structures, determine the fire resistance limit of reinforced concrete structures with changed stiffness characteristics due to the influence of elevated temperatures, as well as the temperature distribution in the nodes of the models. The library of finite element models of thermal conductivity contains one-dimensional, flat and spatial elements. Nonlinear thermal conductivity, implemented for rod, plate and volumetric finite elements, allowed us to estimate the thermal conductivity coefficient, take into account the change in material characteristics due to the influence of temperature heating in
accordance with the requirements of [3].

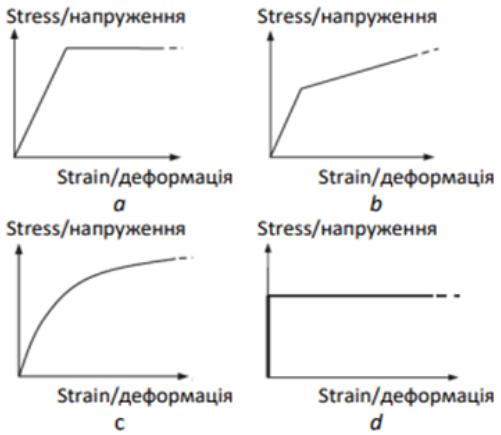


This ensures structural adequacy at all stages of the life cycle of the structure. The functional requirement is to ensure the necessary load-bearing capacity for a sufficient time for safe evacuation and rescue [4]. The specifics of the operation of wooden structures require further study of the characteristics of materials under the influence of fire and improvement of calculation models. One of the key features of the implementation of fire design standards based on characteristics is the assessment of the fire resistance of the structure as a whole and its nodal connections, hence the need to study the thermomechanical behavior of the material at elevated temperatures and develop material models suitable for numerical implementation [10].

For adequate modeling of the structure, the work of the connection is very important. In the case of wooden structures, they are semi-rigid, and their behavior affects the overall stress distribution, the consideration of which leads to a more realistic structural modeling.

The calculation schemes of the considered building structures are required to be as close as possible to the real structure, taking into account the peculiarities of its functioning.

Calculation models are especially complex in relation to wooden structures. They are somewhat conditional, requiring consideration of both the statistically random anisotropic physical and mechanical characteristics of materials and the nature of the operation of different materials in the contact zones.

Depending on the purpose of the calculation, both linear-elastic models and models taking into account geometric and physical nonlinearity can be considered (Fig. 1).

**Fig. 1** Alternative stress–strain relationships commonly used in non-linear analysis:
a - elastic-perfectly plastic; b - elasto-plastic with strain hardening; c - continuously varying; d - rigid plastic behaviour

**Рис. 1** Альтернативні залежності напру-ження-деформації, що зазвичай використо-вуються в нелінійному аналізі: а - ідеально пружно-пластичні; б - пружно-пла-стичні з деформаційним зміцненням; в – безпе-рервно змінні; г - жорстко-пластичні

For calculations of pin-type connections, calculation with limit state analysis for fully plastic behavior of materials is mainly used.

**The purpose of the article** is to analyze the methods for calculating the stressed-deformed state of dowel joints of wooden structures, taking into account non-stationary temperature fields in wood and dowels for a standard fire temperature regime, which make it possible to evaluate the real operation of the connection components and the fire resistance of the joints.

**The materials and methods of research** consist in studying the results of experimental and theoretical research in comparison with the existing theoretical base.

**The object of research** is the directions, methods and experimental data obtained on the basis of the analysis of scientific sour.

## PROBLEM STATEMENT AND RESEARCH ANALYSIS

For room temperature design, the modern design methodology of the Eurocode 5 design code [2] is based on the theory of plastic deformations and the results of Johansen [11] and uses the calculation of the plastic limit state to determine the bearing capacity of the connection [12, 13] (Fig. 2). Further studies are based on the theory of plastic deformations (European Yield Model EYM). With changes and adaptations, this theory is the basis of the design codes for timber structures Eurocode (EC5), similar to the content of the national design codes of the USA (NDS), Canada (CSA 086), which are developed on the basis of EYM.

Dowel joints are theoretically considered semi-rigid [14]. This takes into account the phenomenon of initial slippage, which occurs in joints with a fastener fit and continues until contact with the hole is achieved. Failure at this stage is brittle and is considered unacceptable. In contrast, viscous work (i.e., plastic with significant deformations) is characteristic of well-designed joints [15, 16, 17].

For the calculation of doweis in [2], expressions are proposed that are a function of the density of the timber and the diameter of the fastener. These expressions for the work of the dowel do not take into account some effects, such as the angle of inclination of the load to the grains or the geometry of the joint, which are fundamental for accurate modeling.

The calculation formulas are analyzed in detail by us in the review [29].

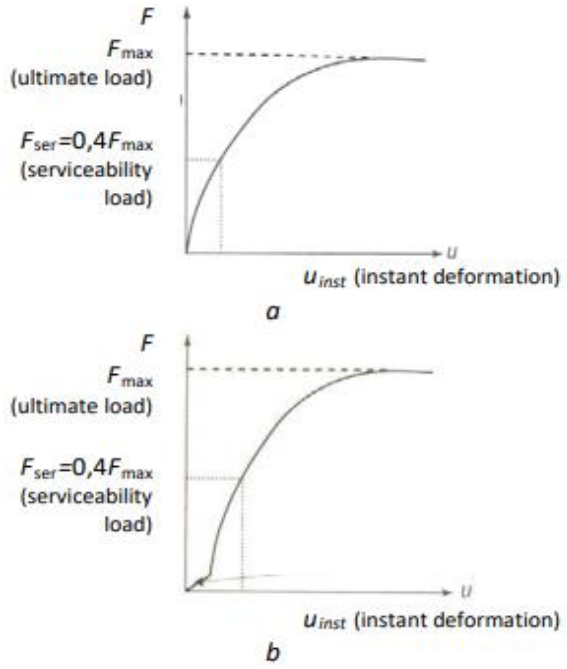


**Fig. 2** Typical "load - shear deformation" relationships for dowel-type connections: a - on screws and nails; b - on bolts and dowels

**Рис.2** Типові залежності "навантаження - деформація зсуву" для з'єднань нагельного типу: а - на шурупах та цвяхах; б - на болтах та нагелях

Numerical simulations of timber joints at room temperature have been carried out by many researchers [17, 18, 19]. In [20, 21, 22] the joints were modelled as three-dimensional, but it was shown that their behaviour can also be analysed using two separate two-dimensional approaches. The behaviour of the timber (perpendicular to the tongue) is actually modelled by two-dimensional finite element models [23-25], while the behaviour of the tongue (parallel to the tongue) is actually modelled by beam finite elements with elastic properties relative to the timber [13, 26, 27, 28].

Examples of finite element modeling of timber joints under fire loading are given in [29, 30] and in [29] a mechanical analysis of the joint is also performed. The conclusion made in [31] is that the influence of the number of

fasteners on the calculation of the load-time-to-failure curves is very small. Thus, the use of a single dowel for modeling timber dowel-type joints under fire should provide accurate results.

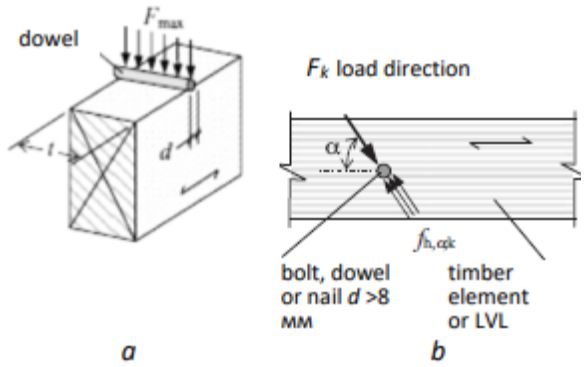


**Fig. 3** Modeling the interaction of timber and dowel elements
**Рис.3** Моделювання взаємодії деревини та нагеля за ЕС5

Wood is a consumable material. However, complete combustion of structural elements is very rare. The development of a growing layer of charcoal acts as an insulator and protects the inner core, but at the same time reduces the efficiency of the transverse surface for transferring loads.

The results of the paper [32] provide an opportunity to analyze the behavior of both timber and dowel under conditions of thermal flow. To achieve this goal, finite element simulations were performed using the specialized finite elements SAFIR [33].

The component model considers the connection as a set of individual components. Each component in the solution proposed here is modeled separately, with its own stiffness and strength. When the connection is loaded, the force distribution in the connection is determined by the relative stiffness/strength and position of the individual components [34]. For a dowel connection with a single fastener, two components can be clearly identified: the wooden element and the steel dowel.

To confirm the modeling results, the authors conducted wood crushing tests in accordance with standard requirements (Fig. 4).

Test results showing a displacement curve are given, for example, in [13, 18, 35]. When the force is applied along the fibers, the ultimate strength and initial stiffness are higher, while the stiffness after plastic deformation is lower than when the force is perpendicular to the fibers [36].

In case the required experimental test results are not available, it is acceptable to use characteristic values, since the model is used for theoretical research, and not for the analysis of a specific wood species or sample.

The materially nonlinear behavior of the dowel cross-section is described discretely using a fiber model, where the cross-section of a steel dowel is considered as a set of fibers, each of which has a one-dimensional stress-strain relationship. In [32], an elastic-ideally plastic stress-strain relationship was considered for the material model of dowels at room temperature.

The scheme proposed in the work is presented in Fig. 5 for the case of a double shear connection. A typical finite element modeling of the connection model uses a series of beam elements to discretize the dowel on an elastic support at each node according to the behavior of the timber.

In paper [32] the properties of the timber components are determined by assuming that these components are continuously distributed along the length of the dowel (the concept of a beam on an elastic base). In the finite element modeling, the strength and stiffness properties of the timber components are determined by the embedding strength.

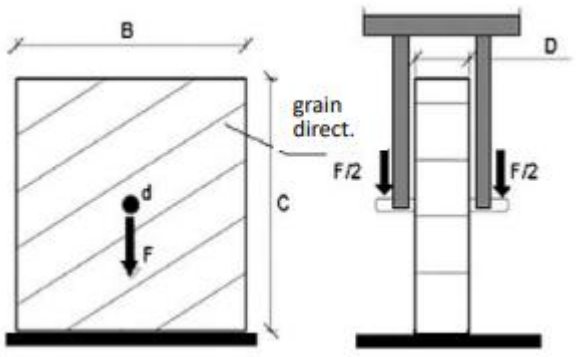


**Fig. 4** Test principle to EN383
**Рис. 4** Схема стандартних випробувань на зминання в отворі

Strength and stiffness characteristics were obtained for the simulated specimens at room

temperature and compared with the results from the Hankinson expressions for the fiber inclination in the connection [2], as well as with the experimental results from [18, 35]. The calculated force-displacement curves are mostly within the range of the experimental results. Both stiffness and strength were simulated accurately.

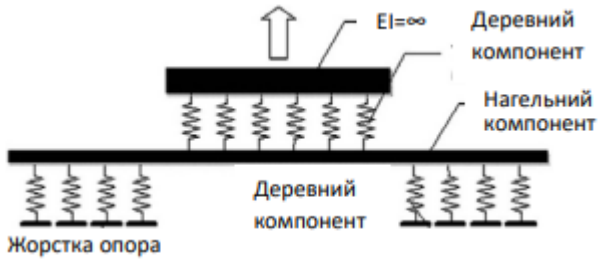


**Fig. 5** Model of a single fastener connection
**Рис.5** Модель однонагельного зєднання

The numerical model of the steel dowel is compared with the experimental one for a symmetric connection (double shear) [18]. The numerical results are in good agreement with the experimental results both in terms of initial stiffness and ultimate strength, both for the case of a load parallel to the fibers and for the case of a transverse member loaded perpendicular to the fibers.

In all cases, the difference between the model failure loads at plastic failure loads is less than 5%. The failure modes of the numerical model are also in agreement with the plasticity theory and Eurocode 5.

In our review, we examine in detail the model presented in [32]. It fully and exhaustively presents both the considerations regarding the node model and the results of calculations, and the obtained results are compared with the experimental ones.

The analysis of the model at elevated temperatures was performed in work [32].

The use of the component model for timber connections under fire loading is performed in a two-step approach: first, a three- dimensional thermal analysis of the connection is carried out that allows the determination of the temperature field in fasteners and timber; second, the component model previously described for the connection is used to determine the mechanical behaviour of the connection.

The three-dimensional thermal analyses of the connections were carried out with material thermal properties defined in Eurocodes [23–25] using the program SAFIR. It is assumed that timber and steel will remain connected during thermal analysis and that no gap develops at the interface.

A different finite element mesh was used for the thermal analysis. In this case, the temperature of the model components was read from the thermal model for further mechanical calculation.

The reduction in the strength and stiffness parameters in compression was taken into account by the coefficients given in Eurocode 5.

The dependences of strength and deformability for different temperatures were constructed.

The non-linear mechanical properties at elevated temperatures for the pins were obtained from the recommendations of Eurocode 3.

.

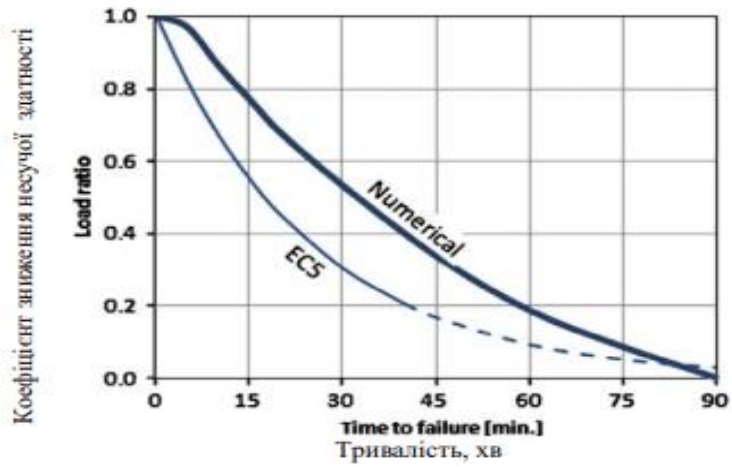


**Fig. 6** Fire resistanc e for a single dowel connection [32]
**Рис.6** Вогнестійкість однонагельного з’єднання [32]

Thermal analysis was performed using the finite element program SAFIR for isolated fastening using a finite element mesh. It is assumed that the connection has symmetry with respect to the axis of the dowel. The model assumes an ideal thermal contact at the interface of wood and steel, and heating is assumed to be one-sided

The temperatures along the axis of the dowel were determined at two different locations: for the steel dowel at the interface between the dowel and the wood, uniform over the entire diameter, and for the wood at a distance of 0.5d from the dowel surface.

It is important that the stiffness of the wood will depend on the temperature profile in the direction perpendicular to the dowel.

Since the temperature in the wood varies with the distance from the dowel, the spring can be considered as a series of springs with different stiffness properties. For simplicity, the model of the wood component along the dowel was used as an equivalent stiffness, i.e. a single temperature.

By calibration, it was found that a distance equal to half the diameter gives a good correlation with the experimental results.

The temperature distribution in the wood at the interface with the pin is obtained by calculation. Temperature curves are given, which are then entered into the component model, and the material properties are adapted accordingly.

After 60 minutes, the joint is still capable of withstanding 20% of its initial load-bearing capacity. The curve obtained from the model is compared with the curve of load factor versus time to failure according to Eurocode 5. The graph shows a fire resistance limit of 40 minutes. Experimental results give a longer time, but it has been shown in [31] that the Eurocode 5 model is a conservativeculation of load-time curves to failure is very small. The comparison showed the correspondence between the numerical and experimental results.

In work [31], a conclusion was made about the sufficient accuracy of approximation, so a longer time to failure can be expected.

The joint was chosen so that all failure modes typical of a timber joint in double shear can be observed: a dowel with two plastic hinges; a single hinge in the central member; and compression of the timber. The behaviour of a double shear symmetrical joint is illustrated in Fig. 7 - 9. The graphs show dotted lines that correspond to the limit of complete charring of wood at time periods. The vertical solid line corresponds to the boundary of the central and lateral elements. The graphs are plotted to the axis of symmetry. Distribution of moments along the dowel (Fig. 7).

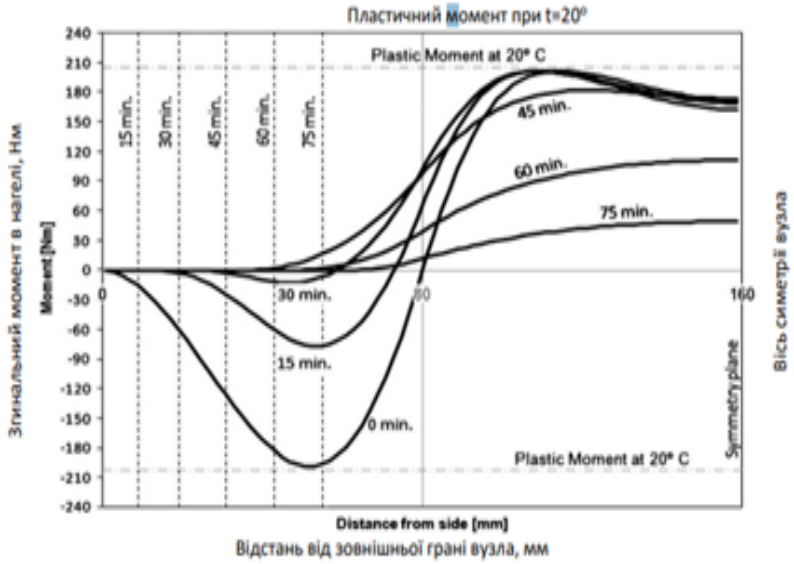


**Fig. 7** Final moment diagrams in the dowel at times 0, 15, 30, 45, 60 and 75 min [32]

**Рис.7** Епюри згинальниз моментів в нагелі у проміжки часу 0, 15, 30, 45 та 75 хв. [32]

At normal temperature, two hinges are fixed in the dowel. When the temperature increases, the moments are redistributed. When the moment in the lateral elements decreases, the fracture occurs in the middle element and a hinge is formed in the middle element. A decrease in the

thickness of the lateral elements is observed and the fracture mode changes again. The moment in the central element decreases again, and the final fracture occurs from the crushing of the wood without the formation of a plastic hinge.

Fig. 8 shows the movement of the dowel, the location of the plastic hinge is clearly visible. The fracture of the wood in the zone of final displacements is observed. Fig. 9 show the stresses in the timber component at the corresponding time intervals. When the temperature increases above 20 degrees, the strength of the wood decreases; the plateau is not constant.

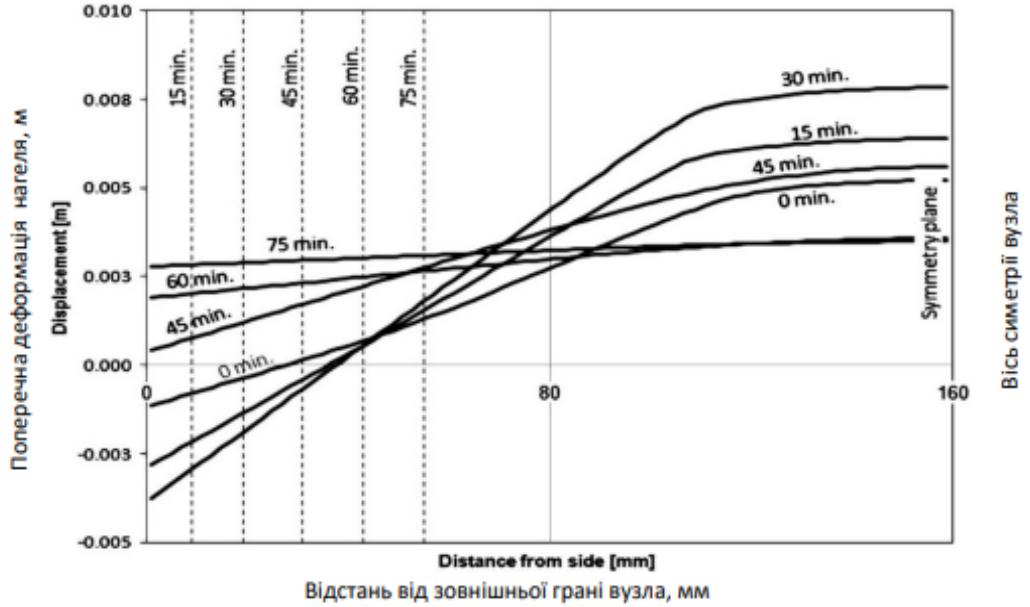


**Fig. 8** Deformation of the dowel at failure at times 0, 15, 30, 45, 60 and 75 min [32]
**Рис.8** Поперечна деформація нагеля у проміжки часу 0, 15, 30, 45 та 75 хв. [32]

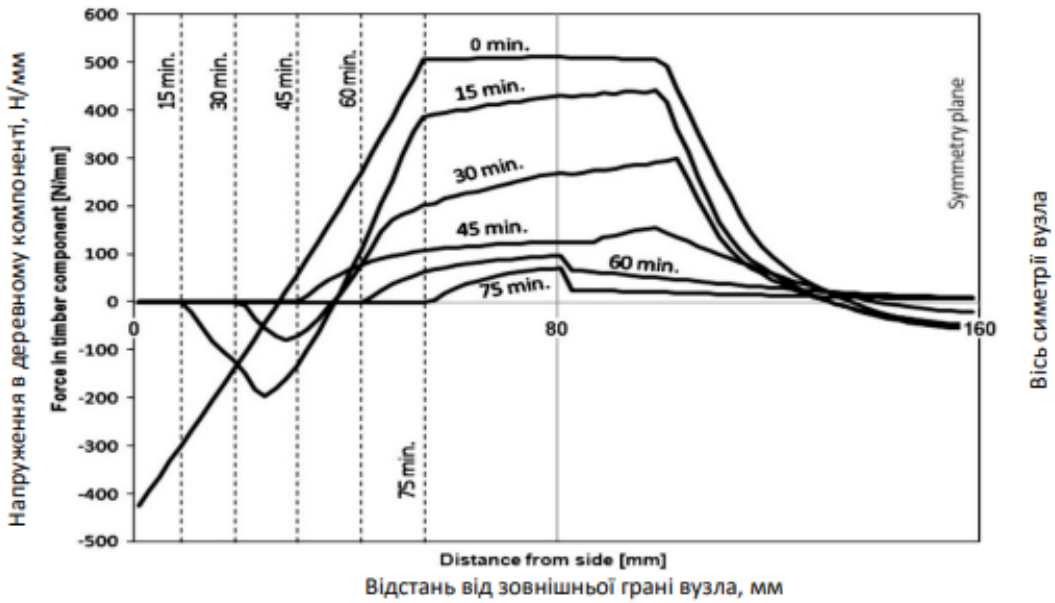


**Fig. 9** Stresses at timber component at times 0, 15, 30, 45, 60 and 75 min [32]
**Рис.9** Епюри напружень при зминанні деревини в отворі з'єднання у проміжки часу 0, 15, 30, 45 та 75 хв. [32]

The obtained numerical results were compared with experimental data. For this purpose, data from works [37] and [31] were used. In experimental studies on multi-nail joints, every fourth nail was made as a bolt to fix the position of the elements during fire tests.

The methodology used for fire resistance analysis was described earlier: first, a thermal analysis is performed, and then the obtained temperatures are applied to the mechanical model. Numerical modeling was performed using a single fastener, since, as noted in [31], the influence of the number of fasteners on the cal the model and the clarify the main mechanisms of the joint obtained.

The model considered is relatively simple, but at the same time validated. It provides specific values of the bearing capacity of the connection under fire exposure and fire resistance values, which are somewhat higher than those given in the standards [2] (Fig. 6).

The theoretical results and directions of experimental work presented are evidence of high research activity in the direction of improving constructive solutions and standards for designing fire resistance of structural components.

Today, the use of computational methods for assessing fire resistance is associated with the introduction and successful operation of the latest software computing complexes, in particular, such as LIRA-SAPR, Ansys Mechanical, Comsol Multi-physics, IdeaStatica [6, 8, 9] and others. New research allows improving information bases for creating tools for numerical modeling of fire resistance of nodal connections on the way to harmonizing international and national standards of Ukraine in the field of construction [7, 39] while taking into account the actual stiffness of wooden structural components under temperature conditions.

## CONCLUSIONS

1. A review of publications on the study of the fire resistance of dowel-type joints was conducted. The results obtained were verified by experimental studies.
2. New models and calculation schemes were considered, which, based on classical approaches, allow for a more accurate determination of the actual stress-strain state of multi-component dowel joints.
3. The obtained research results analysed in the review allow for a refinement of approaches to the calculation of mass types of dowel joints, determination of their bearing capacity resources, and improvement of the information base for further creation of tools for numerical modelling of joint joints on the path of harmonization of international and national standards of Ukraine in the field of construction, taking into account the actual stiffness of wooden structure joints under temperature influences.

## REFERENCES


1. **DSTU-N B EN 1993-1-2:2010**. Yevrokod 3. Proektuvannia stalevykh konstruktsii. Chastyna 1-2. Zahalni polozhennia. Rozrakhunok konstruktsii na vohnestiikist (EN 1993-1-2:2005, IDT) – *Chynnyi vid 2014-01-01 – K.: Minrehion Ukrainy, 2012. – 106 s. – (Natsionalnyi standart Ukrainy)* [in Ukrainian]
2. **DSTU-N B EN 1995-1-2:2012** Yevrokod 5. Proektuvannia derev`ianykh konstruktsii. Chastyna 1-2. Zahalni pravyla. Rozrakhunok konstruktsii na vohnestiikist (EN 1995-1-2:2004, IDT) – *Chynnyi vid 2013-07-01 – K.: Minrehion Ukrainy, 2013. – 96 s. – (Natsionalnyi standart Ukrainy)* [in Ukrainian]
3. **DSTU-N B EN 1992-1-2:2012**. Yevrokod 2. Proektuvannia zalzobetonnykh konstruktsiy. Chastyna 1-2. Zahalni polozhennia. Rozrakhunok konstruktsiy na vohnestiikist (EN 1992-1-2:2004, IDT) – *Chynnyi vid 2013-07-01 – K.: Minrehion Ukraïny, 2012. – (Natsionalnyy standart Ukraïny)* [in Ukrainian]
4. **DBN V .1.1-7:2016**. Pozhezhna bezpeka obiektiv budivnytstva. Zahalni vymohy: – chynni vid 2017-06-01. – *K.: Minrehion Ukrainy, 2017. – 47 s. – (Derzhavni budivelni normy)* [in Ukrainian]
5. **DSTU-N B EN 1991-1-2:2010** Yevrokod 1. Dii na konstruktsii. Chastyna 1-2. Zahalni dii. Dii na konstruktsii pid chas pozhezhi (EN 1991-1-2:2002, IDT) – *Chynnyi vid 2013-07-01 – K.: Minrehion Ukrainy, 2011 – 81 s. – (Natsionalnyi standart Ukrainy)* [in Ukrainian]
6. **Barbash M., Kovalov F., & Romashkina M.** (2022) Calculated assessment of fire resistance of fireproof reinforced concrete building structures by pc LIRA-SAPR tools *Building*

*Constructions. Theory and Practice, (12), 53 – 64* [in Ukrainian] https://doi.org/10.32347/2522-4182.12.2023.53-64

7. **Fesenko O.A., & Momotiuk D.S.** (2021). Fire Resistance Design of Timber Structures According to Eurocode 5. *Tenden-tsii ta vyklyky suchasnoi ahrarnoi nauky: teoriia i praktyka: materialy III mizhnarodnoi naukovoi internet-konferentsii (m. Kyiv, 20-22 Zhovtnia 2021 r.). – K.: NUBiP Ukrainy,. 353* [in Ukrainian]
8. **Khitskov K., & Lavrinenko L.** (2023). Fire resistance design analysis for steel connections using specialized 3d modeling software *Building Constructions. Theory and Practice, (12), 93 – 104* [in Ukrainian]. https://doi.org/10.32347/2522-4182.12.2023.93-104
9. **Fesenko O, Koliakova V., Dmytrenko Ye., & Momotiuk D.** (2022) Fire resistance analysis of bending timber structures according to Eurocode 5. *Building Constructions. Theory and Practice, (10), 94-107* [in Ukrainian]. https://doi.org/10.32347/2522-4182.10.2022.94-107
10. **Nekora V., Sidnei S., Shnal T., Nekora O., Lavrinenko L., & Pozdieiev S.(2021).**.Thermal effect of a fire on a steel beam with corrugated wall with fireproof mineral-wool cladding *Eastern-European Journal of Technologies. – No5/1(113), 24-32.* http://doi.org/10.15587/1729-4061.2021.241268
11. **Johansen K. W.** Theory of Timber Connections *IABSE, Publications No 9, Bern, Switzerland, 1949, pp. 249–262.*
12. **Sawata K, & Yasumura M**. (2003) Estimation of yield and ultimate strengths of bolted timber joints by nonlinear analysis and yield theory *Journal of Wood Scitnce.(49), 383–391* https://doi.org/10.1007/s10086-002-0497-3
13. **Marcolan A. C.. & Dias de Moraes J. P**. (2022). Probabilistic model for determining the failure time of steel-to-timber connections with multiple dowel-type fasteners exposed to fire. *Fire Safety Journal, (133), 103646* https://doi.org/10.1016/j.firesaf.2022.103646
14. **Santana C.L.O., Mascia N.T.**, Determination of fastener stiffness and application in the structural design with semi-rigid connections *Ninth World Conference on Timber Engineering, WCTE 2006, Portland, OR, USA.* https://www.researchgate.net/publication/290841810
15. **Kharouf N., McClure G., Smith I.**, (2003). Elasto-plastic modeling of wood bolted connections// *Comput. Struct. (81), 747–754* .https://doi.org/10.1016/S0045-7949(02)00482-0
16. **Racher P., Bocquet J.F.** (2005). Non-linear analysis of dowelled timber connections: a new approach for embedding modelling Electron. J. Struct. Eng. 5 1–9. https://doi.org/10.56748/ejse.546
17. **Gonzalez Fueyo J., Dominguez M., Cabezas J., Rubio M.**. Design of connections with metal dowel-type fasteners in double shear // *Materials and Structures, 2009.-42(3), pp.385–397.* https://doi.org/10.1617/s11527-008-9389-3
18. **Matsubara D., Teranishi M.,Wakashima, Y.** Elastic interaction in multiple bolted timber joints *Journa of WoodScience, 2022.*-68, 53. https://doi.org/ 10.1186/s10086-022-02060-3
19. **Laplanche K.** Etude du comportement au feu des assemblages de structures bois: approche expe´rimentale et mode´lisation: Ph.D. Dissertation, University Blaise Pascal (Clermont-Ferrand), France, 2006 [in French].
20. **Moses D.M., Prion H.G.L..** (2003). A three-dimen-sional model for bolted connections in wood, *Can. J. Civ. Eng. 30 (3) 555–567.* https://doi.org/10.1139/l03-009
21. **Patton-Mallory M., Smith F.W., Pellicane P.J..** (1998). Modeling bolted connections in wood: a three-dimensional finite-element approach, J. Test Eval. 26 (2) 115–124. https://doi.org/10.1061/(ASCE)0733-9445(1997)123:8(1054)
22. **Resch E., Kaliske M..** (*2010).* Three-dimensional numerical analyses of loadbearing behavior and failure of multiple double-shear dowel-type connections in timber engineering *Computers and Structures, 88 (3-4), p. 165–177.* https://doi.org/ 10.1016/j.compstruc.2009.09.002
23. **Erdodi L., Bodi I..** Experimental and numerical analysis of timber joints, in: C.A. Brebbia, W.P. de Wilde (Eds.). *High Performance Structures and Materials II, WIT Press, Wessex, UK, 2004.*
24. **Chen C.J., Lee T.L., Jeng D.S..** Finite element modeling for the mechanical behavior of dowel-type timber joints//*Comput. Struct. 81 (2003) 2731–2738.* https://doi.org/ 10.1016/S0045-7949(03)00338-9
25. **Reid M., Shin J., Quenneville P..** Capacity predictions for one and two-row bolted timber connections *Eighth World Conference on*

*Timber Engineering, WCTE 2004, Lahti, Finland.*

26. **Jiang L., Chui Y.H.**. Finite element model for wood-based floors with lateral reinforcements// *J. Struct. Eng.—ASCE 130 (7) (2004) 1097–1107.* https://doi.org/10.1061/(ASCE)0733-9445(2004)130:7(1097)
27. **Hwang K., Komatsu K..** Bearing properties of engineered wood products I: effects of dowel diameter and loading direction//*J. Wood Sci. 48 (2002) 295–301*.
28. **Daudeville L., Davenne L., Yasumura. M.** Prediction of the load carrying capacity of bolted timber joints//*Wood Sci. Technol. 33 (1999) 15–29*
29. **Lavrinenko L.I., Afanasieva L.V., & Tonkacheiev V.H.** (2023). Features of behavior and calculation of dowel timber joints with slotted-in plates according to EC5. *Building Constructions. Theory and Practice, (13), 123-138* [in Ukrainian] https://doi.org/10.32347/2522-4182.13.2023.123-138
30. **C. Erchinger, A. Frangi, A. Mischler.** Thermal investigations on multiple shear steel-to-timber connections//*Ninth World Conference on Timber Engineering, WCTE 2006, Portland, OR, USA*
31. **Konig J., Fontana M..** The Performance of Timber Connections in Fire—Test Results and Rules of Eurocode 5 *S. Aicher, H.-W. Reinhardt (Eds.), Proceedings of the RILEM Symposium Joints in Timber Structures, Stuttgart, Germany, 2001, pp. 639–648.*
32. **Cachim P., Franssen J.-M.**. Numerical modelling of timber connections under fire loading using a component model *Fire Safety Journal, 2009. - 44(6), pp. 840–853.* https://doi.org/10.1016/j.firesaf.2009.03.013
33. **Franssen J.-M..** SAFIR. A thermal/structural program modelling structures under fire// *Eng. J. AISC 42 (3) (2005) 143-158* DOI: 10.62913/engj.v42i3.856
34. **Jorissen A.** Double shear timber connections with dowel type fasteners - *Ph.D. Thesis. Delft University of Technology, Delft, Netherlands, 1999 –264 p.*
35. **Sawata K., Yasumura M..** Determination of embedding strength of wood for dowel-type fasteners// *J. Wood Sci. 48 (2002) 138–146.*
36. **Dorn M, Borst K, Eberhardsteiner J**. Experiments on dowel-type timber connections // *Engineering Structures, 2013. – 47, pp. 67–80* https://doi.org/10.1016/j.engstruct.2012.09.010
37. **Kruppa J., Lamadon T., Racher P.**. Fire resistance tests of timber connections, CTICM, INC-00/187-JK/NB – 2000. DOI: 10.1260/2040-2317.3.2.107
38. **Laplanche K., Dhima D., Racher P.** Predicting the behaviour of dowelled connections in fire: fire test results and heat transfer modelling // *Eighth World Conference on Timber Engineering, WCTE, 2004, Lahti, Finland.*
39. **Afanasieva L.V., Kulik T.R.** (2020) Harmonizatsiia mizhnarodnykh i natsionalnykh standartiv yak mekhanizm tekhnichnoho rehuliuvannia budivelnoi haluzi Ukrainy [Harmonization of International and National Standards as a Mechanism of Technical Regulation in the Construction Sector]./*Zbirnyk prats XIV Mizhnarodnoi naukovoi konferentsii «Nauka i osvita». Uhorshchyna, Khaidu-soboslo,3-7* [in Ukrainian]

## LITERATURE

1. **DSTU-N B EN 1993-1-2:2010.** Yevrokod 3. Proektuvannia stalevykh konstruktsii. Chastyna 1-2. Zahalni polozhennia. Rozrakhunok konstruktsii na vohnestiikist (EN 1993-1-2:2005, IDT) – [*Chynnyi vid 2014-01-01] – K.: Minrehion Ukrainy, 2012. – 106 s. – (Natsionalnyi standart Ukrainy)*
2. **DSTU-N B EN 1995-1-2:201**2 Yevrokod 5. Proektuvannia derev`ianykh konstruktsii. Chastyna 1-2. Zahalni pravyla. Rozrakhunok konstruktsii na vohnestiikist (EN 1995-1-2:2004, IDT) – [*Chynnyi vid 2013-07-01] – K.: Minrehion Ukrainy, 2013. – 96 (Natsionalnyi standart Ukrainy)*
3. **DSTU-N B EN 1992-1-2:2012.** Yevrokod 2. Proektuvannia zalzobetonnykh konstruktsiy. Chastyna 1-2. Zahalni polozhennia. Rozrakhunok konstruktsiy na vohnestiikist (EN 1992-1-2:2004, IDT) – [*Chynnyi vid 2013-07-01] – K.: Minrehion Ukraïny, 2012. – (Natsionalnyy standart Ukraïny)*
4. **DBN V .1.1-7:2016**. Pozhezhna bezpeka obiektiv budivnytstva. Zahalni vymohy: – [*chynni vid 2017-06-01]. – K.: Minrehion Ukrainy, 2017. – 47 s. – (Derzhavni budiv-elni normy)*
5. **DSTU-N B EN 1991-1-2:2010** Yevrokod 1. Dii na konstruktsii. Chastyna 1-2. Zahalni dii. Dii na konstruktsii pid chas pozhezhi (EN 1991-1-2:2002, IDT) – *[Chynnyi vid 2013-07-01] – K.: Minrehion Ukrainy, 2011 – 81 s. – (Natsionalnyi standart Ukrainy)*

6. **Barbash M., Kovalov F., Romashkina M**. (2022) Rozrakhunkove otsiniuvannia vohnestiikosti vohnezakhyshchenykh zalizobetonnykh konstruktsii zasobamy PK «LIRA-SAPR». *Budivelni konstruktsiï. Teoriia i praktyka, (12), 53 – 64* https://doi.org/10.32347/2522-4182.12.2023.53-64
7. **Fesenko O.A., Momotiuk D.S.** *(2021).* Rozrakhunok na vohnestiikist derevianykh konstruktsii za Yevrokod 5. *Tendentsii ta vyklyky suchasnoi ahrarnoi nauky: teoriia i praktyka: materialy III mizhnarodnoi naukovoi internet-konferentsii (m. Kyiv, 20-22 zhovtnia 2021 r.). – K.: NU-BiP Ukrainy, 35*3.
8. **Khitskov K., Lavrinenko L.** (2023) Analiz vuzliv metalevykh konstruktsii na vohnestiikist iz zastosuvanniam spetsializovanykh prohramnykh kompleksiv 3D-modeliuvannia. *Budivelni konstruktsiï. Teoriia i praktyka, (12), 93 – 104* https://doi.org/10.32347/2522-4182.12.2023.93-104
9. **Fesenko O, Koliakova V., Dmytrenko Ye., Momotiuk D.** (2022) Rozrakhunok na vohnestiikist derevianykh zghynalnykh konstruktsii za metodykoiu Yevrokodu 5. *Budivelni konstruktsiï. Teoriia i praktyka, (10), 94-107* https://doi.org/10.32347/2522-4182.10.2022.94-107
10. **Nekora V., Sidnei S., Shnal T., Nekora O., Lavrinenko L., Pozdieiev S.**. (2021).Thermal effect of a fire on a steel beam with corrugated wall with fireproof mineral-wool cladding *Eastern-European Journal of Technologies. – No5/1(113), 24-32.* http://doi.org/10.15587/1729-4061.2021.241268
11. **Johansen K. W.** Theory of Timber Connections *IABSE, Publications No 9, Bern, Switzerland, 1949,. 249–262.*
12. **Sawata K, Yasumura M.** (2003). Estimation of yield and ultimate strengths of bolted timber joints by nonlinear analysis and yield theory *Journal of Wood Scitnce.. (49), 383–391* https://doi.org/10.1007/s10086-002-0497-3
13. **Marcolan J. A. C., P. Dias de Moraes.** Probabilistic model for determining the failure time of steel-to-timber connections with multiple dowel-type fasteners exposed to fire. *Fire Safety Journal, 2022, Vol. 133, October 2022,103646* https://doi.org/10.1016/j.firesaf.2022.103646
14. **C.L.O. Santana, N.T.** Mascia, Deter-mination of fastener stiffness and applica-tion in the structural design with semi-rigid connections. *Ninth World Conference on Timber Engineering, WCTE 2006, Portland, OR, USA.* https://www.researchgate.net/publication/290841810
15. **Kharouf N., McClure G., Smith I.,** Elasto-plastic modeling of wood bolted connections // *Comput. Struct. 81 (2003) 747–754* https://doi.org/10.1016/S0045-7949(02)00482-0
16. **Racher P., Bocquet J.F**. Non-linear analysis of dowelled timber connections: a new approach for embedding modelling *// Electron. J. Struct. Eng. 5 (2005) 1–9.* https://doi.org/10.56748/ejse.546
17. **Gonzalez Fueyo J., Dominguez M., Cabezas J., Rubio M..** Design of connections with metal dowel-type fasteners in double shear // *Materials and Structures, 2009.-42(3), pp.385–397.* https://doi.org/10.1617/s11527-008-9389-3
18. **Matsubara, D., Teranishi, M., Wakashima, Y.** Elastic interaction in multiple bolted timber joints *// Journa of WoodScience,2022.-68, 53.* https://doi.org/2010.1186/s10086-022-02060-3
19. **Laplanche. K.** Etude du comportement au feu des assemblages de structures bois: approche expe´rimentale et mode´lisation: *Ph.D. Dissertation, University Blaise Pascal (Clermont-Ferrand), France, 2006* [in French].
20. **Moses D.M., Prion H.G.L**.. A three-dimensional model for bolted connections in wood, *//Can. J. Civ. Eng. 30 (3) (2003) 555–567.* https://doi.org/10.1139/l03-009
21. **Patton-Mallory M., Smith F.W., Pellicane P.J.** Modeling bolted connections in wood: a three-dimensional finite-element approach, *J. Test Eval. 26 (2) (1998) 115–124.* https://doi.org/10.1061/(ASCE)0733-9445(1997)123:8(1054)
22. **Resch E., Kaliske M..** Three-dimensional numerical analyses of loadbear-ing behavior and failure of multiple double-shear dowel-type connections in timber en-gineering // *Computers and Structures, 2010. - 88 (3-4), p. 165–177.* https://doi.org/2010.1016/j.compstruc.2009.09.002
23. **.Erdodi L, Bodi I..** Experimental and numerical analysis of timber joints, in: C.A. Brebbia, W.P. de Wilde (Eds.) *// High Performance Structures and Materials II, WIT Press, Wessex, UK, 2004.*
24. **Chen C.J., Lee T.L., Jeng D.S**. Finite element modeling for the mechanical behavior of dowel-type timber joints *//Comput. Struct. 81 (2003) 2731–2738.* https://doi.org/2010.1016/S0045-7949(03)00338-9

25. Reid M., Shin J., Quenneville P. Capacity predictions for one and two-row bolted timber connections *//Eighth World Confer-ence on Timber Engineering, WCTE 2004, Lahti, Finland.*
26. **Jiang L., Chui Y.H**. Finite element model for wood-based floors with lateral re-inforcements *// J. Struct. Eng.—ASCE 130 (7) (2004) 1097–1107.* https://doi.org/10.1061/(ASCE)0733-9445(2004)130:7(1097)
27. **Hwang K., Komatsu K**. Bearing properties of engineered wood products I: effects of dowel diameter and loading direction .*J. Wood Sci. 48 (2002) 295–301*.
28. **Daudeville L., Davenne L., Yasumura M**. Prediction of the load carrying capacity of bolted timber joints. *Wood Sci. Technol. 33 (1999) 15–29*
29. **Lavrinenko L.I., Afanasieva L.V., Tonkacheiev V.H**. (2023). Osoblyvosti roboty i rozrakhunku nahelnykh ziednan derevianykh konstruktsii z vriznymy plastynamy za EC5. *Budivelni konstruktsii. Teoriia i praktyka. (13), 123-138* https://doi.org/10.32347/2522-4182.13.2023.123-138
30. **Erchinger C., Frangi A., Mischler A**. Thermal investigations on multiple shear steel-to-timber connections *Ninth World Conference on Timber Engineering, WCTE 2006, Portland, OR, USA*
31. **Konig J., Fontana M.** The Perfor-mance of Timber Connections in Fire—Test Results and Rules of Eurocode 5 *S. Aicher, H.-W. Reinhardt (Eds.), Proceedings of the RILEM Symposium Joints in Timber Struc-tures, Stuttgart, Germany, 2001, pp. 639–648.*
32. **Cachim P., Franssen J.-M.** (2009) Numerical modelling of timber connections under fire loading using a component model *// Fire Safety Journal,. 44(6), 840–853*. https://doi.org/10.1016/j.firesaf.2009.03.013
33. **Franssen J.-M.. SAFIR.** (2005) A thermal structural program modelling structures under fire *// Eng. J. AISC 42 (3) 143-158* DOI: 10.62913/engj.v42i3.856
34. **Jorissen A.** Double shear timber connections with dowel type fasteners - *Ph.D. Thesis. Delft University of Technology, Delft, Netherlands, 1999 –264 p.*
35. **Sawata K., Yasumura M.** Determination of embedding strength of wood for dowel-type fasteners *// J. Wood Sci. 48 (2002) 138–146.*
36. **Dorn M, Borst K, Eberhardsteiner J.** Experiments on dowel-type timber connections *// Engineering Structures, 2013. – 47, pp. 67–80* https://doi.org/10.1016/j.engstruct.2012.09.010
37. **Kruppa J., Lamadon T., Racher P.** Fire resistance tests of timber connections, CTICM, *INC-00/187-JK/NB – 2000.* DOI: 10.1260/2040-2317.3.2.107
38. **Laplanche K., Dhima D., Racher P.** Predic-ting the behaviour of dowelled con-nections in fire: fire test results and heat transfer modelling *// Eighth World Conference on Timber Engineering, WCTE, 2004, Lahti, Finland.*
39. **Afanasieva L.V., Kulik T.R.** (2020) Harmo-nizatsiia mizhnarodnykh i natsionalnykh standartiv yak mekhanizm tekhnichnoho rehuliuvannia budivelnoi haluzi Ukrainy. *Zbirnyk prats XIV Mizhnarodnoi naukovoi konferentsii «Nauka i osvita». Uhorshchyna, Khaidusoboslo,3-7.*

## РОЗРАХУНОК НА ВОГНЕСТІЙКІСТЬ КОНСТРУКТИВНИХ ВУЗЛОВИХ З'ЄДНАНЬ ЗА ЄВРОКОД

*Людмила ЛАВРІНЕНКО*
*Людмила АФАНАСЬЄВА*
*Віталій ТОНКАЧЄЄВ*

**Анотація.** Належна оцінка структурної вогнестійкості будівельних конструкцій вимагає точного механічного моделювання роботи матеріалу з урахуванням термічної повзучості в реакції матеріалів на напруження-деформацію при підвищених температурах. Розроблені скінченно-елементні моделі вогнезахищених конструкцій із застосуванням різних типів покриттів [6]. З урахуванням особливостей деревини як конструкційного матеріалу на прикладі нагельних вузлових з'єднань представлено огляд робіт та моделей роботи вузлів.

Огляд проведено на основі наведених в літературі експериментальних результатів та їх застосування до моделей вузлових з'єднань в умовах підвищених температур. Розглядувані в огляді роботи надають великий фактичний матеріал стосовно моделей несучої спроможності з'єднання нагельного типу та його жорсткості.

На сьогодні ці питання досліджуються багатьма дослідниками. Детально аналізується двокомпонентна модель, на основі якої проведено порівняння серії зразків за нормальних умов експлуатації та в умовах пожежі, отримані відповідні коефіцієнти

напружень за різного ступеню вогневого впливу. Як граничні стани нагельного з'єднання розглядаються втрата міцності через пластичний згин нагеля в нагельному гнізді при зминанні деревини стінки отвору. Аналіз чисельних експериментів надає можливість переконатися в надійності чинних правил і норм проектування [1, 2] та імплементованих до них національних норм проектування [3-5], а також дозволяє виявити недоліки та межі застосування правил проектування вогнестійкості стосовно цього виду з'єднання. Результати підкреслюють необхідність включення дійсної роботи нагелів у з'єднаннях дерев'яних конструкцій до сучасних удосконалених структурних розрахунків на вогнестійкість та в інженерну практику. В огляді розглядається приклад симетричного з'єднання з двома площинами зсуву, реалізація скінченно-елементної моделі та отримані результати. На сьогодні застосування розрахункових методів оцінки вогнестійкості пов'язане із впровадженням новітніх програмних обчислювальних комплексів, зокрема таких як Ліра-САПР, Ansys Mechanical, Comsol Multi-physics, IdeaStatica та інші [6, 8, 9]. Нові дослідження дозволяють вдосконалити інформаційні бази для створення інструментів чисельного моделювання складних споруд на шляху гармонізації міжнародних і національних стандартів України в галузі будівництва при урахуванні дійсної жорсткості вузлів дерев'яних конструкцій в умовах температурних впливів.

**Ключові слова:** вузли будівельних конструкцій; нагельні з'єднання; вогнестійкість; Єврокод 2; Єврокод 5.

***Received:*** *October 19, 2025.*
***Accepted:*** *November 30, 2025.*

ISSN 2522-4182

DOI: 10.32347/2522-4182.17.2025.92-101
UDC 624.011

# FRAME STRUCTURES MADE OF COMPOSITE STEEL-TIMBER I-BEAMS WITH CORRUGATED STEEL WEBS

*Ihor SKLIAROV[1], Tetiana SKLIAROVA[2]*

[1,2] Kyiv National University of Construction and Architecture
31, Povitryanykh Syl Avenue, Kyiv, Ukraine, 03037
[1] skliarov.io@knuba.edu.ua, http://orcid.org/0000-0002-6150-5518
[2] skliarova.ts@knuba.edu.ua, http://orcid.org/0000-0001-9162-3999

**Abstract.** Frame structures made of composite steel–timber I-beams with transversely corrugated steel webs represent an innovative composite solution in the construction industry, combining the strength of steel with the environmental benefits of timber. These structures offer significant advantages, including a high strength-to-weight ratio, improved thermal and acoustic performance, enhanced seismic resistance, and high corrosion resistance. From an economic perspective, their use reduces overall construction costs due to lower self-weight, high manufacturability, and ease of installation. The combination of a thin profiled steel web and massive timber flanges ensures optimal utilization of the physical and mechanical properties of both materials, increasing the load-bearing capacity and stiffness of the elements while reducing their weight by a factor of 2–3 compared to traditional steel or solid timber beams The technological aspects of manufacturing elements of constant and variable cross-section are revealed, including the mechanical pressing of the corrugated wall into the wood and glue joints based on two-component epoxy mixtures. The ability to adjust the height of frame cross-sections allows for the optimization of material consumption depending on the bending moment diagram, which increases the efficiency of structures. The advantages of such structures in thermal insulation and prevention of thermal bridges, improved acoustic comfort, long-term durability, and corrosion resistance due to the use of galvanized steel are highlighted.

For Ukraine, the implementation of frame structures made of composite steel–timber I-beams is of strategic importance. They will contribute to increasing the competitiveness of domestic production, reducing dependence on imported materials and technologies, and supporting the development of the country's scientific and engineering potential. Further development and standardization of these structures open broad prospects for creating energy-efficient, reliable, and economically viable buildings, which is critically important in the context of infrastructure reconstruction and modernization.

**Ihor SKLIAROV**
Associate Professor, Department of Steel and Timber Structures,
Assoc. Prof., PhD (Tech. Sci.)

**Tetiana SKLIAROVA**
Aisistant of Department of Steel and Timber Structures

**Keywords:** frame structures; steel-timber beam; composite beam; HTS beam.

## INTRODUCTION

### Definition and concept of steel-timber composite structures

Frame structures made of steel-timber I-beams represent an advanced type of composite profile construction that integrates the properties of two different materials – steel and timber [11, 12].

Steel-timber I-beams are also known as "composite beams" or "HTS beams," indicating their belonging to the category of high-tech hybrid structures.

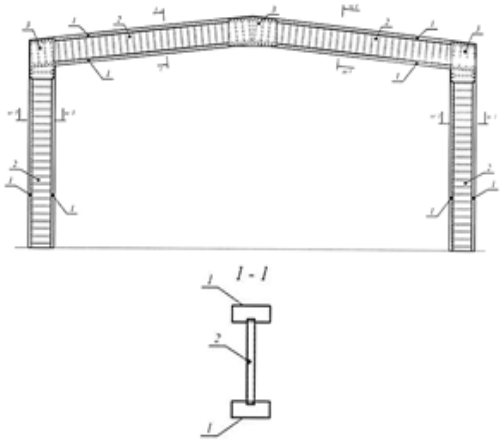


**Fig. 1** Frame made of composite steel-timber I-beams with a transversely corrugated steel web:
1 – timber beam flange;
2 – web made of steel profiled sheet with a trapezoidal corrugation shape;
3 – reinforcing plywood plates

**Рис. 1** Рама композитного металодерев'яного двотаврового перерізу з поперечно гофрованою стінкою:
1 – пояс з клеєної деревини;
2 – стінка з поперечно-гофрованим трапецевидним перерізом;
3 – підсилюючі дерев'яні накладки

The fundamental idea underlying these hybrid solutions is to use the strengths of each material to compensate for their individual weaknesses.

The principle of material optimization is central to the concept of steel-timber I-beams. Steel, especially in a thin corrugated form, is extremely effective in resisting shear forces, making it ideal for the beam web. Timber, in turn, in the form of solid or glued flanges, perfectly withstands significant normal stresses along the fibers and, due to its massiveness, provides the flexural-torsional stability of the beams [1, 2, 6, 13, 17, 23, 24, 25].

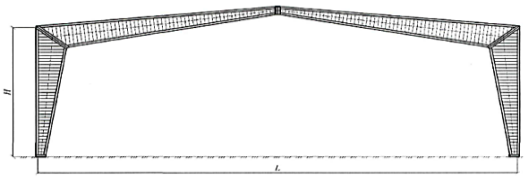

**Fig. 2** Variable cross-section frame made of composite steel-timber I-beams with a transversely corrugated steel web

**Рис. 2** Рама змінного перерізу, виготовлена з композитних метало-дерев'яних дво-таврових балок із поперечно гофрованою сталевою стінкою

Thus, each material is placed in the part of the cross-section where it functions with maximum efficiency under typical loads (bending moments and shear forces). This approach leads to the creation of a significantly more efficient overall cross-section compared to using either of these materials separately for the same structural function [5, 10]. This is a direct application of construction mechanics principles to achieve higher performance.

## Relevance and prospects for development in Ukraine

The current state of the construction market in Ukraine, amidst infrastructure damage and destruction, necessitates the development of new effective structural forms. These forms must have less dependence on production bases, allow for the use of local renewable materials, and ensure speed and ease of building erection [7, 8, 9]. Timber is one of the most accessible materials in this context. The Ukrainian market for metal structures is saturated with proposals from foreign enterprises, leading to capital outflow from the country and a gradual decline in scientific and engineering personnel. An urgent scientific and practical task is to increase the efficiency of metal structures so that domestic factories can compete with foreign manufacturers without fundamental re-equipment. This will allow the country to preserve production capacities, eliminate capital outflow, and maintain a high level of scientific potential in the industry.

## MATERIALS AND METHODS

**Components: transversely corrugated steel web and timber flanges**

The design of frame elements from composite steel-timber I-beams with a transversely corrugated steel web involves milling a longitudinal groove in the timber flanges of the I-beams (element 1 in Fig. 3), into which a steel profiled sheet is glued or pressed (element 2 in Fig. 3). The width of this groove precisely matches the height of the steel profile's corrugation.

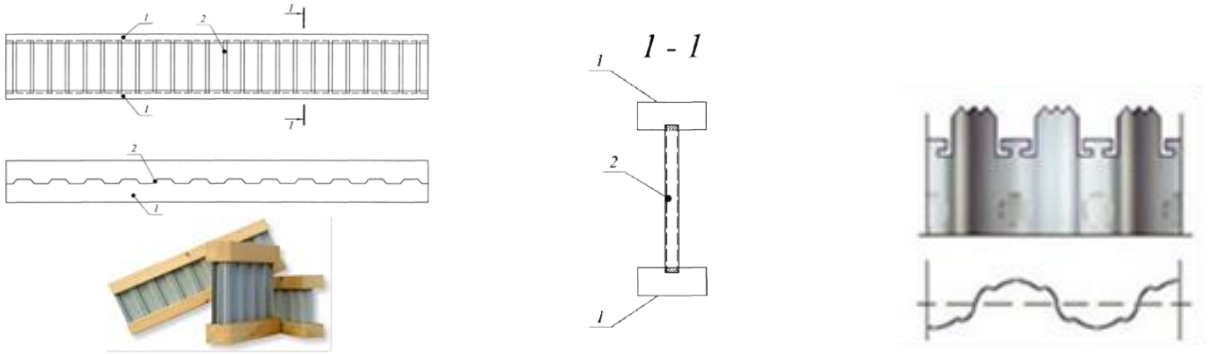


*a* *b* *c*

**Fig. 3** Construction of metal-and-timber I-beam: a – general appearance; b – cross-section; c – shape of the corrugated wall teeth for pressing into the wood belt.

**Рис. 3** Конструкція металодерев'яної двотаврової балки: a – загальний вигляд; b – поперечний переріз; c – форма зубців гофрованої стінки для запресовування в дерев'яний пояс.

Galvanized metal sheet is used as the web, most often made of S550 GD + Z steel according to DIN EN 10147. The thickness of the steel sheet is usually 0,5-0,8 mm. The performance of these beams largely depends on advanced manufacturing technologies and careful material selection. The thinness of the steel web (0,5-0,8 mm) is key to reducing weight, but it is the corrugated profile that provides its stability, and the specific steel grade ensures the necessary strength.

**Connection methods: mechanical pressing and adhesive bonding**

To ensure a reliable connection between the steel profiled sheet and the timber flanges, two main methods are proposed: mechanical pressing of the rigid corrugated steel web into the timber flanges or connection using a two-component epoxy adhesive that demonstrates good adhesion to both metal and timber surfaces [18, 19].

Assembly, pressing, or gluing processes are carried out on specialized technological lines, the length of which can vary depending on the required length of the elements (Fig. 4). The reliability of the composite structure's performance critically depends on the quality of the connection between steel and timber. Mechanical pressing relies on friction and form-fitting, while adhesive bonding is based on chemical adhesion. The use of specialized technological lines indicates industrial, high-precision manufacturing that can be adapted to various element lengths.

**Fig. 4** The technological line for connecting steel joints with timber belts. Photo by *WST Tragwerke GmbH*

**Рис. 4** Технологічна лінія для з'єднання сталевих елементів із дерев'яними поясами. Фото виконано *WST Tragwerke GmbH*

**Features of designing variable cross-section elements**

Steel-timber I-beams can be manufactured as elements of constant cross-section or as structures with variable web height. The web thickness, the height of the steel sheet corrugation, and the dimensions of the timber flanges are determined by calculation.

The ability to vary the cross-section height (and, consequently, stiffness and strength) along the length of the I-beam allows for precise structural optimization (Fig. 5).

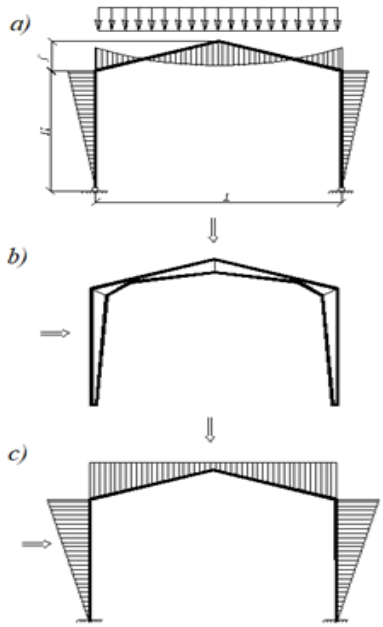


**Fig. 5** Design scheme (a) , construction (b) , and material diagram (c) of a variable cross-section frame.

**Рис. 5** Розрахункова схема (a), конструкція (b) епюра матеріалу (c) рами змінного перерізу

This means that material can be strategically placed in areas with the highest stresses (e.g., at supports or in the middle of the span for bending moments), leading to significant material savings compared to constant cross-section beams designed for peak loads. This principle of material distribution according to the bending moment diagram is directly applicable here, maximizing efficiency and minimizing waste [14, 15, 16, 20, 21, 22]

## RESULTS AND DISCUSSION

The use of a metal profiled web in timber I-beams leads to an increase in the load-bearing capacity and stiffness of the profile, as well as a reduction in the required cross-section height. From a purely static point of view, the use of steel-timber beams is expedient for spans from 7 to 24 meters, where a solid timber cross-section typically cannot be used.

**Reduction of self-weight and its consequences**

Due to the lower density of timber and the use of a thin corrugated web, the self-weight of composite I-beams is 2-3 times less than analogous metal and solid rectangular timber elements. This significantly reduces building construction costs. For example, a steel-timber beam measuring 510/80/140 has a weight of 0,117 kN/m, which corresponds to a self-weight load of 0,25 kN/m². For comparison, a glued laminated timber beam with a cross-section of 140x420 mm weighs 0,28 kN/m, which corresponds to a distributed load of 0,70 kN/m². This significant reduction in self-weight has a cascading effect on the entire construction project. It directly leads to reduced loads on foundations, allowing for the design of smaller, simpler, and cheaper foundation systems. Lighter elements also simplify and accelerate transportation and installation processes, potentially reducing crane usage time, labor costs, and overall project timelines. This provides systemic cost savings that go beyond just the cost of the beam material itself, making the overall construction project more economical and efficient.

**Thermal characteristics and insulation properties**

The very thin steel web (0,5 mm) gives steel-timber I-beams excellent properties for manufacturing thermal insulation building elements. Their insulating properties are significantly better than when using solid or laminated timber beams, especially if the formation of thermal bridges needs to be avoided. With proper insulation installation, condensation will not form in the web area.

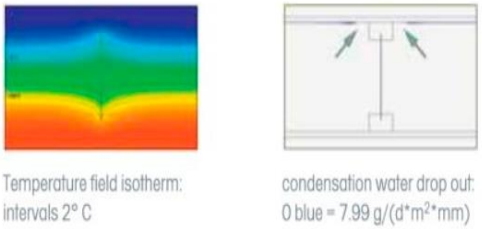


**Fig. 6** Thermal insulation of panels with metal-and-timber beams

**Рис. 6** Теплоізоляція панелей з металево-дерев'яними балками

Steel typically creates thermal bridges in composite structures. However, the thinness and corrugated shape of the steel web in this design, combined with the insulating properties of timber, effectively minimize this problem. The corrugated shape increases the heat transfer path through the web and allows for better integration of insulation into the web cavity, thereby enhancing the overall thermal performance of the composite element [3, 4]. This is a thoughtful design solution to overcome a common problem in hybrid structures.

**Acoustic properties: vibration and noise absorption**

The light steel web in these load-bearing systems reduces the transmission of vibrational oscillations, which positively affects sound absorption. In addition to structural efficiency, this design contributes to human comfort. The combination of materials and specific geometry (thin web, timber flanges) creates a damping effect on vibrations, reducing noise transmission. This means that the beams not only bear loads but also contribute to the overall acoustic performance of the building, making them suitable for applications where noise control is important (e.g., industrial, office, or residential buildings).

**Durability and corrosion resistance**

High corrosion resistance is ensured by the use of galvanized metal webs made of S550 GD + Z steel according to DIN EN 10147, with a zinc layer of at least 275 g/m² (approximately 40 μm). Under operating conditions with high humidity and a medium degree of air aggressiveness (e.g., industrial or urban atmosphere, or coastal climate with low chloride content), the expected service life of the protective zinc coating is 20-30 years. When used indoors, durability can reach 50 to 100 years. Hot-dip galvanizing has significantly better resistance to mechanical impacts compared to painted coatings due to the cathodic protection effect, even with minor surface damage. Additional reliability can be ensured by corrosion protection at the intersection of the flanges with the steel web when used in aggressive operating conditions.

**Seismic resistance**

The reduction of the frame's self-weight and the use of a flexible corrugated web in combination with the characteristics of timber provide building frame structures made of steel-timber profiles with increased seismic resistance. Seismic forces are directly proportional to the mass of the structure. A lighter structure inherently experiences smaller inertial forces during an earthquake, making it more stable. The flexible corrugated web and timber flanges in composite I-beams contribute to energy dissipation and ductility, allowing the structure to deform without brittle failure. This combination enhances the overall dynamic performance and safety of buildings in seismically active zones, making these structures a desirable choice for such applications.

**Aesthetic qualities**

The reduction of the frame's self-weight and the use of a flexible corrugated web in combination with the characteristics of timber provide building frame structures made of steel-timber profiles with increased seismic resistance. Seismic forces are directly proportional to the mass of the structure. A lighter structure inherently experiences smaller inertial forces during an earthquake, making it more stable. The flexible corrugated web and timber flanges in composite I-beams contribute to energy dissipation and ductility, allowing the structure to deform without brittle failure. This combination enhances the overall dynamic performance and safety of buildings in seismically active zones, making these structures a desirable choice for such applications.

**Economic and production aspects**

The assembly, pressing, or gluing of steel-timber beams takes place on specialized technological lines, allowing for the manufacture of both constant and variable height elements. A significant advantage is the manufacturability of these beams: traditional hand building tools are sufficient for their processing. Timber itself is easily processed, and the steel used in the web has a thickness of 0,5-0,8 mm and can be processed with hand circular saws. As noted earlier, the self-weight of composite I-beams is 2-3 times less than analogous metal and solid timber elements, which reduces building construction costs. For comparison, let's consider a frame with a span of 14,0 m at a design load of 3,0 kN/sq.m. The required cross-section of a steel-timber beam with a 510 mm steel web and 80x140 mm flanges will have a weight of 12,30 kg/lin.m. and a current retail price of approximately 28,0 euros/m. In contrast, for the same loads and overall dimensions, the required cross-section of a glued laminated timber beam will be 140x420 mm, with a cost of about 26,0 euros/m. Thus, despite a slight difference in material cost, the significantly lower weight of the steel-timber beam frame leads to substantial savings on foundations and installation costs. This comparison clearly demonstrates that while the initial cost per linear meter may be comparable or slightly higher for steel-timber beams, a compre-hensive economic analysis reveals a significant advantage. The reduction in self-weight directly leads to a cascade of savings: smaller foundations, less need for heavy lifting equipment, faster installation, and potentially reduced labor costs. This provides systemic cost savings that go beyond just the cost of the beam material itself, making the overall construction project more economical and efficient.

**Table 1** Comparative characteristics of metal-timber I-beams and traditional materials.
**Табл. 1** Порівняльні характеристики металево-дерев'яних двотаврових балок і традиційних матеріалів

| *Characteristic* | *Metal-timber I-beam* | *Traditional metal/solid timber beams* |
|---|---|---|
| **Self-weight** (relative to analogous) | 2-3 times lighter | Base (1x) |
| **Load-bearing capacity** | Increased | Lower (relative to composite) |
| **Stiffness** | Increased | Lower (relative to composite) |
| **Optimal span range** | 7-24 m | Solid timber typically limited for such spans |
| **Thermal conductivity** | Significantly better insulation, prevents thermal bridges | Less insulating, potential for thermal bridges |
| **Sound absorption** | Reduces vibrational oscillations, positive impact | Varies, often requires additional measures |
| **Seismic resistance** | Increased due to reduced self-weight and material characteristics | Varies, heavier structures bear higher seismic loads |
| **Corrosion resistance** (steel component) | High (galvanized S550 GD+Z steel, service life 20-100 years) | Unprotected steel prone to corrosion without special treatment |

## CONCLUSIONS AND RECOMMENDATIONS

Frame structures made of composite steel-timber I-beams with transversely corrugated steel webs represent a highly promising direction in modern construction, demonstrating numerous advantages. They provide increased stiffness, significant self-weight reduction, improved thermal and sound insulation properties, high seismic and corrosion resistance, and the aesthetic appeal of natural material. From an economic perspective, these structures allow for significant savings on foundations and installation work, despite the comparable material cost per unit length with traditional counterparts. The simplicity of their processing and the possibility of waste-free production further emphasize their technological and environmental efficiency.

For Ukraine, the implementation of frame structures made of composite steel-timber I-beams is of strategic importance. They will

contribute to increasing the competitiveness of domestic production, reducing dependence on imported materials and technologies, and supporting the development of the country's scientific and engineering potential. Further development and standardization of these structures open up broad prospects for creating energy-efficient, reliable, and economically sound buildings, which is critically important in the context of infrastructure reconstruction and modernization.

REFERENCE


1. **Ivashko Y., Chang P., Dmytrenko A., Kozlowski T. & Mykhailovskyi D.** (2021) Influence of structural schemes on the shaping of historical wooden buildings: On the examples of traditional chinese pavilions, pavilions of the chinoiserie style and Ukrainian wooden churches /*Wiadomosci Konserwatorskie, 2021 (67), pp. 49-60.* [in English] http://doi.org/10.48234/WK67INFLUENCE.
2. **Mykhailovskyi D.** (2021) Method of calculation of panel buildings from cross-laminated timber *Strength of Materials and Theory of Structures.opir Materialiv I Teoria Sporud. (107), 75—78.* [in English] https://doi.org/10.32347/2410-2547.2021.107.75-88
3. **Tsapko Yu., Bondarenko O.** (2020). Determination of the laws of thermal resistance of wood in application of fire-retardant fabric coatings. *Eastern-European Journal of Enterprise Technologies. Vol. 2. (10) (104), 13-18.* [in English] http://doi.org/10.15587/1729-061.2020.200467
4. **Tsapko Yu. Bondarenko O.** (2020). Modeling of thermal conductivity of reed products. *IOP Conf. Series: Materials Science and Engineering. Vol. 907. 012057. 9 p.* [in English] http://doi.org/10.1088/1757-99X/907/1/012057
5. **Mykhailovskyi D., Komar M. (**2021). Reinforcement of Composite Wooden Structures Materials, Condition and Prospects. *Building constructions. Theory and Practice, (09), 72-80.* [in Ukrainian]. https://doi.org/10.32347/2522-4182.9.2021.72-80
6. **Bilyk S., Bashynska O., Bashynskyi O (**2022). Determination of changes inthermal stress state of steel beams in LIRA-SAPR software *Strength of Materials and Theory of Structures-opir Materialiv I Teoria Sporud. —(108), 189-202.* [in English] https://doi.org/10.32347/2410-2547.2022.108.189-202
7. **Göswein V., Reichmann J., Habert G., Pittau F.** (2021) Land availability in Europe for a radical shift toward bio-based construction. *Sustainable Cities and Society – 2021 - №70(3):102929* [in English] https://doi.org/10.1016/j.scs.2021.102929
8. **Kremer, P. D., Symmons, M. A.** (2015) Mass timber construction as an alternative to concrete and steel in the Australia building industry: A PESTEL evaluation of the potential. *International Wood Products Journal – 2015 – №6(3), pp. 138–147.* [in English] https://doi.org/10.1179/2042645315Y.0000000010
9. **Brischke, C; Thelandersson, S.** (2014) Modelling the outdoor performance of wood products – A review on existing approaches. *Construction and Building Materials, 2014, 66, 384-397.* [in English] https://doi.org/10.1016/j.conbuildmat.2014.05.087
10. **Ioannidou, D., Pommier, R., Habert, G., & Sonnemann, G.** (2019) Evaluating the risks in the construction wood product system through a criticality assessment framework. *Resources, Conservation, and Recycling - 2019– №146, pp. 68–76.* [in English] https://doi.org/10.1016/j.resconrec.2019.03.021
11. **Skliarov I.O., Skliarova T.S.** (2022). Synergy of properties of steel and wood in the constructions of metal-timber I-beams with corrugated web. *Building constructions. Theory and Practice, (11), 94-103.* [in Ukrainian] https://doi.org/10.32347/2522-4182.11.2022.94-103
12. **Skliarov, I., Mykhailovskyi, D., & Skliarova, T.** (2023). A the use of metal-timber structures in the reconstruction of industrial buildings for the renewal of residential real estate. *Building constructions. Theory and Practice,, (13), 76–88.* [in English] https://doi.org/10.32347/2522-4182.13.2023.76-88
13. **Mykhailovskyi, D., Skliarov, I., & Skliarova, T.** (2024). Features of determining the design length of shallow arches from glued laminated timber]. *Building constructions. Theory and Practice, (14), 161–169.* [in Ukrainian] https://doi.org/10.32347/2522-4182.14.2024.161-169
14. **Sklyarov, I.** (2016). Application of monosym-

metrical I-beams in light metal frames with variable stiffness. *Proceedings of Odessa Polytechnic University. 1(48) (Ber 2016), 30–34.* [in English] https://doi.org/10.15276/opu.1.48.2016.06

15. **Kánnár A., Karácsonyi Zs., Andor K., Csóka L.** (2019) Analysis of glued-laminated timber structure during five years of outdoor operation. *Construction and Building Materials, (205), Pages 31-38* [in English] https://doi.org/10.1016/j.conbuildmat.2019.01.234
16. **Hansson M., Larsen H.J.** (2005) Recent failures in glulam structures and their causes *Engineering Failure Analysis (12), (5), 808-818* [in English] https://doi.org/10.1016/j.engfailanal.2004.12.020
17. **Lyu C.H., Gilbert B.P., Guan H., Underhill I.D., Gunalan S., Karampour H., Masaeli M.** (2020) Experimental collapse response of post-and-beam mass timber frames under a quasi-static column removal scenario. *Engineering Structures (213), 110562* [in English] https://doi.org/10.1016/j.engstruct.2020.110562
18. **Munch-Andersen J., Dietsch Ph.** (2011) Robustness of large-span timber roof structures — Two examples. *Engineering Structures (33), (11), 3113-3117* [in English] https://doi.org/10.1016/j.engstruct.2011.03.015
19. **Zhi Li , Tao Li , Can Wang , Xiaozhou He , Yan Xiao** (2019) Experimental study of an unsymmetrical prefabricated hybrid steel-bamboo roof truss. *Engineering Structures (201), 109781* [in English] https://doi.org/10.1016/j.engstruct.2019.109781
20. **Yurchenko V.** (*2019)* Searching for shear forces flows in arbitrary cross-sections of thin-walled bars:numerical algorithm and software implementation. *Strength of Materials and Theory of Structures: Scientific-and-technical collected articles. – Kyiv: KNUBA,.(103), 82 – 111.* [in English] https://doi.org/10.32347/2410-2547.2019.103.82-111
21. **Mykhailovskyi, D., Skliarova, T.** (2021). Calculation of large-span glulam structures as a soil base-foundation-above-ground structure system. *ScienceRise, (4),. 17–23*. [in English] https://doi.org/10.21303/2313-8416.2021.002033
22. **Ivanchenko H., Getun G., Skliarov, I. Solomin A., Getun S.** (2025) Application of the low-rank adaptation method on the example of fine-tuning a latent diffusion model. *Strength of materials and theory of structures: scientific and technical collection, (114), 299-310* [in English] https://doi.org/10.32347/2410-2547.2025.114.299-310
23. **Ivashko,Y., Mykhailovskyi,D., Tovbych,V., Kobylarczyk, J., Kuśnierz-Krupa, D., Dmytrenko, A., & Sandu,A.V.** (2023). Problems of plants revitalization in the East of Ukraine after the war. *International Journal of Conservation Science, 14(2). (Apr-Jun 2023): 551-562.* [in English] https://doi.org/10.36868/IJCS.2023.02.12
24. **Hetun, H., Ivanchenko, H., Skliarov, I., Solomin, A., & Hetun, S.** (2025). Application of Neural Networks in Building Architecture and Optimization of Latent Diffusion Models for This Purpose. *Current Problems of Architecture and Urban Planning, (71), 494–509.* [in Ukrainian] https://doi.org/10.32347/2077-3455.2025.71.494-509
25. **Huber, J. A. J., Ekevad, M., Girhammar, U. A., & Berg, S**. (2018). Structural robustness and timber buildings – a review. *Wood Material Science & Engineering, 14(2), 107–128.* [in English] https://doi.org/10.1080/17480272.2018.1446052

## LITERATURE

1. **Ivashko Y., Chang P., Dmytrenko A., Kozlowski T. & Mykhailovskyi D.** (2021) Influence of structural schemes on the shaping of historical wooden buildings: On the examples of traditional chinese pavilions, pavilions of the chinoiserie style and Ukrainian wooden churches /*Wiadomosci Konserwa-torskie, 2021 (67), pp. 49-60.* http://doi.org/10.48234/WK67INFLUENCE.
2. **Mykhailovskyi D.** (2021) Method of calculation of panel buildings from cross-laminated timber *Strength of Materials and Theory of Structures-opir Materialiv I Teoria Sporud. (107), 75—78.* https://doi.org/10.32347/2410-2547.2021.107.75-88
3. **Tsapko Yu., Bondarenko O**. (2020). Determination of the laws of thermal resistance of wood in application of fire-retardant fabric coatings. *Eastern-European Journal of Enterprise Technologies. Vol. 2. (10) (104), 13-18.* http://doi.org/10.15587/1729-061.2020.200467
4. **Tsapko Yu. Bondarenko O**. (2020). Modeling of thermal conductivity of reed products. *IOP*

*Conf. Series: Materials Science and Engineering. (907),. 012057. 9 p* http://doi.org/10.1088/1757-99X/907/1/012057

5. **Mykhailovskyi D., Komar M. (**2021). Armuvannia konstruktsii z derevyny kompozytnymy materialamy, stan i perspektyvy *Budivelni konstruktsii. Teoriia i praktyka, (09), 72-80.* https://doi.org/10.32347/2522-4182.9.2021.72-80
6. **Bilyk S., Bashynska O., Bashynskyi O (**2022). Determination of changes inthermal stress state of steel beams in LIRA-SAPR software *Strength of Materials and Theory of Structures. (108), 189-202.* https://doi.org/10.32347/2410-2547.2022.108.189-202
7. **Göswein V., Reichmann J., Habert G., Pittau F.** (2021) Land availability in Europe for a radical shift toward bio-based construction. *Sustainable Cities and Society – 2021 - №70(3):102929* https://doi.org/10.1016/j.scs.2021.102929
8. **Kremer, P. D., Symmons, M. A.** (2015) Mass timber construction as an alternative to concrete and steel in the Australia building industry: A PESTEL evaluation of the potential. *International Wood Products Journal №6(3), pp. 138–147.* https://doi.org/10.1179/2042645315Y.0000000010
9. **Brischke, C; Thelandersson, S.** (2014) Modelling the outdoor performance of wood products – A review on existing approaches. *Construction and Building Materials, (66), 384-397.* https://doi.org/10.1016/j.conbuildmat.2014.05.087
10. **Ioannidou, D., Pommier, R., Habert, G., & Sonnemann, G.** (2019) Evaluating the risks in the construction wood product system through a criticality assessment framework. *Resources, Conservation, and Recycling , (146),. 68–76.* https://doi.org/10.1016/j.resconrec.2019.03.021
11. **Skliarov I.O., Skliarova T.S.** (2022) Synerhiia vlastyvostei stali ta derevyny v konstuktsiiakh metaloderevianykh dvotavriv z hofrovanoiu stinkoiu. *Budivelni konstruktsii. Teoriia i praktyka (11),. 94-103.* https://doi.org/10.32347/2522-4182.11.2022.94-103
12. **Skliarov, I., Mykhailovskyi, D., & Skliarova, T.** (2023). A the use of metal-timber structures in the reconstruction of industrial buildings for the renewal of residential real estate. *Building constructions. Theory and Practice,, (13), 76–88.* https://doi.org/10.32347/2522-4182.13.2023.76-88
13. **Mykhailovskyi, D., Skliarov, I., & Skliarova, T.** (2024) Osoblyvosti vyznachennia rozrakhunkovoi dovzhyny polozhystykh arok z kleienoi derevyny *Budivelni konstruktsii. Teoriia i praktyka, (14), 161–169* https://doi.org/10.32347/2522-4182.14.2024.161-169
14. **Sklyarov, I.** (2016) Application of monosymmetrical I-beams in light metal frames with variable stiffness. *Pratsi Odeskoho politekhnichnoho universytetu. 1(48) (Ber 2016), 30–34.* https://doi.org/10.15276/opu.1.48.2016.06
15. **Kánnár A., Karácsonyi Zs., Andor K., Csóka L.** (2019) Analysis of glued-laminated timber structure during five years of outdoor operation. *Construction and Building Materials, (205), Pages 31-38* https://doi.org/10.1016/j.conbuildmat.2019.01.234
16. **Hansson M., Larsen H.J.** (2005) Recent failures in glulam structures and their causes *Engineering Failure Analysis (12), (5), 808-818* https://doi.org/10.1016/j.engfailanal.2004.12.020
17. **Lyu C.H., Gilbert B.P., Guan H., Underhill I.D., Gunalan S., Karampour H., Masaeli M.** (2020) Experimental collapse response of post-and-beam mass timber frames under a quasi-static column removal scenario. *Engineering Structures (213), 110562* https://doi.org/10.1016/j.engstruct.2020.110562
18. **Munch-Andersen J., Dietsch Ph.** (2011) Robustness of large-span timber roof structures — Two examples. *Engineering Structures (33), (11), 3113-3117* https://doi.org/10.1016/j.engstruct.2011.03.015
19. **Zhi Li , Tao Li , Can Wang , Xiaozhou He , Yan Xiao** (2019) Experimental study of an unsymmetrical prefabricated hybrid steel-bamboo roof truss. *Engineering Structures (201), 109781* https://doi.org/10.1016/j.engstruct.2019.109781
20. **Yurchenko V.** (*2019).* Searching for shear forces flows in arbitrary cross-sections of thin-walled bars:numerical algorithm and software implementation. *Strength of Materials and Theory of Structure, (103), 82 – 111.* https://doi.org/10.32347/2410-2547.2019.103.82-111

21. **Mykhailovskyi, D., Skliarova, T.** (2021). Calculation of large-span glulam structures as a soil base-foundation-above-ground structure system. *ScienceRise, (4),. 17–23*. https://doi.org/10.21303/2313-8416.2021.002033
22. **Ivanchenko H., Getun G., Skliarov I., Solomin A., Getun S.** (2025) Application of the low-rank adaptation method on the example of fine-tuning a latent diffusion model. *Strength of materials and theory of structures, (114), 299-310* https://doi.org/10.32347/2410-2547.2025.114.299-310
23. **Ivashko,Y., Mykhailovskyi,D., Tovbych,V., Kobylarczyk, J., Kuśnierz-Krupa, D., Dmytrenko, A., & Sandu,A.V.** (2023). Problems of plants revitalization in the East of Ukraine after the war. *International Journal of Conservation Science, 14(2). (Apr-Jun 2023): 551-562*. https://doi.org/10.36868/IJCS.2023.02.12
24. **Hetun, H., Ivanchenko, H., Skliarov, I., Solomin, A., & Hetun, S.** (2025). Zastosuvannia neiromerezh v arhitekturi budivel i optymizatsiia dlia tsioho modelei prykhovanoi dyfuzii. *Suchasni problemy Arkhitektury ta Mistobuduvannia, (71), 494–509*. https://doi.org/10.32347/2077-3455.2025.71.494-509
25. **Huber, J. A. J., Ekevad, M., Girhammar, U. A., & Berg, S**. (2018). Structural robustness and timber buildings – a review. *Wood Material Science & Engineering, 14(2), 107–128*. https://doi.org/10.1080/17480272.2018.1446052

## РАМНІ КАРКАСИ З КОМПОЗИТНИХ МЕТАЛОДЕРЕВ'ЯНИХ ДВОТАВРІВ З ГОФРОВАНОЮ СТАЛЕВОЮ СТІНКОЮ

*Ігор СКЛЯРОВ*
*Тетяна СКЛЯРОВА*

**Анотація.** Рамні конструкції з композитних сталево-дерев'яних двотаврових балок з поперечно гофрованими сталевими стінками є інноваційним композитним рішенням у будівельній галузі, що поєднує міцність сталі та екологічність деревини. Ці конструкції мають значні переваги, зокрема високе співвідношення міцності до ваги, поліпшені теплові та акустичні властивості, підвищену сейсмостійкість та корозійну стійкість. З економічної точки зору, їх використання призводить до зниження загальних витрат на будівництво завдяки меншій власній вазі, високій технологічності та простоті монтажу.

Поєднання тонкої профільованої сталевої стінки та масивних дерев'яних поясів забезпечує оптимальне використання фізико-механічних властивостей обох матеріалів, підвищуючи несучу здатність і жорсткість елементів за одночасного зменшення їхньої маси у 2–3 рази порівняно з традиційними металевими або суцільними дерев'яними балками. Розкрито технологічні аспекти виготовлення елементів постійного та змінного перерізу, включаючи механічне пресування гофрованої стінки в деревину та клеєві з'єднання на основі двокомпонентних епоксидних сумішей. Можливість варіювати висоту перерізу рамних каркасів дає змогу оптимізувати витрати матеріалу залежно від епюри згинальних моментів, що збільшує ефективність конструкцій. Показано переваги таких конструкцій у теплоізоляції та запобіганні утворенню теплових містків, у підвищенні акустичного комфорту, довговічності та корозійній стійкості завдяки використанню оцинкованої сталі.

Для України впровадження рамних конструкцій із композитних метало-дерев'яних двотаврових балок має стратегічне значення. Вони сприятимуть підвищенню конкурентоспроможності вітчизняного виробництва, зменшенню залежності від імпортних матеріалів і технологій, а також підтримці розвитку науково-технічного потенціалу країни. Подальший розвиток і стандартизація цих конструкцій відкривають широкі перспективи для створення енергоефективних, надійних і економічно вигідних будівель, що має вирішальне значення в контексті реконструкції та модернізації інфраструктури

**Ключові слова:** рамні конструкції; метало-дерев'яні балки; композитні балки; HTS-балки.

***Received:*** *November 01, 2025.*
***Accepted:*** *November 30, 2025.*

ISSN 2522-4182

DOI: DOI: 10.32347/2522-4182.17.2025.102-118
UDC 624.012.45

# EXPERIMENTAL TESTING OF A COMPLEX-GEOMETRY FLOOR SLAB MANUFACTURED USING 3DCP TECHNOLOGY

*Oleg KALMYKOV[1], Petro REZNIK[2], Inna FURMAN[3], Ivan DEMIANENKO[4]*

*[1,2,4] O.M. Beketov National University of Urban Economy in Kharkiv, Ukraine*
17, Chornoglazivska Street, Kharkiv 61002
*[3]LLC "3D TECHNOLOGIES UTU"*
2 Maidan Nezalezhnosti, Kyiv 01001, Ukraine
[1] oleg.kalmikov@kname.edu.ua, https://orcid.org/0000-0001-7294-4279
[2] petro.reznik@kname.edu.ua, https://orcid.org/0000-0003-3937-6833
[3] i.furman5@gmail.com, https://orcid.org/0009-0004-3012-0772
[4] ivan.demyanenko.1995@gmail.com, https://orcid.org/0000-0001-9511-7663

**Abstract.** This paper presents the results of an experimental investigation of a thin-walled reinforced concrete slab of complex geometry manufactured using 3D concrete printing (3DCP) technology. The aim of the study was to evaluate the stress–strain behaviour and flexural stiffness of an optimized slab whose internal structure was formed according to the principles of rational cross-sections and topology-based shape design. The tested slab, measuring 2200×2200 mm, incorporated a system of curved ribs printed in 20-mm layers, forming a cellular load-bearing pattern with enhanced material efficiency.

The experimental program was carried out on a rigid spatial steel testing frame with full perimeter support. The load was applied incrementally by placing cast-iron calibration blocks (21 kg) and heavy concrete FBS blocks weighing 518 kg, which ensured an equivalent uniformly distributed load. A total of 12 loading stages were performed with a 15-minute stabilization period at each step, reaching a maximum surface pressure of 25.06 kN/m². Vertical displacements were recorded using three high-precision dial gauges (0.01 mm accuracy), while local strains were measured by ten strain gauges with a 20 mm base installed at characteristic locations on the upper and lower surfaces of the slab.

The obtained results showed that the slab exhibited linear-elastic behaviour throughout the entire loading range. The maximum central deflection reached 2.06 mm, and after complete unloading decreased to 0.63 mm, confirming a significant proportion of recoverable deformation and the absence of damage. Strain gauge readings indicated a uniform development of compressive and tensile strains consistent with the bending moment distribution, with no evidence of localized stress concentrations.

**Oleg KALMYKOV**
Associate Professor, Department of Building Structures,
Assoc. Prof., PhD (Tech. Sci.)

**Petro REZNIK**
Associate Professor, Department of Building Structures,
Assoc. Prof., PhD (Tech. Sci.)

**Inna FURMAN**
LLC "3D TECHNOLOGIES UTU"
Founder

**Ivan DEMYANENKO**
Post-graduate student, Department of building structures

The strain curves contained no sudden jumps or anomalies, indicating the integrity of interlayer bonding and the absence of any signs of structural degradation.

The findings confirm the effectiveness of 3DCP technology for manufacturing load-bearing floor slabs with complex internal geometry. The tested element demonstrated high stiffness, reliable structural performance and highlighted the promising prospects for the development of topologically optimized reinforced concrete structures in modern construction.

**Keywords:** 3DCP; topology optimization; experimental testing; deflections; strains; uniformly distributed load; load-bearing capacity.

## INTRODUCTION

The modern development of additive manufacturing technologies in construction is primarily associated with extrusion-based 3D printing of cementitious and concrete mixtures, which enables the creation of complex spatial geometries and significantly expands the potential for rational structural form-finding. Unlike traditional technologies, 3DCP makes it possible to eliminate formwork, reduce labor intensity, and realize topologically optimized cross-sections that ensure an efficient distribution of material according to the internal force field. Despite the rapid advancement of digital design methods and substantial progress in materials-science research related to 3D printing, experimental data on the actual structural behavior of full-scale slabs with complex geometry remain limited. This highlights the need for comprehensive testing of 3D-printed slab systems to assess their deformability, stiffness, and load-bearing capacity under real loading conditions.

## ANALYSIS OF PREVIOUS RESEARCH

Review studies indicate that concrete 3D printing enables the abandonment of traditional formwork, the fabrication of complex geometries, and the adaptive control of mixture composition and toolpath trajectories. At the same time, it imposes specific requirements on rheological properties, layer formation technologies, and quality control of printed elements [1–4]. Some surveys focus on the selection of sustainable materials, optimisation of toolpath parameters, and criteria for improving the 3D printing process - all of which directly relate to rational structural shaping and the enhancement of material efficiency [3–5].

A significant share of contemporary research is dedicated to integrating digital design, topology optimisation, and digital fabrication of ribbed and funicular slabs using 3D-printed formwork. Studies conducted at ETH Zurich, TU Delft, and other research centres have demonstrated the feasibility of using 3D-printed polymer and composite formwork to create lightweight reinforced concrete slabs with complex geometry [6–13]. It has been shown that combining parametric modelling, shape optimisation, and digital fabrication technologies enables a substantial reduction in material consumption while maintaining or increasing load-bearing capacity, and allows for the creation of integrated slab systems where the geometry of ribs, voids, and zones of material concentration is aligned with the distribution of internal forces [6–13]. Parallel experimental research on shells and beams fabricated using 3D-printed polymeric or composite cementitious materials confirms the fundamental feasibility of structurally efficient shapes and their agreement with numerical models [14,15].

The theoretical foundation of rational structural shaping is grounded in the apparatus of topology optimisation developed for continuum structures [16–18]. Classical approaches - such as density-based methods, evolutionary topology optimisation, and bi-directional evolutionary optimisation (BESO) - allow for determining the material layout that minimises energy functionals or deformation criteria subject to specified constraints [16–18, 32]. Review and applied studies demonstrate the active implementation of these methods for the analysis of steel and reinforced concrete structures, including slabs, shells, and spatial systems, and highlight the connection between topology optimisation, architectural form-finding, and parametric modelling [19–21]. Against this background, Ukrainian researchers have advanced the energy-based approach to

parametric design, introducing the concept of an “energy portrait” of a structural system and using the density of strain energy as a criterion for evaluating and optimising the parameters of shells and slabs [22–25].

One of the key features of 3D-printed concrete is its layered architecture and, consequently, pronounced anisotropy of strength, stiffness, and crack resistance. Experimental studies on interlayer adhesion show a significant dependence of interface strength on the rheological properties of the fresh mix, time intervals between layers, surface condition, and extrusion parameters [26–28]. The mechanical characteristics of 3D-printed concrete are known to vary substantially in the direction of printing, along the layers, and in the vertical direction, with statistical strength parameters exhibiting clear directional dependence [26–28]. Several studies have proposed experimental procedures and statistical analysis methods to quantify anisotropy and account for it in the design of 3D-printed concrete structures [29,30], including the selection of effective design parameters and calibration of material models with regard to printing direction.

Ukrainian research makes a significant contribution to the development of resource-efficient shaping concepts for slabs and shells based on energy criteria. In particular, methods have been proposed for determining the optimal topology of reinforced concrete floor slabs with regard to the distribution of internal forces and deformations, enabling the design of rational ribbed slabs and voided systems [24,25].

Experimental evaluation of the deformability of repaired floor panels in large-panel residential buildings has confirmed the effectiveness of reconstruction strategies and provides grounds for further optimisation of structural schemes [31]. The concept of an energy portrait of a structural system has been introduced as a tool for variant-based design and shown to be applicable to reinforced concrete shells and spatial systems [25]. Additional studies demonstrate the potential of 3D printing for the fabrication of domes and monolithic beams with reinforcement, confirming the overall consistency between numerical modelling and experimental results and highlighting the prospects of integrating additive manufacturing with traditional reinforcement techniques [14,15, 33].

At the same time, the collected research indicates that most studies focus either on topology optimisation and energy-based criteria primarily for traditional reinforced concrete systems [16–22,31], or on technological and material aspects of 3D printing without direct transition to full-scale structural floor elements [1–6]. Studies concerning 3D-printed formwork and thin-walled ribbed slabs are mainly conceptual demonstrations of workflows and prototypes [6–12], whereas comprehensive integration of topology optimisation, energy analysis, and experimental verification of a 3D-printed slab with complex geometry remains insufficiently explored. Under these circumstances, the development of a methodology for designing optimised slab systems based on 3D printing - combining state-of-the-art numerical form-finding methods, energy criteria for assessing stress–strain behaviour, and experimental validation that accounts for material anisotropy - becomes highly relevant. The present study is dedicated to addressing this task.

## OBJECT AND SUBJECT OF THE STUDY

The object of the study is an experimental specimen of a reinforced concrete slab of complex geometry, fabricated by concrete 3D printing (3DCP). The slab has plan dimensions of 2200×2200 mm and is formed as a spatial ribbed–cellular structure. Along the entire perimeter, a 150-mm-wide external frame is provided, ensuring contour stiffness and the transfer of support reactions.

The internal area of the slab is divided into four equal quadrants measuring 875×875 mm, within which a layer-by-layer printed curvilinear topology is formed. The total thickness of the slab is 240 mm, while the height of the internal cavities and the thickness of the printed walls vary according to the geometry of the topologically optimized profile. In the central zone, a cruciform stiffening node is arranged, ensuring the joint

structural action of the four quadrants. Reinforcement of the slab was implemented by placing steel bars between the printed layers.

The general structural layout is shown in Fig. 1. The subject of the study is the deformation behaviour of the investigated element.

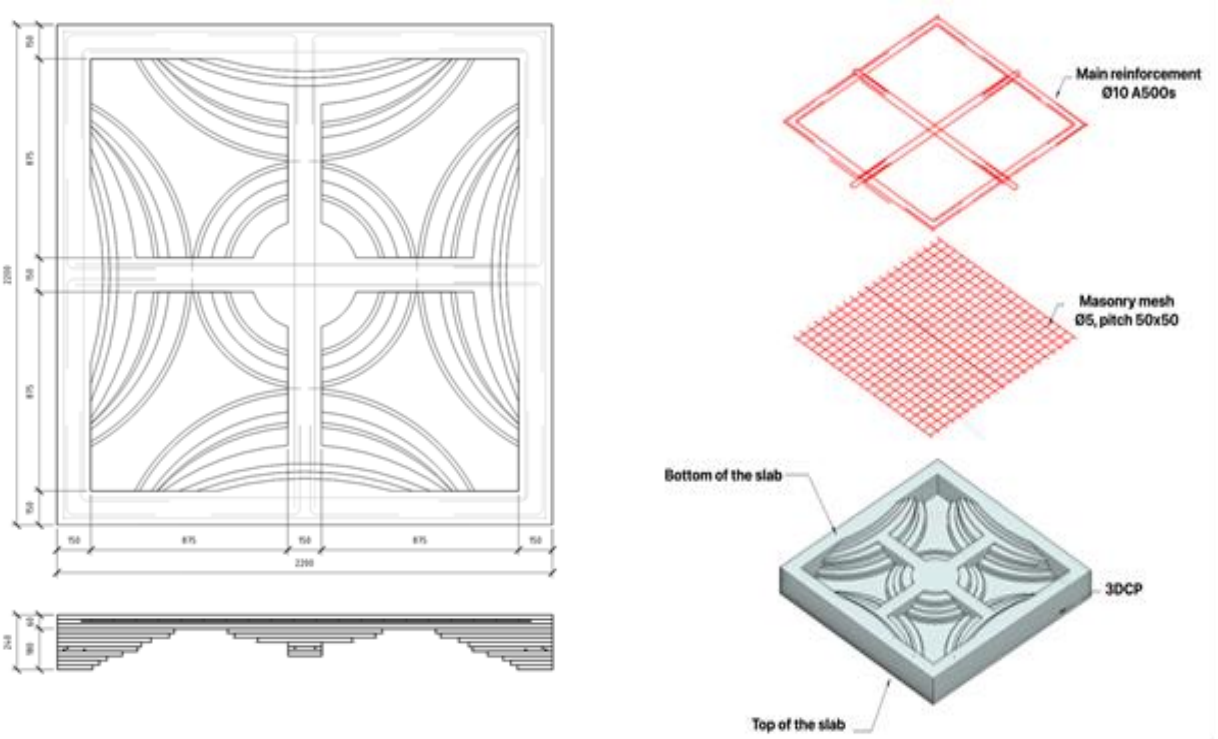


**Fig. 1** Plan view, section, and axonometric representation of the experimental slab
**Рис. 1** Вигляд експериментальної плити в плані, розрізі та аксонометрії

The mechan ical properties of the material used to manufacture the experimental slab were determined in a separate series of laboratory tests on specimens printed using the same layer-by-layer extrusion method as the test element. The preparation procedure, testing protocol and statistical processing of results are described in detail in [28].

Cube specimens were tested in compression in three orthogonal directions: along the extrusion path (X), perpendicular to the extrusion path (Y), and perpendicular to the printed layers (Z). The tests confirmed pronounced orthotropy of the material: the average compressive strength was 12.26 MPa in direction X, 12.44 MPa in direction Y, and 17.32 MPa in direction Z. The highest values were obtained for loading perpendicular to the layers, indicating better performance in the absence of interlayer weaknesses.

The calculated anisotropy indices were: Z/X = 1.41; Z/Y = 1.39; Y/X = 1.01, which is consistent with commonly reported characteristics of extrusion-based cementitious composites, where typical strength ratios between directions reach 1.25–1.6. The lowest coefficient of variation (CV ≈ 16%) was recorded in direction Z, confirming the stability of material properties under loading perpendicular to the printed layers.

The obtained mechanical characteristics are directly used in the analysis of the printed slab, since the material, printing technology and specimen geometry correspond to the conditions presented in [28].

## LOADING SYSTEM

The load was applied to the slab in stages, with a gradual increase in intensity and regulated holding periods between steps. At the first stage, calibrated cast-iron blocks weighing 21 kg each were placed on the slab surface. The blocks were arranged in a checkerboard pattern, providing partial (approximately half) coverage of the surface. A total of 65 blocks were placed, with a combined mass of 1365 kg, corresponding to approximately 282 kg/m² (≈2.8 kN/m²).

At the second stage, additional loading was applied using the same 21 kg cast-iron blocks, which were arranged in the opposite checkerboard pattern - in the gaps between the blocks of the first stage. After this step, the entire slab surface was fully covered with 21 kg blocks. The total number of blocks reached 130 units, with a combined mass of 2730 kg, corresponding to ≈564 kg/m² (≈5.5 kN/m²).

Further load increase was achieved by placing FBS concrete blocks measuring 400×600×900 mm and weighing 518 kg each. The blocks were positioned symmetrically relative to the slab's axes, two blocks at each subsequent loading step. After each loading stage, a 15-minute holding period was implemented to allow deformation stabilization. In total, 12 loading stages were carried out (Table 1).

After reaching the seventh loading stage, the slab was held under constant load for 2 hours, followed by step-by-step unloading in the reverse order. The general view of several loading stages is shown in Fig. 2.

The slab was supported along its perimeter on a rigid testing frame designed as a spatial steel structure. The frame, assembled from rolled steel profiles, ensured stable geometry of the support contour throughout the entire loading cycle. Support was provided by the slab's edge ribs along the perimeter, reproducing the structural behavior of a slab under closed-contour support conditions.

The width of the support strip was 100 mm, which ensured a sufficient contact area between the printed ribs and the elements of the steel frame. This type of support allowed the transfer of forces from the slab to the support system without local stress concentrations and corresponded to the analytical support conditions adopted in the subsequent analysis.

**Table 1** Loading stages
**Табл. 1** Ступені навантаження

| № | 21-kg blocks, pcs. | FBS 518-kg blocks, pcs | Total mass, kg | Uniformly distributed load, kN/m² |
|---|---|---|---|---|
| 1 | 65 | 0 | 1365 | 2.82 |
| 2 | 130 | 0 | 2730 | 5.64 |
| 3 | 130 | 2 | 3670 | 7.58 |
| 4 | 130 | 4 | 4610 | 9.52 |
| 5 | 130 | 6 | 5550 | 11.47 |
| 6 | 130 | 8 | 6490 | 13.41 |
| 7 | 130 | 10 | 7430 | 15.35 |
| 8 | 130 | 12 | 8370 | 17.29 |
| 9 | 130 | 14 | 9310 | 19.24 |
| 10 | 130 | 16 | 10250 | 21.18 |
| 11 | 130 | 18 | 11190 | 23.12 |
| 12 | 130 | 20 | 12130 | 25.06 |

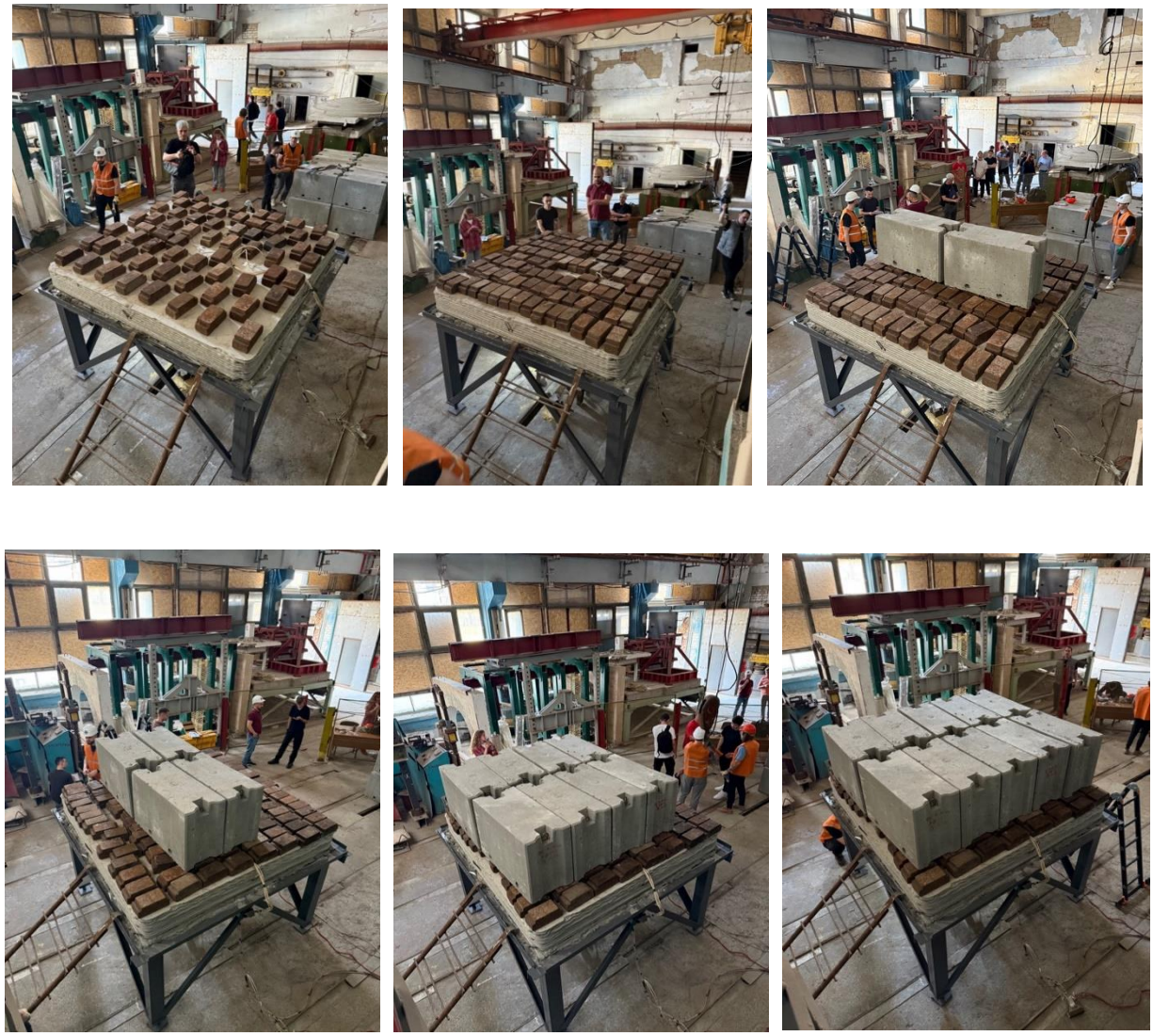

**Fig. 2** Loading stages. Photo by Oleg Kalmykov
**Рис. 2** Етапи завантаження. Автор фото Олег Калмиков

## MEASUREMENT SYSTEM

To monitor the deformation state of the test slab during static loading, a combined measurement system was used, consisting of strain gauges and mechanical deflection gauges. Relative deformations were recorded using foil strain gauges with a 20 mm gauge length, bonded to the surface at ten characteristic locations selected according to the expected zones of maximum bending strains. The sensors were positioned on both the upper and lower surfaces of the slab; their layout was determined based on a pre-developed scheme that covered the central region, the areas near the rigid cross-shaped node, and the peripheral zones within individual quadrants, including points D-0, D-2, D-4, D-6, D-8 on the top surface, and D-10, D-12, D-14, D-16, D-18 on the bottom surface (Fig. 3a, b). This arrangement made it possible to evaluate the behaviour of the slab in both tension and compression fibres and to control section curvature during loading.

Signal acquisition from the strain gauges was performed using the multi-channel measuring system VNP-8, intended for static and repeated-static testing of structural elements.

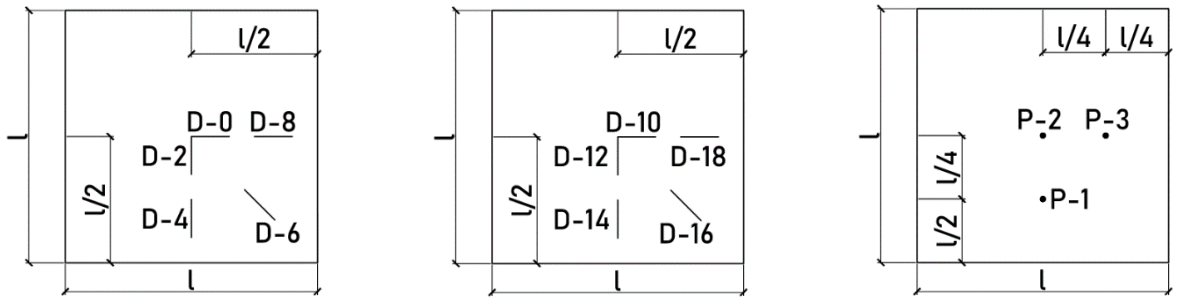


*a* *b* *c*

**Fig. 3.** Layout of measuring devices: a, b – upper and lower strain gauges, respectively; c – dial gauges
**Рис. 3** Схема розташування приладів: а, б – верхні та нижні тензодатчики відповідно; в – прогиноміри

The system recorded changes in the electrical resistance of the strain gauges as digital codes within the range corresponding to resistance variations of ±9999…±39996 μΩ/Ω, depending on the configuration of the measurement bridge. For accurate conversion of electrical signals into mechanical strain, a preliminary calibration of the complete measurement chain – "strain gauge – cable – bridge – ADC"– was carried out in accordance with the procedure provided in the relevant technical documentation.

Calibration was performed on a steel cantilever beam of rectangular cross-section, onto which weights ranging from 1 to 10 kg were sequentially applied. For each load level, several measurements were taken to determine mean code values and their increments. Theoretical strains at the gauge location were calculated using the classical bending formula for prismatic members. Subsequently, the least-squares method was used to determine the conversion coefficient that linearly related the change in digital code to the magnitude of strain. This coefficient was then applied to calculate the actual strains in the test slab during loading.

In addition to strain measurements, three mechanical deflection gauges with an accuracy of 0.01 mm were used to determine the vertical displacements of the slab. They were installed at characteristic control points: P-2 - at the centre of the slab, P-3 - at the right-hand zone of the specimen, and P-1 - in the lower region, which made it possible to monitor the development of deflection in the central area and assess the symmetry of the structural response (Fig. 3c). The gauges were mounted on an independent rigid support system mechanically isolated from both the test frame and the slab, in order to eliminate the influence of frame deformations on the measurement results. The general view of the measuring devices is shown in Fig. 4.


*a* *b*

**Fig. 4** General view of the instruments: a – dial gauges; b – strain gauges. Photo by Oleg Kalmykov
**Рис. 4** Загальний вигляд приладів: а – прогиноміри; б – тензодатчики. Автор фото Олег Калмиков

## RESULTS

*Deflection measurement results*

Deflection measurements were carried out after deformation stabilization at each loading stage, with a 15-minute holding period, which minimized the influence of initial creep of the material.

The maximum vertical displacements were recorded at the central point R2, which corresponds to the expected behavior of the slab as a bending element with maximum curvature at midspan. At the maximum uniformly distributed load of 25.06 kN/m², the deflection at point R2 reached 2.06 mm, while at points R1 and R3 the deflections were 1.65 mm and 1.93 mm, respectively (Table 2). The higher values at points R1 and R3 are attributed to local geometric features, variations in stiffness across the slab, and non-uniform rib distribution beneath the surface.

After complete unloading of the specimen, the deflection at the central point decreased by 1.43 mm, which corresponds to a residual deformation of 0.63 mm, or approximately 30% of the maximum value. A similar trend was observed at points P-1 and P-3, where the residual deflections were 0.37 mm and 0.75 mm, respectively.

Analysis of the loading–unloading curves (Fig. 5) indicates that the structure exhibits elastic–plastic behavior with a high share of recoverable deformation. The degree of shape recovery after unloading was approximately: 77% for P-1, 69% for P-2, and 61% for P-3, indicating the absence of significant plastic damage or macrocrack opening in the zones of maximum stress.

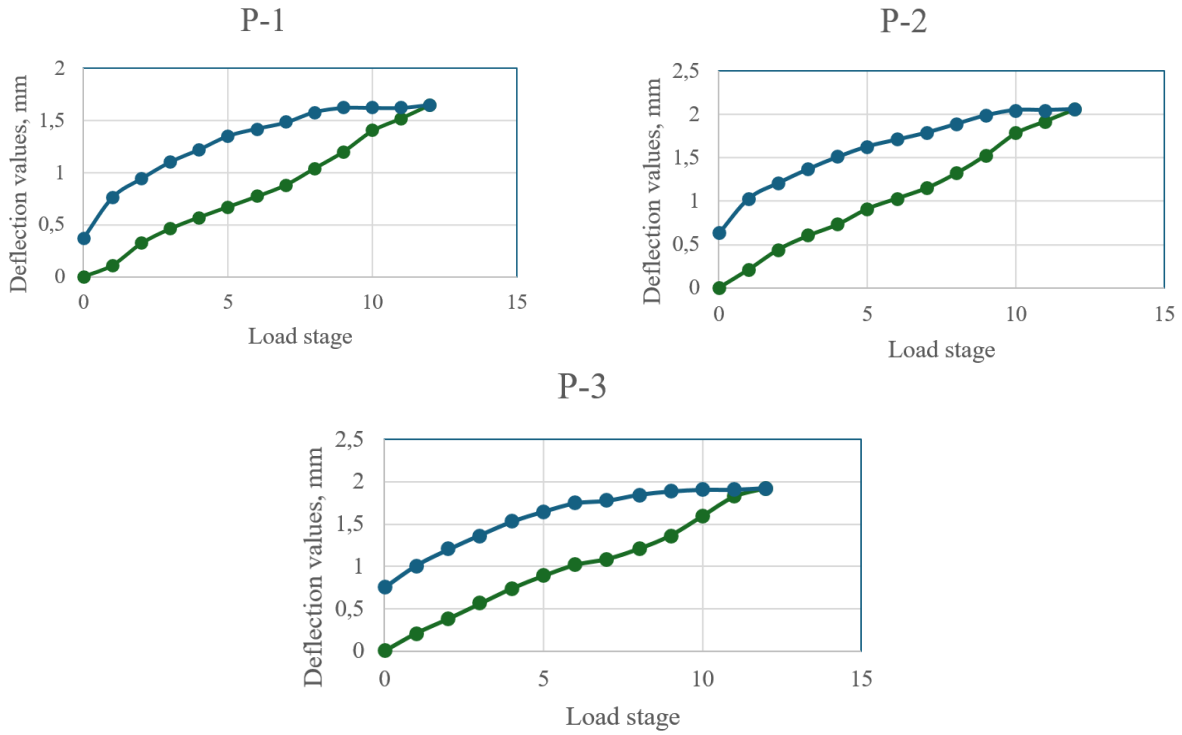


**Fig. 5** Deflection values
**Рис. 5** Значення прогинів

The deflection–load relationships demonstrate behavior typical for thin-walled slabs: an initial quasi-linear segment (0–10 kN/m²), followed by a gradual reduction in stiffness at loads of 10–20 kN/m², and a transition to a nearly horizontal plateau at 20–25 kN/m². The absence of sharp jumps or curve breaks confirms the integrity of the printed slab structure and the absence of brittle failure. The results are summarized in Table 2, and the graphical "load–deflection" plots are presented in Fig. 5.

The deflection–load curves exhibit a characteristic response of thin concrete slabs: the initial segment preserves an almost perfectly linear proportionality between load

and vertical displacements due to the low stress level within the structure. With further increase in load—reaching only about 25% of the structural strength limit—the curve remained close to linear with no visible stiffness degradation.

The absence of sudden drops or discontinuities confirms the integrity of the 3D-printed slab and the absence of brittle cracking at all stages.

It is important to note that the present experiment did not aim to bring the structure to complete failure, as one of its main objectives was to provide a fundamental verification of the feasibility and structural performance of floor slabs fabricated by 3D concrete printing. The results are presented in Table 2, and the load–deflection plots are shown in Fig. 5. The green curve represents loading, while the blue curve represents unloading.

**Table 2** Readings of the deflection gauges
**Табл. 2** Значення прогиномірів

| Load stage | Load | | Instrument readings, mm | | |
|---|---|---|---|---|---|
| | Total, kg | Distributed, kN/m² | P-1 | P-2 | P-3 |
| 0 | 0 | 0 | 0 | 0 | 0 |
| 1 | 1365 | 2.82 | 0.11 | 0.21 | 0.21 |
| 2 | 2730 | 5.64 | 0.32 | 0.44 | 0.38 |
| 3 | 3670 | 7.58 | 0.46 | 0.6 | 0.56 |
| 4 | 4610 | 9.52 | 0.57 | 0.73 | 0.74 |
| 5 | 5550 | 11.47 | 0.67 | 0.91 | 0.89 |
| 6 | 6490 | 13.41 | 0.77 | 1.03 | 1.02 |
| 7 | 7430 | 15.35 | 0.88 | 1.15 | 1.09 |
| 8 | 8370 | 17.29 | 1.04 | 1.32 | 1.21 |
| 9 | 9310 | 19.24 | 1.2 | 1.53 | 1.37 |
| 10 | 10250 | 21.18 | 1.4 | 1.78 | 1.6 |
| 11 | 11190 | 23.12 | 1.52 | 1.92 | 1.83 |
| **12** | **12130** | **25.06** | **1.65** | **2.06** | **1.93** |
| 11 | 11190 | 23.12 | 1.62 | 2.05 | 1.91 |
| 10 | 10250 | 21.18 | 1.62 | 2.05 | 1.91 |
| 9 | 9310 | 19.24 | 1.62 | 1.99 | 1.89 |
| 8 | 8370 | 17.29 | 1.58 | 1.89 | 1.85 |
| 7 | 7430 | 15.35 | 1.48 | 1.79 | 1.78 |
| 6 | 6490 | 13.41 | 1.42 | 1.71 | 1.75 |
| 5 | 5550 | 11.47 | 1.35 | 1.63 | 1.65 |
| 4 | 4610 | 9.52 | 1.22 | 1.51 | 1.53 |
| 3 | 3670 | 7.58 | 1.1 | 1.37 | 1.37 |
| 2 | 2730 | 5.64 | 0.94 | 1.21 | 1.2 |
| 1 | 1365 | 2.82 | 0.76 | 1.03 | 1.01 |
| 0 | 0 | 0 | 0.37 | 0.63 | 0.75 |

*Results of strain measurements*

The deformation readings were recorded after stabilization at each loading stage, with a 15-minute holding time, which made it possible to correctly isolate the elastic component and minimize the influence of short-term creep of the printed concrete. The generalized values are presented in Table 3, and the graphical deformation curves are shown in Fig. 6.

In the areas where compressive behavior of the fibers was expected (sensors D-0, D-2, D-4, D-6), the deformations had a negative sign

(compression) and increased in magnitude with increasing load. Sensor D-0, located closer to the center, exhibited a smooth and well-linearized increase in compressive strains up to approximately $-30\times10^{-6}$ at the maximum load level.

Sensor D-2 showed slightly lower compressive amplitudes but the same stable trend, reaching values of about $-35\times10^{-6}$.Sensors D-4 and D-6, positioned closer to the ribs of the internal topological structure, recorded the highest compressive strains (up to $-70\times10^{-6}$), which was expected because local stiffness concentrators redistribute stresses and increase curvature in these regions.

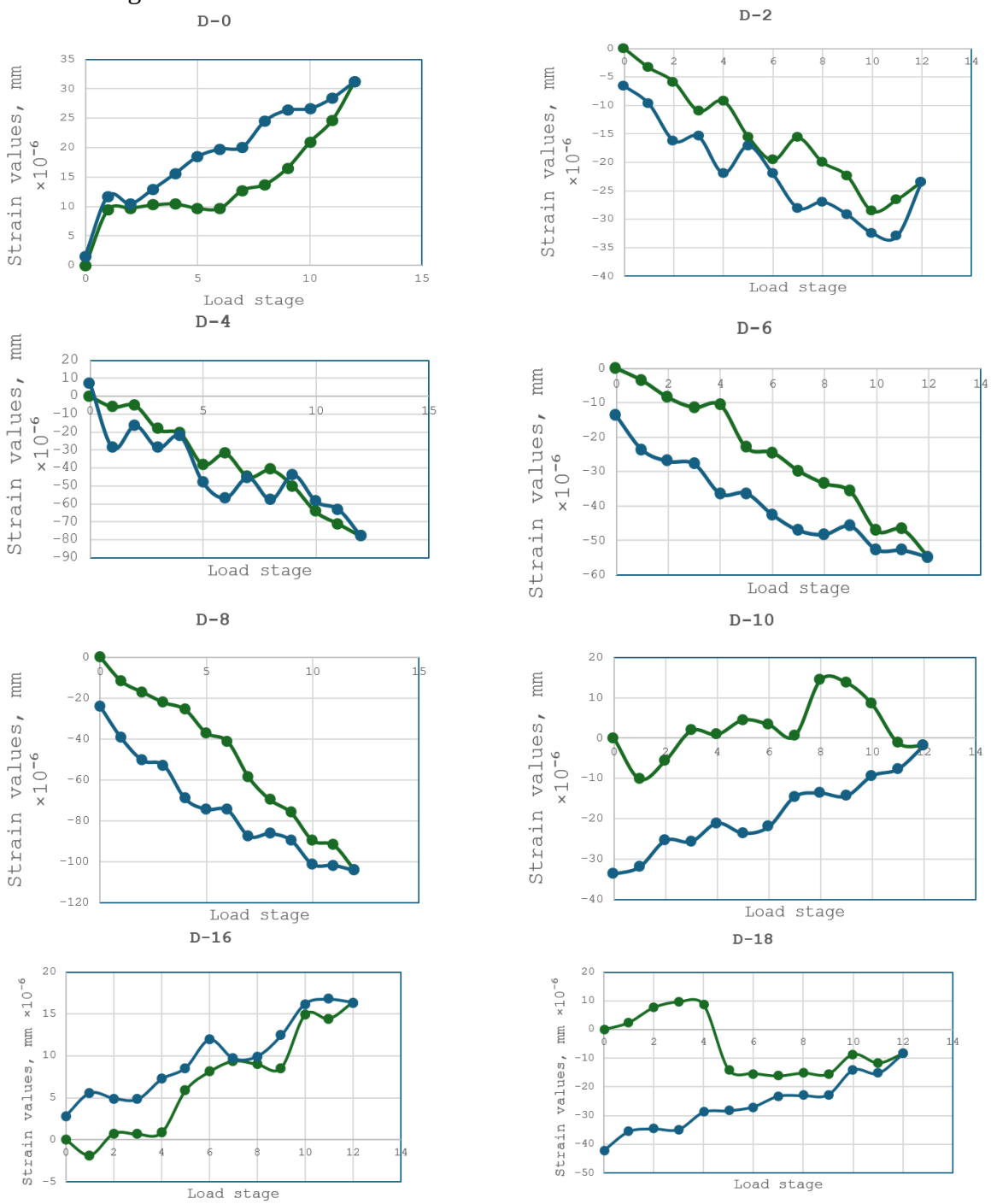


**Fig. 6** Strain values
**Рис. 6** Значення деформацій

**Table 3** Readings of strain gauges – strains
**Табл. 3** Показання тензодатчиків – деформації

| Loading stage | Strain gauges - strain values, mm ×10⁻⁶ | | | | | | | |
|---|---|---|---|---|---|---|---|---|
| | D-0 | D-2 | D-4 | D-6 | D-8 | D-10 | D-16 | D-18 |
| 0 | 0.00 | 0.00 | 0.00 | 0.00 | 0.00 | 0.00 | 0.00 | 0.00 |
| 1 | 9.44 | -3.38 | -5.86 | -3.58 | -11.86 | -10.12 | -1.80 | 2.44 |
| 2 | 9.75 | -5.86 | -5.09 | -8.53 | -17.21 | -5.55 | 0.78 | 7.70 |
| 3 | 10.25 | -10.98 | -18.51 | -11.38 | -22.27 | 1.84 | 0.67 | 9.64 |
| 4 | 10.45 | -9.23 | -20.78 | -10.66 | -25.74 | 0.89 | 0.88 | 8.66 |
| 5 | 9.70 | -15.52 | -38.08 | -23.10 | -37.19 | 4.47 | 5.90 | -13.93 |
| 6 | 9.70 | -19.64 | -32.06 | -24.46 | -41.30 | 3.32 | 8.11 | -15.30 |
| 7 | 12.77 | -15.68 | -45.01 | -29.79 | -58.93 | 0.47 | 9.39 | -16.19 |
| 8 | 13.74 | -20.00 | -41.08 | -33.50 | -69.86 | 14.34 | 9.00 | -15.19 |
| 9 | 16.51 | -22.43 | -50.27 | -35.79 | -76.27 | 13.71 | 8.58 | -15.61 |
| 10 | 20.92 | -28.60 | -64.61 | -47.18 | -89.79 | 8.37 | 14.92 | -8.61 |
| 11 | 24.64 | -26.60 | -71.31 | -46.82 | -92.06 | -1.17 | 14.43 | -11.67 |
| **12** | **31.19** | **-23.42** | **-78.28** | **-54.90** | **-104.56** | **-1.91** | **16.40** | **-8.40** |
| 11 | 28.39 | -33.03 | -63.19 | -52.89 | -101.97 | -7.69 | 16.76 | -15.24 |
| 10 | 26.60 | -32.45 | -58.76 | -52.73 | -101.45 | -9.33 | 16.23 | -14.04 |
| 9 | 26.34 | -29.18 | -43.88 | -45.88 | -89.78 | -14.36 | 12.44 | -22.75 |
| 8 | 24.50 | -26.96 | -57.75 | -48.31 | -86.41 | -13.62 | 9.96 | -23.01 |
| 7 | 20.07 | -28.01 | -45.25 | -47.09 | -87.73 | -14.51 | 9.70 | -23.22 |
| 6 | 19.73 | -22.05 | -56.76 | -42.56 | -74.91 | -21.95 | 11.95 | -26.96 |
| 5 | 18.45 | -17.10 | -48.14 | -36.33 | -74.54 | -23.54 | 8.58 | -28.32 |
| 4 | 15.57 | -21.91 | -22.26 | -36.49 | -69.36 | -21.05 | 7.24 | -28.82 |
| 3 | 12.88 | -15.46 | -28.80 | -27.81 | -53.07 | -25.64 | 4.84 | -34.87 |
| 2 | 10.45 | -16.20 | -16.29 | -27.07 | -50.65 | -25.33 | 4.94 | -34.66 |
| 1 | 11.73 | -9.72 | -28.74 | -23.77 | -39.78 | -31.91 | 5.59 | -35.62 |
| 0 | 1.59 | -6.55 | 7.29 | -13.86 | -24.21 | -33.70 | 2.89 | -42.25 |

All curves of the upper sensors exhibit a clearly monotonic behavior without jumps, inversions, or sharp anomalies, which indicates the integrity of the interlayer bond of the 3D-printed concrete and the absence of local damage or cracking during the test.

In the lower zone of the slab (sensors D-8, D-10, D-16, D-18), the deformations are predominantly tensile, which corresponds to the general bending behavior of the element. Sensor D-8 recorded the highest tensile strains (up to $+100\times10^{-6}$), which corresponds to the region of maximum curvature under bending. Sensor D-10 showed a less uniform but still elastic pattern of strain development, reaching approximately $+20\times10^{-6}$ in tension. Sensors D-16 and D-18, located in peripheral areas, demonstrated smaller but stable tensile strains, which is consistent with the actual bending pattern.

The overall behavior of the strain curves in the lower fibers exhibits an almost linear dependence in the load range of 0–20 kN/m², with minor fluctuations that may be attributed to local features of the printed-layer structure or contact stresses near the ribs.

For all sensors, after the completion of the loading cycle and subsequent unloading, the

strains returned almost entirely to values close to zero. This indicates:

- a predominantly elastic behavior of the slab;
- the absence of plastic strains in the concrete;
- no damage to the interlayer adhesion of the printed contours;
- no accumulation of deformability typical of structures with weak zones.

In fact, the strain diagrams confirm that the applied load—approximately 25 % of the strength limit of the printed concrete—did not create conditions for the development of persistent residual strains in the monitored areas.

## CONCLUSIONS

The experimental testing of a slab with complex topological geometry, manufactured using layer-by-layer 3D concrete printing, confirmed the effectiveness of the selected structural concept and the suitability of 3DCP technology for producing load-bearing floor elements. The slab demonstrated stable and predictable behaviour throughout the entire range of applied loads, which reached 25.06 kN/m² (approximately 25 % of the material's strength limit), without any signs of failure, macrocrack formation, or loss of load-bearing capacity. The maximum recorded deflections were 1.65 mm at the mid-span and up to 2.06 mm in peripheral points. After completing the full loading–unloading cycle, the slab returned to a geometry close to its initial state: the residual deflections did not exceed 0.63 mm, corresponding to a 60–70 % recovery and indicating an elastic mode of structural behaviour.

The results of strain-gauge measurements correlate with the deflection data and show a monotonic and stable development of compressive and tensile strains in the corresponding zones of the slab. The maximum compressive strains in the upper fibres reached approximately $-70\times10^{-6}$, while the tensile strains in the lower fibres were around $+100\times10^{-6}$, which corresponds to the expected behaviour of a bending structural element. After unloading, all sensors recorded an almost complete return of strain values to levels close to zero, indicating the absence of plastic damage, interlayer bond failure, or local stiffness degradation. Sensors D-12 and D-14 were excluded from the analysis due to unstable signals and inconsistency with the expected deformation patterns.

The overall stress–strain behaviour of the slab—both in terms of deflection measurements and strain-gauge data - confirms the high quality of interlayer bonding in the 3DCP material, the proper functioning of the internal ribbed structure, and the uniform transmission of loads through the topologically optimized geometry. The absence of sharp stiffness changes, strain jumps, or anomalies in the readings indicates the integrity of the printed contours and the adequate strength of the material.

The obtained results allow us to conclude that the application of 3D concrete printing technology for manufacturing floor slabs with complex internal geometry is feasible and provides a sufficient level of stiffness, load-bearing capacity, and deformability within service load ranges. The study confirms the viability of the concept and establishes an experimental basis for further scientific research, optimization of geometric parameters, and the development of design recommendations for structural elements produced using 3DCP technology.

## REFERENCES

1. **Buswell, R. A., De Silva, W. L., Jones, S. Z., & Dirrenberger, J.** (2018). 3D printing using concrete extrusion: A roadmap for research. *Cement and Concrete Research, 112, 37–49*. https://doi.org/10.1016/j.cemconres.2018.05.006
2. **Liu, D., Duan, Z., Li, L., Liu, J., & Li, Z.** (2023). 3D printing concrete structures: State of the art, challenges, and opportunities. *Construction and Building Materials, 405, 133364.* https://doi.org/10.1016/j.conbuildmat.2023.133364
3. **Rehman, A. U., Kim, J. H., & Jang, J. G.** (2021). 3D concrete printing: A systematic

review of rheology, mix designs, mechanical, microstructural, and durability characteristics. *Materials, 14(14), 3800.* https://doi.org/10.3390/ma14143800

4. **Fasihi, A., Ghourchian, S., Lark, R. J., et al.** (2024). From pumping to deposition: A comprehensive review of 3D concrete printing material characterization test methods. *Construction and Building Materials, 432, 134968.* https://doi.org/10.1016/j.conbuildmat.2024.134968
5. **Zhuang, Z., Xu, F., Ye, J., et al.** (2024). A comprehensive review of sustainable materials and toolpath optimization in 3D concrete printing. npj *Materials Sustainability, 2, 12.* https://doi.org/10.1038/s44296-024-00017-9
6. **Jipa, A., & Dillenburger, B.** (2022). 3D Printed Formwork for Concrete: State-of-the-Art, Opportunities, Challenges, and Applications. *3D Printing and Additive Manufacturing, 9(2), 86–107.* https://doi.org/10.1089/3dp.2021.0024.
7. **Burger, J. J., Mata-Falcón, J., & Dillenburger, B.** (2022). Design and fabrication of optimised ribbed concrete floor slabs using large-scale 3D printed formwork. *Automation in Construction, 144, 104599.* https://doi.org/10.1016/j.autcon.2022.104599 .
8. **Mata-Falcón, J., Burger, J. J., & Dillenburger, B.** (2022). Digitally fabricated ribbed concrete floor slabs. *RILEM Technical Letters, 7, 68–78.* https://doi.org/10.21809/rilemtechlett.2022.161
9. **Jipa, A., Barentin, C., Javier, C., et al.** (2019). 3D-Printed formwork for integrated funicular concrete slabs. *In Proceedings of the IASS Symposium 2019(6), 1-10.* https://doi.org/10.3929/ethz-b-000387460
10. **Aghaei Meibodi, M., Bernhard, M., Jipa, A., et al.** (2018DF). The Smart Takes from the Strong: 3D printing stay-in-place formwork for concrete slab construction. *In E. Doubrovski, M. R. Tamke, M. R. Thomsen, et al. (Eds.), Fabricate 2017: Rethinking Design and Construction (pp. 210–217). UCL Press.* https://doi.org/10.3929/ethz-b-000237103
11. **Aghaei Meibodi, M., Jipa, A., Giesecke, R., et al.** (2018). Smart Slab: Computational design and digital fabrication of a lightweight concrete slab. *In ACADIA 2018: Recalibration: on imprecision and infidelity (pp. 434–443).* https://doi.org/10.52842/conf.acadia.2018.434
12. **Ma, J., Gomaa, M., Bao, D. W., Rezaee Javan, A., & Xie, Y. M.** (2022). PrintNervi – Design and construction of a ribbed floor system in the digital era. *Journal of the International Association for Shell and Spatial Structures, 63(2), 241–251.* https://doi.org/10.20898/j.iass.2022.017
13. **Bendsøe, M. P., & Sigmund, O.** (2004). Topology Optimization: Theory, Methods and *Applications. Springer.* https://doi.org/10.1007/978-3-662-05086-6
14. **Demchyna, B., Vozniuk, L., Surmai, M., Havryliak, S., & Famulyak, Y.** (2023). Experimental study of the dome model made using a 3D printer from PLA plastic. *AIP Conference Proceedings, 2949(1), 020025.* https://doi.org/10.1063/5.0165270
15. **Demchyna, B., Vozniuk, L., Surmai, M., Burak, D., & Shcherbakov, S.** (2024). 3D printing technology for monolithic beams with the possibility of reinforcing bars. *Bulletin of Lviv National Environmental University. Series Architecture and Construction, 25, 32–37.* [in Ukraine] https://doi.org/10.31734/architecture2024.25.032
16. **Huang, X., & Xie, Y. M.** (2010). Evolutionary Topology Optimization of Continuum Structures: Methods and Applications. *John Wiley & Sons.* https://doi.org/10.1002/9780470689486
17. **Xia, L., Xia, Q., Huang, X., & Xie, Y. M.** (2018). Bi-directional evolutionary structural optimization on advanced structures and materials: A comprehensive review. Archives of *Computational Methods in Engineering, 25(1), 437–478.* https://doi.org/10.1007/s11831-016-9203-2
18. **Stoiber, N., & Kromoser, B.** (2021). Topology optimization in concrete construction: A systematic review on numerical and experimental investigations. S*tructural and Multidisciplinary Optimization, 64(3), 1725–1749.* https://doi.org/10.1007/s00158-021-03019-6
19. **Bialkowski, S.** (2018). Topology Optimisation Influence on Architectural Design Process – Enhancing Form Finding Routine by tOpos *Toolset Utilisation. In Proceedings of the eCAADe 2018 Conference (pp. 139–148).* https://doi.org/10.52842/conf.ecaade.2018.1.139
20. **Tang, T., Wang, L., Zhu, M., Zhang, H., Dong, J., Yue, W., & Xia, H.** (2024). Topology Optimization: A Review for Structural Designs Under Statics Problems. *Materials, 17(23), 5970.*

https://doi.org/10.3390/ma17235970
21. **Hager, I., Maroszek, M., Mróz, K., et al.** (2022). Interlayer bond strength testing in 3D-printed mineral materials for construction applications. *Materials, 15(12), 4112.* https://doi.org/10.3390/ma15124112
22. **Kalmykov, O., Gaponova, L., Reznik, P., & Grebenchuk, S.** (2017). Use of information technologies for energetic portrait construction of cylindrical reinforced concrete shells. MATEC *Web of Conferences, 116, 02017*. [in Ukraine] https://doi.org/10.1051/matecconf/201711602017
23. **Shmukler, V., Petrova, O., Reznik, P., Hamad, F. S., & Sosnowska, M.** (2019). Improvement of the structural parameters of the reinforced concrete support in a mesh cage. *AIP Conference Proceedings, 2077(1), 020048.* https://doi.org/10.1063/1.5091909
24. **Kalmykov, O. O., Reznik, P. A., V'iunkovskyi, V. P., Demianenko, I. M., & Buldakov, O. O.** (2025). Towards the optimization of reinforced concrete slab topology. *Municipal Economy of Cities. Series: Information Technology and Engineering, 192, 228–235*. [in Ukraine] https://doi.org/10.33042/3083-6727-2025-4-192-228-235
25. **Shmukler, V. S., Vozniuk, L. I., & Berezhna, K. V.** (2022). Energy portrait of the structural system as a criteria for option design. *Bulletin of Kharkov National Automobile and Highway University, 98, 136–143.* [in Ukraine] https://doi.org/10.30977/BUL.2219-5548.2022.98.0.136
26. **Sanjayan, J. G., Nematollahi, B., Xia, M., & Marchment, T.** (2018). Effect of surface moisture on inter-layer strength of 3D printed concrete. *Construction and Building Materials, 172, 468–475.* https://doi.org/10.1016/j.conbuildmat.2018.03.232
27. **Skibicki, S., Dvorak, R., Pazdera, L., et al.** (2024). Anisotropic mechanical properties of 3D printed mortar by standard flexural and compression test and acoustic emission. *Construction and Building Materials, 452, 138957*. https://doi.org/10.1016/j.conbuildmat.2024.138957
28. **Reznik, P. A., Petrenko, D. H., Volodymyrov, A. V., Alataiev, D. A., & Maksymenko, V. O.** (2025). Strength anisotropy of 3d-printed concrete: experimental investigation and statistical analysis. *Scientific Bulletin of Construction, 112(1), 248–255.* [in Ukraine] https://doi.org/10.33042/2311-7257.2025.112.1.30
29. **Zhang, K., Lin, W., Zhang, Q., et al.** (2024). Evaluation of anisotropy and statistical parameters of compressive strength for 3D printed concrete. *Construction and Building Materials, 440, 1374417*. https://doi.org/10.1016/j.conbuildmat.2024.137417
30. **Panda, B., Noor Mohamed, N. A., Paul, S. C., Bhagath Singh, G., Tan, M. J., & Šavija, B.** (2019). The Effect of Material Fresh Properties and Process Parameters on Buildability and Interlayer Adhesion of 3D Printed Concrete. *Materials, 12(13), 2149.* https://doi.org/10.3390/ma12132149
31. **Kalmykov, O. O., & Binkevych, K. O.** (2024). Experimental determination of floor panels deformability of a large-panel system building after renovation. *Scientific Bulletin of Construction, 110, 42–52.* [in Ukraine] https://doi.org/10.33042/2311-7257.2024.110.1.7
32. **Kripak, V., Kolyakova, V., & Gaidai, M.** (2021). Research on the effectiveness of reinforced concrete monolithic floors with hollow liners. *Building constructions. Theory and practice,(9), 15–29.*[in Ukraine] https://doi.org/10.32347/2522-4182.9.2021.15-29
33. **Demchyna, B., Voznyuk, L., Burak, D., & Shcherbakov, S.** (2024). 3D printing of beams with the possibility of installing transverse reinforcement, taking into account the peculiarities of the construction printer. *Building construction. Theory and practice, (14), 57–66.* [in Ukraine] https://doi.org/10.32347/2522-4182.9.2021.15-29

## LITERATURE

1. **Buswell, R. A., De Silva, W. L., Jones, S. Z., & Dirrenberger, J.** (2018). 3D printing using concrete extrusion: A roadmap for research. *Cement and Concrete Research, 112, 37–49.* https://doi.org/10.1016/j.cemconres.2018.05.006
2. **Liu, D., Duan, Z., Li, L., Liu, J., & Li, Z.** (2023). 3D printing concrete structures: State of the art, challenges, and opportunities. *Construction and Building Materials, 405, 133364*.

https://doi.org/10.1016/j.conbuildmat.2023.133364

3. **Rehman, A. U., Kim, J. H., & Jang, J. G.** (2021). 3D concrete printing: A systematic review of rheology, mix designs, mechanical, microstructural, and durability characteristics. *Materials, 14(14), 3800.* https://doi.org/10.3390/ma14143800
4. **Fasihi, A., Ghourchian, S., Lark, R. J., et al.** (2024). From pumping to deposition: A comprehensive review of 3D concrete printing material characterization test methods. *Construction and Building Materials, 432, 134968*. https://doi.org/10.1016/j.conbuildmat.2024.134968
5. **Zhuang, Z., Xu, F., Ye, J., et al.** (2024). A comprehensive review of sustainable materials and toolpath optimization in 3D concrete printing. npj *Materials Sustainability, 2, 12.* https://doi.org/10.1038/s44296-024-00017-9
6. **Jipa, A., & Dillenburger, B.** (2022). 3D Printed Formwork for Concrete: State-of-the-Art, Opportunities, Challenges, and Applications. *3D Printing and Additive Manufacturing, 9(2), 86–107.* https://doi.org/10.1089/3dp.2021.0024.
7. **Burger, J. J., Mata-Falcón, J., & Dillenburger, B.** (2022). Design and fabrication of optimised ribbed concrete floor slabs using large-scale 3D printed formwork. *Automation in Construction, 144, 104599.* https://doi.org/10.1016/j.autcon.2022.104599 .
8. **Mata-Falcón, J., Burger, J. J., & Dillenburger, B.** (2022). Digitally fabricated ribbed concrete floor slabs. *RILEM Technical Letters, 7, 68–78.* https://doi.org/10.21809/rilemtechlett.2022.161
9. **Jipa, A., Barentin, C., Javier, C., et al.** (2019). 3D-Printed formwork for integrated funicular concrete slabs. *In Proceedings of the IASS Symposium 2019(6), 1-10.* https://doi.org/10.3929/ethz-b-000387460
10. **Aghaei Meibodi, M., Bernhard, M., Jipa, A., et al.** (2018DF). The Smart Takes from the Strong: 3D printing stay-in-place formwork for concrete slab construction. *In E. Doubrovski, M. R. Tamke, M. R. Thomsen, et al. (Eds.), Fabricate 2017: Rethinking Design and Construction (pp. 210–217). UCL Press.* https://doi.org/10.3929/ethz-b-000237103
11. **Aghaei Meibodi, M., Jipa, A., Giesecke, R., et al.** (2018). Smart Slab: Computational design and digital fabrication of a lightweight concrete slab. *In ACADIA 2018: Recalibration: on imprecision and infidelity (pp. 434–443).* https://doi.org/10.52842/conf.acadia.2018.434
12. **Ma, J., Gomaa, M., Bao, D. W., Rezaee Javan, A., & Xie, Y. M.** (2022). PrintNervi – Design and construction of a ribbed floor system in the digital era. *Journal of the International Association for Shell and Spatial Structures, 63(2), 241–251.* https://doi.org/10.20898/j.iass.2022.017
13. **Bendsøe, M. P., & Sigmund, O.** (2004). Topology Optimization: Theory, Methods and Applications. Springer. https://doi.org/10.1007/978-3-662-05086-6
14. **Demchyna, B.H., Surmai, M., Vozniuk, L.I., Havryliak P.A.** (2023). Eksperymental-ne doslidzhennia modeli kupola, vyhotovle-noi za dopomohoiu 3D-pryntera z PLA-plastyku. *AIP Conference Proceedings, 2949(1), 020025.* https://doi.org/10.1063/5.0165270
15. **Demchyna, B., Vozniuk, L., Surmai, M., Burak D., & Shcherbakov. S.** (2024). Tekhnolohiia 3D-druku dlia monolitnykh ba-lok z mozhlyvistiu vykorystannia armatur-nykh stryzhniv. *Visnyk Lvivskoho natsiona-lnoho ekolohichnoho universytetu. Seriia «Arkhitektura ta budivnytstvo», 25, 32–37.* https://doi.org/10.31734/architecture2024.25.032
16. **Huang, X., & Xie, Y. M.** (2010). Evolutionary Topology Optimization of Continuum Structures: Methods and Applications. *John Wiley & Sons.* https://doi.org/10.1002/9780470689486
17. **Xia, L., Xia, Q., Huang, X., & Xie, Y. M.** (2018). Bi-directional evolutionary structural optimization on advanced structures and materials: A comprehensive review. *Archives of Computational Methods in Engineering, 25(1), 437–478.* https://doi.org/10.1007/s11831-016-9203-2
18. **Stoiber, N., & Kromoser, B.** (2021). Topology optimization in concrete construction: A systematic review on numerical and experimental investigations. *Structural and Multidisciplinary Optimization, 64(3), 1725–1749.* https://doi.org/10.1007/s00158-021-03019-6
19. **Bialkowski, S.** (2018). Topology Optimisation Influence on Architectural Design Process – Enhancing Form Finding Routine by tOpos Toolset Utilisation. *In Proceedings of the eCAADe 2018 Conference (pp. 139–148).* https://doi.org/10.52842/conf.ecaade.2018.1.139

20. **Tang, T., Wang, L., Zhu, M., Zhang, H., Dong, J., Yue, W., & Xia, H.** (2024). Topology Optimization: A Review for Structural Designs Under Statics Problems. *Materials, 17(23), 5970.* https://doi.org/10.3390/ma17235970
21. **Hager, I., Maroszek, M., Mróz, K., et al.** (2022). Interlayer bond strength testing in 3D-printed mineral materials for construction applications. *Materials, 15(12), 4112*. https://doi.org/10.3390/ma15124112
22. **Kalmykov, O., Haponova, L., Reznik, P., & Hrybenchuk, S.** (2017). Vykorystan-nia informatsiinykh tekhnolohii dlia enerhe-tychnoho portretnoho budivnytstva tsylin-rychnykh zalizobetonnykh obolonok. MATEC *Web of Conferences, 116, 02017***.** https://doi.org/10.1051/matecconf/201711602017
23. **Shmukler, V., Petrova, O., Reznik, P., Khammud, M., Sosnovska M. (2019).** Pokrashchennia konstruktyvnykh parametriv zalizobetonnoi opory v sitchastomu kar-kasi. *AIP Conference Proceedings, 2017 (1), 020048***.** https://doi.org/10.1063/1.5091909
24. **Kalmykov, O., Peznik, P., Viunkovskyi, V., Demianenko I., & Buldakov O.** (2025). Pro poshuk optyma-lnoi topolohii zalizobetonnoi plyty perekryttia. *Komunalne hospodarstvo mist. Seriia: Informatsiini tekhnolohii ta inzhe-neriia, 192, 228–235* https://doi.org/10.33042/3083-6727-2025-4-192-228-235
25. **Shmukler, V., Vozniuk, L.,& Berezhna. K. (2022).** Enerhetychnyi portret konstruktyvnoi systemy yak kryterii variantnoho proektu-vannia. *Visnyk Kharkivskoho natsionanoho avtomobilno-dorozhnoho universytetu, 98, 136–143.* https://doi.org/10.30977/BUL.2219-5548.2022.98.0.136
26. **Dzhei H. Sandzhaian, Bekhzad Nemato-llakhi, Min Sia, Teilor Marchment.** (2018). EVplyv poverkhnevoi volohy na mizhsharovu mitsnist betonu, nadrukovanoho za dopo-mohoiu 3d-druku. *Budivnytstvo ta budivelni materialy, 172, 468–475***.** https://doi.org/10.1016/j.conbuildmat.2018.03.232
27. **Skibicki, S., Dvorak, R., Pazdera, L., et al.** (2024). Anisotropic mechanical properties of 3D printed mortar by standard flexural and compression test and acoustic emission. *Construction and Building Materials, 452, 138957.* https://doi.org/10.1016/j.conbuildmat.2024.138957
28. **Reznik, P.A., Petrenko, D.H., Volo-dymyrov, A.V., Maksymenko, V.O., & Alataiev D.A. (2025).** Anizotropiia mitsnosti 3D-drukovanoho betonu: Eksperymentalne doslidzhennia ta statystychnyi analiz. *Naukovyi visnyk budivnytstva, 112(1), 248–255***.** https://doi.org/10.33042/2311-7257.2025.112.1.30
29. **Zhang, K., Lin, W., Zhang, Q., et al.** (2024). Evaluation of anisotropy and statistical parameters of compressive strength for 3D printed concrete. Construction and Building Materials, 440, 1374417. https://doi.org/10.1016/j.conbuildmat.2024.137417
30. **Panda, B., Noor Mohamed, N. A., Paul, S. C., Bhagath Singh, G., Tan, M. J., & Šavija, B.** (2019). The Effect of Material Fresh Properties and Process Parameters on Buildability and Interlayer Adhesion of 3D Printed Concrete. Materials, 12(13), 2149. https://doi.org/10.3390/ma12132149
31. **Kalmykov, O.O., & Binkevych K.O. (2024).** Eksperymentalne vstanovlennia deformatyv-nosti paneei perekryttiv velykopanelnoho zhytlovoho budynku pislia vidnovlennia. *Naukovyi visnyk budivnytstva, (110), 42–52.* https://doi.org/10.33042/2311-7257.2024.110.1.7
32. **Kripak, V., Koliakova, V., & Haidai, M. (2021).** Doslidzhennia efektyvnosti zalizobetonnoho monolitnoho perekryttia z porozhnystymy vkladyshamy. *Budivelni konstruktsii. Teoriia i praktyka, (9), 15–29.* https://doi.org/10.32347/2522-4182.9.2021.15-29
33. **Demchyna, B., Vozniuk, L., Burak, D. & Shcherbakov, S. (2024).** 3D druk balok iz mozhlyvistiu vlashtuvannia poperechnoho armuvannia, vrakhovuiuchy osoblyvosti ro-boty budivelnoho pryntera. *Budivelni konstruktsii. Teoriia i praktyka, (14), 57–66.* https://doi.org/10.32347/2522-4182.9.2021.15-29

# ЕКСПЕРИМЕНТАЛЬНЕ ВИПРОБУВАННЯ ПЛИТИ ПЕРЕКРИТТЯ СКЛАДНОЇ ГЕОМЕТРІЇ, ВИКОНАНОЇ ЗА ДОПОМОГОЮ ТЕХНОЛОГІЇ 3D CP

*Олег КАЛМИКОВ*
*Петро Резнік*
*Інна ФУРМАН*
*Іван ДЕМ'ЯНЕНКО*

**Анотація.** У статті наведено результати комплексного експериментального дослідження залізобетонної тонкостінної плити складної геометрії, виготовленої методом 3D-друку бетоном (3DCP). Метою роботи є оцінювання напружено-деформованого стану, жорсткісних характеристик та загальної працездатності плити з внутрішньою структурою, сформованою на основі принципів раціонального перерізу та топологічного формоутворення. Досліджуваний зразок розміром 2200×2200 мм містив систему криволінійних ребер та комірчастих порожнин, надрукованих шарами завтовшки 20 мм. Така геометрія забезпечувала перерозподіл матеріалу відповідно до очікуваних полів напружень та мала на меті покращення конструктивної ефективності при зменшенні маси.

Випробування здійснювались на жорсткому просторовому сталевому стенді з опиранням плити по контуру. Навантаження прикладалося поетапно шляхом укладання чавунних мірних блоків масою 21 кг та важких бетонних блоків ФБС масою 518 кг, що забезпечували еквівалентне рівномірно розподілене навантаження. Загалом виконано 12 етапів навантаження з витримкою 15 хв на кожному кроці, а максимальний тиск на поверхню становив 25.06 кН/м². Геометричну деформативність контролювали трьома високоточними прогиномірами (0.01 мм), тоді як локальні деформації фіксували десять тензометричних датчиків із базою 20 мм, наклеєних у характерних зонах верхньої та нижньої поверхонь плити.

Аналіз отриманих результатів показав, що плита працює у межах лінійно-пружної деформативності в усьому діапазоні навантажень. Максимальний прогин у центрі досяг 2.06 мм, а після повного розвантаження зменшився до 0.63 мм, що підтверджує значну частку зворотних деформацій та відсутність пошкоджень у матеріалі. Показання тензодатчиків засвідчили рівномірний розвиток стискаючих і розтягуючих деформацій, їх кореляцію з полем згинальних моментів та відсутність локальних зон концентрації напружень. Деформаційні криві не містили стрибків або аномалій, що вказує на цілісність міжшарових з'єднань і відсутність ознак руйнування.

Отримані результати підтверджують ефективність застосування технології 3DCP для створення несучих плит перекриття складної внутрішньої структури, демонструють високу жорсткість та надійність друкованого елемента й підкреслюють перспективи розвитку топологічно оптимізованих залізобетонних конструкцій у сучасному будівництві.

**Ключові слова:** 3DCP; топологічна оптимізація; експериментальне випробування; прогини; деформації; рівномірно розподілене навантаження; несуча здатніст.

***Received:*** *October 28, 2025.*
***Accepted:*** *November 30, 2025.*

ISSN 2522-4182

DOI: 10.32347/2522-4182.17.2025.119-130
UDC 624.012.45

# INFLUENCE OF MIXING TIME OF CONCRETE MIXTURES ON THE DEFORMATIONAL CHARACTERISTICS OF STRUCTURAL CONCRETES

*Alexander KONOPLIANIK[1], Dmitrij ZHUK[2]*

[1,2] Ukrainian State University of Science and Technology,
Educational and Research Institute "Prydniprovska State Academy of Civil Engineering and Architecture"
24a, Oleg Petrov Street., Dnipro, Ukraine, 49005
[1]konoplianik.alexander@gmail.com, http://orcid.org/0000-0003-4664-8809
[2]dmitrij.zhuk.98d@gmail.com, http://orcid.org/0009-0001-2454-4980

**Abstract**. This scientific work is a continuation of studies [1] related to the determination of the class of structural concretes at different mixing times of the concrete mixture. The influence of the mixing time of the concrete mixture on the strength characteristics of concretes has been established. As a result of strength tests of cube and prism specimens, the classes of concretes by strength under axial compression were determined.

However, in the literature sources there are data on the influence of the deformability of concretes on the determination of their class by strength through the study of the modulus of elasticity of concretes. Therefore, the question arises of studying the deformability characteristics of concretes and their comparison with strength characteristics. Based on the results of these two studies, the final class of concrete can be determined.

The analysis of the current state of development and research of concretes has shown that one of the factors influencing the determination of the class of concrete by strength is the determination of the modulus of elasticity of concretes, which characterizes their deformability characteristics. Under laboratory conditions, studies of the modulus of elasticity and the class of concrete were carried out at mixing times of the concrete mixture of 480, 300, 180, and 90 seconds, respectively. For this purpose, 20 prism specimens with dimensions of 100 × 100 × 400 (height) mm were manufactured and tested. In determining the class of concrete, non-force
(volumetric) deformations of concrete and the cost of producing 100 m³ of concrete mixture based on electricity consumption during the mixing time of the mixture were also taken into account.

As a result of the conducted studies, it was determined that to obtain a guaranteed class of structural concrete not less than C16/20 (B20), the optimal mixing time of the concrete mixture is 180 seconds.

The purpose of the study is to investigate the deformational characteristics of structural concretes depending on the mixing time of the concrete mixture and their influence on the determination of the concrete class in terms of compressive strength.

**Keywords:** concrete mixture; mixing time; deformation characteristics; modulus of elasticity of concrete; concrete class

**Alexander KONOPLIANIK**
Associate Professor Department of Reinforced Concrete and Masonry Structures,

**Dmitrij ZHUK**
PhD Student Department of Reinforced Concrete and Masonry Structures,
St

## PROBLEM STATEMENT

This scientific work is a continuation of studies [1] related to determining the class of structural concrete at the optimal mixing time

of the concrete mixture. The influence of mixing time of the concrete mixture on the strength characteristics of concrete has been established. As a result of strength tests of cube and prism specimens, concrete classes were determined according to axial compressive strength.

However, literature sources contain data on the influence of concrete deformability on determining its strength class through the study of the modulus of elasticity of concrete. Therefore, the question arises of studying the deformation characteristics of concrete and comparing them with strength characteristics. Based on the results of these two studies, the final class of concrete can be determined

## ANALYSIS OF PREVIOUS RESEARCH

**Analysis of the current state** of development and research of concrete showed that one of the factors influencing the determination of concrete class by strength is the determination of the modulus of elasticity of concrete, which characterizes its deformation properties. Analysis of publications allows us to state that one of the most successful idealized objects of the general theory of its deformation can be considered the model of a deformed solid body. Such a model made it possible not only to reproduce the elastic–plastic properties of reinforced concrete itself but also to propose their alternative solutions in the form of force, deformation, and improved deformation–force models [2].

Among the deformation characteristics of concrete, two types of deformations can be distinguished: force deformations, which spread in the direction of the applied force, and non-force (volumetric) deformations, which spread in all directions and are mainly caused by shrinkage and swelling of concrete [3,4]. The study by Kongshaug [5] examined how force loading affects expansion and deformation of concrete, and determined that loading acts on concrete synergistically: mechanical characteristics (strength and modulus of elasticity) decrease faster under combined action and change the deformation model of the structure.

The main tool of the deformation calculation model is the actual stress–strain diagram of concrete, which establishes the relationship between its stresses σ and relative deformations ε in the compressed and tensioned zones of the section. Most often such a diagram is obtained by indirect methods, testing standard concrete prisms under eccentric compression [6, 7].

Chinese scientists in [8] proposed a new technology for determining deformability on concrete cubes by simultaneously measuring the modulus of elasticity and Poisson's ratio under a special vibration regime. The authors [9] proposed measuring deformations on porous concrete cylinder specimens by testing these specimens under triaxial compression and tension with significant lateral pressure. At the same time, measuring axial deformation using sensors makes it possible to assess the homogeneity of specimen deformation.

In domestic practice, there are two different approaches to determining the class of concrete by deformability. Authors [3] determine the class of concrete by the initial modulus of elasticity at stresses equal to 20% of ultimate strength, while authors [10] determine the class of concrete by the average value of the initial modulus of elasticity at stresses equal to 30% of ultimate strength. Therefore, two different approaches to determining the class of concrete by deformability require practical studies of both moduli of elasticity, and the class of concrete determined by deformability requires comparison with the class of concrete determined by strength.

It is desirable to supplement the list of Ukrainian studies in which the force loading of prisms was investigated: in [13, 14] the force loading regimes of prisms were studied, analyzing the stress–strain relationship, as well as modeling the stress–strain state of concrete under different loading regimes. The authors [15] conducted tests of prisms under central compression, with emphasis on crack resistance and force deformations.

In the work of the author [16], the modulus of elasticity is considered as the main parameter for stiffness calculations. Examples of determining the initial modulus of elasticity are provided. The study also describes the modulus of elasticity, shrinkage, and creep.

An analysis of the obtained diagrams in our study was carried out using the work of Fomin et al. [17]. The paper also describes the regularities of deformation changes on the graph and how this affects the load-bearing capacity of structures. An analysis of the obtained diagrams was performed in our study.

In the sections [18] devoted to the calculation of deflections and stiffness, the modulus of elasticity is used as a key parameter. It is explained how its value influences the deformation characteristics of structures.

In the works [19, 20, 21], a common approach to the analysis of concrete deformational characteristics can be observed. All authors emphasize the importance of the modulus of elasticity and shrinkage as key parameters determining the durability of structures. Their studies combine experimental methods (testing of prisms) with theoretical deformation models, which provided the foundation for modern international standards (Eurocode, ACI, RILEM).

The textbook [22] covers the fundamental properties of concrete, including prism testing, modulus of elasticity, and shrinkage.

In the works [23, 24, 25], a common approach to the analysis of the modulus of elasticity and concrete deformability can be observed. The authors demonstrate that these characteristics depend on the microstructure, mixture composition, and concrete class. Using this knowledge helped us to analyze the results obtained after conducting the experiments.

The works in the article [26] are used for predicting concrete deformations is used as a practical tool for engineers. It provides practical methods for forecasting concrete creep and shrinkage, which are widely applied in design practice.

## MAIN RESEARCH

Previous studies of cubic and prism strength of structural concretes obtained at mixing times of 90, 180, 300, and 480 seconds showed that the concrete classes determined by cubic strength results, based on calculated coefficients of variation, were identical and corresponded to C16/20 (B20). The concrete classes determined by prism strength results were different; the highest class values, C30/35 (B35) and C25/30 (B30), were observed in mixtures No. 1 and No. 3 at mixing times of 480 and 180 seconds, respectively. The obtained result, where prism strength exceeded cubic strength, is not typical. To confirm or refute the determined concrete classes by strength, studies of the deformative characteristics of concretes were conducted by determining their modulus of elasticity. In addition, linear and volumetric shrinkage of structural concretes, which represent non-strength deformations of concrete, were investigated.

The concrete mixture was prepared in an “Airich” concrete mixer, and specimens for testing were produced by manual compaction in molds and cured for 28 days. The mixing technology and specimen preparation procedure are presented in [1].

In total, 20 prism specimens of dimensions 100 × 100 × 400 mm (height) were produced to determine the modulus of elasticity and concrete class, i.e., 5 specimens of each mixture for the corresponding mixing time. To determine linear and volumetric shrinkage of concretes, 24 cube specimens of dimensions 100 × 100 × 100 mm were produced, i.e., 6 specimens of each mixture.

The relationship between stress and strain of concrete under stepwise loading of prisms was investigated [11]. This relationship characterizes the strength-related deformations of concrete.

For the experiments, dial-type indicators were installed on four opposite faces of the prisms. The prisms were stepwise loaded on a P-125 press with a load of 12.5 kN (Fig. 1). After each loading stage, the indicator readings were recorded, and the average concrete deformations were determined.

**Fig 1**. Determination of the deformative characteristics of concrete prisms using the P-125 press. Photo by D. Zhuk

**Рис 1** Визначення деформативних характеристик бетонних призм на пресі П-125. Автор фото Д. Жук

The load was increased up to failure, and stress–strain diagrams were constructed. On the diagrams, the zones of elastic and elastic–plastic deformations, as well as stresses $\sigma_{02}$ and $\sigma_{03}$ and strains $\varepsilon_{02}$ and $\varepsilon_{03}$, within which Hooke's law is valid, were identified.

The stresses $\sigma_{02}$ were taken as equal to 0.2 $R_b$ (ultimate strength). The initial modulus of elasticity $E_b$ for each mixture was calculated as the ratio of stresses $\sigma_{02}$ to strains $\varepsilon_{02}$ [3]. In addition, the mean modulus of elasticity $E_{cm}$ was determined at loads corresponding to 30% of the ultimate strength [10].

The relationship between the initial modulus of elasticity and the mean modulus of elasticity $E_{cm}$ was established. According to [3], this relationship is defined by the coefficient of elastic–plastic deformations of concrete, which is determined by the following formula:

$$v = E_b / E_{cm} \qquad (1)$$

To study the structure of concrete, one of the prisms was split in a direction perpendicular to the layers of mixture placement, and the uniformity of aggregate distribution on the internal surface of the concrete as well as the condition of the binder was evaluated.

The prism tests were carried out at an air temperature of 18.6–19.7 °C and a relative humidity of 56–62%.

Table 1 presents the results of determining

**Table 1**. Results of compressive strength and modulus of elasticity of concrete prisms (mixing time 180 s)
**Табл. 1** Результати визначення характеристик бетону призм після випробування на стиск

| Specimen labeling | Cross-sectional area $a_{avg} \cdot b_{avg}$ = S, $cm^2$ | Ultimate load, P, kN | Prism strength $R_b$ ($f_{prism}$), MPa | Stresses, $\sigma_{02}$, MPa | Strains, $\varepsilon_{02} \cdot 10^5$ | Initial modulus of elasticity, $E_b \cdot 10^3$, MPa | Stresses, $\sigma_{03}$, MPa | Strain, $\varepsilon_{03} \cdot 10^5$ | Mean modulus of elasticity, $E_{cm} \cdot 10^3$, MPa |
|---|---|---|---|---|---|---|---|---|---|
| $3_{13}$ | 9,975.9,955 =99,3 | 206,25 | 20,77 | 4,15 | 13,91 | 29,86 | 6,23 | 21,76 | 28,63 |
| $3_{14}$ | 9,965.10,2 =101,64 | 225,5 | 22,19 | 4,44 | 13,13 | 33,79 | 6,66 | 21,2 | 31,4 |
| $3_{15}$ | 10,0.10,075 =100,75 | 225,675 | 22,4 | 4,48 | 14,52 | 30,85 | 6,72 | 21,98 | 30,57 |
| $3_{16}$ | 10,0.10,05 =100,5 | 204,51 | 20,35 | 4,07 | 14,08 | 28,91 | 6,1 | 21,19 | 28,81 |
| $3_{17}$ | 10,0.9,975 = 99,75 | 175,11 | 17,55 | 3,51 | 12,49 | 28,11 | 5,27 | 19,91 | 26,45 |

**Note**. The moduli of elasticity with the lowest values are highlighted in yellow

the characteristics of concrete prisms after compression testing, namely the dimensions of the cross-section, applied loads, the results of strength determination, and the modulus of elasticity of concrete produced at a mixing time of 180 seconds. The stress–strain curve of concrete obtained during compression testing of prism P-3$_{14}$ is shown in Fig. 2.

As shown in Table 1, the prism strength of concrete specimens with dimensions of 100 × 100 × 400 mm under axial compression ranged from 17.55 to 22.4 MPa. At the same time, the values of the initial modulus of elasticity were (28.11–33.79) × 10³ MPa, while the mean modulus of elasticity was (26.45–31.4) × 10³ MPa.

Figure 3 presents the structure of the internal surface of prism No. 3$_{14}$ after compression testing.

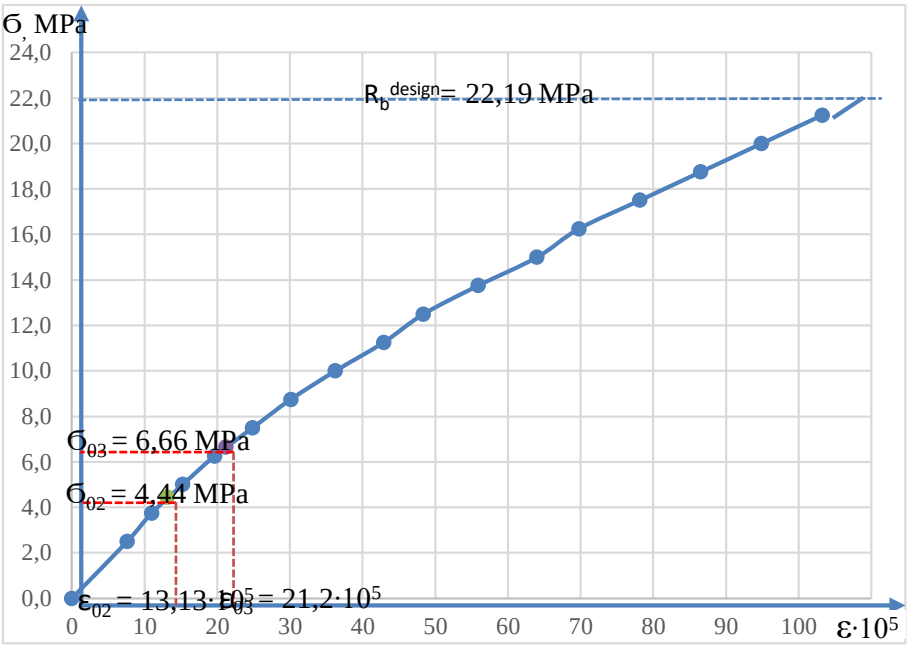


**Fig 2**. Stress–strain relationship of concrete during compression testing of prism P-3$_{14}$
**Рис 2** Залежність між напруженнями і деформаціями бетону при випробуванні призми П-3$_{14}$ на стиск

**Fig 3**. Structure of the internal surface of concrete prism P-3$_{14}$ (Photo by D. Zhuk)
**Рис 3** Структура внутрішньої поверхні бетону призми П-3$_{14}$ (Автор фото Д. Жук)

As shown in Fig. 3, the binder is uniformly distributed between the aggregate grains, while containing only a small number of open pores. The adhesion of the aggregate grains to the binder is good.

Similarly, prism specimens were tested at mixing times of 480, 300, and 90 seconds.

The results of testing structural concretes allowed us to systematize the dependence of prism strength and modulus of elasticity of concretes obtained at different mixing times of the concrete mixture.

Since there are currently two different approaches in the literature to determining the concrete class, in our opinion it is appropriate to analyze the results according to both approaches. The first approach [3] defines the concrete class B based on prism strength $R_b$ under axial compression and the initial modulus of elasticity $E_b$, determined at loads equal to 20% of the ultimate load. According to the second approach [10], the concrete class C is defined based on prism strength $f_{cm,prism}$ under axial compression and the mean modulus of elasticity $E_{cm}$, determined at loads equal to 30% of the ultimate load.

The authors of regulatory document [11, clause 8.6] propose, in our view, a rather ambiguous approach to determining the concrete class, which consists of the following steps:

- when calculating the average values of prism strength and modulus of elasticity within a series of specimens, abnormal (i.e., significantly deviating) test results are preliminarily excluded;
- to justify whether abnormal results should be considered, reference is made to another regulatory document [12, clause 8.8], which requires determining the average intra-series coefficient of variation of compressive strength by testing 30 series of specimens of the same concrete class;
- the obtained intra-series coefficient of variation is then compared with the threshold value [5, Annex A], which should not exceed 8%;
- if the coefficient of variation is greater than 8%, abnormal test results are taken into account;
- if the coefficient of variation is less than 8%, the average prism strength and modulus of elasticity are calculated based on the four specimens with the highest values.

In our opinion, it is necessary to consider the coefficient of variation adopted for calculations and design, which equals 13.5%. If the coefficient of variation is lower than 13.5%, the modulus of elasticity should be calculated based on the four specimens with the highest values. Conversely, if the coefficient of variation exceeds 13.5%, abnormal test results must be taken into account.

Thus, when determining the modulus of elasticity of concrete, the coefficient of variation should be established through mathematical processing of the experimental data[13-17].

The summarized results of prism tests at mixing times of 480, 300, 180, and 90 seconds are presented in Table 2.

As shown in Table 2, the highest concrete class determined by the modulus of elasticity is obtained at a mixing time of 480 s. In this case, the final concrete class is taken as the lower of the two values, namely C30/35 (B35). With a reduction in mixing time to 300, 180, and 90 s, concrete of the same class C20/25 (B25) is obtained. The increase in concrete class to C25/30 (B30), determined at a mixing time of 300 s based on the initial elastic modulus, is not considered, since it was obtained with a coefficient
of variation of 21.06%, which is significantly higher than the design standard value of 13.5%.

In addition, at a mixing time of 300 s, the elastic–plastic strain coefficient of concrete, equal to 0.909, indicates that under stresses up to 0.2 of the ultimate load, the deformation of concrete remains elastic, while under stresses above 0.2 of the ultimate load, elastic–plastic deformation occurs.

**Table 2**. Results of Determining the Modulus of Elasticity and the Class of Structural Concrete
**Табл. 2** Результати визначення модуля пружності та класу конструкційного бетону

| No. | Metrics | Mix No.<br>Mixing Time of Concrete, s | | | |
|---|---|---|---|---|---|
| | | 1<br>480 | 2<br>300 | 3<br>180 | 4<br>90 |
| 1 | Initial Modulus of Elasticity $E_b = 0{,}2 \cdot f_{ck,prism}$ , MPa | 36,16 | 32,445 | 30,85 | 31,94 |
| 2 | Average Initial Modulus of Elasticity $E_{cm} = 0{,}3 \cdot f_{ck,prism}$ , MPa | 35,55 | 29,48 | 29,85 | 30,72 |
| 3 | Coefficient of Elastic–Plastic Deformations of Concrete, ν | 0,983 | 0,909 | 0,968 | 0,962 |
| 4 | Determined Coefficient of Variation for the Initial Elastic Modulus, $V_m$,% | 2,8 | 21,06 | 7,26 | 2,97 |
| 5 | Determined Coefficient of Variation for the Average Initial Elastic Modulus, $V_m$,% | 2,44 | 9,91 | 13,16 | 5,19 |
| 6 | Concrete Class by Initial Elastic Modulus C(B) | C32/40 (B40) | C25/30 (B30) | C20/25 (B25) | C20/25 (B25) |
| 7 | Concrete Grade Based on the Average Initial Elastic Modulus, C(B) | C30/35 (B35) | C20/25 (B25) | C20/25 (B25) | C20/25 (B25) |

**Note.** The values of the initial elastic modulus and the average initial elastic modulus of concrete should be multiplied by $10^3$.

Non-load (volumetric) deformations of concrete were also investigated. For this purpose, both linear and volumetric shrinkage were determined [19-22].

Linear shrinkage of concrete, expressed as a percentage, was determined on six cube specimens of dimensions 100 × 100 × 100 mm as follows. After demolding, four lines parallel to the central axis were marked on four opposite faces (along the specimen height). The initial length of these lines was taken as the reference dimension. Measurements were performed using a caliper.

After curing the specimens for 28 days, the dimensions were measured again, and the linear shrinkage of concrete was calculated according to the following formula:

$$\varepsilon = \frac{l_2 - l_1}{l_1} \times 100 \qquad (2)$$

where:

- $l_1$ — the initial specimen dimension after demolding;
- $l_2$ — the specimen dimension after 28 days of curing.

The volumetric shrinkage of concrete, expressed as a percentage, was determined by recording the change in specimen volume according to the following formula:

$$\varepsilon_v = \frac{V_2 - V_1}{V_1} \times 100 \qquad (3)$$

where:

- $V_1$ — the initial specimen volume after demolding;
- $V_2$ — the specimen volume after 28 days of curing.

Figure 4 presents the graph of the dependence of linear and volumetric shrinkage of concrete on the mixing time of the concrete mixture [19-22].

As shown in Figure 4, the highest linear shrinkage, equal to 0.11%, is observed in concrete produced with a mixing time of 300 s. Overall, the linear shrinkage of concrete changes insignificantly and, in the graph of Figure 4, appears as a straight line with a slight increase in shrinkage values when the mixing time increases from 90 to 300 s. With an increase in mixing time to 480 s, the linear shrinkage of concrete decreases to 0.07%, which practically does not differ from the shrinkage value of concrete produced with a mixing time of 90 s.

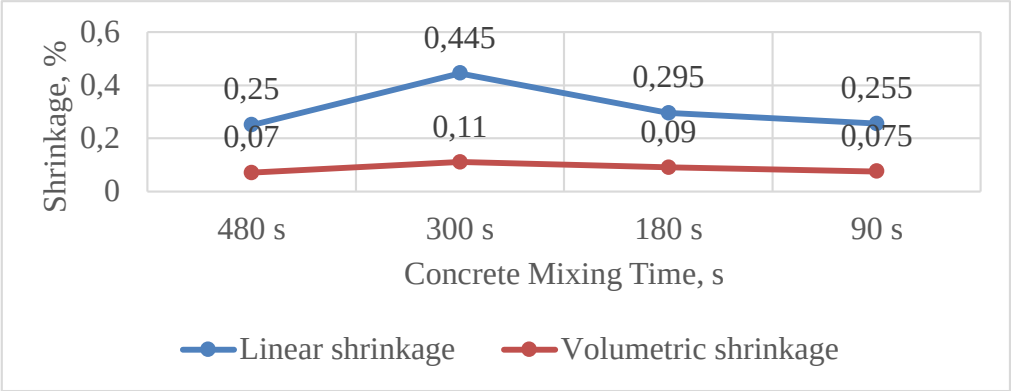


**Fig 4**. Dependence of Linear and Volumetric Shrinkage of Concrete on Mixing Time
**Рис 4** Залежність лінійної та об'ємної усадки бетону від часу перемішування бетонної суміші

The volumetric shrinkage of concrete produced with a mixing time of 300 s increases significantly and reaches 0.445%. This increase on the volumetric shrinkage curve is characterized as a "peak." The volumetric shrinkage of concrete produced with mixing times of 90 and 480 s is practically the same, amounting to 0.255% and 0.25%, respectively.

The elevated values of linear and volumetric shrinkage of concrete produced with a mixing time of 300 s are directly related to the reduction in compressive strength and bulk density of concrete [1].

Studies of concrete deformability at different mixing times showed that, according to the determined values of the elastic modulus and the indicators of linear and volumetric shrinkage, the deformability characteristics of concrete can be distinguished at mixing times of 480 s and 180 s, when the concrete class corresponds to C30/35 (B35) and C20/25 (B25), respectively. However, according to the previously determined prism strength values [1], at mixing times of 480 s and 180 s the concrete class corresponds to C30/35 (B35) and C25/30 (B30), respectively, while according to cube strength values the concrete class is the same and corresponds to C16/20 (B20).

Therefore, the conducted studies demonstrated a significant difference in determining the concrete class based on strength and deformability of specimens.

In the final determination of the optimal mixing time of the concrete mixture with respect to concrete class, the following factors were considered:

1. The cost of producing 100 m³ of concrete mixture at mixing times of 480 s and 180 s in an "Ayrich" concrete mixer, based on electricity consumption of 3.3 kWh and the cost of 1 kWh of electricity for industrial enterprises (6.9 UAH):
   - at a mixing time of 180 s:
     277.8 h×3.3 kWh×6.9 UAH=6325.5 UAH
   - at a mixing time of 480 s:
     740.7 h×3.3 kWh×6.9 UAH=16865.7
2. The concrete class in terms of axial compressive strength is determined by the temporary resistance to compression of concrete cubes with an edge length of 150 mm [2].
3. In this case, the final concrete class is rationally taken as the lower of the obtained values.

Considering the above, it should be concluded that, in order to obtain a guaranteed class of structural concrete not less than C16/20 (B20), the optimal mixing time of the concrete mixture is 180 s.

## CONCLUSIONS

The conducted studies of concrete deformability at different mixing times of 480, 300, 180, and 90 s showed that, according to the determined values of the elastic modulus of concrete and the indicators of its linear and volumetric shrinkage, the deformability

characteristics of concrete can be distinguished at mixing times of 480 s and 180 s, when the concrete class corresponds to C30/35 (B35) and C20/25 (B25), respectively. However, according to the previously determined prism strength values [1], at mixing times of 480 s and 180 s the concrete class corresponds to C30/35 (B35) and C25/30 (B30), respectively, while according to cube strength values the concrete class is the same and corresponds to C16/20 (B20).

In the final determination of the optimal mixing time of the concrete mixture with respect to concrete class, the following factors were taken into account: the cost of producing 100 m³ of concrete mixture in an "Ayrich" concrete mixer; the determination of concrete class by axial compressive strength based on the temporary resistance of concrete cubes; and the rational acceptance of the final concrete class as the lower of the obtained values.

As a result of the conducted studies, it was determined that, in order to obtain a guaranteed class of structural concrete not less than C16/20 (B20), the optimal mixing time of the concrete mixture is 180 s.

## REFERENCE


1. **Konoplyanyk, O. Yu., & Zhuk, D. V.** (2025). Influence of mixing time of concrete mixtures on strength characteristics of structural concretes. *Ukrainian Journal of Construction and Architecture*, 3(027), 81–91. [in Ukrainian] https://doi.org/10.30838/UJCEA.2312.270425.81.1164
2. **Romashko, V. M.** (2020). General fundamentals of reinforced concrete elements and structures deformation mechanics. *Collection of Scientific Works of the Ukrainian State University of Railway Transport* (191), 45–52. [in Ukrainian] https://doi.org/10.18664/1994-7852.191.2020.217288
3. **Dzyuba, A. P., Dzyuba, A. A., & Levitina, L. D**. (2022). Optimal design of shell constructions taking into account the evolution of corrosion damage. *Strenggth of materials and theory of structures*, (108), 17-34. [in English] https://doi.org/10.32347/2410-2547.2022.108.17-34
4. **Neville, A. M., & Brooks, J. J.** (2010). *Concrete Technology* (2nd ed.). 442 p. [in English] ISBN: 9788-131-7294-23
5. **Kongshaug, S. S., Oseland, O., Kanstad, T., Hendriks, M. A. N., Rodum, E., & Markeset, G.** (2020). Experimental investigation of ASR-affected concrete – The influence of uniaxial loading on the evolution of mechanical properties, expansion and damage indices. *Construction and Building Materials*, (245), 118384. **[**in English] https://doi.org/10.1016/j.conbuildmat.2020.118384
6. **EN 1992-1-1.** (2004). Eurocode 2: Design of concrete structures – Part 1-1: General rules and rules for buildings. *European Commission*. [in English] ISBN: 978-058-0420-82-8
7. **Solodei, I. I., Ruvin, O. H., Kolyakova, V. M., & Kulikov, O. P.** (2024). Formulation of the problem of interaction between a structure and a soil plastic medium under dynamic evolutionary processes. *Strength of materials and theory of structures*, (112), 83–92. [in Ukrainian] https://doi.org/10.32347/2410-2547.2024.112.83-92
8. **Sha, X., & Zhu, S.** (2025). Joint measurement of modulus of elasticity and Poisson's ratio of concrete cubes by actuating special vibration modes: A novel baseline-free technique. *Journal of Sound and Vibration*, 618, 119288[in English] https://doi.org/10.1016/j.jsv.2025.119288
9. **Vu, X. H., Malecot, Y., & Daudeville, L.** (2009). Strain measurements on porous concrete samples for triaxial compression and extension tests under very high confinement. *The Journal of Strain Analysis for Engineering Design*, 44(8), 633–657. [in English] https://doi.org/10.1243/03093247JSA547
10. **DBN V.2.6-98:2009.** (2011). Konstruktsii budynkiv i sporud. Betonni ta zalizobetonni konstruktsii. Osnovni polozhennia [Buildings and structures. Concrete and reinforced concrete structures. Basic provisions]. *[Chynni vid 01.06.2011] Kyiv: Minrehionbud Ukrainy. 2011. – 71 s.* . [in Ukrainian]
11. **DSTU B V.2.7-217:2009.** (2010). Betony. Metody vyznachennia pryzmovoi mitsnosti, modulia pruzhnosti i koefitsiienta Puassona [Concretes. Methods for determining prism strength, modulus of elasticity and Poisson's ratio]. *[Chynni vid 22.12.2009]. Kyiv: Minrehionbud Ukrainy. 2010. – 16 s.* [in Ukrainian]

12. **DSTU B V.2.7-214:2009.** (2010). Betony. Metody vyznachennia mitsnosti za kontrolnymy zrazkamy [Concretes. Methods for determining strength by control specimens]. *[Chynni vid 22.12.2009]. Kyiv: Minrehionbud Ukrainy 2010. – 43 s.* . [in Ukrainian]
13. **Krus, Yu. O.** (2022). Connection between stresses and strains of concrete under different force modes of short-term axial compression. *Technical Sciences and Technologies*, (1(27), 184–198. [in Ukrainian] https://doi.org/10.25140/2411-5363-2022-1(27)-184-198
14. **Koliakova, V., & Bozhynskyi, M. (2017).** Settlement and theoretical studies of the temperature distribution in the cross section of concrete staircase folds**.** *Building Constructions. Theory and Practice*, *1*(1), 149–157. [in Ukrainian] https://doi.org/10.32347/2522-4182.1.2017.149-157
15. **Fesenko, O., & Koliakova, V.** (2022). Fire resistance analysis of bending timber structures according to Eurocode 5. *Building Constructions. Theory and Practice*, (10), 94–107. [in Ukrainian] https://doi.org/10.32347/2522-4182.10.2022.94-107
16. **Barashykov, A.**, & **Koliakova V**. *Building Structures: Textbook. VD Slovo, 2011. – 256 s* [in Ukrainian]
17. **Koliakova, V. M., Bozhynskyi, M. O., & Fesenko, O. A. (2016).** Temperature distribution in the cross-section of a reinforced concrete slab. *Modern Technologies and Methods of Calculations in Construction*, (5), 232–239. Lutsk: LNTU. [in Ukrainian]
18. **Pavlikov, A. M.** (2017). Reinforced Concrete Structures: Buildings, Facilities, and Their Parts. *Kyiv: Osnova Publishing House*. 512 p. [in Ukrainian] ISBN: 978-617-6076-88-9
19. **Neville, A. M.** (2011). Properties of Concrete (5th ed.). *Harlow: Pearson Education Limited*. 846 p. [in English] ISBN: 978-027-3755-80-7
20. **Bažant, Z. P., & Jirásek, M**. (2002). Creep and Shrinkage in Concrete Structures. *Berlin: Springer*. 357 p. [in English] ISBN: 978-079-2374-34-0
21. **Lizunov, P. P., Pogorelova, O. S., & Postnikova, T. G.** (2023). Influence of stiffness parameters on vibro-impact damper dynamics. *Strength of materials and theory of structures.*, (110), 21-35. [in English] https://doi.org/10.32347/2410-2547.2023.110.21-35
22. **Bažant, Z. P., & Baweja, S**. (2000). Creep and shrinkage prediction model for analysis and design of concrete structures: Model B3. *Materials and Structures*, 33(6), 357–365. [in English] https://doi.org/10.1007/BF02473152
23. **Zhou, F., Li, Y., Wang, J., et al.** (2022). Concrete elastic modulus experimental research based on theory of capillary tension. *Materials*, 15(3), 1123–1138. [in English] https://doi.org/10.3390/ma15103734
24. **Mehta, P. K., & Monteiro, P. J. M.** (2006). Concrete: Microstructure, properties, and materials — updated perspectives. *Cement and Concrete Composites*, 28(6), 481–489 [in English] https://doi.org/10.1016/j.cemconcomp.2006.02.010
25. **Aïtcin, P. C.** (1998). High-Performance Concrete. *London: E & FN Spon*. 600 p. [in English] https://doi.org/10.4324/9780203475034
26. **Bažant, Z. P., & Li, G. H.** (2008). Comprehensive analytical model for creep and shrinkage of concrete. *Cement and Concrete Research*, 38(6), 751–765. [in English] https://doi.org/10.1016/j.cemconres.2008.01.002

LITERATURE

1. **Konoplyanyk, O. Yu., & Zhuk, D. V.** (2025). Vplyv chasu peremishuvannia betonnykh sumishei na mitsnisni kharakterystyky konstruktsiinykh betoniv *Ukrainian Journal of Construction and Architecture*, 3(027), 81–91. [in Ukrainian] https://doi.org/10.30838/UJCEA.2312.270425.81.1164

2. **Romashko, V. M. (2020).** Zahalni osnovy mekhaniky deformuvannia zalizobetonnykh elementiv I konstruktsii. *Zbirnyk naukovykh prats Ukra-yinskoho derzhavnoho universytetu zaliz-nychnoho transportu, (191), 45–52.* https://doi.org/10.18664/1994-7852.191.2020.217288
3. **Dzyuba, A. P., Dzyuba, A. A., & Levitina, L. D**. (2022). Optimal design of shell constructions taking into account the evolution of corrosion damage. *Strenggth of materials and theory of structures*, (108), 17-34.

https://doi.org/10.32347/2410-2547.2022.108.17-34
4. **Neville, A. M., & Brooks, J. J.** (2010). *Concrete Technology* (2nd ed.). 442 p. [in English] ISBN: 9788-131-7294-23
5. **Kongshaug, S. S., Oseland, O., Kanstad, T., Hendriks, M. A. N., Rodum, E., & Markeset, G.** (2020). Experimental investigation of ASR-affected concrete – The influence of uniaxial loading on the evolution of mechanical properties, expansion and damage indices. *Construction and Building Materials,* (245), 118384. https://doi.org/10.1016/j.conbuildmat.2020.118384
6. **EN 1992-1-1.** (2004). Eurocode 2: Design of concrete structures – Part 1-1: General rules and rules for buildings. *European Commission*. [in English] ISBN: 978-058-0420-82-8
7. **Solodei, I. I., Ruvin, O. H., Kolyakova, V. M., & Kulikov, O. P.** (2024). Postanovka zadachi vzaiemodii sporudy i hruntovoho plastychnoho seredovyshcha v umovakh dynamichnykh evoliutsiinykh protsesiv *Strength of materials and theory of structures,* (112), 83–92. [in Ukrainian] https://doi.org/10.32347/2410-2547.2024.112.83-92
8. **Sha, X., & Zhu, S.** (2025). Joint measurement of modulus of elasticity and Poisson's ratio of concrete cubes by actuating special vibration modes: A novel baseline-free technique. *Journal of Sound and Vibration*, 618, 119288[in English] https://doi.org/10.1016/j.jsv.2025.119288
9. **Vu, X. H., Malecot, Y., & Daudeville, L.** (2009). Strain measurements on porous concrete samples for triaxial compression and extension tests under very high confinement. *The Journal of Strain Analysis for Engineering Design*, 44(8), 633–657. [in English] https://doi.org/10.1243/03093247JSA547
10. **DBN V.2.6-98:2009.** (2011). Konstruktsii budynkiv i sorud. Betonni ta zalizobetonni konstruktsii. Osnovni polozhennia [Buildings and structures. Concrete and reinforced concrete structures. Basic provisions]. *Kyiv: Minrehionbud Ukrainy*.. [in Ukrainian]
11. **DSTU B V.2.7-217:2009.** (2010). Betony. Metody vyznachennia pryzmovoi mitsnosti, modulia pruzhnosti i koefitsiienta Puassona [Concretes. Methods for determining prism strength, modulus of elasticity and Poisson's ratio]. *Kyiv: Minrehionbud Ukrainy*.. [in Ukrainian]
12. **DSTU B V.2.7-214:2009.** (2010). Betony. Metody vyznachennia mitsnosti za kontrolnymy zrazkamy [Concretes. Methods for determining strength by control specimens]. *Kyiv: Minrehionbud Ukrainy*. [in Ukrainian] https://doi.org/10.25140/2411-5363-2022-1(27)-184-198
13. **Krus, Yu. O.** (2022). Zviazok mizh napruzhennyamy i deformat¬siiamy betonu za riznykh sylovykh rezhymiv korotkochasnoho osiovoho stysku [Relationship between stresses and deformations of concrete under different force regimes of short-term axial compression]. *Tekhnichni nauky ta tekhnolohii*, (1), 45–53. [in Ukrainian] https://doi.org/10.25140/2411-5363-2022-1(27)-184-198
14. **Koliakova, V., & Bozhynskyi, M. (2017).** (2017). Rozrakhunkovo-teoretychni - rozpodilu temperatury v pererizi zalizobetonnoi konstruktsii skhidchastykh skladok. *Budivelni konstruktsii. Teoriia i praktyka, 1(1), 149–157.* https://doi.org/10.32347/2522-4182.1.2017.149-157
15. **Fesenko, O., & Koliakova, V.** (2022). (2022). Rozrakhunok na vohnestiikist derevianykh zhynalnykh konstruktsii za metodykoiu Yevrokodu 5. *Budivelni konstruktsii. Teoriia i praktyka, (10), 94–107.* https://doi.org/10.32347/2522-4182.10.2022.94-107
16. **Barashykov, A.**, & **Koliakova V**. Budivelni konstryctsii: Pidrychnyk. *VD Slovo, 2011. – 256*
17. **Koliakova, V. M., Bozhynskyi, M. O., & Fesenko, O. A. (2016).** Temperature distribution in the cross-section of a reinforced concrete slab. *Modern Technologies and Methods of Calculations in Construction*, (5), 232–239. Lutsk: LNTU. [in Ukrainian]
18. **Pavlikov, A. M.** (2017). Zalizobetonni konstruktsii: budivli, sporudy ta yikh chastyny *Kyiv: Osnova Publishing House*. 512 ISBN: 978-617-6076-88-9
19. **Neville, A. M.** (2011). Properties of Concrete (5th ed.). *Harlow: Pearson Education Limited*. 846 p. [in English] ISBN: 978-027-3755-80-7
20. **Bažant, Z. P., & Jirásek, M**. (2002). Creep and Shrinkage in Concrete Structures. *Berlin: Springer*. 357 p. ISBN: 978-079-2374-34-0
21. **Lizunov, P. P., Pogorelova, O. S., & Postnikova, T. G.** (2023). Influence of stiffness parameters on vibro-impact damper dynamics. *Strength of materials and theory of structures.*

(110), 21-35. https://doi.org/10.32347/2410-2547.2023.110.21-35
22. **Bažant, Z. P., & Baweja, S**. (2000). Creep and shrinkage prediction model for analysis and design of concrete structures: Model B3. *Materials and Structures*, 33(6), 357–365. https://doi.org/10.1007/BF02473152
23. **Zhou, F., Li, Y., Wang, J., et al.** (2022). Concrete elastic modulus experimental research based on theory of capillary tension. *Materials*, 15(3), 1123–1138. https://doi.org/10.3390/ma15103734
24. **Mehta, P. K., & Monteiro, P. J. M.** (2006). Concrete: Microstructure, properties, and materials — updated perspectives. *Cement and Concrete Composites*, 28(6), 481–489 https://doi.org/10.1016/j.cemconcomp.2006.02.010
25. **Aïtcin, P. C.** (1998). High-Performance Concrete. *London: E & FN Spon*. 600 ISBN: 041-919-2700 https://doi.org/10.4324/9780203475034
26. **Bažant, Z. P., & Li, G. H.** (2008). Comprehensive analytical model for creep and shrinkage of concrete. *Cement and Concrete Research*, 38(6), 751–765. https://doi.org/10.1016/j.cemconres.2008.01.002

## ВПЛИВ ЧАСУ ПЕРЕМІШУВАННЯ БЕТОННИХ СУМІШЕЙ НА ДЕФОРМАТИВНІ ХАРАКТЕРИСТИКИ КОНСТРУКЦІЙНИХ БЕТОНІВ

*Олександер КОНОПЛЯНИК*
*Дмитро ЖУК*

**Анотація.** Дана наукова робота є продовженням досліджень [1], які пов'язані з визначенням класу конструкційних бетонів при різних часах перемішування бетонної суміші. Встановлений вплив часу перемішування бетонної суміші на міцністні характеристики бетонів. В результаті випробувань міцності зразків-кубів та призм встановлені класи бетонів за міцністю на вісьовий стиск.

Однак в літературних джерелах присутні данні про вплив деформативності бетонів на визначення їх класу за міцністю шляхом дослідження модуля пружності бетонів. Тому постає питання дослідження деформативних характеристик бетонів та їх порівняння з міцністними характеристиками. За результатами цих двох досліджень може бути визначений остаточний клас бетону.

Аналіз сучасного стану розробки та дослідження бетонів показав, що одним з факторів, які впливають на визначення класу бетону за міцністю - є визначення модуля пружності бетонів, який характеризує його деформативні характеристики.

В лабораторних умовах були проведені дослідження модуля пружності і класу бетону при часі перемішування бетонної суміші 480, 300, 180 і 90 секунд відповідно. Для цього виготовлювали та випробували 20 зразків-призм розмірами 100x100x400 (висота) мм. При визначенні класу бетону враховували також несилові (об'ємні) деформації бетону та вартість виготовлення 100 м$^3$ бетонної суміші виходячи з витрат електроенергії за час перемішування суміші.

В результаті проведення досліджень визначено, що для отримання гарантованого класу конструкційного бетону не менш С16/20 (В20) оптимальний час перемішування бетонної суміші складає 180с.

Мета роботи полягає в дослідженні деформативних характеристик конструкційних бетонів в залежності від часу перемішування бетонної суміші та їх впливу на визначення класу бетону по міцності на стиск.

**Ключові слова:** бетонна суміш; час перемішування суміші; конструкційний бетон; деформаційні характеристики, модуль пружності бетону; клас бетону

***Received:*** *November 03, 2025.*
***Accepted:*** *December 05, 2025.*

ISSN 2522-4182

DOI: 10.32347/2522-4182.17.2025.131-140
UDC 624.04: 69.059.1:338.45:69

# TECOREP TECHNOLOGY AND POSSIBILITIES OF ITS ADAPTATION FOR POST-WAR UKRAINE

*Hanna SHPAKOVA[1], Volodymyr KRIPAK [2]*

[1,2] Kyiv National University of Construction and Architecture
31, Povitryanykh Syl Ave., Kyiv, Ukraine, 03037
[1]shpakova.gv@knuba.edu.ua, http://orcid.org/0000-0003-2124-0815
[2] kripak.vd@gmail.com, http://orcid.org/0000-0001-6575-5015

**Abstract**. The article examines modern technologies for dismantling high-rise buildings in the context of the transition of world megacities to the principles of a circular economy and increasing requirements for the environmental safety of construction processes. The article provides an extensive review of the history of the development of dismantling methods. Particular attention is paid to the innovative Japanese technology for internal dismantling of skyscrapers TECOREP (Taisei Ecological Reproduction System), developed by Taisei Corporation for the conditions of ultra-dense urban development. The method involves the gradual internal dismantling of floors using temporary metal supports and jacking systems, which ensures a controlled reduction in the height of the building without the use of external heavy equipment or blasting. The study analyzed the features of the technological process, the advantages of TECOREP in terms of reducing emissions, noise and dust, the possibility of recovering and reusing building materials, as well as the limitations associated with the geometry of facades and the structural system of buildings.

Separately, the potential for applying TECOREP technology in Ukraine in the context of post-war urban reconstruction, where a significant number of high-rise buildings were partially or completely destroyed as a result of hostilities, is considered. It has been shown that internal dismantling allows work to be carried out in dense buildings, minimizing the danger to the population, transport infrastructure, and buildings that have survived nearby. Given the scale of the destruction and the need to recycle millions of tons of construction waste, it is reasonable to believe that the introduction of such technologies will contribute to the formation of an environmentally friendly urban reconstruction system, reducing anthropogenic load, and developing the market for secondary construction materials.

The results of the study may be useful for specialists in the field of construction, urban planning, environmental engineering, and for government agencies dealing with issues of restoration and modernization of urban areas.

**Hanna SHPAKOVA**
Professor Department of Construction Technologies, Prof., D.Sc.

**Volodymyr KRIPAK**
Professor of the Department of Reinforced Concrete and Stone Structures,
Prof., PhD (Tech.Sci.)

**Keywords:** demolition of buildings; TECOREP technology; recycling of materials; post-war reconstruction; energy efficiency of demolition; innovative construction technologies.

## PROBLEM STATEMENT

The problem of dismantling dilapidated or outdated high-rise buildings is becoming increasingly urgent for countries with rapid urban development.

Such structures, built in the 1960s–1990s, often no longer meet modern standards for earthquake resistance, energy efficiency, and safety. In addition, many cities around the world are faced with the need to update urban infrastructure, reconstruct old areas, and modernize the building stock [3].

In Ukraine, the problem of dismantling has gained particular importance due to the war. In 2022–2024 alone, hundreds of high-rise residential complexes in Mariupol, Kharkiv, Bakhmut, Irpen, Borodyanka, Chernihiv, and other cities were seriously damaged or destroyed. Some of these buildings are in a condition that makes it impossible to restore their load-bearing capacity. Traditional demolition methods are generally not suitable for dense construction conditions, especially where intact buildings remain next to the damaged structures [4].

Current trends in construction and demolition reflect the global economy's shift towards sustainability and circularity. The use of environmentally friendly, low-noise, and safe demolition methods is becoming not only desirable, but also economically viable. Japanese TECOREP technology is one of the most progressive in world practice, and its adaptation to Ukrainian conditions can play an important role in post-war reconstruction.

## TRADITIONAL DEMOLITION METHODS

Usually, demolishing a building is almost as difficult as building it – especially if it is a skyscraper located in a densely built-up area. The standard method of destruction used by construction workers has always been to demolish a building using heavy machinery or a controlled explosion. Observers enjoyed the “spectacular” demolition of the 165-meter towers of the Mina Plaza complex in Abu Dhabi in 2020, which entered the Guinness Book of Records as the demolition of the tallest building using explosives, for a full 10 seconds. However, the time to lay 18,000 explosive charges on 144 floors and clear the area of construction debris and dust was over 2 months, with over a thousand specialists working simultaneously.

The most common methods of demolishing tall buildings include:

1. Controlled explosion (implosion). As a result of correct calculations, the building collapses inside its own perimeter. The method is fast, but environmentally and technologically problematic. First, it is an increased noise level. Second, it is a huge dust plume that affects the environment: a high concentration of harmful substances in the air, limited visibility, a layer of solid precipitation that will settle around the site for a long time. Thirdly, the destruction of a significant part of building materials, which makes their secondary use impossible. All these factors sometimes simply make it impossible to use in dense development.

2. Mechanical dismantling using heavy equipment. During the work, hydraulic shears, hydraulic hammers and excavators with extended booms are used. However, this method has a number of disadvantages. The main disadvantage is the duration of the work. Also, a significant amount of free space is required at the construction site. There is also a high risk of collapses, high noise levels, which as a result has a negative impact on the population of the surrounding area.

Such methods have been dominant for decades, but in a world where the quality of the urban environment is becoming increasingly important, they are gradually giving way to innovative technologies.

It should be borne in mind that modern cities are densely built up, and the buildings that need to be demolished are sometimes over 100 m high. Their demolition in the traditional way can lead to serious consequences. In addition, today the world is moving towards a circular economy, the main postulate of which is recycling. Therefore, there has been a trend when demolishing buildings not to destroy building materials, but to reuse them. In 2010-2020, many EU and Asian countries introduced construction waste management programs that encourage: reuse of materials, on-site waste sorting, reduction of construction

waste, reduction of emissions and energy consumption.

In this structure, dismantling ceases to be “demolition” and becomes a technological process of “dismantling,” that is, the controlled, careful removal of materials for reuse.

Therefore, the Japanese construction company Taisei Corporation from Tokyo has developed an unusual technology for the demolition of high-rise buildings, in which the destruction of the building occurs internally [1].

TECOREP technology meets the above requirements as much as possible.

## GENERAL CHARACTERISTICS OF THE TECHNOLOGY

As the world's most populous capital, Tokyo currently has nearly 800 buildings over 100 meters tall. Under a modernization program to comply with Japanese building safety regulations, nearly a hundred of the oldest skyscrapers are to be demolished within 10 years [2]. The method, called Tecorep (Taisei Ecological Reproduction System), is relevant and looks very unusual - looking at a building being dismantled, a decrease in its overall height becomes noticeable over time.

The technology involves the preliminary dismantling of all interior elements and non-load-bearing structures. Compact special equipment and special metal structures are delivered to the skyscraper on its top floor. These metal “rods” are installed inside the building, playing the role of columns and giant jacks. Then the “hat” of the building (the upper floors and roof) is fixed on temporary columns. After that, special equipment begins to remove all the load-bearing walls and floors, thus destroying layer by layer. And the building itself “slides” down on metal scaffolding, decreasing by one upper floor. At the same time, workers calmly dismantle the walls from the inside in comfortable conditions even in bad weather, without fear of harming residents of neighboring houses and passersby. The roof and floor themselves are removed last.

The dismantled structures are lowered through internal elevators and shafts, from where they are removed from the construction site by dump trucks. It should be noted that when lowering materials down, energy is generated on the internal elevator, which is used to power the equipment and tools for dismantling work.

TECOREP technology provides full control over the dismantling process, minimizes environmental impact, reduces noise and dust levels outside, and, which is especially important for dense Tokyo, makes it possible to work in extremely cramped conditions.

What is the main difference in the dismantling technology offered by Taisei Corporation?

The technology includes several key structural components:

- internal metal columns-jacks. They are installed inside the building and temporarily replace its load-bearing elements for the period of dismantling;
- "hat" - a spatial protective module. It performs the functions of noise absorption, dust protection and wind load stabilizer;
- compact dismantling equipment: cutting units, hydraulic platforms, mobile manipulators;
- a floor lowering control system. Jacks synchronously lower the upper structure by one floor after the lower one is dismantled;
- a vertical logistics system. The use of internal elevators and shafts for material removal allows for energy savings through recovery.

## ALGORITHM FOR PERFORMING WORK USING TECOREP TECHNOLOGY

Dismantling using the TECOREP system takes place in several stages, each of which is aimed at maximum safety and environmental friendliness.

At the preparatory stage, the building is completely disconnected from the engineering networks. Before the installation of the necessary equipment, a detailed inspection of the supporting structures is performed. "Light" dismantling of internal elements (partitions,

cladding, furniture, communications) is performed.

The second preparatory stage involves the installation of temporary metal columns. The columns are designed to withstand the load from the upper floors after the column-beam elements are dismantled.

At the third stage of preparatory work, a protective "hat" is installed, which is a key element. It absorbs wind loads, prevents the spread of dust, reduces the noise level for the environment, and provides comfortable conditions for workers even during heavy rainfall or wind.

Fig. 1 shows a visualization of dust distribution during dismantling with and without a “hat”.

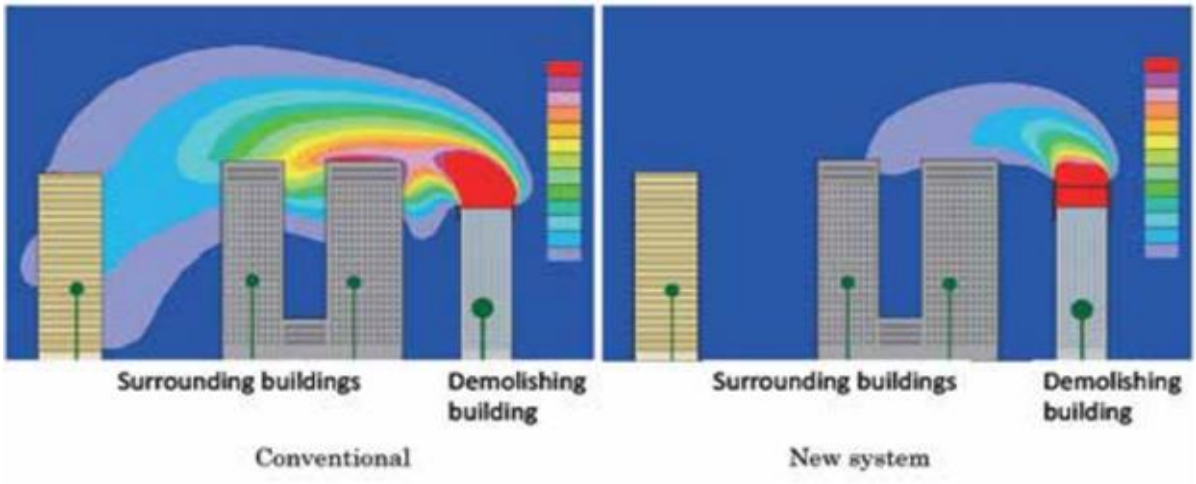


**Fig. 1** Dust dispersion simulation (Source:Taisei Corporation)
**Рис.1** Моделювання дисперсії пилу (Джерело: Taisei Corporation)

Materials and structures are sorted inside the building.

The main dismantling process is carried out in a sequence that corresponds to the structural features of the object, the condition of the main load-bearing walls. The most common sequence is “floor, columns, beams, shafts, etc.” After the floor is completely dismantled, the jacks synchronously lower the "hat" and the entire upper part of the building one floor down.

The cycle is repeated until the building is completely dismantled. The roof and the floor of the lower floor are dismantled last. A fragment of the roof dismantling is shown in Fig. 2.

The dismantled structures are lowered through internal elevators and shafts, from where they are removed from the construction site by dump trucks. It should be noted that when lowering materials down, energy is generated on the internal elevator, which is used to power the equipment and tools for dismantling work.

**Fig. 2** The utilization of the existing roof structure (Source: Taisei Corporation)
**Рис. 2** Використання наявної конструкції покрівлі (Джерело: Taisei Corporation)

This method of dismantling is quite quiet and environmentally friendly compared to traditional methods. Since all work is carried out in a closed space, the noise level outside is

significantly lower than with an open demolition method, and the proportion of dust particles in the air is reduced by 90% for the surrounding areas. In addition, the Tecorep method does not require the use of cranes and heavy equipment, which are known to greatly pollute the environment with harmful emissions. Taisei Corporation uses lifting equipment that allows for an 80% reduction in carbon dioxide emissions compared to cranes operating on traditional fuel.

This is the company's know-how, which is kept secret. And the building materials can be dismantled carefully, allowing them to be reused.

## PRACTICAL APPLICATION: DISMANTLING THE GRAND PRINCE HOTEL AKASAKA

The method was tested during the demolition of the old 140-meter-high Grand Prince Hotel Akasaka back in 2013. The dismantling took over 9 months. Grand Prince Hotel Akasaka became the first building in the world to be dismantled using TECOREP technology. Main results:

- dust levels around the building decreased by 90%;
- $CO_2$ emissions - 80% less than when using traditional cranes;
- noise pollution - 17-23 dB lower;
- possibility of full sorting of materials;
- complete safety for surrounding buildings.

The project became a landmark example of "green" urbanism (Fig. 3).

**Fig. 3** Work proceeding situation (Source:Taisei Corporation)
**Рис. 3** Процес виконання робіт (Джерело: Taisei Corporation)

## PROSPECTS FOR THE APPLICATION OF TECOREP TECHNOLOGY IN UKRAINE

Following Russia’s full-scale invasion of Ukraine, the scale of destruction of residential and public buildings has become unprecedented. According to the World Bank, more than 150,000 buildings have been destroyed or significantly damaged, including a significant number of high-rise buildings.

Particularly difficult cases include:

- partially destroyed 16–25-story buildings in Kharkiv and Mariupol;
- high-rise residential complexes with severely damaged load-bearing structures;
- buildings where only part of the facade is destroyed, but the core remains standing;

- buildings that pose a danger to the environment.

In many cities, the density of buildings does not allow for the use of explosive demolition methods, and the large-scale destruction makes it difficult to use heavy equipment.

That is why internal demolition technology, similar to TECOREP, can become a critically important tool in post-war reconstruction.

Prospects for the application of TECOREP technology in Ukraine

Following Russia's full-scale invasion of Ukraine, the scale of destruction of residential and public buildings has become unprecedented. According to the World Bank, more than 150,000 buildings have been destroyed or significantly damaged, including a significant number of high-rise buildings.

Particularly difficult cases include:

- partially destroyed 16–25-story buildings in Kharkiv and Mariupol;
- high-rise residential complexes with severely damaged load-bearing structures;
- buildings where only part of the facade is destroyed, but the core remains standing;
- buildings that pose a danger to the environment.

In many cities, the density of buildings does not allow for the use of explosive demolition methods, and the large-scale destruction makes it difficult to use heavy equipment.

That is why internal demolition technology, similar to TECOREP, can become a critically important tool in post-war reconstruction.

Dismantling in a confined space with the installation of temporary columns allows you to work safely even when:

- the external facade is partially collapsed;
- the internal structures remain unstable;
- there is a risk of collapse under the influence of wind or vibrations.

In cities such as Kharkiv, Mykolaiv, Chernihiv, the buildings are built extremely close together. Heavy hydraulic shears simply cannot reach the facade.

During post-war reconstruction, it is important to preserve the health of the population and minimize noise, dust, and vibrations. TECOREP's "Hat" reduces dust by 90%, which is especially important for areas with damaged engineering networks and a lack of centralized medicine.

## WHY TECOREP IS POTENTIALLY SUITABLE FOR UKRAINE

Military strikes often destroy only part of the structures, leaving other elements unstable. Ukraine will need millions of tons of construction materials. The TECOREP system allows you to store:

The TECOREP system allows you to store:

- metal structures;
- part of reinforced concrete;
- glass;
- interior elements.

This significantly reduces the cost and speed of reconstruction.

In conditions of electricity shortage, it is important to use low-consumption technologies. Energy recovery in elevators allows you to partially power the equipment.

Despite significant advantages, the application of TECOREP in Ukraine will require serious adaptation:

1. Damage to load-bearing structures due to war. In Japan, the technology is applied to undamaged buildings.
   In Ukraine, many buildings have:
   - missing parts of the facades;
   - damaged columns;
   - damaged core;
   - partially destroyed floors.

   This will require reinforcement or restoration of individual elements before dismantling.
2. Mining of buildings. Some of the destroyed buildings (especially in Mariupol) may contain unexploded ordnance.
3. Heterogeneity of Soviet high-rise projects. Unlike Japanese skyscrapers with a flat cross-section, Soviet buildings often have a variable planning structure.

4. Climatic conditions. The technology must be adapted to severe frosts and large temperature drops.

TECOREP is more expensive than traditional methods, but for post-war Ukraine it can be economically advantageous in conditions of dense development of historical and office and representative centers, in areas of ecological reserves, and with large volumes of work on a city scale (economy in serial application).

## CONCLUSIONS AND PROSPECTS FOR FURTHER RESEARCH

TECOREP technology is one of the most promising solutions in the field of safe dismantling of high-rise buildings and can be extremely useful for Ukraine, especially in the context of post-war reconstruction.

It allows you to work in dense buildings, ensure the safe dismantling of partially destroyed skyscrapers, minimize environmental impact, reuse some materials, and reduce energy consumption.

Given the scale of the destruction, Ukraine has the potential to become a global platform for the implementation of innovative dismantling and reconstruction technologies, shaping new standards of sustainable development.

## REFERENCE


1. **Ichihara H., Kayashima M., Ogura M., Koga T., & Yajima K**. (2013). A new environmental burden-reducing demolition system for high-rise buildings -"TECOREP" system. *Report of Taisei Technology Center*, No. 46. [in English]. https://www.taisei.co.jp/giken/report/2013_46/abstract/detail/B046_006.htm?utm_source=chatgpt.com.
2. **Yamaguchi, K., Masuda, K., Utsugi, J., Nagata, A., Ichihara, H., & Umetsu, K.** (2012). Noise propagation of TECOREP system, a new demolition system for high-rise buildings. *Report of Taisei Technology Center*, No. 45. [in English]. https://www.taisei.co.jp/giken/report/2013_46/abstract/detail/B046_006.htm?utm_source=chatgpt.com.
3. **Shpakova H., Shpakov A., Kripak W., Koliakova V.** (2024). Structural and technological aspects of conservation of street art on buildings damaged during the war. *International Journal of Conservation Science*, 15, pp. 103–118. [in English]. DOI: 10.36868/IJCS.2024.si.09. https://ijcs.ro/public/IJCS-24-SI_09_Shpakova.pdf
4. **Shpakova H., Shpakov A.** (2023). Strategies for post-war reconstruction of Ukraine: institutional and economic dimensions. *Ways to increase the efficiency of construction in the conditions of the formation of market relations*. *No. 51(1). 152-161.* [in Ukrainian].
5. **Bilokon O., Nesevria K., & Naumov M.** (2022). Analysis of the main technical solutions in demolition projects of buildings and structures. *Ukrainian Journal of Civil Engineering and Architecture*, *4*(1), 63–72. DOI:10.30838/J.BPSACEA.2312.050722.15.860.
6. **Kayashima M., Shinozaki T., Koga T., & Ichihara H.** (2013). A new demolition system for high-rise buildings. *Council on Tall Buildings and Urban Habitat.* [in English]. https://global.ctbuh.org/resources/papers/download/940-a-new-demolition-system-for-high-rise-buildings.pdf
7. **Kayashima M., Ichihara H., Koga T., & Shinozaki T.** (2015). Development of a new clean demolition system for tall buildings. *Council on Tall Buildings and Urban Habitat.* [in English]. https://global.ctbuh.org/resources/papers/download/2485-development-of-a-new-clean-demolition-system-for-tall-buildings.pdf
8. **Patel R., & Shah M.** (2014). Demolition of buildings – An overview. *International Journal of Advanced Engineering Research and Development*, *1*(6), 234-242. https://www.ijaerd.org/index.php/IJAERD/article/view/241
9. "High-Tech Demolition Systems for High-Rises" (2013). *Web Japan – Trends in Japan.* https://web-japan.org/trends/11_tech-life/tec130325.html?utm_source=chatgpt.com
10. **Rosenfeld, K.** (2013, January 10). *How to Pleasantly Demolish a High-Rise.* ArchDaily. [in English]. https://www.archdaily.com/317019/how-to-pleasantly-demolish-a-high-rise?utm_source=chatgpt.com.
11. **Stavridis A., Samaras A., & Paschalis A.** (2025). Fundamentals of controlled demolition

in structures: Real-life applications, discrete element methods, monitoring, and artificial intelligence-based research directions. *Buildings, 15*(19), 3501. [in English]. https://doi.org/10.3390/buildings15193501

12. **Bilokon O., Nesevria K., & Naumov M.** (2022). Subject area of demolition of buildings and structures and prerequisites for further research. *Ukrainian Journal of Civil Engineering and Architecture, 3*(2), 39–48. DOI: 10.30838/J.PMHTM.2413.271222.18.907.
13. **Clark, L**. (2013, January 15). Japan's Quiet Skyscraper-Demolition Technique Generates Energy. *WIRED.* [in English]. https://www.wired.com/2013/01/japan-building-demolition/?utm_source=chatgpt.com.
14. **Sormunen, P., & Kärki, T.** (2019). Recycled construction and demolition waste as a possible source of materials for composite manufacturing. *Journal of Building Engineering*, 26, 100742. [in English]. https://doi.org/10.1016/j.jobe.2019.100742.
15. **Chandrappa, R., & Das, D. B.** (2024). Construction and Demolition Waste. In *Environmental Science and Engineering Solid Waste Management (pp. 609–638)*. Springer. [in English]. DOI:10.1007/978-3-031-50442-6_15.
16. **Palii, O. V. (2024).** Environmental aspects of demolition waste utilization in Ukraine: The use of recycled material for sustainable construction. *Environmental Sciences, 1(52), 1–12.* [in Ukrainian]. https://eztuir.ztu.edu.ua/jspui/handle/123456789/8431
17. **Shamrai, V. I., Korobiichuk, V. V., & Sobolevskyi, R. V.** (2017). Management of waste of stone processing in the framework of Euro-integration of Ukraine. *Вісник ЖДТУ. Серія «Технічні науки»,* 1(2(80)), 234–239. [in English]. DOI: https://doi.org/10.26642/tn-2017-2(80)-234-239.
18. **Safranov T. A., Prykhodko V. Yu., Mykhailenko V. I.** (2023). Characteristics of demolition waste management in the regions of Ukraine. *Journal of Environmental Management*, Article 342, 118200. [in English] DOI: https://doi.org/10.31481/uhmj.33.2024.07
19. **Ivanova, T., Martynenko, S., & Kushnir, V.** (2025). Optimization of demolition and reuse of construction materials within a circular economy framework. *Ukrainian Journal of Civil Engineering and Architecture*, 5(1), 112–125. https://uajcea.pgasa.dp.ua/article/view/342716
20. **Kostiuchenko, S., & Petrenko, R.** (2025). Challenges of managing secondary construction waste from urban destruction on urbanized territories. *Modern Technologies in Construction*, 2(51), 44–58. https://stmkvb.vntu.edu.ua/index.php/stmkvb/article/view/936
21. **Osipov, V., & Syhyda, L.** (2019). Demolition technology of buildings and structures of industrial enterprises. *Shliakhy Pidvyshchennia Efektyvnosti Budivnytstva, 41(1), 97–104.* https://ways.knuba.edu.ua/article/view/196404
22. **Alagöz, S.** (2022). Simulation Program for Controlled Demolition of Buildings. *TAS Journal, 2(4), 50–57.* https://tasjournal.com/index.php/tas
23. **Chang** (2025). Debris Simulation in Controlled Demolition of Tall Building Structures: Solid Model-Based Approach. *Buildings, 15(18), 3396.* https://doi.org/10.3390/buildings15183396
24. **Chernenko, K. V.** (2020). Modern methods of dismantling (demolition) of large-panel buildings in dense urban development. *Scientific Bulletin of Construction*, 102(4). [in Ukrainian]. https://svc.kname.edu.ua/index.php/svc/uk/article/view/272?utm_source=chatgpt.com
25. **Yuzbaşi J.** (2025). Debris simulation in controlled demolition of tall building structures: Solid model-based approach. *Buildings, 15(18), 3396.* https://doi.org/10.3390/buildings15183396

## LITERATURE

1. **Ichihara H., Kayashima M., Ogura M., Koga T., & Yajima K**. (2013). A new environmental burden-reducing demolition system for high-rise buildings -"TECOREP" system. *Report of Taisei Technology Center, No. 46.* https://www.taisei.co.jp/giken/report/2013_46/abstract/detail/B046_006.htm?utm_source=chatgpt.com.

**Yamaguchi K., Masuda K., Utsugi J., Nagata, A., Ichihara H., & Umetsu K.** (2012). Noise propagation of TECOREP system, a new demolition system for high-rise buildings. *Report of Taisei Technology Center, No. 45.* https://www.taisei.co.jp/giken/report/2013_46/a

bstract/detail/B046_006.htm?utm_source=chatgpt.com.

3. **Shpakova H., Shpakov A., Kripak W., Koliakova V.** (2024). Structural and technological aspects of conservation of street art on buildings damaged during the war. *International Journal of Conservation Science*, 15, *pp. 103–118.* DOI: 10.36868/IJCS.2024.si.09. https://ijcs.ro/public/IJCS-24-SI_09_Shpakova.pdf.
4. **Shpakova H., Shpakov A.** (2023). Stratehii povoiennoho vidnovlennia Ukrainy: instytutsiini ta ekonomichni vymiry. *Shliakhy pidvyshchennia efektyvnosti budivnytstva v umovakh formuvannia rynkovykh vidnosyn*. *№51(1). 152-161.*
5. **Bilokon O., Nesevria K., & Naumov M.** (2022). Analysis of the main technical solutions in demolition projects of buildings and structures. *Ukrainian Journal of Civil Engineering and Architecture, 4*(1), 63–72. DOI:10.30838/J.BPSACEA.2312.050722.15.860.
6. **Kayashima M., Shinozaki T., Koga T., & Ichihara H.** (2013). A new demolition system for high-rise buildings. *Council on Tall Buildings and Urban Habitat* https://global.ctbuh.org/resources/papers/download/940-a-new-demolition-system-for-high-rise-buildings.pdf.
7. **Kayashima M., Ichihara H., Koga T., & Shinozaki T.** (2015). Development of a new clean demolition system for tall buildings. *Council on Tall Buildings and Urban Habitat.* https://global.ctbuh.org/resources/papers/download/2485-development-of-a-new-clean-demolition-system-for-tall-buildings.pdf.
8. **Patel R., & Shah M.** (2014). Demolition of buildings – An overview. *International Journal of Advanced Engineering Research and Development, 1*(6), 234-242. https://www.ijaerd.org/index.php/IJAERD/article/view/241
9. "High-Tech Demolition Systems for High-Rises" (2013). *Web Japan – Trends in Japan.* https://web-japan.org/trends/11_tech-life/tec130325.html?utm_source=chatgpt.com
10. **Rosenfeld K.** (2013, January 10). *How to Pleasantly Demolish a High-Rise.* ArchDaily. https://www.archdaily.com/317019/how-to-pleasantly-demolish-a-high-rise?utm_source=chatgpt.com.
11. **Stavridis A., Samaras A., & Paschalis A.** (2025). Fundamentals of controlled demolition in structures: Real-life applications, discrete element methods, monitoring, and artificial intelligence-based research directions. *Buildings, 15*(19), 3501. https://doi.org/10.3390/buildings15193501.
12. **Bilokon O., Nesevria K., & Naumov M.** (2022). Subject area of demolition of buildings and structures and prerequisites for further research. *Ukrainian Journal of Civil Engineering and Architecture, 3*(2), 39–48. DOI: 10.30838/J.PMHTM.2413.271222.18.907.
13. **Clark, L.** (2013, January 15). Japan's Quiet Skyscraper-Demolition Technique Generates Energy. *WIRED.* https://www.wired.com/2013/01/japan-building-demolition/?utm_source=chatgpt.com.
14. **Sormunen, P., & Kärki, T.** (2019). Recycled construction and demolition waste as a possible source of materials for composite manufacturing. *Journal of Building Engineering, 26, 100742.* https://doi.org/10.1016/j.jobe.2019.100742.
15. **Chandrappa, R., & Das, D. B.** (2024). Construction and Demolition Waste. In *Environmental Science and Engineering Solid Waste Management* (pp. 609–638). Springer. DOI:10.1007/978-3-031-50442-6_15.
16. **Palii O.V.** (2024). Ekolohichni aspekty utylizatsii vidkhodiv ruinuvan v Ukraini: vykorystannia pereroblenoho materialu dlia staloho budivnytstva. *Ekolohichni nauky, 1(52), 1–12* https://eztuir.ztu.edu.ua/jspui/handle/123456789/8431
17. **Shamrai, V. I., Korobiichuk, V. V., & Sobolevskyi, R. V.** (2017). Management of waste of stone processing in the framework of Euro-integration of Ukraine. *Visnyk ZhDTU. Seriia «Tekhnichni nauky»*, 1(2(80)), 234–239. DOI: https://doi.org/10.26642/tn-2017-2(80)-234-239
18. **Safranov T. A., Prykhodko V. Yu., Mykhailenko V. I.** (2023). Characteristics of demolition waste management in the regions of Ukraine. *Journal of Environmental Management, Article 342, 118200.* DOI: https://doi.org/10.31481/uhmj.33.2024.07.
19. **Ivanova, T., Martynenko, S., & Kushnir, V.** (2025). Optimization of demolition and reuse of

construction materials within a circular economy framework. *Ukrainian Journal of Civil Engineering and Architecture, 5(1), 112–125.* https://uajcea.pgasa.dp.ua/article/view/342716

20. **Kostiuchenko, S., & Petrenko, R.** (2025). Challenges of managing secondary construction waste from urban destruction on urbanized territories. *Modern Technologies in Construction, 2(51), 44–58.* https://stmkvb.vntu.edu.ua/index.php/stmkvb/article/view/936
21. **Osipov, V., & Syhyda, L.** (2019). Demolition technology of buildings and structures of industrial enterprises. *Shliakhy Pidvyshchennia Efektyvnosti Budivnytstva*, 41(1), 97–104. https://ways.knuba.edu.ua/article/view/196404
22. **Alagöz, S.** (2022). Simulation Program for Controlled Demolition of Buildings. *TAS Journal, 2(4), 50–57.* https://tasjournal.com/index.php/tas
23. **Chang** (2025). Debris Simulation in Controlled *Demolition of Tall Building Structures: Solid Model-Based Approach. Buildings, 15(18), 3396.* https://doi.org/10.3390/buildings15183396
24. **Chernenko, K. V**. (2020). Suchasni metody rozbyrannia (demontazhu) krupnopanel-nykh budivel v shchilnii miskii zabudovi. *Naukovyi visnyk budivnytstva, 102(4)* https://svc.kname.edu.ua/index.php/svc/uk/article/view/272?utm_source=chatgpt.com
25. **Yuzbaşi, J.** (2025). Debris simulation in controlled demolition of tall building structures: Solid model-based approach. *Buildings, 15(18), 3396.* https://doi.org/10.3390/buildings15183396

## ТЕХНОЛОГІЯ TECOREP ТА МОЖЛИВОСТІ ЇЇ АДАПТАЦІЇ ДЛЯ ПОВОЄННОЇ УКРАЇНИ

*Ганна ШПАКОВА*
*Володимир КРІПАК*

**Анотація**. У статті досліджено сучасні технології демонтажу висотних будівель у контексті переходу світових мегаполісів до принципів циркулярної економіки та підвищення вимог до екологічної безпеки будівельних процесів. У статті проведено розширений огляд історії розвитку методів демонтажу. Особливу увагу приділено інноваційній японській технології внутрішнього демонтажу хмарочосів **TECOREP (Taisei Ecological Reproduction System)**, розробленій компанією *Taisei Corporation* для умов надщільної міської забудови. Метод передбачає поступове внутрішнє розбирання поверхів із використанням металевих тимчасових опор та домкратних систем, що забезпечує контрольоване зменшення висоти будівлі без застосування зовнішньої важкої техніки чи вибухових робіт. У дослідженні проаналізовано особливості технологічного процесу, переваги TECOREP щодо зменшення викидів, шуму та пилу, можливості відновлення й повторного використання будівельних матеріалів, а також обмеження, пов'язані з геометрією фасадів і конструктивною системою споруд.

Окремо розглядається потенціал застосування технології TECOREP в Україні в умовах післявоєнного відновлення міст, де значна кількість висотних будівель була частково або повністю зруйнована внаслідок бойових дій. Показано, що внутрішній демонтаж дозволяє виконувати роботи у щільній забудові, мінімізуючи небезпеку для населення, транспортної інфраструктури та будівель, які збереглися поруч. Враховуючи масштаб руйнувань та необхідність переробки мільйонів тонн будівельного сміття, обґрунтовано, що впровадження подібних технологій сприятиме формуванню екологічно орієнтованої системи реконструкції міст, зниженню антропогенного навантаження й розвитку ринку вторинних будівельних матеріалів.

Результати дослідження можуть бути корисними для фахівців у галузі будівництва, урбаністики, екологічної інженерії та для органів державного управління, що займаються питаннями відновлення та модернізації міських територій.

**Ключові слова:** демонтаж будівель; технологія TECOREP; рециркуляція матеріалів; відновлення після війни; енергоефективність демонтажу; інноваційні будівельні технології.

***Received:*** *November 02, 2025.*
***Accepted:*** *November 30, 2025.*

**ISSN 2522-4182**

*DOI:* 10.32347/2522-4182.17.2025.141-152
*UDC 624.012*

# TECHNOLOGICAL ASPECTS OF FABRICATING A REINFORCED CONCRETE SHELL USING 3D CONCRETE PRINTING

*Vladyslav TENESESKU*

O.M.Beketov National University of Urban Economy in Kharkiv
17, Chornohlazivska Str., Kharkiv, Ukraine, 61002
[1] vladislav.tenesesku@kname.edu.ua, https://orcid.org/ 0000-0002-4935-4454

**Annotation.** The article focuses on the technological aspects of fabricating a reinforced concrete shell using concrete 3D printing combined with polystyrene formwork. A comprehensive literature review was conducted to analyze recent advancements in additive manufacturing methods for shell structures, with a particular emphasis on the development and application of flexible and stay-in-place formwork systems. A step-by-step manufacturing procedure for the test shell element was implemented, including the generation of a digital parametric model, followed by the fabrication of a custom polystyrene mold. The mold was assembled using layered foam sheets, which were cut according to pre-defined templates, bonded using adhesives, and manually refined to ensure geometric accuracy.
The digital model was processed in CAD software and converted into a format suitable for slicing. The slicing operation was performed to define the layer height, printing path, and tool trajectories. Based on the generated G-code, a robotic concrete printer (console-type, "UTU 3D") was employed to execute the additive layering process. The concrete was deposited layer-by-layer on the pre-installed polystyrene form, beginning from the bottom ring, which was reinforced with embedded steel bars to accommodate lifting hooks. Thixotropic concrete mix was used to maintain the stability of each deposited layer and to prevent slippage on the curved surface of the mold. Short pauses between layers were introduced to manage curing and maintain interlayer bonding.
The finished shell was allowed to cure under ambient conditions until the desired structural strength was achieved. The study confirmed the feasibility and efficiency of combining foam-based formwork and 3D printing for creating thin-walled curved concrete structures, offering significant potential for use in both experimental and industrial-scale applications in the construction industry.
Further research is aimed at conducting full-scale tests of the shell under the action of quasi-uniform static loading in order to determine the bearing capacity and deformability of the structure.

**Vladyslav TENESESKU**
Post-graduate student of the Department of Building Structures

**Keywords:** concrete shell; 3D concrete printing; polysterene formwork; additive technology.

## INTRODUCTION

Shell structures continue to represent one of the most expressive forms of architectural and structural solutions in contemporary construction.
Due to their curved geometry, they provide exceptional spatial rigidity while maintaining minimal thickness and low material consumption, making them highly efficient from an engineering perspective. At the same time, the complex shape of such elements poses a number of technological challenges for both designers and builders. The conventional construction of shells requires the use of custom-made formwork systems of

complex configuration, high-precision layout, and strict geometric control at every stage.

The formation of double curvature is particularly difficult, often demanding expensive molds, flexible materials, numerous temporary supports, and specialized equipment. These processes are generally labor-intensive and resource-demanding, and their implementation is only feasible with the involvement of highly qualified specialists.

In modern construction, there is a growing demand for new approaches to shell fabrication that can preserve architectural freedom while optimizing manufacturing and assembly processes. One of the most promising directions is the use of digital form-generation technologies and three-dimensional concrete printing (3DCP) [1-3], which enables the elimination or significant simplification of complex formwork, transforming it into a flexible auxiliary element.

In this context, the present study investigates the production process of a test sample of a spherical concrete shell fabricated using 3D concrete printing. The experiment was carried out using the technology and industrial capacities of the Ukrainian company "UTU 3D" [4].

## ANALYSIS OF PREVIOUS RESEARCH

An analytical review of recent scientific achievements shows that interest in 3D concrete printing (3DCP) is steadily growing worldwide – including in Ukraine. In recent years, 3D concrete printing has been addressed by the scientific schools of Prof. V. Shmukler [5-6], Prof. M. Savitsky [7-8], and Prof. B. Demchyna [9-10], etc. Specifically, study [11] gives a structural solution for a building frame whose components – beams, columns, and slabs – are manufactured using 3D-printed concrete formwork. The design allows flexibility for use not only in new construction but also in renovation. Work [12] is devoted to a comparative analysis of bridge-type 3D-printer constructions used in construction; an improved model with two extruders was proposed. The results demonstrated a reduction in the cost of producing 1 m³ of products by 1.9–2.7 times and a decrease in metal consumption by 1.8–2.6 times compared to traditional printer designs. In article [13], a solution to the problem of transverse reinforcement in 3D-printed reinforcedconcrete load-bearing beams was proposed. The developed technology enabled vertical reinforcement cages to be placed in their design position without interrupting the printing process, ensuring the ability of the structure to resist both bending moments and shear forces.

Contemporary international publications demonstrate a wide variety of research efforts aimed at automation, serial production, and reduction of the impact of labor-intensive factors in construction. In the field of shell-structure printing, a particularly relevant challenge remains the use of formwork – including stay-in-place formwork. In this regard, the work by A. Jipa and B. Dillenburger [14] should be mentioned, in which a comprehensive review of indirect methods for producing concrete components via 3D-printed formwork is conducted. In that article, five different technologies for 3D-printing concrete formwork (material extrusion, ink- or foam-jet printing, powder binding, etc.) are classified and approximately 30 implemented projects are analyzed. The authors discuss new geometrical possibilities, improvements in efficiency and sustainability in construction enabled by these technologies, and outline their advantages and challenges compared to traditional methods.

In the study by Ivaniuk et al. [15], the concept of assembling reinforced-concrete shell structures using robotic installation of modular falsework was examined. The authors describe the automated placement of rigid components that form the supporting geometry of a shell. The results confirmed the effectiveness of robotics in ensuring geometrical accuracy, reducing labor costs, and enabling the standardization of structural solutions. The method is suitable for serial production of curved shell buildings. Research [6] introduces a new technology called F3DP – robotic 3D printing of mineral foam to create stay-in-place formwork for lightweight, complex concrete

elements. Two experimental demonstrations are provided: a perforated facade panel and an arched slab, where the foam inserts printed served as formwork for the concrete. The results showed up to 50 % savings in concrete volume and more than 60 % reduction in mass without loss of strength. The foam inserts remain within the elements, providing additional thermal and acoustic insulation.

In the article by Li et al. [16], a systematic review of modern formwork systems used in concrete construction is presented, with particular attention to their environmental friendliness, economic efficiency, and technological flexibility. The advantages and drawbacks of various types of formwork – timber, steel, modular, 3D-printed, and pneumatic – are summarized. The authors emphasize the relevance of developing reusable systems with reduced material consumption. A special section is devoted to formwork for geometrically complex shell structures, in which traditional solutions are often inefficient.

In work [17], a method is presented for printing concrete layers onto a temporary flexible formwork to create a thin shell. The researchers combined an adjustable flexible template (developed by TU Delft) with a gantry-type 3D printer, printing part of a shell onto a curved surface; the remaining sections were cast conventionally with concrete. As a result, a thin shell of ~5 m² was obtained: part was 3D-printed and part cast, using a CNC-milled polystyrene mold for support during printing. This work demonstrates the possibility to overcome the limitations of concrete's self-supportiveness during 3D-printing by employing temporary forms.

Article [18] describes the "Eggshell" technology, which consists of 3D-printing an ultra-thin (≈ 1–2 mm) plastic formwork and simultaneously filling it with concrete. This approach combines formwork fabrication and concreting in one process: a robotic system prints a hollow "eggshell"-shaped mold, and then a fast-hardening concrete mix is poured immediately inside. This enables efficient production of geometrically complex reinforced-concrete elements with minimal formwork waste. It was shown that reinforcement can be easily placed inside the thin printed shell; the resulting concrete elements (e.g., branching columns) have optimized geometry and strength unattainable by traditional methods.

In study [19], an innovative technology for creating curved shells using 3D-printed flexible formwork is described. Initially, a flat mesh formwork made of a special polymer is robotically printed; then this mesh is elastically bent into the shell shape and used as a base for applying concrete (e.g., via shotcrete) or laying fibre-reinforced concrete. It was experimentally confirmed that approximately 80 kg of the printed mesh formwork successfully supported about 400 kg of fresh concrete. This method enables the construction of thin, doubly-curved reinforced-concrete shells with complex geometry without traditional rigid formwork; the printed formwork may remain as part of the structure or be reused.

The analytical review leads to the conclusion that current research in 3D-concrete printing, especially for shell structures, is aimed at overcoming the technological limitations of traditional monolithic construction, reducing material consumption, and introducing automated systems. The main trends include the development of stay-in-place and flexible formwork systems, integration of reinforcement during printing, and the use of lightweight forming materials (foam, plastic, polymer meshes), allowing the realization of complex-geometry shells. The most economically efficient technologies proved to be those in which 3D printing is applied not only to concrete itself but also to the production of the formwork.

## PURPOSE AND METHODS

The aim of the study was to test a method for constructing a concrete shell with a diameter of 2200 mm, a thickness of 40 mm, and a rise of 300 mm using 3D concrete printing technology. In this study, the implementation of a rationalized [20] concrete shell formed using expanded polystyrene formwork is presented.

The objectives of the research included:

- the preparation of a digital model of the shell based on preliminary calculations using the finite element method (FEM);
- the cutting and fabrication of the expanded polystyrene mold, which served as a supporting surface for the application of concrete extrusion;
- the printing of the concrete shell using a cantilever-type 3D printer manufactured by UTU 3D.

## MAIN PART OF RESEARCH

To generate the shell geometry and define the contours of the formwork layers, the Autodesk Fusion 360 software package was used in combination with a parametric modeling module. The shell geometry was created as a solid body with adjustable parameters for diameter, height, and thickness. Subsequently, the digital model was stratified into layers according to the thicknesses of the polystyrene foam sheets (50 mm and 20 mm).

The design dimensions of the shell were obtained as a result of FEM analys according the energy rationalization approach [21-22] and defined as follows: a diameter of 2200 mm, a rise of 300 mm, and an average thickness of 40 mm. A general view of the shell with the integrated polystyrene formwork insert is presented in Fig. 1.

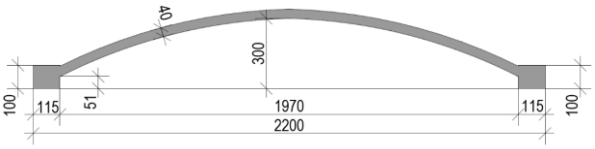


**Fig. 1** General view of the concrete shell
**Рис. 1** Загальний вигляд бетонної оболонки

Given the relatively small dimensions of the test shell, the use of a polystyrene foam screen was considered the most rational solution, as it is capable of withstanding the weight of freshly placed concrete without deformation [23].

Standard expanded polystyrene (EPS) sheets of type PS-30 with dimensions of 1×1 m and thicknesses of 50 mm and 20 mm were used to shape the precise geometry of the shell. This thickness gradation was chosen to increase the accuracy of the form, based on the calculated shell geometry.

A total of four 50 mm layers and five 20 mm layers were cut. Since the overall size of the shell exceeded the width of a standard sheet, most layers had to be assembled by bonding multiple sheets together.

Silicone adhesive and a hot glue gun were used for this purpose. Each prepared layer was marked with the outer and inner contours, after which cutting was performed along the outer line.

The geometry of the shell and the cutting strategy of the EPS screen are shown in Figure 2. Figure 3 presents the cutting layouts for each formwork layer, using EPS blocks measuring 2×2 m and individual sheets of 1×1 m.

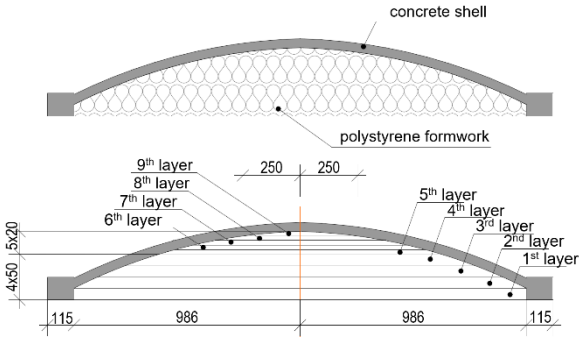


**Fig. 2** Shell with a polystyrene screen (top) and vertical layer-wise cutting of the polystyrene screen (bottom)
**Рис. 2** Оболонка з пінопластовим екраном (вгорі) та розрізання екрану з пінопласту на шари по висоті (внизу)

The cutting of polystyrene sheets was carried out in accordance with layouts prepared in the design software environment. The entire process was performed in several stages:

1. Marking of layer contours was carried out manually.
2. Initial cutting of sheets to the required dimensions and their assembly into blocks of the desired thickness was performed, with staggered joints to enhance structural integrity.
3. Mechanical shaping was conducted using: a construction knife (for rough cutting), a hot knife (for curves and radii), and a wire-type thermal cutter (for precise shaping of curved areas).

The blocks were assembled into the final form sequentially, with visual control of dimensional and geometric accuracy. The layers were glued

together, and surface irregularities at transitions were sanded. A tensioned string and manual visual inspection were used to verify compliance with the design profile.

After cutting the formwork layers, each segment was trimmed along its edge to match the geometric profile of the shell. During the fabrication process, it became evident that small and thin segments were difficult to process using thermal cutting tools due to a sharp drop in accuracy. The high temperature of the equipment caused local melting of the polystyrene, and due to the slow processing speed, the risk of damaging the workpiece beyond correction increased significantly.

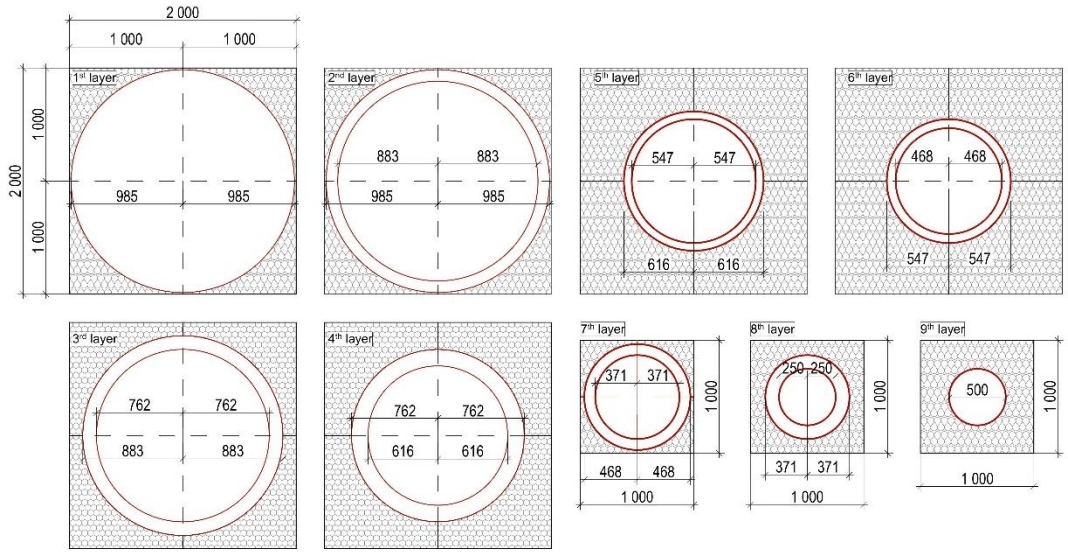


**Fig. 3** Cutting layouts of polystyrene sheets
**Рис. 3** Схеми розкрою листів пінопласту

Fig. 4 shows the results of cutting using a hot knife (Fig. 4a), a heated nichrome wire (Fig. 4b), and a standard utility knife (Fig. 4c). The labor intensity and time required for manual shaping led to a significant increase in production time. For future industrial-scale applications, the use of CNC-controlled equipment is recommended to ensure precision and efficiency.

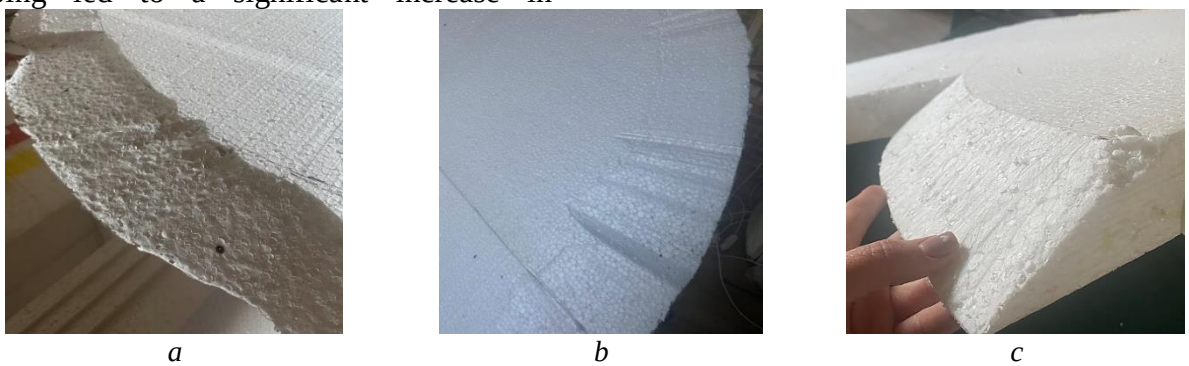

*a* *b* *c*

**Fig. 4** Polystyrene processing: a) with a hot knife, b) with a heated wire, c) with a utility knife. Photo by V. Tenensku
**Рис. 4** Обробка пінопласту: а) термоножем, б) гарячою струною, в) будівельним ножем. Автор фото В. Тенесеску

After all layers had been cut according to the prepared design drawings, the assembly of the polystyrene formwork into a single three-dimensional structure was initiated. The primary objective at this stage was to ensure geometric compliance with the design shape,

provide secure bonding between individual components, and create a smooth, monolithic surface capable of withstanding the load from the concrete mixture.

Before assembly, each layer was carefully cleaned of dust, debris, and glue residue from the previous cutting operations. Any rounding or surface irregularities that could result in deviations from the desired form were manually corrected using sanding mesh or abrasive paper. To bond the polystyrene components, two types of adhesive were employed: a silicone-based construction adhesive was used for bonding large surface areas, providing sufficient working time; and hot melt glue (applied with a glue gun) was used for quick point-fixation at joints and curved sections.

The layers were stacked sequentially, starting from the bottom, with strict adherence to orientation markings. The adhesive was applied in narrow strips, after which the next layer was firmly pressed into position and held under slight pressure for 10–15 minutes to achieve initial bonding.

Upon completion of the assembly, surface alignment and sealing were performed. Some layers were additionally trimmed with a utility knife; joints, gaps, and irregularities were filled using an acrylic-based putty. After drying, the filled areas were sanded using abrasive tools to ensure a smooth transition between layers and an even surface finish.

The step-by-step formwork making is presented in Fig. 5.

*a* *b* *c*

*d* *e* *f*

**Fig. 5.** Procedure for creating polystyrene formwork: a) manual marking of individual polystyrene sheets; b) basic cutting of fragments with a utility knife; c) general view of blanks before edge trimming; d) blanks after edge trimming; e) shape adjustment after assembling the formwork; f) puttying of seams and joints. Photo by V. Tenensku

**Рис. 5.** Процедура створення опалубки з пінопласту: а) розмітка окремих листів пінопласту вручну; б) базове нарізання окремих фрагментів будівельним ножем; в) загальний вигляд заготовок до зрізання країв; в) заготовки після підрізки країв; г) підрізка форми після формування опалубки; г) шпатлювання швів і стиків. Автор фото В. Тенесеску

Subsequent operations involved the transportation of the assembled formwork to the printing site and the concrete 3D printing process itself using a console-type 3D printer. Before initiating the printing, it was essential to properly prepare the digital model. A CAD

program was used to model the volume of the shell structure, taking into account thickness, curvature, and reinforcement layout. The model underwent mesh and geometry validation and was then exported in STL format.

Next, a specialized slicing software was used to divide the model into thin horizontal layers [24]. Parameters such as layer thickness, extruder path, reinforcement insertion levels, and other print settings were defined. Based on this data, the slicing software generated G-code for the 3D printer. When needed, a print simulation was conducted to check for collisions, sagging, or printing errors. Only after this verification process was the print job initiated. This approach allowed for the transformation of complex 3D geometry into an executable construction sequence, while accounting for technological constraints

At the construction site, the polystyrene formwork was installed in its project position, and the printing of the outer concrete ring began (Fig. 6a).

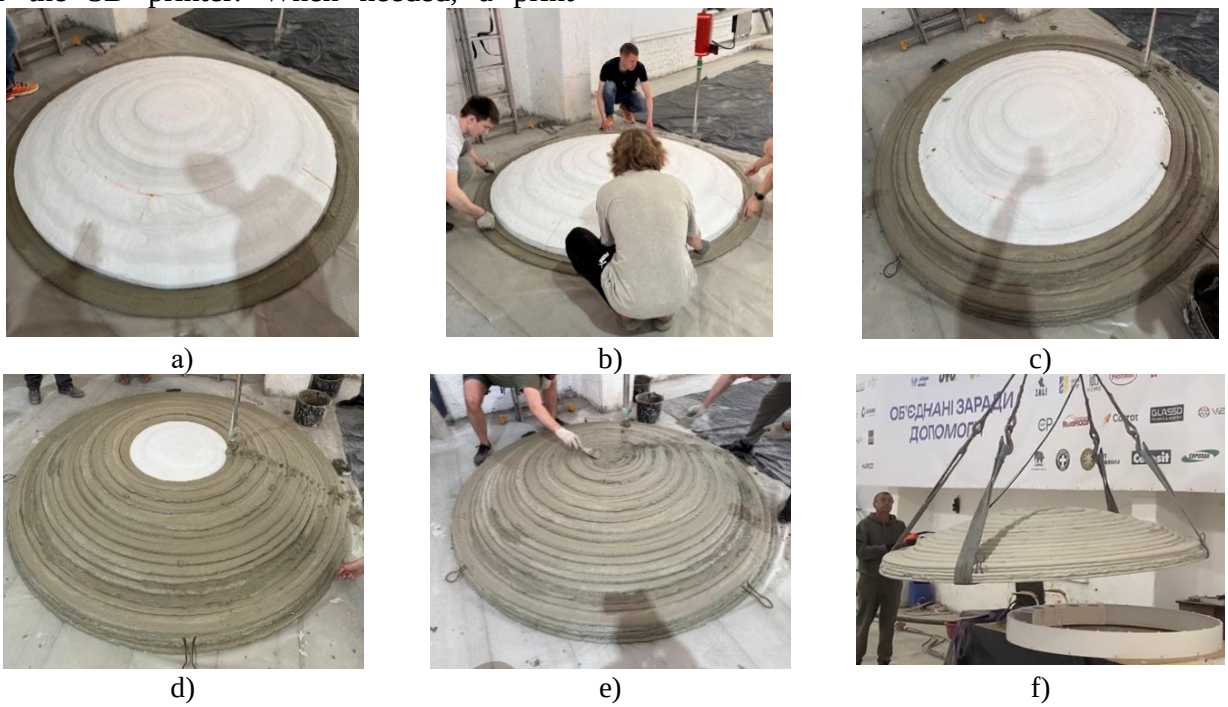


**Fig. 6.** Stages of shell printing: a) installation of the formwork and printing of the support ring; b) placement of reinforcement and mounting loops; c–e) layer-by-layer extrusion of concrete along the height of the formwork; f) transportation of the shell after it has gained sufficient strength. Photo by V. Tenensku

**Рис. 6.** Етапи друку оболонки: а) встановлення опалубки і друк опорного кільця; б) укладання арматури та монтажних петель; в-д) пошарова екструзія бетону по висоті опалубки; ж) транспортування оболонки після набрання нею міцності. Автор фото В. Тенесеску

The printing proceeded vertically from the base of the form upward. The structure was designed without area-wide reinforcement, except for the lower support ring. In this region, 10 mm diameter steel bars were placed to secure four 6 mm mounting loops (Fig. 6b), fastened using steel binding wire. These reinforcement elements were embedded within the initial extrusion layer and subsequently enclosed by additional printed layers (Fig. 6c–d). Technological pauses between layers were allowed, though their duration was minimized to prevent cold joints and ensure interlayer bonding. At the same time, considering the curved geometry of the formwork, short breaks helped prevent sliding of fresh concrete layers due to the weight of upper layers.

The concrete mix used for printing exhibited thixotropic properties, essential for layer-by-layer extrusion. Upon completion of printing, the concrete shell was left to cure under ambient conditions until it reached the required strength (Fig. 6e). After hardening, the structure became suitable for further transportation (Fig. 6f) and integration into larger construction processes.

## CONCLUSIONS AND RECOMMENDATIONS

The article presents the technological sequence of producing a reinforced concrete shell of complex geometry using polystyrene foam formwork and concrete 3D printing. An efficient approach is proposed for shaping the curved surface by means of layer-by-layer assembly of foam formwork, which ensured high geometric accuracy while minimizing material consumption and labor resources. The process of digital model preparation, fabrication and assembly of the polystyrene base, as well as subsequent concrete printing using a 3D printer, confirmed the viability of the proposed technology under real-life experimental conditions.

The proposed method significantly simplifies the fabrication of complex-shaped elements by avoiding the use of traditional rigid formwork and can be adapted for different construction scales. The feasibility of using foam-based formwork as a foundation for printing was confirmed, with subsequent application of concrete mixture without compromising geometric precision or structural integrity.

Further research is aimed at conducting experimental investigations of the concrete shell to determine its deformability and load-bearing capacity.

## AKNOWLEDGMENT

The author sincerely acknowledges the invaluable support provided by “UTU 3D” in the development and realization of the printed concrete shell structure. Special thanks are extended for their expert consultation and technical assistance throughout all phases of preparation, calibration, and execution of the 3D printing process.

## REFERENCES

28. **Buswell, R.A., Leal de Silva, W.R., Jones, S.Z., Dirrenberger, J.** (2018). 3D printing using concrete extrusion: A roadmap for research, *Cement and Concrete Research*, (112), 37-49. ISSN 0008-8846. [in English]. https://doi.org/10.1016/j.cemconres.2018.05.006

29. **Ma G., Buswell R., Leal da Silva W., Wang L., Xu J., Jones S.** (2022). Technology readiness: A global snapshot of 3D concrete printing and the frontiers for development. *Cement and Concrete Research*. [in English]. https://doi.org/10.1016/j.cemconres.2022.106774.

30. **Kimura, T., Hayashi, S., Muto, T., Yamasaki, K., Sakai, Y., Gondo, T.** (2024). Form-finding for free-curved reinforced concrete shell structure considering structural performance and construction formwork. *Engineering Structures*. 301. 117332. [in English]. https://doi.org/10.1016/j.engstruct.2023.117332

31. **UTU-3D.** https://www.utu.com.ua/

32. **Reznik, P., Lugchenko, O., Volodymyrov, A., Tenesesku, V., Alatayev, D., Buldakov, O.** (2025) Chyselne modeliuvannia zalizobetonnykh balok iz neznímnoiu 3D-drukovanoiu opalubkoiu [Numerical analysis of 3D printed permanent formwork for reinforced concrete]. *Collected scientific works of Ukrainian state university of railway transport*, (212), 82–100. [in Ukrainian]. https://doi.org/10.18664/1994-7852.212.2025.336411

33. **Reznik, P., Petrenko, D., Volodymyrov, A., Maksymenko, V., Alatayev, D.** (2025). Anizotropiia mitsnosti 3D-drukovanoho betonu: eksperymentalne doslidzhennia ta statystychnyi analiz [Strength anisotropy of 3D-printed concrete: experimental investigation and statistical analysis]. *Naukovyi visnyk budivnytstva*, (112), 248-257. [in Ukrainian]. https://doi.org/10.33042/2311-7257.2025.112.1.30

34. **Savytskyi, M., Konoplianyk, O., Myslytska, A., Liasota, O.** (2020). Determination of physico-mechanical characteristics of concrete for 3D printing building designs. *Bulletin of Prydniprovs'ka State Academy of Civil Engineering and Architecture*, (2), 59–68. [in Ukrainian]. https://doi.org/10.30838/J.BPSACEA.2312.280420.64.622

35. **Savytskyi, M. V., Ivantsov, S. V., Nikiforova, T. D., Zinkevych, O. H., Khalaf, I.** (2020). Stress-strain state of structural elements of

buildings constructed using 3D printing technology. *Bulletin of Prydniprovs'ka State Academy of Civil Engineering and Architecture*, (3), 265–266. [in Ukrainian] https://doi.org/10.30838/J.BPSACEA.2312.070720.92.645

36. **Vozniuk, L. I., Shcherbakov, S. O., Surmai, M. I., Demchyna, K. B.** (2024). Design and manufacture of arches with reinforcement using 3D printing *Resource-saving materials, structures, buildings and structures, (45), 401–408*. [in Ukrainian]. https://doi.org/10.31713/budres.v0i45.46

37. **Vozniuk, L. I., Burak, D. Yu., Demchyna, K. B., Hovorukha, Yu**. (2025). Test results of a beam produced by 3D printing without transverse reinforcement *Resource-saving materials, structures, buildings and structures*,(48), 133–140. [in Ukrainian].

38. **Shmukler, V., Reznik, P., Krul, Yu., Volodymyrov, A., Binkevych, K.** (2024). Design features of the new system for reconstruction and renovation of large panel buildings. *IOP Conference Series: Earth and Environmental Science*, 1376, 012012. [in English]. https://doi.org/10.1088/1755-1315/1376/1/012012

39. **Shatov, S. V., Savytskyi, M. V., Holubchenko, O. I., Matsiuk, I. M., Shliakhov, E**. (2022). Research of optional equipment solutions for 3D-printing of building products. *Ukrainian Journal of Civil Engineering and Architecture*, 80–88. [in English]. https://doi.org/10.30838/J.BPSACEA.2312.220222.80.836

40. **Demchyna, B. H., Vozniuk, L. I., Burak, D. Yu., Shcherbakov, S. O. (2024).** 3D uvannia poperechnoho armuvannia, printing of beams with the possibility of transverse reinforcement, considering the peculiarities of the construction printer. *Building Constructions. Theory and Practice*, (14), 57-66. [in Ukrainian] https://doi.org/10.32347/2522-4182.14..2024.57-66

41. **Ivaniuk, E., Pukhkaiev, D., Reichle, M., Zhao, W., Mey, J., Krombholz, M., Tošić, Z., Assmann, U., Klinkel, S., Mechtcherine, V.** (2025). Robotic Assembly of Modular Concrete Shells Using Falsework. *Developments in the Built Environment*, 21, 100616. [in English]. https://doi.org/10.1016/j.dibe.2025.100616

42. **Bedarf, P., Calvo Barentin, C., Schulte, D., Şenol, A., Jeoffroy, E., Dillenburger, B.** (2023). Mineral composites: stay-in-place formwork for concrete using foam 3D printing. *Architecture, Structures and Construction*, 3. [in English]. https://doi.org/10.1007/s44150-023-00084-x

43. **Li, W., Lin, X., Bao, D.W., Xie, Y. (2022).** A review of formwork systems for modern concrete construction. Structures. 38. 52-63. [in English]. https://doi.org/10.1016/j.istruc.2022.01.089

44. **Costanzi, C.B., Ahmed, Z.Y., Schipper, H.R., Bos, F.P., Knaack, U., Wolfs, R.J.M**. (2018). 3D Printing Concrete on Temporary Surfaces: The Design and Fabrication of a Concrete Shell Structure. *Automation in Construction*, 94, 395–404. [in English]. https://doi.org/10.1016/j.autcon.2018.06.013

45. **Burger, J., Lloret, E., Scotto, F., Demoulin, T., Gebhard, L., Mata-Falcón, J., Gramazio, F., Kohler, M., Flatt, R.** (2020). Eggshell: Ultra-Thin Three-Dimensional Printed Formwork for Concrete Structures. *3D Printing and Additive Manufacturing*, 7(1), 13–22. [in English]. https://doi.org/10.1089/3dp.2019.0197

46. **Wang, X., Yuan, P.F., Xie, M., Leach, N., Yao, J.** (2020). 3D-Printed Bending-Active Formwork for Shell Structures. In *Architectural Intelligence* (pp. 245–256). Springer, Singapore. [in English]. https://doi.org/10.1007/978-981-15-6568-7_18

47. **Shmukler, V.S.** (2022). Pro odyn pidkhid formuvannia tekhnolohii proiektuvannia ratsionalnykh konstruktsii. [About one approach to the formation of design technology of rational designs]. *Visnyk Kharkivskoho natsionalnoho avtomobilno-dorozhnoho universytetu*, (98), 93–113. [in Ukrainian]. https://doi.org/10.30977/BUL.2219-5548.2022.98.0.93

48. **Lugchenko, O., Reznik, P., Petrova, O., Tenesesku, V.** (2023). Numerical Verification of the Positive Gaussian Curvature Shell Topological Optimization Approach. In *Smart Technologies in Urban Engineering. Lecture Notes in Networks and Systems* (Vol. 807, pp. 164–176). Springer, Cham. [in English]. https://doi.org/10.1007/978-3-031-46874-2_15

49. **Shmukler, V.** (2017). Novi enerhetychni pryntsypy ratsionalizatsii konstruktsii [New energy principles of structures rationalization]. *Zbirnyk naukovykh prats UkrDUZT*, (167), 120–132. [in Ukrainian]. https://doi.org/10.18664/1994-7852.167.2017.97206

50. **Babaev, V., Ievzerov, I., Evel, S., Lantoukh-Liashchenko, A., Shevetovsky, V., Shimanovskyi, O., Shmukler, V., Sukhonos, M.** (2019). *Rational Design of Structural Building Systems*. Berlin: DOM publishers. ISBN 978-3-86922-733-7. [in English]. https://dom-publishers.com/products/rational-design-for-structural-building-systems
51. **Atarihuana, S., Fernández, F., Erazo, J., Narváez, M., Hidalgo, V.** (2024). Optimal Strategies for Filament Orientation in Non-Planar 3D Printing. *Processes*, 12(12), 2811. [in English]. https://doi.org/10.3390/pr1212281
52. **da Silveira Júnior, J.G., de Moura Cerqueira, K., de Araújo Moura, R.C., de Matos, P.R., Rodriguez, E.D., de Castro Pessôa, J.R., Tramontin Souza, M.** (2024). Influence of Time Gap on the Buildability of Cement Mixtures Designed for 3D Printing. *Buildings*, 14(4), 1070. [in English]. https://doi.org/10.3390/buildings14041070

## LITERATURE

1. **Buswell, R.A., Leal de Silva, W.R., Jones, S.Z., Dirrenberger, J.** (2018). 3D printing using concrete extrusion: A roadmap for research, *Cement and Concrete Research*, (112), 37-49. ISSN 0008-8846. https://doi.org/10.1016/j.cemconres.2018.05.006
2. **Ma G., Buswell R., Leal da Silva W., Wang L., Xu J., Jones S.** (2022). Technology readiness: A global snapshot of 3D concrete printing and the frontiers for development. *Cement and Concrete Research*. https://doi.org/10.1016/j.cemconres.2022.106774.
3. **Kimura, T., Hayashi, S., Muto, T., Yamasaki, K., Sakai, Y., Gondo, T.** (2024). Form-finding for free-curved reinforced concrete shell structure considering structural performance and construction formwork. *Engineering Structures*. 301. 117332. https://doi.org/10.1016/j.engstruct.2023.117332 **UTU-3D.** https://www.utu.com.ua/
4. **Reznik, P., Lugchenko, O., Volodymyrov, A., Tenesesku, V., Alatayev, D., Buldakov, O.** (2025) Chyselne modeliuvannia zalizobetonnykh balok iz neznímnoiu 3D-drukovanoiu opalubkoiu *Collected scientific works of Ukrainian state university of railway transport*, (212), 82–100. https://doi.org/10.18664/1994-7852.212.2025.336411
5. **Reznik, P., Petrenko, D., Volodymyrov, A., Maksymenko, V., Alatayev, D.** (2025). Anizotropiia mitsnosti 3D-drukovanoho betonu: eksperymentalne doslidzhennia ta statystychnyi analiz *Naukovyi visnyk budivnytstva*, (112), 248-257. https://doi.org/10.33042/2311-7257.2025.112.1.30
6. **Savytskyi, M., Konoplianyk, O., Myslytska, A., Liasota, O.** (2020). Vyznachennia fizyko-mekhanichnykh kharakterystyk betoniv dlia 3D-druku budivelnykh konstruktsii *Visnyk Prydniprovs'koi derzhavnoi akademii budivnytstva ta arkhitektury, (2), 59–68*. https://doi.org/10.30838/J.BPSACEA.2312.280420.64.622
7. **Savytskyi, M. V., Ivantsov, S. V., Nikiforova, T. D., Zinkevych, O. H., Khalaf, I.** (2020). Naprusheno-deformovanyi stan konstruktyv-nykh elementiv budivel, zvedenykh iz zastosuvanniam tekhnolohii 3D-druku. *Visnyk Prydniprovs'koi derzhavnoi akademii budivnytstva ta arkhitektury, (3), 265–266*. https://doi.org/10.30838/J.BPSACEA.2312.070720.92.645
8. **Vozniuk, L. I., Shcherbakov, S. O., Surmai, M. I., Demchyna, K. B.** (2024). Proiektuvannia ta vyhotovlennia arok iz armuvanniam iz vykorystanniam tekhnolohii 3D-druku. *Resursozberihaiuchi materialy, konstruktsii, budivli ta sporudy, (45), 401–408*. https://doi.org/10.31713/budres.v0i45.46
9. **Vozniuk, L. I., Burak, D. Yu., Demchyna, K. B., Hovorukha, Yu**. (2025). Rezultaty vyprobuvan balky, vyhotovlenoi metodom 3D-druku bez poperechnoho armuvannia. *Resursozberihaiuchi materialy, konstruktsii, budivli ta sporudy, (48), 133–140*.
10. **Shmukler, V., Reznik, P., Krul, Yu., Volodymyrov, A., Binkevych, K.** (2024). Design features of the new system for reconstruction and renovation of large panel buildings. *IOP Conference Series: Earth and Environmental Science*, 1376, 012012. https://doi.org/10.1088/1755-1315/1376/1/012012
11. **Shatov, S. V., Savytskyi, M. V., Holubchenko, O. I., Matsiuk, I. M., Shliakhov, E**. (2022). Research of optional equipment solutions for 3D-printing of building products. *Ukrainian*

*Journal of Civil Engineering and Architecture*, 80–88. https://doi.org/10.30838/J.BPSACEA.2312.220222.80.836

12. **Demchyna, B. H., Vozniuk, L. I., Burak, D. Yu., Shcherbakov, S. O. (2024).** 3D-druk balok iz mozhlyvistiu poperechnoho armuvannia z urakhuvanniam osoblyvostei budivelnoho pryntera. *Budivelni konstruktsii. Teoriia i praktyka*, *(14), 57–66*. https://doi.org/10.32347/2522-4182.14..2024.57-66
13. **Ivaniuk, E., Pukhkaiev, D., Reichle, M., Zhao, W., Mey, J., Krombholz, M., Tošić, Z., Assmann, U., Klinkel, S., Mechtcherine, V.** (2025). Robotic Assembly of Modular Concrete Shells Using Falsework. *Developments in the Built Environment*, 21, 100616. https://doi.org/10.1016/j.dibe.2025.100616
14. **Bedarf, P., Calvo Barentin, C., Schulte, D., Şenol, A., Jeoffroy, E., Dillenburger, B.** (2023). Mineral composites: stay-in-place formwork for concrete using foam 3D printing. *Architecture, Structures and Construction*, 3. https://doi.org/10.1007/s44150-023-00084-x
15. **Li, W., Lin, X., Bao, D.W., Xie, Y. (2022).** A review of formwork systems for modern concrete construction. Structures. 38. 52-63. https://doi.org/10.1016/j.istruc.2022.01.089
16. **Costanzi, C.B., Ahmed, Z.Y., Schipper, H.R., Bos, F.P., Knaack, U., Wolfs, R.J.M**. (2018). 3D Printing Concrete on Temporary Surfaces: The Design and Fabrication of a Concrete Shell Structure. *Automation in Construction*, 94, 395–404. https://doi.org/10.1016/j.autcon.2018.06.013
17. **Burger, J., Lloret, E., Scotto, F., Demoulin, T., Gebhard, L., Mata-Falcón, J., Gramazio, F., Kohler, M., Flatt, R.** (2020). Eggshell: Ultra-Thin Three-Dimensional Printed Formwork for Concrete Structures. *3D Printing and Additive Manufacturing*, 7(1), 13–22. https://doi.org/10.1089/3dp.2019.0197
18. **Wang, X., Yuan, P.F., Xie, M., Leach, N., Yao, J.** (2020). 3D-Printed Bending-Active Formwork for Shell Structures. In *Architectural Intelligence* (pp. 245–256). Springer, Singapore. https://doi.org/10.1007/978-981-15-6568-7_18
19. **Shmukler, V.S.** (2022). Pro odyn pidkhid formuvannia tekhnolohii proiektuvannia ratsionalnykh konstruktsii. *Visnyk Kharkivskoho natsionalnoho avtomobilno-dorozhnoho universytetu*, (98), 93–113. https://doi.org/10.30977/BUL.2219-5548.2022.98.0.93
20. **Lugchenko, O., Reznik, P., Petrova, O., Tenesesku, V.** (2023). Numerical Verification of the Positive Gaussian Curvature Shell Topological Optimization Approach. In *Smart Technologies in Urban Engineering. Lecture Notes in Networks and Systems* (807), 164–176). https://doi.org/10.1007/978-3-031-46874-2_15
21. **Shmukler, V.** (2017). Novi enerhetychni pryntsypy ratsionalizatsii konstruktsii *Zbirnyk naukovykh prats UkrDUZT*, (167), 120–132. https://doi.org/10.18664/1994-7852.167.2017.97206
22. **Babaev, V., Ievzerov, I., Evel, S., Lantoukh-Liashchenko, A., Shevetovsky, V., Shimanovskyi, O., Shmukler, V., Sukhonos, M.** (2019). *Rational Design of Structural Building Systems*. Berlin: DOM publishers. ISBN 978-3-86922-733-7.
23. https://dom-publishers.com/products/rational-design-for-structural-building-systems
24. **Atarihuana, S., Fernández, F., Erazo, J., Narváez, M., Hidalgo, V.** (2024). Optimal Strategies for Filament Orientation in Non-Planar 3D Printing. *Processes*, 12(12), 2811.. https://doi.org/10.3390/pr1212281
25. **da Silveira Júnior, J.G., de Moura Cerqueira, K., de Araújo Moura, R.C., de Matos, P.R., Rodriguez, E.D., de Castro Pessôa, J.R., Tramontin Souza, M.** (2024). Influence of Time Gap on the Buildability of Cement Mixtures Designed for 3D Printing. *Buildings*, 14(4), 1070.. https://doi.org/10.3390/buildings14041070

ISSN 2522-4182

# ТЕХНОЛОГІЧНІ АСПЕКТИ ЗВЕДЕННЯ БЕТОННОЇ ОБОЛОНКИ ЗА ДОПОМОГОЮ 3D-ДРУКУ БЕТОНОМ

*Владислав ТЕНЕСЕСКУ*

**Анотація.** У статті основна увага приділена технологічним аспектам виготовлення залізобетонної оболонки за допомогою 3D-друку бетону в поєднанні з полістирольною опалубкою. Було проведено комплексний огляд літератури для аналізу останніх досягнень у методах адитивного виробництва оболонкових конструкцій, з особливим акцентом на розробці та застосуванні гнучких та незнімних опалубочних систем. Було реалізовано покрокову процедуру виготовлення тестового елемента оболонки, включаючи створення цифрової параметричної моделі, а потім виготовлення спеціальної полістирольної форми. Форму було зібрано з використанням шаруватих пінопластових листів, які були вирізані за заздалегідь визначеними шаблонами, склеєні за допомогою клеїв та вручну вдосконалені для забезпечення геометричної точності.

Цифрову модель було оброблено в програмному забезпеченні CAD та перетворено у формат, придатний для слайсування. Операція слайсування була виконана для визначення висоти шару, напрямку друку та траєкторій руху сопла. На основі згенерованого G-коду для виконання процесу адитивного нашарування було використано роботизований бетонний принтер (консольного типу, «UTU 3D»). Бетон укладався шар за шаром на попередньо встановлену пінополістирольну форму, починаючи з нижнього кільця, яке було армовано вбудованими сталевими стрижнями для розміщення вантажопідйомних гаків. Тиксотропна бетонна суміш використовувалася для підтримки стабільності кожного нанесеного шару та запобігання сповзання по криволінійній поверхні форми. Були введені короткі паузи між шарами для керування твердінням та підтримки міжшарового зчеплення.

Готовій оболонці дали затвердіти в нормальних умовах до досягнення бажаної структурної міцності. Дослідження підтвердило доцільність та ефективність поєднання опалубки на основі полістиролу та 3D-друку для створення тонкостінних криволінійних бетонних конструкцій, що пропонує значний потенціал для використання як в експериментальних, так і в промислових цілях у будівельній галузі.

Подальші дослідження спрямовані на проведення повномасштабних випробувань оболонки під дією кваз-рівномірного статичного навантаження з метою визначення несучої здатності та деформативності конструкції.

**Ключові слова:** бетонна оболонка; 3D-друк бетоном; опалубка з пінопасту; адитивні технології.

***Received:*** *October 22, 2025.*
***Accepted:*** *November 30, 2025.*

ISSN 2522-4182

DOI: 10.32347/2522-4182.17.2025.153-167
UDC 666.19; 677.522

# THE INFLUENCE OF TECHNOLOGICAL FACTORS ON THE PROPERTIES OF REACTION POWDER CONCRETES BASED ON ALKALI-ACTIVATED SLAG PORTLAND CEMENT

*Andrij RAZSAMAKIN*

[1]Kyiv National University of Construction and Architecture
31, Povitryanykh Syl Ave., Kyiv, Ukraine, 03037
razsamakin.a@gmail.com, http://orcid.org/0000-0001-5130-6059

**Abstract.** The development of reactive powder concrete (RPC) based on Portland cements containing varying amounts of granulated blast furnace slag and activated with soluble sodium silicates is of global importance in terms of protecting critical infrastructure.

The article identifies factors influencing the kinetics of strength gain, inherent shrinkage deformation and impact strength of reactive powder concretes when using sodium metasilicate pentahydrate as an alkaline activator in various aggregate states (powder, solution), as well as soluble sodium silicates with a silicate modulus of $M_s$ = 2...3. It has been shown that changing the ratio between slag portland cement and sand from 1:3 to 1:1 and using sodium metasilicate in powder form ensures the production of sand concrete with compressive strengths of 35.7, 63.8, 87.5, 118. 1 and 123.9 MPa after 1, 3, 28, 180 and 360 days, respectively.

The use of sodium metasilicate in the form of an aqueous solution significantly accelerates the kinetics of strength gain and provides a strength of 52.3, 85.0, 108.7, 126.1 and 141.1 MPa after 1, 3, 28, 180 and 360 days, respectively.

The introduction of finely dispersed calcite reduced the shrinkage during drying of RPC by 1.2...1.6 times. Reducing the OPC content from 45 to 5% by mass with a water silicate glass modulus of 2.6...2.7 resulted in a slight decrease in the early compressive strength of ultra-rapid hardening RPC, but provided a significant increase in the compressive strength limit from 112.5 MPa to 132.4 MPa after 28 days. Viscous fracture after 28 days is confirmed by a better brittleness coeffi

**Andrij RAZSAMAKIN**
Postgraduate student of the Department of TBKV

cient of 5.3...5.9 and 10.5...28.7% higher impact toughness of samples on sodium metasilicate and sodium disilicate compared to the analogue based on OPC. RPC with stable long-term strength, high impact toughness and reduced shrinkage during drying has been obtained. The introduction of bleaching agents in the form of $CaCO_3$ and mineral pigments allows decorative RPC to be obtained.

The possibility of obtaining products by extrusion based on alkali-activated RPC with the determination of the main technological parameters of the process is indicated.

**Keywords:** reaction powder concretes, alkali-activated cement, strength, shrinkage.

## INTRODUCTION

Current trends in materials science, as well as the military-political situation in the world and in Ukraine in particular, are leading to growing interest in high-performance concretes with increased resistance to dynamic loads [1-3]. One type of new-generation concrete is reactive powder concrete (further RPC) [4, 5].

The effectiveness of RPC for critical structures has been confirmed [6, 7].

RPC is characterised by high compressive and flexural strength (150...230 MPa and 20...50 MPa after 28 days) [8], crack resistance [9], corrosion resistance [10] and heat resistance [11].

However, despite the undeniable advantages of RPC, questions remain regarding its economic efficiency due to the high content of binder (about 1000 kg/m³), the total cost of production, the shortage of some raw materials and the insufficient study of the technological parameters of its production [6]. RPC requires a high level of production technology and hardening before commissioning [12]. The high binder content and the absence of coarse aggregate emphasise the relevance of significant shrinkage [13]. Another disadvantage of such concretes is their insufficient environmental friendliness. To partially overcome these disadvantages, it is recommended to replace cement (up to 50% by mass) or silica (10…15% by mass) with additional materials such as limestone, various slags, fly ash, glass powder, etc. [14].

The most promising for obtaining reaction-powder concretes are binding compositions obtained by alkali activation of cements containing up to 95% granulated blast furnace slag in accordance with EN 197-1:2011. Alkali-activated slag cements according to DSTU B V.2.7-181:2009 [15] are effective in reducing clinker content and, consequently, $CO_2$ emissions, as well as minimising the use of natural raw materials and energy resources [16, 17]. The most effective activators of alkali-activated cements (further, AAC) are sodium silicates, whose anions are similar to the hydrated primary decomposition products of the alumina-silica-oxygen framework and act as their additional reserve [18].

The use of alkali-activated cements in concrete and mortar, in addition to high strength, provides high heat resistance [11], sulphate resistance [19], frost resistance [20, 21], durability in marine environments [22], and crack resistance [23].

However, along with their advantages, AAC-based materials also have certain characteristics. One of them is greater shrinkage compared to Portland cements, which is explained by the increased content of gel-like and submicroscopic crystalline phases in hydration products, as well as the absence of crystalline phases such as portlandite $Ca(OH)_2$ and ettringite $3CaO{\cdot}Al_2O_3{\cdot}3CaSO_4{\cdot}32H_2O$ [18]. This feature exacerbates the problem of controlling shrinkage deformations in RPC. A well-known approach to reducing shrinkage in AAC is the use of mineral additives (limestone, fly ash, silica fume), chemical additives (shrinkage reducers, expanders, surfactants, superabsorbent polymers, nanoparticles), as well as various types of fibres (steel fibres, polypropylene fibres, carbon fibres, glass fibres) [24-28].

The aim of the study was to determine the influence of technological factors on the long-term physical and mechanical properties of alkali-activated reactive powder concrete based on slag Portland cement, including its compressive strength and impact toughness, as well as shrinkage during drying.

## RAW MATERIALS AND TESTING TECHNIQUES

The following components were used in the AAC:

- Crushed granulated blast furnace slag (further – GBFS) (oxides, % by weight: $CaO$ – 50.98; $SiO_2$ – 32.13; $Al_2O_3$ – 11.48; $Fe_2O_3$ – 0.4; $MgO$ – 1.14; $K_2O{+}Na_2O$ – 0.77; $SO_3$ – 1.8; LOI – 1.3), specific surface area (S) = 400 м$^2$/kg (according to Blaine), basicity modulus $M_b$ = 1.18, glass phase content – 84.0 %.
- CEM I 42,5 N (further – OPC) (oxides, % by weight: $CaO$ – 65.0; $SiO_2$ – 21.0; $Al_2O_3$ – 5.6; $Fe_2O_3$ – 4.8; $MgO$ – 2.5; $SO_3$ – 0.7; $K_2O{+}Na_2O$ – 0.15; LOI – 0.25) for EN 197-1:2011, specific surface area (S) = 390 м$^2$/kg (according to Blaine).
- Sodium metasilicate pentahydrate was used as the alkaline component. ($Na_2O{\cdot}SiO_2{\cdot}5H_2O$) for CAS 497-19-8 in both solid aggregate form (non-hygroscopic powder) and as a solution with a density of 1.24 g/ml; as well as high-modulus soluble sodium glass with $M_s$ = 2...3.

As small aggregates in RPC used:

- Silicon river sand with non-optimised granulometry: 0…0.16 mm – 13.1%, 0.16…0.315 mm – 65.0%, 0.315…0.63 mm – 16.0%, 0.63…1.25 mm – 5.1%, 1.25…2.5 mm – 0.6%; Sand size module $M_{ss}$ = 1.16.
- Silicon sand with optimised granulometry: fraction 0.315 mm – 22.47%, fraction 0.63 mm – 32.36%, fraction 1.25 mm – 45.17%, which was optimised by approximating the general granulometric curve to the ideal Fuller curve [29-31], which ensures minimal intergranular voids. The fraction that passed through a 0.16 mm sieve was not used.

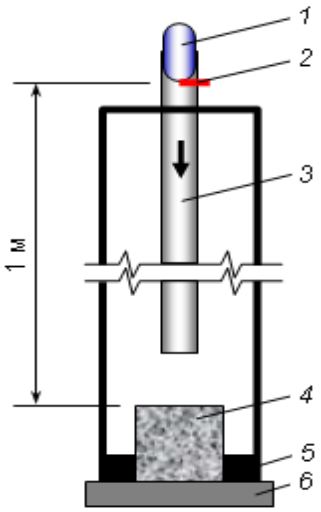


**Fig. 1** Concrete impact strength test procedure:
*1* – 2 kg weight; *2* – weight lock; *3* – vertical guide pipe; *4* – 10×10×10 cm concrete cube sample; *5* – sample position lock; *6* – solid foundation

**Рис. 1** Схема випробування бетону на ударну міцність:
*1* – гиря вагою 2 кг; *2* – фіксатор гирі; *3* – направляюча вертикальна труба; *4* – куб-зразок бетону 10×10×10 см; *5* – фіксатор положення зразка; *6* – масивна основа

The viscosity (crack resistance) of concrete was evaluated based on the ratio of compressive strength to flexural tensile strength.

Shrinkage deformations of fine-grained concrete were determined on samples measuring 40×40×160 mm. After fabrication and hardening in molds with an insulated surface for 24 hours, the samples were removed from the molds and stored for 7 days under normal conditions (t = 20±2°C, R.H. = 95±5%). The samples were then stored above a saturated solution of ammonium nitrate ($NH_4NO_3$) at t = 20±2°C and R.H. = 65% until the control age. The length of the samples after 1 day was taken as the initial (zero) length.

To control shrinkage during drying, finely dispersed calcium carbonate ($CaCO_3$) per CAS 471-34-1 was used in the RPC.

The RPC was prepared in a standard Hobart mixer.

The strength of cement-sand mortars was determined on beam samples measuring 4×4×16 cm with a composition of 1:1, 1:2, and 1:3 (binder : sand) and on 10×10×10 cm cube samples using quartz river sand with $M_{ss}$ = 1.16. Strength was determined after 1, 2, 3, 7, 28, 90, 180, and 360 days.

The RPC impact strength (impact toughness) test was performed according to the method described in [32]. The concrete impact strength test scheme is shown in Fig.1.

## RESULTS AND DISCUSSIONS

As a cementitious matrix for RPC, AACs based on sodium metasilicate (*system 1*) and soluble high-modulus glass (*system 2*) were investigated. System 1 was considered in terms of obtaining RPC as a single-component product [33, 34, 35], while system 2 was used to obtain ultra-fast-setting RPC [18, 36].

*RPC based on AAS system 1*

The effect of the AAC to sand ratio on the strength of RPC was studied using siliceous sand with non-optimized granulometry (Table 1). Sodium metasilicate was used in a solid aggregate state (powder). The compositions were mixed with water.

**Table 1** Physical and mechanical characteristics of fine-grained alkali-activated concretes depending on the ratio of "binder : sand"

**Табл. 1** Фізико-механічні характеристики дрібнозернистих лужно-активованих бетонів залежно від співвідношення "в'яжуча речовина : пісок"

| Compositions of AAC, wt. % | | | AAC-to-sand ratio | Water-to-AAC ratio | Consis-tency (flow), mm | Compressive strength / flexural strength, MPa, at age, day | | | | | | | |
|---|---|---|---|---|---|---|---|---|---|---|---|---|---|
| GBFS | OPC | sodium metasi-licate | | | | 1 | 2 | 3 | 7 | 28 | 90 | 180 | 360 |
| 85 | 5 | 10 | 1:1 | 0.218 | 180 | 35.7 / 5.9 | 55.1 / 6.7 | 63.8 / 7.4 | 73.6 / 10.5 | 87.5 / 14.8 | 104.5 / 17.9 | 118.1 / 19.8 | 123.9 / 20.7 |
| | | | 1:2 | 0.237 | 165 | 27.1 / 6.0 | 42.8 / 7.1 | 50.7 / 8.8 | 57.7 / 9.2 | 67.7 / 11.0 | 78.5 / 13.0 | 88.5 / 15.5 | 92.6 / 16.3 |
| | | | 1:3 | 0.334 | 145 | 20.7 / 5.6 | 31.4 / 5.8 | 35.7 / 6.1 | 42.4 / 8.3 | 49.8 / 10.5 | 57.0 / 12.5 | 61.7 / 14.7 | 64.8 / 15.4 |

As can be seen in Fig.2, the dependence of strength on sand content is practically linear under the condition of Water-to-AAC ratio ≤ 0.35.

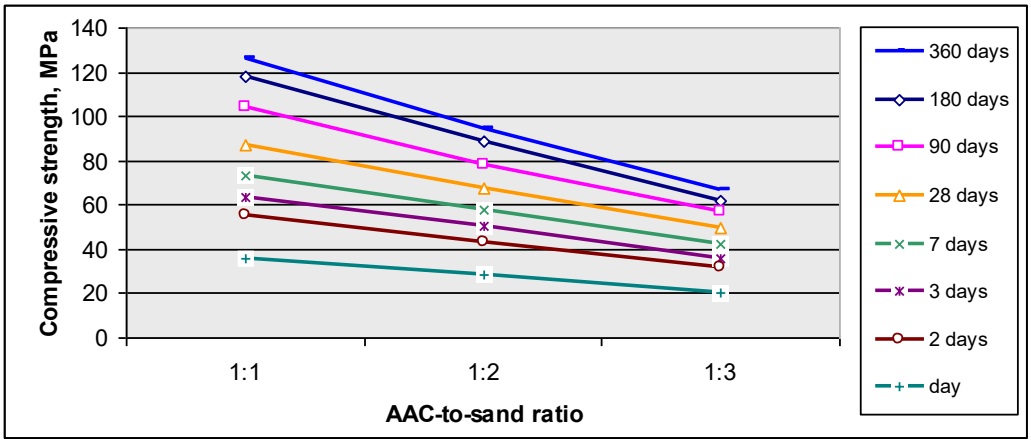


**Fig. 2** Dependence of the strength of cement-sand concretes at different hardening times on the ratio of "binder : sand". Alkaline component – sodium metasilicate

**Рис. 2** Залежність міцності цементно-піщаних бетонів у різні строки твердіння від співвідношення "в'яжуче : пісок". Лужний компонент – метасилікат натрію

As can be seen from the results in Table 1 and Fig. 2, an increase in the binder content in the composition leads to an expected increase in strength. The highest strength was demonstrated by the composition with a "binder : sand" ratio of 1:1 (see Table 1), which is accepted for further research as RPC.

The effect of the aggregate state of sodium metasilicate on the strength of RPC was studied at a ratio of AAS to sand of 1:1. Siliceous sand with optimized granulometry was used. According to previous studies, the use of such sand increases strength by 7…8% due to denser packing of aggregate grains and a reduction in water content for standard consistency according to EN 196-3, which is associated with a decrease in the specific surface area of the aggregate [35].

Sodium metasilicate was added in equal amounts – 10.0% (in terms of dry matter) or 2.9% (in terms of $Na_2O$).

The genesis of RPC strength with different Portland cement contents in the cement-slag mixture when using sodium metasilicate in different aggregate states is shown in Fig.3.

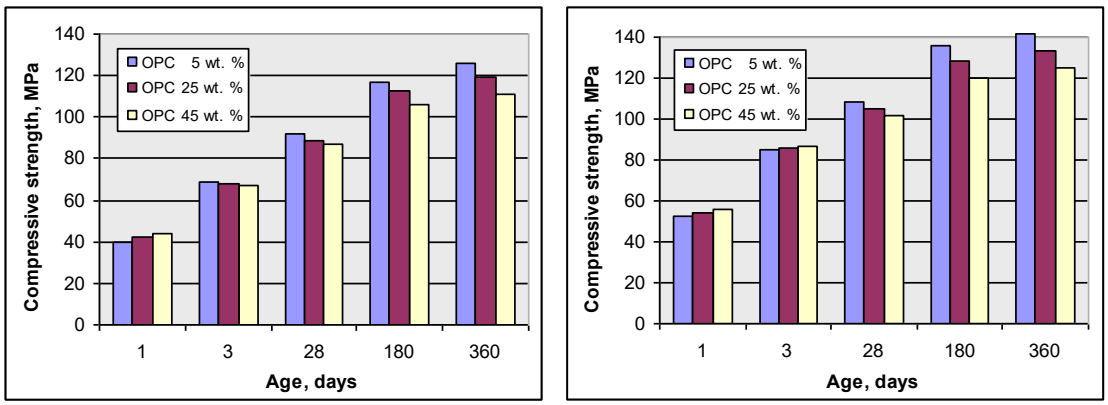


*a* *b*

**Fig. 3** Strength of RPC depending on age and aggregate state of sodium metasilicate: *a* – solid aggregate state (powder); *b* – liquid aggregate state (solution);
**Рис.3** Міцність RPC залежно від віку та агрегатного стану метасилікату натрію: *а* – твердий агрегатний стан (порошок); *б* – рідинний агрегатний стан (розчин)

The use of sodium metasilicate in solution form instead of dry powder ensured maximum reduction in the soluble-binding ratio, which led to a further intensification of concrete strength development by 30.5%, 23.5%, 18.4%, 6.1%, and 3.9%, providing 52.3, 85.0, 108.7, 136.1, and 141.4 MPa at ages 1, 3, 28, 180, and 360 days, respectively.

All compositions showed a stable and monotonous increase in long-term strength, which contradicts the conclusions presented in [37].

The brittleness coefficient was 5.3...5.5, 5.5...5.7, and 5.7...6.0 at 28, 90, and 360 days, respectively, indicating a sufficiently high crack resistance of RPC [38].

The setting times of the compositions using sodium metasilicate powder and a Portland cement content of 5…45% in the slag cement mixture were 19…100 min, and with the addition of 2% LSTM additive, they were 40…118 min. An increase in the Portland cement content causes a reduction in setting times.

The effect of the OPC content in the "GBFS + OPC" mixture on the shrinkage of RPC during drying was investigated using a complete factorial design of type $2^3$ [39]. Shrinkage during drying is a critically important characteristic of concrete in general and RPC in particular [40-42]. To ensure a comprehensive effect on shrinkage reduction, $CaCO_3$ additive was used, the positive effect of which in alkali-activated systems was demonstrated in [27, 35].

The following variables were selected: X1 – $CaCO_3$ content (0...40 wt.%); X2 – OPC content in AAC (5...45 wt.%). The study was conducted with a 1:1 ratio of AAC to sand. The content of sodium metasilicate in the solid state (powder) was 10.0 %. As a result of mathematical processing of the experimental results, adequate regression equations were obtained. Based on the obtained regression equations, a response surface of shrinkage change during RPC drying was constructed (Fig. 4).

Increasing the OPC content from 5 to 45 % by mass and the $CaCO_3$ content from 0 to 20...25 % by mass made it possible to reduce the shrinkage of RPC from 1.23 mm/m to 0.50...0.55 mm/m (by 55...60 %).

In addition, $CaCO_3$ can be considered a whitening additive, so adding it in the optimal amount (20...25 %) allows the resulting RPC to be classified as white and decorative, with a whiteness level of at least 70 %.

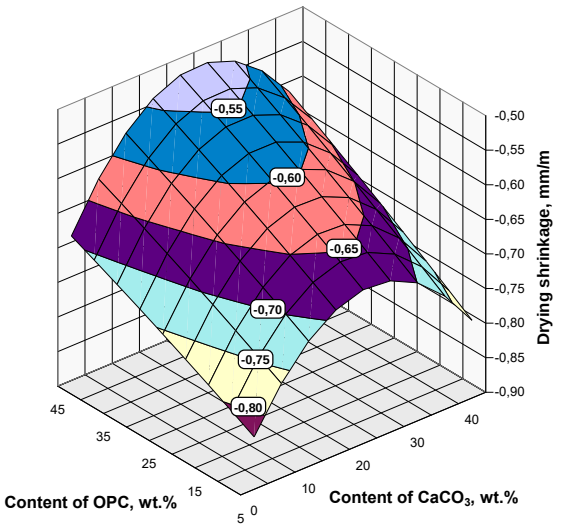


**Fig.4** Drying shrinkage of RPC at 90 days vs. content of OPC vs. content of $CaCO_3$

**Рис.4** Усадка RPC при висиханні на 90 добу залежно від вмісту OPC та вмісту $CaCO_3$

The effect of sodium silicates on the impact strength of RPC was studied using a composition based on AAC with an "OPC : GBFS" ratio of 5 : 95 (compositions #1 and #2). Sodium metasilicate and sodium disilicate were used in a solid aggregate state (powder). RPC based on CEM I 42.5 R with a superplasticizer (composition #3) was used as a comparison analogue. All compositions were mixed with water. The test results are presented in Fig. 5 and Fig. 6. The samples are cubes measuring 10×10×10 cm. The samples were tested at 28 days and 180 days.

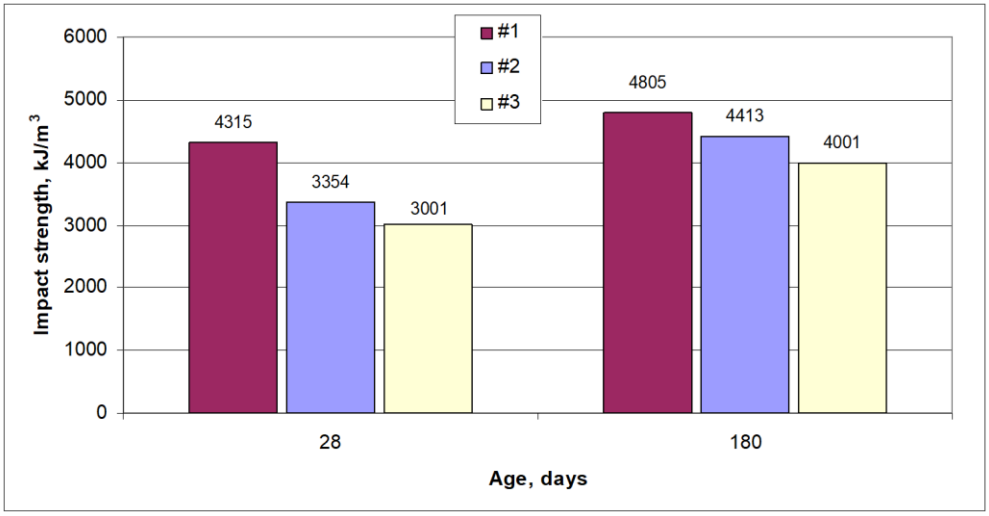


**Fig. 5** Dependence of RPC impact strength on RPC composition and age: #1 - RPC based on AAS with sodium disilicate, #2 - RPC based on AAS with sodium metasilicate, #3 - RPC based on OPC (control)

**Рис. 5** Залежність ударної в'язкості RPC від складу RPC та віку: #1 - RPC на основі ААС з дисилікатом натрію, #2 - RPC на основі ААС з метасилікатом натрію, #3 - RPC на основі OPC (контроль)

As can be seen in Fig. 5, composition #1 based on sodium disilicate demonstrated the highest impact strength. Slightly lower was #2 based on metasilicate. And the lowest was #3 based on OPC (sample for comparison). Fig. 6 also shows that sample *c* based on Portland cement is more brittle, as fragments of the sample broke off, while samples *a* and *b* only developed cracks.

The nature of destruction and higher impact resistance indicators of RPC based on alkali-activated slag Portland cements can be explained by the peculiarities of the phase composition of new formations with a predominance of low-base calcium hydrosilicates and mixed *Na-Ca* composition, the ratio of gel-like and crystalline components of hydraulic new formations with a predominance of the gel-like component [43], which is confirmed by other authors [9, 33]

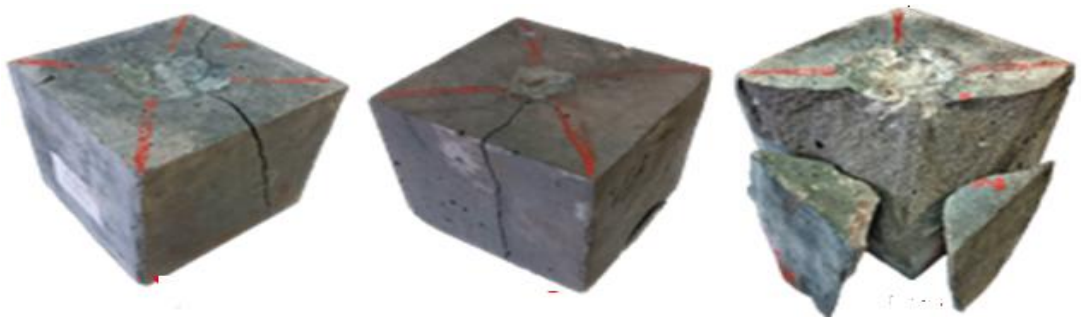

*a* *b* *c*

**Fig. 6** Samples of reaction-powder concretes of different compositions after impact resistance testing after 28 days of hardening: *a* – RPC based on AAC with sodium disilicate, *b* – RPC based on AAC with sodium metasilicate, *c* – RPC based on OPC (control)

**Рис. 6** Зразки реакційно-порошкових бетонів різного складу після випробування на ударна стійкість через 28 діб твердіння: *а* – RPC на основі ААС з дисилікатом натрію, *б* – RPC на основі ААС з метасилікатом натрію, *в*– RPC на основі традиційного портландцементу (контроль)

In addition, concretes of this class have higher adaptive properties and the ability to self-heal defects in the form of cracks if they appear as a result of extreme operating conditions [36].

Regardless of the composition, the impact strength of all RPBs increases over time [34, 35].

*RPC based on AAS system 2*

The influence of the silicate modulus of soluble glass on the strength of RPC was studied using a complete factorial design of experiment type $2^3$. High-modulus sodium glass (density 1.3 g/cm³) was used. Trisodium phosphate (further TNF) was added to the soluble glass in an amount of 12% of the mass of sodium glass. The ratio of AAS to sand was 1:1. Siliceous sand with optimized granulometry was used. The factors, their variation levels, and the results of the experiment are presented in Table 2 and Table 3.

**Table 2** Initial data
**Табл. 2** Вихідна дані

| Factors | Units of measurement | Code | Levels of variation | | |
|---|---|---|---|---|---|
| | | | –1 | 0 | +1 |
| Silicate modulus of glass, Ms | – | X1 | 2 | 2.5 | 3 |
| OPC content in the mixture | % | X2 | 5 | 25 | 45 |

**Table 3** Experiment plan and results
**Табл. 3** План і результати експерименту

| N | Plan matrix in co-codes | | Plan matrix in natural values | | Compressive strength, R compression, MPa, through | | | | | | | |
|---|---|---|---|---|---|---|---|---|---|---|---|---|
| | X1 | X2 | $M_s$ | OPC % | 3 hours | 1 day | 3 days | 7 days | 28 days | 90 days | 180 days | 360 days |
| 1 | +1 | +1 | 3 | 45 | 26.9 | 45.7 | 66.2 | 82.8 | 96.6 | 102.7 | 105.3 | 109.5 |
| 2 | +1 | -1 | 3 | 5 | 24.1 | 40.0 | 62.4 | 89.8 | 119.3 | 126.7 | 129.9 | 134.1 |
| 3 | -1 | +1 | 2 | 45 | 21.1 | 36.2 | 53.2 | 66.4 | 77.7 | 82.7 | 84.8 | 88.2 |
| 4 | -1 | -1 | 2 | 5 | 19.0 | 32.1 | 50.4 | 72.1 | 91.1 | 96.8 | 99.3 | 102.9 |
| 5 | +1 | 0 | 3 | 25 | 25.5 | 40.9 | 64.4 | 86.3 | 108.1 | 114.9 | 117.8 | 121.7 |
| 6 | -1 | 0 | 2 | 25 | 20.1 | 32.0 | 51.9 | 69.2 | 84.5 | 89.8 | 92.1 | 95.7 |
| 7 | 0 | +1 | 2.5 | 45 | 28.0 | 45.4 | 69.2 | 88.9 | 111.9 | 118.9 | 121.9 | 125.8 |
| 8 | 0 | -1 | 2.5 | 5 | 25.6 | 40.7 | 65.9 | 95.3 | 129.8 | 138.0 | 141.5 | 144.6 |
| 9 | 0 | 0 | 2.5 | 25 | 26.8 | 40.8 | 67.6 | 92.1 | 121.0 | 128.6 | 131.8 | 136.1 |

As a result of processing the data in Table 4, regression equations were obtained for all hardening times, which adequately describe the results of the experiment.

$$R_1 = 40.899 + 4.383 \cdot X_1 + 1.657 \cdot X_2 - 9.483 \cdot X_1^2 + 2.117 \cdot X_2^2 + 0.4 \cdot X_1 \cdot X_2 \ (R^2 = 0.99) \quad (1)$$

$$R_{28} = 120.989 + 11.783 \cdot X_1 - 9 \cdot X_2 - 24.683 \cdot X_1^2 - 0.133 \cdot X_2^2 - 2.325 \cdot X_1 \cdot X_2 \ (R^2 = 0.99) \quad (2)$$

$$R_{360} = 132.633 + 13.083 \cdot X_1 - 9.167 \cdot X_2 - 24.35 \cdot X_1^2 - 0.6 \cdot X_2^2 - 2.475 \cdot X_1 \cdot X_2 \ (R^2 = 0.99) \quad (3)$$

Based on the regression analysis of the equations, it was concluded that in the early stages of hardening (up to 3 days inclusive), both factors have a positive effect on strength – equation (1). Moreover, the influence of factor X1 (Ms) is slightly stronger than that of X2 (OPC content).

Subsequently, the picture changes somewhat. Starting from 7 days onwards, the influence of factor X1 (Ms) remains positive, while the influence of factor X2 (ORP) changes to the opposite, i.e., it no longer contributes to an increase in strength—equations (2) and (3).

As a result, it was shown that the use of soluble sodium silicates with $M_s$ = 2...3 ensured the production of ultra-fast-setting high-strength reaction-powder concretes with compressive strength after 3 hours of 19.0...28.0 MPa, 1 day – 32.1…45.7 MPa, after 7 days – 66.4…95.3 MPa, after 28 days – 77.7…129.8 MPa, after 90 days – 82.7… 138 MPa, after 180 days – 84.8…141.5 MPa, 360 days – 88.2…144.6 MPa (Table 3). The optimal solution is to use soluble sodium glass with Ms = 2.6…2.7 (Fig. 7).

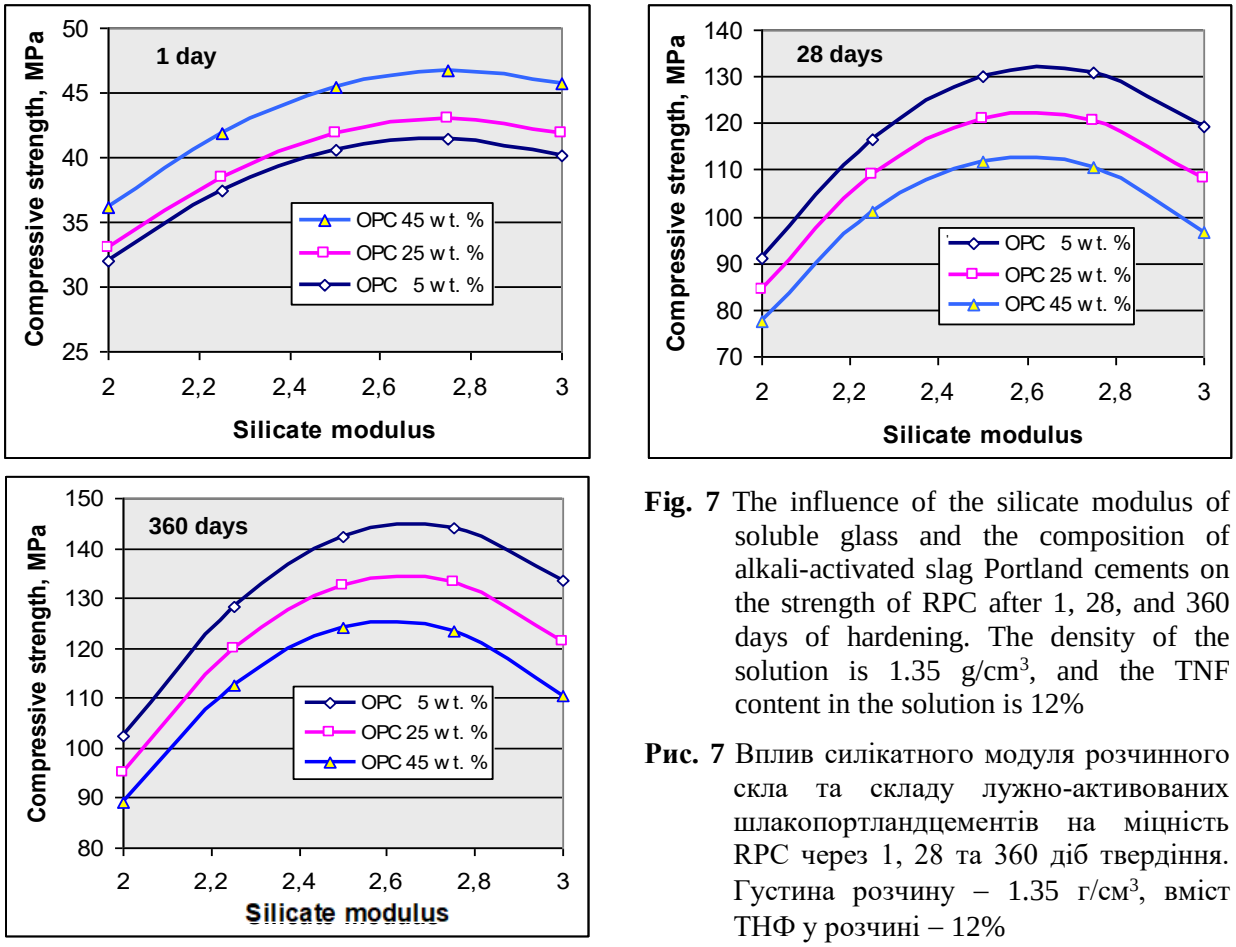


**Fig. 7** The influence of the silicate modulus of soluble glass and the composition of alkali-activated slag Portland cements on the strength of RPC after 1, 28, and 360 days of hardening. The density of the solution is 1.35 g/cm$^3$, and the TNF content in the solution is 12%

**Рис. 7** Вплив силікатного модуля розчинного скла та складу лужно-активованих шлакопортландцементів на міцність RPC через 1, 28 та 360 діб твердіння. Густина розчину – 1.35 г/см$^3$, вміст ТНФ у розчині – 12%

At the same time, the strength ratio "compression : bending" was 5.8 on day 28 and 6.2 after 90 days for the optimal composition with the content of OPC in the mixture "GBFS + OPC" – 5% and $M_s$ = 2.5 (Table 3, item 8), which indicates a sufficiently high impact strength and crack resistance of concrete.

The setting times were 34…46 minutes, but they can be increased to 60…90 minutes by using the complex additive "TNF + glycerin".

Based on the method of absolute volumes of raw components of the concrete mixture, the composition of the RPB per 1 $m^3$ was calculated with a ratio of "binder : sand" of 1:1 using a powdered alkali component and mixing the concrete with water:

- binding agent (slag + Portland cement + alkali component) – 1034 kg/$m^3$;
- fine river sand ($M_{ss}$ = 1.16) – 1034 kg/$m^3$;
- water – 220…230 l/$m^3$ (W/C = 0.213…0.222).

Despite the low W/C ratio, the mixture was fairly easy to lay – the spread on the vibrating table after 30 strokes was 210…220 mm.

The composition was designed taking into account that it would be subjected to vibration during laying and that the air content would not exceed 4…8% by volume.

The option of using RPC for forming products by extrusion or using them in 3D-printers with the determination of the main technological parameters of the process was also considered.

The concrete mixture *extrusion method* is used to manufacture formwork-free products (pipes, panels, floor slabs, blocks, etc.) when the mixture is extruded through a forming head. For this process, concrete must have *special rheological properties* – sufficient plasticity for forming, but at the same time high rigidity so that the product retains its shape after leaving the mold. It has been established that when using RPC based on alkali-activated slag Portland cements, the cone slump should be 1…4 cm (stiffness 7…12 sec.) depending on the volume and configuration of the product, the type of extruder (screw, screw-auger), the pressure and speed of extrusion of the mixture. More specific pressure and speed values vary with the type of extruder. Therefore, follow the equipment instructions and perform a series of routine test mouldings. Fast-setting mixtures with a setting time of 25…40 minutes are recommended.

RPC mixtures for 3D-printing must have the following key characteristics: Suttard spread 12…15 cm, water retention ≥ 97%, setting time ≤ 20 min.

## CONCLUSIONS

1. Stable long-term properties of rapid-hardening, high-strength "GBFS+OPC"-based alkali-activated RPC were achieved by regulating the aggregate state and silicate modulus of soluble sodium silicates, which represent the key technological factors.
2. The use of sodium metasilicate in the form of a solution instead of dry powder ensured the maximum reduction in the soluble-binding ratio, which led to a further intensification of concrete strength development by 30.5%, 23.5%, 18.4%, 6.1%, and 3.9%, ensuring a strength of 52.3, 85.0, 108.7, 136.1, and 141.4 MPa at ages 1, 3, 28, 180, and 360 days, respectively. The ratio of compressive strength to flexural strength in the range of 5.3...5.9 confirmed the high viscosity and crack resistance of concrete..
3. Adding calcite ($CaCO_3$) to RPC in optimal amounts reduced shrinkage during drying at the moment of its stabilization by 1.2...1.6 times, which is explained by a denser microstructure and more intense crystallization processes of hydration products.
4. It has been shown that RPC based on alkali-activated slag Portland cements demonstrate higher ballistic characteristics compared to RPC based on traditional Portland cement.
5. A specific feature of the influence of the age factor on the obtained RPC is stable long-term strengthening. Thus, RPC based on AAC with sodium metasilicate and soluble glass demonstrates increased values of key properties compared to 28-day age: compressive strength after 360 days – up to 141.4 MPa (by 30.1%) and 144.6 MPa (by 9.1%); impact strength after 180 days – up to

4413 kJ/m³ (by 31.6%) and 4805 kJ/m³ (by 11.3%).

6. The approximate parameters of RPC concrete mixtures based on alkali-activated slag Portland cements for the manufacture of products using extrusion and 3D printing technologies have been established.

## ACKNOWLEDGMENTS

The author express their gratitude to the Ministry of Education and Science of Ukraine for financial support of this research that is carried out within the budgetary financing of the topics with registration No 0123U101832 with the implementation period between 2023 and 2025.

## REFERENCES

1. **Dvorkin L.** (2020). Reactive Powder Concretes and Materials Based on Them: A Monograph *Rivne: NUVHP,. 305 s.* [in Ukrainian].
2. **Du J, Meng W, & Khayat KH**. (2021) New development of ultra-high-performance concrete (UHPC). *Composites Part B Engineering*, 224(9): 109220.[in English] https://doi.org/10.1016/j.compositesb.2021.109220
3. **Kryvenko PV, Valerga-Puerta AP, Rivera-Armenta JL, Vinci A.** Ballistic Protection. In: editors. *Aggregated book; 2025; Baech, Switzerland: Trans Tech Publication LTD. 460 p.* [in English] https://doi.org/10.4028/b-6G91y5.
4. **Khan MI, Abbas YM, Fares G.** Review of high and ultrahigh performance cementitious composites incorporating various combinations of fibers and ultrafines. *Journal of King Saud University - Engineering Sciences.* 2017; 29(4): 339–347. [in English] https://doi.org/10.1016/j.jksues.2017.03.006.
5. **Mayhoub OA, Nasr EAR, Ali YA, Kohail M**, The influence of ingredients on the properties of reactive powder concrete: A review. *Ain Shams Engineering Journal*. 2021; 12(1): 145–158. [in English] https://doi.org/10.1016/j.asej.2020.07.016.
6. **Richard P, Cheyrezy M**. Composition of reactive powder concretes. *Cement and Concrete Research*. 1995; 25 (7): 1501–1511. [in English] https://doi.org/10.1016/0008-8846(95)00144-2
7. **Song J, Liu S.** Properties of reactive powder concrete and its application in highway bridge. *Advanced Materials Science*. 2016; 2016: 5460241. [in English] https://doi.org/10.1155/2016/5460241.
8. **Zhang Q, Huang L**. Review of research on durability of reactive powder concrete. *Journal of Physics: Conference Series.* 2020; 1549: 032073. [in English] https://doi.org/10.1088/1742-6596/1549/3/032073.
9. **Sanytsky M, Kropyvnytska T, Vakhula O, Bobetsky Y**. Nanomodified ultra high-performance fiber reinforced cementitious composites with enhanced operational characteristics. *Lecture Notes in Civil Engineering*. 2024; 438: 362–371. [in English] https://doi.org/10.1007/978-3-031-44955-0_36.
10. **Li J, Wu Z, Shi C, Yuan Q, Zhang Z.** Durability of ultra-high performance concrete – A review. *Construction and Building Materials*. 2020; 255: 119296. [in English] https://doi.org/10.1016/j.conbuildmat.2020.119296
11. **Aydın S, Baradan B.** High temperature resistance of alkali-activated slag- and portland cement-based reactive powder concrete. *Materials Journal*. 2012; 109(4): 463–470. [in English] https://doi.org/10.14359/51683921.
12. **Marvila MT, de Azevedo ARG, de Matos PR, Monteiro SN, Vieira CMF**. Materials for production of high and ultra-high performance concrete: review and perspective of possible novel materials. Materials. 2021; 14(15): 4304. [in English] https://doi.org/10.3390/ma14154304.
13. **Aydın S, Baradan B**. Engineering properties of reactive powder concrete without portland cement. *ACI Materials Journal*. 2013; 110(6): 619–627. [in English]
14. **Ahmed S, Al-Dawood Z, Abed F, Mannan MA, Al-Samarai M**. Impact of using different materials, curing regimes, and mixing procedures on compressive strength of reactive powder concrete: a review. *Journal of Building Engineering*. 2021; 44: 103238. [in English] https://doi.org/10.1016/j.jobe.2021.103238.
15. **DSTU B V.2.7-181:2009.** Alkaline cements. Technical specifications *[Chynnyi vid 2009-08-01]. Vyd. ofits. Kyiv: Minrehionbud Ukrainy, 2009. 17 s.* [in Ukrainian].
16. **Naqi A, Jang JG**. Recent progress in green cement technology utilizing low-carbon

17. emission fuels and raw materials: a review. *Sustainability*. 2019; 11: 537. [in English] https://doi.org/10.3390/su11020537.
18. **Sanytsky M, Kropyvnytska T, Ivashchyshyn H**. Sustainable modified pozzolanic supplementary cementitious materials based on natural zeolite, fly ash and silica fume. *IOP Conference Series: Earth and Environmental Science*. 2023; 1254: 012004 [in English] https://doi.org/10.1088/1755-1315/1254/1/012004
19. **Kryvenko P, Rudenko I, Sikora P, Sanytsky M, Konstantynovskyi O, Kropyvnytska** T. Alkali-activated cements as sustainable materials for repairing building construction: a review. *Journal of Building Engineering*. 2024; 90: 109399. [in English] https://doi.org/10.1016/j.jobe.2024.109399.
20. **Aydın S, Baradan B.** Sulfate resistance of alkali-activated slag and Portland cement based reactive powder concrete. *Journal of Building Engineering*. 2021; 43: 103205. [in English] https://doi.org/10.1016/j.jobe.2021.103205.
21. **Krivenko P, Rudenko I, Konstantynovskyi O**. Effect of technological factors on freeze-thaw resistance of alkali-activated slag cement concrete in NaCl solution. *AIP Conference Proceedings*. 2023; 2684: 040011. [in English] https://doi.org/10.1063/5.0120034.
22. **Krivenko P, Rudenko I, Konstantynovskyi O, Razsamakin A.** Sustainable performance of alkali-activated blast furnace cement concrete with high freeze-thaw resistance. *IOP Conference Series: Earth and Environmental Science. IOP Publishing*. 2023; 1254: 012003. [in English] https://doi.org/10.1088/1755-1315/1254/1/012003.
23. **Krivenko P, Rudenko I, Konstantynovskyi O, Boiko O, Vaičiukynienė D**. Effect of sodium phosphate and sodium nitrate on microstructure of alkali-activated slag cement pastes and properties of reinforced concrete under cyclic drying-wetting in sea water. *AIP Conference Proceedings*. 2023; 2840: 020006-1–020006-11. [in English] https://doi.org/10.1063/5.0168007
24. **Yao W, Shi Y, Xia K, Peterson K**. Dynamic fracture behavior of alkali-activated mortars: Effects of composition, curing time and loading rate. *Engineering Fracture Mechanic*s. 2019; 208: 119–130. [in English] https://doi.org/10.1016/j.engfracmech.2019.01.017.
25. **Zhang B, Zhu H, Cheng Y, Huseien GF, Shah KW**. Shrinkage mechanisms and shrinkage-mitigating strategies of alkali-activated slag composites: a critical review. *Construction and Building Materials*. 2022; 318: 125993. [in English] https://doi.org/10.1016/j.conbuildmat.2021.125993.
26. **Wei Y, Dou H, He T, Song K, Zhang Q**. Investigation of shrinkage mechanism of alkali-activated slag. *Case Studies in Construction Materials*. 2024; 21: e03493. [in English] https://doi.org/10.1016/j.cscm.2024.e03493.
27. **Kryvenko PV, Gots VI, Petropavlovskyi OP, Rudenko II, Konstantynovskyi OP**. Complex shrinkage-reducing additives for alkali activated slag cement fine concrete. *Solid State Phenomena*. 2021; 321: 165–170. [in English] https://doi.org/10.4028/www.scientific.net/SSP.321.165.
28. **Lacante M, Delsaute B, Staquet S**. Mitigation of volume changes of alkali-activated materials by using limestone filler. *Materials*. 2025; 18(13): 2963. [in English] https://doi.org/10.3390/ma18132963.
29. **Krivenko P, Rudenko I, Konstantynovskyi O.** Comparison of influence of surfactants on thermokinetic characteristics of alkali-activated slag cement. *Eastern-European Journal of Enterprise Technologies.* 2021; 6(6 (114): 39–48. [in English] https://doi.org/10.15587/1729-4061.2021.245916.
30. **Rudenko, I., Hots, V., Helevera, O., & Razsamakin, A.** (2023). Control of Setting Times of Slag-Containing Cements Activated with Sodium Metasilicate *Building Constructions. Theory and Practice, (13), 110–123.* [in Ukrainian] https://doi.org/10.32347/2522-4182.13.2023.110-123
31. **Rudenko, I., Helevera, O., Konstantynovskyi, O., & Razsamakin, A**. (2024). Reactionary powder concrete based on alkali-activated cement. *Building Constructions. Theory and Practice, (15), 135–145.* [in Ukrainian] https://doi.org/10.32347/2522-4182.15.2024.135-145
32. **Kryvenko, P., Hots, V., Helevera, O., Rohozina, N. (**2022). Performance Characteristics of Slag-Alkali Decorative Cements and Mortars. *Building Constructions. Theory and Practice, (10), 124–135*. [in Ukrainian]

https://doi.org/10.32347/2522-4182.10.2022.124-135

33. **Kryvenko P.V., Pushkarova K.K., Baranovskyi V.B. ta in.** *Building materials science: Textbook*. Kyiv: Vydavnytstvo "Lira-K", 2012. 624 s. [in Ukrainian]
34. **Kryvenko P, Rudenko I, Gelevera O, Konstantynovskyi O**. Effect of sodium metasilicate on the early-age hydration and setting behavior of alkali-activated common cements containing slag. *IOP Conference Series: Earth and Environmental Science*. 2024; 1415: 012070. [in English] https://doi.org/10.1088/1755-1315/1415/1/012070.
35. **Kryvenko P, Rudenko I, Gelevera O, Konstantynovskyi O., Kovalchuk A**. Improvement of early strength of slag containing portland cements. *Advances in Transdisciplinary Engineering*. 2024; 62: 515–521. [in English] https://doi.org/10.3233/ATDE241029.
36. **Helevera O, Razsamakin A, Rudenko I, Konstantynovskyi O., Smeshko V**. Development mix design alkali-activated cement powder concrete. *Advances in Transdisciplinary Engineering*. 2024; 62: 644–650. [in English] https://doi.org/10.3233/ATDE241044.
37. **Kryvenko P, Rudenko I, Kovalchuk O, Gelevera O, Konstantynovskyi O**. Influence of dosage and modulus on soluble sodium silicate for early strength development of alkali-activated slag cements. *Minerals.* 2023; 13(9): 1164. https://doi.org/10.3390/min13091164.
38. **Zhang M, Zunino F, Yang L, Wang F, Scrivener K**. Understanding the negative effects of alkalis on long-term strength of Portland cement. *Cement and Concrete Research*. 2023; 174: 107348. [in English] https://doi.org/10.1016/j.cemconres.2023.107348.
39. **Jamrozy J.** Beton i jego technologie. *Wydawnictwo Naukowe PWN, Warszawa-Krakow, 2000. 485 p*. [in Polska]
40. **Montgomery DC**. Design and analysis of experiments. *2019; EMEA Edition, 10th Edition, Wiley, Hoboken. 688 p*. [in English]
41. **Murali G**. Recent research in mechanical properties of geopolymer-based ultra-high-performance concrete: *A review. Defence Technology. 2023; 32: 2024. 67–88. [in English]* https://doi.org/10.1016/j.dt.2023.07.003.
42. **Yoo DY, Min KH, Lee JH, Yoon YS**. Shrinkage and cracking of restrained ultra-high-performance fiber-reinforced concrete slabs at early age. *Construction and Building Materials*. 2014; 73: 357–365. [in English] https://doi.org/10.1016/j.conbuildmat.2014.09.097.
43. **Yalçınkaya Ç, Yazıcı H**. Early-age shrinkage properties of eco-friendly reactive powder concrete with reduced cement content. *European Journal of Environmental and Civil Engineering*. 2019; 26(19): 456–472. [in English] https://doi.org/10.1080/19648189.2019.1665105.
44. **Ponomar V, Luukkonen T, Yliniemi J**. Revisiting alkali-activated and sodium silicate-based materials in the early works of Glukhovsky. *Construction and Building Materials*. 2023; 398: 132474. [in English] https://doi.org/10.1016/j.conbuildmat.2023.132474.

## LITERATURE

1. **Dvorkin L**. Reaktsiino-poroshkovi betony i materialy na yikh osnovi. *Monohrafiia. Rivne : NUVHP, 2020. 305 s.*.
2. **Du J, Meng W, Khayat KH.** New development of ultra-high-performance concrete (UHPC). *Composites Part B Engineering. 2021; 224(9): 109220.* https://doi.org/10.1016/j.compositesb.2021.109220
3. **Kryvenko PV, Valerga-Puerta AP, Rivera-Armenta JL, Vinci A**. Ballistic Protection. In: editors. *Aggregated book; 2025; Baech, Switzerland: Trans Tech Publication LTD. 460 p.* https://doi.org/10.4028/b-6G91y5.
4. **Khan MI, Abbas YM, Fares G.** Review of high and ultrahigh performance cementitious composites incorporating various combinations of fibers and ultrafines. *Journal of King Saud University - Engineering Sciences. 2017; 29(4): 339–347.* https://doi.org/10.1016/j.jksues.2017.03.006.
5. **Mayhoub OA, Nasr EAR, Ali YA, Kohail M.** The influence of ingredients on the properties of reactive powder concrete: *A review. Ain Shams Engineering Journal. 2021; 12(1): 145–158.* https://doi.org/10.1016/j.asej.2020.07.016.
6. **Richard P, Cheyrezy M.** Composition of reactive powder concretes. *Cement and Concrete Research. 1995; 25 (7): 1501–1511.* https://doi.org/10.1016/0008-8846(95)00144-2

7. **Song J, Liu S.** Properties of reactive powder concrete and its application in highway bridge. *Advanced Materials Science. 2016; 2016: 5460241.* https://doi.org/10.1155/2016/5460241.
8. **Zhang Q, Huang L.** Review of research on durability of reactive powder concrete. *Journal of Physics: Conference Series. 2020; 1549: 032073.* https://doi.org/10.1088/1742-6596/1549/3/032073.
9. **Sanytsky M, Kropyvnytska T, Vakhula O, Bobetsky Y.** Nanomodified ultra high-performance fiber reinforced cementitious composites with enhanced operational characteristics. *Lecture Notes in Civil Engineering. 2024; 438: 362–371* https://doi.org/10.1007/978-3-031-44955-0_36.
10. **Li J, Wu Z, Shi C, Yuan Q, Zhang Z.** Durability of ultra-high performance concrete – *A review. Construction and Building Materials. 2020; 255: 119296.* https://doi.org/10.1016/j.conbuildmat.2020.119296
11. **Aydın S, Baradan B.** High temperature resistance of alkali-activated slag- and portland cement-based reactive powder concrete. *Materials Journal. 2012; 109(4): 463–470.* https://doi.org/10.14359/51683921.
12. **Marvila MT, de Azevedo ARG, de Matos PR, Monteiro SN, Vieira CMF**. Materials for production of high and ultra-high performance concrete: *review and perspective of possible novel materials. Materials. 2021; 14(15): 4304.* https://doi.org/10.3390/ma14154304.
13. **Aydın S, Baradan B.** Engineering properties of reactive powder concrete without portland cement. *ACI Materials Journal. 2013; 110(6): 619–627.*
14. **Ahmed S, Al-Dawood Z, Abed F, Mannan MA, Al-Samarai M.** Impact of using different materials, curing regimes, and mixing procedures on compressive strength of reactive powder concrete: a review. *Journal of Building Engineering. 2021; 44: 103238.* https://doi.org/10.1016/j.jobe.2021.103238.
15. **DSTU B V.2.7-181:2009**. Tsementy luzhni. Tekhnichni umovy. *[Chynnyi vid 2009-08-01]. Vyd. ofits. Kyiv: Minrehionbud Ukrainy, 2009. 17 s.*
16. **Naqi A, Jang JG.** Recent progress in green cement technology utilizing low-carbon emission fuels and raw materials: a review. *Sustainability. 2019; 11: 537.* https://doi.org/10.3390/su11020537.
17. **Sanytsky M, Kropyvnytska T, Ivashchyshyn H.** Sustainable modified pozzolanic supplementary cementitious materials based on natural zeolite, fly ash and silica fume. *IOP Conference Series: Earth and Environmental Science. 2023; 1254: 012004* https://doi.org/10.1088/1755-1315/1254/1/012004
18. **Kryvenko P, Rudenko I, Sikora P, Sanytsky M, Konstantynovskyi O, Kropyvnytska T**. Alkali-activated cements as sustainable materials for repairing building construction: a review. *Journal of Building Engineering. 2024; 90: 109399.* https://doi.org/10.1016/j.jobe.2024.109399.
19. **Aydın S, Baradan B.** Sulfate resistance of alkali-activated slag and Portland cement based reactive powder concrete. *Journal of Building Engineering. 2021; 43: 103205.* https://doi.org/10.1016/j.jobe.2021.103205.
20. **Krivenko P, Rudenko I, Konstantynovskyi O.** Effect of technological factors on freeze-thaw resistance of alkali-activated slag cement concrete in NaCl solution. *AIP Conference Proceedings. 2023; 2684: 040011.* https://doi.org/10.1063/5.0120034.
21. **Krivenko P, Rudenko I, Konstantynovskyi O, Razsamakin A.** Sustainable performance of alkali-activated blast furnace cement concrete with high freeze-thaw resistance. I*OP Conference Series: Earth and Environmental Science. IOP Publishing. 2023; 1254: 012003.* https://doi.org/10.1088/1755-1315/1254/1/012003.
22. **Krivenko P, Rudenko I, Konstantynovskyi O, Boiko O, Vaičiukynienė D**. Effect of sodium phosphate and sodium nitrate on microstructure of alkali-activated slag cement pastes and properties of reinforced concrete under cyclic drying-wetting in sea water. *AIP Conference Proceedings. 2023; 2840: 020006-1–020006-11.* https://doi.org/10.1063/5.0168007
23. **Yao W, Shi Y, Xia K, Peterson K**. Dynamic fracture behavior of alkali-activated mortars: Effects of composition, curing time and loading rate. *Engineering Fracture Mechanics. 2019; 208: 119–130.* https://doi.org/10.1016/j.engfracmech.2019.01.01.
24. **Zhang B, Zhu H, Cheng Y, Huseien GF, Shah KW.** Shrinkage mechanisms and shrinkage-mitigating strategies of alkali-activated slag

composites: a critical review. *Construction and Building Materials. 2022; 318: 125993.* https://doi.org/10.1016/j.conbuildmat.2021.125993.

25. **Wei Y, Dou H, He T, Song K, Zhang Q.** Investigation of shrinkage mechanism of alkali-activated slag. Case Studies in Construction *Materials. 2024; 21: e03493*. https://doi.org/10.1016/j.cscm.2024.e03493.

26. **Kryvenko PV, Gots VI, Petropavlovskyi OP, Rudenko II, Konstantynovskyi OP**. Complex shrinkage-reducing additives for alkali activated slag cement fine concrete. *Solid State Phenomena. 2021; 321: 165–170*. https://doi.org/10.4028/www.scientific.net/SSP.321.165.

27. **Lacante M, Delsaute B, Staquet S.** Mitigation of volume changes of alkali-activated materials by using limestone filler. *Materials. 2025; 18(13): 2963*. https://doi.org/10.3390/ma18132963.

28. **Krivenko P, Rudenko I, Konstantynovskyi O.** Comparison of influence of surfactants on thermokinetic characteristics of alkali-activated slag cement. *Eastern-European Journal of Enterprise Technologies. 2021; 6(6 (114): 39–48*. https://doi.org/10.15587/1729-4061.2021.245916.

29. **Rudenko, I., Hots, V., Helevera, O., & Razsamakin, A.** (2023). Upravlinnia Terminamy tuzhavlennia shlakovmishchuiuchykh tsementiv, aktyvovanykh metasylikatom natriiu. *Budivelni konstruktsii. Teoriia i praktyka, (13), 110–123.* https://doi.org/10.32347/2522-4182.13.2023.110-123

30. **Rudenko, I., Helevera, O., Konstantynovskyi, O., & Razsamakin, A.** (2024). Reaktsiinoporoshkovi betony na osnovi luzhnoaktyvovanoho tsementu. *Budivelni konstruktsii. Teoriia i praktyka, (15), 135–145.* https://doi.org/10.32347/2522-4182.15.2024.135-145

31. **Kryvenko, P., Hots, V., Helevera, O., Rohozina, N.** (2022). Ekspluatatsiini kharakterystyky shlakoluzhnykh dekoratyvnykh tsementiv i rozchyniv. *Budivelni konstruktsii. Teoriia i praktyka, (10), 124–135.* https://doi.org/10.32347/2522-4182.10.2022.124-135

32. **Kryvenko P.V., Pushkarova K.K., Baranovskyi V.B**. ta in. Budivelne materialoznavstvo : pidruchnyk *Kyiv: Vydavnytstvo "Lira-K", 2012. 624 s.*

33. **Kryvenko P, Rudenko I, Gelevera O, Konstantynovskyi O.** Effect of sodium metasilicate on the early-age hydration and setting behavior of alkali-activated common cements containing slag. *IOP Conference Series: Earth and Environmental Science. 2024; 1415: 012070.* https://doi.org/10.1088/1755-1315/1415/1/012070.

34. **Kryvenko P, Rudenko I, Gelevera O, Konstantynovskyi O., Kovalchuk A.** Improvement of early strength of slag containing portland cements. Advances in Transdisciplinary Engineering. 2024; 62: 515–521. https://doi.org/10.3233/ATDE241029.

35. **Helevera O, Razsamakin A, Rudenko I, Konstantynovskyi O., Smeshko V.** Development mix design alkali-activated cement powder concrete. *Advances in Transdisciplinary Engineering. 2024; 62: 644–650.* https://doi.org/10.3233/ATDE241044.

36. **Kryvenko P, Rudenko I, Kovalchuk O, Gelevera O, Konstantynovskyi O.** Influence of dosage and modulus on soluble sodium silicate for early strength development of alkali-activated slag cements. *Minerals. 2023; 13(9): 1164.* https://doi.org/10.3390/min13091164.

37. **Zhang M, Zunino F, Yang L, Wang F, Scrivener K.** Understanding the negative effects of alkalis on long-term strength of Portland cement. *Cement and Concrete Research. 2023; 174: 107348.* https://doi.org/10.1016/j.cemconres.2023.107348

38. **Jamrozy J.** Beton i jego technologie. *Wydawnictwo Naukowe PWN, Warszawa-Krakow, 2000. 485 p.*

39. **Montgomery DC.** Design and analysis of experiments. *2019; EMEA Edition, 10th Edition, Wiley, Hoboken. 688 p*.

40. **Murali G.** Recent research in mechanical properties of geopolymer-based ultra-high-performance concrete: *A review. Defence Technology. 2023; 32: 2024. 67–88.* https://doi.org/10.1016/j.dt.2023.07.003.

41. **Yoo DY, Min KH, Lee JH, Yoon YS.** Shrinkage and cracking of restrained ultra-high-performance fiber-reinforced concrete slabs at early age. *Construction and Building Materials. 2014; 73: 357–365.* https://doi.org/10.1016/j.conbuildmat.2014.09.097.

42. **Yalçınkaya Ç, Yazıcı H.** Early-age shrinkage properties of eco-friendly reactive powder concrete with reduced cement content. *European Journal of Environmental and Civil Engineering. 2019; 26(19): 456–472.* https://doi.org/10.1080/19648189.2019.1665105.
43. **Ponomar V, Luukkonen T, Yliniemi J.** Revisiting alkali-activated and sodium silicate-based materials in the early works of Glukhovsky. *Construction and Building Materials. 2023; 398: 132474.* https://doi.org/10.1016/j.conbuildmat.2023.132474.

## ВПЛИВ ТЕХНОЛОГІЧНИХ ФАКТОРІВ НА ВЛАСТИВОСТІ РЕАКЦІЙНИХ ПОРОШКОВИХ БЕТОНІВ НА ОСНОВІ ШЛАКОПОРТЛАНДЦЕМЕНТУ, АКТИВОВАНОГО ЛУГАМИ

*Андрій РАЗСАМАКІН*

**Анотація.** Розробка реактивного порошкового бетону (РПБ) на основі портландцементів, що містять різну кількість гранульованого доменного шлаку та активовані розчинними силікатами натрію, має глобальне значення з точки зору захисту об'єктів критичної інфраструктури.

У статті встановлено фактори впливу на кінетику набору міцності, власні деформації усадки та на ударну міцність реакційно-порошкових бетонів при використанні метасилікату натрію пентагідрату як лужного активатора у різному агрегатному стані (порошок, розчин), а також розчинних силікатів натрію з силікатним модулем Мс = 2…3. Показано, що зміна співвідношення між шлакопортландцементом і піском від 1:3 до 1:1 та використання метасилікату натрію у вигляді порошку забезпечує отримання піщаного бетону з міцністю на стиск 35.7, 63.8, 87.5, 118.1 та 123.9 МПа через 1, 3, 28, 180 та 360 діб відповідно.

Використання метасилікату натрію у вигляді водного розчину значно прискорює кінетику набору міцності і забезпечує міцність 52.3, 85.0, 108.7, 126.1 та 141.1 МПа через 1, 3, 28, 180 та 360 діб відповідно. Використання розчинного скла з Мс = 2.6 дозволило отримати надшвидкотверднучі високоміцні реакційно-порошкові бетони з міцністю на стиск 19…28, 32.1…45.7, 91.1…129.8 та 102.9…144.6 МПа через 3 години, через 1, 28 і 360 діб відповідно. Введення дрібнодисперсного кальциту зменшило усадку при висиханні РПБ, в 1.2...1.6 рази. Зменшення вмісту портландцементу у шлако-цементній суміші з 45 до 5% мас. при силікатному розчинного скла 2.6...2.7 зумовило незначне зниження ранньої межі міцності на стиск надшвидкотверднучого РПБ, проте забезпечило суттєве підвищення межі міцності на стиск з 112.5 МПа до 132.4 МПа через 28 діб. В'язке руйнування через 28 діб підтверджується кращим коефіцієнтом крихкості 5.3...5.9 та на 10.5…28.7% вищою ударною міцністю зразків на метасилікаті натрію та дисилікаті натрію порівняно з аналогом на основі традиційного цементу. Одержано РПБ зі стабільною довготривалою міцністю, високою ударною в'язкістю та зменшеною усадкою при висиханні. Введення відбілювачів у вигляді $CaCO_3$ та мінеральних пігментів дозволяє отримувати декоративні РПБ. Вказано на можливість отримання виробів екструзією та 3D-друком на основі лужно-активованих РПБ з визначенням основних технологічних параметрів процесу.

**Ключові слова:** реакційно-порошкові бетони; лужно-активований цемент; міцність; усадка; технологічні фактори.

***Received:*** *November 05, 2025.*
***Accepted:*** *November 30, 2025.*

ISSN 2522-4182

DOI: 10.32347/2522-4182.17.2025.168-178
УДК 624.011

# ANALYSIS OF METHODS FOR CALCULATING THE PENETRATING EFFECT OF THE MAIN TYPES OF AMMUNITION AND FRAGMENTATION DAMAGE TO DEFENSIVE STRUCTURES

*Denys MYKHAILOVSKYI[1], Oleg KOMAR[2]*

[1,2]Kyiv National University of Construction and Architecture
31, Povitryanykh Syl Ave., Kyiv, Ukraine, 03037
[1] mykhailovskyi.dv@knuba.edu.ua, https://orcid.org/0000-0003-3151-8630
[2] komar_oa-2023@knuba.edu.ua, http://orcid.org/0009-0004-4507-9178

**Abstract** In the current realities arising from the full-scale armed aggression of the Russian Federation against Ukraine, and in light of the rapid technological development of highly effective weapons, the issue of ensuring the reliability and stability of fortifications and defensive structures has acquired unpreceden-ted relevance. The critical task of engineering defence is to counter a wide range of threats, including the penetrating action of small-arms bullets, cumulative jets, armour-piercing shells, and the destructive impact of high-explosive fragmentation ammunition.

The impact of these factors is not limited to local damages, such as perforation or chipping of structural elements. It determines the overall survivability of the object - its ability to maintain integrity, load-bearing capacity, and essential functional characteristics directly during intense fire exposure. A wide range of methods is used to predict the behaviour of structures: from analytical and empirical approaches to complex numerical modelling.

The reliability and accuracy of such predictions directly depend on the comprehensive consideration of input parameters. Firstly, these are the kinematic characteristics of the striking elements: their mass, velocity vector, angle of encounter with the obstacle, and shape. Secondly, the physico-mechanical properties of the materials of the obstacle itself play a decisive role, in particular dynamic strength, ultimate plasticity, impact strength, and the degree of structural heterogeneity (for example, in reinforced concrete). Thirdly, the geometry and design of protective elements are essential, such as multilayered structures or spaced armor.



**Denys MYKHAILOVSKYI**
Professor of the Department of Metal and Timber Structures, D.Sc. (Eng.)

**Oleg KOMAR**
Postgraduate student of the Department of Metal and Timber Structures

In practical terms, there is a clear division of calculation methods. Empirical formulas, due to their simplicity, are indispensable at the stages of preliminary design for obtaining quick, albeit approximate, estimates. Instead, modern numerical methods, implemented using the finite element method (FEM), allow us to reproduce with high accuracy the mechanisms of interaction between the projectile and the structure in time and space.

**Keywords:** engineering methodology; debris; ammunition; UAV; missile.

## FORMULATION OF THE PROBLEM

The military actions in Ukraine have led to an urgent need to construct a large number of fortifications and protective structures of various purposes and designs, which must

account not only for normal loads and influences but also for special effects related to threats of enemy attack. Such effects include blast wave action, shrapnel damage, partial or complete penetration of ammunition into the body of the protective structure, which may be accompanied by subsequent explosions, temperature changes, and so on.

To our great regret, the enemy is improving and increasing their means to inflict maximum damage on targets. Yes, there have been more frequent cases of using metal shrapnel in the bodies of unmanned aerial vehicles or in missiles (Fig.1).

**Fig. 1** The body of the undetonated missile filled with shrapnel (photo by the Denys Mykhailovskyi)
**Рис. 1** Корпус нездетонованої ракети заповнений шрапнеллю (фото зроблено Денисом Михайловським)

However, despite these threats, Ukraine still lacks regulatory documents that specify the methodology or procedures for calculating the elements of protective structures against the penetrating effects of the main types of ammunition and fragmentation damage. Recommendations for ensuring the thickness of elements to prevent penetration are provided in DBN V.2.2-5:2023 "Civil Defence Protective Structures" [2] in section 14.2.3; however, it does not specify which threats these values are intended to address, and it is not clear how to apply them to current realities.

As part of this work, a comparison was made of the calculation of the penetrating action of the main types of ammunition and fragmentation damage using the following methods:

1. Engineering method of Berezan V.I.;
2. Energy method (or energy balance method);
3. Engineering method of NDRC (National Defence Research Committee).

| № | Material | Reduced coefficient | Min. Thickness, mm |
|---|---|---|---|
| 1 | Concrete heavy C16/20 | 0,917 | 360 |
| 2 | Concrete heavy C20/25 | 0,943 | 350 |
| 3 | Concrete heavy C25/30 | 1,0 | 330 |
| 4 | Concrete heavy C30/35 | 1,032 | 320 |
| 5 | Concrete heavy C32/40 | 1,065 | 310 |
| 6 | Concrete heavy C35/45 | 1,1 | 300 |
| 7 | Concrete heavy C40/50 | 1,138 | 290 |
| 8 | Ordinary soil | 0,134 | 2470 |
| 9 | Clay | 0,189 | 1750 |
| 10 | Sandy loam | 0,267 | 1240 |
| 11 | Loam | 0,228 | 1450 |
| 12 | Sand | 0,267 | 1240 |
| 13 | Pine | 0,152 | 2180 |
| 14 | Maple | 0,271 | 1220 |
| 15 | Oak | 0,341 | 970 |
| 16 | Brick masonry | 0,703 | 470 |
| 17 | Steel | 3,667 | 90 |

**Fig. 2**. Minimum wall thicknesses according to DBN V.2.2-5:2023 "Civil Defence Protective Structures" [2]

**Рис. 2** Мінімальні товщини стін відповідно до ДБН В.2.2-5:2023 "Захисні споруди цивільного захисту"[2]

## MAIN RESEARCH

### Engineering methodology of Berezan V.I.

Berezana V.I.'s method is a classical empirical dependence widely used in the Soviet school of military engineering and fortification to calculate the penetration depth of a penetrator (projectile, fragment) into an obstacle (concrete, soil, brickwork).

According to this formula, the penetration depth is recommended to be determined using an empirical formula:

$$h_p = \lambda k_p \frac{m}{d_{pr}^2} V_{pr} \cos\alpha \qquad (1)$$

where: $h_p$ – the depth of projectile penetra-tion along the normal to the outer surface of the obstacle in metres;

$\lambda$ - the coefficient, which mainly depends on the shape of the projectile, is equal to 1.3 when firing armour-piercing shells at concrete and 1.0 in other cases;

$k_p$ – the coefficient of compliance of this environment to penetration (taken as in Fig. 3);

$m$ - the weight of the projectile at the moment of encountering an obstacle, kg.

$d_{pr}$ - projectile diameter in metres;

$V_{pr}$ - projectile speed at the moment of encountering an obstacle, in m/s.

| Name of the medium | Values of coefficients | | | |
|---|---|---|---|---|
| | Penetration $k_p$ | Explosion $k_b$ | High-explosive action $k_{exp}$ | Spalling, $k_{ch}$ |
| Freshly placed loose soil | 0,0000130 | 0,60 | 1,40 | |
| Ordinary soil | 0,0000065 | 0,53 | 1,07 | |
| Dense sand | 0,0000045 | 0,50 | 1,04 | |
| Sandy loam | 0,0000050 | 0,50 | 1,00 | |
| Loam | 0,0000060 | 0,50 | 1,00 | |
| Dense clay | 0,0000070 | 0,50 | 1,00 | |
| Limestone or sandstone | 0,0000020 | 0,25 | 0,92 | |
| Granite or gneiss | 0,0000016 | 0,20 | 0,86 | |
| Pine | 0,0000050 | 0,30 | 0,60 | |
| Oak, beech, ash | 0,0000040 | 0,30 | 0,60 | |
| Dry brick masonry | 0,0000030 | 0,25 | 0,96 | |
| Dry stone masonry | 0,0000030 | 0,25 | 0,96 | |
| Brick masonry in cement mortar | 0,0000025 | 0,25 | 0,88 | 0,81 |
| Stone masonry in cement mortar | 0,0000020 | 0,20 | 0,84 | |
| Reinforced brick masonry | 0,0000022 | 0,20 | 0,52 | 0,73 |
| Rubble concrete | 0,0000016 | 0,18 | 0,70 | |
| Heavy concrete of class C 8/10, C 12/15. | 0,0000012 | 0,18 | 0,65 | |
| Reinforced concrete of class C 20/25. | 0,0000010 | 0,12 | 0,30 | 0,37 |
| Fortification concrete of class C 40/45 | 0,0000008 | 0,16 | 0,60 | |
| Fortification reinforced concrete of class C 40/45 | 0,0000007 | 0,11 | 0,25 | 0,33 |
| with flexible spall liner | 0,0000008 | 0,13 | 0,52 | |
| with rigid spall liner | 0,0000008 | 0,13 | 0,42 | |
| Monolithic reinforced concrete structures of concrete C45/60 | 0,0000007 | 0,11 | 0,25 | 0,33 |

**Fig. 3** Coefficient of penetrability of the medium dvantages of the method [4]
**Рис. 3** Коефіцієнт податливості середовища проникненню [4]

- Simplicity and convenience: The formula has a linear form and allows for quick calculations without the use of complex software. It is ideal for rapid assessment in field or engineering conditions.
- Clear physical meaning of parameters: All variables (mass, diameter, speed, angle of incidence) are understandable and easily measurable.
- Experimental confirmation: The methodology is based on a large number of field tests; therefore, for typical materials (concrete, reinforced concrete, soil), it provides sufficiently accurate results for engineering purposes.

Disadvantages of the method:

- Empirical nature: The formula depends on empirical coefficients that are selected for specific materials. If the material of the protective structure is non-standard (for example, ultra-strong fibre concrete), the accuracy of the calculation sharply decreases.
- Limited speed range: The formula works correctly within the range of speeds typical for ordinary artillery shells and fragments. At hypersonic speeds or in the case of cumulative jets, the physics of the process change, and the linear dependence ceases to be valid.
- Ignoring the material dynamics: The methodology considers the final result (depth), but does not account for wave processes within the wall, the formation of chips from the back side, or the interaction of the fragment directly with the reinforcement.

## Energy method (or energy balance method)

This method has gained widespread popularity in Western European countries (France, the United Kingdom). It is based on the law of conservation of energy.
According to this method, the penetration thickness is determined by the formula (2)

$$h_t = \left(\frac{4}{\pi}\right)\frac{E_k}{\left(\sigma \times 10^6\right) \times d^2} \quad (2)$$

where $h_t$ - the thickness of the projectile penetration, m;
d - projectile diameter, m;
$E_k$ - kinetic energy of the projectile, J;
σ – average pressure, MPa

The kinetic energy of the projectile (J) should be determined using the formula (3):

$$E_k = \frac{1}{2}mV^2 \quad (3)$$

*m* – mass of the projectile, kg;
*V* – projectile velocity, m/s

The average stresses are determined by the formula (4):

$$\sigma = \left(\alpha + \beta\sqrt{\frac{\rho_t}{\left(\sigma_t \times 10^6\right)}V_i}\right)\sigma_t \quad (4)$$

where $\rho_t$ - density of target material, kg/m$^3$;
$\sigma_t$ - shear strength (Y) of the target material, MPa;
$V_i$ - projectile velocity at impact, m/s.

The alpha (α) and beta (β) coefficients, which depend on the material and shape of the projectile or fragment, are determined from the tables shown in Fig. 4.

Parameter values for steel target

| | $\alpha$ | $\beta$ | $\sigma_t$ | $\xi$ |
|---|---|---|---|---|
| Conical nose | $\frac{1}{2}\left[1+\ln\frac{2E}{(5-4\nu)R_y}\right]$ | $2\sin\frac{\theta}{2}$ | $R_y$ | 0 |
| Flat nose | $\frac{1}{2}\left[1+\ln\frac{2E}{(5-4\nu)R_y}\right]$ | 2 | $R_y$ | - |
| Ogive nose | $\frac{2}{3}\left[1+\ln\frac{E}{3(1-\nu)R_y}\right]$ | $\frac{3}{4\psi}$ | $R_y$ | 0 |
| Hemispherical nose | $\frac{2}{3}\left[1+\ln\frac{E}{3(1-\nu)R_y}\right]$ | $\frac{3}{2}$ | $R_y$ | 0 |
| Eroding penetration | $\frac{2}{3}\left[1+\ln\frac{E}{3(1-\nu)R_y}\right]$ | $\frac{3}{2}$ | $R_y$ | 1 |

Parameter values for concrete and soil targets

| | $\alpha$ | $\beta$ | $\sigma_t$ | $\xi$ |
|---|---|---|---|---|
| Conical nose | $\frac{1}{2}\left[1+\ln\frac{2E}{(5-4\nu)f_c}\right]$ | $2\sin\frac{\theta}{2}$ | $f_c$ | - |
| Flat nose | $\frac{1}{2}\left[1+\ln\frac{2E}{(5-4\nu)f_c}\right]$ | 2 | $f_c$ | - |
| Ogive nose | $\frac{2}{3}\left[1+\ln\frac{E}{3(1-\nu)f_c}\right]$ | $\frac{3}{4\psi}$ | $f_c$ | 2 |
| Hemispherical nose | $\frac{2}{3}\left[1+\ln\frac{E}{3(1-\nu)f_c}\right]$ | $\frac{3}{2}$ | $f_c$ | 2 |

**Fig. 4** Parameter values for mean stress determination [4]
**Рис. 4** Значення параметрів для визначення серед ніх напружень [4]

Advantages of the methodology:

- Fundamentality: It is based on the law of conservation of energy, which makes it physically transparent and understandable for explanation.
- Versatility of input data: Allows operating with energy as a comprehensive parameter, without breaking it down separately into mass and velocity at each stage.
- Ease of adaptation: Convenient for comparative analysis of the effectiveness of different ammunition, if their energy is known.

Disadvantages of the method:

- Idealisation of the process: The method assumes that the resistance force of the material is constant throughout the entire penetration path, which is not the case in

reality (resistance varies depending on speed and depth).

- The absence of a time factor: The energy balance shows the final state but does not describe the dynamics of the process over time (rate of deformation).

**Engineering methodology of the US National Defence Research Committee**

This method is the most common in Western engineering practice (in particular, in the standards of the USA and NATO countries). The difference between this method and the previous two is that it uses its own empirical formula for the main types of materials.

So, to calculate the penetration of ammunition or shrapnel into reinforced concrete, the formula for determining the depth of penetration takes the form (5):

$$h_t = \frac{56.6\left(\frac{m}{d^3}\right)^{0.075} \overline{N} m V^{1.8}}{d^2\sqrt{f_c}}\left(\frac{d}{c}\right)^{0.15} f_{age} + d \qquad (5)$$

where $h_t$ - maximum concrete penetration thickness by projectile, mm;

$d$ - projectile diameter, mm;

$m$ - mass of the projectile, kg;

$V$ - projectile speed, m/s;

$f_c$ - compressive strength of concre-te, MPa; c – maximum stone size, mm (19 mm for heavy concrete and 4 mm for concrete masonry);

$\overline{N}$ - projectile end shape coefficient according to Annex C UFC 4-023-07 [18];

$f_{age}$ – concrete age coefficient, which should be taken as:

1.05 - for concrete less than 28 days old;

1.02 - for concrete aged from 28 to 66 days;

1.01 - for concrete aged from 66 to 360 days;

1.00 - for concrete aged more than 360 days.

$\overline{N}$ = 0.91 – for low threat severity;

$\overline{N}$ = 1.26 – for medium threat severity level;

$\overline{N}$ = 1.39 – for a high level of threat severity;

$\overline{N}$ = 1.31 – for a very high level of threat severity;

The residual velocity of the projectile after penetrating an obstacle can be calculated using the formula (6):

$$V_r = V\left(1 - \frac{t_{conc}}{h_t}\right)^{0.733} \qquad (6)$$

where $V_r$ – residual velocity, m/s;

$V$ – impact velocity, m/s;

$t_{conc}$ – concrete thickness, mm;

$h_t$ – maximum penetration depth, mm

To determine the maximum penetration thickness of a steel obstacle in UFC 4-023-07, it is recommended to use the following formula (7):

$$h_t = d\left(\frac{V m^{0.5}\cos^{0.8}\theta}{1.125 d^{1.5}\log_{10} BHN}\right)^{1.25} \qquad (7)$$

where $h_t$ - maximum steel penetration thick-ness, mm;

$d$ - projectile diameter, mm;

m - ammunition mass, kg;

$V$ – projectile velocity, m/s;

$\theta$ - obstacle inclination angle from steel, degrees;

$BHN$ - Brinell hardness number, for ordinary steels 110–160, for armour steels 220–350.

The residual velocity of the projectile after penetrating steel obstacles in accordance with UFC 4-023-07 21 should be determined using the formula (8):

$$V_r = \left(V^2 - \left[\frac{1.1275\left(\frac{t}{d}\right)^{0.8} d^{1.5}\log_{10} BHN}{m^{0.5}\cos^{0.8}\theta}\right]^2\right)^{0.5} \qquad (8)$$

where $t$ - actual thickness of the steel, m;

$d$ - diameter of the projectile, mm;

$m$ - mass of the ammunition, kg;

$V$ - velocity of the projectile, m/s;

$\theta$ - angle of inclination of the steel obstacle, degrees;

$BHN$ – Brinell hardness number, for ordinary steels 110–160, for armour steels 220–350.

To determine the maximum penetration thickness of an obstacle made of wood, UFC 4-023-07, it is recommended to use the formula (9):

$$h_t = 0.64 \frac{V^{0.4113} m^{1.4897}}{\rho \left( \frac{\pi d^2}{4} \right)^{1.3596} H^{0.5414}} \quad (9)$$

where $h_t$ - maximum drilling thickness of the wood, m;
$d$ - projectile diameter, m;
$m$ mass of the projectile, kg; $V$ – velocity of the projectile, m/s;
$\rho$ - wood density, kg/m³;
$H$- wood hardness, kg.

Although we note that the hardness values are for American and European timber, for our purposes of performing similar calculations, we need to standardise these data for our own timber.

The residual velocity of the projectile after penetrating obstacles made of wood should be determined according to UFC 4-023-07 using the formula (10):

$$V_r = V \left[ 1 - \left( \frac{t}{h_t} \right)^{0.5735} \right] \quad (10)$$

where $t$ - the actual thickness of the wood, m.

Advantages of the method:

- High accuracy for different materials: These formulas are considered the 'gold standard' for calculating concrete barriers, steel plates, and wooden barriers, as they take into account the specific characteristics of the material (for concrete, this includes the concrete strength, aggregate size, and concrete age).
- A wide testing base: The methodology relies on a vast array of experimental data obtained by US military engineers.

Disadvantages of the method:

- Difficulty of calculation: The formula contains fractional exponents, which complicate manual calculation;
- Speed limitation: The formula gives an error at high impact speeds when the projectile begins to deform (it is designed for a 'rigid' non-deformable projectile).

To analyse the results of calculations using different methodologies in this work, a reinforced concrete element was calculated using various concrete classes. The results of the calculation were also compared with the parameters specified in Tables 14 and 13 of DBN B.2.2-5:2023 'Protective Structures of Civil Defence'. The calculation was carried out for threats posed by fragments from the explosions of UAVs and missiles, in accordance with the latest recommendations of the Central Directorate of Military Education and Science of the General Staff of the Armed Forces of Ukraine, as shown in Fig. 5.

| UAV | |
|---|---|
| TNT equivalent weight of warhead charge, kg | 100 |
| Impact velocity, m/s | 145 |
| Impact angle, ° | 20-60 |
| Fragment dimensions, A x B x C (thickness), cm;<br>mass, g | 9 x 2 x 0,7;<br>80 |
| Initial fragment velocity, m/s | 2300 |
| Missile | |
| TNT equivalent weight of warhead charge, kg | 718,2 |
| Impact velocity, m/s | 800 |
| Impact angle, ° | 80-90 |
| Fragment dimensions, A x B x C (thickness), cm;<br>mass, g | 3,5x3,5 (Cylindrical shape) |
| Initial fragment velocity, m/s | 2380 |

**Fig. 5**. Threats from fragments caused by UAV and missile explo-sions in accordance with the latest recommendations of the Central Directorate of Mili-tary Education and Science of the General Staff of the Armed Forces of Ukraine

**Рис. 5** Загрози від уламків при вибуху БпЛА та ракети відповідно до останніх рекомендацій Централь-ного управління військ-кової освіти та науки Генераль-ного штабу Збройних Сил України

**Table 1** Penetration depth of reinforced concrete elements by missile blast fragments
**Табл. 1** Глибина пробиття залізобетонних елементів при враженні уламками від вибуху ракети

| Class of concrete | Depths of drilling into the reinforced concrete element, mm | | | |
|---|---|---|---|---|
| | DBN V.2.2-5: 2023 | Method of Berezan V.I.; | Energy method | Engineering Methodology NDRC |
| C20/25 | 350 | 340 | 497 | 512 |
| C25/30 | 330 | 340 | 457 | 476 |
| C30/35 | 320 | 310 | 440 | 446 |
| C35/42 | 310 | 290 | 425 | 422 |

**Table 2** Penetration depth of reinforced concrete elements by UAV blast fragments
**Табл. 2** Глибина пробиття залізобетонних елементів при враженні уламками від вибуху БпЛА

| Class of concrete | Depths of drilling into the reinforced concrete element, mm | | | |
|---|---|---|---|---|
| | DBN V.2.2-5: 2023 | Method of Berezan V.I.; | Energy method | Engineering Methodology NDRC |
| C20/25 | 350 | 410 | 615 | 458 |
| C25/30 | 330 | 410 | 565 | 425 |
| C30/35 | 320 | 340 | 544 | 399 |
| C35/42 | 310 | 270 | 525 | 377 |

As we can see from the calculation results, the energy method and the engineering methodology of the US National Defence Research Committee give quite similar results, but they significantly exceed the required thickness according to the Berazan method, which in turn is quite close to the thickness values given in DBN V.2.2-5:2023 "Civil Defense Protective Structures"[2].

## CONCLUSIONS AND PROSPECTS FOR FURTHER RESEARCH

Based on these results, it can be concluded that when calculating according to the methodologies of the USA and the United Kingdom, the recommended wall thicknesses are not sufficient in accordance with DBN B.2.2-5:2023 'Civil Defence Protective Structures'. A promising direction for further research is improving the calculation method for penetrative effects on various obstacle materials and all potential damage mechanisms. Developing modern calculation methods, considering existing military threats, will enable the most effective construction of engineering protective and fortification structures, which will significantly support the realisation of the 'Country-Fortress' concept.

It should be noted that a critical task is the development of modern regulatory documents that would regulate the basic requirements and calculation methods for fortification and protective structures of various purposes, taking into account contemporary military threats.

## REFERENCE

*1.***Bobro, D. H**. (2015). Determination of assessment criteria and threats to critical infrastructure. *Stratehichni priorytety. Seriia Ekonomika, 4(37), 83–93*. [in Ukraine]

*2.***Ministerstvo rozvytku hromad, terytorii ta infrastruktury Ukrainy**. (2023). DBN V.2.2-

5:2023. Civil defense protective structures. Kyiv. [in Ukraine].

3. **Krishna Chaitanya, M.** (2015). Progressive collapse of structures. *International Journal of Mechanical, Civil and Control Engineering*, 23–29. [in English]

4. **Mykhailovskyi, D. V., Bilyk, A. S., & Skliarov, I. O.** (2024). Calculation of building structures for the effects of main air strike damage factors [Monograph], 92 p. [in Ukrainian]

5. **Mykhailovskyi, D., & Skliarov, I., (**2023). Methods of calculation and engineering protection of critical infrastructure objects and other strategic facilities against long-range projectiles. *Strength of materials and theory of structures. (111), 155-171.* [in English] https://doi.org/10.32347/2410-2547.2023.111.155-171

6. **Mykhailovskyi, D., Skliarov, I., Khomik, M., Vavilova N., & Skliarova, T. (**2024**).** Analysis of methods for calculating the penetrating effect of the main types of missiles and fragmentation damage to the structures of protective constructions. *Strength of materials and theory of structures: (113), 171-182.* [in English] https://doi.org/10.32347/2410-2547.2024.113.171-182.

7. **Cormie, D., Mays, G., & Smith, S.** (2020) Blast effects on buildings, third edition, *London, 320 P.* (ISBN 978-0-7277-6147-7) [in English]

8. **Khadid et Al**. (2007), BLast loaded stiffened plates *Journal of Engineering and Applied Sciences,VOL. 2(2), 456-461*. [in English]

9. **Bounds, W.L.** (2010) Design of blast-resistant buildings in petrochemical facilities; asce publications: *Reston, VA, USA,. – 300 P.* [in English]

10. **Ministry of Construction** of Ukraine. (2006). *DBN V.1.2-2:2006 System of reliability and safety of construction objects. Loads and impacts [in Ukrainian].

11. **Harlin W.J., Cicci David A.** (2007). Ballistic missile trajectory prediction using a state transition matrix. *Applied Mathematics and Computation 188 pp.1832–1847* [in English]

12. **Hakan Hansson** (2011) Warhead penetration in concrete protective structures. Licentiate thesis in civil and architectural *Engineering. Stockholm, Sweden 126 p. appendix – 47 p.* [in English]
ISSN 1103-4270 –

13. **Brode, H.** (1995) Numerical solution of spherical blast waves. *Journal of Applied Physics, BD. 26(6),. 766 – 775.* [in English]

14. **Mays, G., & Smith, P. (HG.):** (1995). Blast effects on buildings – design of buildings to optimize resistance to blast loading. *Thomas Telford, LondoN,.121*. [in English]

15. **Henrych, J.** (1979) The dynamics of explosion and its use. *Elsevier, Amsterdam, 558 P.* [in English]

16. **Korenev, B., & Rabinovič, I.** (1985). Structural dynamics – Structures under special effects. *Berlin: Veb Verlag für Bauwesen.* [in German]

17. **Kinney, G., Graham, K.,** (1985) Explosive shocks in air. *Springer, New York, 269 P.* ISBN 978-3-642-86682-1. [in English]

18. **U.S. Army Corps of Engineers, Naval Facilities Engineering Command, Air Force Civil Engineer Support Agency** (2017). *UFC 4-023-07. Unified Facilities Criteria. Design to Resist Direct Fire Weapons Effects. Change 1*. 66 p. [in English].

19. **U.S. Army Corps of Engineers, Naval Facilities Engineering Command, Air Force Civil Engineer Support Agency** (2016). *UFC 4-023-03. Design of Buildings to Resist Progressive Collapse. Change 3*. 227 p. [in English].

20. **Kosenko, V. S., Voloshchenko, O. I., & Kushnirenko, M. H**. (2022). Determination of the resistance of closed-type field fortification structures to a nuclear blast wave. *Strength of Materials and Theory of Structures*, 109, 387–402. [in Ukrainian].

21. **Pokrowski, G. I. (**1985) Explosion und Sprenung. Kleine Naturwissenschaftliche Bibliothek, Leipzig. – 293 p. [in English]

22. **Babych, Ye. M., Dvorkin, L. Y., Kochkariov, D. M., et al.** (2018). Recommendations for the design of reinforced concrete fortification structures. *Rivne: NUVHP. 173 p.* [in Ukrainian] ISBN 978-966-327-398-3..

23. **Ministry for Communities, Territories and Infrastructure Development of Ukraine** (2011). DBN V.2.6-98:2009. Structures of buildings and works. Concrete and reinforced concrete structures. Main provisions. Kyiv. 71 p. [in Ukrainian].

24. **Koliakova, V., Dumych, A., & Sumak, A**. (2024, January). Stress-strain state of shelter structures under the action of air shock wave. *Sworld-Us Conference Proceedings, 1*(usc22-01), 49–56. [in Ukrainian] https://doi.org/10.30888/2709-2267.2024-22-00-020

25. **Romashkina, M., Pisarevskyi, B., & Zhuravlyov, O.**. (2024). Analysis of the building on the air shock wave by direct dy-

namic method (with LIRA-FEM soft-ware) . *Building Constructions. Theory and Practice*, (14), 147–160. https://doi.org/10.32347/2522-4182.14.2024.147-160

## LITERATURE


1. **Bobro D.H.** (2015) Vyznachennia kryteriiv otsinky ta zahrozy krytychnii infrastrukturi/ Stratehichni priorytety. – Seriia EKONOMIKA – № 4 (37). – S. 83-93.
2. **DBN V.2.2-5:2023** Zakhysni sporudy tsyvilnoho zakhystu. – chynni vid 2023-11-01.– *Kyiv: Ministerstvo rozvytku hromad, terytorii ta infrastruktury Ukrainy,2023 – 131 s.*
3. **Krishna Chaitanya, M.** (2015). Progressive collapse of structures. *International Journal of Mechanical, Civil and Control Engineering*, 23–29
4. **Mykhailovskyi, D. V., Bilyk, A. S., & Skliarov, I. O.** (2024). Rozrakhunok konstruktsii budivel i sporud na dii osnovnykh faktoriv urazhennia zasobiv povitrianoho napadu [Monograph], 92 c.
5. **Mykhailovskyi, D., & Skliarov, I., (**2023). Methods of calculation and engineering protection of critical infrastructure objects and other strategic facilities against long-range projectiles. *Strength of materials and theory of structures. (111), 155-171.* https://doi.org/10.32347/2410-2547.2023.111.155-171
6. **Mykhailovskyi, D., Skliarov, I., Khomik, M., Vavilova N., & Skliarova, T. (**2024**).** Analysis of methods for calculating the penetrating effect of the main types of missiles and fragmentation damage to the structures of protective constructions. *Strength of materials and theory of structures: (113), 171-182.* https://doi.org/ 10.32347/2410 - 2547.2024.113.171-182.
7. **Cormie, D., Mays, G., & Smith, S.** (2020) Blast effects on buildings, third edition, *London, 320 P.* ISBN 978-0-7277-6147-7
8. **Khadid et Al**. (2007), Blast loaded stiffened plates *Journal of Engineering and Applied Sciences,VOL. 2(2), 456-461.*
9. **Bounds, W.L.** (2010) Design of blast-resistant buildings in petrochemical facilities; asce publications: *Reston, VA, USA,. – 300 P.*
10. **DBN V.1.2-2:2006** systema zabezpechennia nadiinosti ta bezpeky budivelnykh obiektiv. Navantazhennia i vplyvy. normy proiektuvannia– [chynni vid 2007-01-01]. – *Kyiv: Ukrainskyi naukovo-doslidnyi ta proektnyi instytut stalevykh konstruktsii im. V.M.Shymanovskoho– 75 s.*
11. **Harlin W.J., Cicci David A.** (2007). Ballistic missile trajectory prediction using a state transition matrix / Applied Mathematics and Computation 188 pp.1832–1847
12. **Hakan Hansson** (2011) Warhead penetration in concrete protective structures. Licentiate thesis in civil and architectural Engineering. Stockholm, Sweden ISSN 1103-4270 – 126 p. appendix – 47 p.
13. **Brode, H.** (1995) Numerical solution of spherical blast waves. *Journal of Applied Physics, BD. 26(6),. 766 – 775.*
14. **Mays, G., & Smith, P. (HG.):** (1995). Blast effects on buildings – design of buildings to optimize resistance to blast loading. *Thomas Telford, LondoN,.121.*
15. **Henrych, J.** (1979) The dynamics of explosion and its use. *Elsevier, Amsterdam, 558 P.*
16. **Korenev, B., Rabinovič, I. (**1985) **Baudynamik** – Konstruktionen unter speziellen einwirkungen. *Veb Verlag für Bauwesen, Berlin,.41.*
17. **Kinney, G., Graham, K.,** (1985) Explosive shocks in air. *Springer, New York, 269 P.* ISBN 978-3-642-86682-1.
18. **UFC 4-023-07** Unified Facilities Criteria. Design to Resist Direct Fire Weapons Effects. Change 1 *U.S. Army corp of engineers, naval facilities engineering comand, air force civil engineer support agency, 2017 – 66 p.*
19. **UFC 4-023-03** Design Of Buildings To Resist Progressive Collapse. Change 3 / U.S. *Army corp of engineers, naval facilities engineering comand, air force civil engineer support agency*, 2016 – 227 p.
20. **Kosenko, V. S., Voloshchenko, O. I., & Kushnirenko, M. H**. (2022). Vyznachennia stiikosti konstruktsii polovykh fortyfikatsiinykh sporud zakrytoho typu vid udarnoi khvyli yadernoho vybukhu. *Strength of Materials and Theory of Structures*, 109, 387–402.
21. **Pokrowski, G. I. (**1985) Explosion und Sprenung. Kleine Naturwissenschaftliche Bibliothek, Leipzig. – 293 p.
22. **Babych, Ye. M., Dvorkin, L. Y., Kochkariov, D. M., et al.** (2018). *Rekomendatsii z proiektuvannia zalizobetonnykh konstruktsii fortyfikatsiinykh sporud*. Rivne: NUVHP. 173 p. ISBN 978-966-327-398-3. [in Ukrainian].
23. **DBN V.2.6-98 (2009)** Konstruktsii budynkiv i sporud. Betonni ta zalizobetonni konstruktsii. Osnovni polozhennia. – *K.: Minrehionbud Ukrainy, 2011. – 71.*

24. **Koliakova, V., Dumych, A., & Sumak, A.** (2024). Napruzheno-deformovanyi stan konstruk-tsii ukryttia pry dii povitrianoi udarnoi khvyli. Sworld-Us Conference Proceedings, 1(usc22-01), 49–56. https://doi.org/*10.30888/2709-2267.2024-22-00-020*

25. **Romashkina, M., Pisarevskyi, B., & Zhuravlov, O.** (2024). Rozrakhunok budivli na vplyv dii povitrianoi udarnoi khvyli priamym dynamichnym metodom z vykorystanniam PK LIRA-SAPR. *Budivelni konstruktsii. Teoriia i praktyka, (14), 147–160.* https://doi.org/10.32347/2522-4182.14.2024.147-160

# АНАЛІЗ МЕТОДИК РОЗРАХУНКУ ПРОНИКНОЇ ДІЇ ОСНОВНИХ ВИДІВ БОЄПРИПАСІВ ТА ОСКОЛКОВОГО УРАЖЕННЯ КОНСТРУКЦІЙ ЗАХИСНИХ СПОРУД

*Денис МИХАЙЛОВСЬКИЙ,*
*Олег КОМАР*

**Анотація**. У поточних реаліях, що склалися внаслідок повномасштабної збройної агресії рф проти України, а також з огляду на стрімкий технологічний розвиток високоефективних засобів ураження, проблематика забезпечення надійності та стійкості фортифікаційних і захисних споруд набула безпрецедентної актуальності. Критичним завданням інженерного захисту стає протидія широкому спектру загроз, що включає проникну дію куль стрілецької зброї, кумулятивних струменів, бронебійних снарядів, а також руйнівний вплив осколково-фугасних боєприпасів.

Вплив цих факторів не обмежується лише локальними пошкодженнями, такими як пробиття чи відкол елементів конструкції. Він визначає загальну живучість об'єкта — його здатність зберігати цілісність, несучу здатність та основні функціональні характеристики безпосередньо під час інтенсивного вогневого впливу. Для прогнозування поведінки споруд використовується широкий спектр методик: від аналітичних та емпіричних підходів до складного чисельного моделювання.

Достовірність та точність таких прогнозів напряму залежать від комплексного врахування вхідних параметрів. По-перше, це кінематичні характеристики вражаючих елементів: їхня маса, вектор швидкості, кут зустрічі з перешкодою та форма. По-друге, вирішальну роль відіграють фізико-механічні властивості матеріалів самої перешкоди, зокрема динамічна міцність, гранична пластичність, ударна в’язкість та ступінь гетерогенності структури (наприклад, у залізобетоні). По-третє, важливими є геометрія та конструктивні рішення захисних елементів, такі як багатошаровість або наявність рознесеного бронювання.

У практичній площині існує чіткий розподіл застосування методів розрахунку. Емпіричні формули, завдяки своїй простоті, є незамінними на етапах ескізного проєктування для отримання швидких, хоча й наближених оцінок. Натомість сучасні чисельні методи, що реалізуються через метод скінченних елементів (МСЕ) дозволяють з високою точністю відтворити механізми взаємодії снаряду з конструкцією у часі та просторі.

**Ключові слова:** інженерна методика; уламки; боєприпаси; БпЛА; ракета.

***Received:*** *October 30, 2025.*
***Accepted:*** *November 30, 2025.*

ISSN 2522-4182

DOI: 10.32347/2522-4182.17.2025.179-188
UDC 624.012.45:624.04:624.072.2:693.554(091)

# HISTORY OF EMERGENCE AND DEVELOPMENT OF THE SANDWICH MODEL FOR DESIGN OF MEMBRANE, SHELL AND SLAB ELEMENTS ACCORDING TO EN 1992-1-1:2023

*Leonid SKORUK*

Kyiv National University of Construction and Architecture,
31, Povitrianykh Syl Ave., Kyiv, Ukraine, 03037
skoruk.slm@gmail.com, http://orcid.org/0000-0002-7362-1348

**Abstract.** For the first time in European design standards for concrete structures, specifically in Annex G (normative), the new version of Eurocode EN 1992-1-1:2023 pays focused attention to the design of membrane, shell and slab elements and proposes a modern approach for their calculation.

As a method of optimal design for reinforced concrete shells, slabs and membranes, Annex G proposes the so-called **sandwich model** - where the shell is represented as a three-layer model consisting of two load-bearing layers (top and bottom) and an intermediate layer between them.

When designing using the sandwich model – a spatial problem (bending + torsion + membrane forces) is transformed into two membrane problems for the top and bottom layers. That is, transformation of a three-dimensional stress state into two layers (top and bottom) with equivalent membrane stresses.

The sandwich model is a rigorous mechanical model that allows reducing a complex spatial problem (shell with combined forces) to two independent plane problems (membrane elements in the top and bottom layers) through statically equivalent transformation of forces into stresses.

The sandwich model is based on transforming the combination of forces (membrane, bending and torsional) into a statically equivalent system of in-plane stresses acting in the top and bottom layers of the model.

Basic assumptions of the method:

*a*) three-layer model: the shell is represented as a structure with two load-bearing layers (top and bottom) and an intermediate layer between them;

**Leonid SKORUK**
Associate Professor of the Department of Reinforced Concrete and Stone Structures, PhD, Ass. Professor

*b*) static equivalence: internal forces are transformed into in-plane stresses in such a way as to maintain complete static equilibrium;

*c*) independent layer design: each layer (top and bottom) is designed separately as a membrane element according to clause G.3.

The formulations presented in Annex G of EN 1992-1-1:2023 in clauses G.3 and G.4 are consistent with the clauses and design provisions in Section 8 (Ultimate Limit States (ULS)) of the main body of the document, and clause G.5 contains additional provisions to 9.2 (Crack Control) of these standards. Annex G covers the design of planar members without discontinuities in the concrete mass. Other more refined design methods complying with clause 7.3.3 (Plastic Analysis) or clause 7.3.4 (Non-linear Analysis) of Eurocode 2 may be used.

Thus, Annex G (Design of Membrane, Shell and Slab Elements) does not replace, but supplements the main sections of Eurocode 2, namely - general principles, materials (σ-ε diagrams), cross-section design for ULS, crack resistance and SLS.

**Keywords**: design of membrane; shell and slab elements; sandwich model..

## PROBLEM STATEMENT

For the first time, the so-called sandwich model for optimal design of reinforced concrete shells and slabs was proposed in 1974 by Danish scientist Troels Brondum-Nielsen [1]

In his proposed design method, an infinitesimal shell element was divided by height into three layers, including two outer layers and a core layer, called the three-layer **Basic Sandwich Model (BSM)**. In this approach, membrane forces, bending and torsional moments are carried only by the outer layers of the shell.

The Basic Sandwich Model (BSM) has disadvantages due to neglecting different lever arms of all forces and the assumption that the resultant forces in steel act in the mid-plane of the outer layer, which can lead to unsafe design at large torsional moments or high reinforcement ratios.

The core in the basic sandwich model is considered to carry transverse shear forces. The design implementation assumes the absence of diagonal cracks in the core. Under this assumption, a state of pure shear develops in the core, which means that the transverse forces in the section do not affect the membrane forces in the outer layers.

Subsequently, Swiss scientist A. Peter Marti made his contribution to the development of the sandwich model in 1990 [2]. Marti complements Brondum-Nielsen's work by assigning out-of-plane shear forces to the intermediate layer. The three-layer sandwich model was then developed for the design of members subjected to membrane and bending states and to account for transverse shear [3]. The outer layers of the sandwich model (i.e., the outer layers) are considered to carry moments and membrane forces, while transverse shear forces are assigned to the core [4].

The key innovation of Marti's contribution to the development of the sandwich model was the distribution of functions between layers:

- **outer layers** – carry membrane forces + bending moments;
- **core** – carries transverse forces through compression fields inclined at 45°.

The inclination angle of the diagonal compression stress field in the core layer $\theta$ is taken equal to 45°, which corresponds to the traditional Mörsch truss model for reinforced concrete beams.

This leads to additional membrane forces in the top and bottom layers of the slab, equal to $0.5v_0$ in the direction of the principal transverse force.

Later in 2013-2014, Swiss researcher Thomas Jaeger presented the "**Extended Sandwich Model (ESM)**", which combines the sandwich model with basic concepts of the cracked membrane model and a new aggregate interlock relationship for shear stresses transmitted through cracks in the core [5-7].

Thomas Jaeger introduces a compatibility condition to link both outer layers, assuming a linear distribution of strains through the slab thickness, defined as a function of three curvatures and three strains in the mid-plane of the core.

The Extended Sandwich Model includes aggregate interlock in the core, allowing concrete to contribute to the transverse load-bearing capacity of slabs both with and without transverse reinforcement.

The introduction of stressed crack faces in the core allows dividing the applied transverse force into concrete and steel contributions.

Thomas Jaeger's contribution to the development of the sandwich model consisted of the following:

- accounting for cracking in the core;
- aggregate interlock;
- compatibility conditions between layers;
- tension stiffening in the outer layers.

In 2014-2018, E. Hernández-Montes and colleagues conducted a critical analysis and questioned the assumption of reinforcement yielding in the outer layers, which was adopted by Brondum-Nielsen and Marti.

The sandwich model of E. Hernández-Montes concerns an improved model for analysis of reinforced concrete slabs that accounts for limitations of the basic sandwich model. The model accounts for compatibility between tensile reinforcement and the compressive concrete block, which is crucial

for accurate strength calculation, especially in situations with high torsional moments [10-15].

The classical sandwich model assumes that tensile reinforcement reaches yielding ($\sigma_s = f_y$), but this hypothesis was challenged by E. Hernández-Montes and others, who proposed that the strain in tensile reinforcement should be related to the depth of the compressive stress block in the opposite layer.

**Physical meaning:** If concrete in the top layer fails before reinforcement in the bottom layer reaches yielding, the structure will have less load-bearing capacity and less deformability than calculated.

E. Hernández-Montes proposed an additionnal check to ensure that reinforcement actually reached yielding.

Key aspects of the Hernández-Montes model:

- **strain compatibility:** the model refutes the assumption that tensile reinforcement in reinforced concrete slabs always undergoes yielding, proposing instead that its strain is related to the depth of the concrete compressive stress block. This provides a more accurate stress value for reinforcement.
- **stress verification:** it introduces an additional verification step based on the plane section hypothesis. It assumes that the principal compression direction in one outer layer is parallel to the principal tension direction in the opposite outer layer.
- **upper bound theorem:** the model's assumptions ensure that calculated forces are an upper bound of true failure forces, which is a safe design approach.
- **experimental verification:** the accuracy of this approach was experimentally verified by Gil-Martín and Hernández-Montes.
- **basis for advanced models:** the concepts of this work led to the development of the **Advanced Sandwich Model (ASM)**, which solves many shortcomings of the basic sandwich model, such as those related to torsional moments and reinforcement ratios.
- **applications:** this research is particularly relevant for calculating the strength of reinforced concrete slabs subjected to bending and torsional moments. Its principles have also been applied in other areas, such as seismic behavior of coupled walls subjected to shear, and thin reinforced concrete panels [8-12].

The main contribution to the development of the sandwich model by E. Hernández-Montes and colleagues:

- verification of **strain compatibility** between layers;
- **introduction of limitations** on the method's application.

In 2023, a group of researchers [9] proposed the so-called **Developed Advanced Sandwich Model (DASM)**.

This study showed that using DASM reduced steel reinforcement by up to 40% and increased ductility by 10-15%. It was also observed that the ultimate strength of the considered examples, including solid slab and flat slab, decreased slightly by 4.1% and 1.8% (less than 5%) respectively, which has almost no effect on the overall response of the designed structure. These results demonstrate the effectiveness of the developed procedure.

DASM represents a highly accurate, relatively simple and reliable design procedure for plate and shell structures with complex geometry according to multiaxial concrete compression state and accounting for the effect of transverse shear forces.

The first generation of Eurocodes EN 1992-1-1:2004 (2002-2007) did not contain the sandwich method in normative annexes. Although this method was known, it was not standardized.

The second generation of Eurocodes EN 1992-1-1:2023 (2023-2026) contains **Annex G (normative)** – «Design of Membrane, Shell and Slab Elements». This document (EN 1992-1-1:2023) was prepared by Technical Committee CEN/TC 250 «Structural Eurocodes».

In Annex G of EN 1992-1-1:2023, a planar member, depending on the internal forces acting in it, is considered:

- as a **membrane** – a slab with normal and shear stresses (clause G.3) – see Fig. 1;
- as a **shell** – a slab with moments without membrane forces (clause G.4) – see Fig. 2;

- **as a shell or slab with combined forces** (clauses G.4, G.5) – see Fig. 2.

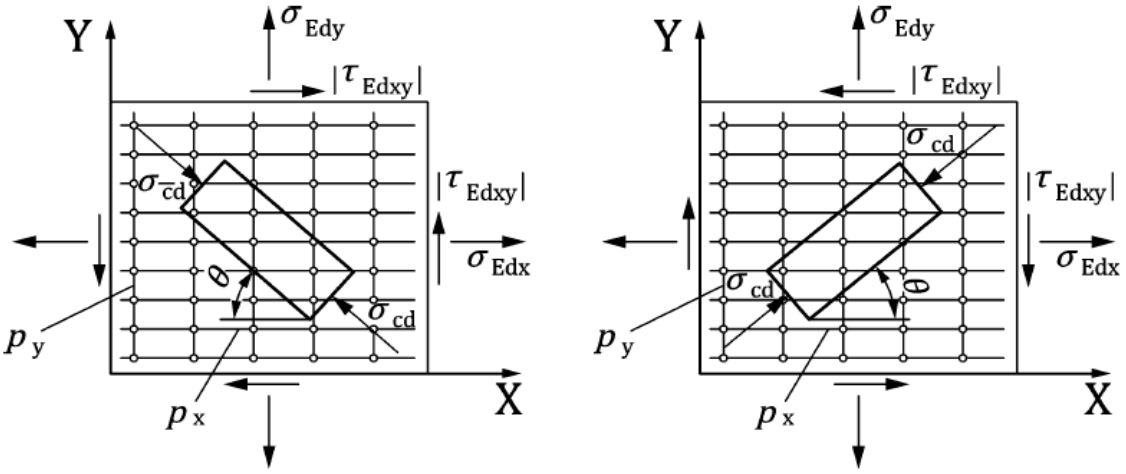


**Fig. 1** In-plane stresses in membrane element and definition of compression stress field inclination (angle θ).

**Рис. 1** Площинні напруження в мембранному елементі та визначення нахилу (кут θ) поля стискаючих напружень.

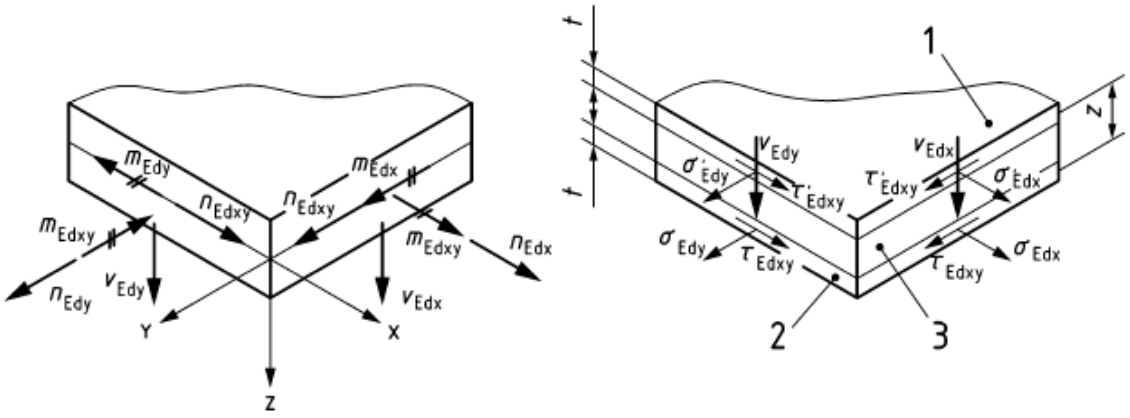


*а* б

**Fig. 2** Shell element (a) and sandwich model (b) with statically equivalent set of in-plane stresses: 1 – top layer, 2 – bottom layer, 3 – intermediate layer.

**Рис. 2** Оболонковий елемент (а) та сендвіч-модель (б) зі статично еквівалентним набором площинних напружень: 1 – верхній шар, 2 – нижній шар, 3 – проміжний шар.

The formulations presented in Annex G of EN 1992-1-1:2023 in clauses G.3 and G.4 are consistent with the clauses and design provisions in Section 8 (Ultimate Limit States (ULS)) of the main body of the document, and clause G.5 contains additional provisions to 9.2 (Crack Control) of these standards. Annex G covers the design of planar members without discontinuities in the concrete mass. Other more refined design methods complying with clause 7.3.3 (Plastic Analysis) or clause 7.3.4 (Non-linear Analysis) of EN 1992-1-1:2023 may be used. Thus, Annex G (Design of Membrane, Shell and Slab Elements) does not replace, but supplements the main sections of

Eurocode 2 EN 1992-1-1:2023, namely – general principles, materials (σ-ε diagrams), cross-section design for ULS, crack resistance and SLS.

Key differences of the new version of standards from the previous version of Eurocode 2 are as follows:

- refined formulas for stresses in layers;
- more detailed tables of optimum reinforcement;

- explicit condition for application of simplified method: $|m_{Edxy}| < 0{,}07d^2f_{cd}$;
- references to specific clauses of other sections.

EN 1992-1-1:2023 uses various methods and models for stress-strain state analysis of structures:

- linear elastic analysis (LEA);
- non-linear finite element analysis (NLFEA);
- yield line method;
- strip method;
- sandwich model.

In particular, when designing using the strip method -- the slab is considered as a system of orthogonal strips working in one direction. The load is distributed between strips in two directions.

The scope of application of the provisions given in Annex G of EN 1992-1-1:2023 may include flat slabs, slabs of constant or variable thickness, slabs with beams, cylindrical and other shells. This annex is also particularly important for design of:

1. **shear walls** – large shear stresses;
2. **deep beam** – non-linear stress distribution;
3. **slabs with concentrated loads** – zone around columns;
4. **bunkers and tanks** – membrane forces + bending;
5. **shells** – complex three-dimensional stress state.

According to clause G.4(1) of EN 1992-1-1:2023 and Fig. 2, the sandwich model is based on transforming the combination of forces (membrane, bending and torsional) into a statically equivalent system of in-plane stresses acting in the top and bottom layers of the model.

**Basic assumptions of the method:**

1. **three-layer model**: the shell is represented as a structure with two load-bearing layers (top and bottom) and an intermediate layer between them;
2. **static equivalence**: internal forces are transformed into in-plane stresses in such a way as to maintain complete static equilibrium;
3. **independent layer design**: each layer (top and bottom) is designed separately as a membrane element according to clause G.3.

The sandwich model formulas (G.12-G.17) of EN 1992-1-1:2023 are **transformed** into formulas for specific cases:

1. **pure membrane elements** (clause G.3) – when moments = 0;
2. **slabs without membrane forces** (clause G.4(5), formulas G.18-G.21) – when n = 0;
3. **shells** – general case with all forces.

Thus, the sandwich model is a generalization that covers all three cases.

**Physical meaning of the sandwich model:**

- **«smears»** the actual stress distribution into two equivalent layers;
- **maintains** equilibrium of forces and moments;
- **allows** using simple membrane formulas (clause G.3).

**Advantages:**

- unified approach for all types of elements;
- explicit physical interpretation;
- simplicity of calculations;
- possibility of manual calculation.

**Disadvantages:**

- approximate stress distribution;
- requires adjustment of coefficients (t, z);
- does not account for exact strain distribution.

**Why was the sandwich model specifically chosen for implementation in EN 1992-1-1:2023.**

**1. Widespread use in software.**

Many modern design software worldwide use Brondum-Nielsen's approach for calculating reinforcement of concrete shells in the ultimate limit state under bending and membrane forces.

Software using the sandwich method:

- SAP2000;
- ETABS;
- RFEM;
- SCIA Engineer;
- Midas Gen.

**2. Need for standardization for shells.**

Existing design codes did not provide specific design methods for reinforced concrete slabs where slabs are subjected to both complex forces and moments.

The problem was that until 2023 there was no standardized method in Eurocode for calculating:

- shells with combination of membrane forces and bending moments;
- bridge slabs with complex load;
- tanks, cooling towers, dome structures.

**3. Scientific consensus and experimental database [1-25].**

Thomas Jaeger and Peter Marti conducted 28 tests to failure on fourteen reinforced concrete slab specimens to investigate the effect of deviation of principal shear and moment direction from reinforcement direction [4].

**Research database:**

- dozens of experimental programs (1974 – 2023);
- hundreds of publications in scientific journals;
- method verification on real structures.

**4. Simplicity and practicality.**

**Method advantages:**

- statically equivalent;
- does not require complex FEM for ordinary cases;
- can be implemented manually;
- conservative (safe).

**5.** Integration with other methods of Eurocode EN 1992-1-1:2023**.**

The sandwich method is consistent with:

- clause 8.2 (Shear design);
- clause 9.2 (Crack control);
- clauses 7.3.3 and 7.3.4 (Non-linear analysis) – as an alternative.

Table 1 presents the chronology of sandwich model development.

**Table 1.** Chronology of sandwich model development
**Табл. 1** Хронологія розвитку сендвіч-моделі

| Year | Development |
|---|---|
| 1974 | Brondum-Nielsen: BASIC SANDWICH MODEL (BSM) [Denmark, Technical University]:<br>• three layers<br>• membrane forces + bending moments in outer layers |
| 1990 | Peter Marti: DEVELOPMENT FOR TRANSVERSE FORCES [Switzerland, ETH Zürich]:<br>• transverse forces in core<br>• angle $\theta = 45°$ for compression fields<br>• publication in ACI Structural Journal. |
| 2004 | EN 1992-1-1:2004 (1st generation):<br>• without sandwich method in normative annexes |
| 2010 | fib Model Code 2010:<br>• contains concepts of sandwich method<br>• creates scientific consensus |
| 2013-2014 | Thomas Jaeger: EXTENDED MODEL (ESM) [Switzerland, ETH Zürich]:<br>• cracking in core<br>• aggregate interlock<br>• strain compatibility |
| 2014-2018 | Hernández-Montes: CRITICAL ANALYSIS:<br>• verification of reinforcement yielding<br>• application limitations |
| 2020-2023 | Preparation of EN 1992-1-1:2023 (2nd generation) [CEN/TC 250]:<br>• working group on shells and slabs<br>• integration of sandwich method |
| 2023 | EN 1992-1-1:2023: OFFICIAL INCLUSION:<br>• Annex G (normative) -- sandwich method<br>• based on Brondum-Nielsen + Marti<br>• simplified version without complex refinements<br>• normative status throughout Europe |
| 2023-2026 | Gradual implementation in national standards |

**What led to the conviction for including the sandwich panel in EN 1992-1-1:2023?**

**A. Recommendations of fib (International Federation for Structural Concrete).**

Fib Model Code 2010 [20] already contained similar concepts, which created scientific consensus.

**B. Pressure from practicing engineers.**

Engineers were already using the method in software, but there was no official standard. This created:

- legal problems;
- different interpretation;
- lack of uniform acceptance criteria.

**C. Successful Swiss experience.**

Swiss standards (SIA) already contained Marti's method, which had been successfully used for decades.

**D. Mandate M/515 of the European Commission.**

Eurocodes were developed under Mandate M/515, issued to CEN by the European Commission and European Free Trade Association.

**The mandate required:**

- harmonization of standards in Europe;
- inclusion of modern design methods;
- consideration of software practice.

## CONCLUSIONS

The sandwich method is the result of half a century of evolution of scientific thought and engineering practice, which has finally received official recognition in the most important European standard for concrete structures.

The inclusion of this method in EN 1992-1-1:2023 became possible thanks to:

1) 50 years of successful application (1974-2023);
2) widespread use in software;
3) need for standardization for shells and slabs;
4) solid experimental database (dozens of studies);
5) simplicity and practicality for engineers;
6) conservatism (safety) of the method;
7) requirement of Mandate M/515 of the European Commission;
8) the scientific consensus reached (fib Model Code 2010).

## REFERENCES


1. **Brondum-Nielsen, T.** (1974). Optimum Design of Reinforced Concrete Shells and Slabs. *Technical University of Denmark, Department of Civil Engineering, (R44), 190-200.*
2. **Marti, P.** (1990). Design of Concrete Slabs for Transverse Shear, *ACI Structural Journal, 87(2), 180-190.*
3. **Denton, S., Shave, J., Bennetts, J., & Hendy, C.** (2010). Design of concrete slab elements in biaxial bending. *Conference Paper: Bridge Design to Eurocodes: UK Implementation At: London. UK: ICE publishing; 2011, p. 1–20.*
4. **Jaeger, T., & Marti, P.** (2006). Versuche zum Querkraftwiderstand und zum. *Verformungsvermögen von Stahlbetonplatten, Institut für Baustatik und Konstruktion, Eidgenössische Technische Hochschule Zürich, Monograph, 358.* https://doi.org/10.3929/ethz-a-005195576
5. **Jaeger, T., Marti, P.** (2009). Reinforced Concrete Slab Shear Prediction Competition: Experiments, *ACI Structural Journal, 106(3), 300-308.* http://hdl.handle.net/20.500.11850/11646
6. **Jaeger, T.** (2013). Extended sandwich model for reinforced concrete slabs in flexure, *Engineering Structures, (56), 2229-2239.* https://doi.org/10.1016/j.engstruct.2013.08.032
7. **Jaeger, T.** (2014). Extended sandwich model for reinforced concrete slabs: Shear strength with transverse reinforcement, *Engineering Structures, (74), 218-228.* https://doi.org/10.1016/j.engstruct.2014.05.025
8. **Jensen, T.W., Poulsen, P.N., Hoang L.C.** (2019). Layer model for finite element limit analysis of concrete slabs with shear reinforcement, *Engineering Structures, (195), 51-61.* https://doi.org/10.1016/j.engstruct.2019.05.038
9. **Makhloof, D.A., Ibrahim, A.R., & Ren, X.** (2023). Robust design procedure for RC plates and shell structures using developed advanced sandwich model, *Journal of Building Engineering, (76), 107212.* https://doi.org/10.1016/j.jobe.2023.107212
10. **Gil-Martín, L.M., & Hernández-Montes, E.** (2019). Strain compatibility in the strength design of RC slabs, *Engineering Structures, (178), 423-435.* https://doi.org/10.1016/j.engstruct.2018.10.045
11. **Gil-Martín, L.M., & Hernández-Montes, E.** (2016). Safety levels of the traditional strength design of RC slabs under bending and torsion.

*Engineering Structures, (127), 374-387*. https://doi.org/10.1016/j.engstruct.2016.08.063

12. **Hernández-Montes, E., Carbonell-Márquez, J.F., & Gil-Martín, L.M.** (2014). Limits to the strength design of reinforced concrete shells and slabs. *Engineering Structures, (61), 184-194*. https://doi.org/10.1016/j.engstruct.2014.01.011
13. **Gil-Martín, L.M., & Hernández-Montes, E.** (2020). Influence of the lever arm in the strength design of RC slabs. *The 7th International conference "Civil engineering – science and practice", Kolasin, Montenegro*.
14. **Palermo, M., Gil-Martín, L.M., Trombetti, T., & Hernández-Montes, E.** (2013). In-plane shear behaviour of thin low reinforced concrete panels for earthquake re-construction. *Materials and Structures, (46), 841-856*. https://doi.org/10.1617/s11527-012-9937-8
15. **Lantsoght, E.O.L., van der Veen, C., & Walraven, J.C.** (2013). Shear in One-Way Slabs under Concentrated Load Close to Support. *ACI Structural Journal, (110), 275-284*. https://doi.org/10.14359/51684407
16. **Alchaar, A., & Abed, F.** (2020). Finite element analysis of a thin-shell concrete sandwich panel under eccentric loading. *Journal of Building Engineering, (32), 101804*. https://doi.org/10.1016/j.jobe.2020.101804
17. **Wang, R., Hu, H., & Guo, Z.** (2021). Analytical study of stiffened multibay planar coupled shear walls. *Engineering Structures, (244), 112770*. https://doi.org/10.1016/j.engstruct.2021.112770
18. **Lipari, A.** (2020). A comparative study of shear design methods for straight and skew concrete slabs. *Engineering Structures, (208), 109515*. https://doi.org/10.1016/j.engstruct.2019.109515
19. **Lantsoght, E.O.L., van der Veen, C., Walraven, J.C., & de Boer, A.** (2015). Experimental investigation on shear capacity of reinforced concrete slabs with plain bars and slabs on elastomeric bearings. *Engineering Structures, (103), 1-14*. https://doi.org/10.1016/j.engstruct.2015.08.028
20. FIB. Model Code 2010. Model Code 2010 – Final draft, vol. 1. Fib Bulletin No. 65. Internatio. Lausanne: 2012.
21. **Muttoni, A., Fernandez Ruiz, M., Cavagnis, F. & Simoes, J.T.** (2023). Background document to clauses 8.2.1 and 8.2.2 - Shear in members without shear reinforcement. *Background Document for FprEN 1992-1-1. CEN/TC 250/SC 2 N2087, 298- 310.*
22. **Muttoni, A.** (2023). Background document to clauses 4.3.3 and Annex A – Partial safety factors for materials. *Background Document for FprEN 1992-1-1. CEN/TC 250/SC 2 N2087, 12-32.*
23. **Lipari, A.** (2025). The shear design and assessment of skew reinforced concrete slabs in the new Eurocode 2. *Engineering Structures, (343), 120393*. https://doi.org/10.1016/j.engstruct.2025.120393
24. **Miguel, P.F., Fernandez, M.A., Hegger, & J., Schmidt, M.** (2023). Shear resistance of members without shear reinforcement in presence of compressive axial force in the next Eurocode 2. *Hormigon y Acero 74(299-300), 41-60*. https://doi.org/10.33586/hya.2023.3112
25. **Henze, L., Rombach, G.A., & Harter M.** (2020). New approach for shear design of reinforced concrete slabs under concentrated loads based on tests and statistical analysis. *Engineering Structures, (219), 110795*. https://doi.org/10.1016/j.engstruct.2020.110795

## LITERATURE

1. **Brondum-Nielsen, T.** (1974). Optimum Design of Reinforced Concrete Shells and Slabs. *Technical University of Denmark, Department of Civil Engineering, (R44), 190-200.*
2. **Marti, P.** (1990). Design of Concrete Slabs for Transverse Shear, *ACI Structural Journal, 87(2), 180-190.*
3. **Denton, S., Shave, J., Bennetts, J., & Hendy, C.** (2010). Design of concrete slab elements in biaxial bending. *Conference Paper: Bridge Design to Eurocodes: UK Implementation At: London. UK: ICE publishing; 2011, p. 1–20.*
4. **Jaeger, T., & Marti, P.** (2006). Versuche zum Querkraftwiderstand und zum *Verformungsvermögen von Stahlbetonplatten, Institut für Baustatik und Konstruktion, Eidgenössische Technische Hochschule Zürich, Monograph, 358*. https://doi.org/10.3929/ethz-a-005195576
5. **Jaeger, T., Marti, P.** (2009). Reinforced Concrete Slab Shear Prediction Competition: Experiments, *ACI Structural Journal, 106(3), 300-308.* http://hdl.handle.net/20.500.11850/11646
6. **Jaeger, T.** (2013). Extended sandwich model for reinforced concrete slabs in flexure, *Engineering Structures, (56), 2229-2239.* https://doi.org/10.1016/j.engstruct.2013.08.032
7. **Jaeger, T.** (2014). Extended sandwich model for reinforced concrete slabs: Shear strength with

transverse reinforcement, *Engineering Structures, (74), 218-228.* https://doi.org/10.1016/j.engstruct.2014.05.025

8. **Jensen, T.W., Poulsen, P.N., Hoang L.C.** (2019). Layer model for finite element limit analysis of concrete slabs with shear reinforcement, *Engineering Structures, (195), 51-61.* https://doi.org/10.1016/j.engstruct.2019.05.038
9. **Makhloof, D.A., Ibrahim, A.R., & Ren, X.** (2023). Robust design procedure for RC plates and shell structures using developed advanced sandwich model, *Journal of Building Engineering, (76), 107212.* https://doi.org/10.1016/j.jobe.2023.107212
10. **Gil-Martín, L.M., & Hernández-Montes, E.** (2019). Strain compatibility in the strength design of RC slabs, *Engineering Structures, (178), 423-435.* https://doi.org/10.1016/j.engstruct.2018.10.045
11. **Gil-Martín, L.M., & Hernández-Montes, E.** (2016). Safety levels of the traditional strength design of RC slabs under bending and torsion. *Engineering Structures, (127), 374-387.* https://doi.org/10.1016/j.engstruct.2016.08.063
12. **Hernández-Montes, E., Carbonell-Márquez, J.F., & Gil-Martín, L.M.** (2014). Limits to the strength design of reinforced concrete shells and slabs. *Engineering Structures, (61), 184-194.* https://doi.org/10.1016/j.engstruct.2014.01.011
13. **Gil-Martín, L.M., & Hernández-Montes, E.** (2020). Influence of the lever arm in the strength design of RC slabs. *The 7th International conference "Civil engineering – science and practice", Kolasin, Montenegro*.
14. **Palermo, M., Gil-Martín, L.M., Trombetti, T., & Hernández-Montes, E.** (2013). In-plane shear behaviour of thin low reinforced concrete panels for earthquake re-construction. *Materials and Structures, (46), 841-856.* https://doi.org/10.1617/s11527-012-9937-8
15. **Lantsoght, E.O.L., van der Veen, C., & Walraven, J.C.** (2013). Shear in One-Way Slabs under Concentrated Load Close to Support. *ACI Structural Journal, (110), 275-284.* https://doi.org/10.14359/51684407
16. **Alchaar, A., & Abed, F.** (2020). Finite element analysis of a thin-shell concrete sandwich panel under eccentric loading. *Journal of Building Engineering, (32), 101804.* https://doi.org/10.1016/j.jobe.2020.101804
17. **Wang, R., Hu, H., & Guo, Z.** (2021). Analytical study of stiffened multibay planar coupled shear walls. *Engineering Structures, (244), 112770.* https://doi.org/10.1016/j.engstruct.2021.112770
18. **Lipari, A.** (2020). A comparative study of shear design methods for straight and skew concrete slabs. *Engineering Structures, (208), 109515.* https://doi.org/10.1016/j.engstruct.2019.109515
19. **Lantsoght, E.O.L., van der Veen, C., Walraven, J.C., & de Boer, A.** (2015). Experimental investigation on shear capacity of reinforced concrete slabs with plain bars and slabs on elastomeric bearings. *Engineering Structures, (103), 1-14.* https://doi.org/10.1016/j.engstruct.2015.08.028
20. FIB. Model Code 2010. Model Code 2010 – Final draft, vol. 1. Fib Bulletin No. 65. Internatio. Lausanne: 2012.
21. **Muttoni, A., Fernandez Ruiz, M., Cavagnis, F. & Simoes, J.T.** (2023). Background document to clauses 8.2.1 and 8.2.2 - Shear in members without shear reinforcement. *Background Document for FprEN 1992-1-1. CEN/TC 250/SC 2 N2087, 298- 310.*
22. **Muttoni, A.** (2023). Background document to clauses 4.3.3 and Annex A – Partial safety factors for materials. *Background Document for FprEN 1992-1-1. CEN/TC 250/SC 2 N2087, 12-32.*
23. **Lipari, A.** (2025). The shear design and assessment of skew reinforced concrete slabs in the new Eurocode 2. *Engineering Structures, (343), 120393.* https://doi.org/10.1016/j.engstruct.2025.120393
24. **Miguel, P.F., Fernandez, M.A., Hegger, & J., Schmidt, M.** (2023). Shear resistance of members without shear reinforcement in presence of compressive axial force in the next Eurocode 2. *Hormigon y Acero 74(299-300), 41-60.* https://doi.org/10.33586/hya.2023.3112
25. **Henze, L., Rombach, G.A., & Harter M.** (2020). New approach for shear design of reinforced concrete slabs under concentrated loads based on tests and statistical analysis. *Engineering Structures, (219), 110795.* https://doi.org/10.1016/j.engstruct.2020.110795

# ІСТОРІЯ ВИНИКНЕННЯ ТА РОЗВИТКУ СЕНДВІЧ-МОДЕЛІ ДЛЯ РОЗРАХУНКУ МЕМБРАННИХ, ОБОЛОНКОВИХ ТА ПЛИТНИХ ЕЛЕМЕНТІВ ЗГІДНО З EN 1992-1-1:2023

*Леонід СКОРУК*

**Анотація.** Вперше в європейських нормах проектування бетонних конструкцій, зокрема в Додатку G (обов'язковий), у новій версії Єврокоду EN 1992-1-1:2023 приділено прицільну увагу проектуванню мембранних, оболонкових та плитних елементів та пропонується сучасний підхід для їх розрахунку.

У якості методу оптимального розрахунку залізобетонних оболонок, плит та мембран в Додатку G пропонується, так звана, **сендвіч-модель** – коли оболонка представляється як тришарова модель з двох несучих шарів (верхній і нижній) та проміжного шару між ними.

При розрахунку за сендвіч-моделлю – просторова задача (згин + крутіння + мембранні зусилля) перетворюється у дві мембранні задачі для верхнього та нижнього шарів. Тобто перетворення просторового напруженого стану на два шари (верхній і нижній) з еквівалентними мембранними напруженнями.

Модель сендвіча – це строга механічна модель, яка дозволяє звести складну просторову задачу (оболонка з комбінованими зусиллями) до двох незалежних плоских задач (мембранні елементи у верхньому та нижньому шарах) через статично еквівалентне перетворення зусиль у напруження.

Сендвіч-модель базується на перетворенні комбінації зусиль (мембранних, згинальних і крутних) у статично еквівалентну систему плоских напружень, які діють у верхньому та нижньому шарах моделі.

Основні припущення методу:

а) тришарова модель: оболонка представляється як конструкція з двох несучих шарів (верхній і нижній) та проміжного шару між ними

б) статична еквівалентність: внутрішні зусилля перетворюються у плоскі напруження так, щоб зберегти повну статичну рівновагу

в) незалежний розрахунок шарів: кожен шар (верхній і нижній) розраховується окремо як мембранний елемент згідно п. G.3

Формулювання, що представлені в Додатку G EN 1992-1-1:2023 у пунктах G.3 та G.4, узгоджуються з пунктами та положеннями щодо проектування у розділі 8 (Граничні стани міцності (ULS)) основного тіла документу, а пункт G.5 містить додаткові положення до 9.2 (Контроль тріщин) зазначених норм. Додаток G охоплює проектування плоских елементів без розривів бетонного масиву на окремі частини. При цьому можуть бути використані інші, більш вдосконалені методи розрахунку, що відповідають п.7.3.3 (Пластичний аналіз) або п.7.3.4 (Нелінійний аналіз) Єврокоду 2.

Таким чином, Додаток G (Проектування мембранних, оболонкових та плитних елементів) не замінює, а доповнює основні розділи Єврокоду 2, а саме – загальні принципи, матеріали (діаграми σ-ε), розрахунок перерізів на ULS, тріщиностійкість та SLS

**Ключові слова**: розрахунок мембранних, оболонкових та плитних елементів; сендвіч-модель

***Received:*** *November 04, 2025.*
***Accepted:*** *December 05, 2025*

ISSN 2522-4182

DOI: 10.32347/2522-4182.17.2025.189-199
УДК624.9

# ANALYSIS OF SOME CASES RESIDENTIAL BUILDINGS DESTRUCTION AS A RESULT OF COMBAT ACTIONS

*Valeriy NUZHNYI[1], Vira KOLIAKOVA[2]*

[1,2] Kyiv National University of Construction and Architecture
31, Povitryanykh Syl Ave., Kyiv, Ukraine, 03037
[1] nuzhnyi.vv@knuba.edu.ua https://orcid.org/0000-0002-0400-3204
[2]koliakova.vm@knuba.edu.ua, http://orcid.org/0000-0001-6879-8520

**Abstract.** The problem of residential infrastructure destruction as a result of the aggression of the Russian Federation is very relevant in Ukraine. If houses are subject to major repairs, they may have various damages, from major to relatively minor. Also, during inspections, the consequences of long-term fires that were not extinguished and the structures from the fire have completely lost their load-bearing capacity are often found. Such damages can be severe and localized within the framework of the frame cells, apartments, rooms on the lower floors, which makes it impossible to carry out radical actions, such as complete replacement. For example, replacing structures could require dismantling the floors above, which is not advisable.

This article provides examples of failures that have been encountered in practice when developing major renovation projects. It highlights aspects of deeper problems that are not obvious at first glance. Insufficient consideration of these factors leads to inappropriate decisions that require adjustments during the work process. This actually leads to an increase in the cost of major renovations that were not previously taken into account.

The article provides recommendations for making optimal, and often the only possible, decisions when developing major building renovation projects.

**Keywords:** damage**;** building structures; destruction; fire damage; major repairs.

**Valeriy NUZHNYI**
Lector Department of Steel and Timber Structures,
PhD (Tech. Sci.)

**Vira KOLIAKOVA**
Associate Professor, Department of Reinforced Concrete and Stone Structures
Assoc. Prof., PhD (Tech. Sci.)

## INTRODUCTION

In the modern realities of Ukraine, unfortunately, the topic of damage to buildings and structures as a result of hostilities is very relevant. Since 2022, a number of publications have been published on this topic in professional publications, which characterize various aspects of this issue. These works also propose methods for performing major repairs and strengthening building structures.

In this article, I would like to present somewhat more in-depth research into rather narrow aspects of this issue. I would like to mainly present interesting practical examples that the authors encountered when inspecting buildings and structures and when choosing a method of reparation.

## ANALYSIS OF CURRENT RESEARCH

The topic of the impact of wars and terrorist acts on building structures in peacetime is a topic of a narrow circle of scientists involved in military science, weapons development and

civil defense, including standards [1, 2, 3, 4]. In a broader sense, in the field of civil engineering, this topic arises and acquires wide and deep relevance only when, unfortunately, the country's society is faced with the consequences of tragic periods of its history during wars and armed conflicts. Ukraine is no exception in this case..

Modern research can be conditionally divided into several directions. The first direction is the study of the features of the action of weapons on structures, the analysis of force effects, methods for calculating penetration, shock waves, etc. [5, 6, 7]. The second direction of research is the topic of designing civil defense structures and protecting civil infrastructure [8, 9, 10, 11]. The third direction of research can be called the generalization and study of the consequences of the impact of weapons on structures, the phenomenology of destruction and methods of major repairs of damaged building structures. Such works include a comparison of the survivability and features of destruction of buildings with different structural schemes, as well as methods of their restoration and strengthening [12,13,14, 15,16,17, 18, 19, 20]. Also, in recent years, state standards and building codes have been significantly improved [21, 22]. Thus, the DSTU [21] already contains typical schemes and recommendations for assessing the technical deterioration of buildings damaged as a result of hostilities and terrorist acts.

This article also belongs to the direction of research on destruction, in which some practical examples from empirical experience are presented and their evaluation and generalization are provided.

## STATEMENT OF RESEARCH GOALS

When examining the structures of buildings and structures damaged by combat operations, mechanical destruction caused by the action of weapons can be observed.

The effect of ammunition on building structures is characterized by the following effects:

1. Shock-impulse action due to a direct impact from the arrival of the ammunition;
2. The explosion of an ammunition, which causes a direct explosive high-explosive effect, is also characterized by the following effects:
   - Damage by the scattering of primary fragments from the explosion of the ammunition;
   - Damage by the scattering of secondary fragments from destroyed structures, furniture, doors, etc.;
   - Damage by a blast wave that creates excessive pressure on the structure and can lead to serious destruction and can break glass in a radius of up to 200..250 m depending on the presence of obstacles in the wave path [1];
3. The effect of high temperatures and fire.

The peculiarity of this impact is that the fire spreads quickly, massively and cannot always be quickly and effectively extinguished by fire brigades due to the fact that either hostilities are taking place in the given area or an air raid is ongoing.

At the same time, the force and temperature effects exceed any calculated and permissible factors that were taken into account when designing buildings and structures.

To correctly assess the consequences of the effects that arose when a weapon hit, it is necessary to understand the nature of the impact itself, the force factors that acted and caused the consequences. Also very useful is any information on the studied precedents and analogues of destruction, which would allow a more accurate assessment of the consequences, make an adequate decision and more accurately recognize the technical and economic indicators and parameters of major repairs at the design stage. Therefore, the purpose of this article is to show and summarize some typical cases of damage that the authors encountered in practice.

## MATERIALS AND RESEARCH METHODS

The authors investigated specific cases that were considered during detailed inspections of multi-storey residential buildings in the Kyiv

region in Bucha, Irpen, and Gostomel, where active hostilities took place in February-March 2022.

These houses were completely renovated. During the clearing and reinforcement of the affected areas, some damaged structural elements had more hidden defects and damage than it seemed at first glance. As a result, it was necessary to adjust the design solutions..

The second serious impact is the prolonged action of the fire, which was not extinguished. The structures were severely damaged beyond the fire resistance limit, which required adequate assessment and decision-making..

## TEACHING THE BASIC MATERIAL

All mechanical damage is short-term in action and very strong, being beyond the working limit of materials. This is manifested both in the impulse action of a direct impact by a munition upon impact, and in the action of a blast wave.

An interesting case may be the one that occurred in the city of Bucha, when a mortar shell hit the balcony slab of a residential building on the 7th floor of a 8-story residential building with brick longitudinal load-bearing walls.

The damage diagram is shown in Fig. 1. Photo in Fig. 2. Thus, as a result of the impact of a mortar shell, a balcony slab was damaged. A corner was knocked out and destroyed in the slab, and at the same time, deep cracks were visible in the partition wall, in which this slab was pinched from the side of the affected corner. The nature of the cracks development, depth, and area of distribution were not visible at first glance. The facade insulation on the wall was also destroyed and the wall surface itself was damaged by blast fragments. At the same time, beacons were installed on the cracks, which showed further progression of the crack opening, as a result of which the company operating the building decided to install supports within the opening.

When attempting to pull the wall together with a metal clamp, it was discovered that it had delaminated across the entire height and area within the 7th floor and as a result required complete re-laying. This was accomplished with sequential dismantling, re-supporting, and re-laying of the masonry in sections.

In the final conclusion, such destruction can be considered typical when ammunition hits the balcony slab and it can lead to progressive destruction of the wall within the upper floors with the collapse of the slabs. In the described case, it was fortunate that the impact occurred on the penultimate floor and the load on the laminated partition was not large and measures for temporary support were taken in time.

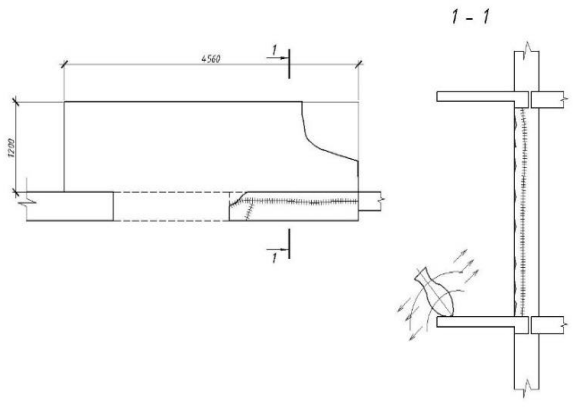


**Fig. 1** Diagram of structural damage due to a mortar shell hitting a balcony slab

**Рис. 1** Схема конструктивних пошкоджень, спричинених влучанням мінометного снаряда в плиту балкону

**Fig. 2** Appearance of the crack from the end of the wall. Photo by V. Nuzhnyi

**Рис. 2** Тріщини на торці стіни. Автор фото В.Нужний

Another type of damage worth paying attention to is massive damage to monolithic reinforced concrete frame buildings from impacts, shell explosions, and fire.

Thus, a multi-storey residential building in the city of Irpin was located in a combat zone and suffered massive damage. The exterior of the building is presented in Fig. 3.

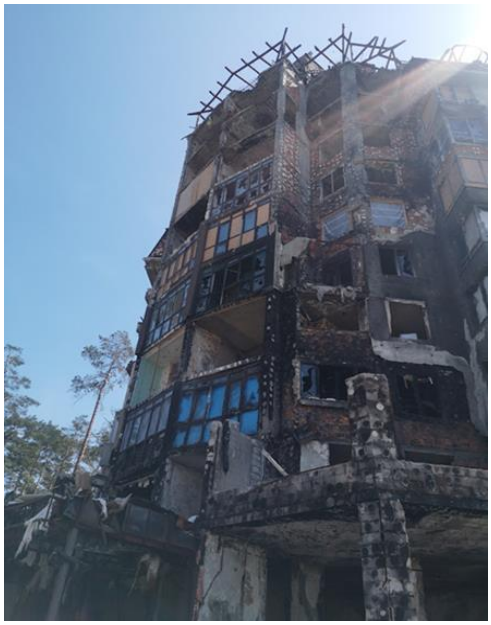

**Fig. 3** Exterior view of a section of a building with a monolithic reinforced concrete frame that was damaged during hostilities. Photo by V. Nuzhnyi

**Рис. 3** Зовнішній вигляд фрагмента будівлі з монолітним залізобетонним каркасом, пошкодженої під час бойових дій. Автор фото В. Нужний

In this building, the consequences of the arrival of shells, mortar shells were observed, which caused both mechanical damage and long-term fires. The roof with the attic floor was completely destroyed and all the damage was localized - within the apartments, rooms. The total amount of damage did not exceed 30..35%. Therefore, it was decided to save the house and carry out its major repairs. The structures of the corner section, which is presented in Fig. 3, were especially damaged. Starting from the 6th floor, the frame elements had massive damage (see Fig. 4, 5, 6, 7).

**Fig. 4** External view of the damage within the floor. Photo by V. Nuzhnyi

**Рис. 4** Зовнішній вигляд пошкоджень у межах перекриття. Автор фото В. Нужний

**Fig. 5.** Pylon hit by a projectile. Photo by V. Nuzhnyi

**Рис. 5** Пілон, уражений снарядом. Автор фото В. Нужний

**Fig. 6** Damage to the frame slab and columns. Photo by V. Nuzhnyi

**Рис. 6** Пошкодження плит перекриття та колон каркаса. Автор фото В. Нужний

**Fig. 7** Damage to the frame plate from Fig. 6, bottom view. Photo by V. Nuzhnyi

**Рис. 7** Пошкодження плити каркаса з рис. 6, вигляд знизу. Автор фото В. Нужний

After damage analysis, it was considered appropriate to dismantle the building frame, starting from the 6th floor. The main factor in making this decision was the significant damage to the columns and pylons (see Fig. 5 and 6). With such crushing of the concrete with the exposure of the reinforcement, the integrity of the structure is completely lost. There are also distortions of the floors located above, which, even if they are relatively intact, require dismantling.

Some damage to floors from shell and mine impacts leads to significant damage around it, which must be taken into account when designing major repairs. Thus, the floor penetration shown in Fig. 6 and 7 was cleared of splintered and cracked concrete around it, and as a result, the damage zone turned out to be almost equal in area to a cell (see Fig. 8).

Similarly, it is possible to classify less extensive damage at first glance, for example, through-hole damage to a pylon by a projectile, which leads to a 50..60% loss of strength (see Fig. 9). Moreover, any through-hole damage is characterized by a small hole at the entrance and large-scale chipping of concrete with destruction of the reinforcing frame at the exit.

**Fig. 8** Cleared impact zone from Figs. 6 and 7, which nearly corresponds to the dimensions of a structural bay. Photo by V. Nuzhnyi

**Рис. 8** Розчищена зона ураження з рис.6 і 7, що майже відповідає розмірам чарунки каркаса. Автор фото В. Нужний

**Fig. 9** Through-hole damage to the pylon. Photo by V. Nuzhnyi

**Рис. 9** Сквозне пошкодження пілона. Автор фото В. Нужний

An example of clearing a small hole from a small-caliber projectile or mortar in a ceiling with a total diameter of up to 150 mm can also be given. Despite the fact that such an impact did not cause significant deformations and damage to the reinforcing frame at first glance, the concrete damage zone was about 1x1 m and had to be cleared (see Fig. 10).

**Fig. 10** Cleaning damaged concrete after a pinpoint hit by a small-caliber projectile. Photo by V. Nuzhnyi

**Рис. 10** Очищення пошкодженого бетону після точкового влучання дрібно-каліберним снарядом. Автор фото В. Нужний

Another impact on the elements of the building frame was the action of fire, which was not extinguished. In addition to explosive special agents in high-explosive ammunition and chemical cumulative action. The structures were affected by the repeated long-term burning of furniture, interior decoration elements, etc. If a fire occurs in round-hole prefabricated panels, the phenomenon of their destruction is described in [13, 19] and they are usually subject to replacement with monoline sections, steel beam floors with reinforced concrete roll, etc.

In the case of prolonged burning of a reinforced concrete frame, the following phenomena occur in structures:

- dehydration of cement, change in color of concrete to whitish-grayish, yellow, sometimes pink with a significant decrease in concrete strength to zero;
- tempering of heat-strengthened reinforcement produced in recent years. Any heating to a temperature above 400˚C leads to the beginning of tempering and a decrease in the mechanical properties of steel;
- destruction of the protective layer, exposure of reinforcement, temperature deformations, destruction of reinforcement and, as a result, destruction of the calculated reinforced concrete cross-section;
- development of large-scale cracks in the frame, especially in floors adjacent to diaphragm elements - stairwells, basement walls, etc. During a fire, the local area of the floor is unevenly squeezed between neighboring rigid vertical structures under conditions of thermal expansion. This causes cracking and the appearance of serious cracks.

The last described phenomena are characteristic both for floor slabs and for vertical monolithic reinforced concrete elements - diaphragms, pylons. The consequences of typical large-scale fire damage to floor sections are shown in Fig. 11 and 12.

**Fig. 11** Effects of fire on floor slab. Photo by V. Nuzhnyi

**Рис. 11** Наслідки пожежі на плиті перекриття. Фото В. Нужного

The bearing capacity of such structures cannot be assessed in any way according to [23, 24, 25], since the structural integrity of the calculated cross-section is completely destroyed. The picture is complicated by the fact that such damage is not massive in nature but is localized within certain cells (where there were rooms in which the fire occurred, and there were no neighboring ones). Thus, demolishing the house is not economically feasible, and replacing the floor in the conditions of the existing frame is complicated by the impossibility of complete replacement and re-supporting of the columns.

**Fig. 12** Complete destruction of the working reinforcement in the ceiling after prolonged exposure to fire. Photo by V. Nuzhnyi

**Рис. 12** Повне руйнування робочої арматури в перекритті після тривалого впливу вогню. Автор фото В. Нужний

Fig. 12 shows the complete destruction of the reinforcing mesh of the basement floor as a result of a multi-day fire in the basement, where office premises were located. When clearing the affected areas of concrete, it turned out that the cross-section of the slab had completely lost its strength throughout. As a result, a relatively large section of the floor was removed (see Fig. 13).

**Fig. 13.** Cleared area of the ceiling after the fire, shown in Fig. 12. View from the upper floor. Photo by V. Nuzhnyi

**Рис. 13.** Розчищена ділянка перекриття після пожежі, показаної на рис. 12. Вид з верхнього поверху. Автор фото В. Нужний

The described destructions are complex from the point of view of capital repairs. Replacing floors, re-supporting new ones on existing columns is a rather complex and sometimes impossible task. Its complexity lies in the impossibility of restoring the adhesion of the new part to the existing one, the impossibility of restoring the support prisms of the thrust on the columns that continue to the higher floors, etc. Therefore, the simplest of the proposed methods of repairing such floors is to introduce steel brackets on the columns and arrange steel beam cells on them using welded I-beams and closed double-walled sections, paired I-beams, etc. (see Fig. 14). The main condition for such a beam system is a small height. Provided that the beams are made with a height of up to 140..150 mm and they are covered with a plasterboard ceiling, the height and functional purpose of the room do not significantly decrease.

**Fig. 14** Reinforcement of the floor slab after a fire by adding steel beams. Photo by V. Nuzhnyi
**Рис. 14** Армування плити перекриття після пожежі шляхом додавання сталевих балок. Автор фото В. Нужний

## CONCLUSIONS AND PROSPECTS FOR FURTHER RESEARCH

Unfortunately, the problem of destruction, while hostilities are ongoing, remains relevant. The boundaries of this problem cannot be determined, because the action of weapons is random in nature. Damage and injuries can be diverse and are the consequences of a complex action - impact, explosive action, fragmentation with penetration and thermal and chemical effects of fire..

Minor mechanical damage can lead to a chain of events that will lead to large-scale collapsive collapse. For example, the example of a balcony slab being hit by a small-caliber mortar shell shows how load-bearing walls can be damaged.

When performing spot repairs on the scale of the entire frame, where it is not advisable to dismantle the floors located above, it has been shown that it is advisable to use reinforcement by introducing steel beam cells.

Therefore, such cases, their patterns, require descriptions and the creation of a kind of database with recommendations and typical reinforcement solutions for mass implementation.

## REFERENCE


1. **David Cormie, Geoff Mays, Peter Smit**h Blast Effects on Buildings. *Third edition ICE Publishing – London -2020*
2. **NATO - ATP-3.12.1.8** Test Procedures and Classification of the Effects of Weapons on Structures. *nsa, 2021.2.*
3. **UFC 4-023-07**: Design to Resist Direct Fire Weapons Effects (Change 1). *U.S. Department of Defense. (2017) Washington, D.C.: Unified Facilities Criteria.*
4. **H. M. Wen** (2002) Predicting the penetration and perforation of targets struck by projectiles at normal incidence*, Mec*hanics of Structures and Machines, (30:4), 543-577 DOI: 10.1081/SME-120015076
5. **Mykhaylovskyi, D. ., Skliarov, I., & Komar, O.** (2025). Comparison of methods for calculating the parameters of an explosion shock wave for the design of protective engineering structures. *Building Constructions. Theory and Practice, (16), 110–122.* [in English] https://doi.org/10.32347/2522-4182.16.2025.110-122
6. **Chyrva, T., Martynov, V., & Koliakova, V.** (2022). The influence of blasting on buildings and constructions. *Building Constructions. Theory and Practice*, (10), 143–149**.** [in English] https://doi.org/10.32347/2522182.10.2022.143-149
7. **Ivanchenko, G., Getun, G., Bezklubenko, I., Solomin, A., & Posternak., O.** (2023) Influence of explosive loads on buildings and structures of the population civil protection. *Strength of Materials and Theory of Structures (111), 108–117.* [in Ukrainian] https://doi.org/10.32347/2410-2547.2023.111.39-48
8. **Getun, G., Bezklubenko, I., Solomin, A., & Balina, O.** (2023). Features of volume-planning decisions of civil defense protective structures. *Current Problems of Architecture and Urban Planning*, (67), 203–220. [in Ukrainian] https://doi.org/10.32347/2077-3455.2023.67.203-220
9. **Vadimov, V., & Pydko, M.** (2024). Problems of civil protection of residential buildings in the cities of Ukraine in the context of sustainable development. *Current Problems of Architecture and Urban Planning*, (69), 140–156 [in Ukrainian]

https://doi.org/10.32347/2077-3455.2024.69.140-156

10. **Getun, G., Koliakova, V., Bezklubenko, I. ., & Solomin, A.** (2023). Constructive solutions for explosion-resistant buildings with civil protection facilities. *Building Constructions. Theory and Practice*, (13), 41–50. [in Ukrainian] https://doi.org/10.32347/2522-4182.13.2023.41-50.
11. **Mykhaylovskyi, D. (2025). E**volution of fortification and protective structures. *Building Constructions. Theory and Practice*, (16), 183–211. [in Ukrainian] https://doi.org/10.32347/2522-4182.16.2025.183-211
12. **Shekhovtsov, V. ., Fesenko, O., Malakhov, V., & Bondarenko, O.** (2024). Renovation with height increasing of residential buildings of the 1960s made of precast concrete. *Building Constructions. Theory and Practice*, (14), 67–78. [in Ukrainian] https://doi.org/10.32347/2522-4182.14.2024.67-7813.
13. **Dobrokhlop, M., & Dobrokhlop, Y.** (2024). Results of the technical investigation of the Logistics Center in Brovary after the rocket and artillery fire in March 2022. *Building Constructions. Theory and Practice*, (15), 66–74. [in Ukrainian] https://doi.org/10.32347/2522-182.15.2024.66-74
14. **Binkevych, K., Volodymyrov, A., & Kolchanov, A.** (2024). Analysis of destructions and strengthening methods of precast reinforced concrete floor panels. *Collection of Scientific Works of the Ukrainian State University of Railway Transport, (208), 67-79* [in Ukrainian] https://doi.org/10.18664/1994-7852.208.2024.308565
15. **Melashenko, Yu., Sliusarenko, Yu., Ishchenko, Yu., & Pavliuk, Ye.**. (2023). Experience in surveying of panel houses damaged from hostilities. *Science and Construction, 36(2), 41-50.* [in Ukrainian] https://doi.org/10.33644/2313-6679-2-2023-5.
16. **Tabarkevych, N., Serhiichuk, V., Belokon, A., & Tabarkevych, O.** (2023). Details of the survey and assessment of the state of residential building damaged due to military actions. Suitability for further operation *Abstract. Science and Construction, 35(1), 27-42* [in Ukrainian] https://doi.org/10.33644/2313-6679-1-2023-4
17. **Lisenyi, O., Hlukhovskyi, V., Marienkov, M., Dubovyk, S., Liubchenko, I., & Yakovenko, M.** (2023). Survey, Assessment of the Technical Condition, and Conditions for the Restoration of a Residential Building at 6-A V. Lobanovskyi Avenue in Kyiv Damaged as a Result of Military Actions. *Science and Construction*, 33(3–4). [in Ukrainian] https://doi.org/10.33644/10.33644/2313-6679-34-2022-6
18. **Donets, T.** (2024). Characteristics of damage to buildings with different structural systems as a result of military actions. *Science and Construction*, *40*(2). [in Ukrainian] https://doi.org/10.33644/2313-6679-2-20246
19. **Nuzhny, V.** (2022). First investigations of damage to buildings and structures as a consequence of combat actions. *Building Constructions. Theory and Practice*, (11), 104–114. [in Ukrainian] https://doi.org/10.32347/2522-4182.11.2022.104-114
20. **Менейлюк, О. І., Менейлюк, І. О., & Русский, В. В.** (2024). Research of the condition of buildings and structures damaged due to military actions. *Building Production*, (75), 17-26. [in Ukrainian] https://doi.org/10.36750/2524-2555.75.17-26.
21. **DSTU 9273:2024.** Guidelines for the Inspection of Buildings and Structures for Determining and Assessing Their Technical Condition. Mechanical Resistance and Stability: *[Entered into force on 2024-02-01]. Kyiv: State Standard of Ukraine, 2024. 47 p. (National Standard of Ukraine).*
22. **DBN V.2.2-5:2023** Protective Structures of Civil Protection: [Effective from 2023-09-01]. *Kyiv: Ministry for Communities and Territories Development of Ukraine, 2023. 140 p. (State Building Codes of Ukraine).*
23. **DBN V.1.1-7:2016** Fire Safety of Construction Sites. General Requirements [Text]: *[Effective from 2017-06-01] / Ministry for Communities and Territories Development of Ukraine. Kyiv: [s.n.], 2016. 60 p. (State Building Codes of Ukraine).*.
24. **Колякова, В.М., Божинський. М.О., & Фесенко О.А.** (2016) Розподіл температури в перерізі залізобетонної плити. *Сучасні технології та методи розрахунків у будівництві. Луцьк: ЛНТУ.(5), 232-239.*
25. **Поклонський, В.Г. Фесенко, О.А. & Тарасюк В.Г.** та ін. (2016). Розрахунок залізобетонних конструкцій на вогнестій-

кість відповідно до Єврокоду 2. Практичний посібник. *К.:Інтертехнологія,* 83 с

LITERATURE


1. **David Cormie, Geoff Mays, Peter Smit**h Blast Effects on Buildings. *Third edition ICE Publishing – London -2020*
2. **NATO - ATP-3.12.1.8** Test Procedures and Classification of the Effects of Weapons on Structures. *nsa, 2021.2.*
3. **UFC 4-023-07**: Design to Resist Direct Fire Weapons Effects (Change 1). *U.S. Department of Defense. (2017) Washington, D.C.: Unified Facilities Criteria.*
4. **H. M. Wen** (2002) Predicting the penetration and perforation of targets struck by projectiles at normal incidence*, Mec*h*anics of Structures and Machines, (30:4), 543-577* DOI: 10.1081/SME-120015076
5. **Mykhaylovskyi, D. ., Skliarov, I., & Komar, O.** (2025). Comparison of methods for calculating the parameters of an explosion shock wave for the design of protective engineering structures. *Building Constructions. Theory and Practice, (16), 110–122.* https://doi.org/10.32347/2522-4182.16.2025.110-122
6. **Chyrva, T., Martynov, V., & Koliakova, V.** (2022). The influence of blasting on buildings and constructions. *Building Constructions. Theory and Practice*, (10), 143–149**.** https://doi.org/10.32347/2522182.10.2022.143-149
7. **Ivanchenko H. M., Hetun H. V., Bezklubenko I. S., Solomin A. V.** (2023). Vplyv vybukhovykh navantazhen na budivli ta sporudy tsyvilnoho zakhystu naselennia *Opir materialiv i teoriia sporud.(111), 108–117.* https://doi.org/10.32347/2410-2547.2023.111.39-48
8. **Hetun H. V., Bezklubenko I. S., Solomin A. V., Balina O. I. (**2023). Osoblyvosti obiemno-planuvalnykh rishen zakhysnykh sporud tsyvilnoho zakhystu *Suchasni problemy arkhitektury ta mistobuduvannia. (67), 216–225* https://doi.org/10.32347/2077-3455.2023.67.203-220
9. **Vadimov, V.M., & M.O. Pydko.** (2024). Problemy tsyvilnoho zakhystu zhytlovoi zabudovy v mistakh Ukrainy v konteksti staloho rozvytku Suchasni problemy arkhitektury ta mistobuduvannia. (69), 140–156. https://doi.org/10.32347/2077-3455.2024.69.140-156
10. . **Hetun, H., Koliakova, V., Bezklubenko, I., & Solomin, A.** (2023). Konstruktyvni rishennia vybukhostiikykh budivel z prymishchenniamy tsyvilnoho zakhystu naselennia. *Budivelni konstruktsii. Teoriia i praktyka, (13), 41–50.* https://doi.org/10.32347/2522-4182.13.2023.41-50
11. **Mykhailovskyi, D.** (2025). Evoliutsiia fortyfikatsiinykh i zakhysnykh sporud. *Budivelni konstruktsii. Teoriia i praktyka, (16), 183–211.* https://doi.org/10.32347/2522-4182.16.2025.183-211
12. **Shekhovtsov , V., Fesenko, O., Malakhov , V., & Bondarenko, O. (**2024). Vidnovlennia iz nadbudovoiu zhytlovykh budynkiv masovykh serii 1960-kh rokiv zi zbirnoho zalizobetonu. *Budivelni konstruktsii. Teoriia i praktyka, (14), 67–78.* https://doi.org/10.32347/2522-4182.14.2024.67-78.
13. **Dobrokhlop , M., & Dobrokhlop , Ye.** (2024). Rezultaty tekhnichnoho obstezhennia lohistychnoho tsentru u m.Brovary, pislia raketno - artyleriiskoho obstrilu u berezni 2022 roku. *Budivelni konstruktsii. Teoriia i praktyka, (15), 66–74* https://doi.org/10.32347/2522-182.15.2024.66-74
14. **Binkevych, K., Volodymyrov, A., & Kolchanov, A.** (2024). Analiz destruktsii i metodiv pidsylennia zbirnykh zalizobetonnykh panelei perekryttiv. *Zbirnyk naukovykh prats Ukrainskoho derzhavnoho universytetu zaliznychnoho transportu, (208), 67-79* https://doi.org/10.18664/1994-852.208.2024.308565
15. **Melashenko Yu., Sliusarenko Yu., IshchenkoIu., & Pavliuk, Ye.** (2023). Dosvid obstezhennia panelnykh budynkiv, poshkodzhenykh vnaslidok boiovykh dii. *Nauka ta budivnytstvo. 36(2),41-50.* https://doi.org/10.33644/2313-6679-2-2023-5.
16. **Tabarkevych, N., Serhiichuk, V., Bielokon A., & Tabarkevych., O..** (2023). Osoblyvosti obstezhennia ta otsinky tekhnichnoho stanu zhyt-lovoho budynku, poshkodzhenoho vnaslidok viiskovykh dii, shchodo yoho prydatnosti do podalshoi ekspluatatsii. *Nauka ta budivnytstvo..(1),. 27-42* **.** https://doi.org/10.33644/2313-6679-1-2023-4
17. **Lisenyi, O.M., Hlukhovskyi , V.P., Marienkov, M.H., Dubovyk, S.O., Liubchenko, I.H., & Yakovenko M.S.** (2022). Obstezhennia, otsinka tekhnichnoho stanu ta umovy

vidnovlennia zhytlovoho budynku na prospekti Lobanovskoho, 6-A v m. Kyievi, poshkodzhenoho vnaslidok voiennykh dii. *Nauka ta budivnytstvo. (3-4), 55-68.* https://doi.org/10.33644/10.33644/2313-6679-34-2022-6

18. **Donets, T.** (2024). Kharakterystyka posh-kodzhen budivel z riznymy konstruktyvnymy systemamy vnaslidok voiennykh dii.. *Nauka ta budivnytstvo, 40(2).* https://doi.org/10.33644/2313-6679-2-2024-6
19. **Nuzhnyi, V.V.** 2022. .Pershi doslidzhennia ushkodzhennia budivel i sporud vnaslidok boiovykh dii *Budivelni konstruktsii. Teoriia i praktyka. (11), 104-114* https://doi.org/10.32347/2522-4182.11.2022.104-114
20. **Meneiliuk, O., Meneiliuk, I., & Russkyi V.** (2023). Doslidzhennia stanu budivel ta sporudposhkodzhenykh vnaslidok voiennykh dii. *Budivelne vyrobnytstvo. (75), 17-26.* https://doi.org/10.36750/2524-2555.75.17-26**.**
21. **DSTU 9273:2024.** Nastanova shchodo obstezhennia budivel i sporud dlia vyznachennia ta otsiniuvannia yikhnoho tekhnichnoho stanu. Mekhanichnyi opir ta stiikist : [Nabuv chynnosti 2024–02–01]. Kyiv : Derzhstandart Ukrainy, 2024. 47 s. (Natsionalnyi standart Ukrainy).
22. **DBN V.2.2-5:2023** Zakhysni sporudy tsyvilnoho zakhystu : [Chynnyi vid 2023-09-01]. Kyiv : Minrehion Ukrainy, 2023. 140 s. (Derzhavni budivelni normy Ukrainy).
23. **DBN V.1.1-7:2016** Pozhezhna bezpeka obiektiv budivnytstva. Zahalni vymohy [Tekst] : [chynnyi vid 2017-06-01] / Minrehion Ukrainy. — Kyiv : [B. v.], 2016. — 60 s. — (Derzhavni budivelni normy Ukrainy).
24. **Koliakova, V.M., Bozhynskyi, M.O., & , O.A. (**2016). Rozpodil temperatury v pererizi zalizobetonnoi plyty. *Suchasni tekhnolohii ta metody rozrakhunkiv u budivnytstvi. Lutsk: LNTU.(5), 232-239.*
25. **Poklonskyi, V.H. Fesenko, O.A. & Tarasiuk V.H.** ta in (2016). Rozrakhunok zalizobeton-nykh konstruktsii na vohnestiikist vidpovidno do Yevrokodu 2. Praktychnyi posibnyk *K.: Intertekhnolohiia,– 83 s*

***Received:*** *November 01, 2025.*
***Accepted:*** *December 05, 2025*

# АНАЛІЗ ДЕЯКИХ ВИПАДКІВ РУЙНУВАНЬ ЖИТЛОВИХ БУДИНКІВ ВНАСЛІДОК БОЙОВИХ ДІЙ

*Валерій НУЖНИЙ,*
*Віра КОЛЯКОВА*

**Анотація.** Дуже актуальною в Україні є проблема руйнувань житлової інфраструктури внаслідок агресії Російської Федерації. Якщо будинки підлягають капітальному ремонту, то вони можуть мати різні ураження, від великих до відносно не значних. Також при обстеженнях часто наявні наслідки тривалих пожеж, котрі не гасилися і конструкції від вогню втратили повністю несучу здатність. Такі ураження можуть носити важкий характер і локалізуватися в межах, чарунок каркасу, квартир, кімнат в нижніх поверхах, що унеможливлює виконання радикальних дій., Наприклад заміна конструкцій могла б вимагати демонтажу розашованих вище поверхів, що не є доцільним.

В даній статті наведені приклади уражень, з якими довелося стикнутися на практиці при розробці проектів капітального ремонту. Вказані аспекти більш глибоких проблем, які не є очевидними на перший погляд. Недостатнє врахування цих факторів призводить до прийняття невідповідних рішень, які потребуюь коригування в процесі робт. Це фактично призводять до збільшення витрат на капітальний ремон, які були попередньо не враховані.

В статі наведені рекомендації щодо прийняття оптимальних а часто і єдино можливих рішень при розробці проектів капітального ремонту будівель.

**Ключові слова**: ураження; будівельні конструкції; руйнування; вогневі ураження; капітальний ремонт.

ISSN 2522-4182

DOI: 10.32347/2522-4182.17.2025.200-210
UDC 624.042.8: 624.074.7: 69.059.25

# ANALYSIS OF THE DYNAMIC BEHAVIOR OF A FRAME BUILDING CONSIDERING THE MULTILAYERED NATURE OF THE SOIL FOUNDATION

*Olha LUKIANCHENKO[1], Denys KOSTIN[2],*

[1,2] Kyiv National University of Construction and Architecture
[1]Research institute of structural mechanics
31, Povitrianyh Syl Avenue, Kyiv, Ukraine, 03037
[1]lukianchenko.oo@knuba.edu.ua, https://orcid.org/0000-0003-1794-6030
[2]kostin.dy@knuba.edu.ua, https://orcid.org/0009-0000-2191-933X

**Abstract**. The influence of rolling stock loading on a twenty-three-story frame building located near the movement of railway trains in an urban area was investigated. Mathematical modeling of the dynamic behavior of multi-story buildings subjected to rolling stock loading was performed using a two-stage numerical method.

In the first stage, a finite element model of the multilayer soil foundation along with the ballast prism was created in the NASTRAN software complex, represented as a planar elastoplastic half-space with a length of 200 m and a depth of 30 m. A real geological cross-section consisting of five layers with different physical characteristics was used. The rolling stock load is represented as a vertical periodic excitation, concentrated at the center of mass of the system consisting of the bogie frame, the wheelsets of a freight wagon, and the ballast prism.

Modal analysis of the soil foundation and the ballast prism was performed using the Lanczos method. The influence of rolling stock loading on the dynamic behavior of the soil foundation was investigated using the fourth-order Runge-Kutta method. Horizontal and vertical displacements and accelerations of the soil were obtained at various distances and depths of the foundation model from the railway track axis.

In the second stage, a 3D model of the monolithic frame building was created in the SCAD software complex. Modal analysis of the structure was performed using the subspace iteration method.

**Olha LUKIANCHENKO**
Professor of the Department of Structural Mechanics, Prof. D.Sc. (Eng.)

**Denys KOSTIN**
PhD student of the Department of Structural Mechanics

Two calculation options for the multi-story building were considered.

The first calculation was performed for the action of design load combinations: permanent, sustained, and short-term (snow, wind load). In the second calculation option, the stress-strain state of the building was investigated using the spectral method under the action of design loads and kinematic soil excitation, applied along the height of the building's foundation in the form of acceleration vectors. The accelerations were considered in two directions and added to the design combinations along the two directions of wind load influence.

A comparison of the two calculation options was performed to check the reliability and structural safety of the building.

**Keywords:** dynamics; finite element method; multi-story frame building; multilayer soil model; modal analysis; forced vibrations.

## PROBLEM STATEMENT

Rolling stock serves as a source of ground vibrations that affect buildings adjacent to railway corridors. These vibrations can cause uneven settlement of foundations and additional stress in structural elements of buildings, potentially leading to defects or even structural failures.

For buildings and structures erected in the train traffic zone, there is a need to evaluate the stress-strain state of the structures under the action of ground accelerations caused by rolling stock loading. To obtain reliable results for the analysis of the stress-strain state of structures, it is necessary to select a soil foundation model that closely approximates the real soil environment. In practice, the model of a linearly deformable layer of finite width is the most common, as it only requires specifying the deformation characteristics of the soil - the modulus of deformation E and Poisson's ratio $\nu$.

The dynamics of rolling stock are determined by the complex interaction of contact forces, geometric parameters, spring suspension systems, vehicle mass, and damping coefficients [1]. Even when moving on a straight track at low speeds, problems associated with hunting oscillations arise. At higher speeds, significant vertical oscillations and forced lateral oscillations of the wheelset system occur. The dynamic interaction between the train and the railway track changes depending on the nature of the track bed section, wheel and rail irregularities, operating conditions, as well as climatic conditions. Rolling stock loads on railway tracks and the stress-strain state parameters of the track superstructure were in many cases determined using the generally accepted methods of V.V. Bolotin, S.P. Timoshenko, B.G. Korenev, and I.M. Rabinovich.

This work is devoted to the investigation of the influence of rolling stock loads on a high-rise building located in the train traffic zone. A numerical method was developed that allowed determining the foundation soil accelerations caused by the periodic rolling stock load and, considering these accelerations, analyzing the dynamic behavior of a multi-story monolithic frame building located near the train movement.

## ANALYSIS OF PREVIOUS RESEARCH

The soil foundation significantly affects the natural frequencies and mode shapes of the building. Ignoring soil properties during the interaction between the foundation and the building can lead to significant errors. This class of problems requires an additional analysis of the soil medium to create correct foundation models and develop effective calculation methods oriented towards the use of powerful computing complexes [2 - 4].

Many publications by domestic and foreign scientists, including [5 – 7], are devoted to the analysis of dynamic loads on buildings, particularly seismic loads, and wave propagation in elastic media. Works [8, 9] are dedicated to recommendations for creating design schemes for building structures.

In studies [10 – 12], the influence on buildings of ground vibrations from the movement of underground trains was investigated. And in a relatively small number of works, methods and models for calculating structures subjected to ground vibrations caused by the movement of surface trains are presented [13 – 16].

In previous publications [17 – 20,25], the authors of this article considered various problems and proposed a methodology for analyzing the influence of ground vibrations on a building using a single-layer soil foundation model. This work demonstrates the calculation results using a multilayer model.

## MAIN RESEARCH

In the article, an analysis of the dynamic behavior of a high-rise building under rolling stock loading acting on a multilayer soil foundation was performed. The maximum vertical and horizontal displacements and accelerations of the soil at the boundaries of

individual layers of the model were determined. The obtained accelerations were applied to the foundation of the multi-story building. The influence of soil accelerations on the building, located near the train movement, more precisely: at a distance of 60 m, was evaluated.

**1. Finite-element modeling of single-layer and multilayer soil foundations**

Figure 1 shows the multilayer soil foundation model. The single-layer foundation has already been described in the authors' previous works. The properties of the ballast prism and the parameters of the rolling stock, whose influence on the frame building was investigated in previous publications [17 - 19], are also given there.

The multilayer foundation was modeled in the NASTRAN software complex [20] based on a real geological cross-section that has a depth of 30 m and consists of five soil layers. The physical characteristics of all soils layer by layer are given in Table 1.

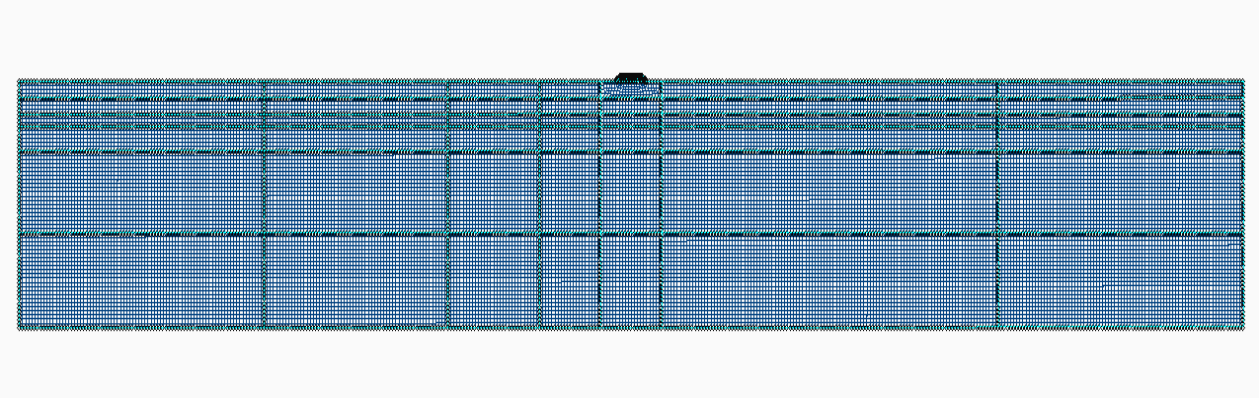

**Fig. 1.** Finite element model of the multilayer soil foundation
**Рис. 1** Скінченно-елементна модель багатошарової ґрунтової основи

**Table 1**. Physical properties of the soils in the multilayer foundation model
**Табл. 1** Фізичні властивості ґрунтів у багатошаровій моделі фундаменту

| Layer of soil | Density, g/sm$^3$ | Porosity coefficient | Angle of friction, degrees | Adhesion coefficient, kPa | Modulus of deforma-tion, MPa | Liquidity index | Soil resistivity, kPa |
|---|---|---|---|---|---|---|---|
| 1 | 1.64 | 0.61 | 28.2 | 0.7 | 17.3 | – | 300 |
| 2 | 1.95 | 0.61 | 30.9 | 0.7 | 28.1 | – | 200 |
| 3 | 1.82 | 0.85 | 14.8 | 15.3 | 6.7 | 0.69 | 120 |
| 4 | 1.86 | 0.9 | 16.5 | 22.0 | 12.5 | 0.34 | 215 |
| 5 | 1.94 | 0.9 | 18.3 | 28.7 | 18.5 | 0.18 | 220 |

The rolling stock load is represented as a vertical periodic excitation, concentrated at the center of mass of the system, which consists of the bogie frame, the wheelsets of a freight wagon, and the ballast prism. Fig. 2 shows the horizontal and vertical displace

ments of the nodes of the multilayer soil model at different distances from the railway tracks to the building. Figure 3 demonstrates the horizontal and vertical accelerations at distances of 30, 60, and 95 meters.

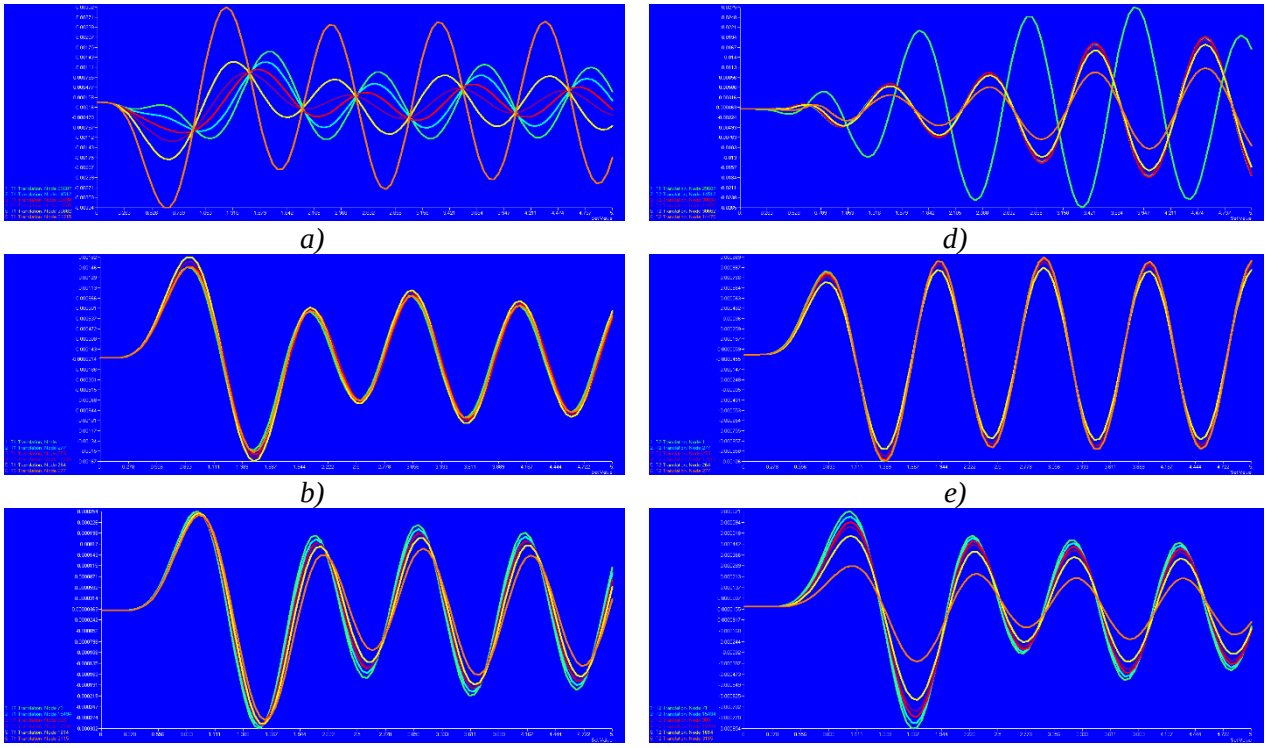

*a)* *d)*

*b)* *e)*

*c)* *f)*

**Fig. 2** Displacements of model nodes at distances of 30, 60, and 95 m from the building:
*a), b), c)* horizontal displacements; *d), e), f)* vertical displacements.

**Рис. 2** Переміщення вузлів моделі на відстані 30, 60 і 95 м від будівлі:
*а), б), в)* горизонтальні переміщення; *г), д), є)* вертикальні переміщення.

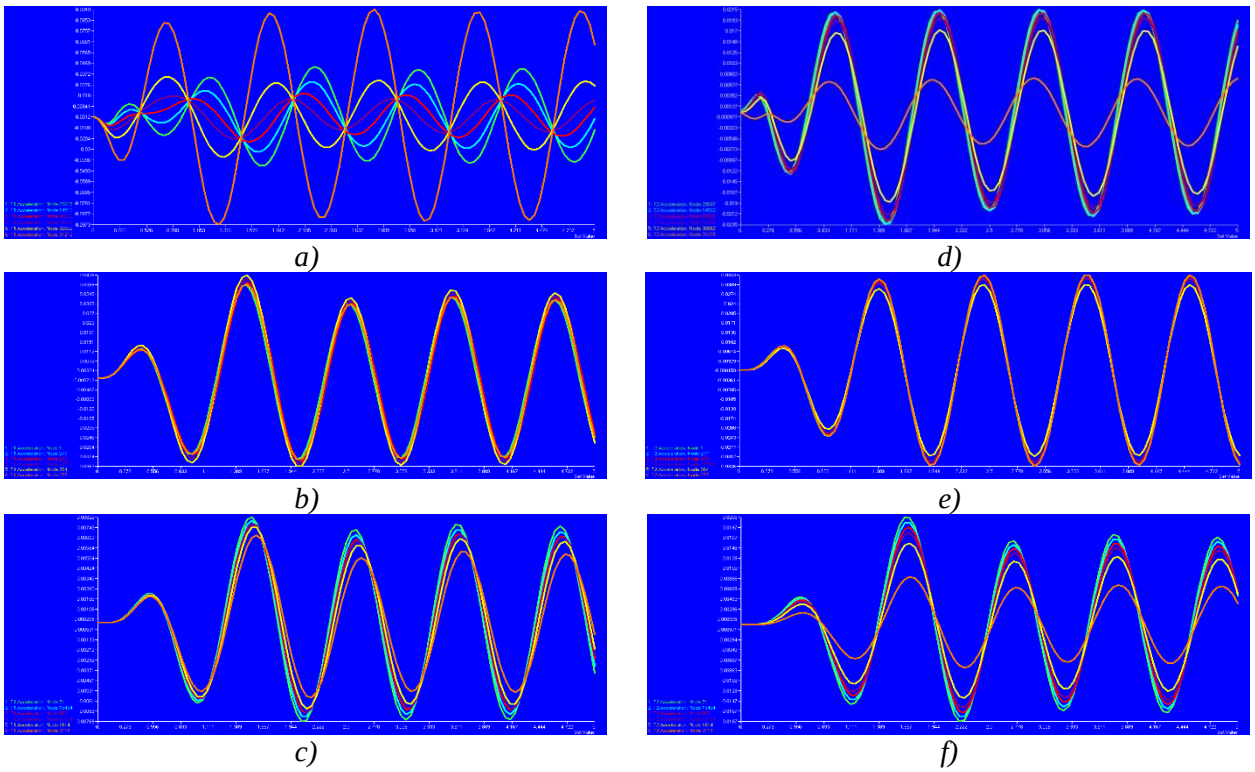

*a)* *d)*

*b)* *e)*

*c)* *f)*

**Fig. 3** Accelerations of model nodes at distances of 30, 60, and 95 m from the building:
*a), b), c)* horizontal accelerations; *d), e), f)* vertical accelerations.

**Рис. 3** Прискорення вузлів моделі на відстані 30, 60 і 95 м від будівлі:
*да), б), в)* горизонтальні прискорення; *г), д), є)* вертикальні прискорення.

**Table 2**. Maximum soil characteristics at distances of 30, 60, and 95 m from the building
**Табл. 2** Максимальні характеристики ґрунту на відстанях 30, 60 і 95 м від будівлі

| Distance / Depth, m | Total Disp., m | Horiz. Disp., m | Vert. Disp., m | Total Accel., m/s$^2$ | Horiz. Accel., m/s$^2$ | Vert. Accel., m/s$^2$ |
|---|---|---|---|---|---|---|
| 30 м / 0 м | - | - | 0,0008 | - | - | 0,0235 |
| 30 м / 18,5 м | 0,0034 | 0,0034 | - | 0,0973 | 0,0949 | - |
| 60 м / 0 м | - | - | 0,0011 | - | - | 0,0346 |
| 60 м / 8,5 м | 0,0018 | 0,0016 | - | 0,0503 | 0,0428 | - |
| 95 м / 0 м | 0,0009 | 0,0003 | 0,0007 | 0,0217 | 0,0082 | 0,0206 |

## 2. Modal analysis of the soil foundation

The dynamic calculation of the soil foundation was performed for the action of a vertical periodic load from the movement of a wagon with a load of 230.0 kN; the natural oscillation frequency of the wagon is 6.046 s$^{-1}$. Modal analysis was carried out using the Lanczos method, retaining 10 mode shapes. In the article [17], the authors described in detail the modal analysis of the single-layer soil foundation model.

This work is devoted to the analysis of the influence of the multilayered nature of the soil. Therefore, modal analysis of the multilayer soil foundation was performed, retaining 10 mode shapes. The mode shapes and natural frequencies of oscillations are presented in Fig. 4.

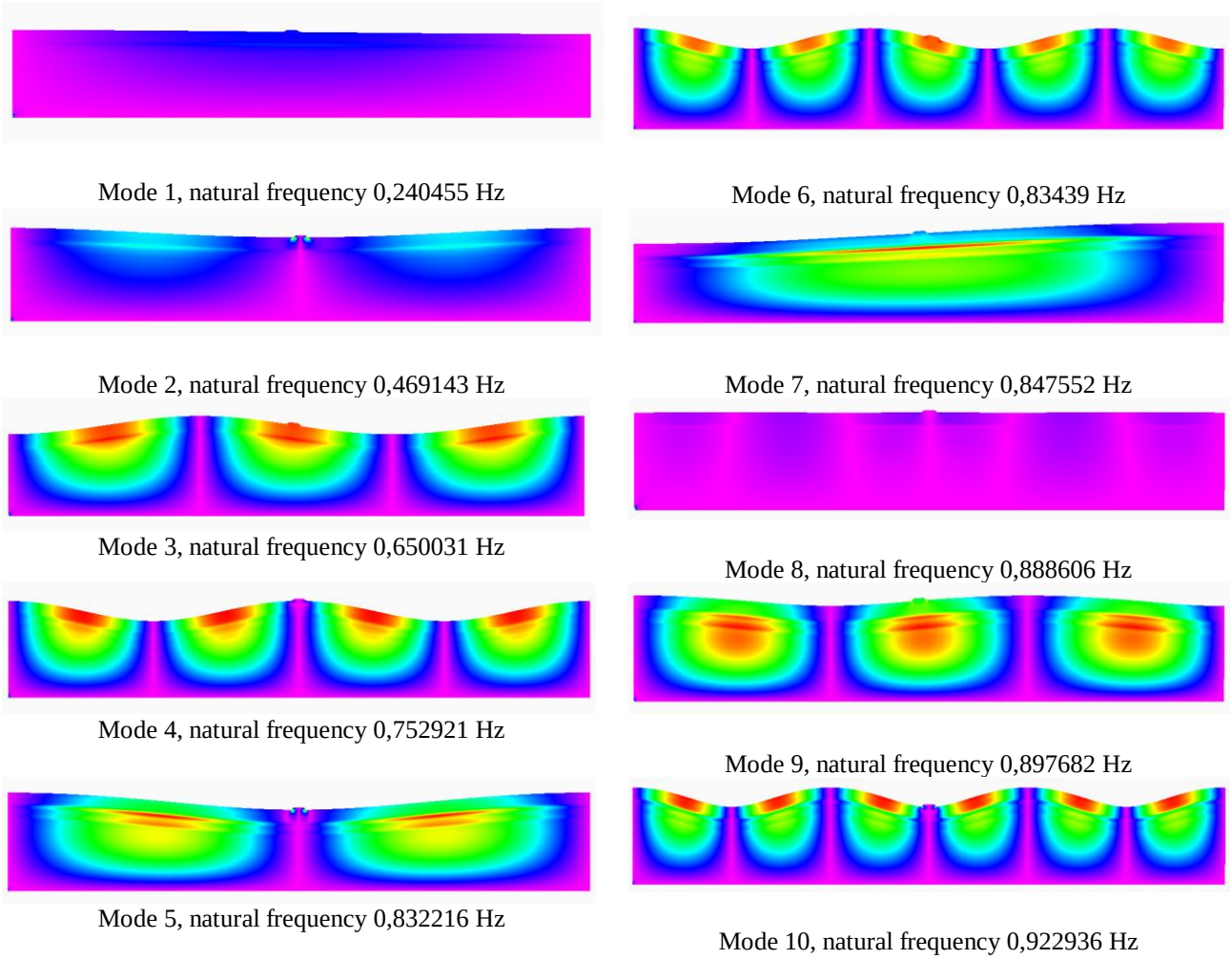


**Fig. 4.** Mode shapes and natural frequencies of the multilayer soil foundation
**Рис. 4.** Форми і частоти власних коливань багатошарової ґрунтової основи

For comparison, we present the natural frequencies of the single-layer soil foundation [17]: ν = [0.237372; 0.460532; 0.629739; 0.724444, 0.804174; 0.82192; 0.8382; 0.88234; 0.892783; 0.894094] Hz.

Compared to the single-layer foundation, the natural oscillation frequencies of the multilayer foundation have values 2 - 3% higher, and the mode shapes demonstrate the influence of the multilayered nature.

**3. Finite element model of the frame building**

A frame multi-story building was investigated, whose finite element model was created using the SCAD office computing complex [21] and is presented in Fig. 5.

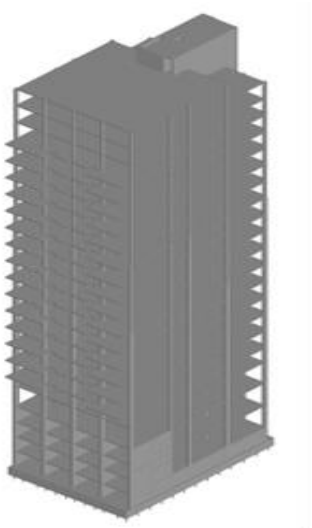

**Fig. 5.** 3D scheme of the building
**Рис. 5.** 3D схема будинку

The twenty-three-story building has the following technical characteristics: monolithic reinforced concrete frame, total height 71.9 m, plan dimensions – 24.0 x 21.3 m. A monolithic reinforced concrete raft on a pile foundation with bored piles was adopted as the foundation. The floors and roof are monolithic reinforced concrete flat slabs (beam-free). The wall material is inter-frame infill made of brick and aerated concrete blocks. The height of a typical floor is 3.3 m. The structural system of the building is a moment-resisting frame with bracing (frame-braced system). Two calculation options were considered: the first was performed for the action of design load combinations, and in the second option, the stress-strain state of the building was additionally investigated using the spectral method under kinematic soil excitation, applied along the height of the building's foundation in the form of acceleration vectors. The accelerations were considered in two directions and added to the design combinations along the two directions of wind load influence.

**4. Dynamic behavior of the frame building from rolling stock action**

The dynamic calculation of the building was performed for the action of soil accelerations, assuming that the rolling stock is located at a distance of 60 m. In this case, 10 mode shapes of the building's natural oscillations were retained. The frequencies and periods of oscillations are summarized in Table 3. Figure 6 shows the total horizontal displacements of the frame in two directions, both without and with consideration of the rolling stock influence.

**Table 3**. Dynamic characteristics of the building's natural oscillations
**Табл. 3** Динамічні характеристики власних коливань будівлі

| Форма коливань /Mode Shape | Частота коливань Frequency, Гц/Hz | Період коливань /Period, c/s |
|---|---|---|
| 1 | 0.2723 | 3.6724 |
| 2 | 0.3133 | 3.1920 |
| 3 | 0.6662 | 1.5010 |
| 4 | 1.3782 | 0.7256 |
| 5 | 1.9380 | 0.5160 |
| 6 | 2.2416 | 0.4461 |
| 7 | 2.2655 | 0.4414 |
| 8 | 2.5773 | 0.3888 |
| 9 | 2.6961 | 0.3709 |
| 10 | 3.0694 | 0.3258 |

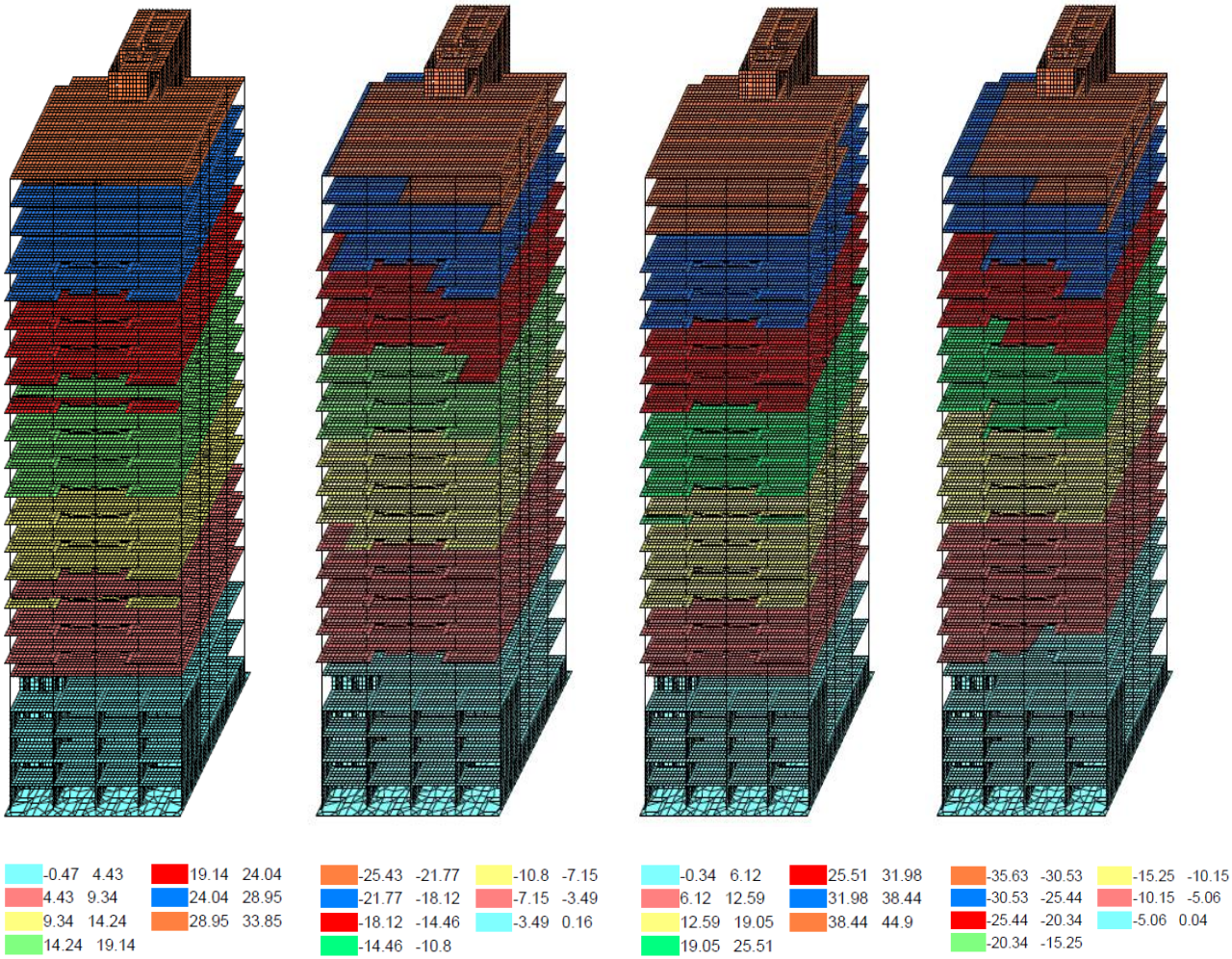


**Fig. 6** Horizontal displacements of the building frame considering rolling stock influence:
a) in the X-axis direction; b) in the Y-axis direction.
**Рис. 6** Горизонтальні переміщення каркасу будівлі з урахуванням впливу рухомого складу:
c) у напрямку осі X; d) у напрямку осі Y.

In the direction of the X-axis, the maximum displacement for the combination of permanent, sustained, and short-term loads is 33.85 mm. Upon adding the dynamic load to the combination along this axis, the maximum displacement is 44.9 mm. Similarly, an increase in horizontal displacements is observed in the direction of the Y-axis. The maximum displacement for the first combination is -25.43 mm. For the second combination, the maximum displacement is -35.63 mm.

## CONCLUSIONS AND PROSPECTS FOR FURTHER RESEARCH

1. A numerical method has been developed that allows assessing the influence of rolling stock loads on a frame building constructed in the railway track area.
2. Dynamic calculation of the multilayer soil foundation was performed. Horizontal and vertical soil accelerations were obtained at three different distances from the building.

3. The accelerations were applied to the foundation of the multi-story frame building. Two calculation options for the building frame were performed: static, for the action of design load combinations, and dynamic, for the action of load combinations considering soil accelerations.
4. Comparative analysis demonstrated an increase in total horizontal displacements along the X-axis by 30 percent, and in the Y-axis direction by 40 percent.

At the same time, the total horizontal displacement of the frame does not exceed 0.001, which is within the permissible displacements according to building codes.

## REFERENCES


1. **Ustenko O.V.** (2021) Fundamentals of the theory of vibrations and stability of rolling stock *posibnyk, Kharkiv:* – 130 s. [in Ukrainian].
2. **Boyko I., Sakharov V.** (2009) Interaction of multi-storey buildings as elements of the system "base - foundation - overground constructions" under static and dynamic loads. *Modern technologies, materials and structures in construction, scientific and technical collection. - Vinnytsia. - Universum-Vinnytsia . – p. 53-59*
3. **Solodei I.I., Ruvin O.H., Koliakova V.M., Kulikov O.P. (**2024) The problem of the structure and the soil plastic environment interaction in the conditions of dynamic evolutionary processes. *Strength of Materials and Theory of Structures: Scientificand-technical collected articles*. (112), 83-92. DOI: 10.32347/2410-2547.2024.112.83-92
4. **Solodei, I., Petrenko, E., Zatyliuk, Gh.** (2020). Nonlinear problem of structural deformation in interaction with elastoplastic medium. *Strength of Materials and Theory of Structures:* (105), 48 – 63. DOI: 10.32347/2410-2547.2020.105.48-63
5. **Ivanchenko H.M., Vorona Yu.V.** (2019) Numerical study of wave propagation in elastic media: *Vyd-vo "Karavela*", 150 s. [in Ukrainian].
6. **Dubovyi S.V.** (2021) Explicit and implicit schemes in numerical dynamics of mechanical systems. *Tekhnika — 450 s.* [in Ukrainian]
7. **Morgun A.S.** (2013) Plastic flow theory in soil mechanics. *Vinnytsya: VNTU – 108 s.* [in Ukrainian]
8. **Gorodetskyi, A.S., Barabash, M.S., Pysarevskyi, B.Yu., & Genzerskyi Yu.V.** (2021) Modeling of seismic loading on the "above-ground structure-soil" system. *Nauka ta budivnytstvo 4 – S. 51–57.* [in Ukrainian]
9. **Perelmuter A.V.** (2001) Design models of structures and their analysis capabilities. *VPP «Kompas». – 352 s.* [in Ukrainian]
10. **Hussein, M. F. M &. Hunt, H. E. M** (2006) A power flow method for evaluating vibration from underground railways, *Journal of Sound and Vibration 293, no. 3-5, pp. 667–679.*
11. **S. Jones, K. A. Kuo, M. F. M. Hussein, and H. E. M. Hunt (**2012) Prediction uncertainties and inaccuracies resulting from common assumptions in modelling vibration from underground railways, *Proc. Inst. Mech. Eng. F J. Rail Rapid Transit, vol. 226, no. 5, pp. 501–512.*
12. **X. Sheng, C.J.C. Jones, and D.J. Thompson** (2004) A theoretical model for ground vibration from trains generated by vertical track irregularities. *Journal of Sound and Vibration, 272(3-5), 937–965.*
13. **X. Sheng, C.J.C. Jones, & M. Petyt** (1999) Ground vibration generated by a load moving along a railway track. *Journal of Sound and Vibration 228(1), - P.129 – 156.*
14. **Xia, H., Cao, Y.M., Roeck, G. De.** (2010) Theoretical modeling and characteristic analysis of moving-train induced ground vibrations, *Journal of Sound and Vibration, 329: 819–832.*
15. **Zhang, Y., Zhang, N., Cao, Y., & Yu Y.** (2016) A prediction model and its validation of railway-induced building vibrations, *Advances in Mechanical Engineering, 8(10): 1 – 10.*
16. **Nielepowiczi, K. Bakowska, A. & Maslakowski, M.** (2018) The influence of train-induced ground motion in assessments of dynamic impact on structures. *Sciendo, Archives of civil engineering, Vol. LXIV,(4), 49 – 63.*
17. **Lukianchenko O.O., Kozak A.A., Kostin D.Ye.** (2025) Analysis of dynamic behavior of a multi-storey frame building in the railway traffic area. *Strength of Materials and Theory of Structures: (*114), 127 - 134. https://doi.org/10.32347/2410-2547.2025.114
18. **Lukianchenko, O., Kozak, A., & Kostin, D..** (2025). Investigation of the influence of ground accelerations In different directions on a building In the railway traffic zone. *Building*

*Constructions. Theory and Practice*, (16), 77–86. https://doi.org/10.32347/2522-4182.16.2025.77-86.**Lukianchenko O.O., Kostina O.V., Geraschenko O.V. (**2014) Influence of loading is from a rolling stock on the dynamic behavior of multi-storey building // *Strength of Materials and Theory of Structures:(*93), 100-109. http://opir.knuba.edu.ua/files/zbirnyk-93/14.pdf

19. **MSC NASTRAN 2021** Reference Guide November 29, 2020. NA:V2021:Z:Z:Z:DC-REF-PDFhttps://help-be.hexagonmi.com/bundle/MSC_Nastran_2021_Reference_Guide/raw/resource/enus/MSC_Nastran_2021_Reference_Guide.pdf
20. **SCAD Office. Versia 23.** Computing complex SCAD++] V.S. Karpilovskyi, E.Z. Kriksunov, A.A. Malyarenko, A.V. Perelmuter, M.A. Perelmuter, S.Y. Fialko. — *Izdatelstvo «SCAD SOFT», 2024.— 992 s.* [in Russian]
21. **DBN B.1.2-2:2006.** (2020) Navantazhennya I vplyvy. Normy proektuvannya [Loads and influences. Design standards]. *Kyiv,* Ministerstvo regionalnoho rozvytku ta budivnytstva Ukrainy – *68 s.* [in Ukrainian]
22. **DBN B.1.2-14:2018.** (2022) Systema zabezpechennya nadiinosti ta bezpeky budivelnyh obiektiv. Zagalni pryntsypy zabezpechennya nadiinosti ta konstruktyvnoii bezpeky budivel i sporud [System for ensuring the reliability and safety of construction sites. General principles for ensuring the reliability and structural safety of buildings and structures] *Kyiv,* Ministerstvo regionlnoho rozvytku ta budivnytstva Ukrainy. – *35 s.* [in Ukrainian]
23. **DBN V.1.1-12:2006.** (2014) Budivnytstvo u seismichnyh raionah Ukraiiny [Construction in seismic regions of Ukraine] *Kyiv,* Ministerstvo regionlnoho rozvytku ta budivnytstva Ukrainy – *110 s.* [in Ukrainian]
24. **Kripak, V., & Koliakova, V.** (2021). Interdependence of constructive and settlement schemes of the building. *Building Constructions. Theory and Practice, 1(8), 17–24.* [in Ukrainian] https://doi.org/10.32347/2522-4182.8.2021.17-24

## LITERATURE

1. **Ustenko O.V.** (2021)**.** Osnovy teorii kolyvan ta stiykosti ruhomogo skladu *posibnyk, Kharkiv:* – 130 s.
2. **Boyko I., Sakharov V.** (2009) Interaction of multi-storey buildings as elements of the system "base - foundation - overground constructions" under static and dynamic loads. *Modern technologies, materials and structures in construction, scientific and technical collection. - Vinnytsia. - Universum-Vinnytsia . – p. 53-59 .*
3. **Solodei I.I., Ruvin O.H., Koliakova V.M., Kulikov O.P. (**2024) The problem of the structure and the soil plastic environment interaction in the conditions of dynamic evolutionary processes. *Strength of Materials and Theory of Structures: Scientificand-technical collected articles*. (112), 83-92. DOI: 10.32347/2410-2547.2024.112.83-92
4. **Solodei, I., Petrenko, E., Zatyliuk, Gh.** (2020). Nonlinear problem of structural deformation in interaction with elastoplastic medium. *Strength of Materials and Theory of Structures:* (105), 48 – 63. DOI: 10.32347/2410-2547.2020.105.48-63 http://opir.knuba.edu.ua/files/zbirnyk-105/05-105_solodey_petrenko_zatiluk.pdf
5. **Ivanchenko H.M., Vorona Yu.V.** (2019) Chyselne doslidzhennya poshyrennya hvyl u pruzhnyh seredovyschah *Vyd-vo "Karavela*", 150 s.
6. **Dubovyi S.V.** (2021) Yavni ta neyavni skhemy v chyslovii dynamitsi mekhanichnykh system *Tekhnika — 450 s.*
7. **Morgun A.S.** (2013) Teoriia plastychnoii techii v mehanitsi gruntiv: *Monografia. Vinnytsya: VNTU – 108 s.*
8. **Gorodetskyi, A.S., Barabash, M.S., Pysarevskyi, B.Yu., & Genzerskyi Yu.V.** (2021) Modelyuvannya seismichnogo navantazhennya na system "nadzemna sporuda - grunt" *Nauka ta budivnytstvo 4 – S. 51–57.*
9. **Perelmuter A.V.** (2001) Rozrakhunkovi modeli konstruktsii ta mozhlyvosti ih analizu *VPP «Kompas». – 352 s.*
10. **Hussein, M. F. M &. Hunt, H. E. M** (2006) A power flow method for evaluating vibration from underground railways, *Journal of Sound and Vibration 293, no. 3-5, pp. 667–679.*
11. **S. Jones, K. A. Kuo, M. F. M. Hussein, and H. E. M. Hunt (**2012) Prediction uncertainties and inaccuracies resulting from common assumptions in modelling vibration from underground railways, *Proc. Inst. Mech. Eng. F J. Rail Rapid Transit, vol. 226, no. 5, pp. 501–512.*
12. **X. Sheng, C.J.C. Jones, and D.J. Thompson** (2004) A theoretical model for ground vibration from trains generated by vertical track irregularities. *Journal of Sound and Vibration, 272(3-5), 937–965.*

13. **X. Sheng, C.J.C. Jones, & M. Petyt** (1999) Ground vibration generated by a load moving along a railway track. *Journal of Sound and Vibration 228(1), - P.129 – 156.*
14. **Xia, H., Cao, Y.M., Roeck, G. De.** (2010) Theoretical modeling and characteristic analysis of moving-train induced ground vibrations, *Journal of Sound and Vibration, 329: 819–832.*
15. **Zhang, Y., Zhang, N., Cao, Y., & Yu Y.** (2016) A prediction model and its validation of railway-induced building vibrations, *Advances in Mechanical Engineering, 8(10): 1 – 10.*
16. **Nielepowiczi, K. Bakowska, A. & Maslakowski, M.** (2018) The influence of train-induced ground motion in assessments of dynamic impact on structures. *Sciendo, Archives of civil engineering, Vol. LXIV,(4), 49 – 63.*
17. **Lukianchenko O.O., Kozak A.A., Kostin D.Ye.** (2025) Analysis of dynamic behavior of a multi-storey frame building in the railway traffic area. *Strength of Materials and Theory of Structures: (*114), 127 - 134. https://doi.org/10.32347/2410-2547.2025.114
18. **Lukianchenko, O., Kozak, A., & Kostin, D..** (2025). Investigation of the influence of ground accelerations In different directions on a building In the railway traffic zone. *Building Constructions. Theory and Practice*, (16), 77–86. https://doi.org/10.32347/2522-4182.16.2025.77-86.
19. **Lukianchenko O.O., Kostina O.V., Geraschenko O.V. (**2014). Influence of loading is from a rolling stock on the dynamic behavior of multi-storey building. *Strength of Materials and Theory of Structures:(*93), 100-109. http://opir.knuba.edu.ua/files/zbirnyk-93/14.pdf
20. **MSC NASTRAN 2021** Reference Guide November 29, 2020. NA:V2021:Z:Z:Z:DC-REF-PDF https://help-be.hexagonmi.com/bundle/MSC_Nastran_2021_Reference_Guide/raw/resource/enus/MSC_Nastran_2021_Reference_Guide.pdf
21. **SCAD Office. Versia 23.** Computing complex SCAD++] V.S. Karpilovskyi, E.Z. Kriksunov, A.A. Malyarenko, A.V. Perelmuter, M.A. Perelmuter, S.Y. Fialko. — *Izdatelstvo «SCAD SOFT», 2024.— 992 s.*
22. **DBN B.1.2-2:2006.** (2020) Navantazhennya I vplyvy. Normy proektuvannya *Kyiv,* Ministerstvo regionalnoho rozvytku ta budivnytstva Ukrainy – *68 s.*
23. **DBN B.1.2-14:2018.** (2022) Systema zabezpechennya nadiinosti ta bezpeky budivelnyh obiektiv. Zagalni pryntsypy zabezpechennya nadiinosti ta konstruktyvnoii bezpeky budivel i sporud *Kyiv,* Ministerstvo regionlnoho rozvytku ta budivnytstva Ukrainy. – *35 s.*
24. **DBN V.1.1-12:2006.** (2014) Budivnytstvo u seismichnyh raionah Ukraiiny *Kyiv,* Ministerstvo regionlnoho rozvytku ta budivnytstva Ukrainy – *110 s.*
25. **Kripak, V., & Koliakova, V.** (2021). Vzaiemozalezhnist konstruktyvnykh i rozrakhunkovykh skhem budivli. *Budivelni konstruktsii. Teoriia i praktyka, 1(8), 17*–24 https://doi.org/10.32347/2522-4182.8.2021.17-24

# АНАЛІЗ ДИНАМІЧНОЇ ПОВЕДІНКИ КАРКАСНОЇ БУДІВЛІ З УРАХУВАННЯМ БАГАТОШАРОВОСТІ ҐРУНТУ ОСНОВИ

*Ольга ЛУК'ЯНЧЕНКО*
*Денис КОСТІН*

**Анотація**. Досліджено вплив навантаження від рухомого складу на двадцятитрьохповерхову каркасну будівлю, що розташована поблизу руху залізничних потягів у міській забудові. Математичне моделювання динамічної поведінки багатоповерхових будівель при дії навантаження від рухомого складу виконано за допомогою чисельної методики, що складається з двох етапів.

На першому етапі у програмному комплексі NASTRAN сформована скінченно-елементна модель багатошарової ґрунтової основи разом їз баластовою призмою у вигляді плоского пружнопластичного напівпростору довжиною 200 м і глибиною 30 м. При цьому використаний реальний геологічний розріз, утворений з п'яти шарів з різними фізичними характеристиками. Навантаження від рухомого складу подано у вигляді вертикального періодичного збурення, зосередженого в центрі мас системи, що складається з рами візка, колісних пар вагону вантажного потягу та баластової призми.

Модальний аналіз ґрунтової основи і баластової призми виконано методом Ланцоша. Досліджено вплив навантаження від рухомого складу на динамічну поведінку ґрунтової основи

методом Рунге-Кутти четвертого порядку. Визначені горизонтальні і вертикальні переміщення та прискорення ґрунту на різних відстаннях і глибинах моделі основи від осі залізничної колії. На другому етапі у програмному комплексі SCAD створена 3D модель монолітної каркасної будівлі. Модальний аналіз споруди виконано методом ітерацій підпросторів. Розглянуто два варіанти розрахунку багатоповерхової будівлі. Перший розрахунок виконаний на дію розрахункових сполучень навантажень: постійних, тривалих, короткочасних (снігове, вітрове навантаження).

У другому варіанті розрахунку за допомогою спектрального методу досліджено напружено-деформований стан будівлі при дії розрахункових навантажень та кінематичного збурення ґрунту, прикладеного по висоті фундаменту будинку у вигляді векторів прискорень. Прискорення враховані у двох напрямках і додані у розрахункові сполучення по двох напрямках вітрового впливу.

Виконано порівняння двох варіантів розрахунку для перевірки надійності і конструктивної безпеки будівлі.

**Keywords:** динаміка; метод скінченних елементів; багатоповерхова каркасна будівля; багатошарова модель ґрунту; модальний аналіз; змушені коливання.

***Received:*** *November 01, 2025.*
***Accepted:*** *December 05, 2025.*

ISSN 2522-4182

DOI: 10.32347/2522-4182.17.2025.211-220
UDC 624.012.4-183.2

# RATIONAL STEEL CANOPY STRUCTURES OVER STADIUM STANDS USING WELDED I-BEAMS WITH VARIABLE FLANGE WIDTH AND WEB HEIGHT

*Liubomyr DZHANOV*

Kyiv National University of Construction and Architecture
31, Povitryanykh Syl Avenue, Kyiv, Ukraine, 03037
angeldl@ukr.net, http://orcid.org/0000-0001-5144-3424

**Abstract.** An improved methodological approach has been developed for determining the optimal structural form of a cantilever welded steel I-beam with variable flange width and web height under combined loading: uniformly distributed along the length and an applied concentrated bending moment at the free end. These steel structures demonstrate a high efficiency of steel use, serving as primary load-bearing elements of canopies over stadium stands.

The structural efficiency is achieved through redistribution of steel along the length of the element and over the section height in such a way as to attain an optimal structural form. The selection of the optimal configuration is based on numerical studies focused on determining the rational gradient of the I-beam's height variation and selecting the gradient value of flange width, while satisfying the strength conditions for each cross-section. It is assumed that the rational distribution of steel over the section height corresponds to the optimal ratio between the flange and web areas according to the criterion of minimizing steel consumption for each elementary segment of the beam.

The optimization problem of a conical welded I-beam under the adopted loading conditions with a linear variation of flange width and web height is formulated in the traditional manner as a single-criterion constrained optimization problem, where the criterion is the minimization of steel consumption, and strength constraints in each cross-section (which depend on the gradients of variation of flange width and web height under combined loading) are imposed.

The problem is solved with the aim of complying with the strength constraints and determining the limiting values of the gradients of change of web height and flange width of the cross section of the steel I-beam for a generalized loading scheme.

Numerical investigations were carried out to find the gradients of variation of web height and flange width based on the criterion of minimizing steel consumption and satisfying strength constraints in each cross-section along the length of the structure.

The results obtained show that the optimal gradient of variation of section height is $\gamma_h \le 0{,}6$ for $P_1 l/M_{x,0} \le 2{,}0$, and $\gamma_h \le 0{,}5$ for $P_1 l/M_{x,0} \le 1{,}0$.. It has been established that for $P_1 l/M_{x,0} \le 0{,}25$ and $\gamma_h \le 0{,}9$, the strength conditions are satisfied for all cross-sections of the rational structural form of the welded steel I-beam. A methodological approach has been developed for solving problems of this type in a generalized form.

**Keywords:** steel structures; stadium coverings; optimal web height and flange width of a welded I-beam and their variation gradient; modeling; numerical studies.

**Liubomyr DZHANOV**
assistant lecturer, Department of Metal and Timber Structures

## PROBLEM STATEMENT

Spatial cantilever steel structural systems are predominantly used for canopies over stadium stands.

This is due to the functional purpose of canopies: protecting spectators from atmospheric precipitation and providing shade for the stadium seating areas. The cantilever span of such structures always exceeds 8–10 m, and the extensive use of these systems highlights the relevance of the task of identifying the most steel-efficient main load-bearing beam structure. The research presented in this paper continues the author's previous works published in [5, 10, 11]. The scientific novelty lies in the generalization of the problem formulation in terms of analyzing and identifying the most rational structural form under the action of combined loading: uniformly distributed load and concentrated loads applied at the free end.

## ANALYSIS OF PREVIOUS RESEARCH

In previous research, the author performed an analysis of methodological approaches for determining the best structural form of a welded steel I-beam with variable web height and flange width under uniformly distributed loading [1–3, 9–11, 14, 16, 18, 22–24]. It was shown in [5, 10, 11] that most often the criterion of minimum material consumption (by a reduced parameter) [5, 10, 11, 12, 22] and the criterion of safe long-term performance under static and seismic loads [19] are used. For critical structures, the criterion of minimum steel consumption is combined with the natural vibration frequencies and the shape of the variable cross-section [6, 13, 23]. The criterion of uniform stress (constant stress) in the most heavily loaded sections is used for investigating combined steel systems [12, 15]. Works [10, 11, 14, 16, 18, 21, 23, 24], including those with corrugated web [20] and flexible web sections, are devoted to finding the optimal height of constant cross-section beams. This article is a continuation of research on such structures previously conducted by the author at the Department of Metal and Timber Structures of KNUBA [5, 10, 11].

## PURPOSE AND METHODS

The purpose of the research is to determine the optimal structural form of a conical steel welded I-beam with linear variation of flange width and web height according to the criterion of minimal steel consumption, while satisfying the strength conditions at each cross-section along the length of the structure under combined loading: a uniformly distributed load and a concentrated vertical transverse force at the free end.

To achieve the stated objective, the methodology of Lagrange multipliers is used to find the optimum of the objective function in terms of steel consumption, along with the necessary Kuhn-Tucker conditions for the optimal solution. The flexibility of the beam's web is variable along its length; the flexibility of the web at the support cross-section is .

$$\lambda_\omega \approx h_0/t_\omega.$$

Local buckling (stability) of the flanges and web is assumed to be ensured. The dimensions of the support cross-section, where the maximum bending moment occurs, are denoted as ($b_{f0}$), ($h_0$).

The bending moment variation is assumed according to equation (1).

$$M_{x,z} = M_{x,0}(1-\frac{z}{l})^2 + P_1 l(1-\frac{z}{l}). \quad (1)$$

The flange width ($b_{fz}$) and web height ($h_z$) of the variable cross-section steel beam vary linearly along the length of the structure from the support section to the free end:

$$b_{f,z} = b_{f,0}\left(1-\frac{\gamma_b\, z}{l}\right); h_z = h_0\left(1-\frac{\gamma_h\, z}{l}\right);$$

*l*– is the span of the steel beam.

The web thickness is assumed constant (2). The web slenderness of the beam is variable along the length; the slenderness of the web at the support section is given by an expression in (2) $\lambda_\omega \approx h_0 / t_\omega$.

$$h_z = h_0 f_{hz} = h_0\left(1-\gamma_h\frac{z}{l}\right); b_{f,z} = b_{f,0} f_{bz} = b_{f,0}\left(1-\frac{\gamma_b\, z}{l}\right)$$
$$f_{hz} = (1-\gamma_h\frac{z}{l}).\ f_{bz} = (1-\gamma_b\frac{z}{l}). \quad (2)$$

The spatial stability of the beam against loss of stability in the plane of bending is ensured by out-of-plane bracing.

The optimization problem of the conical welded I-beam with linear variation in flange width and web height is formulated as a single-criterion constrained optimization problem, where the objective is minimization of steel consumption [10]. To identify a saddle (stationary) point, strength constraints in each cross-section of the structure are imposed. Since satisfying these strength conditions requires finding two independent parameters – the rational distribution of steel along the cross-section depth and the gradient of cross-section variation for the flange and web ($\gamma_h$ , $\gamma_b$) according to (2) – the problem is converted to an unconstrained optimization. Following the findings in [10] he assumption is made that if the beam is optimal in each cross-section, then the entire structure is optimal as well. However, with linear variation of flange width and web height, the strength constraints take the form of an equality for the cross-section where the maximum stress occurs, and inequalities for the other sections. «The problem is tackled in two stages: first, using Lagrange multipliers, it was determined [10], that under linear variation of flange width and web height, the optimal cross-sectional geometry satisfies:
$2A_{f,z} = 2b_{f,z}t_f = h_z t_w; 2b_{f,0}t_f = h_0 t_w$ - the area of the two flanges equals the area of the web, and the variation gradients of flange width and web height are equal ($\gamma_h = \gamma_b$)». In the second stage, numerical studies determined the limiting values of the cross-section variation gradient for the steel I-beam.

The stresses in each cross-section of the steel I-beam structure are given by

$$\sigma_z = \frac{\left(M_{x,z} + P_{1z}\right)}{h_0^2 t_{w,0}(1-\gamma_h\frac{z}{l})^2\left(\frac{t_f b_{f0}(1-\gamma_b\frac{z}{l})}{t_{w,0}h_0(1-\gamma_h\frac{z}{l})}+\frac{1}{6}\right)} \le R_y\gamma_c. \quad (3)$$

Taking into account the equality of the web height and flange width variation gradients ($\gamma_h = \gamma_b$) the strength condition can be written in the form:

$$\sigma_z = \frac{M_{x,0}}{h_0^2 t_{w,0}} \frac{\left[(1-\frac{z}{l})^2 + \frac{P_1 l}{M_{x,0}}(1-\frac{z}{l})\right]}{(1-\gamma_h\frac{z}{l})^2\left(\frac{t_f b_{f0}(1-\gamma_h\frac{z}{l})}{t_{w,0}h_0(1-\gamma_h\frac{z}{l})}+\frac{1}{6}\right)} \le R_y\gamma_c. \quad (4)$$

Applying the optimality conditions yields
$2A_{f,z} = 2b_{f,z}t_f = h_z t_w; 2b_{f,0}t_f = h_0 t_w$ the analytical expression:

$$\frac{2t_f b_{f0}(1-\gamma_h\frac{z}{l})}{t_{w,0}h_0(1-\gamma_h\frac{z}{l})} = 1 \rightarrow \frac{M_{x,z}+P_{1z}}{t_{w,0}h_0(1-\gamma_h\frac{z}{l})^2\left(\frac{1}{2}+\frac{1}{6}\right)} = R_y\gamma_c \quad (5)$$

$$\frac{3}{2}\frac{M_{x,z}+P_{1z}}{t_{w,0}h_0(1-\gamma_h\frac{z}{l})^2} = R_y\gamma_c. \quad (6)$$

Equation (6), the last strength condition, gives a formula for determining the optimal height of the support section, as for steel I-beams of constant cross-section. [15]

Since, depending on the variation gradient of the cross-section, the strength condition may not be satisfied in some sections, analytical and numerical studies were conducted using the criterion that the stresses do not exceed the yield strength of the steel. In other words, the strength constraints serve as the criterion for determining the cross-section variation gradient.

$$z = 0 \to h_0 = \sqrt{\frac{3}{2}\frac{M_{x,z} + P_z}{t_{w,0} R_y \gamma_c}}.$$

$$\frac{\sigma_z}{R_y \gamma_c} = \frac{\left[(1 - \frac{z}{l})^2 + \frac{Pl}{M_{x,0}}(1 - \frac{z}{l})\right]}{\left[1 + \frac{Pl}{M_{x,0}}\right](1 - \gamma_h \frac{z}{l})^2} \le 1. \quad (7)$$

Now the gradient of variation of the web height and flange width must satisfy an algebraic inequality:

$$\gamma_h \le 1 - \frac{l}{z}\sqrt{\frac{\left[(1 - \frac{z}{l})^2 + \frac{Pl}{M_{x,0}}(1 - \frac{z}{l})\right]}{\left[1 + \frac{Pl}{M_{x,0}}\right]}}. \quad (8)$$

Numerical studies using analytical expressions (7) and (8) were carried out to determine the maximum value of the variation gradient of the web height and flange width for the conical beam.

He calculation results showed (Fig. 1) that the optimal gradient of cross-section change at $Pl/M_{x,0}=1,0$ should be considered $\gamma_h=0,7$. With this topology, the strength conditions are satisfied in all cross-sections along the length of the cantilever conical I-beam structure.

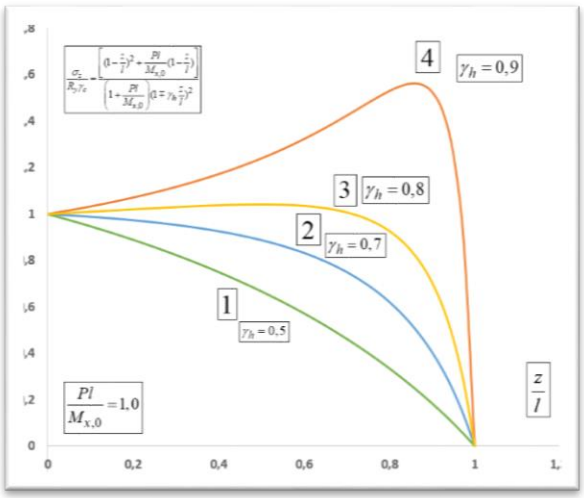


**Fig. 1** Ratio of current stress to the design steel strength in a welded steel I-beam with symmetric cross-section at different gradients of linear variation of web height and flange width (2.52) and at a ratio of bending moments from external loads Pl/Mx,0=1,0: graph 1 - γh≤0,5; graph 2 - γh=0,7; graph 3 - γh=0,8; graph 4 - γh=0,9.

**Рис. 1** Відношення поточних напружень до розрахункового опору сталі у зварному сталевому двотаврів симетричного перерізу при різних градієнтах лінійній змінності висоти стінки і та полиці (2.52) та відношенні між згинальними моментами від зовнішніх зусиль $Pl/M_{x,0}=1,0$: графік 1 - $\gamma_h \le 0,5$; графік 2 - $\gamma_h=0,7$; графік 3 - $\gamma_h=0,8$; графік 4 - $\gamma_h=0,9$.

With an increase in the ratio of bending moments from external loads to 2.0, i.e. $Pl/M_{x,0}$=2,0 (Fig. 2), the optimal value of the cross-section variation gradient is $\gamma_h$=0,6. Thus, it is established that with an increasing influence of the linear distribution of bending moments from concentrated forces, the flange width and web height variation gradients decrease, and the optimal I-beam topology becomes flatter.

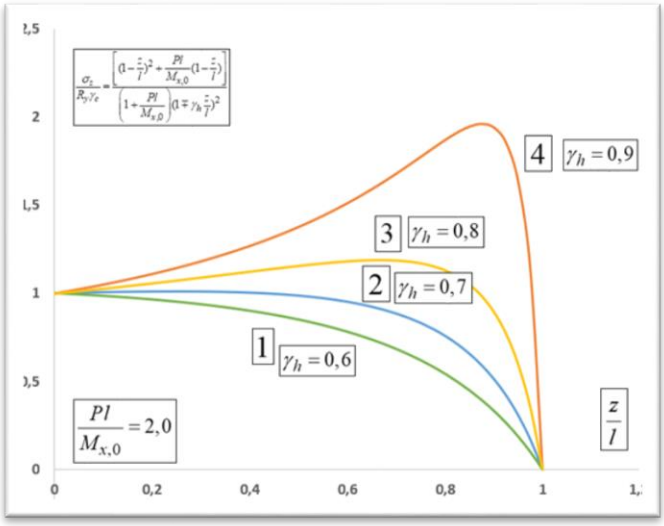


**Fig. 2** Ratio of current stress to the design steel strength in a welded steel I-beam with symmetric cross-section at different gradients of linear variation of web height and flange width (2.52) and at a ratio of bending moments from external loads $Pl/M_{x,0}$=2,0: graph 1 - $\gamma_h \leq 0,5$; graph 2 - $\gamma_h$=0,7; graph 3 - $\gamma_h$=0,8; graph 4 - $\gamma_h$=0,9.

**Рис. 2** Відношення поточних напружень до розрахункового опору сталі у зварному сталевому двотаврів симетричного перерізу при різних градієнтах лінійній змінності висоти стінки і та полиці (2.52) та відношенні між згинальними моментами від зовнішніх зусиль $Pl/M_{x,0}$=2,0: графік 1 - $\gamma_h \leq 0,5$; графік 2 - $\gamma_h$=0,7; графік 3 - $\gamma_h$=0,8; графік 4 - $\gamma_h$=0,9.

Additional studies were carried out at lower values of the ratio $Pl/M_{x,0}$= 0.5 (Fig. 3) and $Pl/M_{x,0}$= 0.25 (Fig. 4). The results show that when the applied load ratio decreases to $Pl/M_{x,0}$= 0.5 (Fig. 3), a more conical structural form with $\gamma_h$ = 0.75 can be considered rational.

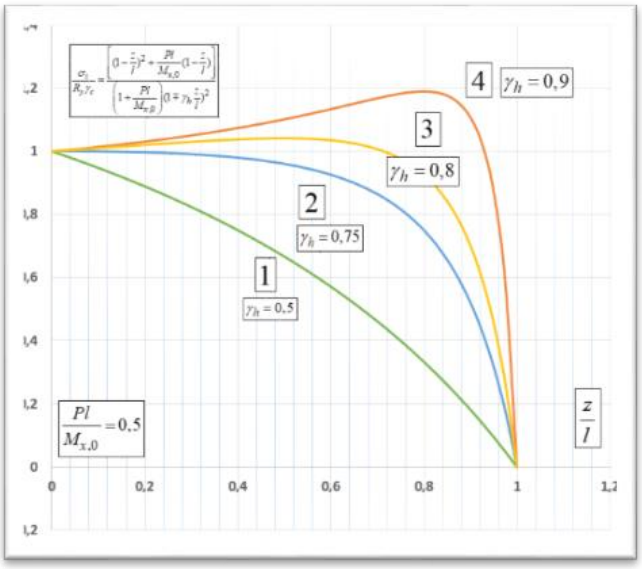


As the ratio approaches $Pl/M_{x,0}$= 0.25 (Fig. 4), a sufficiently rapid transition to the optimal conical beam form occurs: at $\gamma_h$ = 0.9, the strength conditions are satisfied along the entire length of the structure.

**Fig. 3.** Ratio of actual stresses to the design steel strength in a welded steel I-beam with a symmetrical cross-section under various gradients of linear variation in web height and flange width (2.52), and the ratio of bending moments from external loads $Pl/M_{x,0}$=0,5: curve 1 - $\gamma_h \leq 0,5$; curve 2 - $\gamma_h$=0,75; curve 3 - $\gamma_h$=0,8; curve 4 - $\gamma_h$=0,9

**Рис. 3** Відношення поточних напружень до розрахункового опору сталі у зварному сталевому двотаврів симетричного перерізу при різних градієнтах лінійній змінності висоти стінки і та полиці (2.52) та відношенні між згинальними моментами від зовнішніх зусиль $Pl/M_{x,0}$=0,5: графік 1 - $\gamma_h \leq 0,5$; графік 2 - $\gamma_h$=0,75; графік 3 - $\gamma_h$=0,8; графік 4 - $\gamma_h$=0,9.

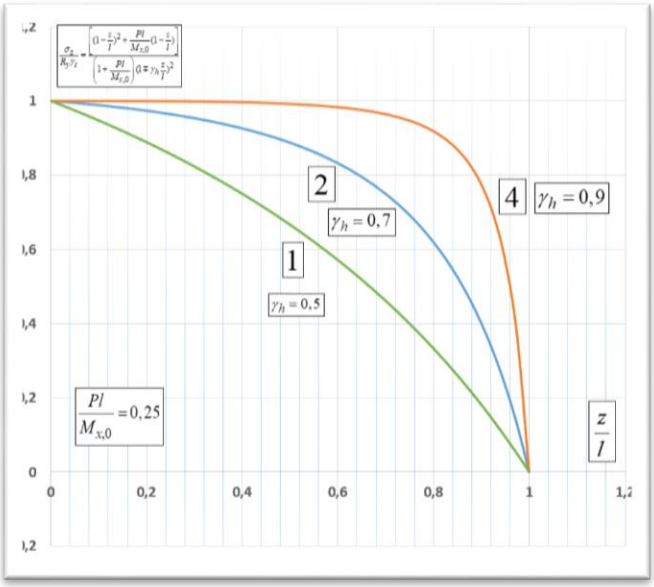


**Fig. 4**. Ratio of actual stresses to the design steel strength in a welded steel I-beam with a symmetrical cross-section under various gradients of linear variation in web height and flange width (2.52), and the ratio of bending moments from external loads $Pl/M_{x,0}= 0.5$: curve 1 - $\gamma_h \leq 0.5$; curve 2 - $\gamma_h = 0.7$; curve 3 - $\gamma_h = 0.9$

**Рис. 4** Відношення поточних напружень до розрахункового опору сталі у зварному сталевому двотаврів симетричного перерізу при різних градієнтах лінійній змінності висоти стінки і та полиці (2.52) та відношенні між згинальними моментами від зовнішніх зусиль $Pl/M_{x,0}=0,5$: графік 1 - $\gamma_h \leq 0,5$; графік 2 - $\gamma_h=0,7$; графік 3 - $\gamma_h=0,9$.

## CONCLUSIONS AND RECOMMENDATIONS

The results obtained indicate that the rational gradient of cross-section variation is $\gamma_h$=0,6 for $P_1l/M_{x,0} \leq 2,0$ and $\gamma_h$=0,5 for $P_1l/M_{x,0} \leq 1,0$.
A methodological approach for finding the optimal design of a welded I-beam with variable cross-section under linear variation of flange width and web height has been developed.

A more conical structural form of the I-beam with $\gamma_h = 0.75$ can be considered a rational design solution. As the ratio approaches $Pl/M_{x,0}= 0.25$ (Fig. 4), a sufficiently rapid transition to the optimal conical form of the steel I-beam occurs: at $\gamma_h = 0.9$, the strength conditions are satisfied along the entire length of the structure.

## REFERENCES


1. **Bazhenov, V.A. Vorona Yu.V., & Perelmuter A.V.** (2016) Construction mechanics and the theory of structures. Essays on history. *Karavela, p. 428* [ in Ukrainian]
2. **Bazhenov, V.A.** (2012). Variational principles and methods of structural mechanics. *Karavela. -720 c.*
*ISBN 978-966-2229-44-8.* [in Ukrainian]
3. **Paola Bertolini, Martin A. Eder Luca Taglialegne Paolo Sebastiano Valvo**. (2019) Stresses in constant tapered beams with thin-walled rectangular and circular cross sections *Thin-Walled Structures (137), 527-540.* [in English]
https://doi.org/10.1016/j.tws.2019.01.008.
4. **Bendse M. P., Sigmund O.** (2004) Topology Optimization. *Berlin, Heidelberg: Springer Berlin Heidelberg, XIV, p.370* [in English]
https://doi.org/10.1007/978-3-662-05086-6
5. **Bilyk, A., Bilyk, S., Hlítin, O., & Dzhanov, L.** (2022). Optimal height of steel I-beams with variable flange width. *Building Constructions. Theory and Practice, (12), 42–52.,* [in Ukrainian]
https://doi.org/10.32347/2522-4182.12.2023.42-52..
6. **Bilyk, A., Nuzhniy, V., Dzhanov, L., & Perestiuk, V.** (2020). Features of the analytical solution of the problem of displacement cantilever steel beams with variable flange depth. *Building constructions. Theory and Practice*, (7), 85–92. [in Ukrainian]

https://doi.org/10.32347/2522-4182.7.2020.85-92

7. **Bilyk S.I., Bilyk A.S., Nilova T.O., Shpynda V.Z., Tsyupyn E.I.** (2018) Buckling of the steel frames with the I-shaped cross-section columns of variable web height. *Strength of Materials and Theory of Structures: Scientific-and-technical collected articles (100), 140-154.* [in English] http://opir.knuba.edu.ua/files/zbirnyk-100/11-100_bylik.pdf.
8. **Thomas Buhl, Claus BW PedersenOle Sigmund.** (2014) Stiffness design of geometrically nonlinear structures using topology optimization. *Structural and Multidisciplinary Optimization (2000) Research paper, (19), p 93–104* [in English] 10.1007/s001580050089
9. **Haidaichuk, V.V., Koshevyi, O.O., & Kosheva, O.V.** (2018). Parametric optimization of columns with various cross-sectional shapes. *Mistobuduvannia ta terytorialne planuvannia, (66), 78–89.* [in Ukrainian].
10. **Dzhanov L.V., Bilyk S.I., Bilyk A.S.** (2025) Rational topology of steel i-beams with various gradients of changing wall height and shelf width at specified sections along the length of the beam. *Strength* of *Materials and Theory of Structures. Scientific-and-technical collected articles, (114), 155-164.* [in English] https://doi.org/10.32347/2410-2547.2025.114.155-164
11. **Bilyk, A.S., Dzhanov, L.V., & Ternovyi, M.I.** (2025). Determination of the optimal height of variable-section steel I-beams using the Lagrange multipliers method. *Spatial Development: Scientific Collection, (11), 282–297.* [in Ukrainian] https://doi.org/10.32347/2786-7269.2025.11.282-297
12. **Hohol M., Marushchak U., Peleshko I., Sydorak D.** (2022) Rationalization of the Topology of Steel Combined Truss. In: Bieliatynskyi A., Breskich V. (eds) *Safety in Aviation and Space Technologies. Lecture Notes in Mechanical Engineering. Springer, Cham, 97-106* [in English] https://doi.org/10.1007/978-3-030-85057-9_9
13. **Ivanchenko G.M., Koshevyi O.O., Koshevyi O.P.** (2023) A numerical study of the multicriteria parametric optimization of the displacement and weight of a two-connected conical shell of minimal surface under thermal and power loading. *Strength of Materials and Theory of Structures: Scientific-and-technical collected articles , (111), 102-112.* [in English] https://doi.org/10.32347/2410-2547.2023.111.102-112
14. **Lavrinenko L., Oliynyk, D.** (2020). Optimal parameter area for steel corrugated web beams. *Building constructions. Theory and Practice, (7), C.45–56.* [in Ukrainian] https://doi.org/10.32347/2522-4182.7.2020.45-56 .
15. **Bilyk, S.I., Shymanovskyi, O.V., Nilov, O.O., Lavrinenko, L.I., & Volodymyrskyi, V.O.** (2021). Metal structures. Vol. 2. Structures of metal frames for industrial buildings. *Kamianets-Podilskyi: Drukarnia "Ruta" p. 448* [in Ukrainian].
16. **Daji Lin a, Liang Gao b, Jie Gao.** (2025) The Lagrangian-Eulerian described Particle Flow Topology Optimization (PFTO) approach with isogeometric material point method / *Computer Methods in Applied Mechanics and Engineering.(440), 117892* [in English] https://doi.org/10.1016/j.cma.2025.117892.
17. **Nuzhnyj, V., & Bilyk, S.** (2024). Revealing the influence of wind vortex shedding on the stressed-strained state of steel tower structures with solid cross-section. *Eastern-European Journal of Enterprise Technologies, 3(1 (129), 69–79.* [in English] https://doi.org/10.15587/1729-4061.2024.306181.
18. **Nguyen, T-T., Lee, J**., (2017) Optimal design of thin-walled functionally graded beams for buckling problems, *Composite Structure, (179), 459-467.* [in English] http://dx.doi.org/10.1016/j.compstruct.2017.07.024
19. **Shugaylo, O., Bilyk, S.** (2023). Development of Safety Assessment Methods for Steel Support Structures of Nuclear Power Plant Equipment and Piping under Seismic Loads. *Nuclear and Radiation Safety, 1 (97), 20–29.* [in English] https://doi.org/10.32918/nrs.2023.1(97).03.
20. **Sudeok Shon, Sengwook Jin, Seungjae Lee** (2017) Minimum Weight Design of Sinusoidal Corrugated Web Beam Using Real-Coded Genetic Algorithms. *Mathematical Problems in Engineering, (7), 1-13/* [in English] https://doi.org/10.1155/2017/9184292.
21. **Harmut Pasternak, Zheng Li.** (2021) Design of steel frame with variable crosssection considering stability usinggeneral method according to EN 1993-1-1. *Scientific Journal of Civil Engineering, (10(2)),* p *59-63* [in English]. https://doi.org/10.55302/SJCE21102059

22. **W. Prager, J. E. Taylor**. (1968) Problems of Optimal Structural Design. J. *Appl. Mech, (35(1)), 102-106* [in English] https://doi.org/10.1115/1.3601120.
23. **Perelmuter A, Yurchenko V**. (2013) Parametric Optimization of Steel Shell Towers of High-Power Wind Turbines. *11th International Conference on Modern Building Materials, Structures and Techniques, Procedia Engineering, (57) 895 – 905.* [in English] https://doi.org/10.1016/j.proeng.2013.04.114200
24. **Trayana Tankova, Luís Simões da Silva, Liliana Marques.** (2018) Buckling resistance of non-uniform steel members based on stress utilization: *General formulation. Journal of Constructional Steel Research, (149), 239-256* [in English] https://doi.org/10.1016/j.jcsr.2018.07.022.
25. **Trayana Tankova, João Pedro Martins, Luís Simões da Silva, Rui Simões, Helder D.** (2018) Experimental buckling behaviour of web tapered I-section steel columns Craveiro *Journal of Constructional Steel Research, (147), 293-312*[in English] https://doi.org/10.1016/j.jcsr.2018.04.015

## LITERATURE

1. **Bazhenov, V.A. Vorona Yu.V., & Perelmuter A.V.** Budivelna mekhanika i teoriia sporud. Narysy z istorii *Karavela, 2016. 428 p*. [in Ukrainian]
2. **Bazhenov V.A.** Variatsiini pryntsypy i metody budivelnoi mekhaniky: *Pidruchnyk. — Kyiv.: Karavela, 2012. 720 s.* ISBN 978-966-2229-44-8
3. **Paola Bertolini, Martin A. Eder Luca Taglialegne Paolo Sebastiano Valvo**. Stresses in constant tapered beams with thin-walled rectangular and circular cross sections *Thin-Walled Structures*. *Volume 137*, *April 2019, Pages 527-540*. https://doi.org/10.1016/j.tws.2019.01.008.
4. **Bendse M. P., Sigmund O.** (2004) Topology Optimization. Berlin, Heidelberg : Springer Berlin Heidelberg, XIV, p.370 https://doi.org/10.1007/978-3-662-05086-6
5. **Bilyk, A. ., Bilyk, S. ., Hlitin, O. ., & Dzhanov, L.** (2022) Optymalna Vysota stalevykh dvotavrovykh balok zi zminnoiu shyrynoiu polyts. *Budivelni konstruktsii. Teoriia i praktyka, (12), 42–52***.** https://doi.org/10.32347/2522-4182.12.2023.42-52.
6. **Bilyk, A., Nuzhniy, V., Dzhanov, L., & Perestiuk, V**. (2020). Osoblyvosti analitychnoho rozviazku zadachi pro peremishchennia konsolnykh stalevykh balok zi zminnoiu shyrynoiu polyts *Budivelni konstruktsii teoriia i praktyka,(7), 85–92.* https://doi.org/10.32347/2522-4182.7.2020.85-92
7. **Bilyk S.I., Bilyk A.S., Nilova T.O., Shpynda V.Z., & Tsyupyn E.I.** Buckling of the steel frames with the I-shaped cross-section columns of variable web height. *Strength of Materials and Theory of Structures: (100), 140-154.* http://opir.knuba.edu.ua/files/zbirnyk-100/11-100_bylik.pdf.
8. **Thomas Buhl, Claus BW PedersenOle Sigmund.** (2014). Stiffness design of geometrically nonlinear structures using topology optimization. *Structural and Multidisciplinary Optimization Research paper*, (19), 93–104, https://doi.org 10.1007/s001580050089
9. **Haidaichuk, V., Koshevyi, O., & Kosheva V.** (2018). Parametrychna optymizatsiia kolon pry riznii heometrychnii formi poperechnoho pererizu. *Mistobuduvannia ta terytorialne planuvannia, (66), 78-89.*
10. **Dzhanov L.V., Bilyk S.I., Bilyk A.S.** (2025) Rational topology of steel I-beams with various gradients of changing wall height and shelf width at specified sections along the length of the beam. *Strength of Materials and Theory of Structures. Scientific-and-technical collected articles.*(*114), 155-164.* https://doi.org/10.32347/2410-2547.2025.114.155-164
11. **Bilyk A.S., Dzhanov L.V., Ternovyi M.I.** (2025) **V**yznachennia optymalnoi vysoty stalevykh dvotavriv zminnoho pererizu za metodykoiu mnozhnykiv Lahranzha *Prostorovyi rozvytok (11), 282-297.* https://doi.org/10.32347/2786-7269.2025.11.282-297
12. **Hohol M., Marushchak U., Peleshko I., & Sydorak D.** (*2021).* Rationalization of the Topology of Steel Combined Truss. *In: Bieliatynskyi A., Breskich V. (eds) Safety in Aviation and Space Technologies. Lecture Notes in Mechanical Engineering. Springer, Cham. P. 97-106* https://doi.org/10.1007/978-3-030-85057-9_9
13. **Ivanchenko G.M., Koshevyi O.O., Koshevyi O.P.** (*2023)* A numerical study of the multicriteria parametric optimization of the displacement and weight of a two-connected

conical shell of minimal surface under thermal and power loading.*Strength of Materials and Theory of Structures: Scientific-and-technical collected articles* (*111), 102-112.* https://doi.org/10.32347/2410-2547.2023.111.102-112

14. **Lavrinenko L., & Oliynyk, D.** (2020) Oblasti optymalnykh parametriv stalevykh hofrovanykh balok. *Budivelni konstruktsiyi. Teoriya i praktyka*. *(7),.45–56.* https://doi.org/10.32347/2522-4182.7.2020.45-56 .
15. **Metalevi konstruktsii.** Kamianets -Podilskyi: «Drukarnia «Ruta» (2021). T2: Konstruktsii metalevykh karkasiv promyslovykh budivel. / Bilyk S.I., Shymanovskyi O.V., Nilov O.O., Lavrinenko L.I., Volodymyrskyi V.O., 448 s.
16. **Daji Lin a, Liang Gao b, Jie Gao.** The Lagrangian-Eulerian described Particle Flow Topology Optimization (PFTO) approach with isogeometric material point method *Computer Methods in Applied Mechanics and Engineering*. *2025.Vol. 440, 117892* https://doi.org/10.1016/j.cma.2025.117892.
17. **Nuzhnyj, V., & Bilyk, S.** (2024) Revealing the influence of wind vortex shedding on the stressed-strained state of steel tower structures with solid cross-section. *Eastern-European Journal of Enterprise Technologies*, 3(1) (129), 69–79. https://doi.org/10.15587/1729-4061.2024.306181 .
18. **Nguyen, T-T., Lee, J.**, (*2017)* Optimal design of thin-walled functionally graded beams for buckling problems, *Composite Structures,. (179), 459-467* http://dx.doi.org/10.1016/j.compstruct.2017.07.024
19. **Shugaylo, O., & Bilyk, S.** 2023. Development of Safety Assessment Methods for Steel Support Structures of Nuclear Power Plant Equipment and Piping under Seismic Loads. *Nuclear and Radiation Safety, Vol.1 (97), 20–29.* https://doi.org/10.32918/nrs.2023.1(97).03.
20. **Sudeok Shon, Sengwook Jin, Seungjae Lee** (2017) Minimum Weight Design of Sinusoidal Corrugated Web Beam Using Real-Coded Genetic Algorithms. *Mathematical Problems in Engineering*. *(7),.1-13* https://doi.org/10.1155/2017/9184292 .
21. **Harmut Pasternak, Zheng Li.** Design of steel frame with variable crosssection considering stability usinggeneral method according to EN 1993-1-1. *Scientific Journal of Civil Engineering*, 2021. Vol. 10(2). P. 59-63 https://doi.org/10.55302/SJCE21102059p
22. **W. Prager, J. E. Taylor.** Problems of Optimal Structural Design. *J. Appl. Mech. 1968. Vol.35(1) P.102-106* . https://doi.org/10.1115/1.3601120.
23. **Anatoly Perelmuter, Vitalina Yurchenko**. Parametric Optimization of Steel Shell Towers of High-Power Wind Turbines. *11th International Conference on Modern Building Materials, Structures and Techniques, Procedia Engineering 2013. Vol.57. P. 895 – 905.* https://doi.org/10.1016/j.proeng.2013.04.114
24. **Trayana Tankova, Luís Simões da Silva, Liliana Marques**. Buckling resistance of non-uniform steel members based on stress utilization: General formulation. *Journal of Constructional Steel Research*. *2018. Vol. 149 P. 239-256* https://doi.org/10.1016/j.jcsr.2018.07.022.
25. **Trayana Tankova , João Pedro Martins, Luís Simões da Silva, Rui Simões, & Helder D.** (*2018).* Experimental buckling behaviour of web tapered I-section steel columns Craveiro *Journal of Constructional Steel Research.. (147), 293-312* https://doi.org/10.1016/j.jcsr.2018.04.015

ISSN 2522-4182

# РАЦІОНАЛЬНІ СТАЛЕВІ КОНСТРУКЦІЇ НАВІСІВ НАД ТРИБУНАМИ СТАДІОНІВ ІЗ ВИКОРИСТАННЯМ ЗВАРНИХ ДВОТАВРІВ ІЗ ЗМІННОЮ ШИРИНОЮ ПОЛИЦІ І ВИСОТИ СТІНКИ

*Любомир ДЖАНОВ*

**Анотація.** Розроблено удосконалений методичний підхід для визначення оптимальної конструктивної форми консольної зварної сталевої двотаврової балки зі змінною шириною полиці та висотою стінки при комбінованому навантаженні: рівномірно розподіленому по довжині та зосередженому згинальному моменті, прикладеному на вільному кінці. Такі сталеві конструкції демонструють високу ефективність використання сталі, виступаючи основними несучими елементами покриттів над трибунами стадіонів.

Ефективність конструкції досягається завдяки перерозподілу сталі по довжині елемента та по висоті поперечного перерізу з метою досягнення оптимальної конструктивної форми. Підбір оптимальної конфігурації базується на числових дослідженнях визначення раціонального градієнта змінності висоти балки та підбору значення градієнта ширини полиці з урахуванням виконання умов міцності для кожного перерізу. Вважається, що раціональний розподіл сталі по висоті перерізу відповідає оптимальному співвідношенню площі полиці і стінки за критерієм мінімізації витрат сталі на кожну елементарну ділянку балки.

Задача оптимізації зварного двотавра конічної форми при прийнятих умовах навантаження з лінійною зміною ширини полиці та висоти стінки сформульована традиційно як однокритеріальна задача умовної оптимізації, в якій критерієм є мінімізація витрат сталі за умов дотримання умов міцності у кожному поперечному перерізі (що залежать від градієнтів змінності ширини полиці та висоти стінки при комплексному навантаженні).

Задача вирішується з метою дотримання обмежень умов міцності та визначення граничних значень градієнта зміни висоти стінки та ширини полиці в поперечному перерізі сталевої двотаврової балки для узагальненої схеми навантаження. Проведено числові дослідження для визначення градієнтів змінності висоти стінки та ширини полиці за критерієм мінімізації витрат сталі та дотримання умов міцності в кожному перерізі вздовж довжини конструкції.

Отримані результати показують, що оптимальним градієнтом змінності висоти перерізу є $\gamma_h \leq 0{,}6$ при $P_1 l/M_{x,0} \leq 2{,}0$ та $\gamma_h \leq 0{,}5$ при $P_1 l/M_{x,0} \leq 1{,}0$. Встановлено, що при $P_1 l/M_{x,0} \leq 0{,}25$ та $\gamma_h \leq 0{,}9$ умови міцності виконуються для всіх перерізів раціональної конструктивної форми зварної сталевої балки. Розроблено методологічний підхід до вирішення такого типу задач в узагальненому вигляді.

**Ключові слова:** сталеві конструкції; покриття стадіонів; оптимальна висота стінки та ширина полиці зварного двотавра; моделювання; числові дослідження

***Received:*** *October 25, 2025.*
***Accepted:*** *November 30, 2025.*

ISSN 2522-4182

DOI: 10.32347/2522-4182.17.2025.221-231
UDC 624.012.4

# INVESTIGATION OF FIBER-REINFORCED CONCRETE BEHAVIOR UNDER SHORT-TERM COMPRESSION

*Oleg SKORUK*

Kyiv National University of Civil Engineering and Architecture,
31, Povitryanykh Syl Ave., Kyiv, Ukraine, 03037
2120756@ukr.net, http://orcid.org/0000-0001-7106-4368

**Abstract**. During the design and subsequent construction of structures, both abroad and in domestic projects, concrete reinforced with various types and forms of fibers—fiber-reinforced concrete—is being used increasingly often. Compared to ordinary concrete, it exhibits enhanced strength characteristics and numerous other properties that indicate improvements in its physical and mechanical performance.

The use of fiber-containing concretes in the production of various structures and their individual elements continues to grow. The combination of the properties of the individual components that make up fiber-reinforced concrete results in a material with improved operational characteristics. As a composite material, fiber-reinforced concrete largely depends on the type and variety of fibers incorporated into its structure, since these determine the key characteristics of the final composite.

Among the different types of fibers, steel fiber is considered one of the most efficient and widespread options, both from an economic standpoint and in terms of its availability across various regions of our country. Different types of fibers are used in manufacturing fiber-reinforced concrete elements and structures to enhance their performance.

The percentage of fiber reinforcement significantly influences the properties of the manufactured specimen or structure as a whole. The characteristics of steel fiber-reinforced concrete also depend heavily on the selected reinforcement percentage, which is determined before production begins.

Compared to ordinary concrete, steel fiber-reinforced concrete exhibits improved strength and deformation characteristics [5,7,9]. This has a positive effect on the economic aspects of production and further operation, as such structures require less maintenance and fewer potential repairs during their service life.

To conduct a deeper analysis of the influence of the quantity, type, and characteristics of steel fibers on axial compression, experimental studies were carried out, the results of which are presented below.

**Oleg SKORUK**
assistant of the Department
of Reinforced Concrete and Stone
Structures

**Keywords**: deformation; fiber concrete; prismatic strength; fiber.

## INTRODUCTION

In the production of fiber-reinforced concrete elements, various types of fibers-including metallic fibers - are used to increase their strength characteristics compared to ordinary concrete. As noted by various researchers [3, 4, 15, 17], their addition significantly improves the strength and deformation properties of the material and the structure as a whole.

The type of fibers used, their length, and their percentage content in the mixture must be selected according to the requirements for the product or structure while strictly adhering to the manufacturing technology.

Deviations from the optimal values of these parameters, whether upward or downward, reduce the effectiveness of dispersed reinforcement and lead to the formation of fiber clumps ("hedgehogs") that are not evenly distributed throughout the volume. Conversely, the absence of fiber reinforcement reduces the overall strength characteristics of the element.

## RESEARCH PURPOSE

Experimental studies of fiber-reinforced concrete prisms in axial compression using metal fibers of various types.

## RESEARCH OBJECTIVES

When performing these studies, the following research tasks were solved:

1. Selection of elements included in the composition of concrete.
2. Search and use of fibers produced by Ukrainian factories.
3. Casting experimental samples.
4. Testing samples.
5. Processing the results and drawing up appropriate conclusions based on the results of the studies.

## MAIN PART

To achieve the set goal and implement the specified tasks, samples were manufactured and tested, and experimental studies of the operation of prisms reinforced with different types of fibers were conducted (Table 2), with subsequent comparison with concrete samples without reinforcement. This made it possible to determine their strength and deformation characteristics.

The formed experimental samples [5] are presented in Fig. 1.

**Fig.1.** Forming samples for an experiment. Photo by Oleg Skoruk
**Рис.1.** Формування зразків для проведення експерименту. Автор фото Олег Скорук

The types of samples of each type are given in Table 1.

**Table 1** Types of test specimens
**Табл. 1** Види дослідних зразків

| № series | Type of samples | Sample size, mm | Quantity, pcs | Notes |
|---|---|---|---|---|
| 1 | prisms | 100×100×600 | 6 | concrete matrix on fine aggregate |
| 2 | prisms | | | fiber concrete matrix made of wavy fibers |
| 3 | prisms | | | fiber-reinforced concrete element made of fiber having anchor ends |
| 4 | prisms | | | reinforced concrete matrix |
| 5 | prisms | | | fiber concrete matrix - fiber mix |

The prisms were tested after storage in accordance with the requirements of DSTU for 28 days.

In total, 30 prisms of different matrix composition and with and without reinforcement were manufactured.

Before testing, clock-type indicators with a division value of 0.001 mm were attached to the surface of the prisms, see Fig. 2.

**Fig.2** Installing sensors on fiber-reinforced concrete prisms. Photo by Oleg Skoruk
**Рис.2** Влаштування датчиків на фібробетонних призмах. Автор фото Олег Скорук

The compression testing of the prisms was performed on a hydraulic press, using the appropriate methodology. The process of testing the test specimens on the equipment, see Fig. 3.

**Fig.3** The process of testing prototypes on equipment. Photo by Oleg Skoruk
**Рис.3** Процес випробування дослідних зразків на устаткуванні. Автор фото Олег Скорук

The loading on the samples was performed in steps, the value was taken to be about 10% of the expected destructive force. At each step, there was a delay of 10 minutes to stabilize internal stresses and deformations, as well as to take readings from the sensors.The indicators on the samples were placed using special mounts and fixed to them with screws.

**Table 2** Types of fibers used
**Табл. 2** Types of fibers used

| Name | General view(sketch) |
|---|---|
| Wave-shaped wire fiber | 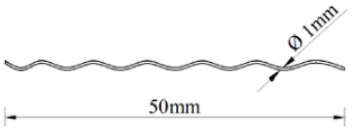  |
| Wire fiber having anchor ends | 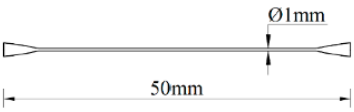  |

Before the start of the tests on the press, the samples were centered relative to the actual axis. For this, the samples were loaded with a test load, which is 5% of the expected destructive force. This load corresponded to σc=1.5 MPa. After that, the difference in the indicators was recorded.

SAMPLE – 1 SERIES

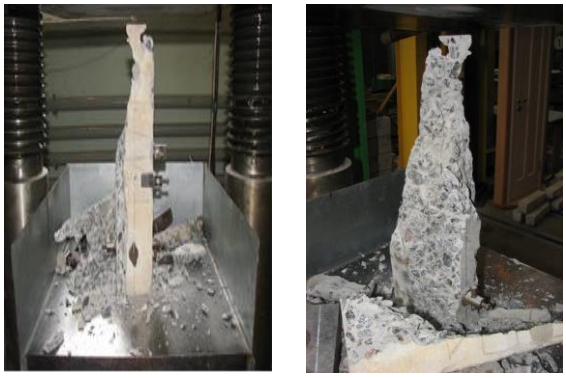

**Fig.4** Test results and nature of destruction. Photo by Oleg Skoruk

**Рис.4** Результати випробування та характер руйнування. Автор фото Олег Скорук

If significant discrepancies in the indicators on four sides were detected, i.e. more than 10%, the test sample was moved along the support plate several times until uniform values were achieved for all arranged indicators. Accordingly, the sample was placed in the desired position in two to four attempts. Then, each sample was tested to determine longitudinal deformations. The general appearance of the fracture of the samples is shown in Fig. 5-8. During the study of experimental research elements, the applied load and the deformation changes that developed were recorded. The applied load and the resulting deformations for sample №1-5 are given in the Tables 3-7.

**Table 3** Change in deformations of test specimen №1.

**Табл. 3** Зміна деформацій дослідного зразка №1.

| Sample № | Load, % | $f_{c,prism}$, MPA |
|---|---|---|
| 1 | 15 | 19,7 |
| | 30 | 20,3 |
| | 45 | 20,4 |
| | 60 | 19,9 |
| | 75 | 19,5 |
| | 85 | 20,2 |

SAMPLE – 2 SERIES

Side surface

**Fig.5** Test results and nature of destruction. Photo by Oleg Skoruk

**Рис.5** Результати випробування та характер руйнування. Автор фото Олег Скорук

**Table 4** Change in deformations of test specimen №2.

**Табл. 4** Зміна деформацій дослідного зразка №2.

| Sample № | Load, % | $f_{c,prism}$, MPA | $\rho_{fv}$ |
|---|---|---|---|
| 2 | 15 | 32,8 | 1,5 |
| | 30 | 33,5 | 1,5 |
| | 45 | 33,4 | 1,5 |
| | 60 | 33,0 | 1,5 |
| | 75 | 32,9 | 1,5 |
| | 85 | 33,1 | 1,5 |

SAMPLE – 3 SERIES

Side surface

**Fig. 6** Test results and nature of destruction. Photo by Oleg Skoruk

**Рис. 6** Результати випробування та характер руйнування. Автор фото Олег Скорук

**Table 5** Change in deformations of test specimen №3.
**Табл. 5** Зміна деформацій дослідного зразка №3.

| Sample № | Load, % | $f_{c,prism}$, MPA | $\rho_{fv}$ |
|---|---|---|---|
| 3 | 15 | 34,2 | 1,5 |
| | 30 | 34,6 | 1,5 |
| | 45 | 34,0 | 1,5 |
| | 60 | 33,8 | 1,5 |
| | 75 | 34,1 | 1,5 |
| | 85 | 33,9 | 1,5 |

SAMPLE – 4 SERIES

Side surface

**Fig.7** Test results and nature of destruction. Photo by Oleg Skoruk
**Рис.7** Результати випробування та характер руйнування. Автор фото Олег Скорук

**Table 6** Change in deformations of test specimen №4.
**Табл. 6** Зміна деформацій дослідного зразка №4.

| Sample № | Load, % | $f_{c,prism}$, MPA |
|---|---|---|
| 1 | 2 | *3* |
| 4 | 15 | 27,9 |
| | 30 | 28,1 |
| | 45 | 28,3 |
| | 60 | 27,8 |
| | 75 | 28,0 |
| | 85 | 28,2 |

SAMPLE – 5 SERIES

Side surface

**Fig. 8** Test results and nature of destruction. Photo by Oleg Skoruk
**Рис. 8** Результати випробування та характер руйнування. Автор фото Олег Скорук

**Table 7** Change in deformations of test specimen №5.
**Табл. 7** Зміна деформацій дослідного зразка №5.

| Sample № | Load, % | $f_{c,prism}$, MPA | $\rho_{fv}$ |
|---|---|---|---|
| 5 | 15 | 38,2 | 0,75+0,75 – fiber mix |
| | 30 | 37,8 | 0,75+0,75 – fiber mix |
| | 45 | 38,6 | 0,75+0,75 – fiber mix |
| | 60 | 39,4 | 0,75+0,75 – fiber mix |
| | 75 | 38,7 | 0,75+0,75 – fiber mix |
| | 85 | 39,1 | 0,75+0,75 – fiber mix |

After testing various series of samples, the corresponding parameters were determined, which are listed in Table 8.

**Table 8** Results of testing of experimental samples.
**Табл. 8** Результати випровування дослідних зразків.

| Sample series | $\rho_{fv}$ | $f_{cf,prism}/f_{c,prism}$ | $f_{cf,prism,m}/f_{c,prism,m}$ | $E_{cf} \times 10^{-3}$ | $E_{cf,m} \times 10^{-3}$ | $\nu$ | $\nu_m$ | $\varepsilon_{cf1}$ | $\varepsilon_{cf1,m} \times 10^{-3}$ |
|---|---|---|---|---|---|---|---|---|---|
| 1.1 | 0 | 19,7 | 19,8 | 17,2 | 17,3 | 0,18 | 0,18 | 0,2 | 0,2 |
| 1.2 | 0 | 20,3 | | 17,3 | | 0,19 | | 0,2 | |
| 1.3 | 0 | 20,4 | | 17,2 | | 0,18 | | 0,2 | |
| 1.4 | 0 | 19,9 | | 17,4 | | 0,18 | | 0,2 | |
| 1.5 | 0 | 19,5 | | 17,3 | | 0,19 | | 0,2 | |
| 1.6 | 0 | 20,2 | | 17,2 | | 0,19 | | 0,2 | |
| 2.1 | 1,5 | 32,8 | 33,2 | 34,4 | 34,4 | 0,23 | 0,23 | 0,24 | 0,25 |
| 2.2 | 1,5 | 33,5 | | 34,3 | | 0,24 | | 0,25 | |
| 2.3 | 1,5 | 33,4 | | 34,5 | | 0,23 | | 0,25 | |
| 2.4 | 1,5 | 33,0 | | 34,4 | | 0,24 | | 0,24 | |
| 2.5 | 1,5 | 32,9 | | 34,5 | | 0,23 | | 0,25 | |
| 2.6 | 1,5 | 33,1 | | 34,4 | | 0,23 | | 0,25 | |
| 3.1 | 1,5 | 34,2 | 34,1 | 35,6 | 35,6 | 0,23 | 0,24 | 0,25 | 0,25 |
| 3.2 | 1,5 | 34,6 | | 35,7 | | 0,24 | | 0,25 | |
| 3.3 | 1,5 | 34,0 | | 35,6 | | 0,24 | | 0,25 | |
| 3.4 | 1,5 | 33,8 | | 35,5 | | 0,25 | | 0,24 | |
| 3.5 | 1,5 | 34,1 | | 35,6 | | 0,25 | | 0,24 | |
| 3.6 | 1,5 | 33,9 | | 35,6 | | 0,24 | | 0,25 | |
| 4.1 | 0 | 27,9 | 28,1 | 25,4 | 25,3 | 0,2 | 0,25 | 0,21 | 0,21 |
| 4.2 | 0 | 28,1 | | 25,4 | | 0,21 | | 0,21 | |
| 4.3 | 0 | 28,3 | | 25,3 | | 0,21 | | 0,2 | |
| 4.4 | 0 | 27,8 | | 25,2 | | 0,2 | | 0,2 | |
| 4.5 | 0 | 28,0 | | 25,3 | | 0,21 | | 0,2 | |
| 4.6 | 0 | 28,2 | | 25,3 | | 0,2 | | 0,2 | |
| 5.1 | 1,5 | 38,2 | 38,3 | 39,1 | 39,3 | 0,26 | 0,25 | 0,27 | 0,26 |
| 5.2 | 1,5 | 37,8 | | 39,2 | | 0,25 | | 0,26 | |
| 5.3 | 1,5 | 38,6 | | 39,3 | | 0,26 | | 0,26 | |
| 5.4 | 1,5 | 39,4 | | 39,2 | | 0,26 | | 0,27 | |
| 5.5 | 1,5 | 38,7 | | 39,3 | | 0,26 | | 0,26 | |
| 5.6 | 1,5 | 39,1 | | 39,2 | | 0,25 | | 0,26 | |

For series of samples where there was no fiber in the composition, the prismatic strength was denoted by - $f_{c,prism.}$

The prismatic strength was determined using the formulas [1]:

$$f_{cf,prism} = f_{c,prism} + (k^2_n \varphi_f \rho_{fv} f_f)$$

in this formula

$$\varphi_f = (5+L)/(1+4,5L),$$

$$L = (k2\rho fvf_f)/( f_{cf,prism}),$$

where

$f_f$ – tensile strength of individual fibers;
$k_n$ – coefficient that takes into account the work of fibers in a cross section perpendicular to the direction of the external compressive force;
$\varphi_f$ – коефіцієнт ефективності непрямого армування фібрами;
$\rho_{fv}$ – коефіцієнт фібрового армування $E_{cf}$.

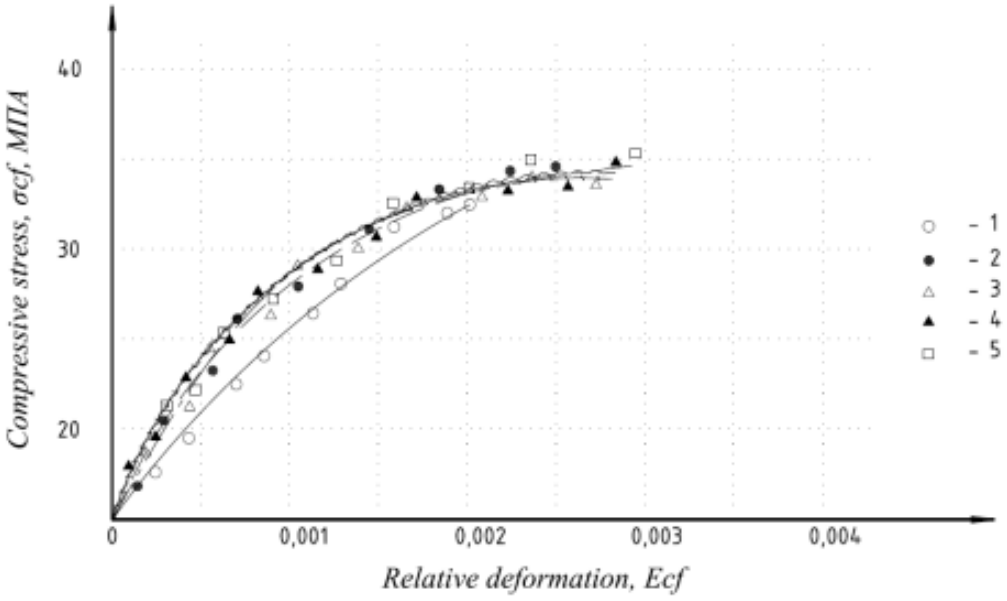


**Fig.9** Diffraction diagram of sample deformation
**Рис. 9** Дифракційна діаграма деформування зразка

## CONCLUSIONS

1. The data obtained from the results of the experiment showed that samples with the addition of any type of fiber demonstrate significantly higher strength indicators in axial compression compared to conventional concrete and reinforced concrete samples.
2. The type of fiber used has an impact on the load-bearing capacity of the element under axial compression, which is evident from the nature of the destruction of the samples and the obtained indicators.
3. Using a mix of different fibers does not significantly improve the load-bearing capacity of the element under axial compression, but remains within the average values.
4. According to the results of the study, the influence of fiber reinforcement on the strength and deformability of elements using fiber was analyzed.
5. The obtained data make it possible to recommend the use of fiber reinforcement in the structures of the country's defense fortifications that perceive static dynamic impacts.

## REFERENCES

1. **DSTU-N B V.2.6-218:2016:** Guidelines for the design and manufacture of constructions from dispensable reinforced concrete *[Effective from 01.07.2016 p.]. - K.: SE "UkrNDNC" 2017 – 32.* [in Ukraine] https://online.budstandart.com/ua/catalog/doc-page?id_doc=65793
2. **Skoruk, O., Cherny, I., & Tatarchenko, G.** (2017). Deflections of thin steel-reinforced concrete slabs supported along the contour. *Scientific news of Daliv University, (12).* [in Ukraine] https://nvdu.snu.edu.ua/wp-content/uploads/2020/03/2017_12_7.pdf
3. **Ksyonshkevych, L., Barabash, I., Danylo-nko, A.** (2015). The effect of basalt fiber on the strength of cement stone. *Resource-saving materials, constructions, buildings and structures, (31), 55-64.* [in Ukraine] https://doi.org/10.31713/budres.v0i31.31
4. **Drobhynets, S.** (2004). The influence of low-cycle loads on the change in the modulus of elasticity of steel-reinforced concrete under axial compression. *Resource-saving materials, constructions, buildings and structures: Collection of scientific papers, (11), 178-183..* [in Ukraine] https://budres.org/index.php/budres/issue/archive

5. **Skoruk, O.** (2015). Features of production of single- and two-layer concrete, steel fiber concrete, steel fiber reinforced concrete slabs. *City-building and territorial planning, (58), 468-475.* [in Ukraine] https://library.knuba.edu.ua/books/zbirniki/02/2015/201558.pdf
6. **Koliakova, V.** (2020). About the requirements for articles published in the collection of scientific works. *Building structures. Theory and practice, (6), 114-118.* [in Ukraine] https://doi.org/10.32347/2522-4182.6.2020.114-118
7. **Skoruk, O.** (2020). Study of the dynamic influence of technological equipment on the operation of steel-reinforced concrete floor slabs. *Building structures. Theory and practice: coll. of science works, (7), 121-128.* [in Ukraine] https://doi.org/10.32347/2522-4182.7.2020.121-128
8. **Rudneva, I., Pryadko, M., Pryadko, & Tonkacheev, G.** (2020). Peculiarities and prospects of the use of technologies for strengthening building structures with composite materials during the reconstruction of buildings. *Building structures. Theory and practice, ( 7), 12-22.* [in Ukraine] https://doi.org/10.32347/2522-4182.7.2020.12-22
9. **EN 1992-1-1:2004 Eurocode 2**: Design of concrete structures – Part 1-1: General rules and rules for buildings. - *Brussels: GEN, 2004. -226*
10. **EN1990 Eurocode 0**: Basis of structural design.
11. **Shmukler, V., Petrova, O., Reznik, P., Hamad, F., & Sosnowska, M.** (2019). Improvement of the structural parameters of the reinforced concrete support in a mesh cage. *Conference Proceedings, (2077), 020048.* https://doi.org/10.1063/1.5091909
12. **Grassl, P., Davies, T.** Lattice modeling of corrosion induced cracking and bond in reinforced concrete. *Cement and Concrete Composites, (9), 918–924.* https://doi.org/10.48550/arXiv.1103.4162
13. **Klymov, Y., Soldatchenko, O., & Oreshkin, D.** (2010). Experimental studies of adhesion of composite non-metallic reinforcement with concrete. *Bulletin of the National University "Lviv Polytechnic", (662), 207-214.* [in Ukraine] https://ena.lpnu.ua/items/c30c5f80-46ce-460f-9302-9120efdffb68
14. **BS 449:2005 A2:2009** Steel for the reinforcement of concrete-Welded reinforcing steel-Bar, Coil and decoiled product. *Specification, Brit-ish Standarts, BSi, 28p.*
15. **Zhuravskyi, O., Zhuravska, N., & Bambura, A.** (2022). Features of calculation of prefabricated steel fiber concrete airfield slabs. *International Journal on Technical and Physical Problems of Engineering, (14), 103-107.* https://www.iotpe.com/IJTPE/IJTPE-2022/IJTPE-Issue50-Vol14-No1-Mar2022/15-IJTPE-Issue50-Vol14-No1-Mar2022-pp103-107.pdf
16. **Zhuravskyi, O.** (2020). Bearing capacity of steel-fiber-concrete slabs with biaxially prestressed reinforcement. *Strength of Materials and Theory of Structures, (105), 292-301.* [in Ukraine] https://doi.org/10.32347/2410-2547.2020.105.292-301
17. **Zhuravskyi, O., Horobets, A.** (2020). Strength and crack resistance of biaxially prestressed reinforced concrete slabs in transverse bending. *Building structures. Theory and practice, (1) 194-204.* [in Ukraine] https://repositary.knuba.edu.ua/server/api/core/bitstreams/055dc236-fdb5-4cb3-af98-d7d2f4a1ebe5/content
18. **Smorkalov, D.** (2022) Monolithic reinforced concrete structures with pre-tensioned ropes. *Building structures. Theory and practice, (10), 136-142.* [in Ukraine] https://doi.org/10.32347/2522-4182.10.2022.136-142
19. **Posternak, O., Posternak, M.** (2022)**.** Influence of the uncertainty of the calculation model of reinforced bending elements. *Building structures. Theory and practice, (10), 158-165.* [in Ukraine] https://doi.org/10.32347/2522-4182.10.2022.158-165
20. **Vyhnanets, M.** (2019). Properties of fiber-reinforced concrete under short-term and long-term loading. *Bulletin of the Odessa State Academy of Civil Engineering and Architecture, (77), 46-57.* [in Ukraine] http://visnyk-odaba.org.ua/2019-77/7.pdf
21. **Kuznietsova, I.** (2022) Findings of modern engineering research and developments. *Findings of modern engineering research and developments: Scientific monograph, 214-232.* https://doi.org/10.30525/978-9934-26-207-4-8
22. **Neutov, S., Surianinov, M., & Korneieva, I**. (2017). Experimental researches of fiber concrete creep. *Structures, Buildings and Facilities, (116).* https://doi.org/10.1051/matecconf/201711602021

23. **Andriichuk, O., Kysliuk, D., & Ninichuk, M**. (2020). Calculation of bearing capacity of normal cross-sections of combined-reinforced sfrc bending elements. *Modern technologies and calculation methods in construction, (13), 15-23*. [in Ukraine] https://doi.org/10.36910/6775-2410-6208-2020-3(13)-02
24. **Kripak, V., Kolyakova, V., & Gaidai, M**. (2021). Research on the effectiveness of reinforced concrete monolithic floors with hollow liners. *Building constructions. Theory and practice, (9), 15–29.*[in Ukraine] https://doi.org/10.32347/2522-4182.9.2021.15-29
25. **Kuznietsova, I.** (2021). Strength of concrete under local compression taking into account the ratio of the element height to the size of the loading area. *Ukrainian Journal of Construction and Architecture, (5), 61-67.* https://doi.org/10.30838/J.BPSACEA.2312.261021.61.802
26. **Koliakova, V. M., & Sharmakov, Ye. L.** (2014). Features of the behavior of steel–reinforced concrete span structures when ensuring their anchoring within the span. *Interuniversity Collection "Scientific Notes", 46, 280–285. Lutsk,* [in Ukraine]

## LITERATURE

1. **DSTU-N B V.2.6-218:2016.** Nastanova z proektuvannia ta vyhotovlennia konstruk-tsii z dyspesno armovanoho betonu. – *K.: DP «UkrNDNTs» 2017. – 32* https://online.budstandart.com/ua/catalog/doc-page?id_doc=65793
2. **Skoruk, O., Chornyi, I., & Tatarchenko H.** (2017). Prohyny tonkykh stalefibrobetonnykh plyt opertykh po konturu. *Naukovi visti Dalivskoho universytetu, (12)* https://nvdu.snu.edu.ua/wp-content/uploads/2020/03/2017_12_7.pdf
3. **Ksonshkevych, L., Barabash, I., & Danylenko, A.** (2015). Vplyv bazaltovoi fibry na mitsnist tsementnoho kameniu. *Resource-saving materials, constructions, buildings and structures, (31), 55-64* https://doi.org/10.31713/budres.v0i31.31
4. **Drobyshynets, S.** (2004). Vplyv malo-tsyklovykh navantazhen na zminu modulia pruzhnoplastychnosti stalefibrobetonu pry osovomu stysku. *Resursoekonomni materialy, konstruktsii, budivli ta sporudy: Zbirnyk naukovykh prats, (11), 178-183* https://budres.org/index.php/budres/issue/archive
5. **Skoruk, O.** (2015). Osoblyvosti vyhoto-vlennia odno-, dvosharovykh betonnykh, sta-lefibrobetonnykh, stalefibrozalizobeton-nykh plyt. *Mistobuduvannia ta terytoria-lne planuvannia, (58), 468-475* https://library.knuba.edu.ua/books/zbirniki/02/2015/201558.pdf
6. **Koliakova, V.** (2020) Pro vymohy shchodo statei, yaki publikuiutsia u zbirnyku naukovykh prats «Budivelni konstruktsii. Teoriia i praktyka». *Budivelni konstruktsii. Teoriia i praktyka.(6), 114-118* https://doi.org/10.32347/2522-4182.6.2020.114-118
7. **Skoruk, O.** (2020). Doslidzhennia dyna-michnoho vplyvu vid tekhnolohichnoho obladnannia na robotu stalefibrobetonnykh plyt perekryttia. *Budivelni konstruktsii. Teoriia i praktyka, (7), 121-128* https://doi.org/10.32347/2522-4182.7.2020.121-128
8. **Rudnieva, I., Priadko, M. & Tonkacheiev, H.** (2020). Osoblyvosti ta perspektyvy vykorystannia tekhnolohii pidsylennia budivelnykh konstruktsii kompozytsiinymy materialamy pry rekonstruktsii sporud. *Budivelni konstruktsii. Teoriia i praktyka, (7), 12-22.* https://doi.org/10.32347/2522-4182.7.2020.12-22
9. **EN 1992-1-1:2004 Eurocode 2**: Design of concrete structures – *Part 1-1: Generalrules and rules for buildings. – Brussels: GEN, 2004. –226 p.*
10. **EN1990 Eurocode 0**: *Basis of structural design.*
11. **Appa Rao G, Kadhiravan, D.** (2013) Nonlinear FE modeling of anchorage bond in reinforced con-crete. *International Journal of Research in Engineering and Technology, (9), 377-382.* https://doi.org/10.1063/1.5091909
12. **Grassl, P., Davies ,T.** (2011). Lattice modelling of cor-rosion induced cracking and bond in reinforced concrete. *Cement and Concrete Composites, (33), 918–924* https://doi.org/10.48550/arXiv.1103.4162
13. **Klymov, Iu., Soldatchenko, O., Orieshkyn, D.** (2010). Eksperymentalni doslidzhennia zcheplennia kompozytnoi nemetalevoi armatury z betonom. *Visnyk Natsionalnoho universytetu "Lvivska Poli-tekhnika", (662), 207-214* https://ena.lpnu.ua/items/c30c5f80-46ce-460f-9302-9120efdffb68

14. **BS 449:2005 A2:2009** Steel for the reinforcement of concrete-Welded reinforcing steel-Bar, Coil and decoiled product. *Specification, British Standarts, BSi, 2009- 28p.*
15. **Zhuravskyi, O., Zhuravska, N., Bambura. A.** (2022). Features of calculation of prefabricated steel fiber concrete airfield slabs. *International Journal on Technical and Physical Problems of Engineering, (14), 103-107.* https://www.iotpe.com/IJTPE/IJTPE-2022/IJTPE-Issue50-Vol14-No1-Mar2022/15-IJTPE-Issue50-Vol14-No1-Mar2022-pp103-107.pdf
16. **Zhuravskyi, O.** (2020). Bearing capacity of steel-fiber-concrete slabs with biaxially prestressed reinforcement. *Strength of Materials and Theory of Structures, (105), 292-301* https://doi.org/10.32347/2410-2547.2020.105.292-301
17. **Zhuravskyi, O., Horobets, A.** (2020). Mitsnist ta trishchynostiikist dvokhosno poperedno-napruzhenykh stalefibrobetonnykh plyt pry poperechnomu zghyni. *Budivelni konstruktsii. Teoriia i praktyka, (1), 194-204* https://repositary.knuba.edu.ua/server/api/core/bitstreams/055dc236-fdb5-4cb3-af98-d7d2f4a1ebe5/content
18. **Smorkalov, D.** (2022). Monolitni zalizobetonni konstruktsii z poperedno napruzhenymy kanatamy. *Budivelni konstruktsii. Teoriia i praktyka, (10), 136-142* https://doi.org/10.32347/2522-4182.10.2022.136-142
19. **Posternak, O., Posternak, M.** (2022). Vplyv nevyznachenosti rozrakhunkovoi modeli pidsylenykh zghynalnykh elementiv. *Budivelni konstruktsii. Teoriia i praktyka, (10), 158-165* https://doi.org/10.32347/2522-4182.10.2022.158-165
20. **Vyhnanets, M**. (2019). Vlastyvosti fibrobetonu pry dii korotkochasnoho ta tryva-loho navantazhennia. *Visnyk Odeskoi derzhavnoi akademii budivnytstva ta arkhitektury, (77), 46-57.* http://visnyk-odaba.org.ua/2019-77/7.pdf
21. **Kuznietsova, I.** (2022). Mitsnist fibrobetonnykh elementiv pry mistsevomu stysnenni. *Findings of modern engineering research and developments: Scientific monograph, 214-232* https://doi.org/10.30525/978-9934-26-207-4-8
22. **Neutov, S., Surianinov, M., Korneieva, I**. (2017). Experimental researches of fiber concrete creep. *Structures, Buildings and Facilities, (116)* https://doi.org/10.1051/matecconf/201711602021
23. **Andriichuk, O., Kysliuk, D., & Ninichuk, M**. (2020). Vyznachennia nesuchoi zdatnosti normalnykh pereriziv kombinovano-armovanykh stale-fibrobetonnykh zghynalnykh elementiv. *Suchasni tekhnolohii ta metody rozrakhunkiv u budivnytstvi, (13), 15-23* doi.org/10.36910/6775-2410-6208-2020-3(13)-02
24. **Kripak, V., Koliakova, V., & Haidai, M. (2021).** Doslidzhennia efektyvnosti zalizobetonnoho monolitnoho perekryttia z porozhnystymy vkladyshamy. *Budivelni konstruktsii. Teoriia i praktyka, (9), 15–29.* https://doi.org/10.32347/2522-4182.9.2021.15-29
25. **Kuznietsova, I.** (2021). Mitsnist betonu za mistsevoho stysnennia z urakhuvanniam vidnoshennia vysoty elementa do rozmiru dilianky navantazhennia. *Ukrainskyi zhurnal budivnytstva ta arkhitektury, (5), 61-67.* https://doi.org/10.30838/J.BPSACEA.2312.261021.61.802
26. **Koliakova, V. M., Sharmakov, Ye. L.** (2014). Osoblyvosti roboty stalezalizobetonnykh prolotnykh konstruktsii pry zabezpechenni yikh ankeruvannia u proloti. *Mizhvuzivskyi zbirnyk "Naukovi notatky". (46),.280- 285*

## ДОСЛІДЖЕННЯ РОБОТИ ФІБРОБЕТОНУ ПРИ КОРОТКОТРИВАЛОМУ СТИСКУ

*Олег СКОРУК*

**Анотація.** При проектуванні та подальшому будівництві як за кордоном так і у вітчизняних проектах все частіше застосовують бетон армований різними типами і видами волокон - фібробетон, який має у порівнянні зі звичайним бетоном підвищені характеристики міцності та багато інших властивостей, що вказують на покращення його фізико-механічних характеристик.

Застосування бетонів з вмістом фібри під час виготовлення різноманітних конструкцій і окремих їх елементів постійно зростає. Поєднання властивостей окремих компонентів, що входять до складу

фібробетону, створює і форм матеріал з покращеними експлуатаційними якостями. Як композиційний матеріал, фібробетон значною мірою залежить від типу та різновиду фібри, що вводиться до його структури, адже саме вона визначає основні характеристики готового композиту.

Серед різних видів волокон сталева фібра вважається однією з найбільш ефективних та поширених з економічної точки зору так із точки зору доступності у різних куточках нашої держави.

Різні види фібр використовують при виготовлені елементів і конструкцій з фібробетону для підвищення характеристик виробу.

Відсоток армування фібрами елементів з фібробетону значною мірою впливає на властивості виготовленого зразка чи конструкції в цілому.

Властивості сталефібробетону також багато в чому залежать від обраного відсотка армування, який розраховується перед початком виготовлення конструкції.

Сталефібробетон, в порівнянні зі звичайним бетоном, має підвищену міцнісні і деформативні характеристики [5,7,9]. Це сприє. Це впливає на економічну складову вартості конструкції при виготовленні і подальшій експлуатації, так як вимагає у подальшому меншого догляду та можливих поточних ремонтів при експлуатації.

З метою глибшого аналізу впливу кількості, типу та характеристик металевих волокон на осьовий тиск було виконано експериментальні дослідження, результати яких наведено нижче.

**Ключові слова:** деформація; фібробетон; призмова міцність; фібра.

***Received:*** *November 01, 2025.*
***Accepted:*** *December 05, 2025.*

Наукове видання

# БУДІВЕЛЬНІ КОНСТРУКЦІЇ. ТЕОРІЯ І ПРАКТИКА

Збірник наукових праць

Випуск 17/2025


Редакція залишає за собою право редагувати та скорочувати подані матеріали.
Усі статті одержали позитивну оцінку незалежних рецензентів.

Оригінал-макет виготовлено в редакції збірника наукових праць
Будівельні конструкції. Теорія і практика.

| | |
|---|---|
| Головний редактор | Журавський О.Д. |
| Комп’ютерне верстання | Колякова В.М. |
| Редагування і коректура | Колякова В.М., |
| Макетування | Колякова В.М., Постернак О.М. |
| Обкладинка | Лисюк С.А., Постернак О.М. |

Підписано до друку 25.12.2025. Формат 60 х 84 1/8.
Ум. друк, арк. _ Обл.-вид. арк. _
Тираж 100 прим.

**Редакція збірника наукових праць:**
03037, Україна, м. Київ, проспект Повітряних Сил, 31, КНУБА, к. 104,114
Телефон редакції: (044) 241-55-04; (044)245-48-42
knubazbk@gmail.com
http://bctp.knuba.edu.ua

Виготовлювач: «Видавництво Ліра-К»
Свідоцтво № 3981, серія ДК.
03142, м. Київ, вул. В.Стуса, 22/1.
тел./факс (044) 247-93-37; 228-81-12
Сайт: lira-k.com.ua, редакція:zv_lira@ukr.net